GROUND MOVEMENTS ASSOCIATED WITH TRENCHLESS PIPELAYING OPERATIONS

by

DAVID NEIL CHAPMAN, B.Sc.

A Doctoral Thesis submitted in partial fulfilment of the requirements for the award of Doctor of Philosophy of the Loughborough University of Technology.

September 1992

To my wife

CONTENTS

ABSTRACT

A comprehensive review of the published work is presented on field, laboratory modelling and theoretical data relating to ground movements associated with trenchless pipelaying techniques. Due to the similarities with convergent trenchless techniques, soft ground tunnelling work is also reviewed.

The factors that influence these ground movements are isolated and the ability to investigate these considered in terms of model tests. A test facility based on a 1.5m long,1.5m high and 1.0m wide steel tank has been developed and this is described together with the philosophy behind its use. The development of appropriate methods of simulating both pipejacking and pipebursting trenchless techniques using the test facility, based on the installation of a 200mm diameter semicircular steel pipe section, are described. The use of a stereo-photogrammetry technique for the ground movement data acquisition is also reported and assessed.

Three programmes of model tests were conducted: open shield pipejacking, closed shield pipejacking and pipebursting. The test programmes included investigations into the effects on the soil movements of variations in cover depth, overcut ratio (pipejacking tests), bursting ratio (pipebursting tests) and the effect of using different dry sands at different densities.

From the photographs obtained during the tests, the sand displacements were determined in both the longitudinal and perpendicular planes to the pipe installation. These displacements allowed contour plots to be produced for the horizontal and vertical components of these displacements. This allowed the interaction of the various areas of sand movement to be appreciated, and the extents and magnitudes to be investigated for the changes in the factors made between each test.

The extension of the results to other test conditions not directly investigated and also to the limited field data available, is made by using interpolation and extrapolation of graphical plots of the test data. These graphical plots also allowed trends in the data to be highlighted.

This project involved a fundamental study of ground movements. However, guidance is given on how the results obtained from the tests can be used to determine the effects on adjacent services and structures. This is presented bearing in mind that the test results were for laboratory model simulations rather than prototype operations.

Two simple theoretical analyses are described, one based on the error function curve and one using a fluid flow method. The error function analysis is used to predict ground movements in the perpendicular plane to the installation, while the fluid flow analysis, with dilation and compression capabilities, is developed to enable ground movements to be predicted in both the perpendicular and longitudinal planes. The analyses were applied to the laboratory model tests and the results correlated very well.

The results of the laboratory model tests and the theoretical analyses developed, considerably extend the understanding and knowledge on the ground movements associated with trenchless pipelaying techniques.

ACKNOWLEDGEMENTS

I would firstly like to thank the Science and Engineering Research Council for providing the funding for the research, without whose support, this project, and this thesis, would not have come about.

I wish to thank Dr. C. D. F. Rogers who supervised this project and provided support and encouragement to me and took an enthusiastic interest in the research throughout the past three years.

For the construction and development of the equipment, I owe a great debt to Mr. M. Gould and Mr. J. Robinson, technicians in the Department of Civil Engineering, whose enthusiastic and skillful work provided the excellent quality equipment to solve a quite complex engineering problem. They also helped me cope through some very frustrating times during the equipment development.

The numerous figures for this thesis would not have been completed without the help and hard work of my father, my wife and Mrs J. Redman.

I would also like to thank the other members of the Department of Civil Engineering, particularly the other researchers, who provided a stimulating and interesting environment in which to work.

Finally, I wish to thank my wife, Sam, who I married towards the end of the research project. She provided a great source of strength and happiness in my life throughout this period. I would also like to thank her for her support, encouragement and help, especially with my written English, while I was producing this thesis.

NOTATION

CAPITAL LETTERS

C	Cover depth
C_c	Coefficient of curvature
C_u	Coefficient of uniformity
D	Outside diameter of pipe/tunnel
D_o	Original pipe diameter
D_f	Final diameter after expansion (pipebursting)
E_h	Horizontal surface strain
G_s	Specific gravity of soil
J	Forward jacking distance
K	Empirical constant (equation 2.17)
K_o	Ratio of the horizontal and vertical stress
K_{cr}	Critical horizontal and vertical stress ratio separating Mode I and Mode II (Wong and Kaiser (1991))
M	Refractive index of glass
N	Stability ratio
N_c	Stability ratio at collapse
P_i	Support pressure inside tunnel
P_o	Vertical pressure above tunnel (soil and surcharge)
R	Outside radius of pipe
R_o	Original radius of pipe prior to bursting operation
R_f	Expansion value during a pipebursting operation
δR	Allowable movement at radius R due to ground loss in fluid flow analysis
V	Volume loss
V_s	Volume loss at ground surface
V_t	Volume loss at tunnel level
W	Ground movement
W_c	Ground movement at crown of tunnel
W_h	Horizontal ground movement
W_{max}	Maximum observed movement at ground surface
Z	Depth from ground surface to pipe/tunnel axis

LOWER CASE LETTERS

a	Radius of a circular sink or source, equivalent to produce the required volume loss or gain associated with an operation
c_u	Undrained shear strength of soil
d	dense soil state
d_{10}	Particle size for which 10% of total passes
d_{30}	Particle size for which 30% of total passes
d_{60}	Particle size for which 60% of total passes
e	Void ratio
$e_{d(l)}$	Void ratio obtained from actual measurements of density made during a dense (loose) sand state test
e_{max}	Maximum void ratio obtainable from standard test in BS1377, 1991;Part 4
e_{min}	Minimum void ratio obtainable from standard test in BS1377, 1991;Part 4
i	Trough width parameter (error function curve)
k	Spring constant (Fig. 2.62)
k	constant (Equation 6.5)
l	Loose state sand
n	Factor for fluid flow analysis formulae (Chapter 6)
r	Radial distance
t	Specific δR value (volume loss dimension) or overcut value in pipejacking tests
t_b	Overburst value in pipebursting operations
x	Horizontal Cartesian coordinate
y	Vertical Cartesian coordinate
z	Longitudinal Cartesian coordinate

GREEK CHARACTERS

α	Compressibility factor in fluid flow analysis (Chapter 6)
α_a	$(1-\sin\psi/1+\sin\psi)$
β	Angle of the line from the vertical joining the tunnel axis to a point on the ground surface, 2.5i from the tunnel centreline (Table 2.2)

δ_v	Maximum surface heave (mm), (Fig. 2.9b)
ϕ'	Angle of shearing resistance
γ	Unit weight of soil
μ	$(1-\sin\phi/1+\sin\phi)$
ρ	Density (Kg/m^3)
ρ_d	Dry density of soil (Kg/m^3)
ρ_w	Density of water (Kg/m^3)
σ	Normal stress
σ_o	Applied stress
σ_c	Confining stress
σ_t	Tunnel support pressure
τ	Shear stress
ψ'	Dilation angle of soil

ABBREVIATIONS

C	Cohesive soil
CPJ	Closed shield pipejacking test
ID	Inside diameter of pipe or tunnel
LF	Load factor (Potts (1976))
NC	Cohesionless soil
OD	Outside diameter of pipe or tunnel
OFS	Overload factor
OPJ	Open shield pipejacking test
PB	Pipebursting test
Rd	Relative density

CHAPTER ONE

1 INTRODUCTION

1.1 A BRIEF BACKGROUND TO TRENCHLESS TECHNOLOGY

Nature has been building tunnels and caves since the world began, and animals have been tunnelling for millions of years. So far as building tunnels is concerned, humans are relatively recent developers of the technique. Although humans had lived in natural caves and tunnels for thousands of years, it was not until humans began to move from the Stone Age to the Bronze Age and subsequently to the Iron Age, that they found it necessary to tunnel, as everything they required up to this time could be found above ground. The requirement for tunnelling thus came about due to the need to quarry stone and mine for metal ores.

It was not until 2180BC and the Babylonians in Mesopotamia that the first tunnel of any importance was constructed, for transporting men and goods under the River Euphrates, and it was thousands of years before another tunnel was constructed under a river. The ancient Egyptians dug many tunnels as part of elaborate tombs and also to obtain building stones. The Greeks were among the early developers of mining techniques and by 700BC they were building elaborate tunnels for water supply purposes.

As might be expected from the many things they achieved in war, public administration, road building and other engineering and construction works, the Romans were the most prolific tunnel builders among the ancient civilizations. Most of their tunnels were built in connection with water supply systems, especially the aqueducts that supplied Rome. The tunnels were required due to the topography of the land and also to hide the water from enemies in times of war. Very few road tunnels were constructed at this time because of the difficulties of construction and especially the lack of adequate equipment. Therefore they prefered to go round obstacles.

Up until the eighteenth century, the use of tunnels was mainly restricted to mining, military and water supply purposes, however the industrial revolution caused a massive increase in tunnelling for transportation, such as railways and canals.

There are basically three types of tunnel, defined by their construction technique. The first is a tunnel dug through rock or soil. The second is a 'cut and cover' tunnel which is constructed by digging a trench, assembling a long tube within the trench and then covering it over. The third technique is the immersed tube type tunnel which is similar to the 'cut and cover' method except under water. The second type, the 'cut and cover' method, can be classed as the most widely used technique for installing the smaller sized services such as sewers, gas and water mains, which are loosely defined as pipelines if smaller than suitable for man entry. Tunnelling thus covers the full spectrum of construction from Channel Tunnel scale projects of tens of metres, to tunnels of tens of millimetres.

There are basically two reasons for constructing tunnels, either to allow humans to move from one point to another, or to allow some other material, such as sewage and water, to be transported from one point to another. As mentioned previously, most of the latter type (pipelines) are constructed using the 'cut and cover' or 'trenching' technique and until recently this was accepted as the cheapest and easiest form of construction. A natural progression was to use some form of subsurface tunnelling technique to avoid the wasted effort of digging a trench, laying a pipe and backfilling, and also to overcome problems where access to the ground surface is impossible, or the depth of the required service too great for trenching methods. Methods known as 'trenchless techniques' have thus developed over recent years for both the virgin installation and renewal of old services.

Virgin installation trenchless techniques derived from a pipejacking method. Pipejacking had been around for many years and had been developed for installing continuous tunnel lining systems to minimise problems of watertightness compared with segmental linings and also for installing linings that were structurally stronger than segmental linings. The earliest records of pipejacking date back to the late nineteenth century in the United States. Since the first pipejacking operations were carried out in Britain in the late 1950s, there has been a wide acceptance of the method in its traditional role for use in sensitive operations, such as excavations under canals and through road and railway embankments. Over the last decade however, this traditional use of the pipejacking technique has been broadened to include all types of service installation including sewers, and water and gas mains, with application to smaller pipe diameters and longer drives. Trenchless technologies provide alternative installation methods for these services and particularly where reduction of surface disruption, through the use of minimal surface excavation, is of great importance. These more recent uses have been brought about through the development of new technologies, including remotely controlled microtunnelling machines. These machines are similar to those used for large scale soft ground tunnelling operations, enabling full face support during excavation, and have meant that even the smallest of pipes (0.1m) can be installed using a pipejacking approach through most ground conditions. The development of trenchless techniques for pipeline renewal, such as pipebursting, has also developed rapidly alongside the pipejacking work. Development has occurred in particular by British Gas and the water companies, who need to renew and upsize many kilometres of pipework each year.

Although the development of technology has made rapid progress, the acceptance of trenchless pipelaying techniques by the public utilities has been slower. Thus although trenchless techniques have been used fairly extensively, the traditional open trench operations still predominate for smaller services. This is true even in urban areas where it has been shown that traffic disruption and other associated problems are greatly reduced by the use of trenchless technology, and where there is increasing pressure from the public to reduce congestion in urban areas during construction works. As this is an indirect cost, and therefore is difficult to assess, it has been neglected in tendering and so generally makes trenchless pipelaying techniques more expensive (UMIST(SRRG) et al, 1987). The New Roads and Street Works Act (1991), which comes into force in autumn 1992, will place tighter controls on street works. The strict settlement criteria for the reinstatement of trenches, which will require much more time and effort to achieve and thus increase costs, in the new Act are likely to provide a breakthrough for trenchless techniques. Trenching costs are liable to increase with the new requirements for improved signing, lighting and guards, and much stricter control over backfill materials and compaction. Stein et al (1989) showed that the direct costs of trenching only rose above those for trenchless methods at a depth greater than about 3m, although these do vary depending on the service diameter. With the new Act, however, this depth could be reduced significantly and, with the associated indirect cost benefits of trenchless techniques becoming more important in the minds of clients, will make for a much more competitive and larger market.

There are, however, problems associated with trenchless techniques. There is the fact that open trenching is much less sophisticated and so allows the use of less skilled operatives to conduct the work. Renewed services with many house connections are a particular problem due to reconnections, although the technology for coping with these situations is developing (Stein et al, 1989). Problems can also occur due to ground deformations caused by trenchless technology, affecting adjacent services and structures: indeed any subsurface disturbance will alter the insitu stresses within the ground and consequently lead to ground deformations. Although, ground movements associated with convergent trenchless techniques have been shown to be less than those for comparable open trenching (O'Reilly & Rogers (1990) compares pipejacking and trenching and Taylor (1984) compares general soft ground tunnelling and trenching) a thorough understanding of likely deformations is important for future developments and may aid the promotion and wider acceptance of the techniques. An investigation into the mechanisms affecting ground movements around trenchless pipelaying techniques is the subject of this thesis.

1.2 TRENCHLESS PIPELAYING TECHNIQUES

The requirements of trenchless pipelaying techniques are to install or renew services as efficiently as possible with minimal surface excavation, and no adverse affects on adjacent structures or services. There are two main groups of trenchless pipelaying techniques. These are classified by how a particular operation affects the surrrounding soil as either convergent techniques or expansive techniques.

When the volume of excavated soil exceeds the volume of the pipe installed the surrounding ground will generally displace, or converge, towards the opening. Construction methods associated with a net volume loss in the insitu soil are referred to as "convergent" installation techniques. These techniques include small diameter (0.9 up to, typically, 2.0m) tunnelling, microtunnelling (less than 0.9m diameter), and various types of thrust boring and jacking, all of which are derived from the original pipejacking principle. Fig. 1.1 shows a cross section through a typical pipejacking operation. The pipejacking technique involves the excavation of two pits, a jacking or start pit and a target pit. The pipejack is initiated at the jacking pit and this is where all the work is executed. The method involves jacking forward the whole pipe train from the jacking pit as excavation is carried out at the face, within a shield on the lead pipe. As the process proceeds new pipe sections are added at the jacking pit. Excavation at the face is carried out either manually or by machine. Spoil is removed from the face through the installed pipe either manually or pumped as a slurry in the case of machine excavation. Plate 1.1 shows a typical microtunnelling machine. Ground deformations occur with these techniques in two ways. The first is due to the excavation process. The subsurface excavation performed with these methods can cause stress relief at the face and subsequent movement of the soil into the shield. Also, to help steering and reduce friction on the jacked pipe sections, the shield is made slightly larger than the outside diameter of the installed pipe. This means that there is convergence of the soil onto the pipe as the shield moves forward (Fig. 1.2). There is also the possibility of long-term consolidation of soil around the installed pipe as the pore pressures dissipate. The second cause of ground movements is due to the forward thrusting of the shield and possible draw-along of soil due to friction with the pipe sections.

When the volume of the installed pipe or construction equipment exceeds the volume of the excavated soil, the surrounding ground will generally displace outwards from the opening. Construction methods associated with a net volume increase in the insitu soil are referred to as "expansive" installation techniques. These techniques include percussive moling, pipe driving and on-line replacement by pipebursting. The work described in this dissertation concentrates on the pipebursting technique. Fig. 1.3 shows a cross section through a typical pipebursting operation. Pipebursting is used primarily as a pipeline renewal technique, and involves mechanical expansion or a pneumatic hammer action to break out the old pipe and force it into the surrounding ground. The amount of expansion obviously depends on the size of the pipe being installed. The bursting head is generally pulled through the pipe being replaced from the target pit by a winch. The new pipe sections are either added at the staring pit and are jacked in behind the bursting head, or, in the case of polyethylene pipes, are pulled through directly behind the bursting head. One type of pipebursting unit is shown in Plate 1.2. Ground movements using these techniques are caused mainly from the soil being thrust outwards by the bursting head as the old pipe is broken out (Fig. 1.4). In order to reduce the friction on the pipes being jacked or pulled in behind the bursting head, it may be of slightly larger diameter than the pipe sections; this can lead to subsequent convergence of the soil onto these pipes. Draw-along of soil due to friction with the pipe section can also occur depending on the convergence rate.

1.3 THE APPROACH ADOPTED FOR THE RESEARCH

The aim of this research project is to investigate the ground movements that occur during the installation or renewal of services using trenchless techniques. The results will help to improve the understanding of the reasons behind the occurrence of ground movements, their likely magnitudes and extents, and their possible effects on adjacent structures and services. This will help engineers, both developing and using trenchless techniques, to obtain a more visual appreciation of the likely effects that changes to their designs will have on the surrounding ground during use in the field.

In the past the development seems to have been conducted on a somewhat "trial and error" basis, as experienced by some dramatic failures of trenchless operations both early on in their introduction and also more recently, resulting in machines having to be retrieved by costly and inconvenient excavations. Such failures seem to be largely due to lack of understanding or inadequate investigation of the problem before field use. The lack of a rigorous approach to development has been detrimental to the industry in terms of loss of confidence, and there is therefore an even greater need for improved understanding in several areas. One such area is that of ground behaviour during the various trenchless operations.

The investigations in this thesis follow the general pattern for a fundamental, laboratory-based research project with practical application in order to obtain a thorough understanding of the problems and their solutions.

A thorough review of the literature is presented in order to ascertain what information, in the form of field observations, experimental investigations and methods of theoretical analysis, is available on the ground movements caused during trenchless pipelaying operations. Work on soft ground tunnelling is also reviewed due to similarities with some of the trenchless pipelaying operations. The quality of the published work is assessed and areas in which work is outstanding are detailed. This work is presented in Chapter 2.

Chapter 3 discusses the philosophy behind the adopted research approach with discussion of other possible approaches, and why these were not chosen.

Full details of the experimental investigations are given in Chapters 4 and 5. Theoretical modelling is considered in Chapter 6. This looks at two simple closed form solutions, mainly concentrating on a fluid flow theory and developing various analyses to model different aspects of trenchless pipelaying techniques. The results are compared with those obtained from the experimental work and also field data where possible. Conclusions are drawn from the project in Chapter 7 and suggestions are made for further work.

1.4 TERMINOLOGY

In order to avoid confusion in the use of varied terminology, particularly when discussing the work of others, standard terms have been used throughout this thesis. These are defined below.

"Trenchless" techniques are operations which are conducted in an attempt to minimise the amount of excavation that is necessary at the ground surface.

"Jacking" is the process of pushing a pipe train forwards into the ground using hydraulic jacking equipment.

"Bursting" is the breaking up of an existing service line and forcing the old pipe fragments into the surrounding ground, to allow a new pipe to be installed.

"Microtunnelling" is a trenchless technique based on the pipejacking principle and using a full face tunnelling machine for the excavation and face support. Generally the machines are less than 2.5m in diameter.

"Overcut" is the extra circumferential excavation that occurs because of the greater outside diameter of the pipejacking shield than the outside diameter of the installed pipe, i.e. it is that material excavated outside the required perimeter of the works. This is used to help steering of the pipejack, via the movements of the shield and it also helps to reduce friction on the installed pipes as they are jacked forwards.

"Overburst" is the additional radial expansion that occurs during a pipebursting operation in order to reduce the friction on the installed pipes behind the bursting head.

"Insitu" soil is that which occurs naturally on a site.

"Prototype" refers to the full scale trenchless technique, as opposed to a scaled down version used for modelling purposes.

The "crown" of the pipe or tunnel is the uppermost point on the pipe curvature and the "invert" lowermost, both points lying on the vertical axis. The pipe or tunnel "springings" are the diametrically opposite points on the circumference that lie on the horizontal axis. The "shoulders" are points that lie equally between the "crown" and the "springings", and the "haunches" are points lying between the "springings" and the "invert".

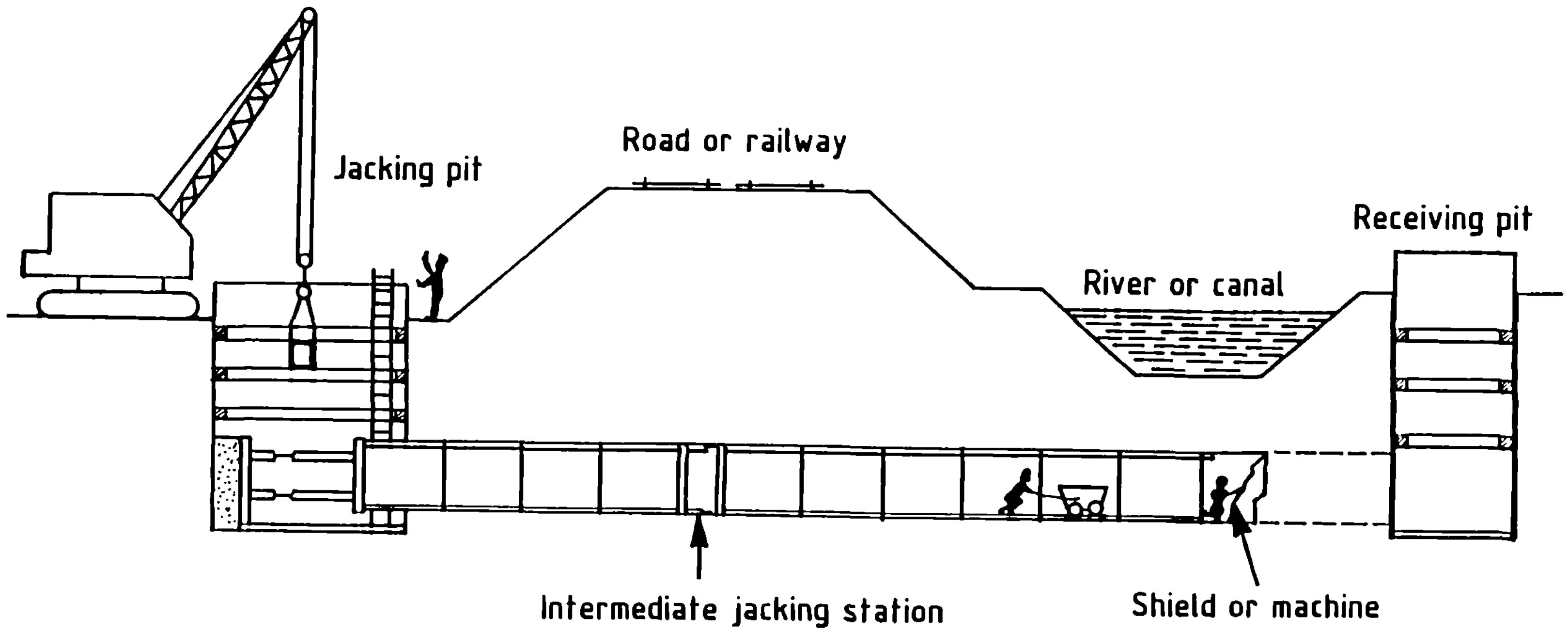

Fig. 1.1 Cross section through a typical pipejacking operation (after Chapman and Rogers, 1991)

Plate 1.1 Typical microtunnelling machine

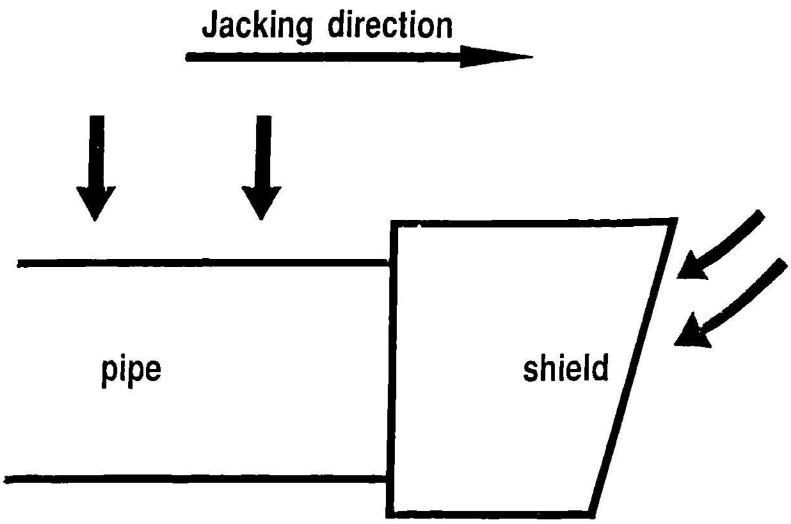

Fig. 1.2 Areas of ground movement during pipejacking

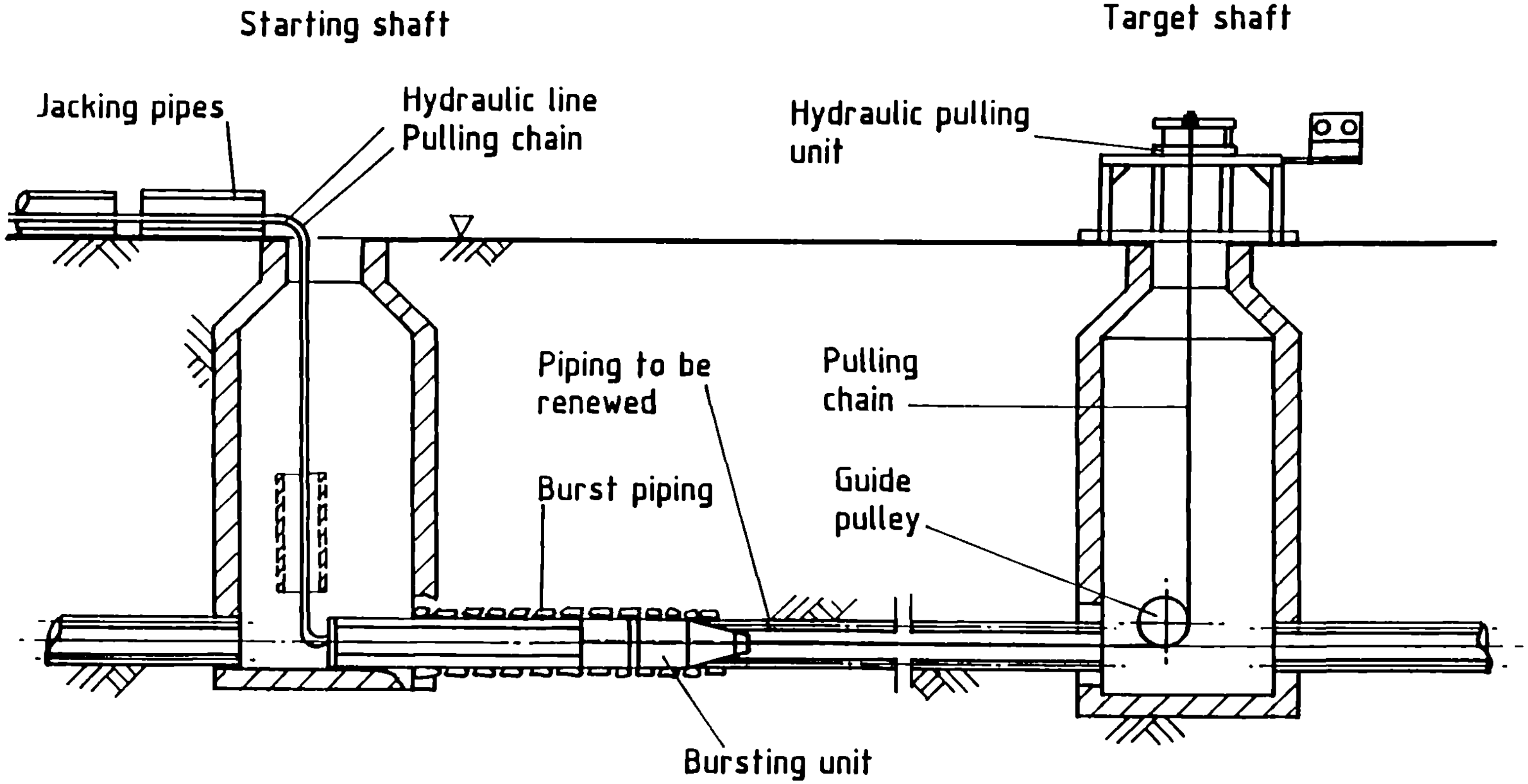

Fig. 1.3 Cross section through a typical pipebursting operation (after Chapman and Rogers, 1991)

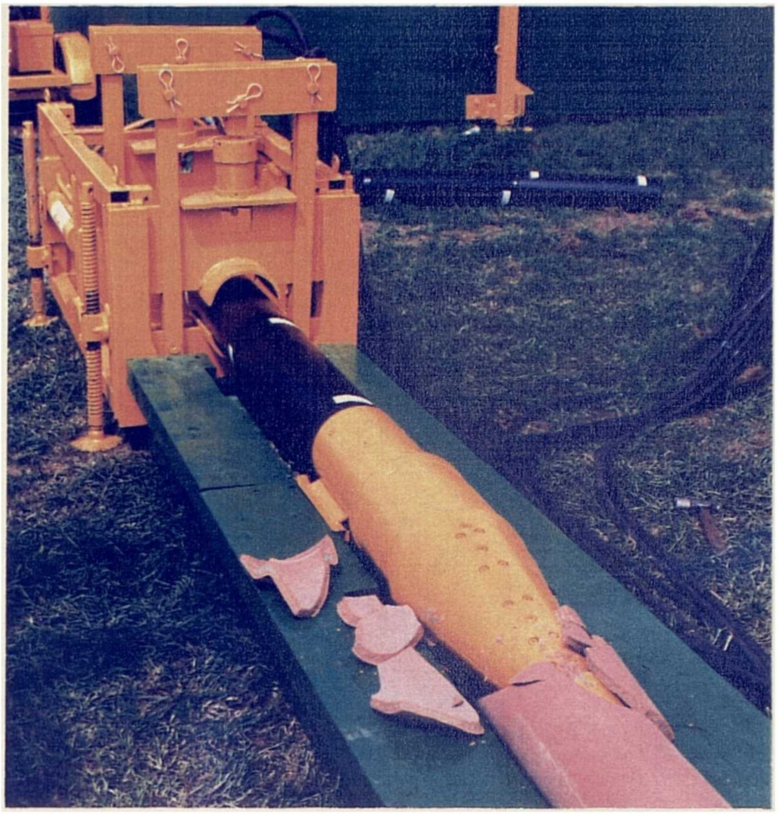

Plate 1.2 Typical pipebursting unit

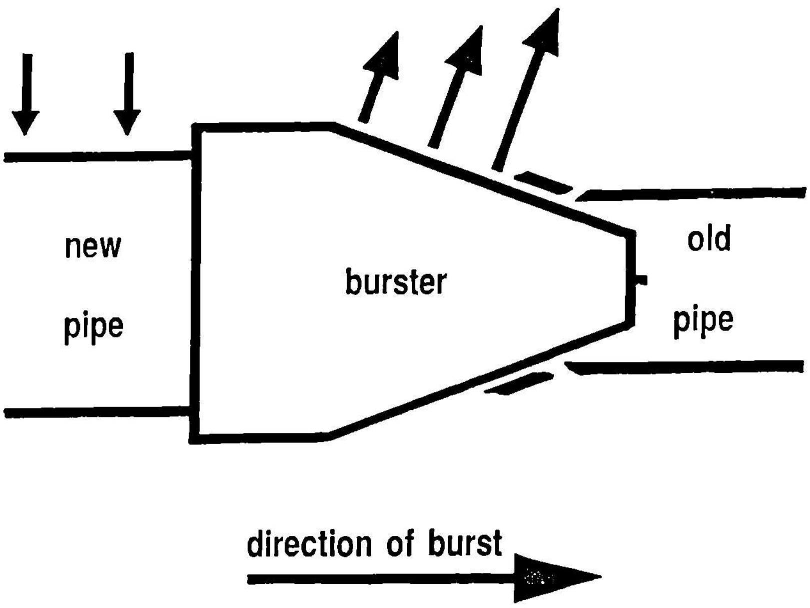

Fig. 1.4 Areas of ground movement during pipebursting

CHAPTER TWO

2 LITERATURE REVIEW

2.1 INTRODUCTION

The literature review has been divided into two sections to allow the broad scope of the subject to be presented. Section 2.2 covers work specifically related to ground movements around trenchless pipelaying techniques. This section is subsectioned into convergent and expansive techniques depending on the means by which the ground is disturbed during construction. Section 2.3 examines the previous investigations into, and observations of, ground deformations associated with segmental lined soft ground tunnelling operations. These show many similarities with convergent trenchless technology and so thorough discussion of this work is important.

Within each of these sections the previous work is discussed in terms of the field investigations (ie. during prototype construction), and experimental investigations (ie. simulating the prototype construction), and theoretical modelling of the prototype observations.

2.2 TRENCHLESS PIPELAYING TECHNIQUES

2.2.1 Convergent Installation Techniques

Stein et al (1989) provide a very detailed description of equipment and methods used for convergent trenchless operations. They show the diverse types of equipment available and outline the suitable soil conditions through which each can be used. This reference is primarily concerned with the equipment aspects of these operations rather than the effects on the surrounding ground. No mention is made of the likely ground movements associated with any of these types of equipment.

Clarkson and Ropkins (1977) made some very pertinent observations on ground movements caused during pipejacking operations. These researchers stated that excavations within the shield can cause disturbance and that this is similar to any soft ground tunnelling operation. Two cases occur: one from failure of the working face and another from over-excavation of the bore. Ground disturbance caused by forward movement of the pipeline during jacking, however is particular to pipejacking. They continued by stating that movement of the roof of the unit (a pipe in general) in contact with the ground above, can cause three forms of ground displacement. Firstly, irregularities in the surface of the pipeline, particularly at the joints, provides in effect a bearing surface that can carry ground forwards. Second, if installed at shallow depths a complete block of soil can be moved forwards, which depends on whether the force transmitted into the block is greater than the restraint offered by the shear and passive resistance of the soil along the sides of the block. Third, friction between the moving units and the soil will cause stresses to be set up within the soil causing reorientation of the soil particles and subsequent movements within the soil. The amount and extent of the movements are very dependent on the type of soil surrounding the units, although this is not qualified in the paper. No other reference is made in the paper to likely ground movements, with the remainder of this paper referring to other aspects of the pipejacking operation, such as the choice of system to use, and the presentation of some case histories, none of which refer to ground movements.

2.2.1.1 Field Measurements

Since the first U.K. pipejacking job was reported by Lanz (1973), there have been many published case histories involving pipejacking. However, most do not consider ground movements. For example, the ten case histories described in a pipejacking association publication (1984) cover a wide variety of applications. These include a 1.5m diameter hand excavated service tunnel under a fully operational runway at Warton Aerodrome in which the only mention of settlement was that "the surface was monitored throughout the project and showed that work had been completed with no settlement recorded", which is hard to believe.

Also described in this publication is an urban trunk sewer renewal contract at Tameside partly constructed using a 1.6m diameter full face tunnelling machine through permeable alluvial glacial sands and gravels. This states only that "settlement at surface level was minimal".

There are numerous other published case histories. Cole (1986) described the construction of a 2.1m diameter hand dug sewer at Greenwich in Thanet Sands. No mention is made of the settlements that must have occurred.

The main problem with this aspect of the literature is that companies reporting case histories are very reluctant to publish ground movement data, for obvious reasons (it could prove detrimental to the companies' reputation). Unfortunately, this makes the data available for analysis very limited and therefore investigations into ground movements are made very difficult, with the result that any possibility of improving the techniques is reduced.

Rogers et al (1989) describe pipejacking beneath Burnham-on-Sea. It involved the construction of a 1.2m diameter sewer (320m long) using a mechanical earth pressure balance machine at 5-6m below ground level. The soil conditions at tunnel level consisted of soft to very soft alluvium. Surface settlements were measured perpendicular to the line of the drive during construction as the machine passed. The measurements indicated an initial settlement and then a heave of material above the tunnel (Fig. 2.1), indicating outward movement of the face at the tunnelling machine. However, examining the magnitudes of the vertical ground movements moving away from the centreline seems to suggest that the values are increasing. This is particularly evident for the data on the right hand side of the figure.

These researchers replotted the movement data by redefining the datum to positions at 11m and 8m from the left and right of the centreline respectively in order to diminish the effects of heave. This gives a rather different picture and indicates a settlement profile as the construction progressed with a maximum settlement of 3-4mm. It must be remembered however, that the measuring points were in the road pavement which would be likely to reduce the observed movements due to slab action of the pavement.

The most comprehensive monitoring of a pipejacking operation was reported by De Moor and Taylor (1989 and 1991). These researchers described the construction of a 2.1m diameter sewer tunnel in very soft alluvium at Tilbury. The operation used the pipejacking technique involving an Iseki slurry shield Crunching mole to support and excavate the soil. The ground movements were monitored both at the surface and subsurface via magnetic extensometers and inclinometers. Pore pressures were also monitored before during and after the tunnel construction. The ground movement observations showed interesting results. As the tunnel construction passed the monitoring points there was a large degree of movement away from the face (up to 300mm) due to over-pressurisation of the slurry at the shield, rather than the expected convergence movements normally associated with tunnelling. The subsurface movements quickly reduced towards the surface due to peat strata above the tunnel. The measured subsurface vertical movements are quite poorly presented in the reports, possibly because of the high reduction in movement just above the pipe caused by the peat layer compressing and thus absorbing much of the movement. The inclinometer data clearly show the outward movements as the tunnel passed (Fig. 2.2), and these do not fully recover after construction. The movements resulted in a maximum surface heave of approximately 25mm in the short term and a maximum settlement of approximately 52mm in the long term, due to consolidation (Fig. 2.3). The pore pressure monitoring showed a positive excess pore pressure response when the tunnel construction was 5m away from the monitored section. The positive excess pore pressures above and ahead of the tunnel indicate a support pressure at the tunnel face above the overburden pressure. The pore pressure was quite variable, although the trend was for the pore pressures to increase until the tunnel construction was approximately 10m beyond the monitored section, at which point they began to dissipate. Pore pressure dissipation was 90% to 95% complete ten months after completion of the tunnel construction. A lot of data are presented for the various monitored sections, however all the results show the same general trends. This case history clearly illustrates the importance of careful construction procedure in controlling ground movements.

2.2.1.2 Laboratory Modelling

There is no published work directly related to investigating, experimentally, ground movements associated with convergent trenchless techniques. (See Section 2.3.2 on the modelling of soft ground tunnels). However, there has been some research work conducted by Uesugi et al (1988) into the sand movements close to steel interfaces. This is indirectly linked to draw-along effects that occur during pipejacking operations. The work was conducted as laboratory experiments using a test apparatus similar to a direct shear box, with a glass side to allow observations of the sand movements. A shearing action was applied to the apparatus. The formation of the shear zone, and in particular the extent and general movements of the sand particles in the region of the sand/steel interface, were investigated. The effect of various surface roughnesses was investigated and this revealed that the greater the roughness, the more erratic and more rolling the sand particle movements became, such that there was not a smooth horizontal slip. The experiments indicated quite clearly the random nature of the sand movements within the shear zone. For the rough interface the shear zone during the tests varied from 5mm to 8mm, however for the smooth interface no such shear zone was observed.

2.2.1.3 Theoretical Analysis

Due to the limited ground movement data available, only limited theoretical predictions of convergent trenchless techniques have been produced. O'Rourke (1985) proposed that the same method could be used as for soft ground tunnelling, due to the similarities between the operations. This means that the surface movements could be predicted using an error function curve (See Section 2.3.1 for a detailed description). De Moor and Taylor

(1991) applied this curve to the surface heave profile obtained during construction and found a very good correlation between the observed and predicted distributions (Fig. 2.4). However, applying the error function curve to observed consolidation settlement profiles did not give a good agreement.

O'Reilly and Rogers (1990) took the surface settlement data presented in Rogers, O'Reilly and Atkin (1989) from a pipejack at Burnham-on-Sea and compared these to the surface movements predicted by a fluid flow model suggested by Sagaseta (1987). (This model is discussed in detail in Section 2.3.3.7.) This seemed to provide a fairly good agreement to the rather variable surface data, although the lateral extent of the predicted movements is questionable (Fig. 2.5).

2.2.2 Expansive Installation Techniques

Stein et al (1989) provide a thorough discussion of various techniques and equipment. As for the convergent trenchless techniques, no mention is made of the ground movements liable to result from the use of the equipment described. A small section relates to theoretical determination of the likely ground movements and this is referred to in Section 2.2.2.3, although this is rather inadequate.

Underground (1986) presented a focus on pipebursting, describing case histories. One example operation used the pipebursting technique to replace and upsize a water main from 75mm to 100mm at Heathrow airport. The cost compared with open trenching was only one third and the technique proved quick and effective. However, there is no mention of ground movements being monitored in this or any other of the case histories.

Microtunnelling (1987) carried an article which assessed the state-of-the-art of pipebursting, the development of the technique and the areas of future research. The technique is not new since in 1959 W.R. Lindsay applied for a USA patent for a pipe splitter and insitu replacement techniques. This article still however lacked any reference to ground displacements.

2.2.2.1 Field Measurements

Several pipebursting case histories have been published, although the ground disturbance caused during the construction operation is often described in terms of visual effects rather than measured data.

Poole et al (1985) describe three case histories where pipebursting techniques were used. The equipment and operating techniques are described, but there is no mention of monitored ground disturbance except for Case History 1. This used an instrumented pipe laid 1.5m away from the 3m deep 229mm diameter clayware foul sewer being replaced. Initially the old sewer was enlarged to 260mm diameter, which was 10mm larger than the 250mm O.D. of the pipe to be installed. However, the ground closed onto the new pipe very quickly and increased the jacking forces considerably; thereafter an overburst of 25mm was employed, which solved this problem. The instrumented pipe only recorded a slight increase in strain, which was negligible, as the burster passed. This was probably due to the instrumented pipe being too far away from the bursting operation in these particular ground conditions.

Noden (1987) describes a case history involving a sewer replacement contract in Oxford clay. The contract involved the replacement of foul sewers at depths ranging from 2.0m to 3.5m. No mention is made of the original size of the sewers or the new installed pipe size. Problems were encountered in the Oxford clay soil on certain lengths of the contract due to leakage of the sewers locally softening the clay. This softened, sticky clay gripped the new pipe immediately after the burster had passed and reduced rates of burst considerably. The solution was to inject bentonite slurry around the new pipe to lubricate it and so reduce the drag. Ground movements are only mentioned briefly, although they were found to be small except when the mole came within two metres of the ground surface. Ground heave at these places was found to be quite significant and damaged a large area of road pavement. As with many of the case histories, the ground movements are qualitative rather than quantitative. It would have been of interest in this case to know the precise effect on the ground movements caused by the bentonite injection.

Asquith et al (1989) describe a case history involving a pipebursting contract in Yorkshire, but concentrate on the equipment and its favourable results in terms of disruption to traffic and costs. There is no mention of any ground movements.

Howe and Hunter (1985) briefly outline a proposed field trial programme to be carried out by British Gas plc. This would involve the monitoring of ground movements during the upsizing of 3inch, 4inch and 6inch cast iron mains using 130mm, 170mm and 245mm moles respectively. However, the results of this work have never been published.

Reed (1987) provides a thorough description of how pipeline renewal techniques have been applied to the British Water Industry. He highlights the factors to be taken into account when considering renewing pipes using trenchless methods and the equipment to be used. It also gives some brief details of controlled field trials, conducted by the Water Research Centre (WRC), to determine the effects of pipebursting on adjacent pipelines in uniform ground conditions. For each of the trials a strain gauged ductile iron pipe was installed above and perpendicular to the pipelines that were subsequently to be replaced. The strain gauges in effect recorded the movements of the pipe during the moling operation (ie. the field monitoring was relatively limited). The results of two of the tests are presented in the paper. The first of these trials involved the replacement of a 300mm internal diameter clay pipe with a 400mm external diameter polyethylene pipe. The trial was conducted on pipelines with a granular surround and installed in Kimmeridge clay (c_u=86kPa). Fig. 2.6 shows how the strain gauges reacted during the moling operation. The instrumented pipe was approximately 700mm from the replaced pipe. The maximum values of strain are only realised with the pipeburster in close proximity to the point of crossing. The strain values are transient and the residual values are small and occurred quickly after the passsage of the pipeburster. The strain values, as the pipeburster continued to pass away from the instrumented pipe were similar to those of the approaching pipeburster. Displacement transducers were installed 300, 600 and 900mm above the pipe being replaced, to record ground movements. Fig. 2.7 shows these results. More displacement measurements would have been beneficial to assess the lateral extent of the movements.

Leach and Reed (1989) combine the work of both British Gas plc and the WRC, and expand on the field work presented by Reed (1987). Ground movements are discussed in some detail, Figs 2.8 a and b illustrating some of the ideas presented. The close proximity of the ground surface, a layer of hard ground below the pipe and trench conditions, all tend to concentrate the outwards movements caused by the burster to be directed more vertically upwards. During a pipebursting operation the ground is initially forced away from the burster, due to the expansion. The ground then converges back onto the new pipe, which is generally of a slightly smaller diameter than the bursting head. This convergence gradually increases at the pipe/soil interface, increasing the jacking loads. A permanent heave is generally left at the ground surface, depending on the soil conditions, replaced and installed pipe sizes and the cover depth.

In addition to the field trials conducted by the WRC and discussed in Reed (1987), British Gas has monitored the effect of pipe replacement during the course of contract works in a similar way to the controlled WRC trials. British Gas also carried out extensive surface monitoring of a variety of moling geometries and ground conditions. These data are presented in a non-dimensional form in Figs. 2.9 a and b, assuming an approximate isoceles triangular profile for the surface heave. Fig. 2.9a shows a general trend of a linear increase in the spread of movement with increased depth, the increase occurring steeply at shallow depths and more gently at depths exceeding approximately 1m. Fig. 2.9b shows that as the cover depth increases, the maximum surface heave decreases, as expected. The relationship seems to form an exponential type of curve which tends to infinity as the axes are approached. The effects of soil type have been excluded from the results in both figures. Using the data collected in the field, a simplified surface damage chart is presented, together with safe proximity charts for adjacent services to bursting operations (Figs. 2.10 a and b). These provide useful guides for engineers considering the use of pipebursting techniques. From the strain gauge readings, an interpretation is made of the effect on a service crossing the replaced pipeline, which is shown in Fig. 2.11, the result of which is that the final position of the pipe is displaced forwards and raised up compared to its original position. There is also some residual rotation of the pipe.

Rogers et al (1991) present some ground movement data obtained from a pipebursting field trial. The field trial was carried out primarily to test the performance of a new ductile iron pipe. The trial involved the replacement of a 200mm internal diameter grey iron pipe at approximately 1.2m depth using a 290mm pipebursting mole to install the 250mm outside diameter ductile iron pipe. The indigenous soil was an overconsolidated firm to stiff clay. Table 2.1 shows the surface ground movements observed both as the burster passed and three months after completion. The lateral extent of significant movements occurred between 50^{o} and 70^{o} to the horizontal. Limited subsurface ground movements were also recorded and these are reported in Section 2.2.2.3. Plotting these case history's results onto Figs. 2.9 a and b, shows them to fall neatly into the pattern of results of other case histories.

Iliffe and Spedding (1990) describe the upsizing of a sewer pipe by the pipebursting technique. The upsizing involved the breaking out of the existing, unreinforced concrete pipe (230mm O.D.) and expanding this to 400mm O.D. in stiff to firm glacial clay. The equipment is discussed, with the disadvantages and advantages of using pipebursting in close proximity to other sewers and services, and the surface highlighted. The problems encountered were mainly concerned with the new pipe installation. The pipe joints caused problems, as did the reliability of the equipment. The surface movements caused by the bursting were monitored. Fig. 2.12 shows a typical heave profile for a 2.2m deep burst in this case with a maximum vertical heave of 50mm, which returned over a period of time to within 5mm of its original level. This seems at first quite strange, as the increase in size is 170mm, which, due to the relatively shallow depth, would have been mostly directed upwards. However, these measurements were taken on the road surface above the bursting operation. This

Distance from centerline	0m	0.5m	1.2m	1.6m
Burster 2.0m away	0	0	0	0
Burster 1.5m away	1	0	0	0
Burster 1.0m away	2	1	0	0
Burster 0.5m away	9	4	0	0
Above burster	19	12	1	0
After 3 months	10	3	0	0

Table 2.1 Surface ground movements (mm) observed during a pipebursting field trial (after Rogers et al (1991))

would provide considerable restraint and therefore reduce the maximum surface heave and widen the significant heave surface profile. When a 700mm thick road surface lay above the bursting operation, this restrained the upwards movement even more, giving a maximum of only 3mm heave in these areas.

2.2.2.2 Laboratory Modelling

Howe and Hunter (1985) describe experiments conducted by British Gas using an X-ray technique to measure soil displacements. Plates are given in the paper illustrating the method used in one particular test. Unfortunately, no movement data are given for any of the tests conducted, so it is of limited use. No data collected from these tests have been published.

Robins et al (1990) describe the development of ductile iron pipes for use with pipebursting. As part of the proof testing of these pipes, a full scale laboratory test was conducted. The trial involved 229mm internal diameter cast (grey) iron pipes being buried in sand at a depth of 1m. The pipes were burst out by an expansive mole having an external diameter of 287mm and replaced by the 250mm diameter smooth bore ductile iron pipes. A few ground movement monitoring instruments were installed, both perpendicular to, and along the centreline of, the pipe. The positions of these instruments are shown in Fig. 2.13, together with some of the movement data collected. The movement data indicate that an area up to 300mm above the pipe is being compressed due to the bursting, and above this the sand moves as a single mass, indicated by the similar movements at this level and at the ground surface. One problem with these measurements is that the lateral extent of the movements perpendicular to the pipe centreline cannot be identified very precisely, and thus only a general picture of the movements is obtained.

The most comprehensive laboratory study to date has been carried out at Oxford University and is reported by Swee and Milligan (1990). These scale model tests of the pipebursting operation (a 55mm diameter burster was used) were conducted in dry Leighton Buzzard 14/25 sand, saturated Speswhite Kaolin clay and a typical sandy clay backfill. The tests in sand provided the upper bound movements and the backfill tests gave the lower bound movements. The test configuration consisted of a constant diameter bar on the front of a varying diameter bar to simulate the bursting (expansion) operation. This means the replaced pipe moves along and up with the burster as it moves forward. This is obviously an approximation compared with the prototype situation. Typical displacement vector plots in sand in both the perpendicular and longitudinal plane, are shown in Figs. 2.14 a and b. This illustrates the highly vertical upward nature of the movements with very little movement below the pipe axis. No attempt was made to investigate the effect of overburst. Fig. 2.15 shows heave profiles in sand for various cover depths. The effect of increasing cover depth in increasing the lateral extent and reducing the maximum vertical magnitude, can be clearly identified. Results for the tests conducted in clay and backfill were not presented in this paper. Swee and Milligan stated that the main factors influencing the magnitude of the ground movements due to the pipebursting operation were soil properties, geometry and drainage characteristics.

2.2.2.3 Theoretical Analysis

O'Rourke (1985) assumed that the conditions of on-line replacement could be approximated by an expanding cylindrical cavity under plane strain in a perfectly elastoplastic undrained clay that is radially homogeneous and isotropic. Due to the assumption of radial uniform expansion, the pipe must be buried at great depth with respect to the ground surface. This is a rather limiting requirement, as most pipebursts are carried out at relatively shallow cover depths. Solutions for this cavity expansion problem are well documented by Vesic (1972), with the development of the cavity expansion theory, and in relation to soil pressuremeters (Gibson & Anderson, 1961 and others). O'Rourke develops the equations, relating them more specifically to pipebursting and permitting the determination of both strain in pipelines crossing the bursting operation and the pressure required for expansion. These provide upper bound solutions for the deformations in the field. Stein et al (1989) take the cavity expansion theory developed by O'Rourke (1985), but concentrate only on the force required for expansion rather than the displacements caused.

Howe and Hunter (1985) considered a similar approach to that of O'Rourke(1985) for high depth/diameter ratios. In order to consider the influence of the ground surface on the ground movements, the finite element method of stress analysis was used. The analysis assumed a saturated cohesive soil, again deforming at constant volume. Fig. 2.16 shows a contour plot of the finite element analysis for a 65mm mole with a cover depth of 0.46m. There is a good indication of the preferential movement towards the free surface. The ratio of upwards to downwards movement is approximately 4.5 to 1. The maximum surface movement is approximately 3.0mm. The few results presented are rather inconclusive and therefore are of limited value.

Leach and Reed (1989) used a stress analysis approach to quantify longitudinal bending effects on a pipe running perpendicular to the bursting operation. The method involves the creation of a stress analysis model to predict the displacement field with the crossing pipe influencing the movements. This is based on the geometry, the material behaviour, boundary conditions and loading conditions. Limited information is given about the method, although it is stated that only approximate results were obtained when it was used.

Rogers and O'Reilly (1991) applied the incompressible fluid flow theory, described in O'Reilly and Rogers (1990) for modelling pipejacking results, to pipebursting data. Specifically, the model is applied to the pipebursting laboratory trial described in Robins et al (1990, see Section 2.2.2.2). A maximum upward burst of 90mm was used at the crown of the pipe varying to zero at the soffit. This was considered appropriate due to the shallow depth of the trial, which would concentrate the movements upwards. Fig. 2.17 shows the total displacement vector plot obtained from the model, with a comparison with measured values at specific positions. There is reasonable correlation, although the lateral extent of the movements seems to be too great.

This same modelling technique was used by Chapman and Rogers (1991) to predict the ground movements for the pipebursting field trial described by Rogers et al (1991). Theoretically, in this case there should be 45mm of expansion all round the pipe, although in reality due to the shallow cover depth, most movement would be directed upwards. This gives 90mm maximum vertical movement above the existing pipe. These researchers applied the model by using a variable expansion around the pipe of zero at the pipe soffit to 90mm at the pipe crown, as for Robins et al (1990). The results of this analysis are shown in Fig. 2.18. There is remarkably good agreement between the measured and theoretical values of ground movement. The lateral extent of the surface heave profile is, however, overestimated by the flow model, which is consistent with the findings of Rogers and O'Reilly (1991).

Swee and Milligan (1990) propose a method of predicting the lateral extent of the movements caused by a bursting operation in dense sand. This is based on the assumption that the shear planes are angled to the vertical by the angle of dilation of the sand (ψ'), which is based on the assumption that the sand reaches the critical state in these regions. Fig. 2.19 shows the proposed method. By using the relationship

$$\varnothing'_{max} - \varnothing'_{crit} = 0.8\psi'_{max}, \qquad (2.1)$$

after Bolton (1986), and inserting appropriate values for the sand, Swee and Milligan found a good agreement between the observed range of surface heave in the model tests and that predicted using the angle of dilation. The position of the start of the plane defining the movements zone close to the burster is rather difficult to determine, particularly for deeper bursts when some outward movement is bound to occur in this region.

2.3 SOFT GROUND TUNNELLING

As mentioned in the introduction, soft ground tunnelling operations with segmental linings have many similarities with convergent trenchless pipelaying techniques, certainly enough to consider the published work on ground movement observations.

The main difference between the two construction techniques is the fact that the trenchless techniques are generally carried out on smaller diameter pipelines (diameter < 1.5m). Another difference is that the pipelines are jacked forwards from the starting pit, where the new pipe sections are added, rather than constructed segmentally immediately behind the shield. In addition, in segmental tunnelling the gap between the ground and the lining is grouted.

2.3.1 Field Measurements

2.3.1.1 Short Term Ground Movements

Ground movements caused during soft ground tunnel construction have been monitored for many years, although this has mainly been in terms of ground surface movements. This was primarily due to the lack of adequate sub-surface measuring equipment which was not developed until the 1970s. Since Peck's (1969) state-of-the-art review on soft ground tunnelling there has been continued work aimed at improving the understanding of ground movements around tunnel construction. A major step in settlement prediction was the proposed use of the now well-known error function curve for describing the perpendicular settlement profile above tunnels, shown in Fig. 2.20 and defined by

$$W = W_{max} \exp(-x^2/2i^2) \qquad (2.2)$$

This was initially developed as an empirical rule by Schmidt (1969, after Martos,1958, who proposed the curve for describing settlement above tabular mine workings based on statistical evaluation of field observations) and taken up by Peck (1969). These workers also developed empirical relationships between the 'width' of the trough (i) and the dimensionless depth of the tunnel (C/D) for broad types of intervening ground. These empirical rules provide useful practical guidelines, but the major problem is to predict the magnitude of the settlement before construction starts. To this end Peck (1969) took available field data and divided them into four classic soil categories (cohesionless granular soils, cohesive granular soils, non-swelling stiff to hard clays and stiff to soft saturated clays). He then tried to relate the volume of the surface settlement profile (i.e. the ground loss at the surface during construction based on the error function curve), to likely volume losses, and hence determine maximum settlement during tunnel construction. This work has been continued by other researchers, with Attewell et al (1986) producing the most comprehensive list to date (Table 2.2 shows some of this list).

The error function curve has been shown to be adequate for describing surface settlement profiles in cohesive soils by many researchers, including Attewell (1978) and Attewell and Woodman (1982). However, Schmidt (1969) and Hansmire (1975) showed that for predominantly non-cohesive granular soils, the error function curve did not fit the data well. O'Reilly and New (1982) recognised that the error function profile is unlikely to fit surface settlement profiles over granular materials, due to dilation effects and the narrow funnelling effect of the material into the void created by the tunnel (discussed later in Section 2.3.2).

When producing linear regression lines to predict the width parameter, i, for the surface profile, using data obtained from tunnelling operations conducted in the UK, O'Reilly and New split the data into cohesive and non-cohesive materials. The evidence suggested the following relationships:

$$i = 0.43\ (Z_o - Z) + 1.1 \quad (3 < Z_o < 34) \qquad (2.3)$$

for cohesive soils and

$$i = 0.28\ (Z_o - Z) - 0.1 \quad (6 < Z_o < 10) \qquad (2.4)$$

for cohesionless soils, where Z_o is the dpth to the tunnel axis and Z is the depth from the surface to the stratum level at which i is required. These equations are reaffirmed by New and O'Reilly (1991) and they also introduce similar equations for a two layered medium above tunnels.

The stability ratio, N, was defined by Broms & Bennermark (1967) as

Table 2.2 Details of some monitored soft ground tunnelling operations (after Attewell et al, 1986)

Tunnel	Tunnel data: Depth z_0 (m)	Tunnel data: Diameter $2R$ (m)	Maximum recorded surface settlement: $\frac{z_0}{2R}$	Maximum recorded surface settlement: w (mm)	Ground geotechnical properties: c_u (kN/m²)	Ground geotechnical properties: $\frac{\gamma z_0}{c_u}$	Volumes: V_t (m³/m)	Volumes: V_s (m³/m)	Volumes: V_s (%)	Settlement trough width: i (m)	Settlement trough width: i/R	Settlement trough width: $3i$ (m)	Settlement trough width: $w = 2.5i$ (m)	Tunnelling method and soil conditions
London Transport Fleet Line, Green Park (Attewell and Farmer, 1974 *a, b*)	29.3	4.15	7.06	6.17	270	2.1	13.52	0.199	1.4	12.6	6.1	37.8	32.0 $(\beta = 46)$	Shield construction. Cast iron lining. 7 segments per ring, erected in shield tail. Annulus behind rings contact grouted every shove. Stiff, fissured, overconsolidated London Clay. Tunnel horizon blue clay overlain by weathered brown clay.
N.W.A. Sewerage Scheme, Willington Quay Syphon, Contract 32 (Attewell *et al.*, 1978)	13.375	4.25	3.15	81.5	33	9.4	24.37	1.86	13.1	9.1	4.28	27.3	22.7 $(\beta = 57°)$	Shield construction. Compressed air pressure 90 kN/m². 7-segment precast concrete lining per ring erected in shield tail. Annulus behind rings contact grouted every 3 rings. Silty alluvial clay with sand and gravel lenses containing water at artesian pressure.
N.W.A. Sewerage Scheme, Howdon, Tyneside (Glossop, 1978)	14.18	3.625	3.91	11.2	100	2.98	0.37	0.194	1.9	6.9	3.81	20.7	17.25 $(\beta = 47°)$	Shieldless construction. 5-segment precast concrete lining per ring erected up to the face. Annulus behind rings contact grouted every three rings. Boulder/stony clay.
London Transport Fleet Line, Regent's Park Northbound Tunnel (Barratt and Tyler, 1975)	20	4.15	8.2	7	230	1.70	13.52	0.18	1.3	10.3	4.96	30.9	25.75 $(\beta = 50°)$	Shield construction. Expanded concrete segmental lining. Stiff fissured, overconsolidated London Clay.
London Transport Fleet Line, Regent's Park, Southbound Tunnel (Barratt and Tyler, 1976)	34	4.15	8.2	5	230	1.7	13.52	0.19	1.4	15.2	7.32	45.6	38 $(\beta = 47°)$	Shield construction. Expanded concrete segmental lining. Stiff fissured, overconsolidated London Clay.

Table 2.2 Details of some monitored soft ground tunnelling operations (after Attewell et al, 1986), continued

Tunnel	Tunnel data: Depth z_0 (m)	Tunnel data: Diameter $2R$ (m)	Maximum recorded surface settlement: $\frac{z_0}{2R}$	Maximum recorded surface settlement: w (mm)	Ground geotechnical properties: c_u (kN/m²)	Ground geotechnical properties: $\frac{\gamma z_0}{c_u}$	Volumes: V_t (m³/m)	Volumes: V_s (m³/m)	Volumes: V_s (%)	Settlement trough width: i (m)	Settlement trough width: i/R	Settlement trough width: $3i$ (m)	Settlement trough width: $w = 2.5i$ (m)	Tunnelling method and soil conditions
Washington D C Metro, Lafayette Square (Butler and Hampton, 1975)	11.6	6.4	2.25	112.8	—	—	4.60	1.21	3.8	4.5	1.4	13.5	11.25 ($\beta = 35$)	Shield construction with bucket digger. Primary liner of steel ribs and hardwood lagging boards expanding during and after the shove. Sand cement bentonite grout injected originally through liner but later through shield at the front. Sand and gravel, interbedded silty sand, sand and clay.
Washington D C Metro, Treasury Yard (Hansmire, 1975)	11.6	6.4	1.8	280	75	3	6.02	1.4	4.3	1.9	0.6	5.7	5 ($\beta = 9$)	Shield construction with ripper bucket digger. Primary liner of steel ribs (4 section) placed on 4 ft centres with full timber lagging. Lining expansion during and after shove. Medium dense silty sand and gravel interbedded with sand, silty clays.
Washington DC. F2a-1 Route Tunnels (Cording *et al.*, 1976).														Articulated (3-segment) shield construction. Excavation by large, half-moon shaped, hydraulically-operated digger spade. Tunnelling below the the water table, but ground dewatered by deep well pumping in advance of tunnel construction. Segmental steel lining erected in tail of shield. Serves as both a primary and secondary or temporary support. Very variable medium stiff-to-hard clays; clayey sands–sandy clays; coarse sand and gravel.
1 IB	20.3	5.5	3.7	5	—	—	0.06	0.12	0.5					
3 IB	20.3	5.5	3.7	3	—	—	0.02	0.07	0.3					
9 IB	22.5	5.5	4.1	8	—	—	0.16	0.2	0.8	8.52	3.1	25.56	21 ($\beta = 39°$)	
10 IB	21.4	5.5	3.9	13	—	—	0.42	0.32	1.3				26	
11 IB	22.0	5.5	4.0	10	—	—	0.23	0.23	1.0	9.90	3.6	27.7	25 ($\beta = 45°$)	

Table 2.2 Details of some monitored soft ground tunnelling operations (after Attewell et al, 1986), continued

Tunnel	Tunnel data: Depth z_0 (m)	Tunnel data: Diameter $2R$ (m)	Maximum recorded surface settlement: $\frac{z_0}{2R}$	Maximum recorded surface settlement: w (mm)	Ground geotechnical properties: c_u (kN m^{-2})	Ground geotechnical properties: $\frac{\gamma z_0}{c_u}$	Volumes: V_t (m^3 m)	Volumes: V_s (m^3 m)	Volumes: V_s (%)	Settlement trough width: i (m)	Settlement trough width: i/R	Settlement trough width: $3i$ (m)	Settlement trough width: $w = 2.5i$ (m)	Tunnelling method and soil conditions
Mission Line, B.A.R.T., San Francisco (Peck, 1969)	10.97	5.33	2.06	10.5 (9.12)	—	—	22.31	0.11	0.5	4.2	1.57	12.6	10.5	Mechanical shield tunnelling with 90 kN m^{-2} compressed air. Dense, silty *fine sand (SPT N = 30) with occasional* thin lenses of peat. Dewatering by deep wells.
Toronto Subway (Peck, 1969)	11.89 (13.41 10.36)	30.5	—	—	—	—	21.07	0.21	1.0	2.7	1.04	7.1	6.7	Shield tunnelling, hand excavation Medium-to-fine uniform dense sand (SPT N-value = 40 to 60) above the water table
Mission Line, B.A.R.T., San Francisco (Peck, 1969)	10.97	5.33	2.06	1.5	—	—	22.31	0.03	0.13	8.0	3.0	24.0	20.0	Mechanical shield tunnelling with 62 kN m^{-2} air pressure. Slightly cemented dense silty fine sand (SPT N-value = 40 to 60). Dewatering by deep wells.
Stockton-on Tees Stage I Interceptor sewer, Measurement Section D (McCaul, 1978)	6.28	1.26	4.98	43.7	30.5	2.7	1.25	0.38	30.4	3.48	3.47	5.51	8.70	Mini-Tunnel system. Hand excavation from shield. 3-segment, smooth, precast concrete lining. Soft, silty, sandy clay.
New Cross L.T.E. Experimental Tunnel (Boden and McCaul, 1974)	10	4.15	2.4	21.5	—	—	13.52	0.27	2.0	5	1.82	15	12.5	Slurry (bentonite) shield. Sandy gravel.
Thames Water Authority, Sutton Sewer (O'Reilly and New, 1982)														Hand-excavated; stiff fissured London Clay. Hand-excavated; firm to stiff weathered London Clay. Full-face machine (mini-tunnel) excavated; firm to stiff weathered London Clay.
(a)	17.1	1.78	9.61	3.8	180	1.89*	2.49	0.096	3.86	10.0	1.12	30.0	25.5	
(b)	3.4	1.78	1.91	3.7	90	0.76*	2.49	0.019	0.75	2.0	2.25	6.0	5.0	
(c)	4.9	1.52	3.22	7.1	9	1.09*	1.81	0.054	2.98	3.0	3.95	9.0	7.5	

$$N = \frac{\sigma_o - \sigma_c}{c_u} \qquad (2.5)$$

where σ_o is the applied stress, σ_c is the confining stress and c_u is the undrained shear strength of the soil (see Section 2.3.2 for more details). This was first recognised by Schmidt (1969) to be a major factor influencing ground loss at the face during tunnel construction. Schmidt derived expressions for the ground loss into tunnels in clays as a function of the stability ratio. Glossop (1977) tried to relate volume loss (V%) to stability ratio, which he called simple overload factor OFS. His analysis produced the equation

$$V\% = -1.4 + 1.33OFS \qquad (2.6)$$

Obviously equation 2.6 can become negative if OFS is small (i.e. less than 0.86) and as an approximate guide Glossop suggested OFS>1.3. This and other work (eg. Attewell and Boden,1971, Davis et al.,1980) was reported by Attewell et al (1986). Fig. 2.21 shows an estimation of the ground losses and surface settlement volumes for the overload factor for tunnels in cohesive soils. The open circles are field data from shield driven tunnels after Schmidt (1969) and the solid cicles are for field data from various other sources which are unknown. The figure indicates quite a considerable spread of the volume loss data. When equation 2.6 is plotted onto the figure, it fits in with only some of the data points. Even the maximum theoretical values of ground loss or surface settlement volumes proposed by Schmidt (1969) (i.e. an upper bound), do not contain all the data points. The proposed relationship for design purposes is also shown on this figure and is based on a best fit with 75% of cases lying below the line.

Boden and McCaul (1974) produced one of the first published works that attempts to record the total field displacement occurring during a tunnel construction. Measurements were obtained using inclinometers, magnetic ring extensometers and precise levelling. The tunnel was constructed at New Cross, London, using an experimental bentonite tunnelling machine. The 4.12m OD tunnel was constructed at a depth of about 10m in a mixture of sandy gravels, coarse sands and clayey sands/silts. Six extensometer boreholes were used, arranged perpendicular to the tunnel direction. Two inclinometers were also used.

Figs. 2.22 and 2.23 show the vertical movements recorded at borehole B2 and the lateral ground movement recorded at borehole C1 0m and 2.5m from the centreline respectively. The vertical movements indicate quite clearly how they are in phase with the progress curve. The total settlement of the lowest magnetic ring is 23mm, the vertical settlements appearing to increase with reduction in depth and then decrease as the surface is approached. This is rather strange as a constant decrease would have been expected. However, as pointed out by the authors, several of the magnetic rings produced unreliable readings due to bad installation.

The lateral movements show that the upper soil layers tended to migrate towards the centre of the settlement trough in the normal way, whilst the ground around the tunnel was displaced outwards by the passage of the shield and the associated slurry pressure. Fig. 2.24 shows the longitudinal ground movements recorded as the shield passed. A similar pattern was found as for the lateral ground movements. The upper soil layers migrated towards the advancing settlement trough, whilst the ground adjacent to the tunnel face tended to be displaced away from the approaching machine. This indicates overpressurisation of the face, which seems to be a problem with pressure balance machines (eg De Moor and Taylor, 1991, reported in Section 2.2.1.1).

Hansmire (1975) carried out a comprehensive study of the soil deformation around a 3.5m diameter shield driven tunnel at Lafayette Park, as part of the Washington DC Metro system. The tunnel was constructed at a depth of approximately 13m in sands, silty sands and gravels. The measurement instruments, inclinometers and extensometers, gave lateral and vertical soil displacements. From these measurements total deformation, geometric strains and volumetric strains were computed. Figs. 2.25 a, b and c show a selection of the contour plots. Considerable interpolation was required between the recorded measurements to obtain the complete contour patterns. This could make the results close to the tunnel rather inaccurate. The total displacement plots show a high degree of concentrated vertical movement as expected from the soil conditions. The shear strain contours exhibit an 'ear' shape emerging from between the tunnel crown and springings, showing the soil failing along an almost vertical plane. These also illustrate the concentrated lateral nature of the soil deformations. The volumetric strain contour plot shows dilatency occuring within the soil directly above the tunnel, although it also indicates an area of compression close to the tunnel which is unexpected. This is presumably due to arching effects transfering the stresses within the displacing soil over the tunnel, to the soil at the tunnel shoulders. There is also a small amount of compression at the surface, probably corresponding to the inflection point on the surface settlement profile. These volume changes will influence the difference between the volume loss at the tunnel and that reaching the surface.

Fig. 2.26 illustrates a typical inclinometer record for lateral displacements. This indicates a similar response to that observed by Boden & McCaul (1974), at the surface, with the soil moving into the settlement trough. However, the movements at the tunnel level are inwards, i.e. the face was hand dug and not slurry pressurized. There is however, a small outwards movement at the tunnel springing after the tail passed (readings D&E), due to a combined result of lining expansion and the outward deflection of the lining as it took load. This is an interesting observation which is not mentioned anywhere else in the literature. It seems to be either ignored or not detected. The surface settlement profiles do not conform well to the error function profile, a finding that has been recognised by other researchers when tunnelling in sands.

Barratt and Tyler (1976) reported ground movement measurements made during the construction of two 4.15m diameter tunnels for the Fleet Line of the London Underground at Regents Park. The two tunnels, at 34m and 20m depth, were hand driven through London Clay. Surface settlement measurements for the southbound tunnel recorded approximately 5mm of vertical displacement over the tunnel centreline, with a 63m wide trough. The volume of the surface settlement trough for the southbound tunnel was 0.19 $\pm$ 0.01 m^3/m, i.e. 1.4% of the excavated volume. Fig. 2.27 shows the surface settlement trough. The settlements are quite variable and are thus similar in trend to those reported by Rogers et al (1989). The variability presumably occurs due to inaccuracies in the measuring technique, combined with the small range over which the movements occur (a few millimetres). The vertical movements obtained indicated that there was approximately a 2mm heave as the shield approached the instruments and then settlement after passing. Fig. 2.28 shows the movements above the southbound tunnel along the centreline. These show a consistent increase in movements with depth, although there seems to be a disproportionate difference in the movements at 12.72m and 18.80m. There is no information in the summary of soil properties to account for this. Fig. 2.29 shows the final vertical settlements for all the boreholes and depths. It should be noted that there is some heave just below the tunnel axis, indicating some compression in this region. A volumetric strain plot might be of use, to provide a better understanding of these movements. The lateral movements for the southbound tunnel, shown in Fig. 2.30, are rather inconclusive, as no datum is given. There is however, evidence of movement towards the tunnel at just above its axis level, due to the ground loss at the tunnel face. Similar movements are shown for the northbound tunnel.

Glossop (1977) describes very detailed ground measurements obtained during the construction of three tunnels in the Newcastle Upon Tyne area, only two will be considered here. The Willington Quay tunnel has an O.D. of 4.3m and an axis depth of 13.375m, and was constructed through stoney clay and some silty alluvium. The Hebburn tunnel has an O.D. of 2m and an axis depth of 7.5m, constructed through stiff stoney clay. At Hebburn 12 boreholes were used, 6 along the centreline and 6 in two arrays perpendicular to centreline. At Willington Quay there were 4 boreholes perpendicular to the centreline.

Fig. 2.31 shows a typical plot of lateral and vertical displacement contours at Willington Quay. The vertical measurements show a reasonably uniform decrease above the tunnel. The lateral movements are consistent with other researchers, with maximum lateral movement towards the tunnel near the tunnel axis and another maximum at the surface, at the point of inflection of the surface settlement profile. Figs. 2.32 a and b, show the total displacement vector plots for Hebburn and Willington Quay. These help to give a more visual picture of the movements towards the tunnel, and indicate that there is a small amount of ground movement below the tunnel axis. The movements for the Hebburn tunnel seem to be more directed towards the tunnel than those for Willington Quay, possibly due to differnces in soil properties. Fig. 2.33 a and b show strain contour plots for Willington Quay and Hebburn. These plots indicate where the soil is in tension or compression. For both plots there is as area of lateral compression near to the tunnel centreline extending to the surface. The lateral extent of this area at the surface coincides with the inflection point for the surface settlement profile. The area outside this compression zone is in tension. The vertical strains are quite different for the two plots. The plot for Willington Quay shows an area of tension directly above the tunnel which changes to compression and then back to a large amount of tension close to the surface. For Hebburn there is only a compression area extending from the tunnel shoulder to the invert level. This indicates that there must be a 'block' movement of the soil directly above the tunnel. These differences between the tunnels must be related to the differences in soil conditions.

Ryley et al (1980) reported on three tunnels at Warrington, constructed in loose cohesionless soils. Although three tunnels were monitored only the Acton Grange Trunk Outfall sewer surface and subsurface results are thoroughly presented. For the other tunnels only surface movements are presented in figures together with some tabular results.

The Acton Grange tunnel has an external diameter of 2.87m and is constructed at a depth of approximately 6.0m through mainly fine-medium grained sands. A bentonite tunnelling machine was used for the excavation. Two sections of the tunnel were monitored for comparison, using two boreholes at each, one on the centreline and one borehole perpendicularly offset by 0.5m. This seems rather a small number to interpret the whole displacement field caused by the tunnel. Similar results were obtained at both monitored sections. Taking section A, the subsurface vertical movements seemed to produce some inconsistent results (Fig. 2.34). The measurements in borehole A1 are very similar for different depths implying 'block' settlements above the tunnel. In borehole A2 the movements do not follow much of a pattern. The measurement ring at 1.6m gives more settlement than the 2.6m ring. The ring at the tunnel axis (5.8m) is showing heave, whilst the two rings either side are settling. These results are not well explained or discussed in the paper. The irregularities in the results are presumably due to either bad installation or variable soil conditions, which are not indicated in the borehole logs. The surface settlement profiles (Fig. 2.35) seem to follow an error function curve, which is suprising as the tunnel was constructed in predominantly cohesionless materials. The field measurements obtained from this monitoring show that settlements can vary appreciably over quite short distances in ostensibly uniform situations.

Eisenstein et al (1981) describe the monitoring of an experimental tunnel constructed using a shielded mole through a stiff silty clay at a depth of approximately 24m. An extensive array of measuring equipment was used at the test section to obtain the full displacement field. Results from one section perpendicular to the tunnel centreline are presented. The vertical and horizontal displacement contours for an area close to the tunnel are shown in Fig. 2.36 a and b. The contours would appear to be computer generated, and there would seem to have been problems in some areas, since there are discontinuities. The vertical displacement plot indicates settlements directly above the tunnel decreasing and spreading laterally as expected for a deep tunnel. There is however an area of settlement directly below the tunnel, which is below the zero settlement line and is thus puzzling. It would be expected that movement would be upwards, if caused by ground loss at the tunnel face. The lateral displacement plot shows inward movement on either side of the tunnel both above and below the tunnel axis. This is consistent with a deep tunnel in stiff soil. From these displacement plots the authors go on to produce contour plots of major and minor principal strains, volumetric strains and maximum shear strains.

The volumetric strain plot, Fig. 2.37 a, indicates more volume change to either side of the tunnel due to the large lateral movements at the axis level, which again is consistent with the other tunnelling observations (Glossop, 1977). Applying soil strength (i.e. failure) criteria to the maximum shear strain plots failure zones can be plotted around the tunnel (Fig. 2.37b). This suggests that arching effects are playing an important role in distributing load away from the tunnel. It would have been expected that a more uniform distribution would develop around the relatively deep tunnel (Wong and Kaiser, 1987, Section 2.3.3.9). This same data is also thoroughly investigated by El-Nahhas (1980) in both the perpendicular and longitudinal planes. The longitudinal plane displacements are due to the soil converging onto the tunnel lining due to the cavity left by the overcut on the tunnelling machine. Although the measurements are taken quite close to the tunnel the resolution is low and therefore only general patterns emerge. The data are however good as far as they go and is the only field monitoring found with this sort of data. The main body of this work is however concerned with the lining performance rather than the ground movements directly.

McCaul and O'Reilly (1987) describe the ground movement measurements obtained during the construction of the Tyne and Wear Metro, Newcastle Upon Tyne. The tunnels were shield driven and excavated in compressed air using a boom header, through boulder clay (including saturated sand banks). The tunnel diameter is 5.21m O.D. and was constructed at a depth of 12.5m. Ground movements were measured both at the surface and subsurface along two instrumented sections, both perpendicular to the tunnel centreline. Expected patterns of surface movements were obtained above the tunnel, with settlements decreasing to zero at approximately 30m from the tunnel centreline. The maximum surface settlement at the monitored section was 13mm and the settlement profile approximated to the error function curve. The subsurface movements measured 2m from the centreline increased with depth, whereas the measurements 5m from the centreline decreased with depth. This indicates a steepening and narrowing of the subsurface settlement trough as the depth from the surface increases. The maximum measured subsurface movement was 33mm at a depth of 4.8m.

Ward and Pender (1981) make some important observations on the ground displacements around tunnelling operations in their general report. These researchers state that most field studies, although obtaining a general picture of the ground displacements, do not record the behaviour of the ground close to the tunnelling operation, where every detail of the progress of excavation, temporary support or shield support, and final lining determines how much the ground is allowed to yield. In most field cases, the location and components of the displacement vectors that are measured are limited. They appealed for more comprehensive studies in different types of ground and with different tunnelling techniques. This has happened to a certain extent since then, with more field studies being conducted, however the records are still relatively limited. Another point noted by these reporters is that a considerable proportion of the total displacement takes place in the ground ahead of the tunnel face. The displacements close to an advancing tunnel develop gradually in a three-dimensional pattern ahead of the face with a rotation of vectors as the face passes. Material elements thus go through a series of different stress paths during tunnel driving. The understanding of these displacements is improving, with more case histories and monitoring in advance of tunnelling operations.

There has been much interest in relating the amount of ground loss around the tunnel (Vt) and the amount of ground loss appearing at the surface (Vs) during tunnel driving (Cording et al, 1976 and Attewell et al, 1986). The volume loss at the tunnel, however, is difficult to measure. As an alternative to this, Atkinson and Potts (1977b) sought a relationship between the vertical displacement above the crown of the tunnel (W_c), which is relatively easy to measure, and the maximum settlement (W_{max}) at the ground surface. Using the error function curve a simple relationship is obtained between (Vs/Vt) and (W_{max}/W_c). However, as these reporters pointed out, there is a dependency on the volume changes that occur in the ground between the tunnel and the surface, caused by stress changes occuring in the ground due to tunnel driving. Generally, there will be a reduction in mean normal stress which will tend to cause dilation, and an increase in shear stress which may cause either compression or dilation depending on the nature of the ground. Stress changes due to the shield thrusting, bentonite shield pressures, compressed air and pressure grouting must not be overlooked in such an analysis. Ward and Pender (1981) go into more detail, using field data from case histories.

2.3.1.2 Long-Term Ground Movements

Long-term ground movements seem to have been neglected in terms of monitoring of field sites and the extent of published data is limited. Variation in pore pressures after the construction of the tunnel will lead to consolidation of the soil and additional settlement. This is wholly dependent on the soil properties and the permeability of the tunnel, and it can take years for the settlements to stabilise.

Glossop (1977) presents some of the first field measurements on relatively long-term settlements at the Willington Quay tunnel construction site described earlier. Fig. 2.38 shows the transverse settlement profile for this tunnel at 504 days after the finish of construction. It can be seen quite clearly that the settlement trough has deepened and widened compared with the earlier measurements.

O'Reilly et al (1991) discuss the long term settlements recorded over an eleven year period for a sewer tunnel at Grimsby located in very soft clay. The 3.0m O.D. tunnel was hand excavated. Field measurements were taken at three locations:

Array A - depth 8.0m to axis
Array B - depth 5.3m to axis
Array C - depth 6.5m to axis

Fig. 2.39a shows the development of the centreline settlements over the eleven year period. Fig. 2.39b shows how the transverse settlement profiles developed. These researchers found that although the maximum short term settlement above the tunnel at the three arrays varied by a factor of about 2, the maximum value of settlement occurring between 7 days and final equilibrium at arrays A and B was remarkably consistent at 48mm and 44mm respectively. There is, therefore, no simple relationship between the magnitude of initial, and time dependent maximum, settlements in terms of depth or face stability. Although the long term settlement profile deepened and widened, the magnitudes of the angular distortions, which affect structures, remain remarkably unchanged. Finite element predictions allowing for possible drainage through the tunnel linings gave promising results.

An empirical method for the prediction of long-term surface settlements above shield driven tunnels in soil is discussed by Hurrell (1984). The general error function curve, used for short-term settlement profiles from ground loss considerations, does not fit observed long-term settlement profiles, which are generally deeper and wider than those of short-term settlements. Using case history data Hurrell suggests a method for predicting the ultimate transverse settlement profile. This involves the superposition of the short-term, ground loss, settlement profile and two discrete consolidation settlement profiles, shown in Fig. 2.40. The final formula for this profile is given below:

$$W_t = W_{maxs} \exp\left[\frac{-y^2}{2i_s^2}\right] + W_{maxc} \exp\left[\frac{-(y+D)^2}{2i_i^2}\right] + \exp\left[\frac{-(y-D)^2}{2i_i^2}\right] \qquad (2.7)$$

where W_{maxs} is the maximum short-term settlement, i_s is the short-term trough width parameter, i_i is the trough width parameter for the two consolidation settlement profiles, y is the distance from the tunnel centreline, D is the tunnel diameter and W_{maxc} is the consolidation element of settlement and can be evaluated from the equation below:

$$W_{maxc} = (W_{maxt} - W_{maxs}) / (2 \exp\left[\frac{-D^2}{2i_s^2}\right]) \qquad (2.8)$$

where W_{maxt} is the maximum long-term settlement.

When compared to the limited field data available on long-term settlements, the method seems to predict the surface profiles well.

A second method was proposed by Attewell (1988). It is based on the definition of the long term trough width parameter i_t defined below:

$$i_t = \frac{i_s}{\exp\left(-D^2/(2i_s^2)\right)} \qquad (2.9)$$

This leads to a value for the long-term surface loss V_{st} shown below:

$$V_{st} = \sqrt{2\pi}\, i_t W_{maxt} \qquad (2.10)$$

The two methods are compared by Selby and Attewell (1989) using one example, and only minor differences are detectable in the final settlement trough. These researchers recommend the second approach, however, as it is easier to apply and is conservative.

In terms of the effects of long-term settlements on adjacent services and structures, there is more chance of them being affected due to the wider lateral extent of the movements. However, the associated reductions in the curvature and hence the differential movements implies that the induced strains would be reduced.

2.3.2 Laboratory Modelling

There are two areas of laboratory experiments related to tunnelling construction: those tests relating to the more fundamental parameters involved, such as unsupported face stability and those tests simulating more closely the prototype tunnelling situation.

Laboratory investigations have been mainly concentrated in one area, namely the stability of tunnel faces. This is important as yielding of the tunnel face contributes a large proportion of the total ground loss occuring during a tunnelling operation. The stability of clay at vertical circular openings was investigated by Broms and Bennermark (1967). For undrained behaviour, they proposed that failure does not occur by flow of soil into the opening, if the ratio between vertical pressure in the ground at tunnel axis level and the undrained shear strength of the material (c_u) is less than six,

$$\text{i.e.} \quad \frac{(\sigma_o - \sigma_c)}{c_u} < 6 \qquad (2.11)$$

where σ_o is the applied stress and σ_c the confining stress.

Attewell and Boden (1971) proposed another stability ratio based on extrusion tests, which involve measurement of the soil creep displacement through a circular hole in the side of a container. Examining the failure concepts, upon which previous similar works were based, suggested that a ratio, derived from the maximum acceleration of intrusive movement more appropriately defines the critical depth of interest, the depth at which face collapse occurs, in a practical tunnelling situation.

The advantage of the extrusion test is that it facilitates prediction of the rate of soil intrusion at a tunnel face for any depth of tunnel axis, and by measuring the actual extrusion movement, prediction of the levels of criticality for the applied stress can be obtained. This prediction is an invaluable parameter in any attempt to relate ground loss to the tunnel construction process.

In order to investigate stability of tunnels more specifically, a series of laboratory experiments was commissioned by the TRRL at Cambridge University in the early 1970s, which testing continued through to 1979. These model tests were not intended to reproduce, precisely to scale a real tunnel during construction, together with all the details of the method of excavation and support. Instead their purpose was to illustrate the way in which the soil around a circular cavity deforms as the cavity pressure is reduced, since this approximates to the stress conditions during construction. This allows stability of the soil to be investigated and gives an indication of the resulting ground displacements and behaviour. Five projects were undertaken as part of this research. Cairncross (1973) conducted small scale model tests on unlined tunnels in clay. Orr (1976) extended the work of Cairncross (1973) to include lined tunnels in stiff clay. Potts (1976) investigated the behaviour of both lined and unlined tunnels in sand. Seneviratne (1979) conducted fully drained tests on plane-section tunnels in soft normally consolidated clay. Finally, Mair (1979) investigated the stability of shallow tunnels under construction in soft clay. The investigations by Potts (1976) and Mair (1979) will be discussed in more detail.

Potts (1976) carried out tests both under static conditions and in a centrifuge. These tests investigated the behaviour of lined and unlined tunnels. Potts carried out the tests using both loose and dense sand, and they were conducted in one plane perpendicular to the tunnel centreline. A rubber membrane filled with compressed air provided the internal tunnel support. Potts defined the load factor (LF) as the ratio between the actual stability ratio (N), as defined in equation 2.5, and the stability ratio at collapse (Nc). Thus at collapse LF=1 and at the start of the test when the support pressure equals the overburden pressure, N=0 and LF=0. In the tests, the deformations about the tunnel were measured as LF was increased from 0 to 1 by reducing the support pressure. The sand deformations were recorded using a radiographic technique with lead balls in the sand. Fig. 2.41 shows some typical results, with substantial settlements being restricted to soil contained within a region immediately above the tunnel. It also shows that the soil displacements were relatively small below and to the sides of the tunnel. In the dense sands at low stresses it was found that the vertical settlement attenuates rapidly above the tunnel in association with dilation close to the crown. However, for the loose sand there was little dilation and much less attenuation of displacements with distance above the tunnel. This produces a wider settlement trough for the loose sand and a greater surface settlement. Figs. 2.42a and b show shear strain and volumetric strain contours for the loose and dense sands close to failure. The contours of shear strain show zones of intense shearing developing in the sand close to the tunnel shoulders, the effects being most prominent in the dense sand. The volumetric strains show, as expected, the dense sand dilating faster than the loose sand. Fig. 2.43a and b shows the direction of the major principal strains around the model tunnels, for the same tests as before. These directions are approximately tangential to the tunnel in zones above the tunnel axis and illustrate quite clearly the arching effect where the soil tries to shed the overburden stresses away from the tunnel crown. Potts also noted that increasing the surcharge pressure caused a narrowing of the lateral extents of the movements, probably due to an increased arching effect.

Mair (1979) conducted tests using similar equipment to Potts (1976), but was concerned with the stability of shallow tunnels under construction in soft clay. Experimental studies were undertaken to investigate the relationship between support pressure, deformation and overall stability of unlined tunnels in soft clay. A first series of two-dimensional tests, on plane-section tunnels in clay, of constant undrained shear strength with depth, investigated overall stability. In a second plane-section test series the clay was brought into equilibrium in an overconsolidated state on the centrifuge before tunnel cutting. Deformation and pore pressure responses around the tunnel were then compared with finite element predictions for the clay with this known stress history.

The mechanisms of collapse, illustrated by the displacement plots shown in Fig. 2.44a and b (with depth to diameter ratios of 1.6 and 2.6 respectively), reveal a region of almost constant displacement above the shallow tunnel with some inward movement at the tunnel shoulders. A much wider region is affected for the deeper tunnel and significant inward movement is observed at the tunnel springings and haunches. The shear strain patterns corresponding to the displacements in Fig. 2.44a & b are shown in Fig. 2.45a & b respectively. The pattern observed in Fig. 2.45a is characterisd by a region of intense shearing, spreading upwards and outwards at the tunnel shoulders. In the deeper tunnel (Fig. 2.45b), the region of intense shearing emanates more from the tunnel springings. The general pattern of movements are similar to those observed by Potts (1976) for loose sand. A further test series, carried out by Mair, modelled three-dimensional tunnel headings and investigated the influence of heading geometry on deformation, behaviour and stability. These tests showed the stability to be strongly influenced by the heading geometry, the length of the unlined tunnel back from the face, and the diameter of the unlined heading. The reduction in stability as the length of the unsupported heading increased was accompanied by the deformation behaviour becoming increasingly two-dimensional. This is illustrated by Figs. 2.46a and b, although they do not give a very detailed picture of the soil movements.

Cording et al (1976) used model tests to investigate the relationship between volume loss into the tunnel, the shape of the settlement trough and volume changes developed in the soil. The tests involved a tank filled with sand in which were buried two pipe sections, one inside the other. The test involved the withdrawal of the outer pipe allowing the sand to displace into the cavity formed around the inner pipe. Different diameter outer pipes were used in the tests to simulate a range of ground loss values. The subsurface ground displacements were observed only in the plane perpendicular to the pipe by stereo-photogrammetry measurements. Surface measurements were also taken and compared to those recorded by the photographic technique. There was found to be good correlation. However, only three different tests are reported so the data presented are limited. The three tests were carried out at a constant depth with only the volume loss being varied.

The shape of the surface settlement troughs in the models corresponded closely to those observed in the field by Hansmire (1975). In both the model and the prototype, settlements were large and were therefore concentrated near the centre of the trough. The surface profiles did not fit the normal probability curve. The subsurface vector displacements, shown for two of the model tests in Fig. 2.47a and b, illustrate a similar pattern to Potts (1976) with very concentrated movements (i.e. of little lateral extent). The movements are predominantly vertical with greater horizontal magnitudes at the tunnel shoulders and towards the soil surface, illustrating a funnelling effect. There is very little movement below the tunnel springings. This is somewhat unexpected since the simulated ground loss in these tests is uniformly distributed all around the tunnel. The development of the ground displacements at different depths as the tunnel passed a specific plane are shown in Fig. 2.48. These show a very uniform increase in vertical diplacement with increasing depth.

An interesting feature of these results is the amount of movement occuring well behind the tail of the shield. It would have been thought that the movements would have been more concentrated in the sand.

Taylor (1984) carried out two-dimensional model tests using a similar approach to other researchers at Cambridge University (Potts, 1976 and Mair, 1979). However, these more recent tests were looking more at time dependent effects on the ground deformations, such as 'stand up' and squeeze effects. Two series of tests were conducted for tunnels. The first series involved tests using incompressible silty soils, which clearly illustrated the destructive effect of water flow into excavations. Seepage water flow into the tunnel caused progressive damage in the soil near the tunnel wall which led to instability and collapse as the internal tunnel pressure was reduced. The second test series involved tunnels in clay and investigated the effects of transient seepage flow towards unlined tunnels. The tunnel pressure was held constant for a period of time to observe the effect on settlements and pore pressure changes. These results compared well with the tests conducted by Mair (1979). The test results allowed a relationship to be derived between the pressure and load factor (N/Nc). This was found to be independent of the cover depth ratio of the tunnel. The observed soil displacements were predominantly vertical within a lateral area spreading from the tunnel springing to a distance of one half of the cover depth to the tunnel invert. The dissipation of pore pressures, during the stand up period in these tests caused settlements to develop, the nature of the response being a bi-linear increase with the logarithm of time. There was a low rate of pore pressure change early on in the tests, the rates increasing towards failure. Pore pressure changes close to the tunnel indicated that initially the soil behaved elastically, but later plastic yielding developed near the tunnel. Water inflow was not obvious in these tests, but plays an important role in stability and deformations in the soil around tunnels.

Face stability of shallow tunnels in granular soils was investigated by Chambon et al (1991), who describe model tests in dry sand from two research teams. The model used a similar idea as Mair (1979) for his three-dimensional model tests in soft clay. A rubber membrane and compressed air is used to support the face, the compressed air is reduced until collapse is initiated. The tests allowed investigation of the internal limiting pressure needed to ensure face stability, how this pressure is influenced by tunnel geometry and soil conditions, how failure can be predicted to be imminent and how the displacement field can be charaterised at collapse. The tests revealed that face collapse is a sudden process, preceded by only limited displacements, as shown in Fig. 2.49. Movements of the ground surface may be detected only once failure has propagated. The minimum uniform internal pressure that is necessary to support the face was found to be very low and is only affected marginally by soil density. The failure mechanism involves the displacement of a rigid block of soil, the shape of which remains nearly the same whatever the diameter, the depth and the soil density. Fig. 2.50 shows some typical results.

Steensen-Bach and Steenfelt (1991) describe a series of trapdoor model tests to investigate displacements around tunnels using a pin model, similar to Terzaghi (1943). Two model shapes were used, a hemispherical (tunnel) and a rectangular (trapdoor) shape. Surface subsidence profiles obtained from the tests showed good agreement with the error function curve. This is strange as other results in cohesionless soils do not show this agreement. Using a simple beam analogy, horizontal surface displacements were calculated and these predictions compared well with those measured in the model tests. Arching effects observed in the tests correspond well to other model tests using real sands. It was therefore concluded that pin models can provide information about both kinematic behaviour and stress distributions for a trapdoor/tunnel arrangement in loose sand.

2.3.3 Theoretical Analysis

2.3.3.1 Introduction

Geotechnical design and analysis methods for tunnels concern the issues of stability, loads on support systems, water flows, and movements. Most conventional methods of predicting tunnel behaviour were developed from elastic solutions or limit theory, or were derived from empirical data. Reviews of these methods are provided by Peck (1969), Clough and Schmidt (1977) and Ward and Pender (1981). These methods underline the basic approach to design. The conventional design tools are not characteristically coupled, i.e. loads are determined by one technique, movements by another, and neither is linked to the other. In the prototype situation, all behaviour is coupled. Numerical procedures, such as the finite element method, provide a framework that allows this coupling in a theoretical technique. This is not to say, therefore that the finite element method makes other analysis techniques redundant, far from it, but it does help to fill gaps that exist in conventional approaches, and thereby helps improve existing techniques.

It should not be forgotten that tunnelling in soft ground is basically a problem of soil mechanics, and all the principles of soil mechanics apply. Atkinson and Mair (1981) have examined the problem in terms of critical-state soil mechanics, but primarily by considering the magnitude of internal support needed in the tunnel to achieve stability and avoid collapse. The paper does, however, provide a rational understanding of tunnel deformation behaviour which can help interpretation of field data.

2.3.3.2 Numerical Solutions

Numerical solutions include the finite element method. This is a powerful and versatile method and allows the solution of many boundary value problems in continuum mechanics. The most comprehensive review to date of the finite element method as a means of analysing soft ground tunnels was reported by Clough and Leca (1989). They point out that soft ground tunnelling has proved resistant to finite element modelling, because of its complex nature and that it often involves parameters that are not well defined. The method is unforgiving if the data used do not adequately model both the soil and tunnel supports, as well as the construction process. The sensitivity of the finite element method to these factors has meant that it has proven a less reliable method for ground movement prediction than other less sophisticated methods. At the present time, the finite element method has a place in tunnelling for assessment of new technology, to investigate alterations for difficult design situations, and to improve understanding of the effects of variables that may potentially affect the tunnel performance. Improvements in computer technologies will reduce the costs of a full three-dimensional analysis to within the budget of most tunnelling applications. Presently, two-dimensional analyses are common and Clough and Leca discuss the reliability of these for predicting the three-dimensional situation. Although these analyses will only approximate the three-dimensional situation, with careful simulation reasonable results can be obtained. Fig. 2.51a and b show typical finite element meshes for two-dimensional and three-dimensional analyses respectively. One of the biggest problems in the use of the finite element method is constitutive modelling of the soil behaviour, and in particular which model to use (for example linear-elastic or non-linear elasto-plastic models). This area is discussed by Clough and Leca in some depth and no simple answer is given. The more complex soil models generally give more accurate results, but these models require a large number of soil parameters to be input and inaccuracy in any of these can affect the accuracy of the results. The simpler models allow a much quicker and easier analysis, but the accuracy is reduced.

The flexibility of finite element models can, however, be exploited when back analysis is carried out from observed ground movements, and can assist in understanding the movements at particular sites by extending conventional design techniques.
Recent developments in laboratory testing of soils, particularly with regard to the measurement of small strains during triaxial testing (Mair, 1992), has improved the constitutive models for soils. With regard to tunnelling, this induces small strains (0.001% to 1%) into the surrounding ground. In order to develop constitutive models for finite element analyses, the stiffness of the soil is required. Until recently, the stiffness/strain relationship could not be obtained for small strains during triaxial tests and so was assumed to be linear. However, developments of 'on sample'

strain measurement have revealed a highly non-linear behaviour for almost all circumstances. Tying these results in with in-situ measurements from pressuremeter testing has resulted in a much greater understanding of the soil at small strains. Using this information to develop improved constitutive soil models will result in improved results from finite element analyses.

2.3.3.3 Stochastic Theory

Interesting estimates of surface settlement were developed by Litwiniszyn (1955) and by Sweet and Bogdanoff (1965) based on "stochastic" theories of ground movements. A "stochastic" process is one obeying statistical rather than deterministic laws, normally with time as the dominant, independent variable. The "stochastic" approach assumes that the soil is represented by discs or spheres, depending on whether the analysis carried out in two-dimensions or three-dimensions respectively. All the model particles have the same size. The removal of any particle within the media is regarded as analogous to the tunnel excavation process. This removal creates an empty space that could be filled by either of the two particles above and adjacent to it. These particles, however, would have to be replaced in turn by the particles immediately above them. The downward movement of the particles (each particle movement downwards having an obvious and simply-specifiable probability) will take place until the void reaches the ground surface. As a result of this mechanism a settlement trough will develop in the surface.

The "stochastic" theory of subsidence was investigated by Schmidt (1969). He found that although the shape of the subsidence profile compares well with observed field profiles, the "stochastic" theory cannot properly predict the width of the profile. Glossop (1977) developed the "stochastic" model and found that settlements, lateral displacement and lateral strain at a transverse distance from the tunnel centreline, caused by volume losses in the tunnel, can be predicted using the "stochastic" model provided that the magnitude of the volume loss is known and assumed to be equal to the settlement trough. Glossop (1977) developed the relationships shown by the equations below:

Surface settlement

$$W = \left[\frac{2V_s}{2\,y}\right] \exp\left[\frac{-x^2}{y^2}\right] \qquad (2.12)$$

Lateral surface displacement

$$W_h = \left[\frac{x}{y}\right] W \qquad (2.13)$$

Lateral surface strain

$$E_h = \left[1 - \frac{4x^2}{y^2}\right] \frac{W}{y} \qquad (2.14)$$

where V_s is the volume of the surface settlement trough and y and z are horizontal and vertical dimensions respectively, from the tunnel axis. Glossop found that subsurface movements were less well predicted. The "stochastic" model assumes linear spread of movement from the tunnel springings to the ground surface at approximately 45 degrees, which is not borne out by the field observations.

2.3.3.4 Method of Associated Fields

Sokolowski (1960) states the equations governing the distribution of stress in a material deforming plastically. Corresponding equations for strain were given, among others, by Davis (1968). Using these two sets of equations together with constitutive equations for the material behaviour and known boundary conditions, complete solutions may be found for boundary value problems in soil deforming plastically. This approach is known as the method of associated fields (Smith, 1972). The complexity of the partial differential equations describing the stress and strain fields does not allow a closed solution for this method of analysis. The strategy adopted by Potts (1976) was to assume an initial value for one variable and, by numerical solution of the two sets of field equations using finite differences, to approach a complete solution by an iterative procedure.

Atkii. Potts (1974) used the method of associated fields to predict the stresses and displacements around unlined tunnels in sands. This method has not been widely used for tunnels in cohesive materials, or for lined tunnels, because the assumption of wholly plastic behaviour is unlikely to be valid for cohesive materials, and because the boundary stresses around a lined tunnel are generally not known. In subsequent work, Potts (1976) investigated the behaviour of tunnels in sand using the same sophisticated soil model in both associated fields and finite element analyses. Comparing the two predictions with experimental data, it was concluded that, at least for the particular boundary value problem considered, the associated fields method was superior. A disadvantage of the associated fields method, particularly relevant to the model tunnels, is the necessity to know both stress and displacement boundary conditions. In the case of the unlined tunnels, two stress boundary conditions are known, but no displacements. Potts avoided this problem by assuming a particular pattern of displacements at the tunnel centreline. It has been found that the predictions of the associated fields method can be improved if experimental data for the deformations of the tunnel wall are used as the displacement boundary condition.

2.3.3.5 Upper and Lower Bound Solutions

Ward and Pender (1981) review upper and lower bound solutions for both perfectly plastic materials (Davis et al, 1980) and in dry cohesionless materials (Atkinson and Potts, 1977a). Davis et al (1980) derived solutions for two undrained cases: (a) the stability of the face of a circular tunnel lined up to the face, and (b) for a long unlined circular tunnel. The safe lower bound solutions for the two cases is shown in Fig. 2.52. As expected the long unlined circular tunnel is less stable, has a smaller value of N (stability number), and would require a greater fluid pressure in the tunnel to prevent collapse than the tunnel lined right up to the face. One practical rule emerges from the above work. Immediate collapse will not occur in an unpressurised tunnel for a surface surcharge of zero, and any value of C/D, provided $\rho g D/c_u$ is less than unity. For example, instability is imminent in a 1m diameter tunnel in very soft clay (c_u<20kN/m^2), and in an 8m diameter tunnel in stiff clay (c_u<150kN/m^2).

Atkinson and Potts (1977a) derive an expression for the lower bound to the tunnel support pressure required for stability of long unlined circular tunnels in dry cohesionless materials. The solution is given by

$$\frac{\sigma_t}{\rho g D} = \frac{\mu}{(\mu^2 - 1)} \tag{2.15}$$

where σ_t is the support pressure, μ = (1+sin ϕ')/(1-sin ϕ') and ϕ' is the effective angle of shearing resistance, D is the tunnel diameter and based on the assumption that $\phi'=\psi'$, where ψ' is the dilation angle for the soil. This solution was verified for model tests carried out by Potts (1976). An interesting feature of the solution is its independence between support pressure and tunnel depth (similar findings for model tests were described by Chambon et al, 1991).

These researchers also derive an upper bound (unsafe) solution to the collapse pressure. This solution can be found by selecting any kinematically possible collapse mechanism and performing an approximate work rate calculation. The accuracy of the solution is dependent on the closeness of the assumed failure mechanism to the real one, and model tests proved to be of value in selection of this collapse mechanism. Fig. 2.53 shows the proposed collapse mechanism chosen by Atkinson and Potts. As with the lower bound solution, it is assumed that $\phi'=\psi'$, where ψ' is the dilation angle for the soil. This leads to the formula

$$\frac{\sigma_t}{2\gamma R} = \frac{1}{4\cos\phi'}\left[\frac{1}{\tan\phi'} + \phi' - \frac{\pi}{2}\right] \tag{2.16}$$

provided C/R > (1/sinϕ') – 1, to ensure that the apex of the sliding wedge at B is below the ground surface. This is discussed in much greater detail in the paper.

2.3.3.6 Stress Path Method

The stress path method (Atkinson and Bransby, 1978) is an analytical approach well suited for examining the actual ground conditions around a tunnel in clay. This method is a procedure that may be used to estimate either the strength or the deformation of representative elements of soil in the deformation field. The basic idea involves determining, in the laboratory, how a soil element behaves when subjected to specific in-situ loading conditions. Thus, the procedure followed in this method of analysis is to remove several undisturbed samples of soil from the ground, and subject them to the estimated changes in total or effective stresses that occur in the soil element during the construction process. Both the deformations and the failure strength are observed, and they may be used to estimate the overall deformation of the ground. It is important to notice that the effect of drainage in the field can be modelled by allowing the soil sample to drain between each stage of loading, if construction is slow, or only at the end of loading if the construction is rapid.
Although the stress path method has several advantages, there are certain difficulties with this method which must be faced. The major difficulty, if not an impossibility, is to simulate the actual field loading conditions in the laboratory. There is the difficulty of obtaining good quality undisturbed samples, although as reported by Mair (1992) the development of thin-walled sampling has improved this situation enormously. In addition there are the recently recognised problems associated with small strain behaviour, and the ubiquitous problem of assumed soil homogeneity. Despite many difficulties, and accepting that the method provides only qualitative and generalised solutions, certain results and conclusions can usefully be noted for practical purposes.

2.3.3.7 Closed Form Solutions

Although finite element analysis is a powerful tool, there are many cases where the available information on the soil properties is scarce and does not justify the use of a complex constitutive soil model and a refined numerical method. The use of a closed form solution is therefore preferable. One such closed form solution is presented by Sagaseta (1987) for obtaining the strain field in an initially isotropic and homogeneous incompressible soil due to near-surface ground loss, in this case due to tunnelling. This problem fits into the category of cases in which the imposed boundary conditions are only, or mainly, in terms of displacements (strain controlled problems). The stresses can be eliminated and the strains obtained by using the incompressible condition. The presence of the free surface is considered by means of both a virtual image technique and some results for an elastic half-space. The results can be obtained simply, especially for movements of the soil surface. The calculated movements presented by Sagaseta agree well with field observations and compare favourably with commonly used numerical methods. Rogers and O'Reilly (1991) applied this analysis method to soft ground tunnelling ground movement data. One such application was to the data obtained during the construction of a tunnel at Willington Quay (Glossop (1976)). Fig. 2.54 shows the results of this analysis with a comparison to some of the field data. The results appear to be quite accurate for the limited points being compared, even below the tunnel springing level. This method of analysis is discussed in greater detail in Chapter 6, Section 6.3, where it is adapted and extended.

Another closed form solution was proposed by O'Reilly and New (1982) based on the error function curve, as representing the surface settlement profile above a tunnel. Based on field measurements, the assumption is made that all movements of the subsurface soil occur along radial paths towards a 'sink', which is located at a point just below the axis level of the tunnel. The adoption of this assumption means that the width of the zone of deformed ground decreases linearly with depth below the ground surface. This results in the magnitude of the ground movements increasing linearly with depth below the surface to conform with the plane strain constant volume conditions:

$$i_y = Ky \tag{2.17}$$

where i_y is the trough width at a height y above the tunnel axis and K is an empirical constant. This leads to

$$H(x,y) = (x/y)\ W(x,y) \qquad (2.18)$$

where $H(x,y)$ and $W(x,y)$ are, respectively, the horizontal and vertical components of the soil displacement at a tranverse distance, x, and a vertical distance, y, from the tunnel axis. The equations for the generalised displacements are given by

$$W(x,y) = W(max,x,y)\ \exp(-x^2/2i_y{}^2) \qquad (2.19)$$

$$H(x,y) = (x/y)\ W(max,x,y)\ \exp(-x^2/2i_y{}^2) \qquad (2.20)$$

The researchers state, however, that these equations are not applicable in the region close to the tunnel, within about one diameter, due to the simplifying assumptions made. Within one diameter, construction and other influences will affect the displacements. The above equations are combined with the equations for the trough width parameter, i, given in Section 2.3.1. The researchers do not actually compare their theoretical predictions with field observations. One such comparison was conducted by Rogers and O'Reilly (1991). They compared the predicted displacements using the above method with those observed at Willington Quay (Glossop, 1976). The results are presented in Fig. 2.55, which shows good agreement, although the movements below the springing level of the tunnel appear to be poorly predicted.

Vafaeian (1991) describes an interesting analysis for predicting ground movements around tunnels, particularly surface settlements. The method is based on incompressible radial movements towards the tunnel. The variation of the movements is dependent on the angle to the vertical for a line drawnbetween the point being considered and the tunnel axis. The radial assumption is based on hypothetical slices of soil moving towards the tunnel at the same radial angle from the vertical. For the subsurface lateral extents of the movements a parabola is assumed, which passes through the tunnel invert and two points on the ground surface. This assumption has not been substantiated in the paper. The surface profiles obtained using this method are compared to the error function curve. The comparison is good. The method is also compared to Sagaseta's incompressible fluid flow analysis and shows a much narrower trough for similar field parameters and produces a much better comparison with the actual data. The lateral extent of the surface profile is, however, based on empirical data, which makes comparison with existing data relatively accurate but predition of likely movements above tunnels more difficult. Centreline values of ground movement directly above the tunnel, using this analysis, also compare well with field data. The analysis looks quite promising as an alternative to the O'Reilly and New analysis mentioned earlier (based on the error funtion curve). A more thorough investigation would be advantageous, as the information presented in the paper is quite limited.

2.3.3.8 Predicting Settlements above Soft Ground Tunnels using Flow Net Construction.

Another method of predicting the settlements above soft ground tunnels, which has been investigated by Glossop (1977) and by Howland (1980), is by considering the ground water response with the aid of flow net constructions. The method involves producing a model whereby the settlement above a tunnel is determined mechanistically. When a tunnel is driven through saturated soft ground it acts as a drain, and the ground water responds by flowing towards it. The response can be modelled by a flow net construction in a similar way to those used in other groundwater seepage situations. The result of the hydraulic gradient, initiated by this drainage, is to lower the original pore water pressures in the ground in a way fully described by the net. Assuming that full saturation is maintained, an increase in effective stress in the ground around the tunnel can be determined, if the hydraulic gradient is quantified and the original pore pressure is known.

By producing the flow net for any tunnel geometry, a distribution of effective stress increase brought about by the pore pressure reduction can be determined at any point. According to consolidation theory, the ground will settle as a response to an increased effective stress. Since the increase is variable according to the equipotential distribution of the flow net, it follows that the settlement will not be uniform. By taking a vertical line through the flow net adjacent to the tunnel, the increase in effective stress can be substistuted into consolidation formulae to give a measure of the settlement at that point. In order to check the hypothesis, Howland applied the method to two published case histories, Willington Quay (Attewell et al, 1978) and Stockton-on-Tees (McCaul, 1978). Good agreement was found between settlements predicted in this way, both in terms of magnitude and distribution, and those reported in the two case histories. Fig. 2.56a & b show the flow net constructions at Willington Quay and Fig. 2.57 shows comparisons between the actual and calculated settlements, also at Willington Quay. The method allows the prediction of long term settlements, which would be expected since it is based on a drainage related method.

2.3.3.9 Other Approaches

Another method of predicting collapse mechanisms associated with soft ground tunnels, which is difficult to put into any of the above sections, has been proposed by Wong and Kaiser (1986,1987 and 1991). The ideas presented in these papers are based on theoretical studies, observed field behaviour and model test results. The first of these papers, in 1986, proposed a conceptual model that the ground behaviour near a soft ground tunnel may be characterised by two distinct modes of yielding (Modes I and II), separated by a critical K_o value, the ratio of the horizontal and vertical stresses, (K_{cr}). For Mode I ($K_o<K_{cr}$), yielding induced by stress relief, ie a reduction in internal tunnel pressure, is initiated at the shoulders of a tunnel and localised yield zones propagate to the surface with further stress relief (Fig. 2.58a). For Mode II ($K_o>K_{cr}$) a continuous yield zone surrounds the tunnel opening and no localised shearing takes place (Fig. 2.58b). Due to the different modes, Wong and Kaiser suggested that these would produce different surface profiles as a result of differences in the subsurface displacement patterns. This means that Mode I settlements are larger than Mode II, because of differences in the arching effect above the opening. It also means that the trough width for Mode I is narrower than for Mode II, which would seem sensible. This implies that the potential for damage due to surface settlement becomes more critical for Mode I than for Mode II. For normally consolidated soils, where K_o = (1-sinϕ), the expected mode of yielding is generally Mode I. Hence, there is a need to minimise crown deformation by high support pressures near the crown, possibly by the use of expanding segments or by immediate pressure grouting. These researchers compare the ideas with numerical simulations, and Fig. 2.59 shows reasonably good agreement with the proposed patterns. These ideas are also compared with case history data and model test data, and is discussed below.

In the 1987 paper, the theory is developed further from the original ideas. Fig. 2.60 shows the various modes of tunnel behaviour for various P_i/P_o values (the ratio of support pressure inside the tunnel to the vertical pressure above the tunnel) and stress ratio K_o. This paper has similar finite element analyses and case history comparisons as the earlier paper. It does, however, introduce the concept of the ground convergence curve, which relates support pressure to displacement or settlements. The case history used in the paper shows that the ground convergence curve is an effective technique to evaluate field obervations in terms of support pressure and surface displacements.

The most recent paper, Wong and Kaiser (1991) propose similar ideas to the previous papers and do not really present any new information, although comparison with another case history is used to reinforce the ideas. Comparison with the model test results of Potts (1976) and Cording et al (1976) substantiate the findings that Mode I takes place for $K_o<K_{cr}$. These gravity type model tests were carried out in confined plane-strain conditions, and hence the K_o value should be much less than the value of K_{cr}. The mode of yielding therefore should be Mode I-1 or I-2 (Fig. 2.61). The observed shear-strain patterns compare well with those predicted for Mode I. Mode II yielding was observed in model tests on tunnels in over-consolidated kaolin at K_o=1.0

(Cairncross, 1973). During the initial stage of stress relief the shear-strain contours are approximately concentric. As roof collapse is approached the gravity effect above the roof dominates and a pair of high shear-strain zones develop locally at the shoulders of the tunnel (Mode II-1). These observations verify that Mode II develops at $K_o=1$.

The in-situ stress ratio not only governs the mode of yielding but also influences the displacement pattern. Potts (1976) reported surface settlement profiles for a set of model tests in sand with $K_o=0.5$ and 1.0 (Fig. 2.61). The surface settlement profile for $K_o=1.0$ is much smaller than that for $K_o=0.5$, even at much lower support pressures. This difference is attributed to the fact that tangential arching is enhanced by higher horizontal stresses at $K_o=1.0$. This causes an increase in resistance against the downward movement of the soil above the crown and reduces the surface settlements. It also implies that the potential for damage due to surface settlement becomes more critical for Mode I than for Mode II, as proposed by Wong and Kaiser (1986).

2.4 THE RESPONSE OF STRUCTURES AND BURIED SERVICES TO GROUND MOVEMENTS CAUSED BY TUNNELLING IN SOFT GROUND

Structures and buried services respond to ground movements by different degrees of deformation, according to their rigidity and the position of their constitutive elements. There has been much work conducted in this area and the papers discussed here give a broad overview of this.

Several researchers have studied the effect of movements on buildings and presented recommendations on allowable settlements of structures. Among these, and perhaps the best known studies, are those of Skempton and McDonald (1956), Polshin and Tokar (1957) and Burland and Wroth (1975). More recently Wahls (1981) has studied this matter in more detail. There is, however, a basic feature in the tunnelling process that is not entirely compatible with these recommendations: buildings impose long-term self-weight settlement and deformations, and much of any potential damage can be prevented by taking up deformation during the construction stage, while tunnel construction induces most of the movements in a structure very quickly and prevention against damage cannot thus be achieved.

Once the ground deformations due to tunnelling have been estimated, their effects on nearby structures and services may be predicted. The analysis of interactions between structures and the ground are invariably complex because of the uniqueness of conditions at each site; both the ground and buildings vary so much from one site to another. The problem is inherently less difficult for services because of the relative geometrical simplicity of the system. It is well-known that ground movements may be modified by soil-structure interaction but the behaviour of structures or buried services, subsequent to initial damage, is not usually considered in analyses. Such complexities cannot be taken into account in any analytical solutions, and these methods can be used only for certain simplified situations. In order to tackle the problem of soil-structure interaction, it is necessary to have a clear and consistent set of definitions describing the types of movements and deformation experienced by structures of services.

Attewell, Yeates and Selby (1986) look at structural response to tunnelling settlement. A study is made of a two-dimensional ground-structure interaction problem of an open frame. Initially they consider the simplest form of analysis, the Winkler ground model (Winkler, 1867), in which the soil is considered as a series of discrete linear-elastic vertical springs. The structure is assumed to act as a simple beam in bending, which limits the application of this analysis to plain walls, rafts and shallow service pipes. They extend the method via a finite element analysis to make it more applicable to a wider range of structures. Using the finite element analysis, brickwalls are analysed on various soils, a steel framed building is analysed on clay soil and infill panels are also analysed. The results are compared with field measurements wherever possible and there seem to be some discrepancies in the results, presumably due to the simplifying assumptions made in the analyses.

Selby (1987) looks at some of the variables involved when trying to calculate the effects of tunnelling induced settlements on floor slabs. The parameters considered include the shape of the transverse settlement profile, the elastic modulus of the soil and the three-dimensional nature of the advancing settlement trough. The conclusions are based on a linear-elastic analysis, assuming no soil/slab separation. It was found that there is negligible difference, in effect, between a normal probability transverse settlement profile and a triangular settlement profile of similar maximum settlement and width. There was some difficulty in assigning a realistic value of soil elastic modulus, as the maximum moments in the slabs were very variable depending on the elastic modulus used. This is obviously a sensitive relationship. When considering the three-dimensional effects, it was concluded that the extra expense of a three-dimensional soil plate finite element model is generally of little value. The additional sagging moments induced into the slab were relatively small.

The stresses and displacements developed in a buried pipe during tunnel excavation are very difficult to predict theoretically because they are strongly influenced by the nature of the soil-pipe interaction. The problem is further complicated by other factors such as the age of the pipe, its in-trench construction, traffic loading and other long-term stresses. When a pipe is laid in the ground it will obviously be affected to some extent by the movement of that ground. In the context of soft ground tunnelling the area where the ground is under tension is of the greatest concern with regard to the possible failures of pipelines. The level of risk to a main is, in practice, very wide because of a large variation of material propertites. In many cases, old pipes might be highly stressed because of deterioration in material quality and changes in past loading conditions. It is known that when the tunnel face progresses, buried pipelines within the ground settlement trough may respond by compressing, stretching, bending, shearing, warping and twisting. Such a complex response will depend largely on the relative stiffness between the pipe and surrounding soil and relative position of the pipeline to the tunnel drive.

An extensive field study on the effects of shallow tunnels on buried services was carried out by Owen (1984). The observations were made during two large resewerage schemes carried out in tunnels beneath established urban areas. The sewers ranged up to 2.0m in diameter and were constructed through predominantly glacial and alluvial silts and clays. The predicted ground movements based on the error function curve compared favourably with those observed. The problem found was that the gas and water mains tend to be interwoven, forming something similar to "reinforced earth". Due to essential items such as stop valves, air valves, bends and tees, movement tended to be restricted and stresses concentrated at certain points, which were difficult to predict and sometimes caused failure in the pipes. Owen found that by exposing pipe connections, i.e. uncoupling them from the ground, reduced the observed pipe strains significantly. However, this is obviously not a practical solution for all pipe connections.

In an initial study, it may be assumed that the pipe deforms conformably with the predicted ground deformations that develop without the presence of the pipe. A pipe on, or close to, and roughly parallel to the tunnel centreline could thus fail in bending, particularly if above a shallow tunnel where the induced radii of the ground curvature could be small. This same mode of failure could apply to a jointless pipeline transverse to the tunnel centreline. Additional direct horizontal tensions towards the limbs of a settlement trough could supplement the induced bending tensions to facilitate failure. The ground-pipe interaction associated with horizontal movements is somewhat analogous to the skin friction problem in piles (Poulos and Davies, 1980). Major difficulties in such an analysis relate to the definition of fixity (zero movement) points in the pipeline and to the definition of appropriate soil physical properties.

Attewell, Yeates and Selby (1986) study thoroughly the problem of movements induced in buried services, induced by tunnelling. As with the structure-ground interaction method described previously, the Winkler subgrade reaction model is used. This is characterised by the assumption that the pressure in the pipeline is proportional at every point to the deflection occuring at that point. Fig.2.62 shows the general application of this method to a pipeline. Various assumptions are made to simplify the analysis:

1. The soil is already precompressed and always remains in contact with the pipe.
2. The pipe material is linear-elastic, homogeneous and isotropic.
3. The soil around the pipe is linear-elastic and homogeneous.
4. The pipeline is homogeneous (i.e. rigid joints).

The analysis is carried out with the pipe parallel to the tunnel centreline and with the pipe transverse to the tunnel centreline, for both rigid and non-rigid joints. These researchers also consider the elastic analysis of Poulos and Davies (1980) applied to pipelines.

Once the result is obtained using a selected method of calculation, comparison is then made with appropriate allowable pipe deformation in order to ascertain whether damage may occur. Generally, axial tensile stress (compounded from components of direct tension and bending tension) may be chosen as the most appropriate limiting criterion for failure of brittle pipe materials. Occasionally limitations of extension on a pipeline joint may be important.

A recent report by Herbert and Leach (1990), for British Gas provides some interesting results and observations on the effects of ground movements on distribution mains. This report investigates the soil-pipe interaction. It states that the backfill around pipes, its density and its moisture content will combine to influence the backfill material compressibility, strength and shear stiffness, which in turn will affect the load transfer to the pipe. This is investigated in field tests and by numerical modelling. The soil-pipe interaction model used is similar to that described by Attewell, Yeates and Selby (1986). Prediction of the likely ground movements caused by tunnelling close to services, to input into the model, derives from the error function curve. The effect of pipebursting on adjacent services is discussed with reference to model tests at Oxford Univ. and pipeline responses to ground movements (Reed, 1987). Fig.2.63 shows a breakdown of the pipebursting problem for the stress analysis method.

In order to simplify the assessment of the magnitude of movement induced into structures or services by tunnel-induced ground movements, Attewell, Yeates and Selby (1986) have reproduced the equations relating to ground displacements and strains above tunnels in a graphical form. Some of the plots produced are illustrated in Fig. 2.64. The tunnel face is theoretically positioned at the origin. In order to find the displacements of a foundation or pipeline, it needs to be drawn to an appropriate scale and overlaid onto the contour plots in the correct position. The values of displacement can then be read off directly. It is important to know the damage threshold of angular distortion for buildings and services, which will depend on their construction. Norgrove et al (1979) gives some indication of these values.

O'Reilly and Rogers (1990) look briefly at the effect of ground movements caused by trenching and pipejacking on structures and compare the likely deformations. It is clear that for comparable situations, trenching causes the largest movements and greatest differential deformations. This conclusion was also borne out by model tests conducted by Taylor (1984), which compared the movements caused by trenching to those caused by soft ground tunnels.

2.5 CONCLUDING DISCUSSION

As shown by the previous sections, there has been only a relatively small amount of research conducted into ground movements around trenchless pipelaying operations and a little more into soft ground tunnelling movements. It is interesting to note that most of the work presented on trenchless technology is British based. It seems strange that the technologies which have developed rapidly in other countries, particularly Japan, have produced virtually no published work on the effects of these techniques on the surrounding ground.

The main problem with the section relating to trenchless pipelaying techniques, is that the data presented contains only a small amount of information. There are no detailed studies, and therefore it is difficult to obtain a good understanding of, or comparisons between, the work. The work also suffers from the fact that it is not really of a fundamental nature (with the exception of Swee and Milligan, 1990). It is mostly based on field observations, which are very site specific and require a lot of data to enable good interpretation. However, the work being conducted at British Gas and the WRC, based on field observations of pipebursting operations, is obviously relatively comprehensive. Field observations become much more valuable once the fundamentals of the movements have been investigated and established under controlled conditions.

Much of the field data for soft ground tunnelling have been presented in a list format rather than a critical review. The quantity of field data collected is growing and the quality of the information is also improving, presumably as experience increases and improved measuring techniques become available. However, information on the subsurface movements around tunnels is still relatively limited, and in many case histories only surface data are presented. It has not been the intention to cover all of the available case history data here, but only to investigate those that appear more useful in terms of relationships to trenchless techniques and those illustrating the full displacement field around tunnels. This will enable comparisons to be made with the results presented later in this thesis.

Most of the soft ground tunnelling laboratory modelling has concentrated on investigating the stability of tunnels during construction (Cambridge University work), with only Cording et al (1976) looking briefly at the overcut effect on ground movements. The stability investigations, although related to the face support in trenchless techniques, are not totally applicable due to the construction differences.

Various theoretical techniques have been outlined in the previous sections. Numerical modelling, particularly finite element analysis, is obviously becoming an area of increasing importance, not only due to the increases in computing power at lower costs, but also due to the improvements in constitutive soil models and thus improvements in the accuracy of the analyses. However, these techniques need a large amount of expertise and knowledge to produce good quality results and to understand the limitations of the analyses. They are therefore quite specialised and at present not quick and simple enough for general use. Other analysis techniques mentioned are less sophisticated, for example, the method proposed by O'Reilly and New (1982) and that proposed by Sagaseta (1987). Although these techniques have limitations, they are quick and simple to use, and are of value as long as the likely accuracy of the results is appreciated. In terms of specific analyses conducted for trenchless pipelaying techniques, there are very few, with O'Reilly and Rogers (1990), Rogers and O'Reilly (1991) and Chapman and Rogers (1991) providing the most detailed investigations, based on the closed form solutions mentioned above.

This literature review has highlighted differences in the behaviour of soils when subjected to subsurface disturbance and stress changes. It has shown how the behaviour of cohesionless soils, due to subsurface excavation, causes a very concentrated area of movements, when compared with cohesive soils in which the movements influence a much wider region of soil. It has also illustrated the varied nature of tunnelling and trenchless pipelaying techniques, and that a high proportion of the movements occuring around these operations are due to the different construction techniques. The excavation process is very variable and this makes assessment of ground movements and their prediction very subjective. However, certain factors associated with these operations, and which influence the ground movements, can be investigated under controlled conditions. A fundamental investigation of mechanisms affecting ground movements associated with trenchless pipelaying techniques is thus necessary.

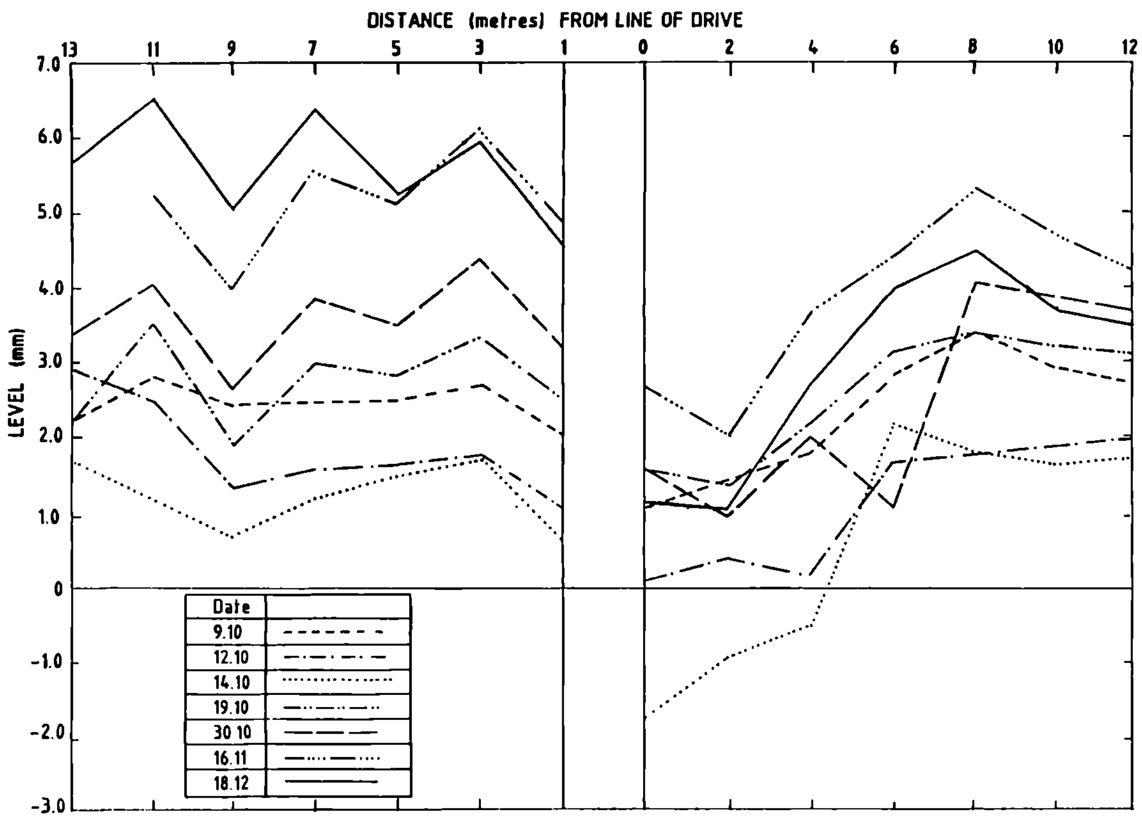

Fig. 2.1 Surface movements observed during a pipejack beneath Burnham-on-Sea (after Rogers et al, 1989)

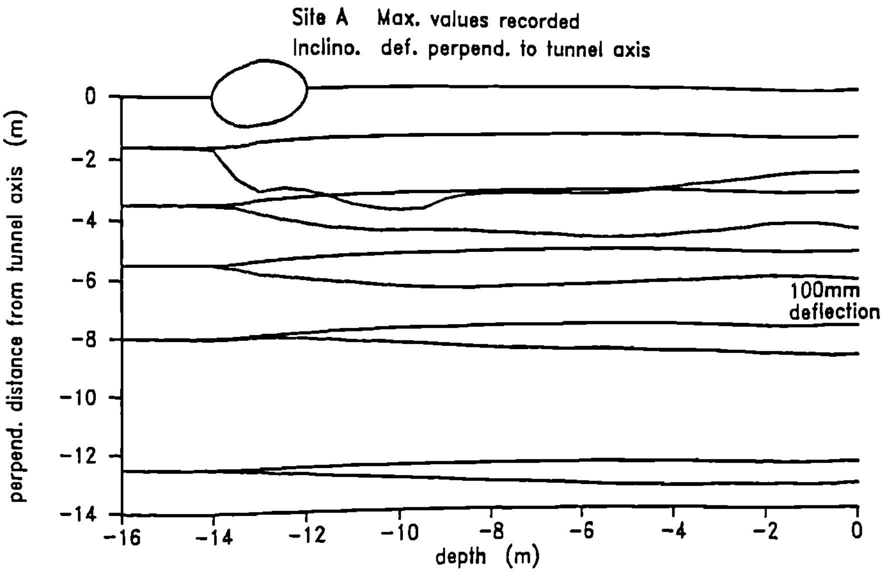

(a) Maximum inclinometer deflections

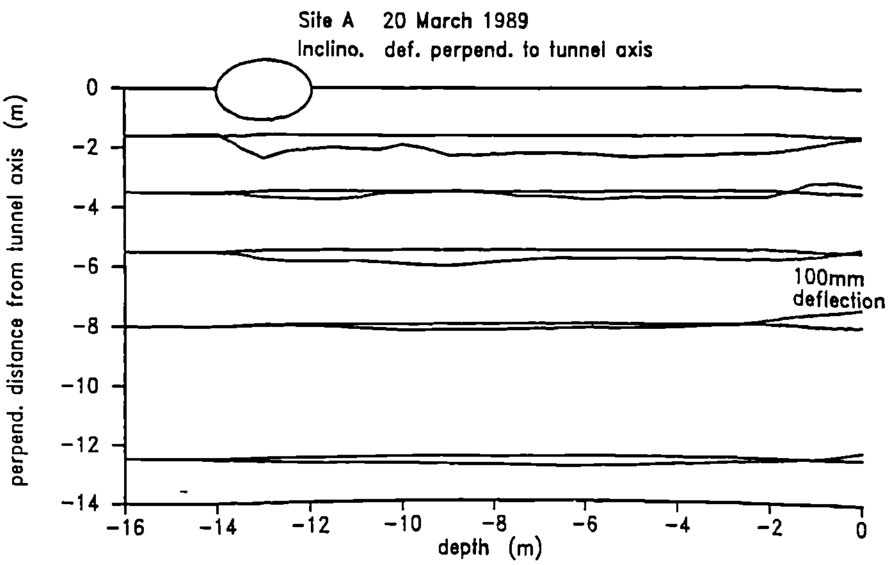

(b) Inclinometer deflections 8 months after construction

Fig. 2.2 Inclinometer data obtained during the construction of a sewer tunnel using pipejacking at Tilbury (after De Moor and Taylor, 1989)

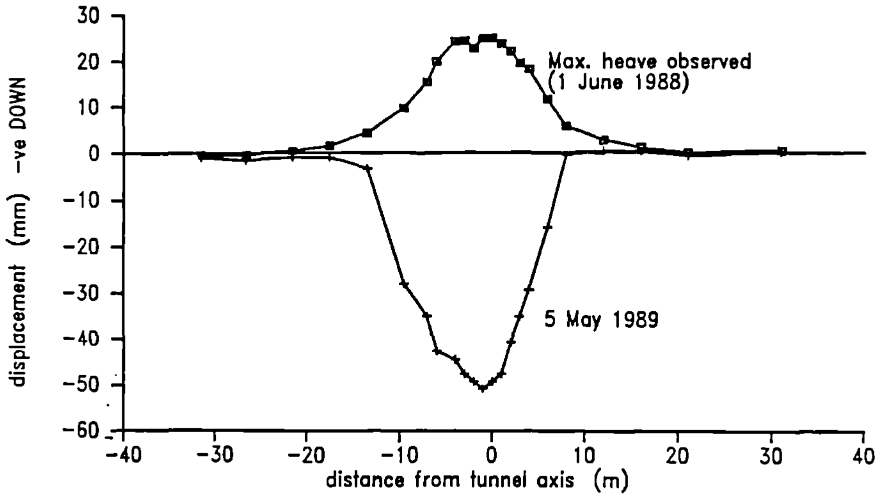

Fig. 2.3 Surface displacement profile perpendicular to tunnel axis (after De Moor and Taylor, 1989)

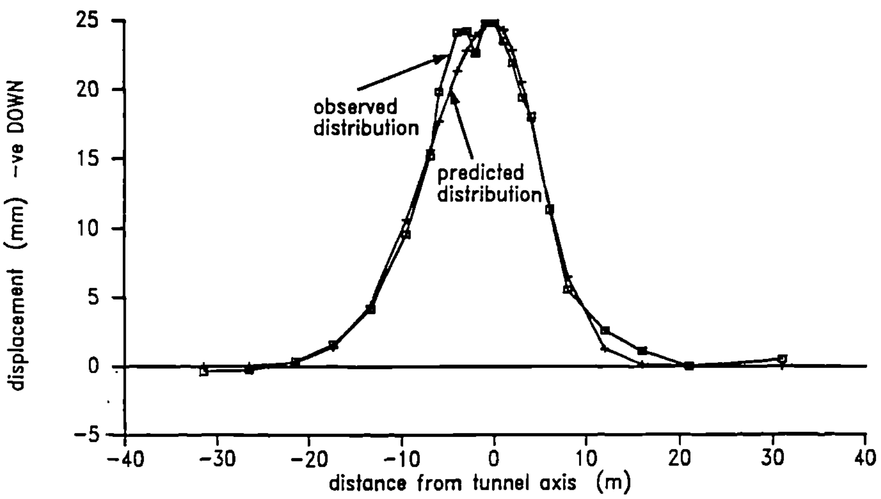

Fig. 2.4 Observed surface heave profile, compared to results calculated using the error function curve (after De Moor & Taylor, 1991)

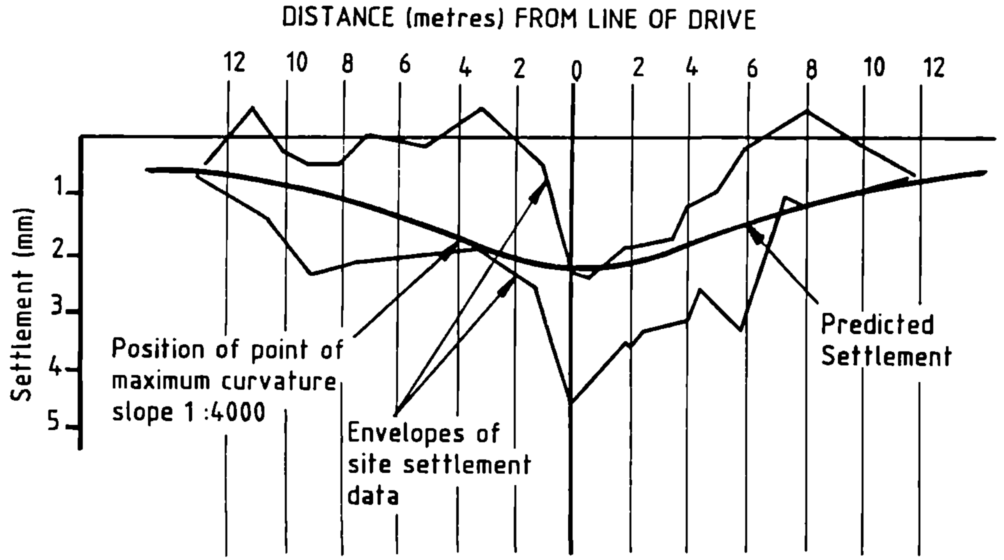

Fig. 2.5 Comparison between predicted surface settlements and field data from Burnham-on-Sea (after O'Reilly and Rogers, 1990)

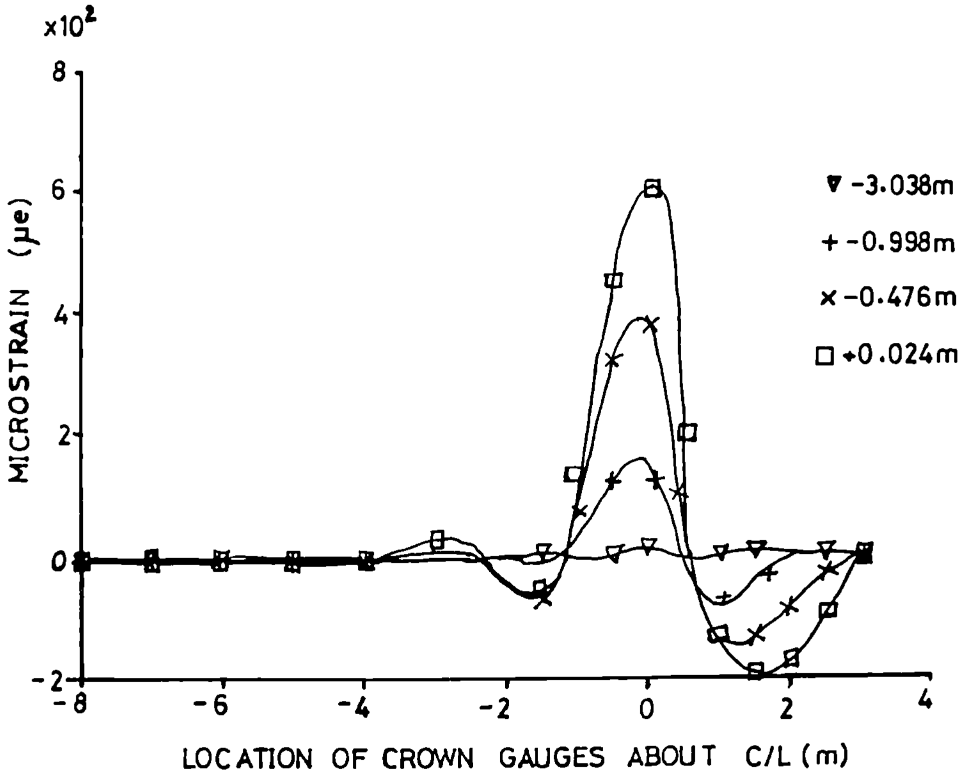

Fig. 2.6 Strain gauge readings during a moling operation (after Reed, 1987)

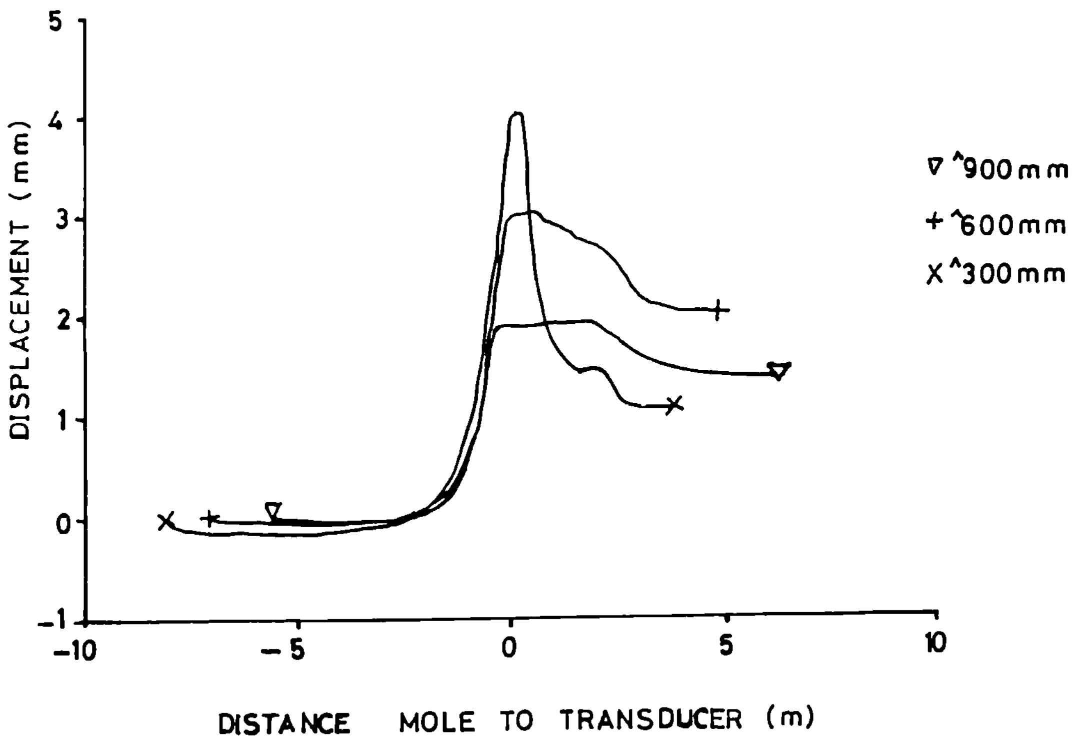

Fig. 2.7 Displacement measurements above a moling operation (after Reed, 1987)

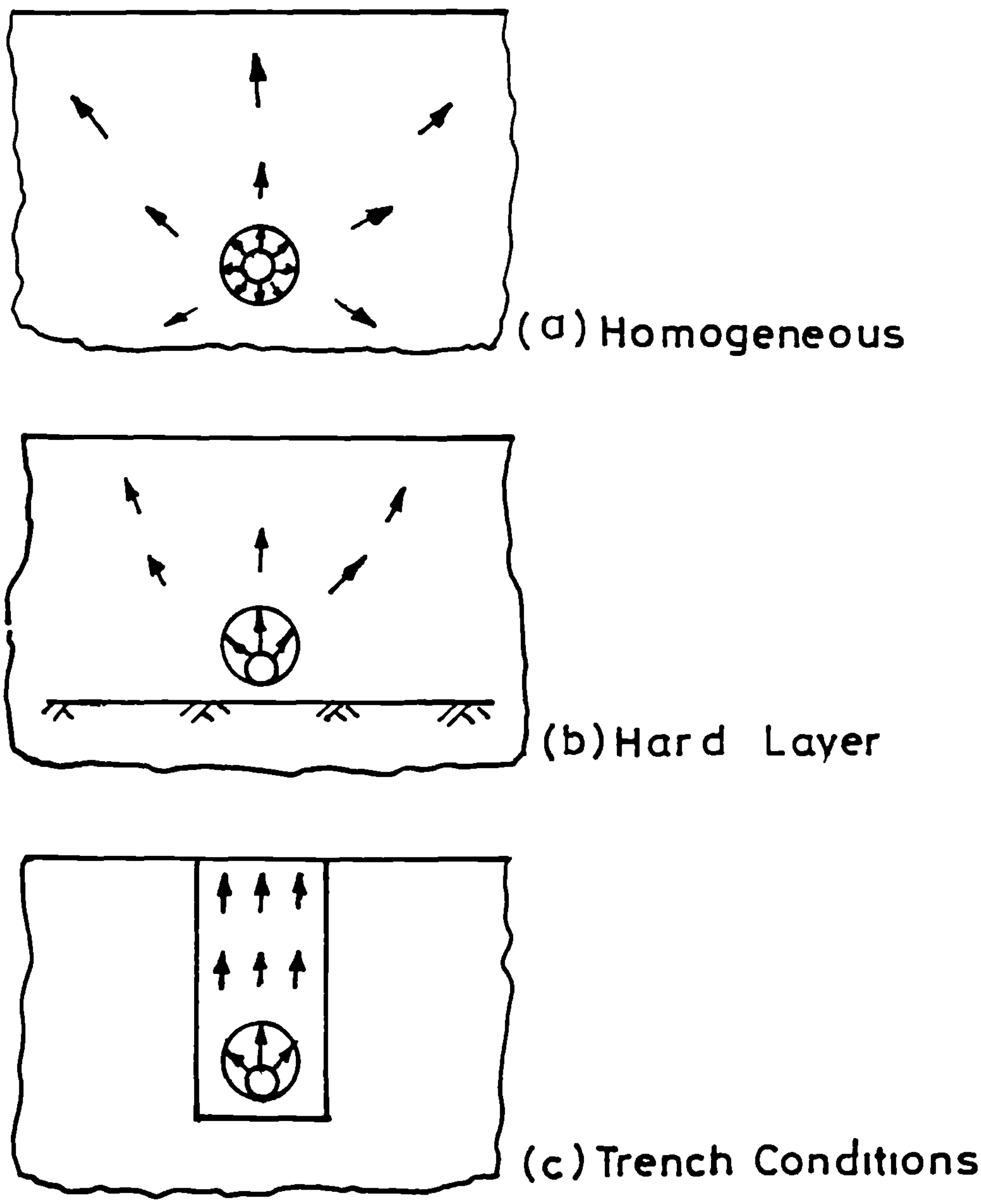

(a) Effects on movements of different ground conditions

Fig. 2.8 Likely ground movements caused by pipebursting operations (after Leach and Reed, 1989)

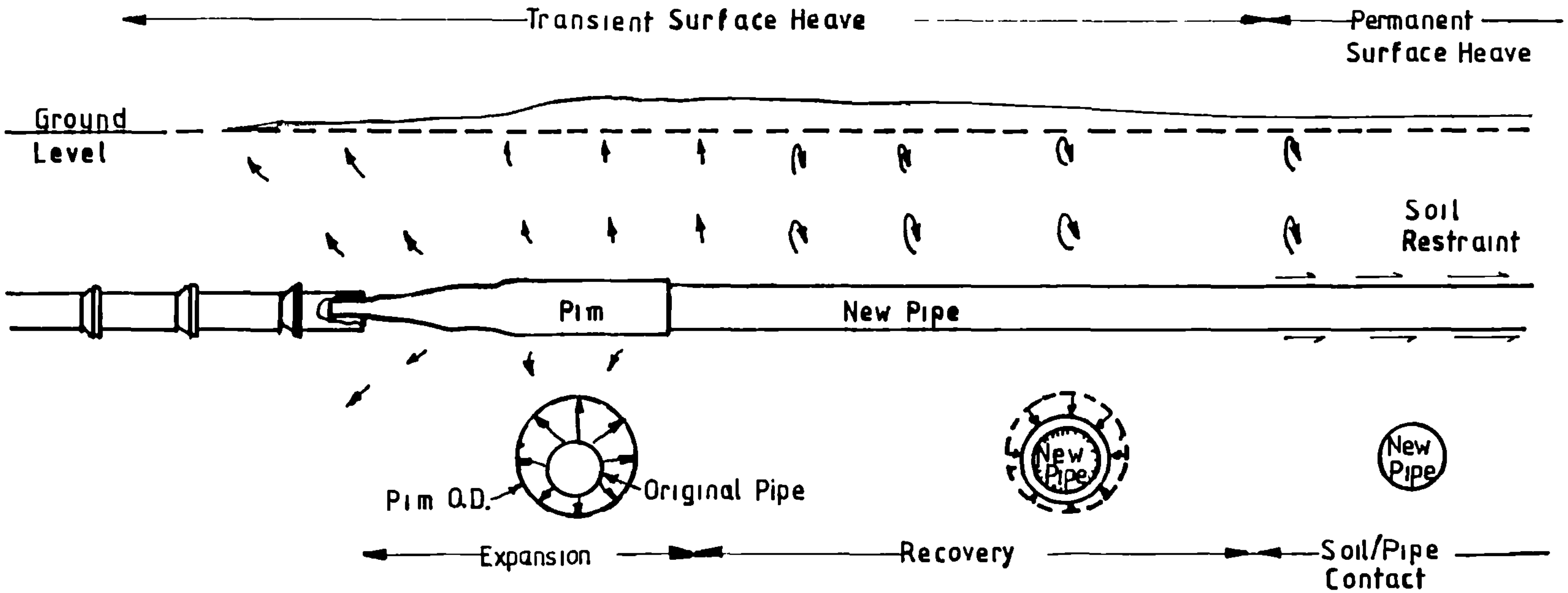

(b) Ground movements during a pipebursting operation

Fig. 2.8 Likely ground movements caused by pipebursting operations (after Leach and Reed, 1989)

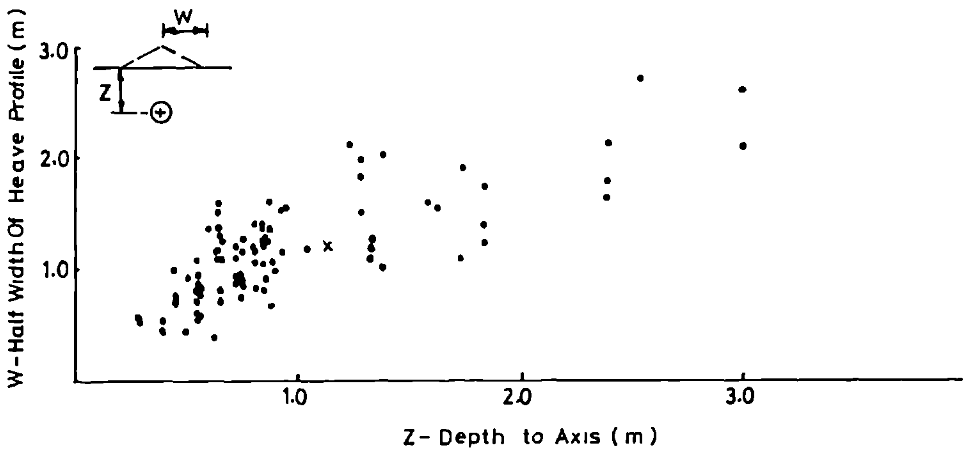

(a) Graph of half width of heave profile against depth to axis (x - data by Rogers et al, 1991)

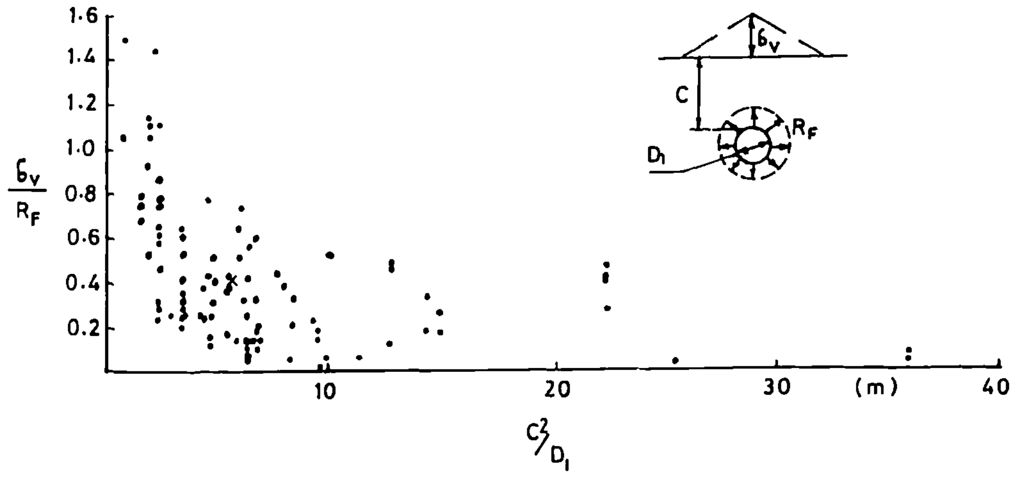

(b) Graph of surface heave to expansion ratio against C^2/D_1 (x - data by Rogers et al, 1991)

Fig. 2.9 Data collected during field operations (after Leach and Reed, 1989)

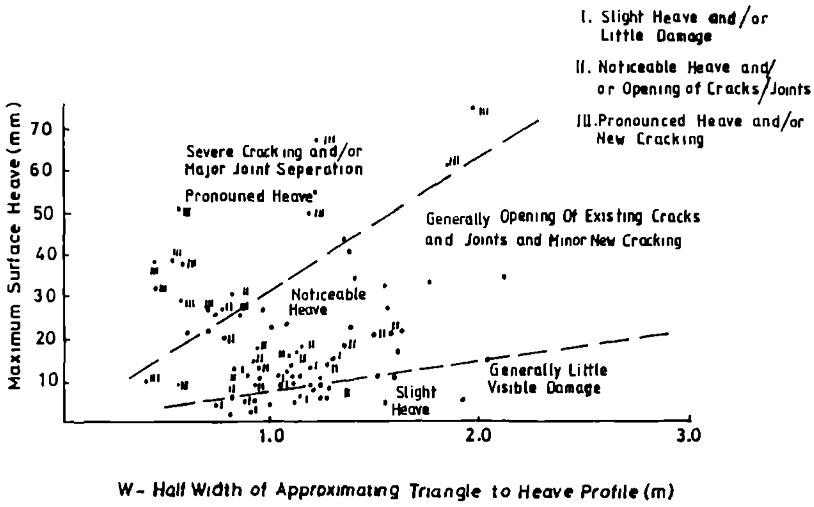

(a) Surface damage chart

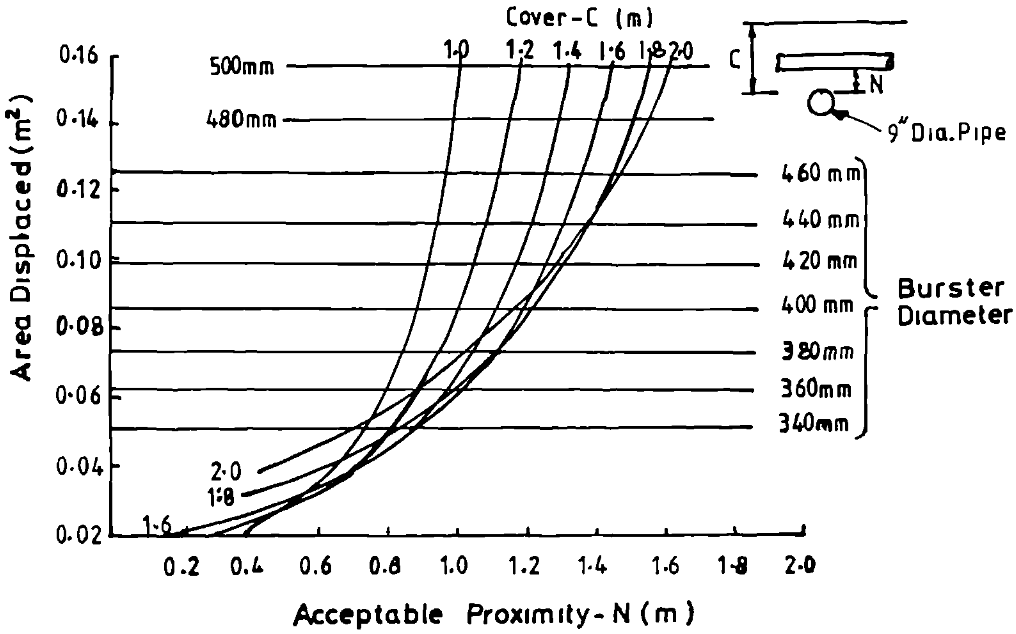

(b) Safe proximity chart

Fig. 2.10 Data collected during field operations (after Leach and Reed, 1989)

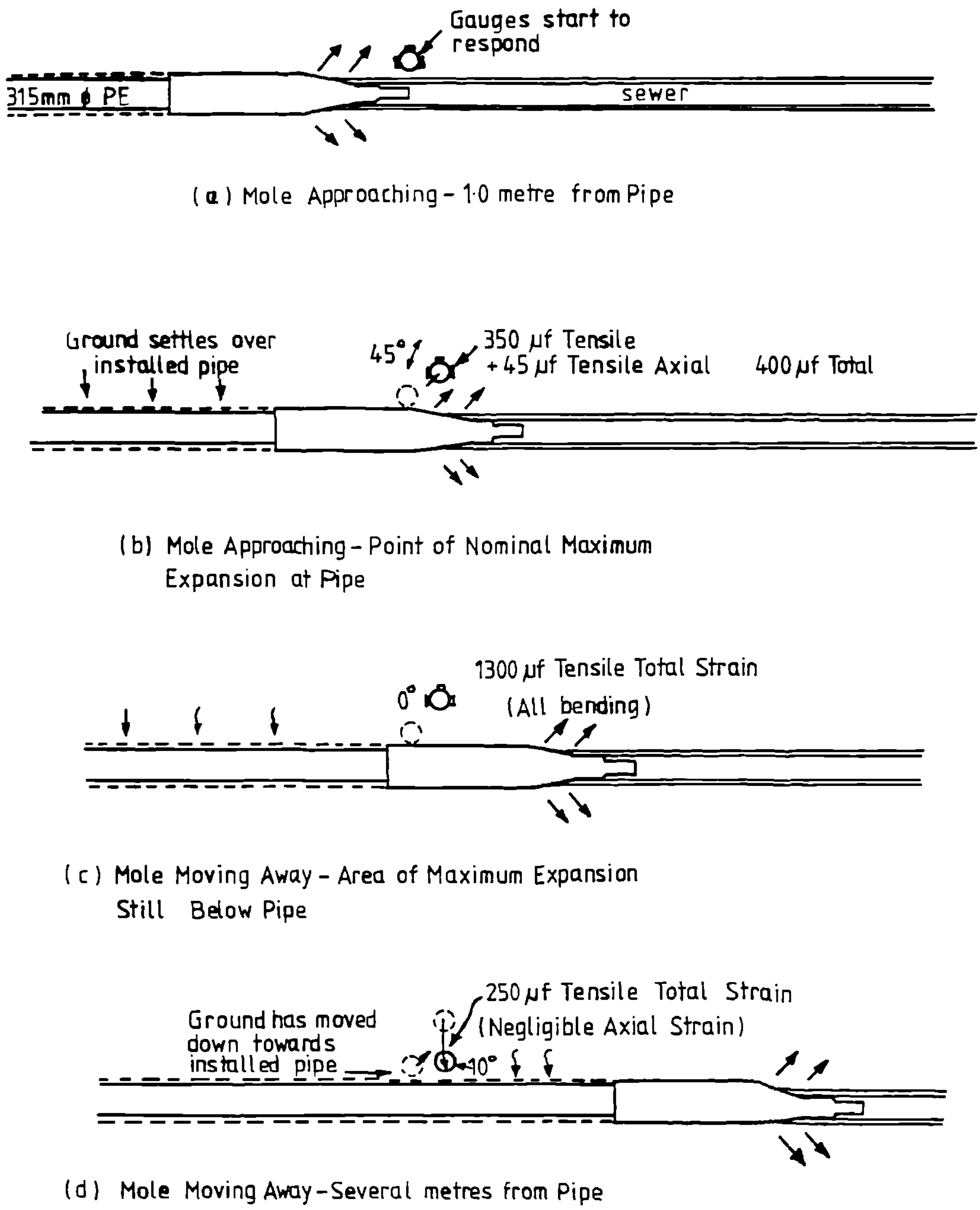

Fig. 2.11 Interpretation of strain gauge readings during a pipebursting operation (after Leach and Reed, 1989)

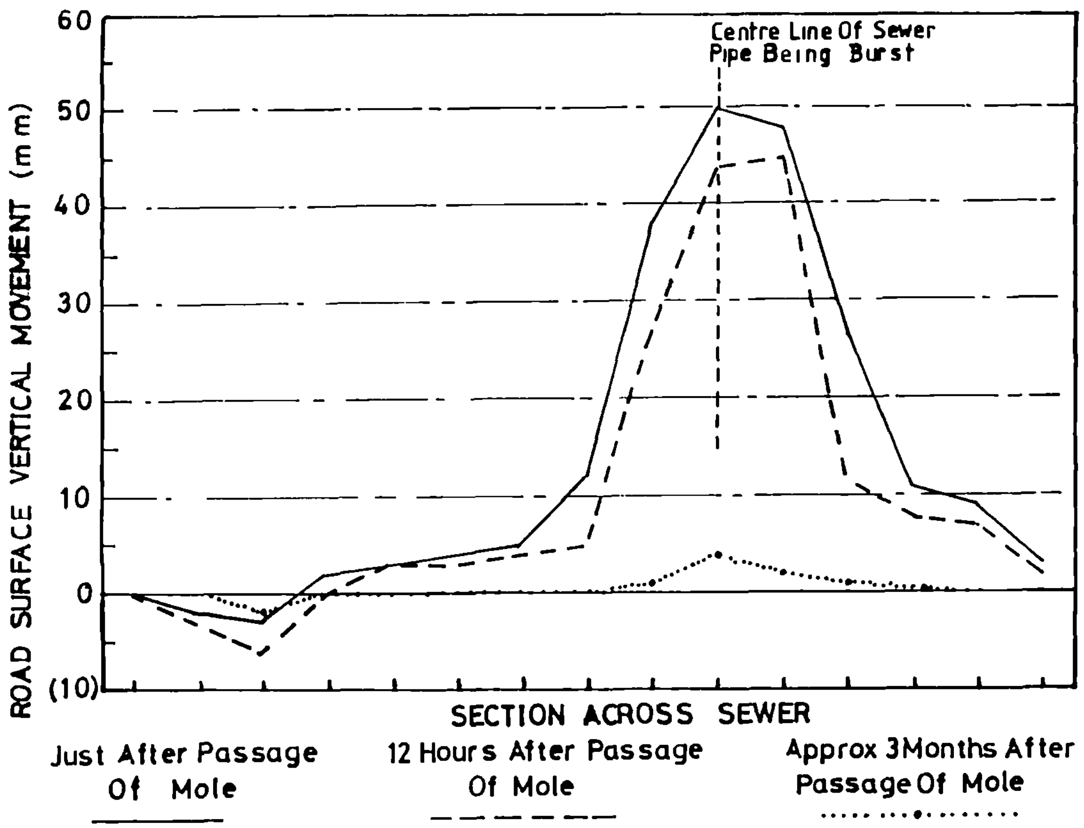

Fig. 2.12 Surface movements during the upsizing of a sewer (after Iliffe and Spedding, 1990)

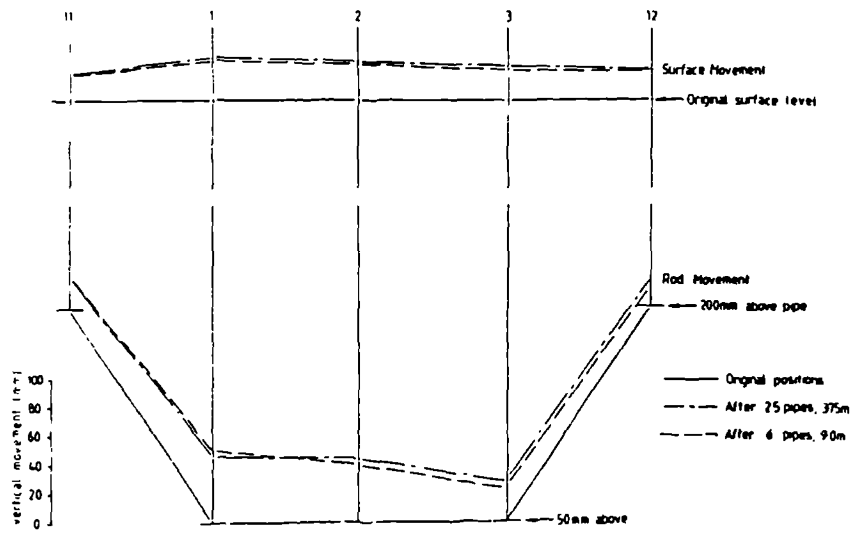

(a) Perpendicular plane

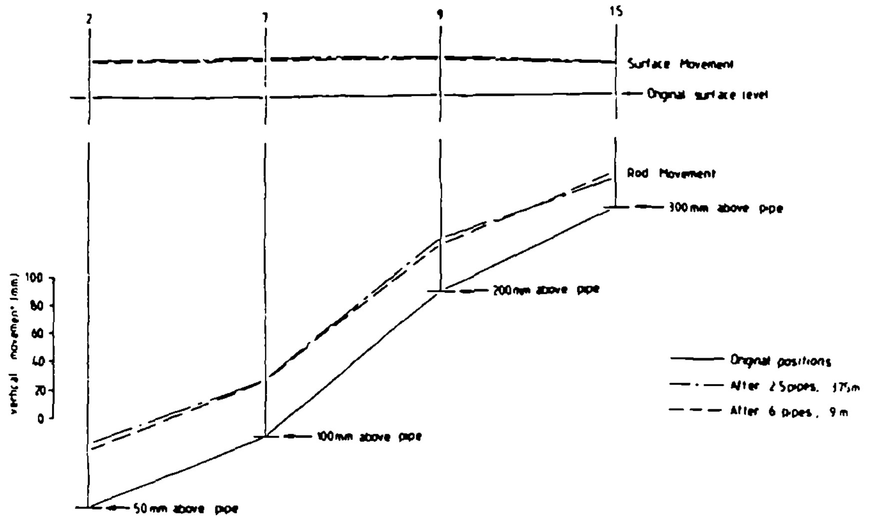

(b) Longitudinal plane

Fig. 2.13 Instrument positions and movements obtained during a pipebursting trial in sand (after Robins et al, 1990)

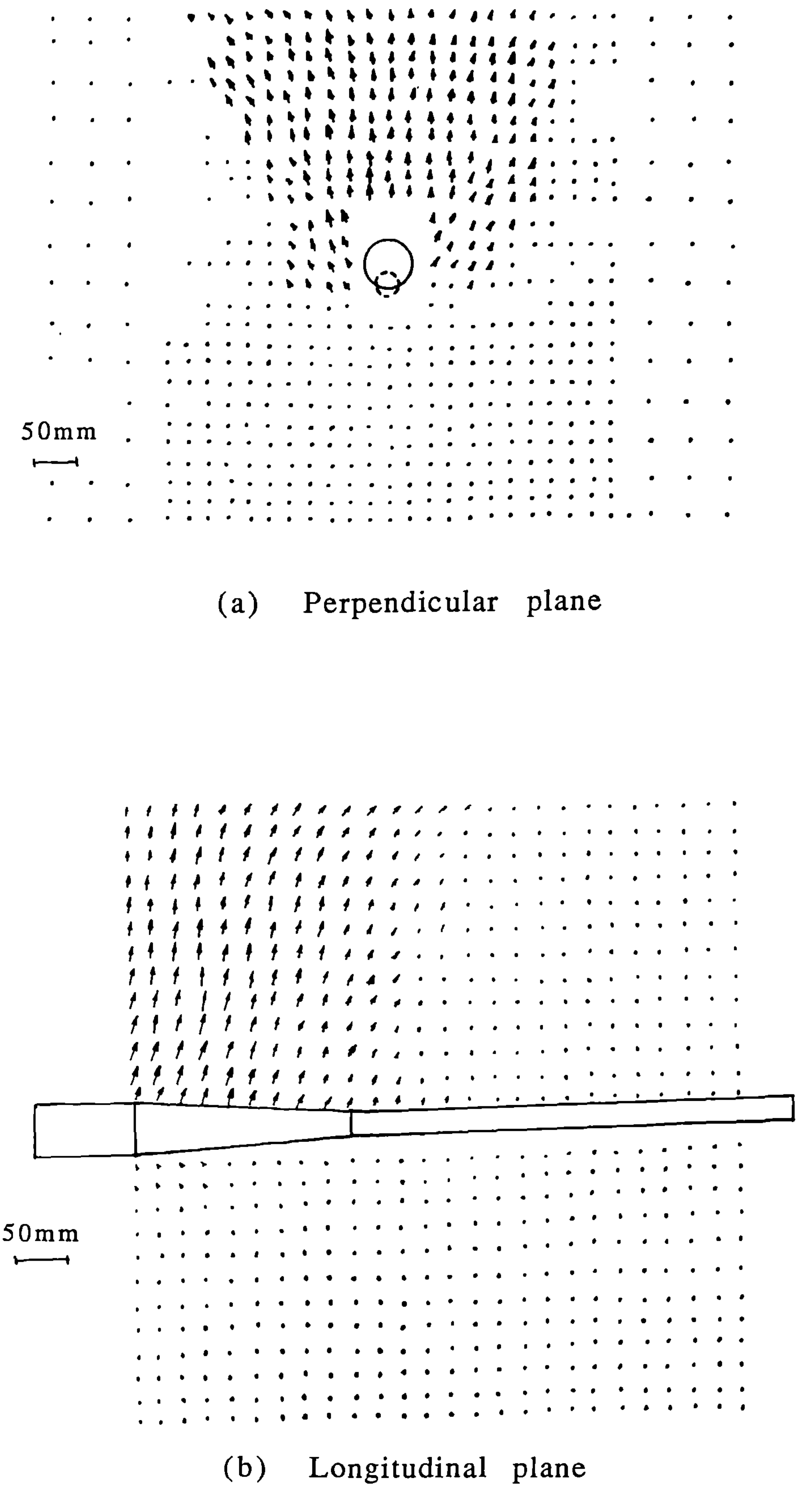

Fig. 2.14 Sand displacements observed during pipebursting model tests (after Swee and Milligan, 1990)

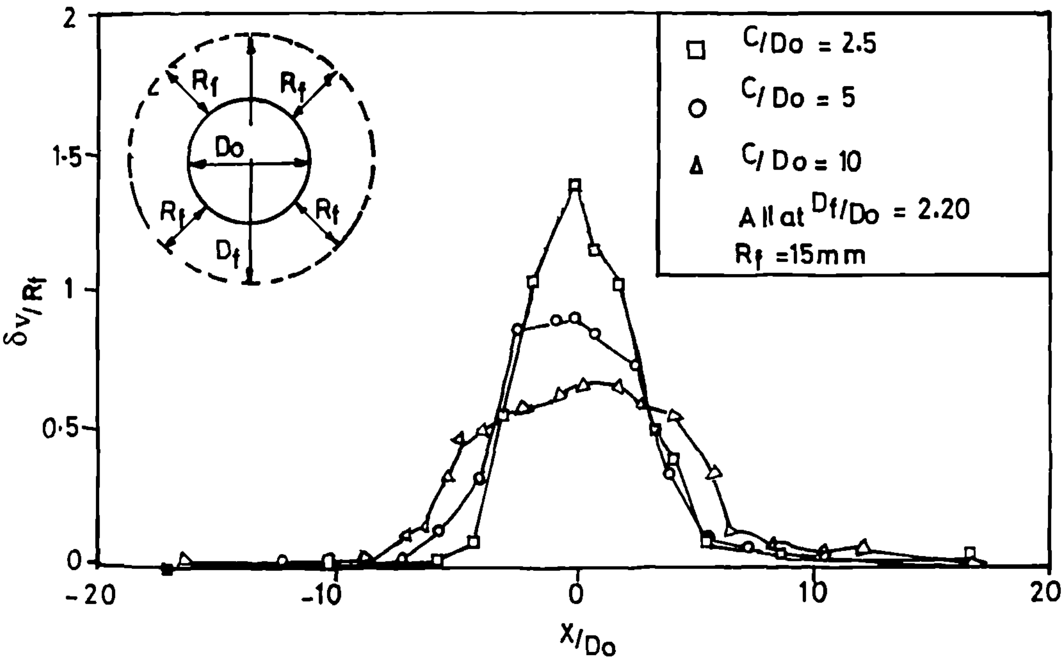

Fig. 2.15 Surface heave profiles for pipebursting model tests in sand (after Swee and Milligan, 1990)

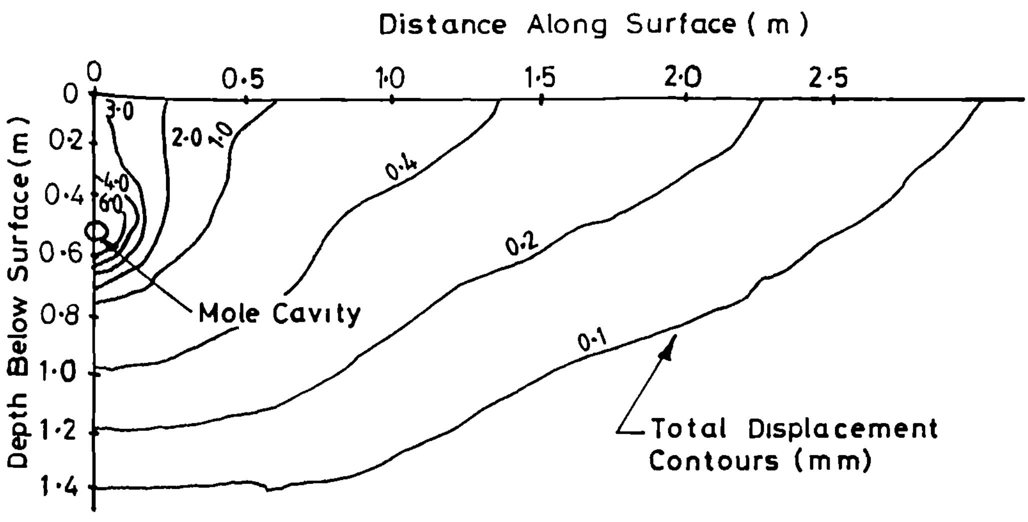

Fig. 2.16 Finite element analysis results for a pipebursting operation (after Howe and Hunter, 1985)

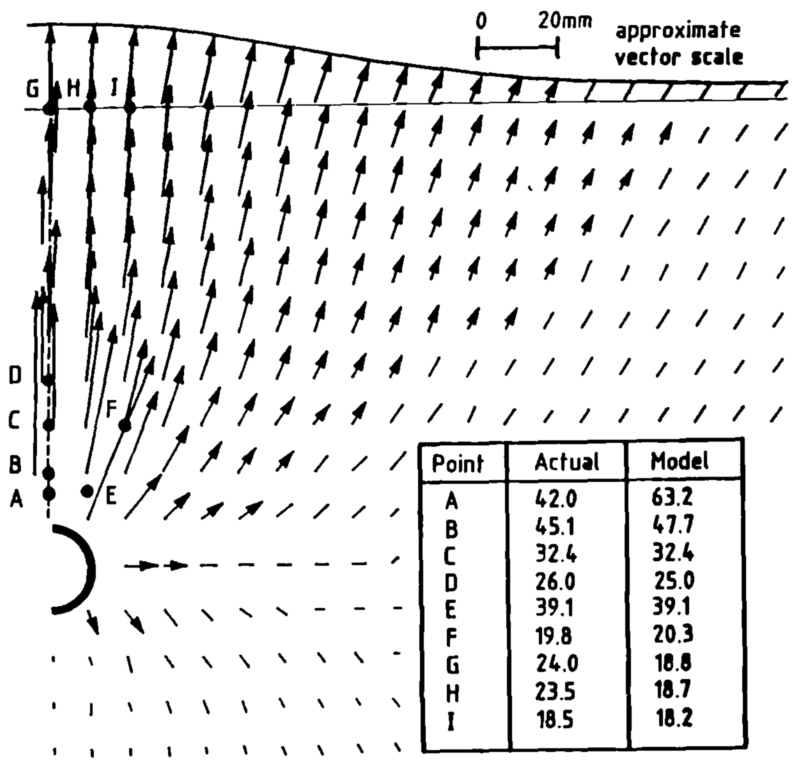

Point	Actual	Model
A	42.0	63.2
B	45.1	47.7
C	32.4	32.4
D	26.0	25.0
E	39.1	39.1
F	19.8	20.3
G	24.0	18.8
H	23.5	18.7
I	18.5	18.2

Fig. 2.17 Displacement vectors obtained from applying an incompressible fluid flow theory model to a pipebursting laboratory trial in sand (after Rogers and O'Reilly, 1990)

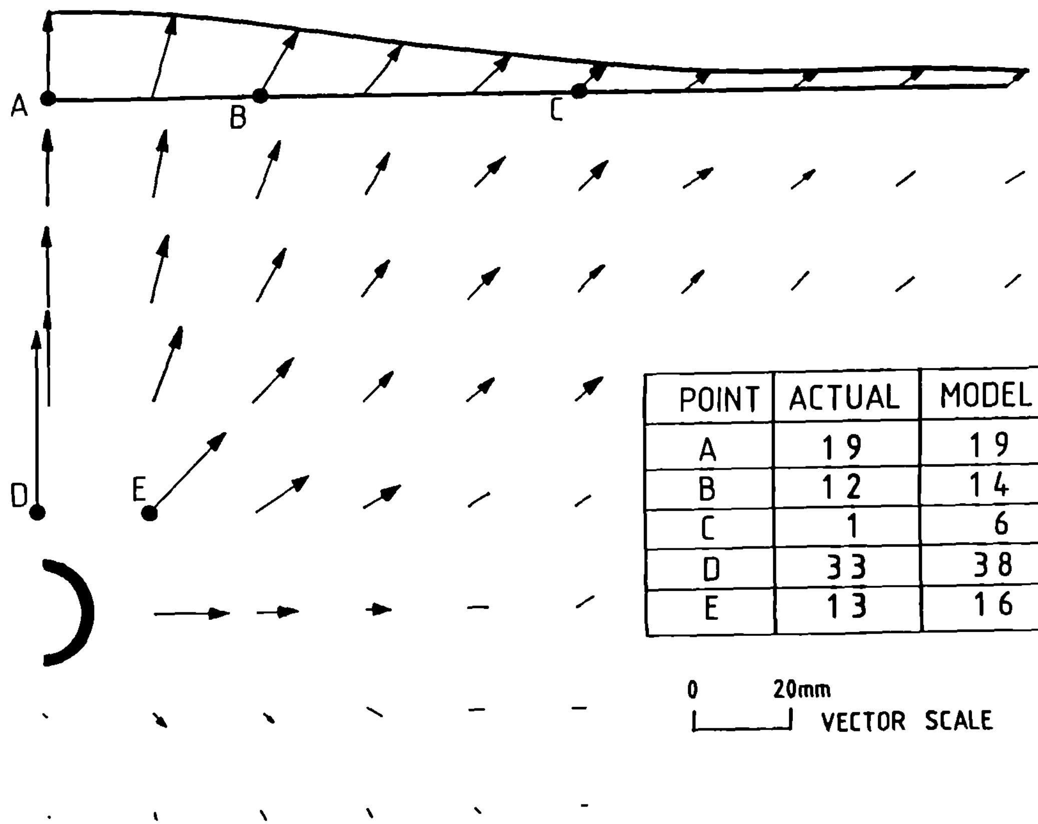

POINT	ACTUAL	MODEL
A	19	19
B	12	14
C	1	6
D	33	38
E	13	16

Fig. 2.18 Displacement vectors obtained from applying an incompressible fluid flow theory model to a pipebursting field trial in stiff clay (after Chapman and Rogers, 1991)

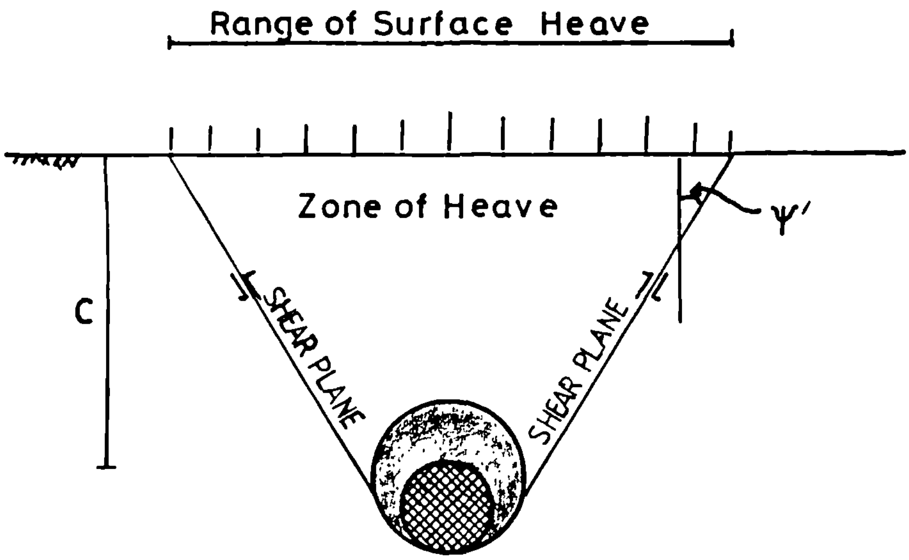

Fig. 2.19 Proposed zone of ground movements above a pipebursting operation based on the dilation angle of the soil (after Swee and Milligan, 1990)

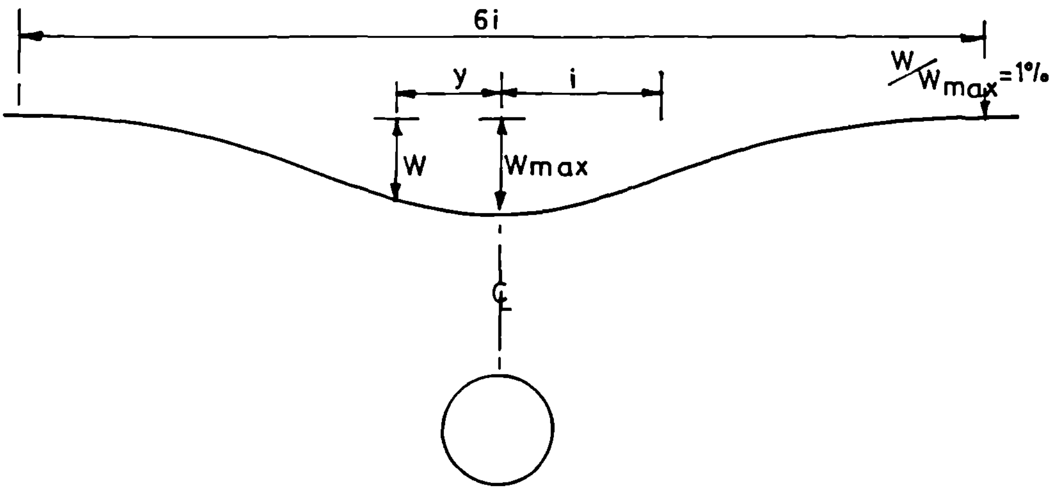

Fig. 2.20 Error function curve

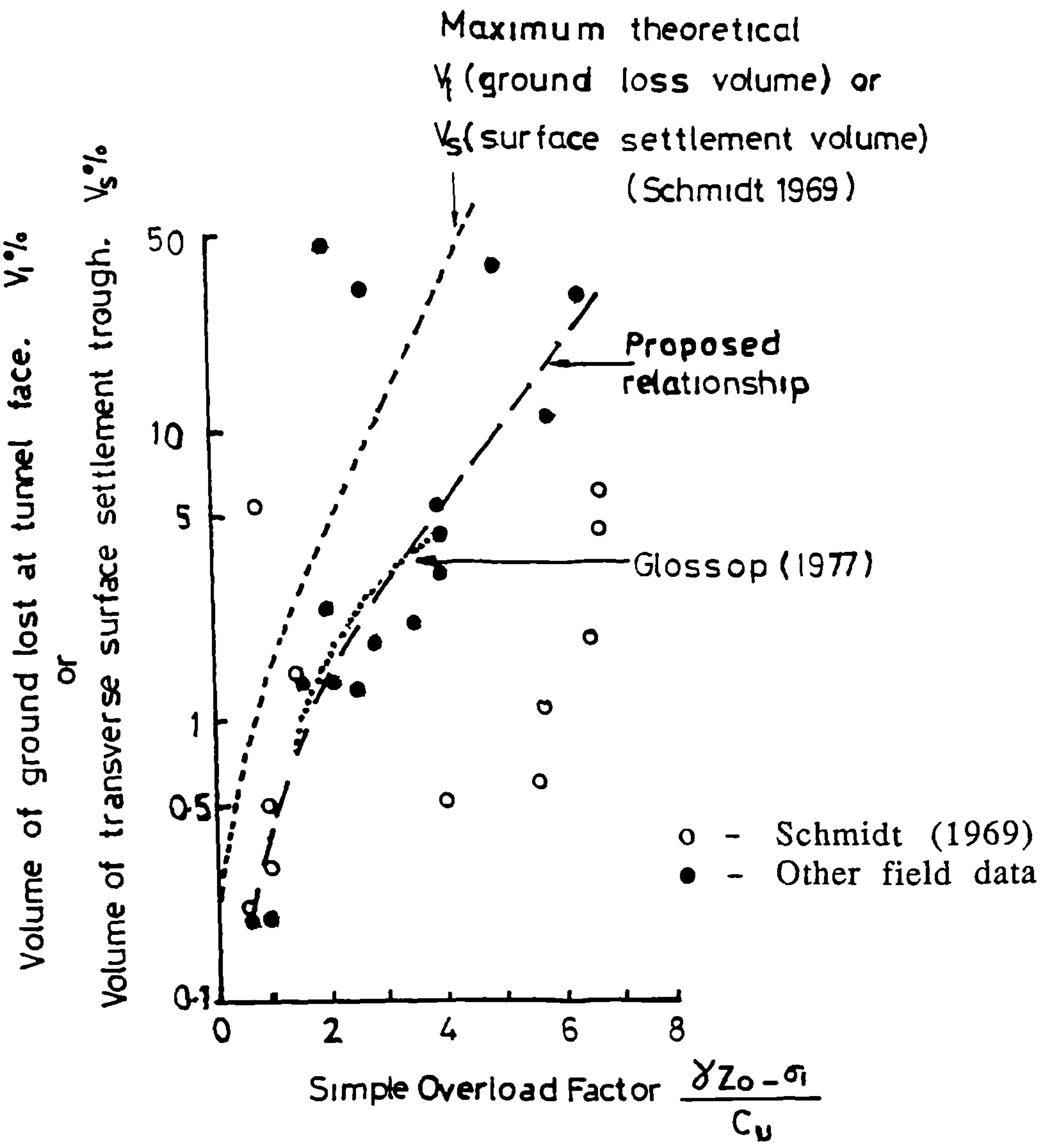

Fig. 2.21 Relationships between volume loss and simple overload factor (after Attewell et al, 1986)

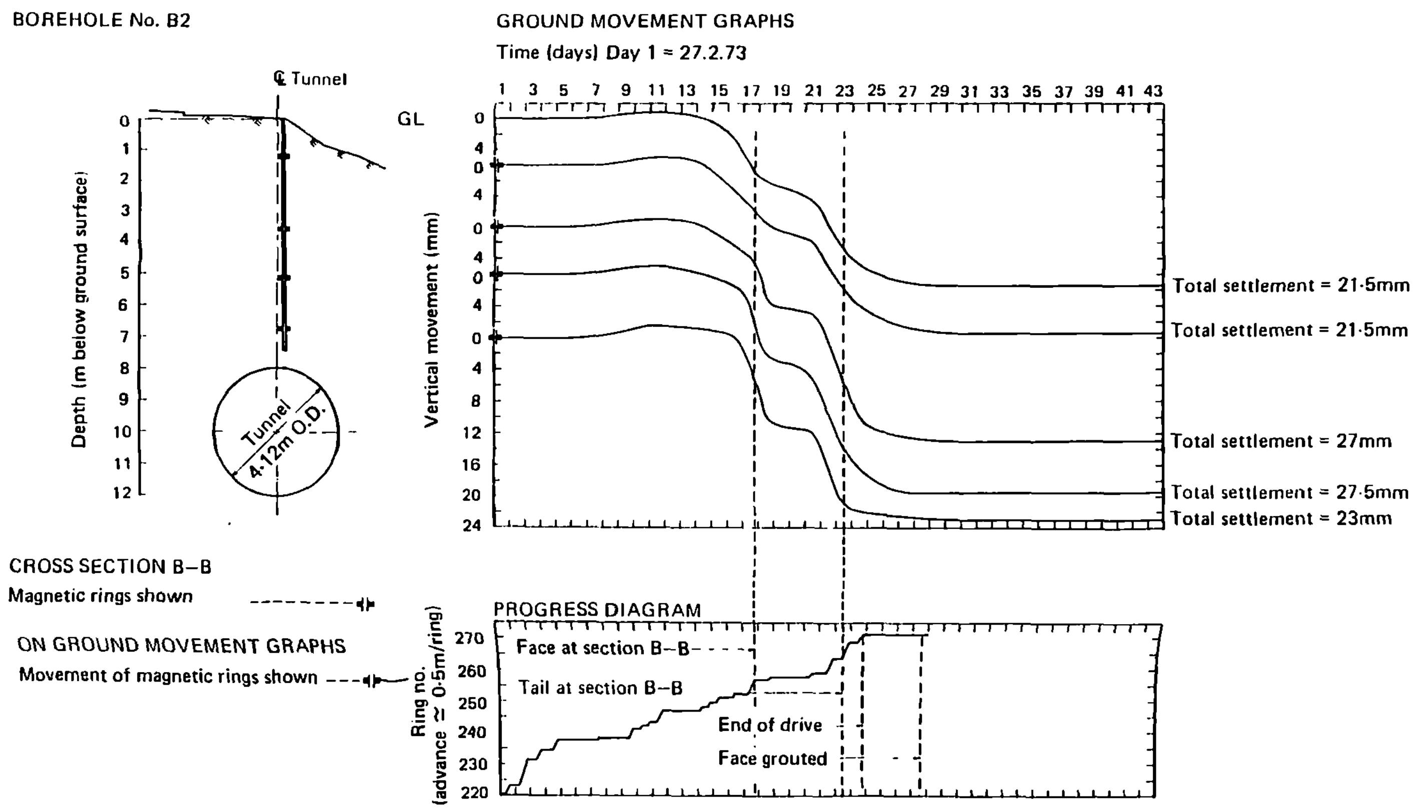

Fig. 2.22 Vertical ground movements recorded above a tunnel construction at New Cross, London (after Boden and McCaul, 1974)

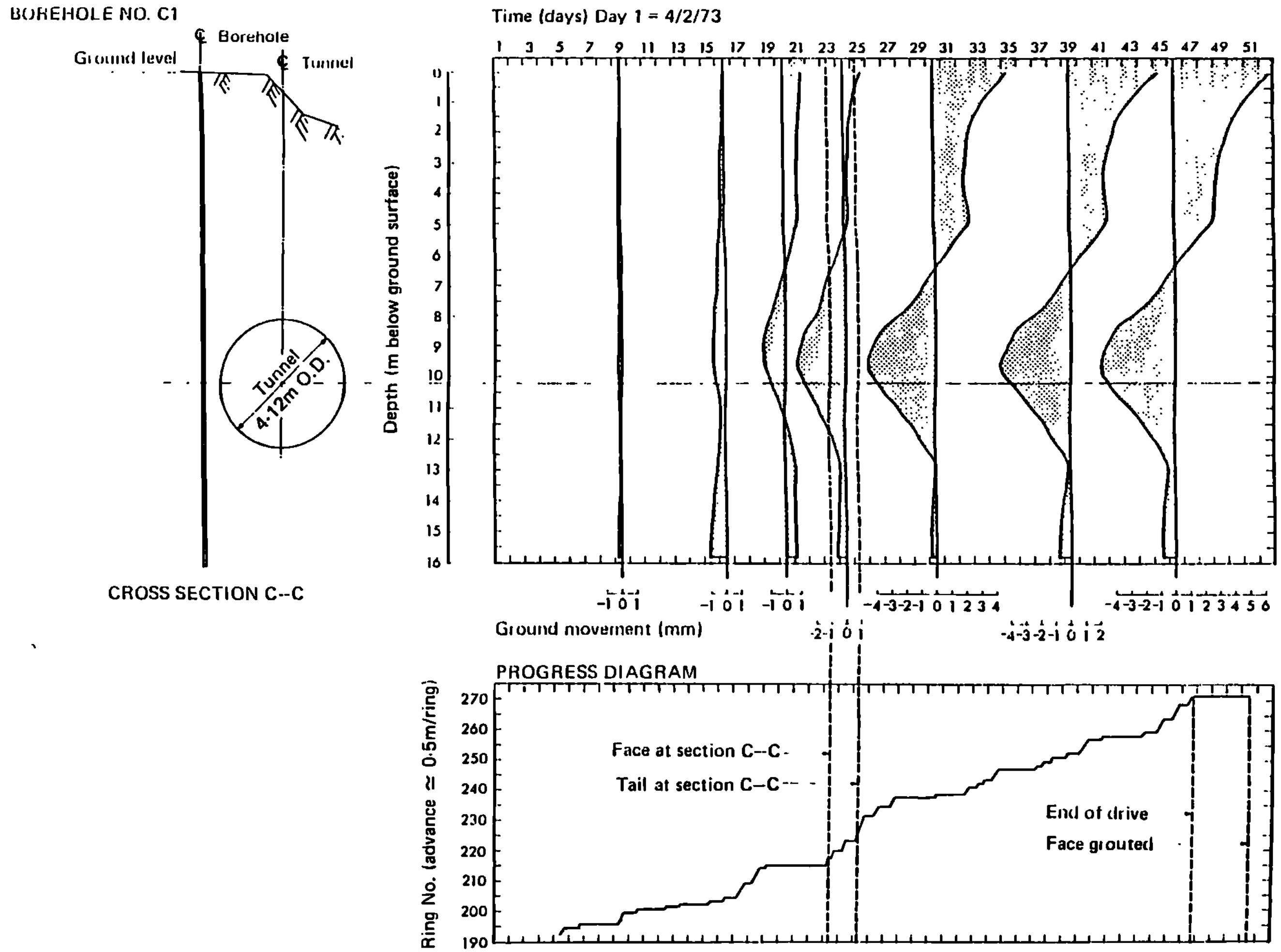

Fig. 2.23 Lateral ground movements recorded during the construction of a tunnel at New Cross, London (after Boden and McCaul, 1974)

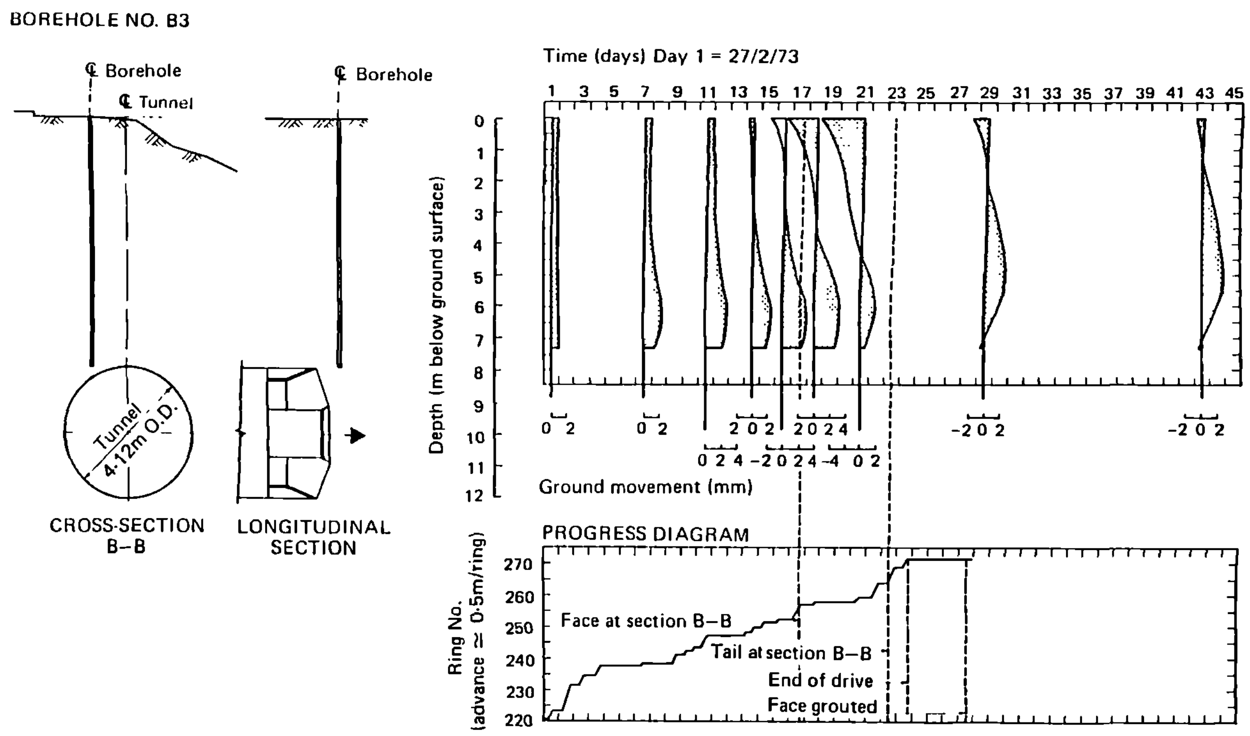

Fig. 2.24 Longitudinal ground movements recorded during the construction of a tunnel at New Cross, London (after Boden and McCaul, 1974)

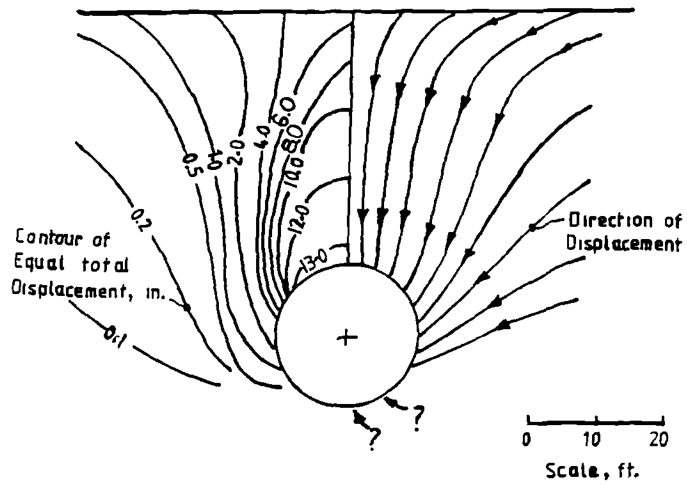

(a) Total displacements

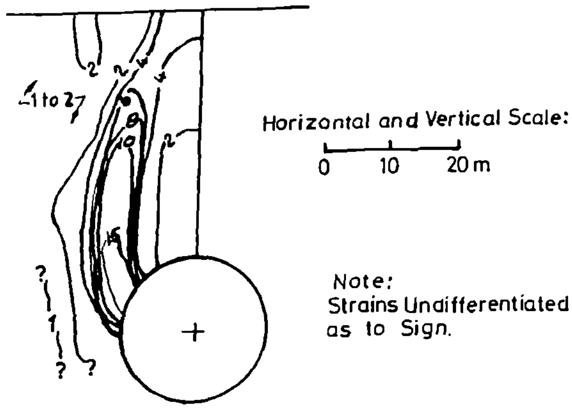

(b) Geometric strains

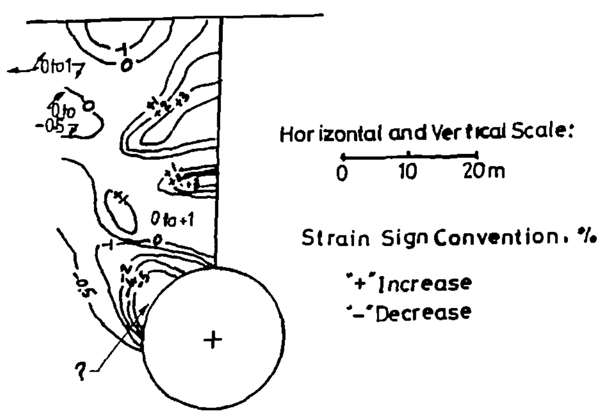

(c) Volumetric strains

Fig. 2.25 Information on ground movements observed around a tunnel at Lafayette park, Washington D.C. (after Hansmire, 1975)

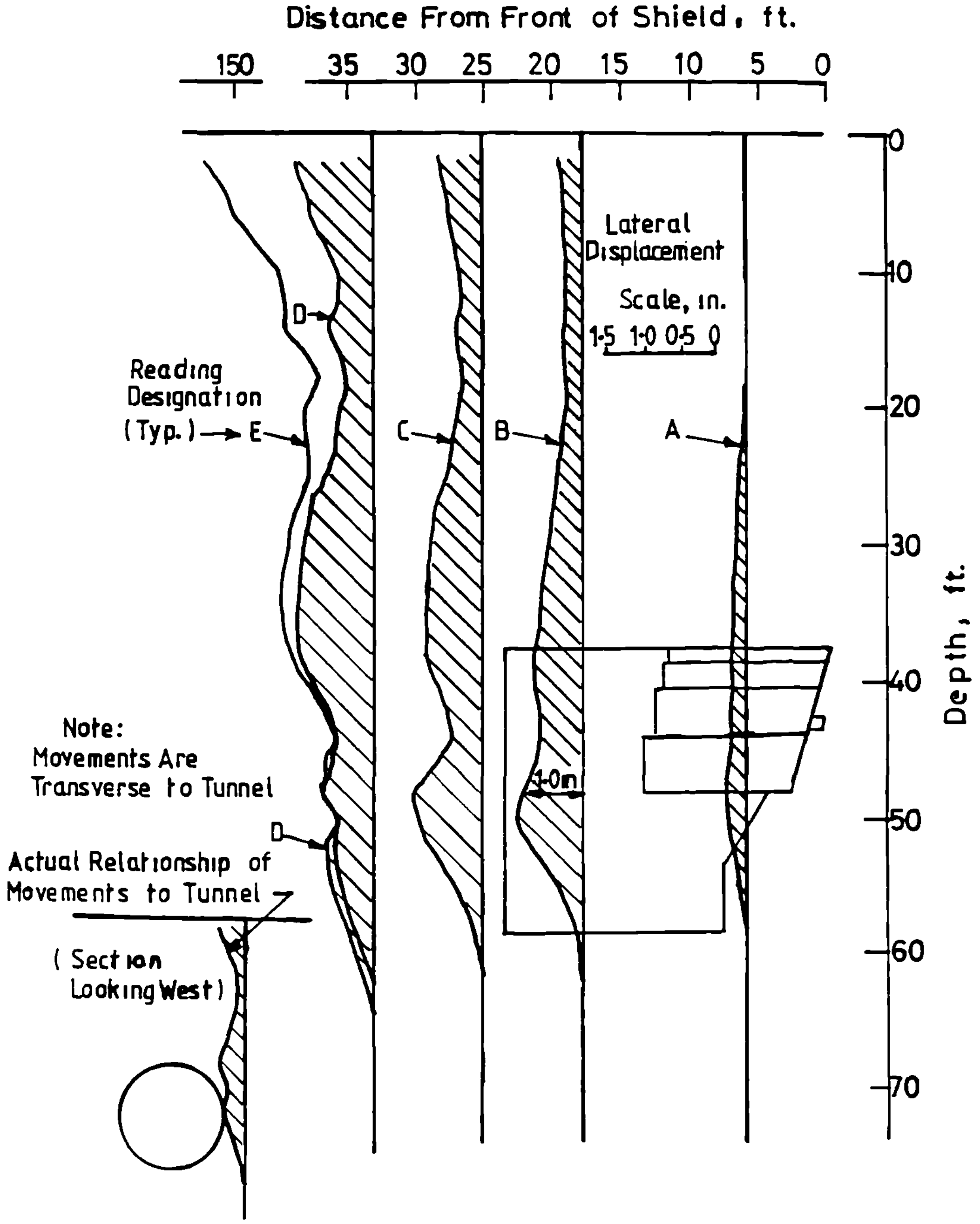

Fig. 2.26 Inclinometer data for lateral displacements during a tunnel construction at Lafayette Park, Washington D.C. (after Hansmire (1975))

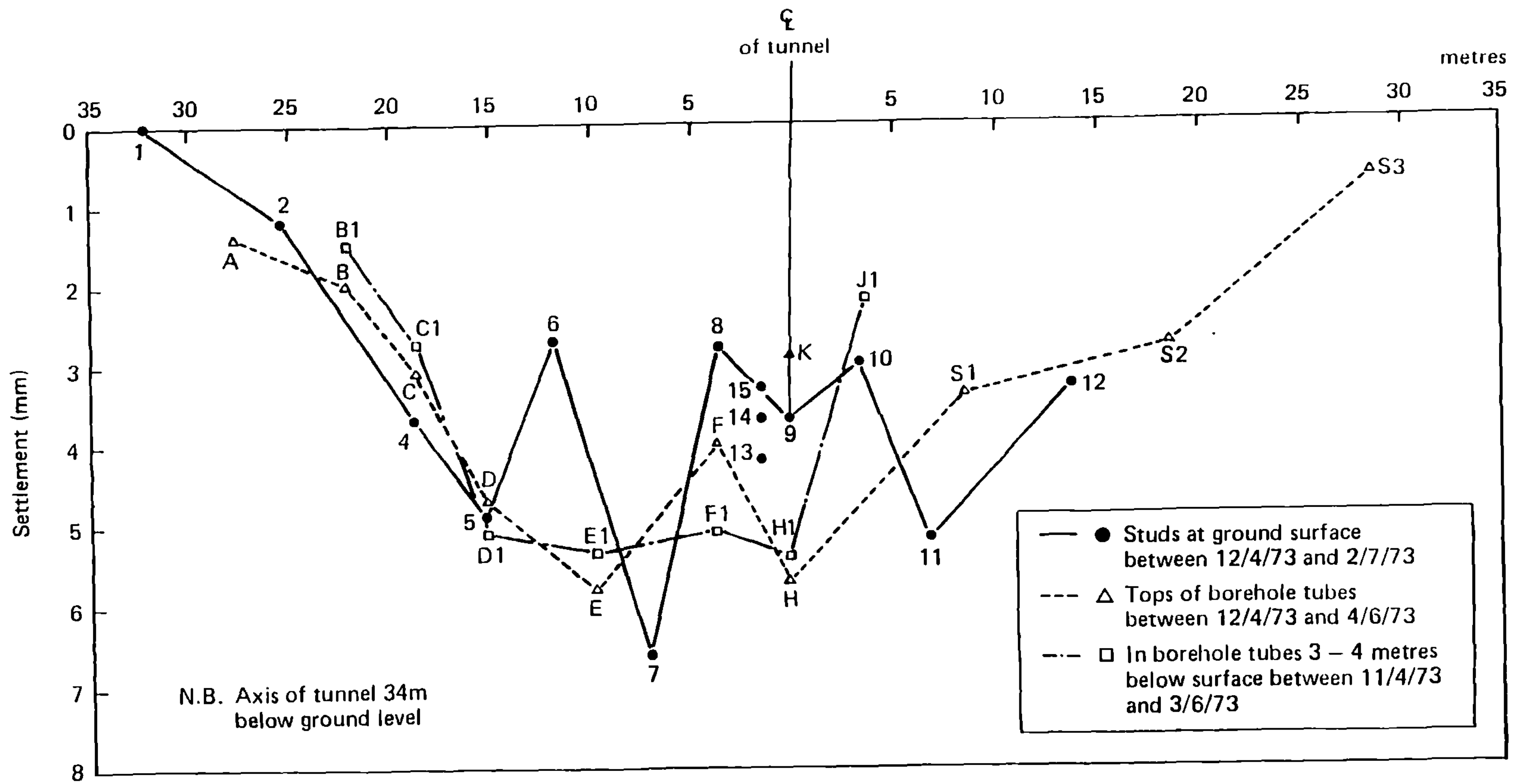

Fig. 2.27 Surface settlement trough above a tunnel construction at Regents Park, London (after Barratt and Tyler, 1976)

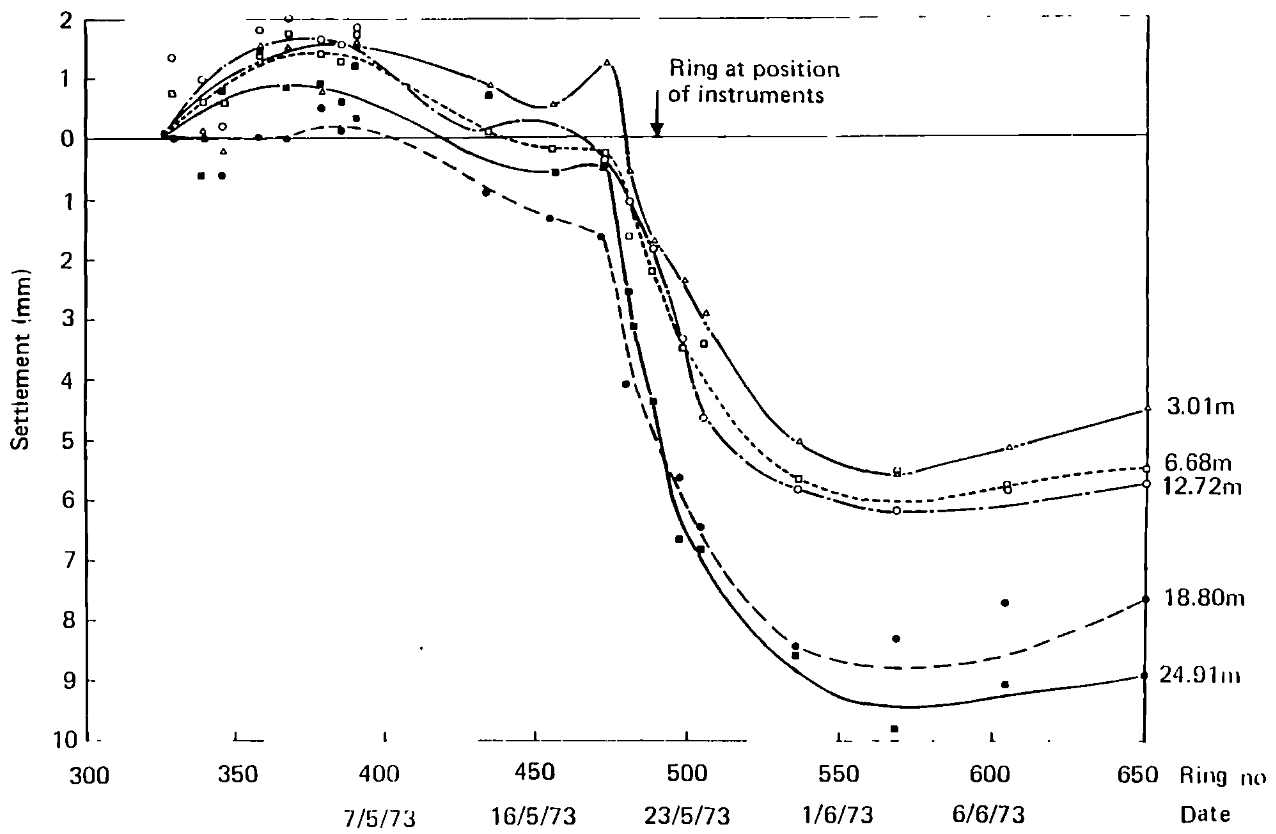

Fig. 2.28 Settlements along the centreline of a tunnel construction at Regents Park, London (after Barratt and Tyler, 1976)

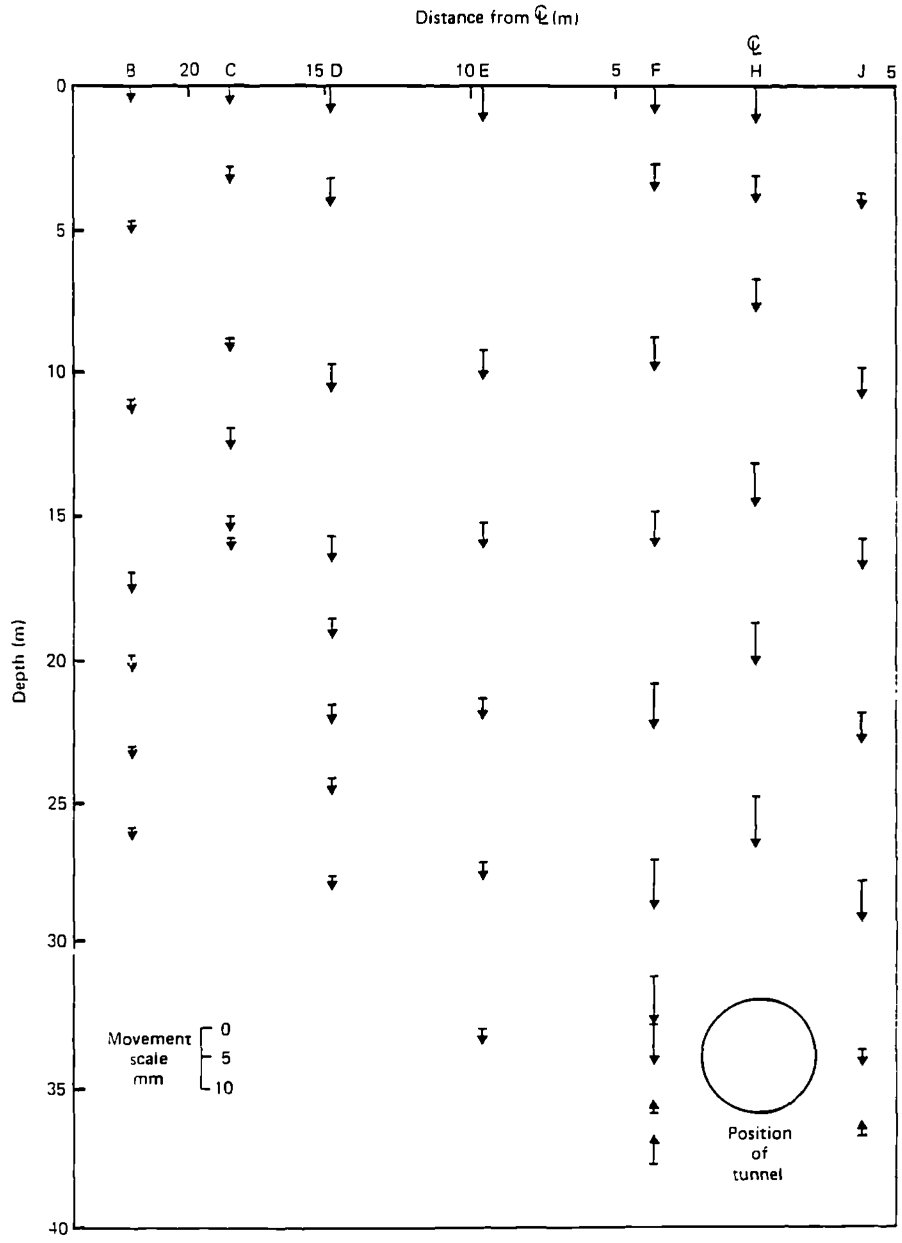

Fig. 2.29 Final vertical settlements in the perpendicular plane for a tunnel constructed at Regents Park, London (after Barratt and Tyler, 1976)

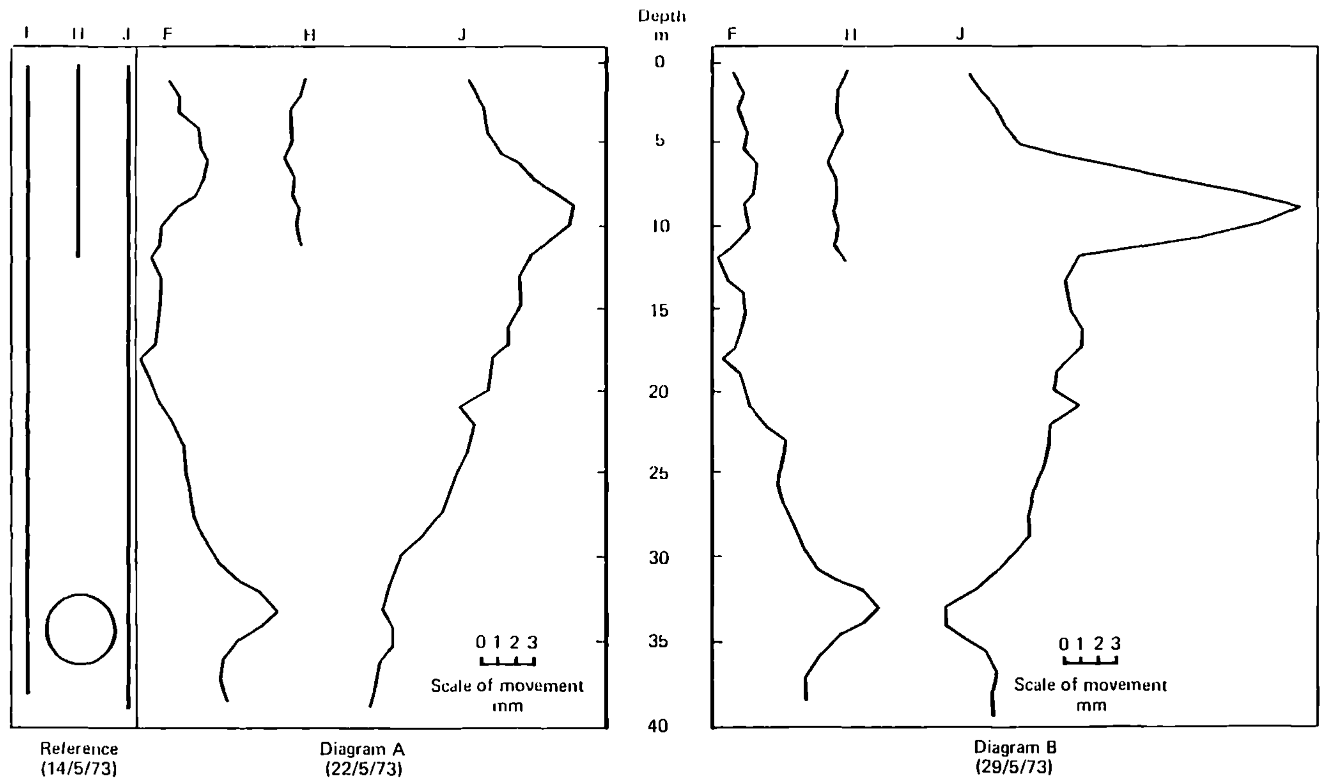

Fig. 2.30 Lateral movements during a tunnel construction at Regents Park, London (after Barratt and Tyler, 1976)

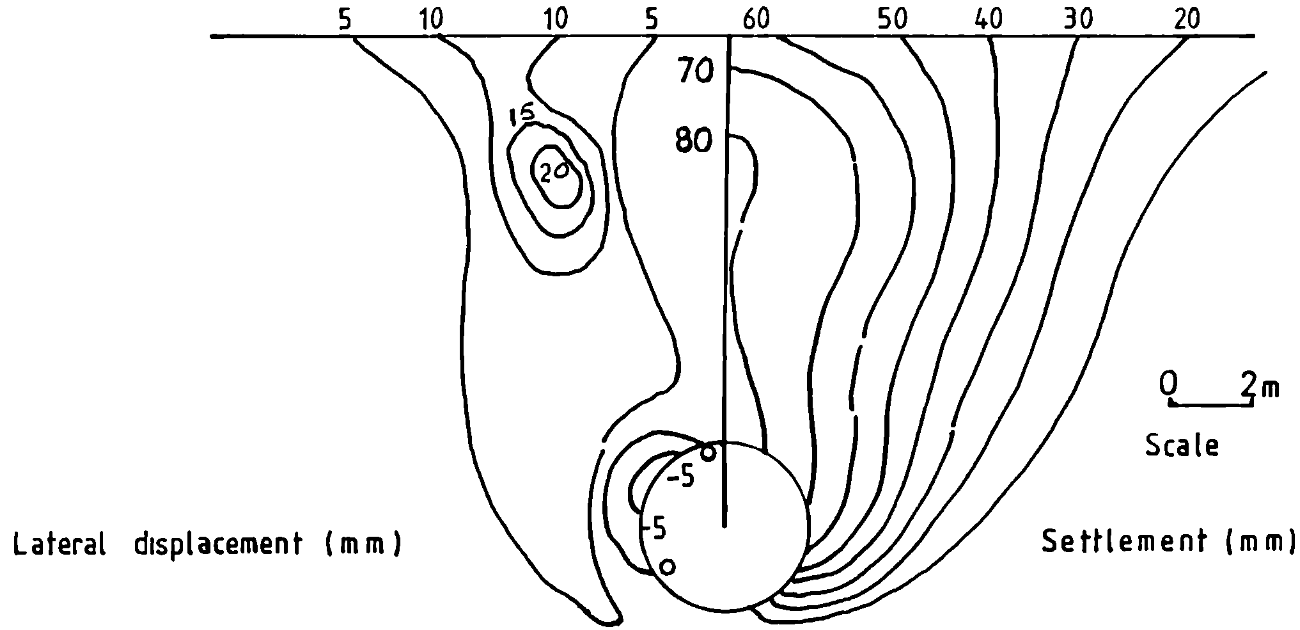

Fig. 2.31 Lateral and vertical displacement contours during a tunnel construction at Willington Quay (after Glossop, 1977)

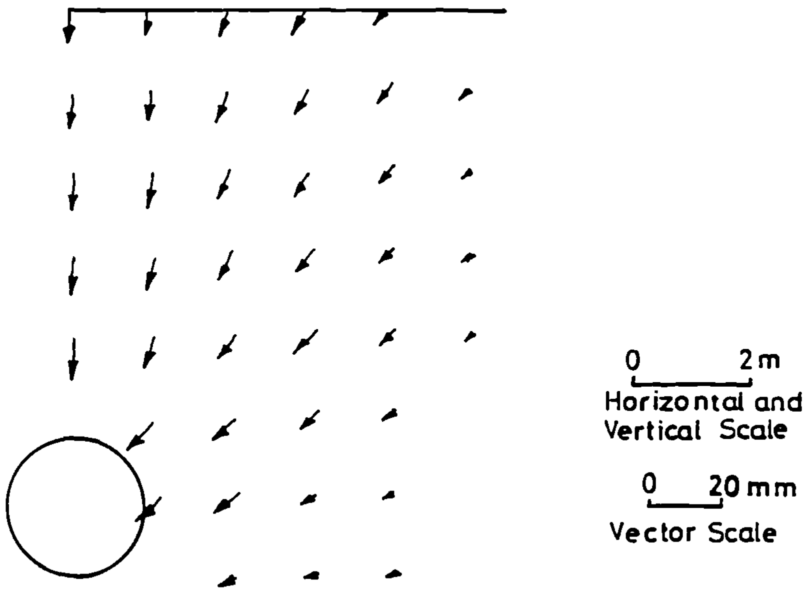

(a) Tunnel constructed at Willington Quay

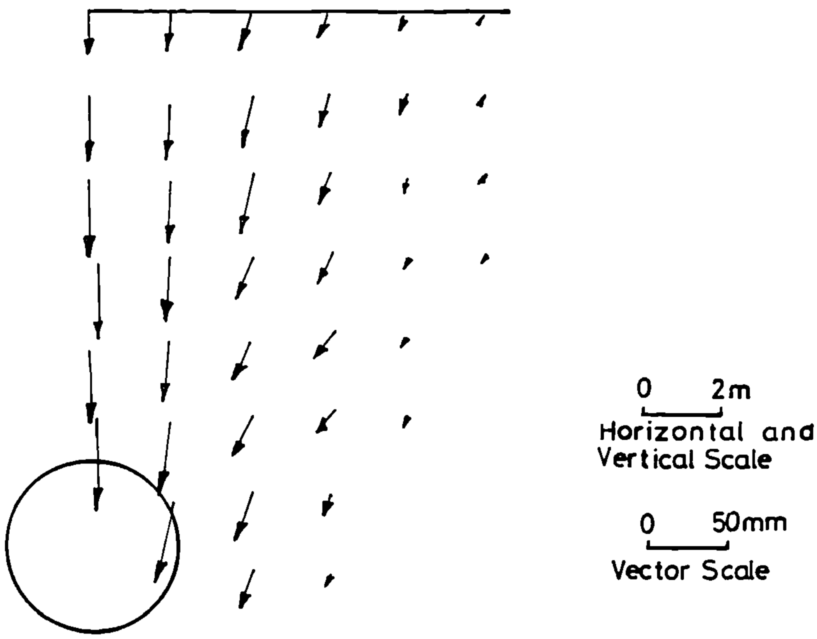

(b) Tunnel constructed at Hebburn

Fig. 2.32 Total displacement vector plots (after Glossop, 1977)

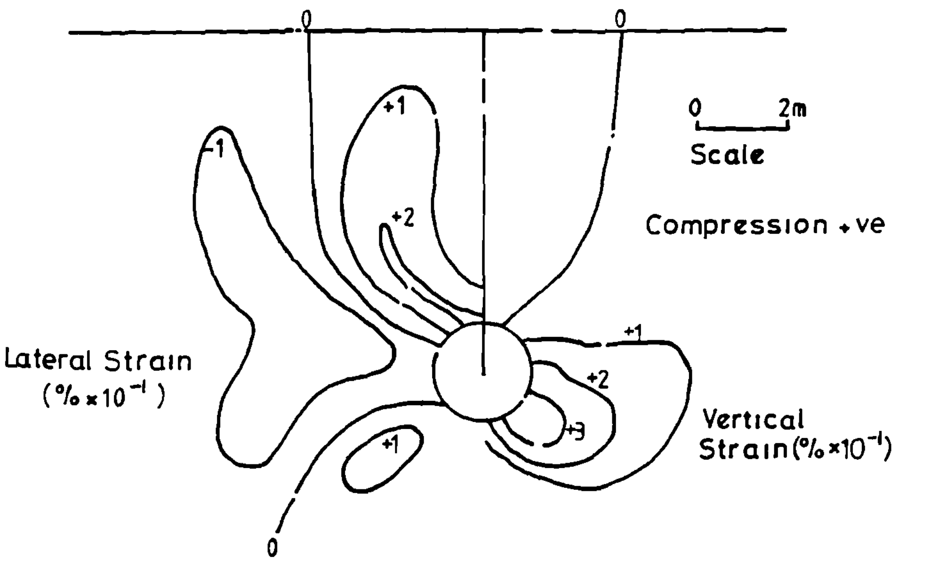

(a) Tunnel constructed at Willington Quay

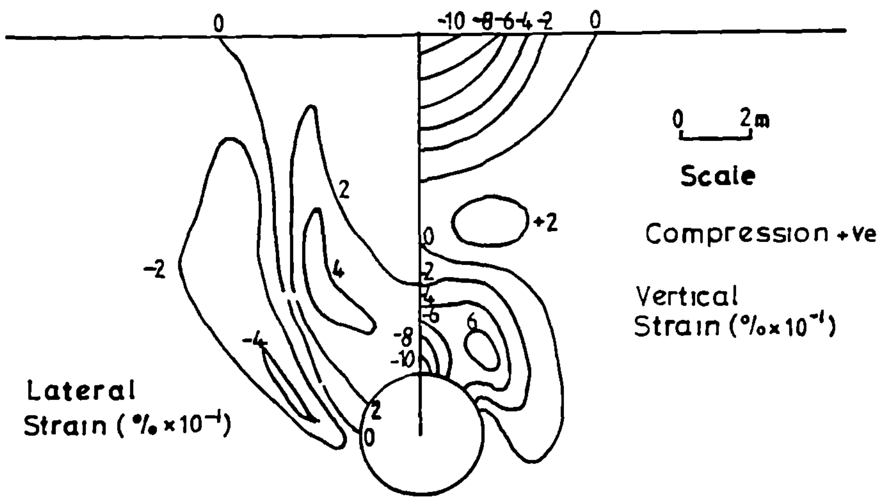

(b) Tunnel constructed at Hebburn

Fig. 2.33 Strain contour plots (after Glossop, 1977)

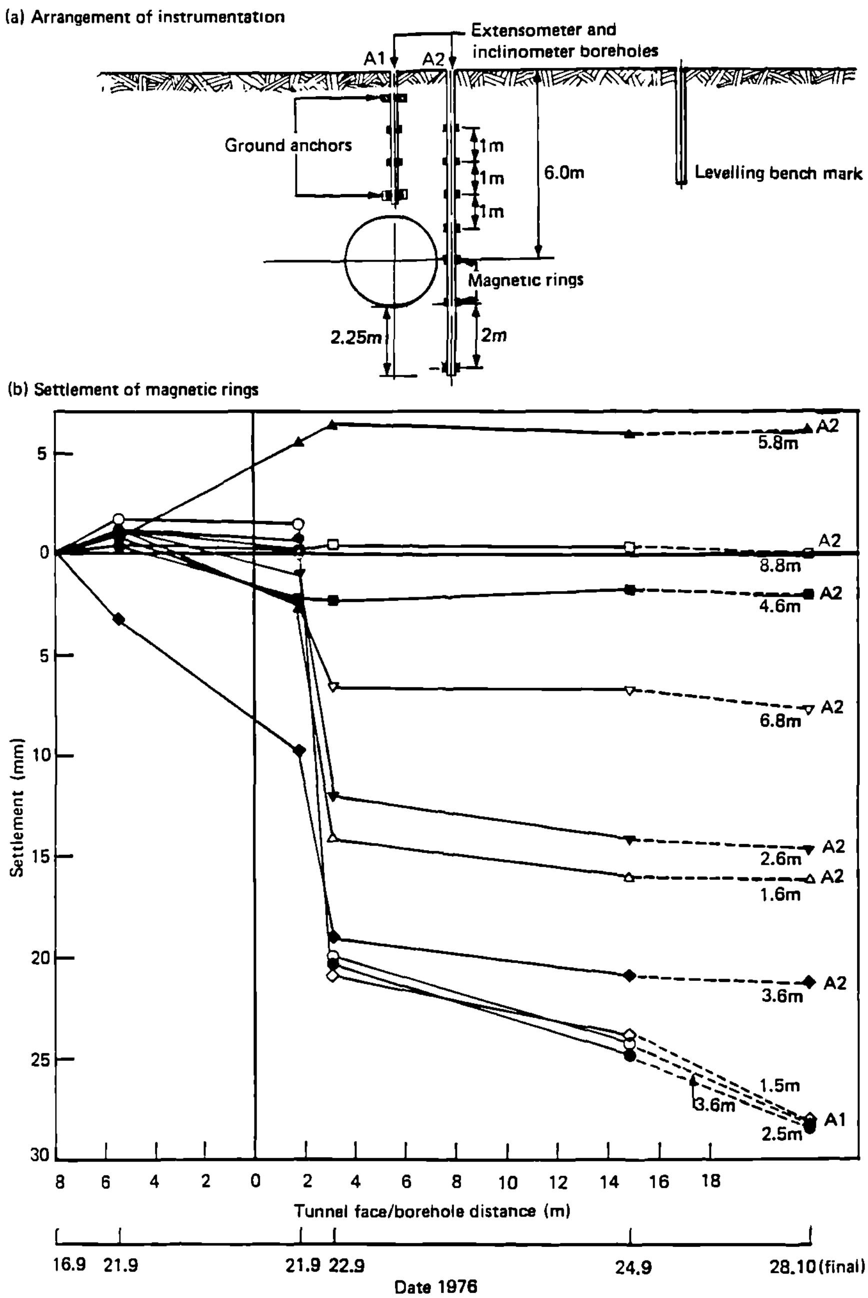

Fig. 2.34 Vertical ground movements around a tunnel constructed at Acton Grange (after Ryley et al, 1980)

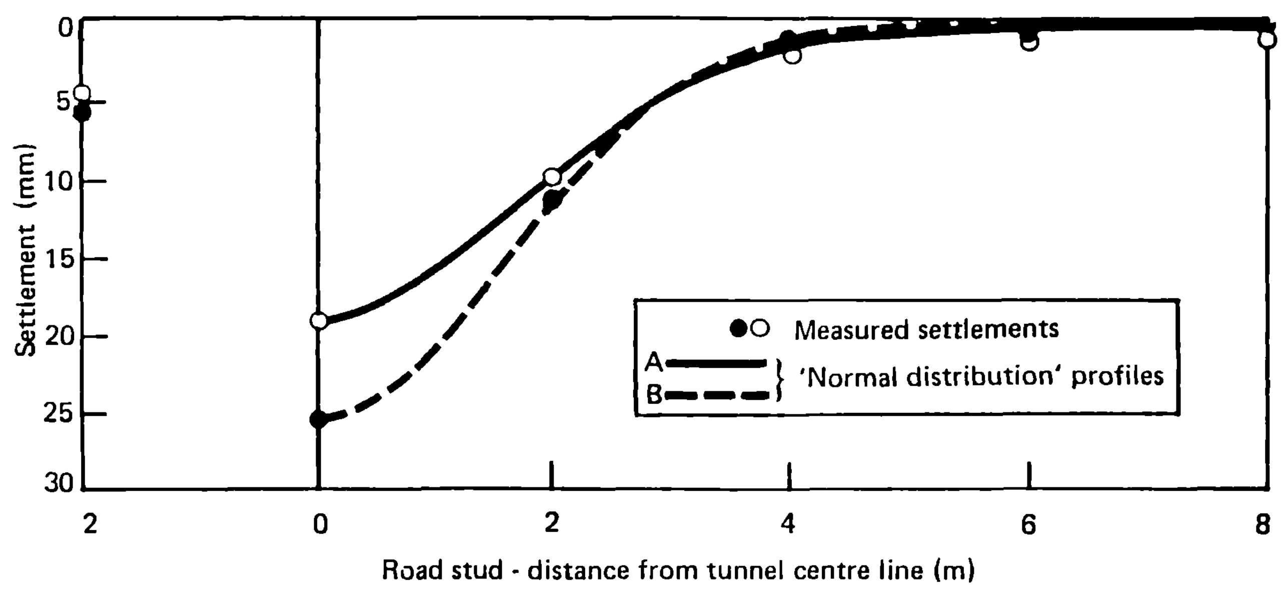

Fig. 2.35 Surface settlement profiles obtained during the construction of a tunnel at Acton Grange (after Ryley et al, 1980)

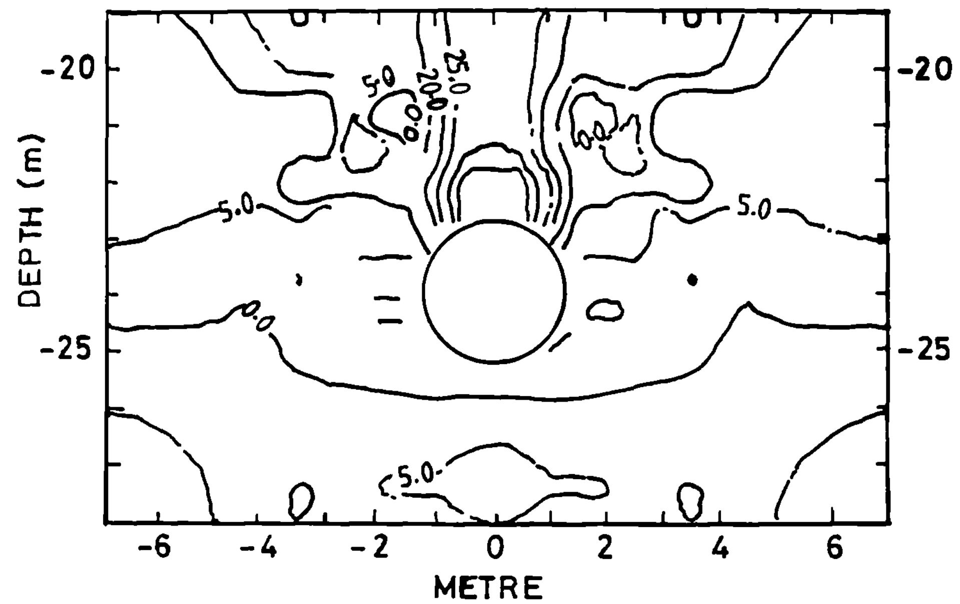

(a) Vertical displacement contours (displacements in mm, positive values are downwards)

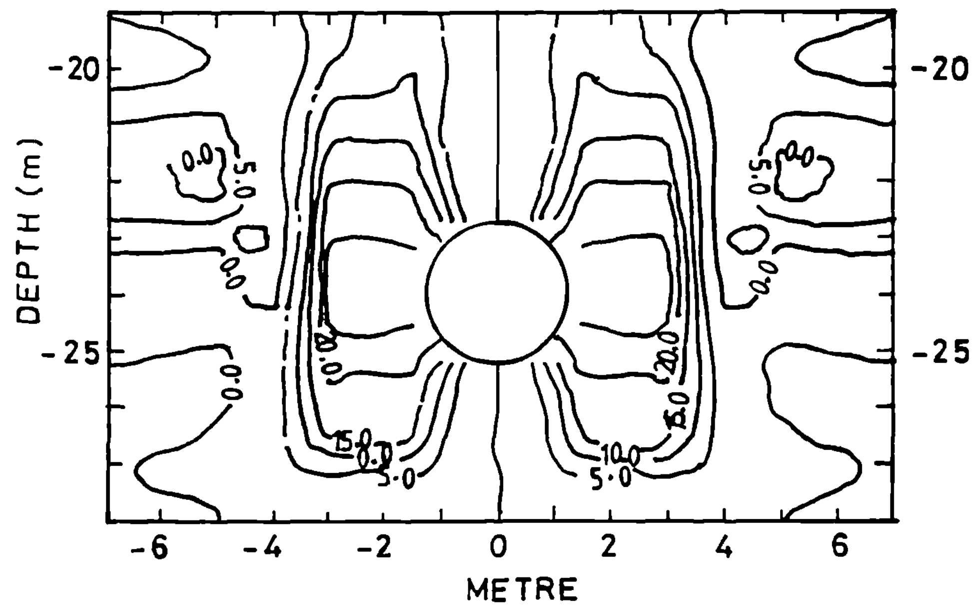

(b) Horizontal displacement contours (displacements in mm, positive values are towards tunnel)

Fig. 2.36 Displacement contours around a tunnel constructed using a shielded mole (after Eisenstein et al, 1981)

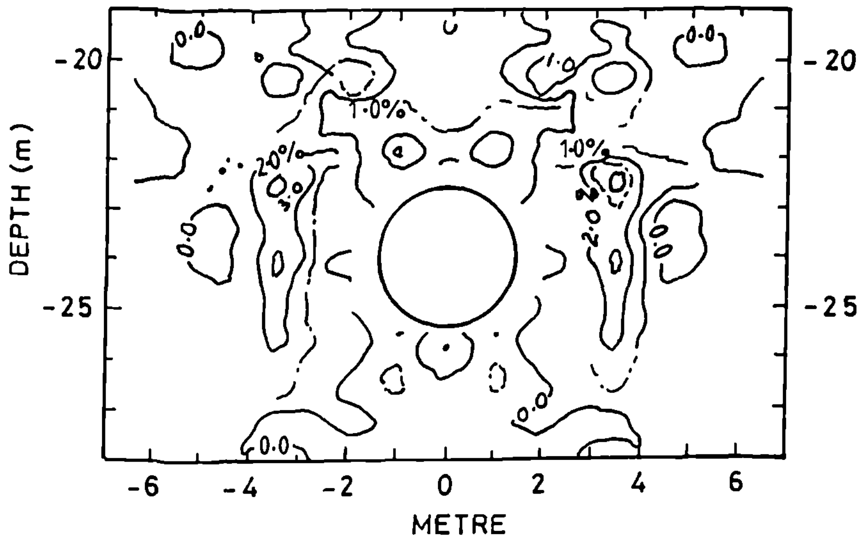

(a) Volumetric strain contours

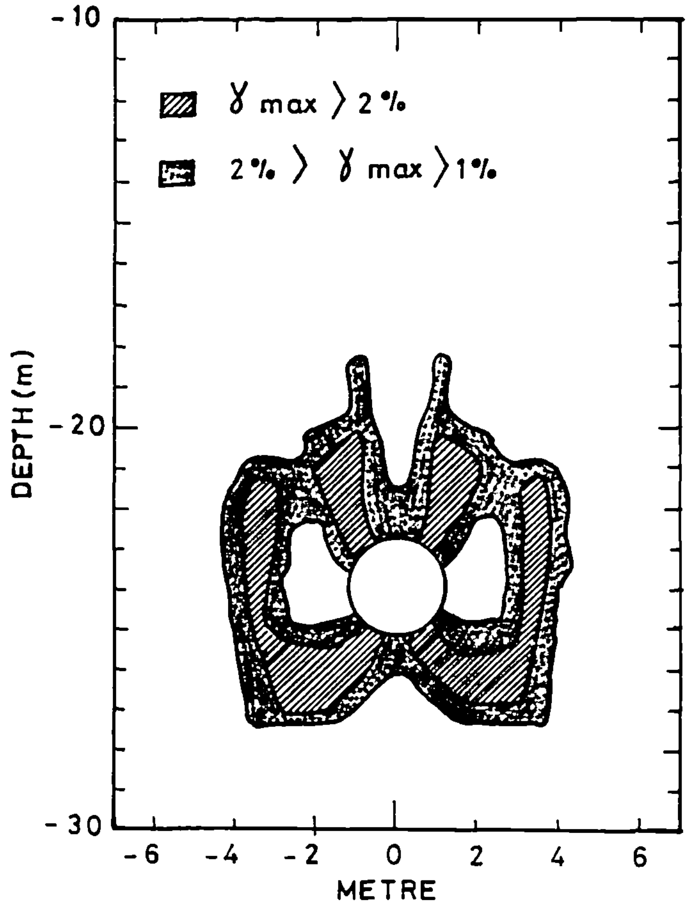

(b) Failure zones around tunnel

Fig. 2.37 Ground behaviour around a tunnel construction using a shielded mole (after Eisenstein et al, 1981)

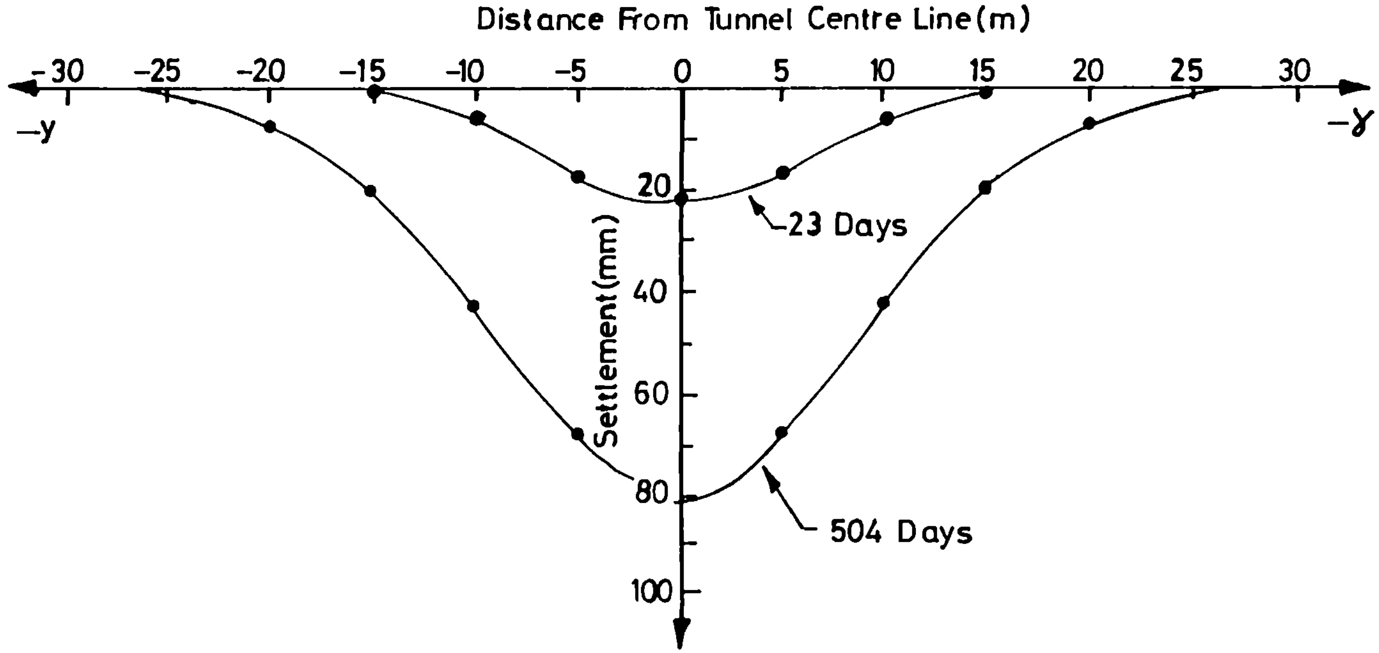

Fig. 2.38 Long term surface settlements for a tunnel constructed at Willington Quay (after Glossop, 1977)

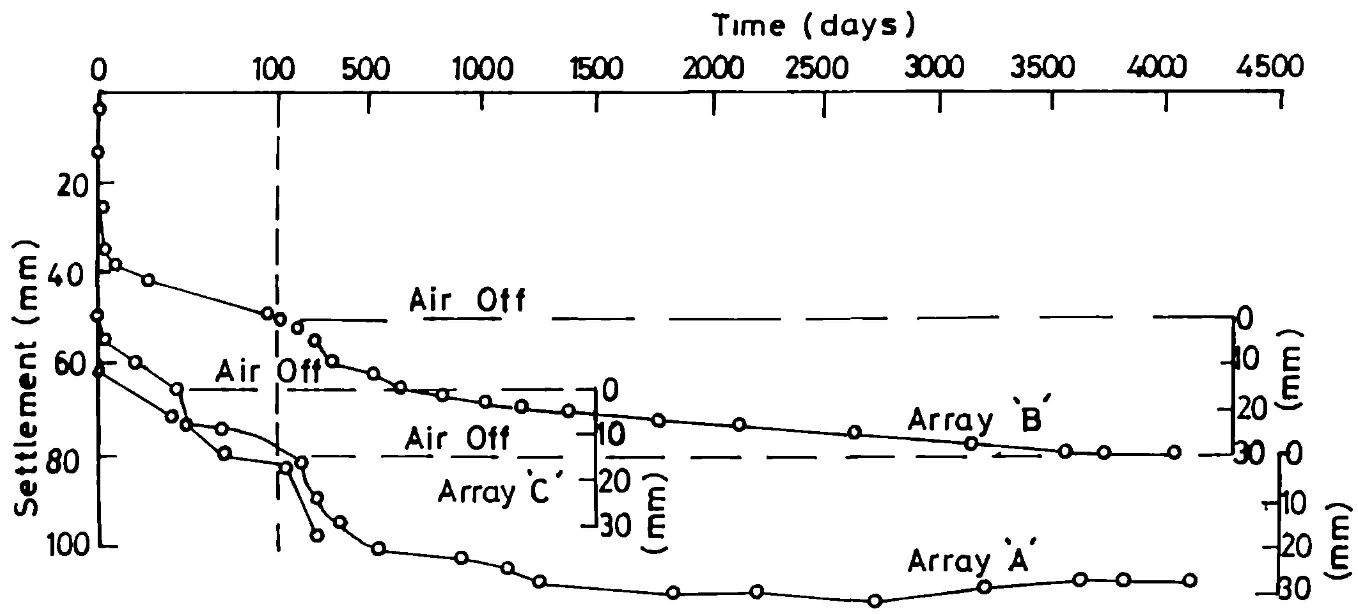

(a) Centreline settlements

Fig. 2.39 Development of long term surface settlements above a tunnel constructed at Grimsby (after O'Reilly et al, 1991)

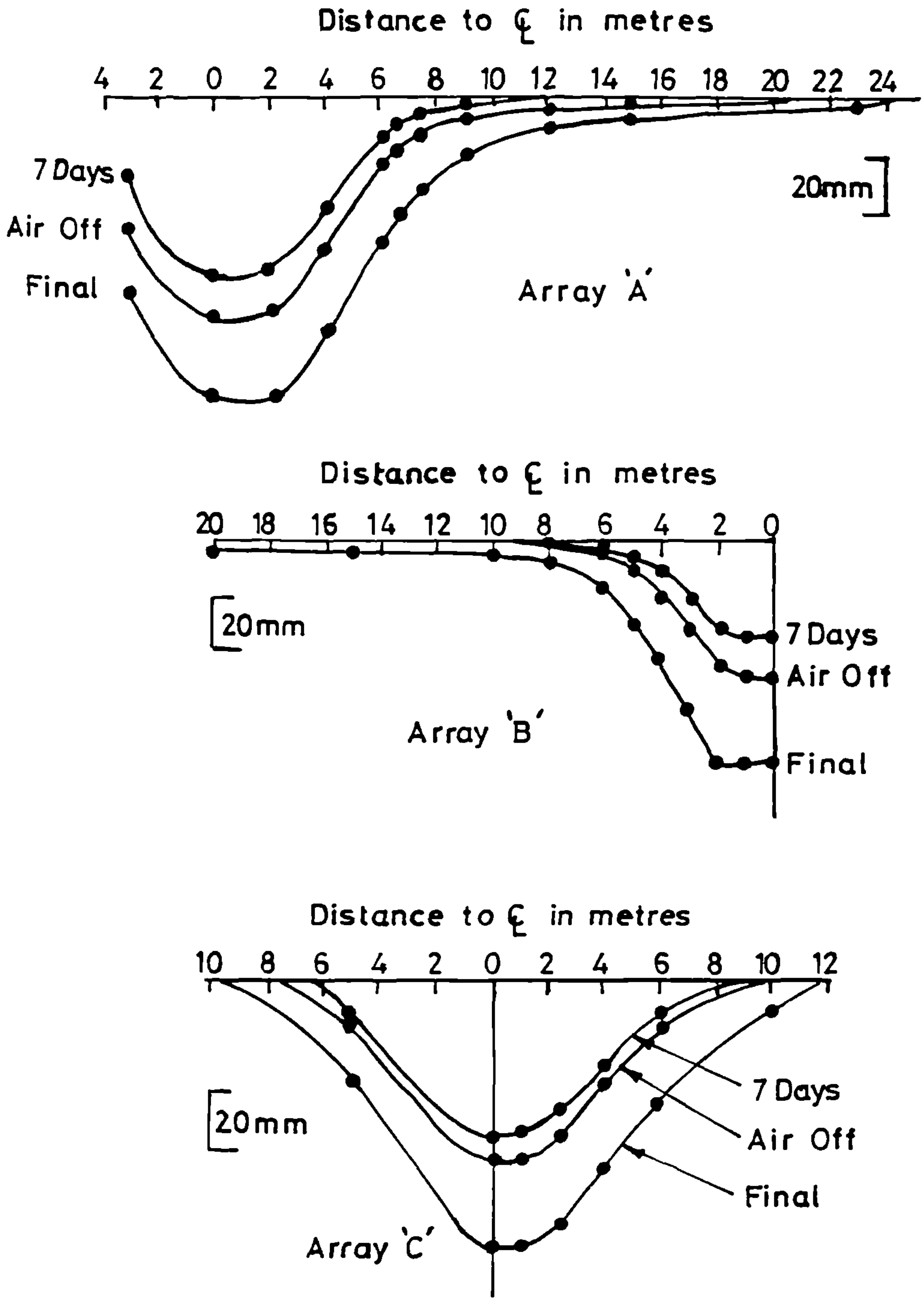

(b) Transverse settlements

Fig. 2.39 Development of long term surface settlements above a tunnel constructed at Grimsby (after O'Reilly et al, 1991)

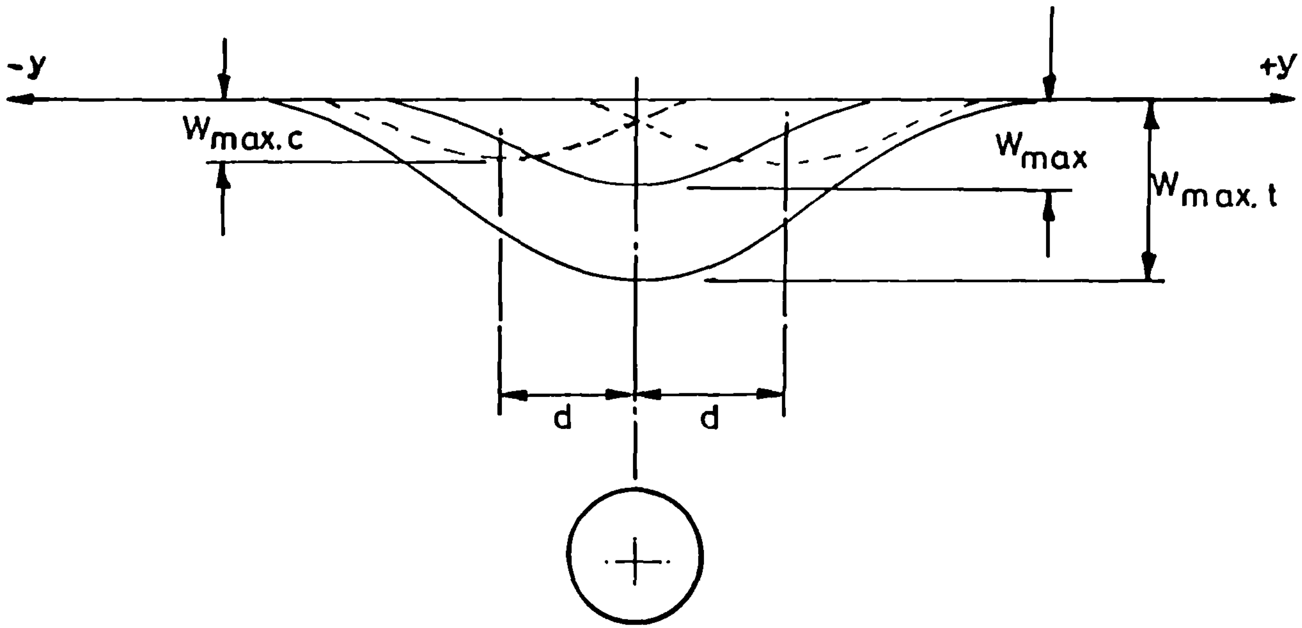

Fig. 2.40 Method of predicting the long term settlement profiles above tunnels (after Hurrell, 1984)

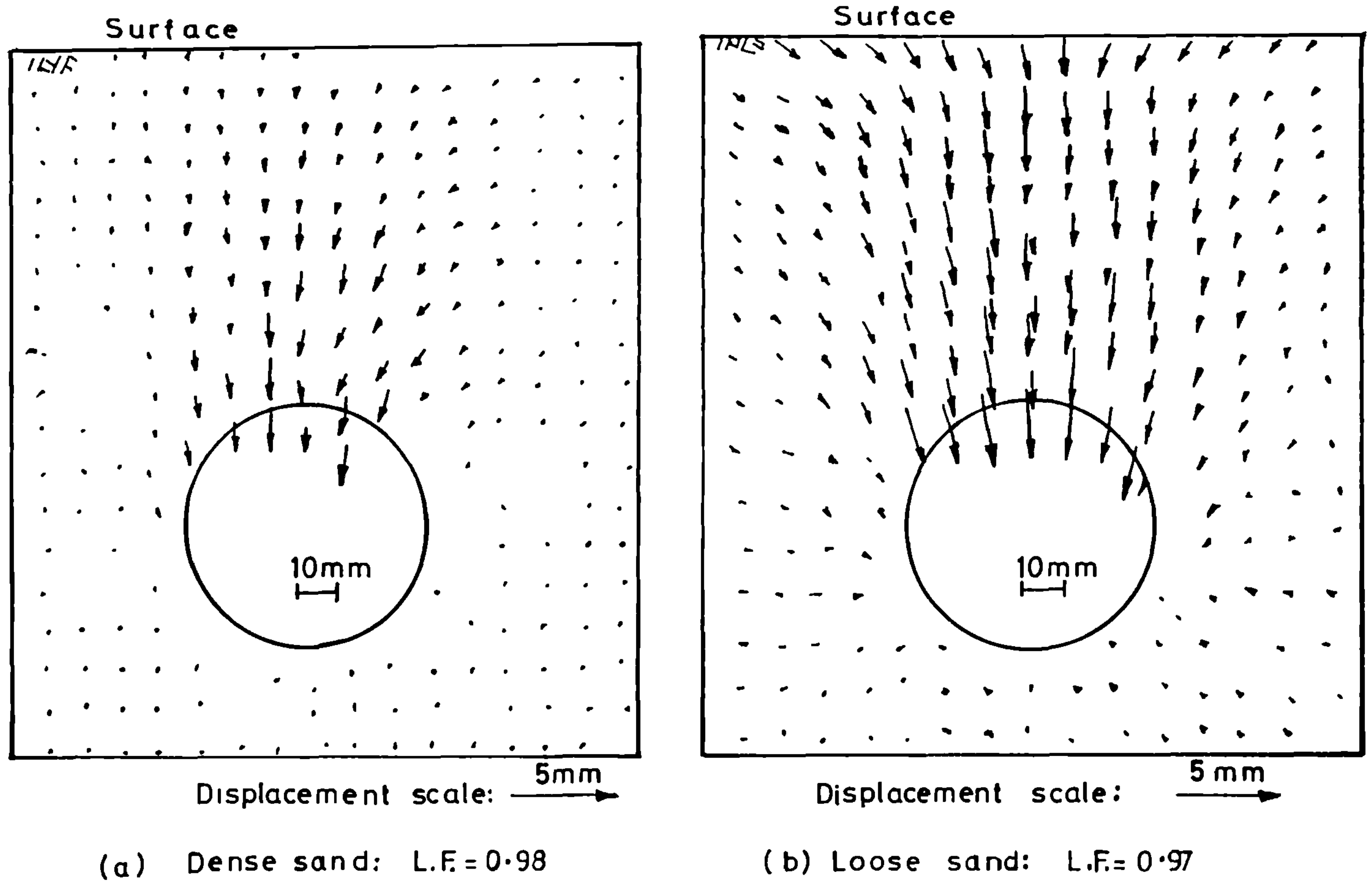

Fig. 2.41 Total displacement vectors obtained during the collapse of model tunnels in sand (after Potts, 1976)

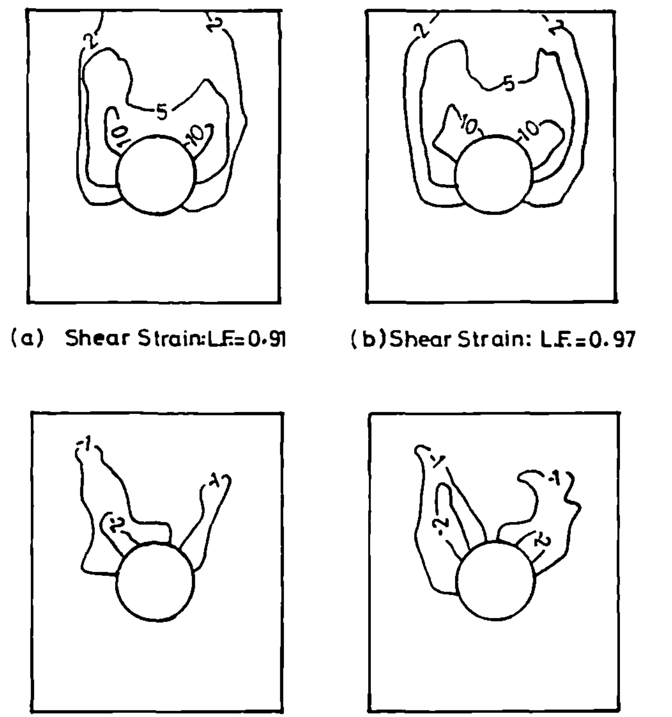

(a) Sand in a loose state (values are percentages, for volumetric strains positive is compression)

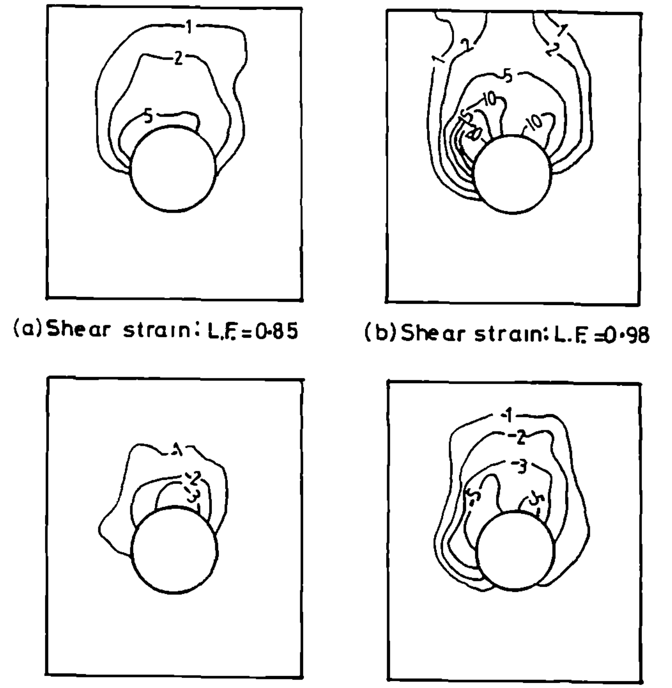

(b) Sand in a dense state (values are percentages, for volumetric strains positive is compression)

Fig. 2.42 Shear strain and volumetric strain contours close to tunnel collapse in sand (after Potts, 1976)

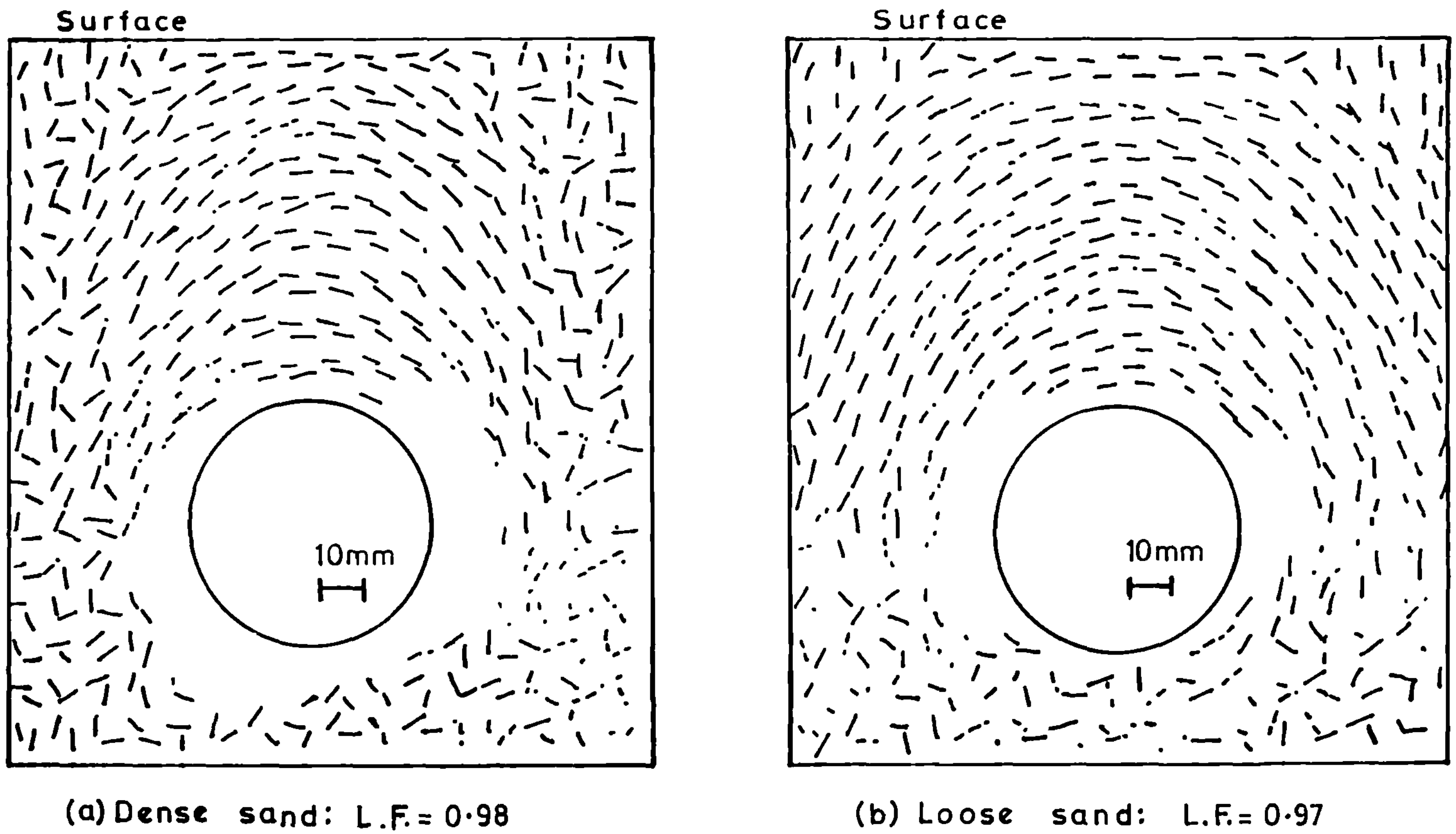

Fig. 2.43 Directions of the major principal strains around tunnels in sand (after Potts, 1976)

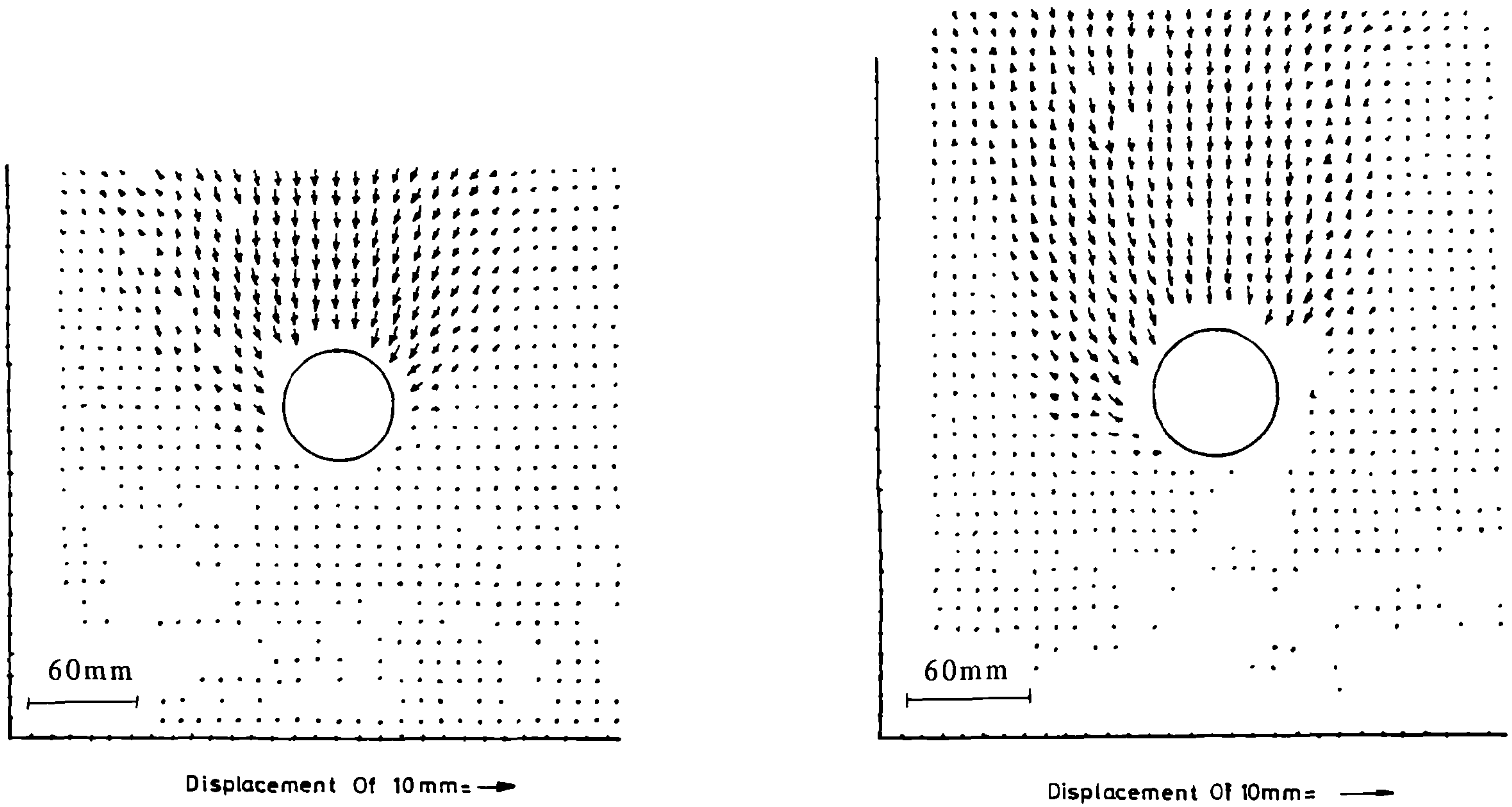

(a) Cover depth/diameter ratio of 1.6

(b) Cover depth/diameter ratio of 2.6

Fig. 2.44 Total displacement vector plots for model tunnels close to collapse in soft clay (after Mair, 1979)

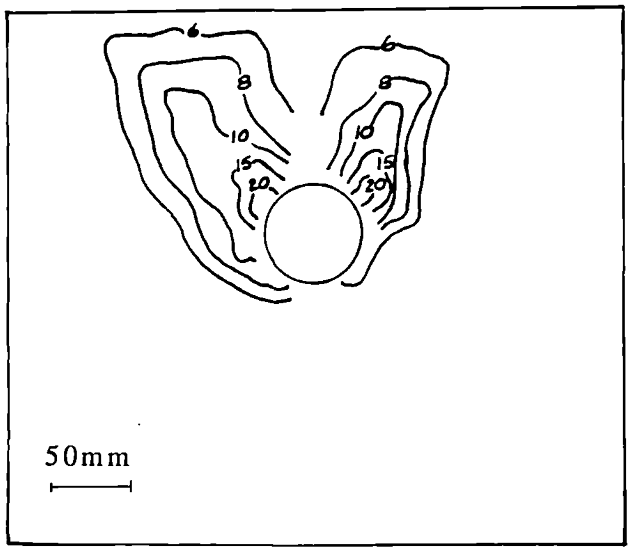

(a) Cover depth/diameter ratio of 1.6

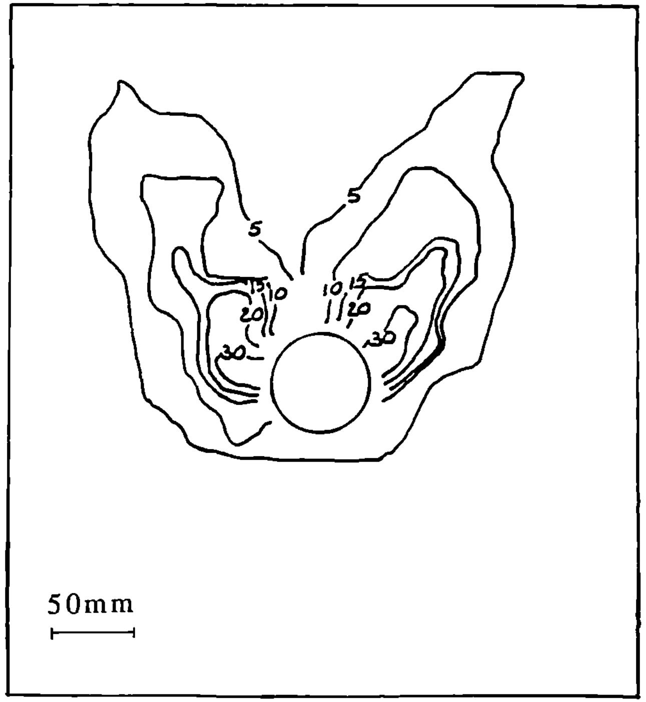

(b) Cover depth/diameter ratio of 2.6

Fig. 2.45 Shear strain (%) contour plots for model tunnels close to collapse in soft clay (after Mair, 1979)

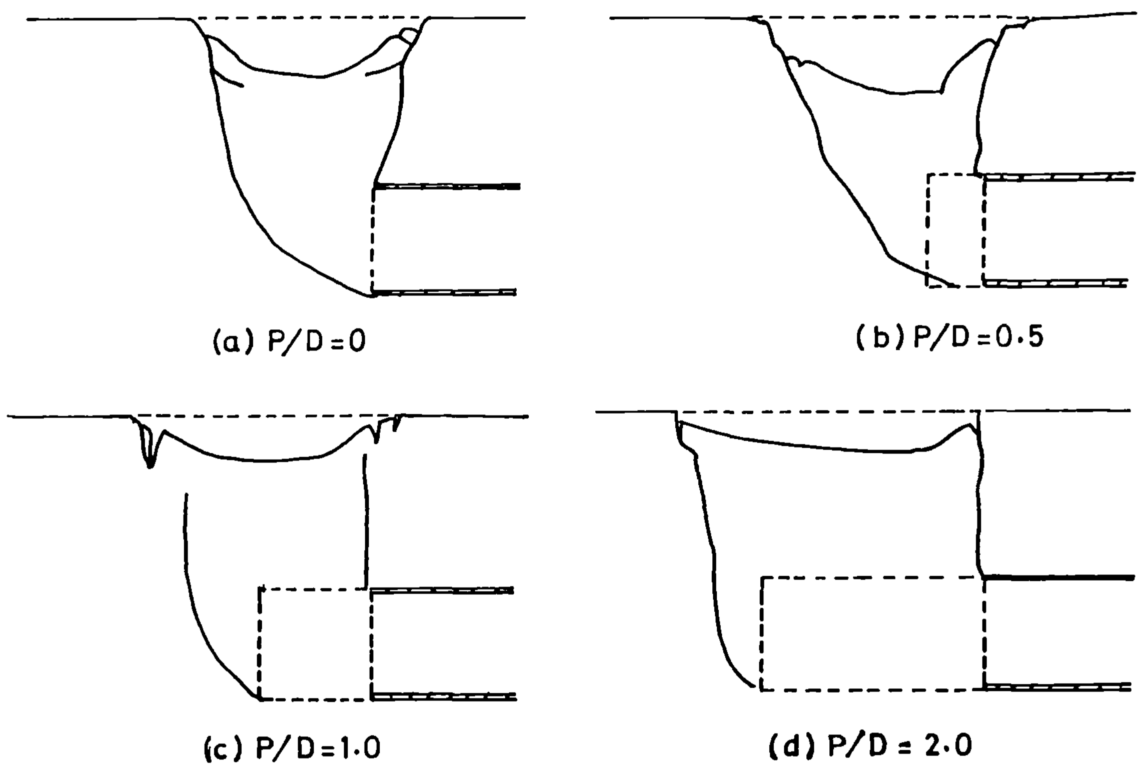

(a) Cover depth/diameter ratio of 1.6

Fig. 2.46 Tunnel heading collapse patterns for different geometries (after Mair, 1979)

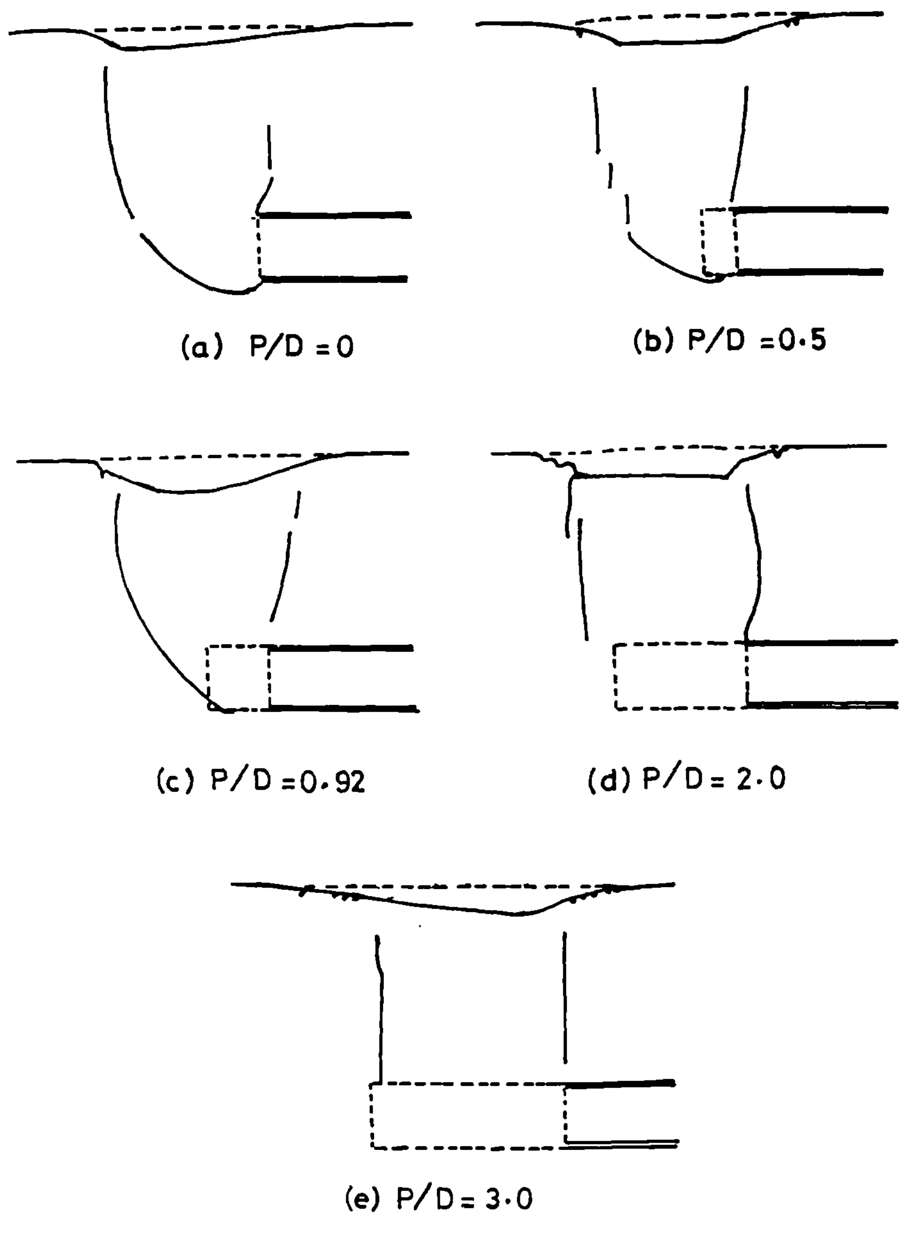

(b) Cover depth/diameter ratio of 2.6

Fig. 2.46 Tunnel heading collapse patterns for different geometries (after Mair, 1979)

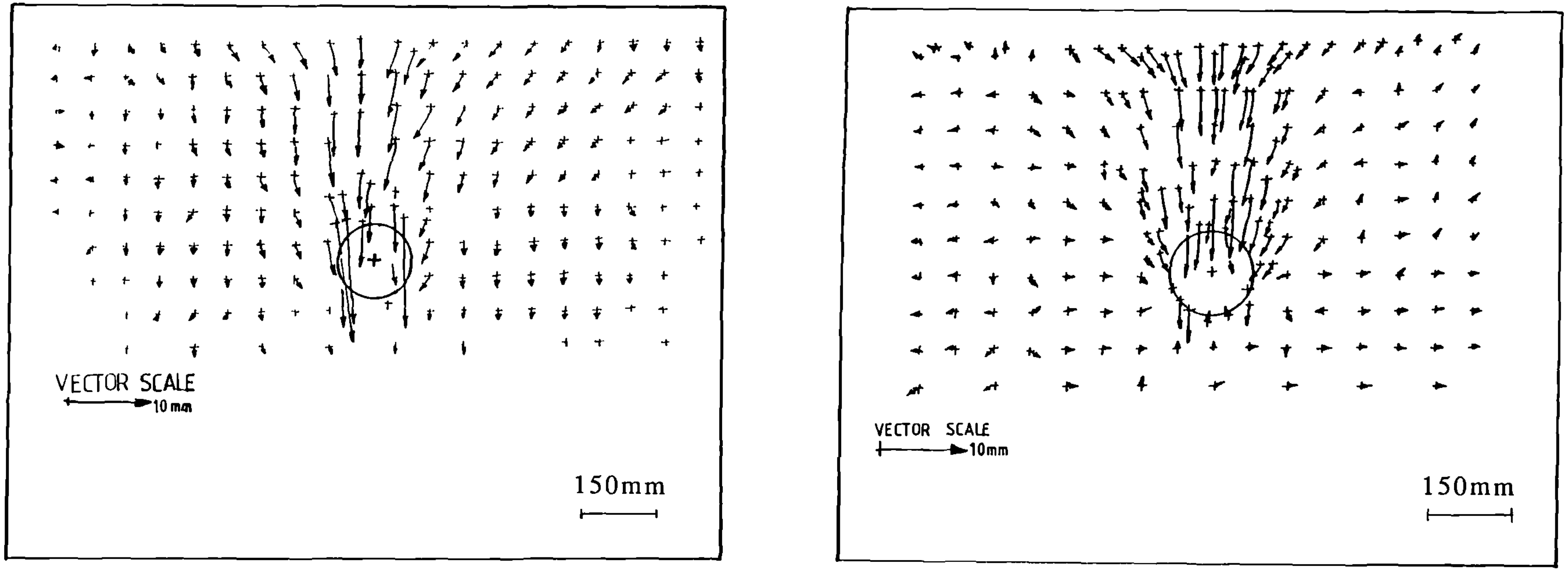

(a) Test 1 (b) Test 2

Fig. 2.47 Subsurface total displacement vector plots for model tests in sand (after Cording et al, 1976), the parameters relating to these tests are given in Table 5.7

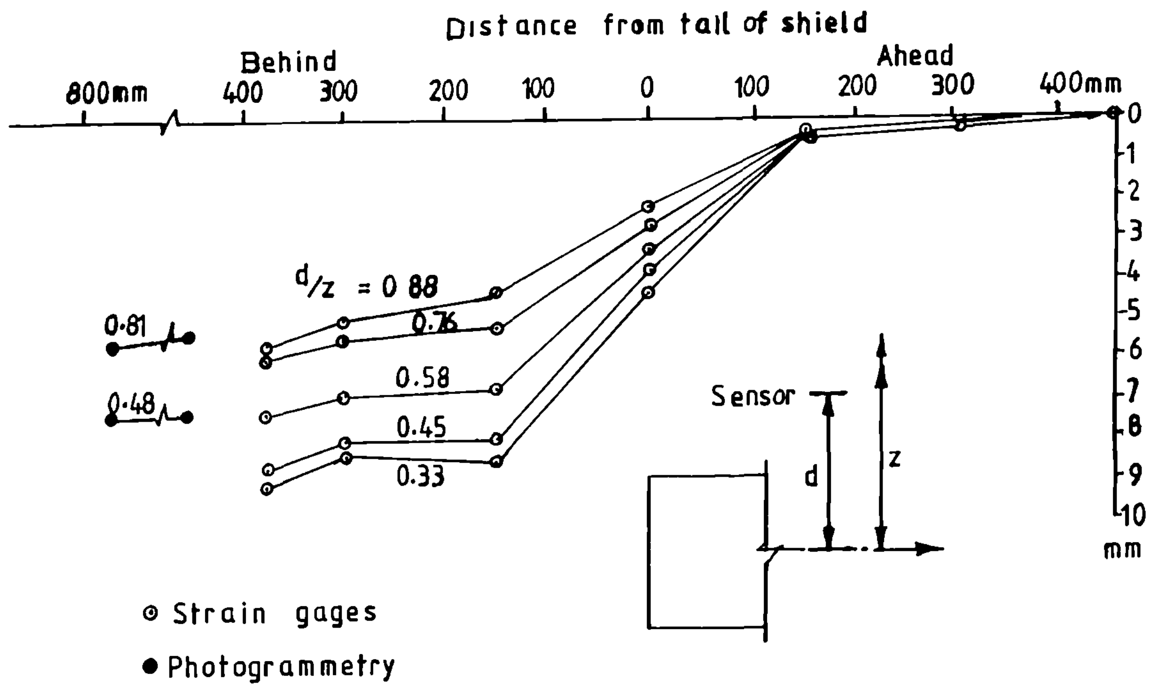

Fig. 2.48 Centreline movements above model tunnels in sand (after Cording et al, 1976)

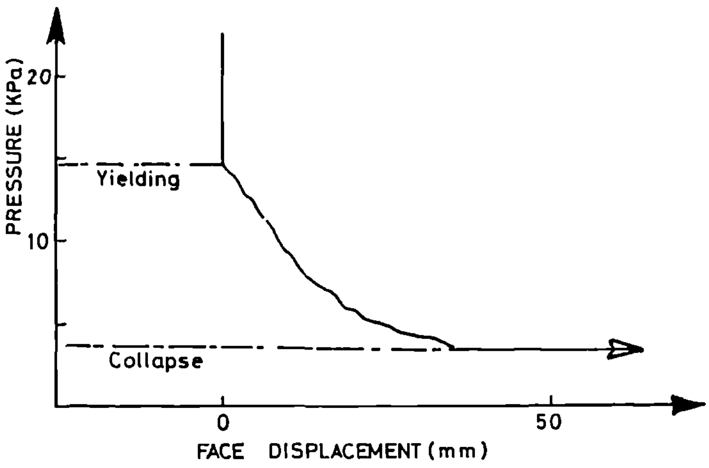

Fig. 2.49 Relationship between face displacement and tunnel pressure for model tests in sand (after Chambon et al, 1991)

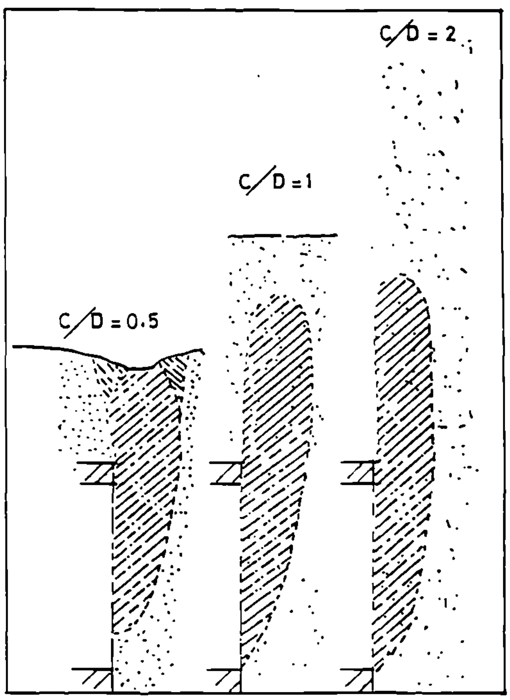

Fig. 2.50 Failure mechanisms at a tunnel face for different C/D ratios in sand (after Chambon et al, 1991)

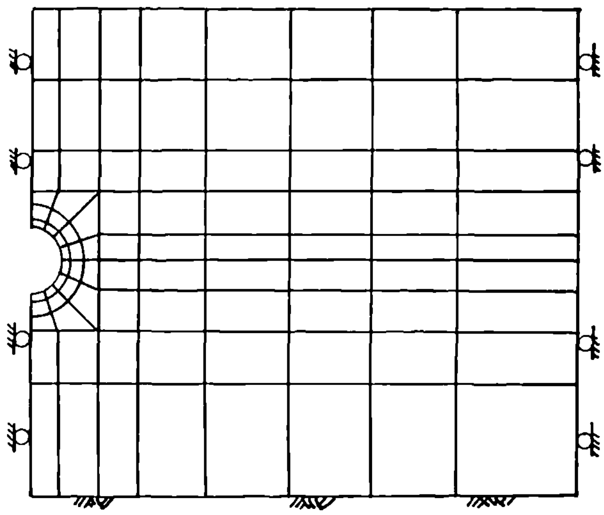

(a) two dimensional

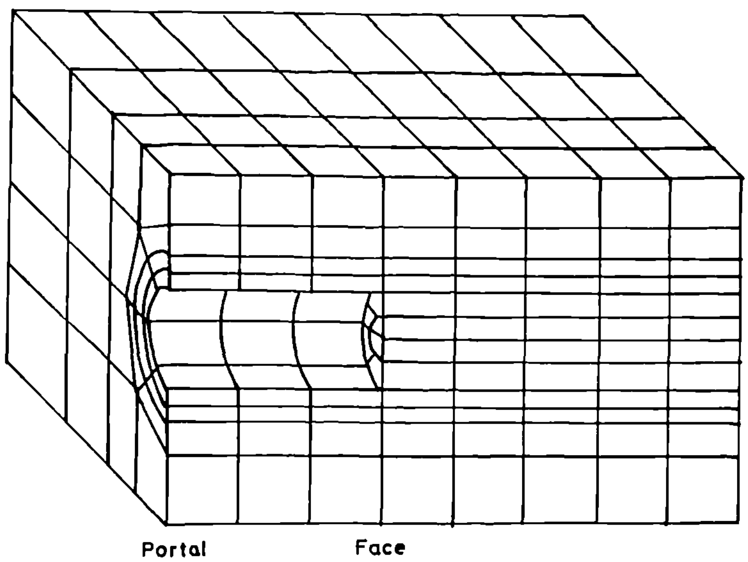

(b) three dimensional

Fig. 2.51 Typical finite element meshes

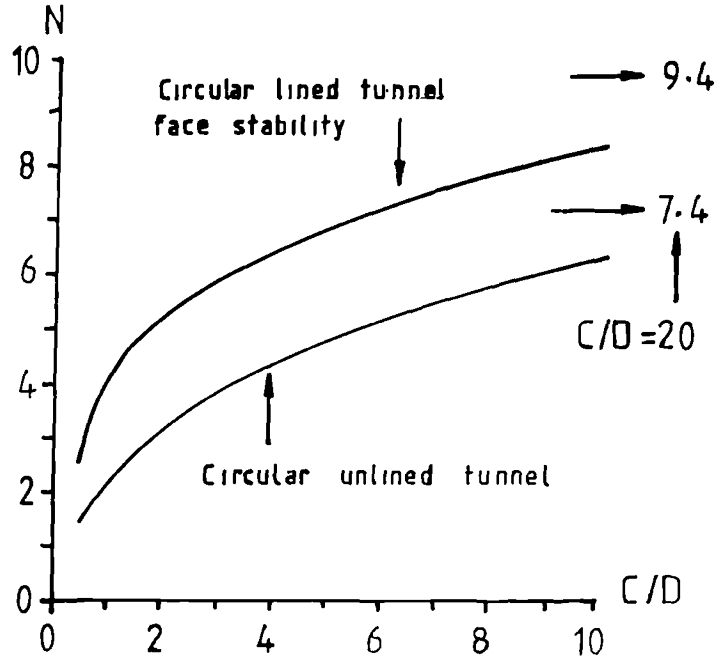

Fig. 2.52 Lower bound solutions for tunnels for C/D ratios against stability number, N (after Davis et al, 1980)

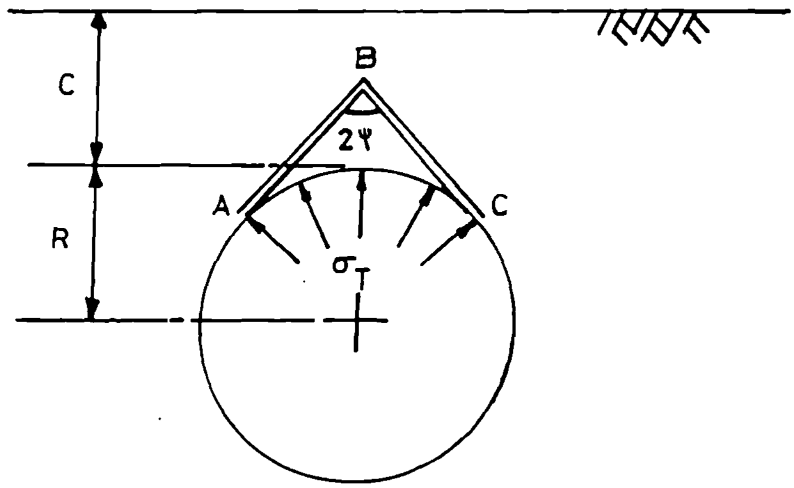

Fig. 2.53 Upper bound collapse mechanism (after Atkinson and Potts, 1977)

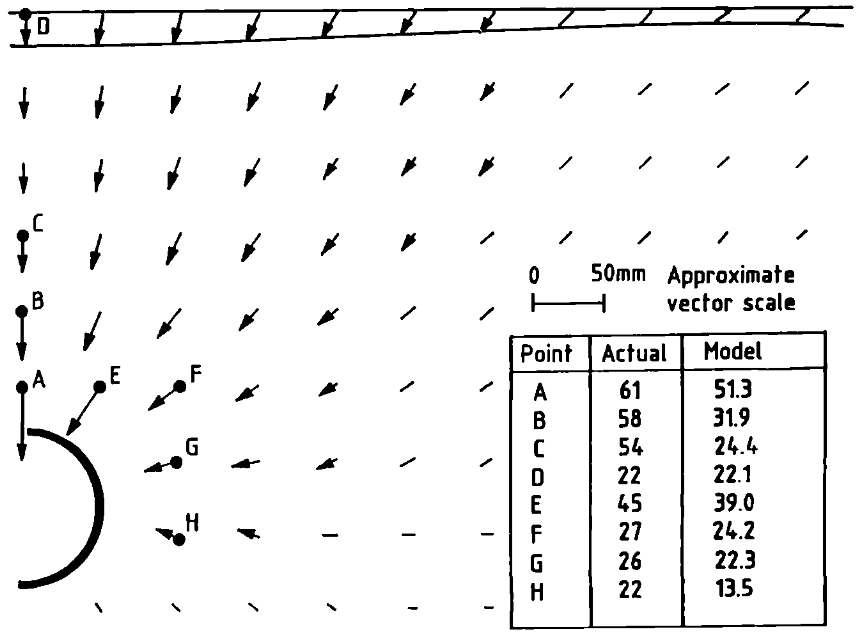

Point	Actual	Model
A	61	51.3
B	58	31.9
C	54	24.4
D	22	22.1
E	45	39.0
F	27	24.2
G	26	22.3
H	22	13.5

Fig. 2.54 Application of Sagaseta's incompressible flow theory analysis to a tunnel at Willington Quay (after Rogers and O'Reilly, 1991)

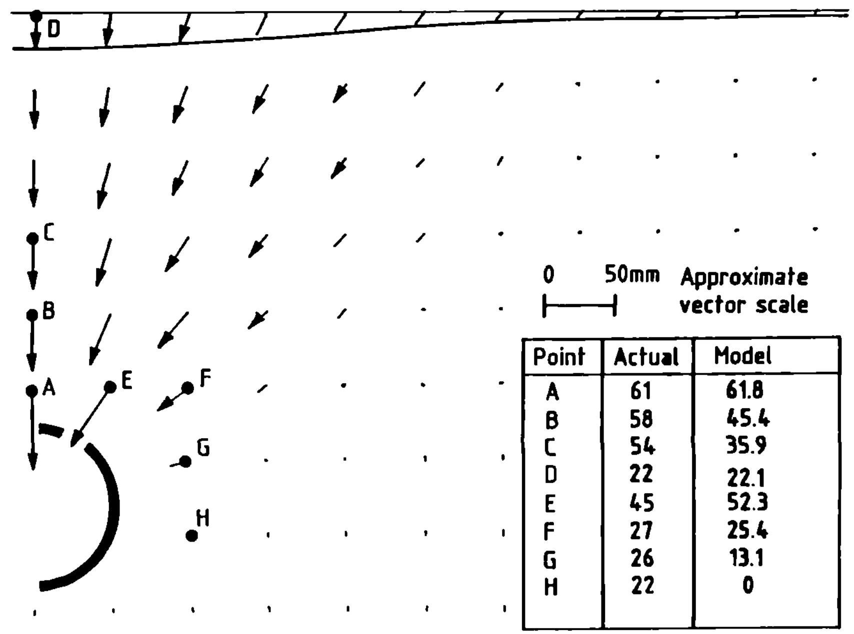

Point	Actual	Model
A	61	61.8
B	58	45.4
C	54	35.9
D	22	22.1
E	45	52.3
F	27	25.4
G	26	13.1
H	22	0

Fig. 2.55 Application of the O'Reilly and New method of ground movements prediction to a tunnel at Willington Quay (after Rogers and O'Reilly, 1991)

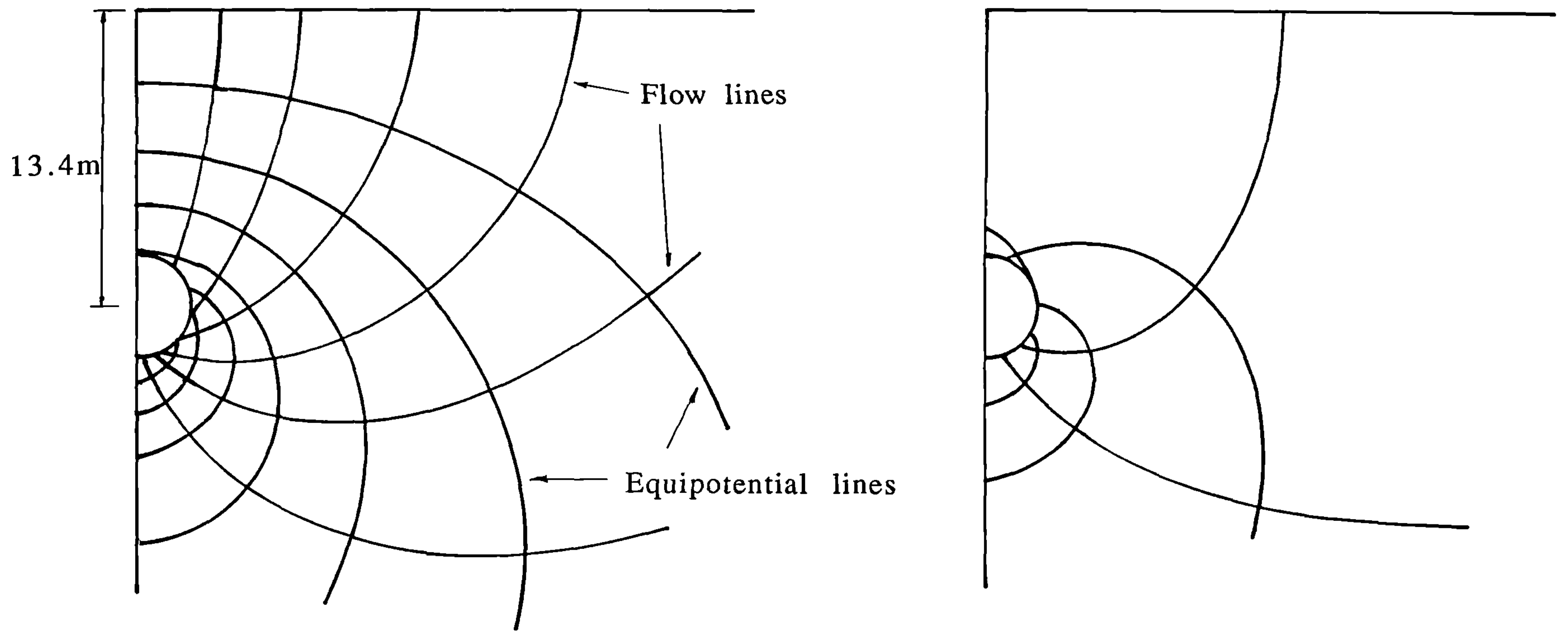

(a) Without compressed air

(b) With compressed air

Fig. 2.56 Flow net construction for prediction of ground movements around a tunnel at Willington Quay (after Howland, 1980)

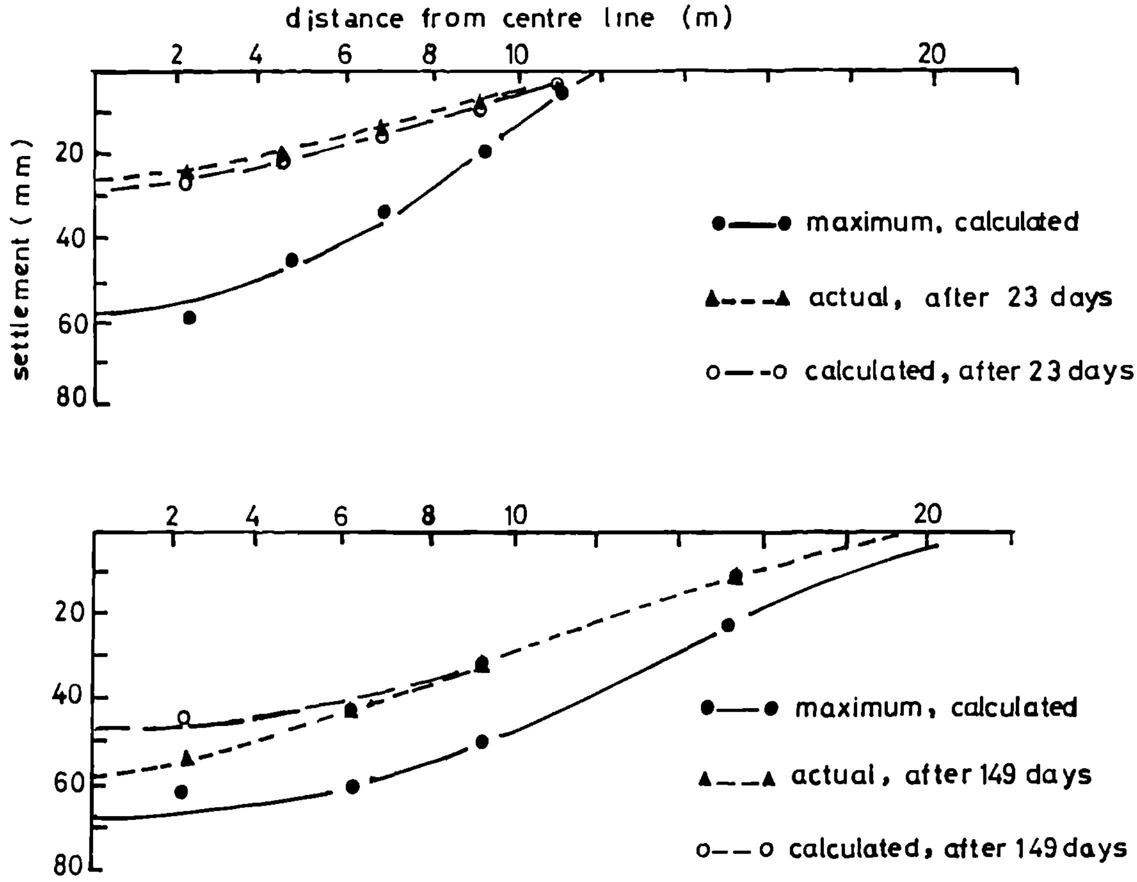

Fig. 2.57 Comparison between the actual and calculated surface settlements by using flow net construction for a tunnel at Willington Quay (after Howland, 1980)

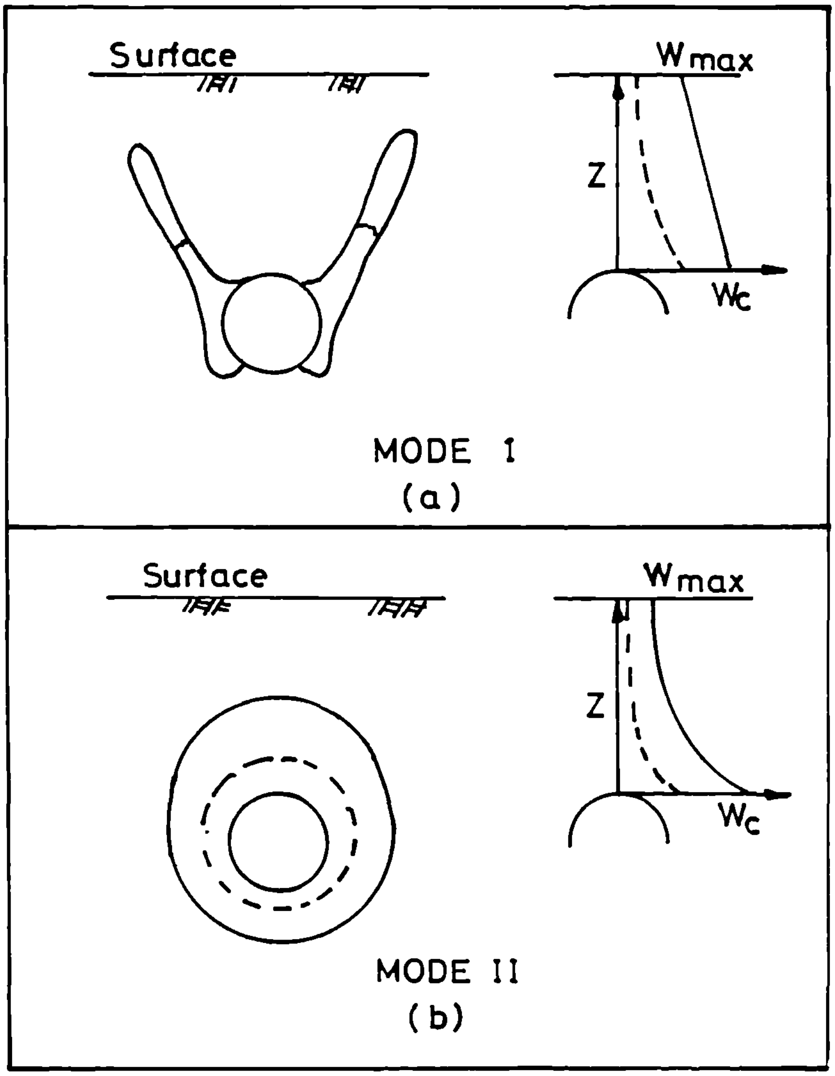

Fig. 2.58 Modes of yielding around a tunnel (after Wong and Kaiser, 1986)

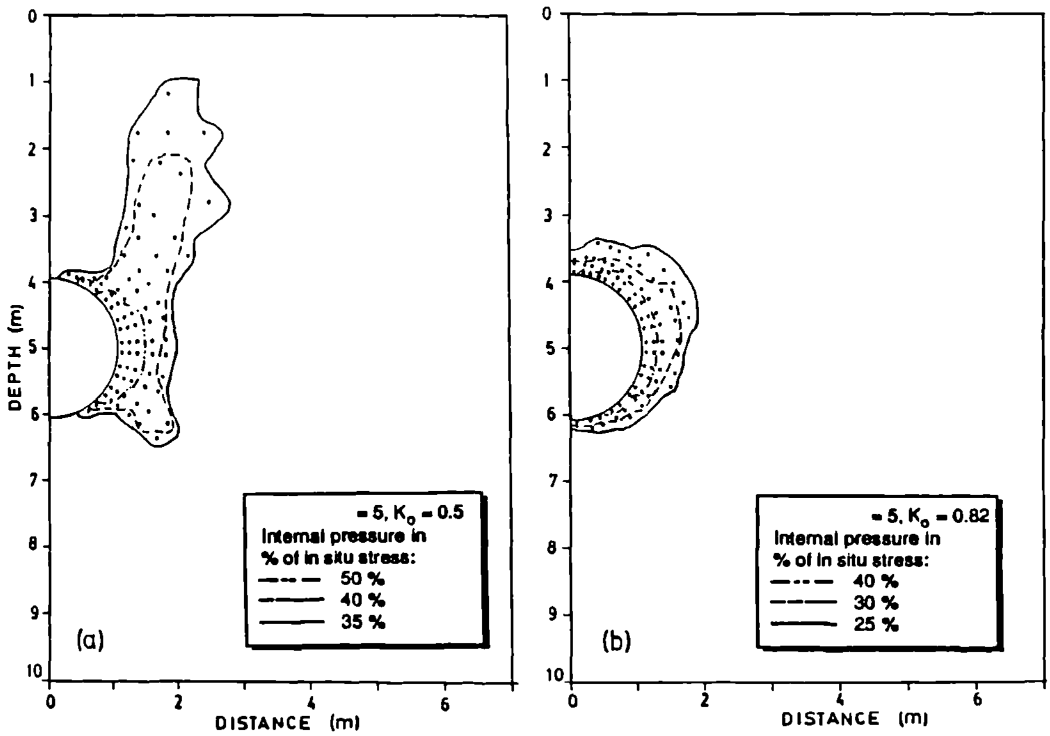

Fig. 2.59 Numerical simulations of tunnel collapse (after Wong and Kaiser, 1986)

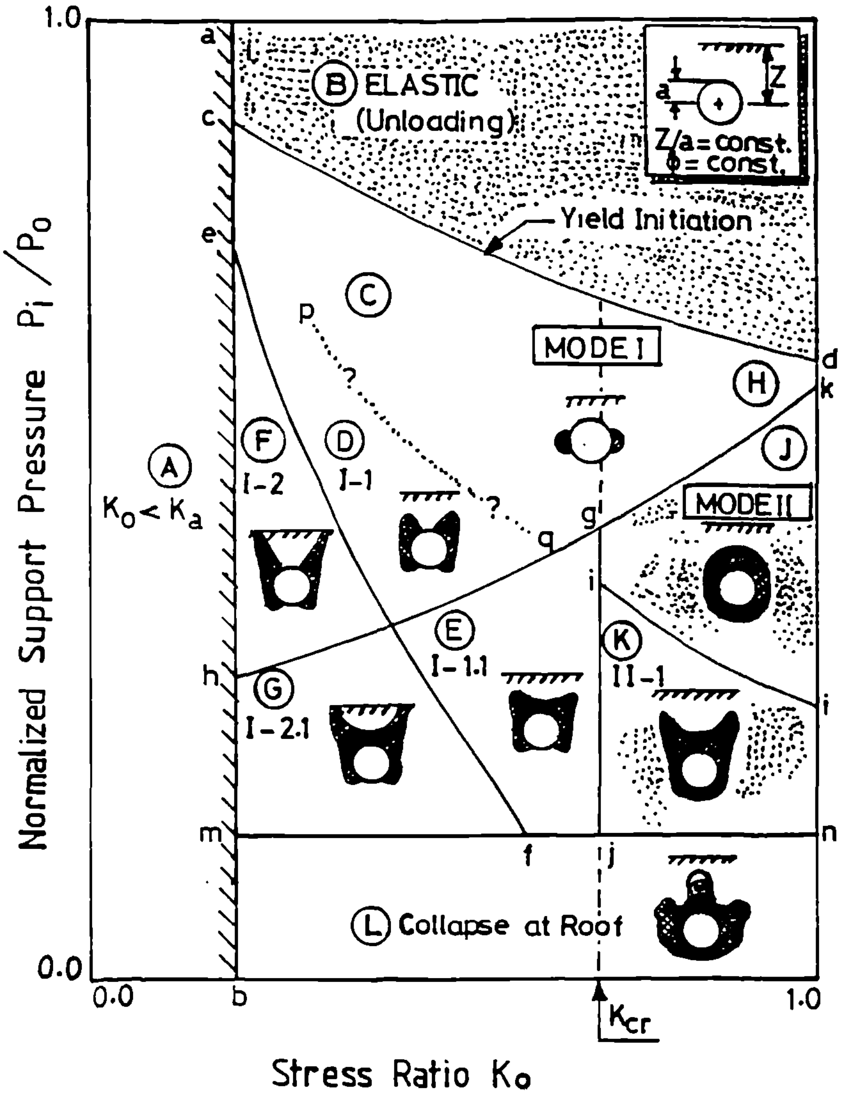

Fig. 2.60 Modes of tunnel behaviour for various P_i/P_o ratios against stress ratios, k_o (after Wong and Kaiser, 1987)

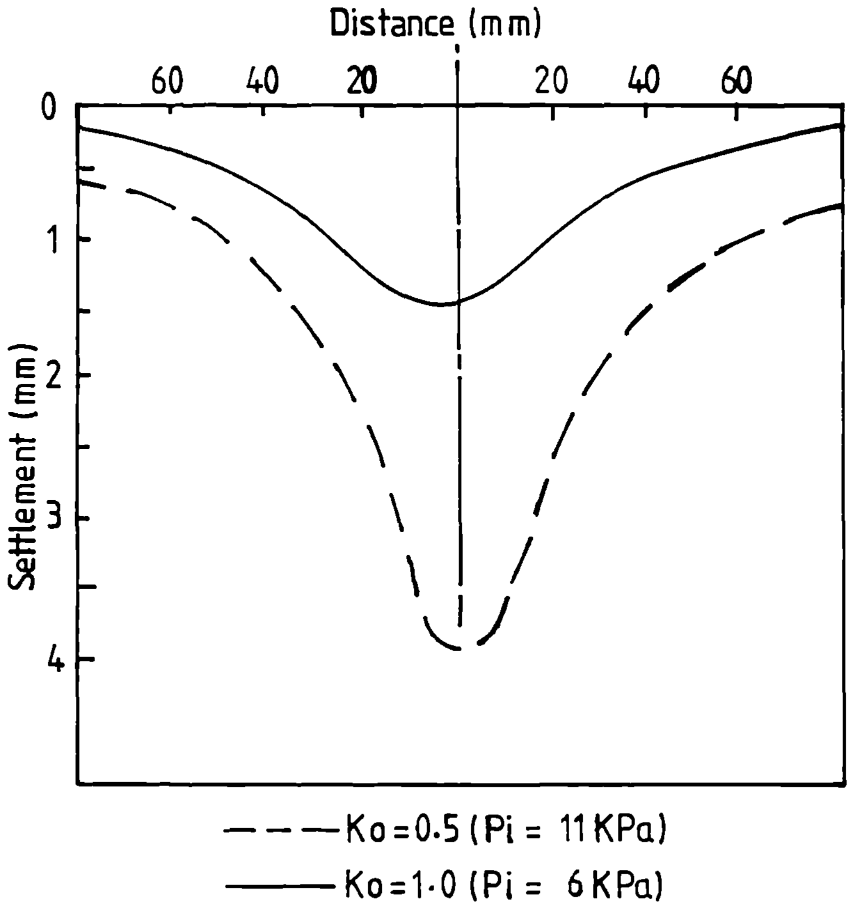

Fig. 2.61 Comparison of surface settlement profiles for different stress ratios, k_o (after Wong and Kaiser, 1991)

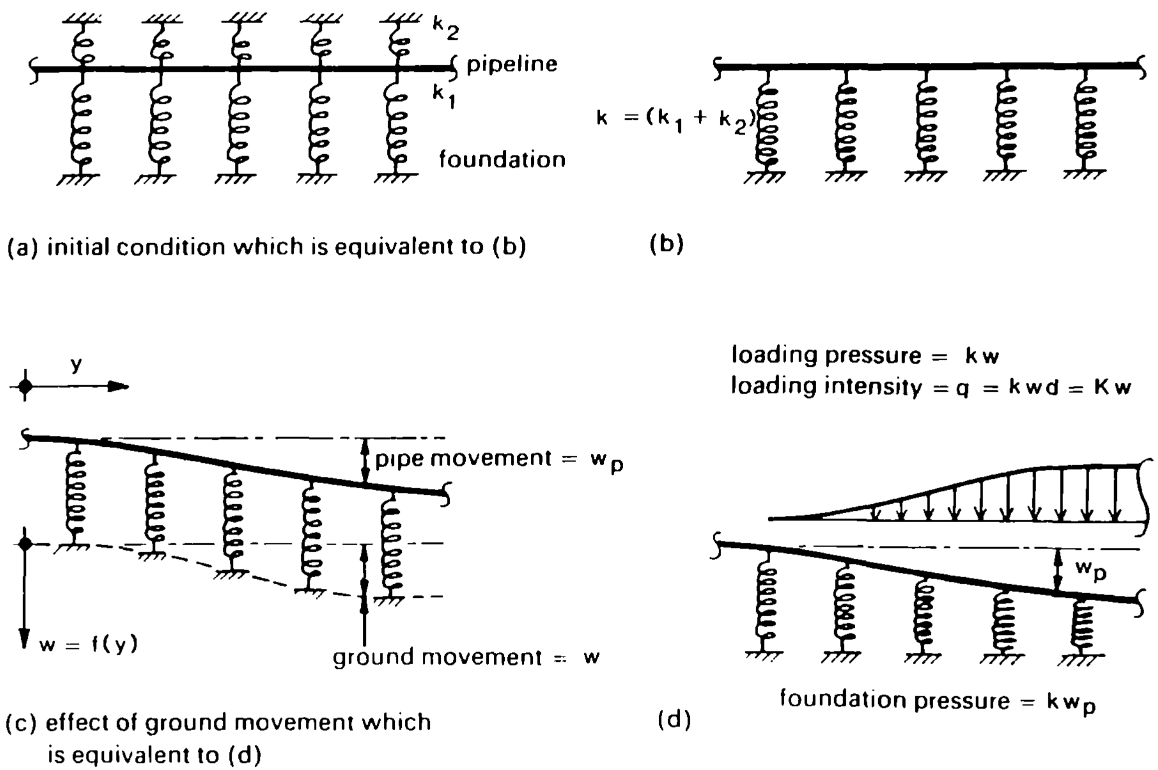

Fig. 2.62 Application of the Winkler spring model analysis to a pipeline (after Attewell et al, 1986)

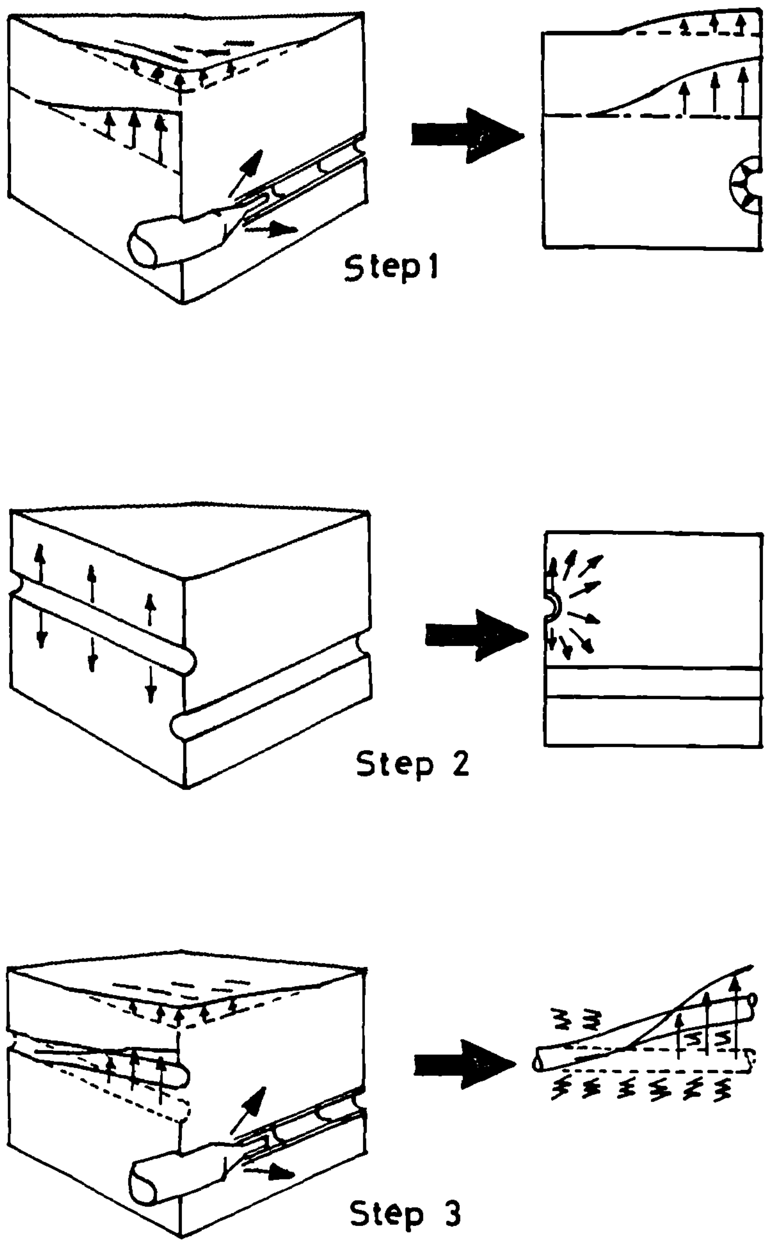

Fig. 2.63 Stress analysis method applied to a pipebursting operation (after Herbert and Leach, 1990)

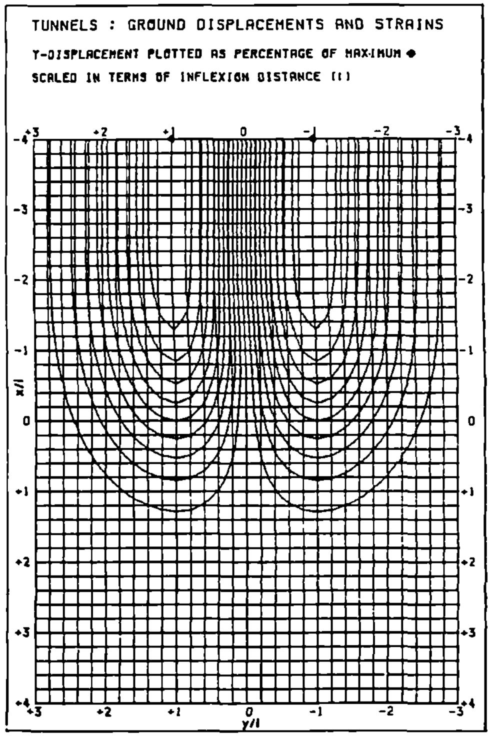

10% incremental ground displacement (v) curves, y-axis.

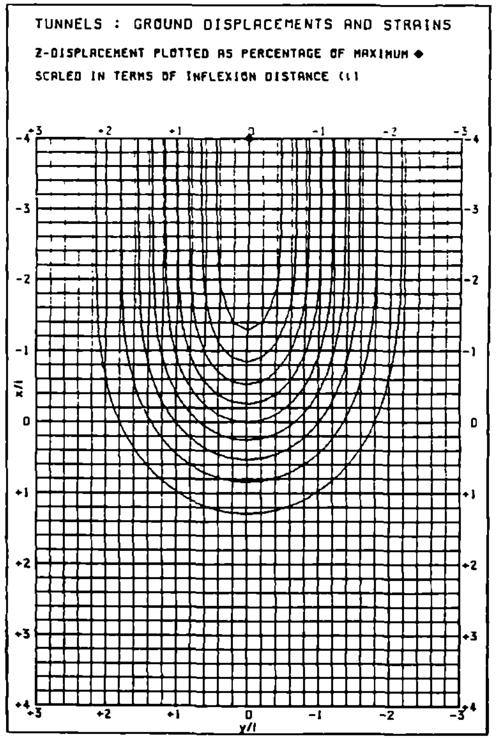

10% incremental ground displacement (w) curves, z-axis.

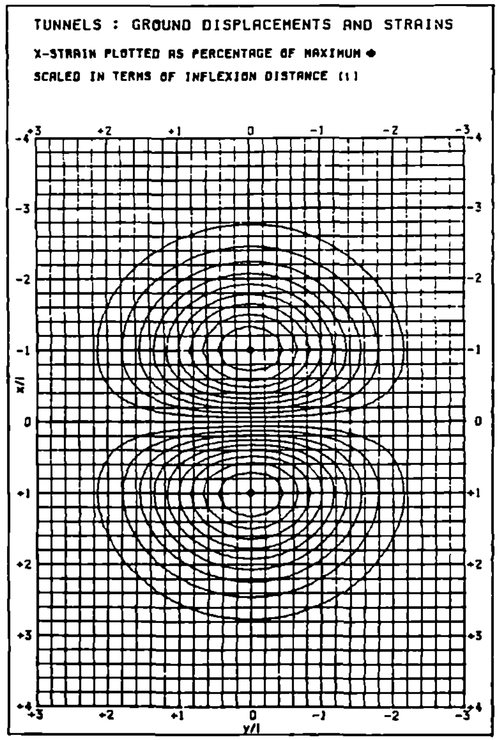

10% incremental ground strain (ε_x) curves, x-axis.

Fig. 2.64 Predicting tunnel induced movements using contour plots (after Attewell et al, 1986)

CHAPTER THREE

3 RESEARCH PHILOSOPHY

3.1 INTRODUCTION

All aspects of research previously conducted into the ground deformations associated with trenchless pipelaying techniques and soft ground tunnelling have been extensively reviewed in Chapter 2. The work is, as a whole, lacking in all areas, with only general results emerging. This might be expected, certainly from the field observations which are very dependent on the site conditions and construction details. Although the work reported on soft ground tunnelling is more comprehensive, care must be taken when applying this to convergent trenchless pipelaying techniques. Some aspects of the two techniques are similar but, as discussed previously, there are differences. Taking this into account, the reported work relevant to trenchless techniques, and particularly convergent trenchless techniques, is very sparse and inadequate in the area of ground movement investigation.

This chapter initially draws on the information within the literature review concerning the different methods available for investigation and discusses the reasons behind the decision to use a laboratory modelling technique. The decision thus takes into account the previous work that has been conducted. The subsequent section lists the basic factors, that have emerged from the literature review, which contribute to the likely ground movements during trenchless pipelaying operations. Section 3.4 discusses the factors highlighted in the previous section, considering the practicalities of investigation and the relative importance of the factors in achieving the overall aims of the project. Section 3.5 outlines the experimental considerations relating to the design of the laboratory equipment in which the simulation of the trenchless techniques are to be conducted. The final section in this chapter shows the philosophy behind the test programme.

3.2 METHODS OF INVESTIGATION

There are several approaches that can be adopted when investigating practical situations and each has its advantages and disadvantages.

Monitoring of full scale field jobs is one method of obtaining information on ground movements. Precise information is required on the initial soil conditions and a large number of insitu ground measuring instruments need to be installed both subsurface and on the surface, in order to obtain the full three-dimensional displacement field. This would, depending on the number of instruments used, lead to reasonably comprehensive data at the monitored sections. It does, however, require the precise conditions to be known at the pipe level (construction details) as the pipe installation operation passes the monitored section in order to interpret the observed movements precisely. The main problem is that control is limited and the data are only obtained for a 'one-off' situation, ie with solely one set of conditions. This is not to say that field monitoring is unimportant, far from it, but in areas such as trenchless pipelaying techniques, where the information available is very limited, a more controlled situation is preferable initially to allow better interpretation of the field data.

An alternative is to reproduce the field conditions in a laboratory test. This would create a more controlled situation in terms of soil properties. Unfortunately, repeating full-scale trenchless pipelaying techniques in the laboratory would be expensive and complicated because of the test facility required (Robins et al, 1991 , carried out a full scale laboratory test for a pipebursting operation, which proved successful but required an exceptionally large test facility). There would also be the problem of the limited number of tests that could be conducted in the time available, and this would still leave the problem of accurately obtaining measurements of the soil deformations that occur.

A further laboratory technique that could be employed involves the testing of models. These are capable of investigating a wide variety of conditions with a high degree of control. Model tests fall into three main categories (Potts, 1976):

a) Model tests of a real structure, the object being to simulate exactly the behaviour of the prototype.

b) Model tests of idealised problems, the object being to investigate the validity of existing theoretical analysis.

c) Model tests of simple idealised problems for which no theoretical solution exists, the object of these tests being to identify mechanisms so that appropriate theoretical investigations may be developed and investigated.

Tests of the first type are usually expensive and complicated, as it is difficult to produce an exact similarity between model and prototype. On the other hand tests of the other types are both cheaper and easier to conduct and can be extremely valuable, particularly when investigating more fundamental aspects of the prototype. However, there are problems, the main one probably being scaling effects which could make the model behave differently from the prototype situation.

The final option involves the use of theoretical techniques for prediction of the ground movements during trenchless operations. However, full scale trial data would be required to validate the model. Finite element analysis would provide the most suitable medium, but, as described earlier, tunnelling type operations are very complicated to simulate accurately using these methods. Three-dimensional analyses would be required for best results. The constitutive soil models available, or requiring development, are also critical to the accuracy of the analysis. Although the development would be slow, if proved accurate when compared with field data, an infinite number of permutations of site conditions could be calculated to produce design charts.

Full scale experiments are the most accurate in terms of reproducing site conditions and allow a high degree of control, however the high cost to develop a suitable facility and low test rate would make it very difficult to execute the very throrough and more fundamental investigation which trenchless pipelaying operations require at this stage (Chapter 2). Moving to the other extreme of small scale modelling, this also presents the problems mentioned above. Although providing a high degree of control and reasonable test rate, scaling problems are particularly important. Great care is therefore required when developing model tests in order to minimise these effects.

For this research project it was decided to use a compromise between the full scale experiments and the small scale modelling. A 200mm diameter pipe was used as the basis for the project which, although in many prototype situations is still classed as modelling, does represent the smaller range for the prototype pipebursting and pipejacking operations. This scale of modelling also minimises scaling effects and, by certain simplifications to the prototype situation, allows a more fundamental approach to the understanding of basic areas, whilst ensuring a fairly realistic simulation. It is important to make any type of modelling a good simulation of the prototype situation, in order to gain appreciation of the interelationship of the factors causing the ground movements. This is true even for the more fundamental type investigations, since if they are too far removed from the field situation practical interpretation of the results becomes very difficult.

3.3 FACTORS INFLUENCING GROUND MOVEMENTS DURING TRENCHLESS PIPELAYING OPERATIONS

The factors that contribute to the likely ground movements caused during trenchless pipelaying operations are outlined below and need to be considered when investigating this subject area. Some general factors are presented initially, followed by other more specific factors for convergent and expansive techniques.

3.3.1 <u>General Factors</u>

3.3.1.1 Soil Type and Density

Soil type affects the extent of any displacements caused by the trenchless pipelaying operation, ie how the diplacements propogate through the soil. In areas of compression, compressible materials will absorb a large proprotion of the movements and conversely stiff materials will transmit movements further. However, the reverse is true in areas of expansion: cohesive materials will cause much greater long-term movements, whereas cohesionless materials will produce a much more immediate response.

3.3.1.2. Water Table

If the water table is above the pipe invert level it will tend to influence the stability of the face in pipejacking operations and therefore affect the soil movements in this area. The effect will be very dependent on the type of soil and its permeability. For pipebursting operations the primary problem arises from water/soil encroachment into the old pipe during breaking out.

3.3.1.3 Pipe Alignment

Pipe sections during the jacking process can rotate at the joints by up to 1 degree, which means that the pipeline is not perfectly straight (Fig. 3.1). This allows material to converge erratically onto the pipe. It may also affect the ground movements as the pipe is jacked forwards.

3.3.1.4 Rate of Installation or Renewal

The excavation at the face during pipejacking operations is required to match the forward progress of the shield and pipe. For pipebursting operations faster rates of progress (both burster and pipe are linked) may lead to less chance of leakage of soil into the old pipe during breaking out. The type of soil will influence the rate of installation for both pipejacking and pipebursting.

3.3.1.5 Long-Term Movements

Consolidation of soils caused by pore pressure dissipation, as the pipe acts as a drain either due to leakage or due to water moving along the pipe soil interface, leads to settlements long after the pipe has been installed. When pipebursting in stiff clays, there is likely to be a considerable period of time before the soil converges onto the new pipe. This movement can reduce the surface heave over the pipeline quite significantly (Robins et al, 1991). It is important to realise this effect. If damage is caused during the pipebursting operation and repairs are carried out too quickly after the event, long-term movements may cause more damage.

3.3.1.6 Draw-Along Effects

As the pipe and shield are jacked forwards, material is carried forwards with the pipe by friction, and also in some cases due to the slightly larger pipe collars or by a limited bearing area caused by gaps at joints. There is also the movement of material due to pipe alignment. These movements are very dependent on the soil type.

3.3.1.7 Cover Depth

Increased depth of soil causes greater stresses at the pipe level and, as a result, will influence the soil deformations that occur. There is also the effect of arching within granular materials, which is greatly influenced by increased stresses (Potts, 1976), which again will affect the deformation.

3.3.2 Convergent Techniques

3.3.2.1 Overcut Ratio (t/R)

The ratio between overcut (t) and pipe radius (R) will influence the ground loss as excavation proceeds, allowing material to converge into the excavated cavity onto the installed pipe behind the shield.

3.3.2.2 Face Support and Excavation Technique

Stability of the face is important as this will influence the ground losses and movements into the shield. An over-pressurised face causes movements away from the shield (DeMoor and Taylor, 1991). The soil type will have a large influence at the face. The support of granular materials is crucial as catastrophic collapse can occur very suddenly.

3.3.2.3 Yawing

Yawing is an operational technique whereby the shield is angled upwards slightly in order to stop it, and the pipeline, diving downwards as installation proceeds (Fig. 3.2). Excavation within the shield therefore causes an oval shaped cavity, which means greater ground loss and larger ground displacements.

3.3.3 Expansive techniques

3.3.3.1 Overburst Ratio (t_b/R_o)

As with the pipejacking overcut ratio, this affects the amount of convergence onto the new pipe. For pipebusting operations there is no ground loss so all the material is pushed away in front of the burster and subsequently tends to converge back onto the pipe. The soil therefore goes through a greater cycle of displacements than for pipejacking operations.

3.3.3.2 Bursting Ratio (D_f/D_o)

The ratio of the old pipe (D_o) to the new pipe (Df) is of obvious importance as this governs the the amount of expansion that takes place during a bursting operation. If a large increase in capacity is required for the new pipeline, i.e. a large bursting ratio, then this may be carried out using a two-stage-expansion burster.

3.3.3.3 Type of Burster

For the expansive type of burster, the soil is simply pushed away as the burster passes, although the angle of movement will depend on the design of the burster. The ramming type of buster induces a high vibration into the soil, causing greater movements in granular materials, and these vibrations can be transmitted to adjacent services and structures.

3.3.3.4 Trench Conditions and Hard Strata

This is particularly relevant to renewal techniques, the influence of the original trench construction tending to concentrate the movements above the bursting operation and thereby causing greater differential movements within the soil. Depending on the age of the trench, some mixing of the surrounding ground and the trench backfill will occur, reducing the effect of the trench with time.

The effect of a relatively hard stratum below the bursting operation can also direct the ground movements, caused by the bursting operation, upwards. This would become a more important influence on the ground movements at greater cover depths, when the influence of the ground surface, in attracting the movements, decreases.

3.4 BOUNDARY CONDITIONS

It is clear from the above, that to reproduce, and try to investigate, all of the relevant factors would be very difficult. It was therefore decided to concentrate on several and investigate these as thoroughly as possible, bearing in mind the laboratory technique to be used. Each of the factors is considered below.

Soil type and density are obviously very important and will greatly influence the ground movements produced. The choice of material is therefore critical. Typical soils found during field trials would constitute one possibility, although a more controlled material would be more advantageous for the controlled models.

However, other factors need to be considered. As the tests were to be conducted in a large tank and a large number of tests were envisaged, the material had to facilitate a quick turn around of the tests and provide consistent and repeatable conditions. Dry sand was the obvious choice for this material. It is relatively easy to move and place, and there are no drainage problems, so the tests can be conducted instantly with the observation of the movements being instantaneous. The particulate nature also enables the stereo-photogrammetry technique to be employed for observing the sand displacements.

The initial sand chosen was a standard Leighton Buzzard sand, whose properties are well defined. The uniform nature and particle size of the sand also meant that the displacements would be easily visible. To act as a comparison and to provide a more 'realistic' well graded material, a second sand was chosen. This was a 25B grade gravel, chosen as it provided the correct particle size range without requiring sieving and was readily available. The use of dry sand automatically makes investigation into the effects of the water table level and long-term movements impracticable. It has been highlighted, in the literature review, that most of the important movements caused by tunnelling, occur as the construction process is taking place, and thus this limitation was considered to be of secondary importance.

Pipe alignment is not as important when considering ground movements as it is when investigating forces during jacking, since the excavated volume is the same whether the pipe sections are straight or not and the maximum ground displacements are the same, although not as uniform for an irregular pipe alignment. Draw-along effects at the pipe/soil interface will be altered and possibly increased, but the effects would be very problematic to simulate and it would be difficult to obtain repeatability between tests.

The effect of the rate of installation can be investigated in any test arrangement by varying the jacking speed and so can the draw-along effects of different pipe materials. However, the draw-along would be difficult to observe clearly and would probably need to be investigated seperately at a much larger scale (Uesugi et al, 1988).

The cover depth ratio is an important factor. For the scale of modelling being used, the only feasible way of simulating increased depths is by the use of a water bag to apply a surface surcharge onto the sand.

For the convergent techniques, it was decided to simulate the most basic principle, that of pipejacking. The overcut ratio is very important in this case and can be simulated by varying the outside diameter of the shield. The simulation of face support and excavation technique accurately in model tests presents an immense difficulty (especially with the semi-circular arrangement subsequently chosen). In any case, these two parameters are very dependent on the site conditions and construction technique, so that any accurate simulation would be of limited value, with repeatability being difficult and becoming far too sophisticated for the investigation required. It was therefore decided to use the simplest case of no face support, and the simplest excavation technique, a careful use of suction. These conditions could easily be repeated for each test. To act as a comparison, a completely closed shield was also used to represent a fully supported face. The effect of yawing of the shield, although important, can be thought of as an approximate increase in the overcut ratio.

For the expansive technique it was decided to investigate expansive pipebursting, as this represented the simplest technique to simulate accurately. There will thus be some similarity to the tests described by Swee and Milligan (1990), but, due to the larger scale and a more practical simulation (the scale permitted the introduction of a pipe to be burst out), there will be slightly different emphasis. To some extent, other types of burster have different effects on the ground movements, but the basic opening up of a cavity, i.e. causing expansion, is the same whether this is by inducing vibration to split the old pipe or by some other method. Simulating the basic, static expansive burster is therefore the best initial approach.

The overburst ratio can be simulated by varying the difference in diameter between the burster and the installed pipe. The bursting ratio is similarly investigated, but by varying the size of the old pipe being broken out. Investigating the effect of the trench conditions imposes many complications and difficulties into the test procedure. Also the wide range of conditions that would be required to be investigated and the ageing effects of the trench would make it very difficult to simulate adequately. Also for this initial investigation a uniform medium is required in order to establish a general picture of the ground movements produced by pipebursting operations. This similarly applies to investigating the effects of hard strata below the bursting operation; this is a rather too specific condition for the general investigation required. The effect of hard underlying strata could be considered as similar to providing a shallower cover depth, in terms of the soil being directed upwards.

3.5 EXPERIMENTAL CONSIDERATIONS

Before the design of the equipment could begin, the method of determining the ground movements during the tests needed to be finalised as this would largely influence the general equipment arrangement.

There were two options available for the equipment design. The first option was to simulate the trenchless techniques using a whole pipe being jacked through the centre of a tank, which would have been similar to a previous pipejacking research programme investigating jacking forces. This would require remote measurement of the subsurface soil movements. Several methods were considered for achieving this. One involved an X-ray technique using lead ball bearings layered within the soil mass. However, this technique suffers from several drawbacks. The equipment is expensive and, because of the dangers associated with the use of X-rays, considerable safety precautions are required. There is also the problem of the ball bearings within the soil mass affecting the uniformity of the soil and influencing the observed movements. Another method involved the use of miniature extensometer rods within the soil mass. Again these would interfere with the uniformity of the soil mass and they can only provide localised measurements, insufficient for the detailed movements required.

The second option was to split the trenchless techniques along the pipe centreline. This would require the equipment to be designed to use a semi-circular pipe section being jacked along up against a glass viewing panel. One advantage of this approach is that it allows direct observation of the displacement field longitudinally, and by also using glass end panels on the tank, displacements could also be observed in the perpendicular plane. This would mean that a stereo-photogrammetry technique could be used to determine the soil displacements externally to the tank, avoiding affecting the soil uniformity. There is one disadvantage of using this approach, and that is the friction between the soil and the glass. However, this has been shown by other researchers (Cording et al, 1976) to be small at the stress levels being considered (see Chapter 4, Section 4.3)

After careful consideration of all the facts, it was decided that option two would provide the best equipment to meet the required objectives.

Once the approach for the equipment arrangement had been chosen, the size of the tank had to be decided upon. The size of the tank was based on several considerations. One was the decision to use a 200mm pipe section and another was the likely extents of any soil displacements caused during the tests. From the results of previous researchers (Potts, 1976, Cording et al, 1976 and Swee and Milligan, 1990), the likely spread of movements could be estimated in the perpendicular plane. By taking a 1m depth of soil above the pipe as a reasonable value, the maximum spread of any movements would not exceed 45^o, i.e. a 1m lateral surface extent. Allowing 0.5m below the pipe axis as a sensible value to avoid any boundary effects from the base of the tank, a total height of 1.5m and a width of 1.0m was chosen. The length of the tank was based on the requirement of a reasonable amount of pipe entering the tank; 1.5m was thought adequate. The length was also based on the possible extents of the movements in the longitudinal plane, an idea being gained from the results of Swee and Milligan (1990). The chosen length was thought to give the upper bound to the likely movements. The final internal tank size was therefore chosen to be 1.5m high x 1.5m long x 1.0m wide.

The remaining equipment arrangement was dictated by the requirement of jacking a semi-circular pipe into the tank from one end, up against one of the longer faces. Chapter 4 describes the development process for this equipment in more detail.

3.6 PHILOSOPHY BEHIND THE TEST PROGRAMME

The results from the laboratory tests are to be related to field conditions and prototype trenchless pipelaying techniques. Therefore the aim was to include as much realism as possible in the laboratory tests, bearing in mind the modelling difficulties and the requirements of a more fundamental understanding of the ground movements involved.

The equipment proposed for the tests was to be wholly new and therefore required a large amount of development. Also, there was a degree of uncertainty about how it would perform and whether certain aspects of the design would need altering. This would mean that it may not be possible to investigate certain factors of the simulation of the trenchless pipelaying operations. As a result, the test programme drawn-up was based largely on the performance and nature of many initial trial runs during the development stage. The experimental work was however, designed to provide as much information as possible about the behaviour of the ground around trenchless pipelaying operations, bearing in mind that the development of the equipment was a major part of the project and would provide a plane strain test facility for this project and future research.

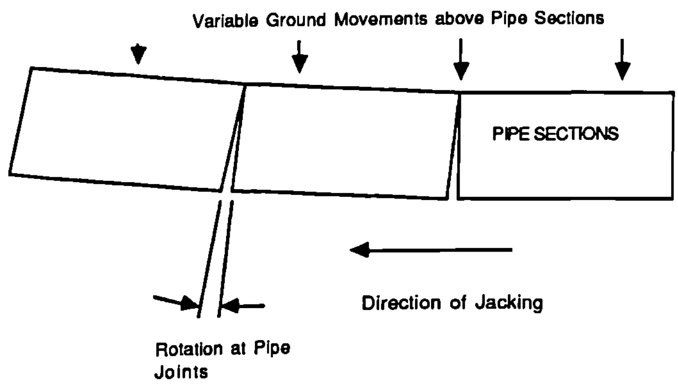

Fig. 3.1 Rotation at pipe section joints

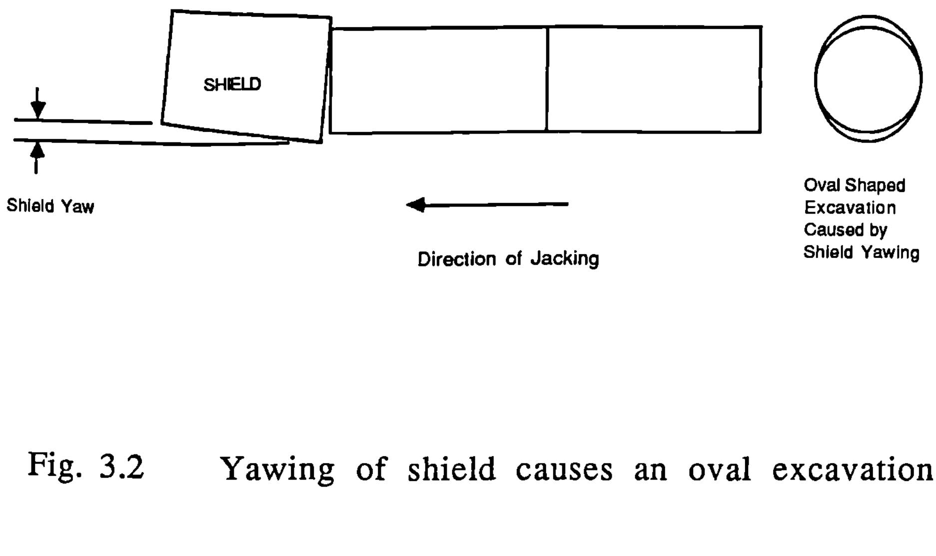

Fig. 3.2 Yawing of shield causes an oval excavation

CHAPTER FOUR

4 EXPERIMENTAL INVESTIGATION OF GROUND MOVEMENTS ASSOCIATED WITH TRENCHLESS PIPELAYING TECHNIQUES

4.1 INTRODUCTION

Many of the factors considered in the design of the experimental equipment have been discussed in Chapter 3. This chapter gives an explanation of the equipment and data acquisition, and their use.' Brief details have been given elsewhere (Chapman and Rogers, 1991). These details will be enlarged upon and the reasons behind the design decisions and the development of the experimental techniques will be described. The apparatus was designed to enable pipejacking and pipebursting operations to be simulated in the laboratory under controlled conditions. It allows the total displacement field associated with these operations to be observed. The sands used in the tests are classified and the methods for obtaining desired densities for the tests are described. The test procedure is outlined for both the pipejacking and pipebursting tests. Test programmes are presented for each test series (pipejacking and pipebursting). These were based on trial tests to investigate the performance of the equipment and test procedure, which were conducted in order to understand the limitations and turn-around timings for the tests. Thus the test programmes presented in this thesis are given with hindsight. There was a need for the test programme to be highly efficient, since the requirement of researching, designing, constructing and testing the equipment took a considerable period of time. The data acquisition technique of stereo-photogrammetry is described, together with how it is applied to these tests. The accuracy of the technique is assessed based on past research work and data collected from the tests described in this thesis.

4.2 LABORATORY APPARATUS

4.2.1 The Test Tank

The most important development for this largely experimental project was a suitable test facility in which to carry out the work. Plate 4.1 shows the general arrangement of the laboratory equipment and Fig. 4.1 illustrates the construction of the tank. The tank consists of a frame constructed of rolled hollow (RH) steel sections and infilled with sheet steel on two sides and glass on two sides. The internal dimensions of the tank are 1.5m long, 1.5m high and 1.0m wide. The design of the tank was based on a design pressure of 200kPa (approximately 12.5m of soil, creating a vertical stress with a K_o value of unity) inside the tank, which, although high for this project, would allow flexibility in any future work. In fact, it turned out that it was the limitation of the pipe strength that prevented any higher surcharge pressures than 50kPa being used for the experimental work.

The size of the glass viewing panels was a major factor affecting the design of the steelwork. A 500mm x 500mm panel was considered to be adequate to view areas of the sand around the pipe. With this size of panel 30mm thick glass was required, using a factor of safety of 2 on assumed applied stress. Once this panel size had been established, the steelwork was designed based on deflection rather than load capacity. The design was based on two continuous steel rings constructed of 120 x 80 RH section, one around the base and one around the top of the tank. The rings provided the strength to prevent any outward bursting effects due to the pressure in the tank. These two structural rings were tied together vertically using 120 x 80 RH section members. The vertical members were designed to reduce the deflection of the glass to within acceptable limits. Limiting the deflection was important to ensure low stresses in the glass and also for the requirement of plane strain conditions within the tank, which has to be assumed when analysing the results. Smaller 100 x 60 RH sections were used for the horizontal members to tie the vertical members together. These provided hoop strength within the height of the tank and also, more importantly, provided support for the glass. The glass was bonded directly onto the steel work using an approved adhesive compound. Consideration was given to other types of construction, including designs where the glass is brought vertical after application of the load using adjustable supports. However, this type of design is more complicated and with the chosen thickness of the glass and adequate steelwork, the deflections for the adopted design would be small. Measurements during proof testing of the tank showed that the maximum deflection under the full design load was approximately 0.25mm.

Due to the limiting size of the viewing panels caused by the glass design, more horizontal steel supporting members were required than actually desirable. In order to reduce this viewing obstruction at lower tank pressures, they were made removable on the two glass sides, i.e. they were bolted into position rather than welded and special rubber padding was used at the glass/steel interface.

4.2.2 Tank Lid and Water Bag

In order to simulate various cover depths to the pipe, a water bag arrangement was devised. This means that by varying the pressure of water in the bag, a different uniform vertical surcharge can be applied to the surface of the sand in the tank. The general arrangement for the water bag and lid is shown in Plates 4.2 a and b. The rubber is secured in place by sandwiching it between a 50mm wide steel strip along its edges and the main steel plate of the lid. The steel strip is bolted tightly onto the rubber and provides a watertight seal. The lid was designed to minimize deflection due to the pressure. This was achieved by providing steel RH sections welded horizontally across the steel plate of the lid. The lid is bolted to the top of the tank around its edge using sixteen, 15mm diameter steel bolts. The pressure gauge and valve system allow control of the pressure in the bag which can be maintained at a constant value throughout each test.

Although surcharging the surface of the sand in the tank is only an approximate method of simulating depth, as it does not reproduce exactly the stresses within the sand, it was the only feasible way for these experiments. Also, the relatively shallow

depths simulated in these tests, 4.0m maximum, means that the simulation of depth is not so inaccurate.
One of the problems with the water bag simulation of depth occurs when trying to model situations causing heave at the surface, which are expected to occur during the pipebursting tests. The rubber membrane of the water bag would try to restrict the movements and cause a reinforcing effect at the soil surface in the tank. This would be unlike the restraint offered if there was an equivalent depth of soil above this level

4.2.3 Guides and Guide Rails

The guide rails are positioned externally to the tank and are designed to hold the pipe sections securely, but to allow horizontal movement during the jacking process (Plate 4.3).

The guide rails are fully adjustable and so can cater for various sizes of pipe and any irregularities in the pipe. Plate 4.4 shows the adopted guide system. This system simply holds the pipe along its length and is a simplified design of the original method used to restrict the pipes (described in Section 4.2.6), which held the pipe edges away from the guides to prevent damage to the plastic edging strip along the pipes. This was found to be unnecessary as the plastic was tough enough to cope with the applied frictional forces. This simplified design for the guide rails proved to be far more accurate than the original design. A major problem encountered with the guide system, was the accuracy required when positioning it outside the tank. The tolerance on the pipe moving along the glass inside the tank was fractions of a millimetre, whereas the realistic tolerance on positioning of the guides outside the tank was of the order of millimetres. This problem was very difficult to overcome, and yet had to be solved to prevent the pipe section from moving away from the glass. The problem was partly solved by angling the guides very slightly, to direct the pipe onto the glass, rather than positioning the pipe to run exactly parallel to it. This caused higher forces in the pipe sections, but helped to keep them tight against the glass. The rest of the solution to the problem involved time-consuming setting and resetting the position of the guide rails holding the pipe. This eventually led to a satisfactory result.

4.2.4 Jacking Station

This part of the equipment provides the horizontal thrust to the pipe to move it through the sand (Plate 4.5). The jacking station consists of a 30 tonne capacity hydraulic jack fixed to a steel frame. The jack has a stroke of approximately 100mm and is driven by an electric compressor unit. The two smaller hand operated jacks above and below the main jack are provided to draw the main jack back at the end of each stroke. Hinges on one side of the jacking frame allow the whole jacking unit to swing out of position, allowing easier insertion of new pipe sections and spacers in the guide rails.

4.2.5 Seals to Inlet Hole in Tank

The hole through which the pipe enters the tank has to be sealed to avoid any sand leakage. The seal consists of a piece of rubber sandwiched between a steel plate and the glass. The plate and rubber are removable to allow renewal of the rubber, which becomes worn due to the abrasive nature of the sand.

For the pipebursting tests the expanding size of the front burster had to be allowed for in the seal. This was accomplished very simply using a thinner piece of rubber which stretched as the burster passed. No leakage at all occurred during any of the tests using this technique. Sand movements within the tank were not affected by the forward movement of the external rubber seal as the burster entered the tank. This was because the rubber, even at the full expansion of the burster, did not move a greater distance than the glass thickness (Fig. 4.7).

4.2.6 Semi-Circular Jacking Pipe

The pipe sections used are manufactured from a drawn mild steel tube (203mm O.D. and 9.5mm wall thickness). This was the second type of pipe used as the first tube section (hot rolled mild steel tube 193mm O.D. and 4.5mm wall thickness) was found to be too weak, and buckled under the applied loads. Plate 4.6 shows some of the pipe sections. (A black PVC edging strip was used along the full length of each pipe section.)

With a circular tube there is an inherent strength in the shape. However problems occur when a circular section is cut in half. It becomes very susceptible to 'squashing' and twisting. These problems manifested themselves in the first pipe sections during the trial pipejacks and, in order to overcome these problems for the second pipe sections, it was decided to use steel plate and form a closed "D" section. This would help prevent the squashing and possibly the twisting. The steel plates are bolted to blocks along the sections and can be removed to provide access to the pipe section joints. In addition these plates allow more control of the sand as it is excavated from the face and removed by vacuum cleaner. The pipe sections are 500mm long and have a PVC edging strip along the length of each side. This helps to prevent scratching of the glass, and also provides a smoother finish to eliminate sand leakage and to reduce friction during jacking.

4.2.7 Pipe Section Joints

The joints between the pipe sections needed careful design, as these were areas of weakness and therefore created possible problems. The main criterion for the joints were that they needed to make accurate alignment of the pipe sections within the guide rails simple and to minimize disruption to the jacking procedure. They also needed to be strong enough to resist the large bending and twisting forces acting on the pipe, as it is jacked forwards into the tank. The initial designs proved in testing to be either too weak or inadequate to alignment of the pipe sections accurately enough. The joint system finally adopted for the second pipe sections uses three accurately milled blocks fixed to the inside of both the pipe sections, which when bolted together brings them exactly into line every time (Plate 4.7).

4.2.8 Pipejacking Shield Design

The shield is placed at the front of the lead pipe and is designed to provide a cutting edge and steering capabilities for the pipejacking work. A typical prototype pipejacking shield is shown in Plate 4.8. The design for one of the open face pipejacking shields, with an overcut ratio of 0.1, is shown in Fig. 4.2. A similar design was used for the shield having an overcut ratio of 0.2. The shield design is based on the prototype design, although somewhat simplified. The shields used in the laboratory tests are shown in Plate 4.9. They have a cutting edge angled at 35^{o}, which is approximately the natural angle of repose of the Leighton Buzzard sand used in the tests. The overcut dimensions for these shields are large when scaled up: for example, for a 1m diameter prototype shield, a 20 mm overcut on the model represents 100mm of overcut on the prototype. (In reality a 1m diameter prototype shield would typically overcut by 20mm, or possibly 10mm.) The large overcuts on the model were necessary in order to produce movements that could be measured easily. The general patterns of movements and the distributions observed in the model, however, are likely to be similar to the prototype situation, within the ranges of the overcut commonly used. The magnitudes and the extents of the movements can be scaled down to represent smaller overcut ratios.

The original design for the model shields did not include the flat steel plate. However, a problem with this design soon became apparent during the first trial tests. Figs. 4.3a and b illustrate the problem. As the pipe was jacked forwards the sand entering the shield was compressed, the shield diameter being larger than the pipe diameter. This generated a force on the inside of the shield and against the glass. As the shield/pipe is not fixed to the glass, it was pushed away by the forces. In order to remove these resultant forces on the inside of the shield, a steel plate was added to the shield to form a closed "D" shape. This removes the forces on the glass and contains them within the shield, thereby removing any resultant force on the shield. However, this additional plate must influence the forward motion of the sand in front of the shield, but the plate was made as thin as possible and, due to a shallow cutting edge on this plate, the effects will be small. The effect is however, unavoidable.

4.2.9 Pipebursting Head Design

The pipebursting head consists of an accurately milled half steel cone, the design of which is shown is shown in Fig. 4.4. This was used to simulate the expansion type bursters. A typical prototype pipebursting head is shown in Plate 4.10. The constructed pipebursting head used in the laboratory tests is shown in Plate 4.11. The burster has an angle of attack to the horizontal of 12^{o}. This angle was chosen based on several considerations. Perhaps of most importance is that this angle is typical of prototype bursters. In addition it allowed the plaster pipe, used as the pipe being replaced in the bursting tests, to be broken out effectively, by pushing the plaster pipe outwards rather than causing it to crush, to which it is susceptible. The bursting head is 500mm long with a maximum diameter of 210mm, i.e. 10mm larger than the steel pipe being installed. This allows a small overburst to represent the over-expansion carried out during prototype bursting operations to reduce the friction on the installed pipe. The model burster is attached to the same steel pipe used in the pipejacking tests and this pipe therefore acts as the installed pipe. In order to simulate the renewal process, a plaster pipe is fixed to the glass inside the tank and is broken out as the burster is jacked forwards. This is explained in greater detail in Section 4.2.11.

The model burster is the simplest design possible that adequately represents the prototype situation. More complex versions were envisaged, including an expanding burster and a vibration type burster, but these would have been very complicated to model accurately and would probably have only yielded limited additional results.

4.2.10 Filling and Emptying the Test Tank

The procedure for filling and emptying the test tank involved the use of a Floveyor auger to convey the sand from the skip into the tank and vice-versa. Plate 4.12 shows the general set up of the auger during the tank filling. The auger uses a rotating steel wire to which are attached plastic discs. As these rotate they cause an air draught which carries the sand particles upwards. The technique means that there is minimal contact of the sand with any moving parts, which could crush the sand particles. Even so, some dust was inevitably generated and this was sucked out of a polythene tent arrangement placed over the tank. The auger technique used did allow the large quantity of sand, required to fill the tank, to be moved relatively quickly. This enabled a more efficient test programme. The methods of obtaining different densities using this equipment are described in Section 4.6.

4.2.11 Plaster Pipe Manufacture

Plaster pipe sections were required for the pipebursting tests to act as the old pipe and were sacrificial during the tests. The pipe sections were 500mm long and manufactured using a Kafir-D plaster mix. To manufacture the pipes, two different sized moulds were developed, giving plaster pipes having external diameters of 169mm and 125mm. This allowed investigation of two D_f/D_o ratios, of 1.2 and 1.7, in the tests. The moulds are shown in Plate 4.13. The plaster mix was poured into the semi-circular section of the mould, the inside surface of which had been previously coated with olive oil to stop the plaster sticking to the mould. The cylindrical section was then pushed down into the mould to spread the plaster. The whole mould was then vibrated to remove any air bubbles. The Kafir-D plaster was used as it has a setting time of only a few minutes. To remove the set plaster pipe section from the mould, the end plates to the mould were removed and compressed air blown between the interface of the plaster and the mould. The plaster pipe section was lifted up by this pressure and could be removed. Excellent plaster pipe sections were produced. The wall thicknesses of the plaster pipe is 6mm, which was found to be strong enough to support the weight of the sand once positioned in the test tank, but weak enough to be broken out during the test. The Kafir-D actually performed very well during the tests. It did not crumble, but broke into larger fragments in a similar fashion to cast iron pipes during pipebursting operations.

4.3 MEASUREMENT OF SAND DISPLACEMENTS

As mentioned in Section 3.2, the choice of equipment arrangement was made with consideration to the technique for soil displacement measurement. The technique used is called stereo-photogrammetry and is described in detail by Butterfield et al (1970). The technique is also described in detail by Wong and Vonderohe (1978), with reference to the model tests reported by Cording et al (1976). These researchers estimated the overall accuracy of their technique to be ± 0.15mm (approximately 1%) for the measurement of the sand displacements. The technique involves taking photographs from the same camera position, one prior to the movements and one after the movements have occurred. Once these photographs have been developed, the movements can be observed by viewing them in stereoscopic projection using a stereo-viewer. The particle movements appear as a three-dimensional image. The image shows peaks and troughs across the surface of the photographs and these correspond to different directions of movements in one plane, either horizontal or vertical. The heights or depths of these surface irregularities are a measure of the magnitude of the movements. Different orientations of the photographs provides information on movements in different planes.

The stereo-viewer gives a good indication of the different areas of movement and in which direction these are occurring. It is also useful for observing the boundaries of different areas of movement and the variations in magnitude. Definition of the actual magnitudes of the movements is, however, not very accurate using the available instrument. Consideration was given to digitizing individual sand grains from successive photographs to obtain their movements. However, there were problems with this method, such as lack of suitable software, the length of time to develop a working system, the small size of the photographs and thus, the small size of the movements to be measured. Therefore this idea was not used. The only alternative was to carry-out the sand movement measurements by hand, using dividers and a scale. The photographs were magnified and individual sand grains selected on the pair of photographs. Dividers and a scale were used to obtain measurements from fixed points to the chosen sand grain on each of the photographs. Three measurements were required to fix the grain in space on each photograph. The measurements were input into a computer program which, using the scaling factor for the photographs, was able to calculate the horizontal and vertical displacements for the sand grain. This process was carried out for 5 to 10 sand particles per 50mm square section of the photographs. This measurement frequently depended on the intensity of the movements within that area, obtained from the stereo-viewing procedure. Although, this seems to be a very laborious method of measuring the sand displacements, other methods such as the digitising technique, would also have taken a long time to carry out. The other consideration was that the accuracy using the manual technique was very high.

Four sources of error were isolated when using the stereo-photogrammetry technique: alignment of the cameras, production of the photograph, measurement from the photograph and reduced sand movements due to friction of the sand against the glass.

The camera position is quite critical to the success of the stereo-photogrammetry technique. The camera needs to be set exactly perpendicular to the glass in the observation panels in three dimensions. This was a lengthy operation and involved the use of squares and spirit levels. Plate 4.14 shows the arrangement of the three cameras set up at one position to observe the movements in the longitudinal plane. The camera position had to be fixed between photographs, otherwise they would not be simply recording the sand movements alone. This was achieved by avoiding touching the cameras once set in position, by the use of motor winds and remote shutter releases.

Plates 4.15 and 4.16 show some typical photographs taken during a pipejacking and a pipebursting test. The white crosses stuck to the inside of the glass, which did not move, helped to emphasise the three-dimensional images obtained from the stereo-viewer by giving a zero movement reference plane.

Distortion of the image during its production can arise from several sources and this would lead to non-linearity across the print. Optical distortion can occur if the object being photographed is in different parts of the field of view. This can be minimised by the use of good quality photographic equipment, in these tests Minolta and Canon. Also, by limiting measurements to the central part of the photographs and using photographs from other cameras to compare the movements obtained, i.e. overlapping fields of view, optical distortion can be both minimised and checked for. Film distortion, whether in the camera or during developing and printing, is reduced by the use of good quality film, in these tests Kodak film was used, and also by using high quality, automatic processing services. Comparing the consistency of the photographs produced, these sources of error were found to be insignificant.

To test the accuracy of the camera set up, i.e. camera movements between photographs, the development process and the measurement technique, two successive photographs were taken without sand displacements occurring. Comparison of these photographs, by measuring sand displacements on each, would reveal any errors if movements were detected. No measurable movements were detected between the photographs, i.e. the errors must be less than ± 0.1mm. Several pairs of photographs were examined in this way to check this. Other inaccuracies can occur due to the refraction of the glass, particularly at the edges of the field of view. However, as long as the movements being detected are relatively small, only 20mm in the pipebursting tests, this effect will cause very small errors. A calculation given in Appendix A shows that this error, with the 30mm thick glass and the maximum measurement distances, is approximately 0.2mm. The movements of the sand cannot be much greater than 20mm at any one time, otherwise particles tend to get 'lost', i.e. they move out of plane strain or they rotate and look different making identification impossible. This is more likely for the more well graded 25B sand. A further check on the accuracy was conducted by simply measuring the movement of the pipejacking shield. This forward movement of 10mm was accurately known. The maximum inaccuracy detected for numerous photographs examined was ± 0.1mm, even for movements close to the edge of the field of view. In most cases no detectable errors were observed.

There was no means of checking the effect of friction between the glass and the sand during a test. A comparison could not be made between those measurements obtained at the surface and those obtained in the perpendicular plane using the stereo-photogrammetry technique because of the draw-along effects, which do not occur at the end face but do occur away from this face. The only possible gauge of the friction effects was that the movements at the overcut were approximately of the correct magnitude, i.e. for a 20mm overcut, 18mm of movement in the sand was detected at a short distance above the crown. Due to the seals around the inlet, measurements could not be obtained within an area of about 30mm from the pipe circumference. Cording et al (1976) were able to investigate the effects of friction in their tests. These researchers found that the errors were less than 5%. Simple shear box tests were also conducted to investigate the friction at the glass/sand interface. These were carried out for the load range encountered in the laboratory tests, for both sands at different densities. It was discovered that the maximim force required to shear the glass/sand interface as a percentage of the applied normal force, was 0.6%, i.e. very small. It was estimated that the overall error for the photogrammetry technique used for the tests conducted in this thesis, based on the various errors, was no more than 5%.

In addition to the sand displacement measurements recorded through the glass viewing panels, surface movements were also measured for several of the tests. These were thought useful in order to help tie in the longitudinal and perpendicular plane observations. Surface measurements could only be made when the sand movements actually reached the surface during a test and when there was no lid on the tank, so this limited the results that could be obtained. The measurements were obtained using a scale to record the vertical distance between an accurately positioned datum above the sand surface and small ball bearings positioned on a grid arrangement over the surface of the sand. Readings could be taken to $\pm$0.1mm. Comparative measurements were also taken using dial gauges positioned over a small plastic plates on the sand surface. The dial gauges could read to 0.01mm.

The results from both techniques compared well, although the dial gauges were more reliable and precise.

4.4 SAND CLASSIFICATION

As mentioned in Section 3.4, two different dry sands were chosen in which to conduct the experiments, a Leighton Buzzard sand and a 25B grade sand. The particle size distribution for the Leighton Buzzard sand is given in Fig. 4.5. This shows a uniformly graded sand of particle size values D_{10}, D_{30} and D_{60} of 1.18mm, 1.40mm, and 1.60mm respectively. The particle size distribution for the 25B grade sand is given in Fig. 4.6. This shows it to be a well graded sand with particle size values D_{10}, D_{30} and D_{60} of 0.67mm, 0.92mm, and 1.90mm respectively. Table 4.1 outlines various other parameters for the two sands. The shearing angles were obtained from simple shear box tests using normal stress ranges comparable to those experienced in the model tests. The shear angles at critical state were obtained from standard quick undrained triaxial tests. Specific gravity tests (BS1377:1990, Part 4) gave Gs as 2.6 for the Leighton Buzzard sand and 2.57 for the 25B grade sand. The void ratios determined for the densities obtained during the laboratory tests for the loose and dense states are also shown in the table. The maximum and minimum void ratios were obtained for each sand from the standard tests described in BS1377:1990, Part 4. The void ratios given are mean values from a number of tests, although the variation was only about 2%. The dilation angle for each density was calculated from the formula proposed by Bolton (1986), equation 2.1, which relates the dilation angle to the angle of shearing for the sand at its original state and at the critical state.

4.5 TEST SET UP

The methods for obtaining consistent densities were very important for these experiments. Any variation in density between tests or within tests, would have the greatest influence on the observed sand displacements. Two states of density were

Table 4.1 Soil parameters obtained for the two sands used in the laboratory tests

Soil Parameters	Sand Type Leighton Buzzard	 25B Grade
Gs	2.60	2.57
Maximum Density*	1667kg/m^3	1709kg/m^3
Minimum Density*	1493kg/m^3	1563kg/m^3
Cu	1.36	2.84
Cc	1.04	0.66
Natural Slope Angle	35^o	36^o
ϕ'_{dense}^	48^o	50^o
ϕ'_{loose}^	39^o	40^o
ϕ'_{crit}	34^o	36^o
ψ_{dense}"	17.5^o	17.5^o
ψ_{loose}"	6^o	5^o
e_{max}	0.74	0.64
e_{min}	0.56	0.52
e_{dense}'	0.60	0.53
e_{loose}'	0.70	0.59
Rd_{dense}	88%	90%
Rd_{loose}	22%	39%

Notes:
- * Obtained from standard laboratory tests (BS1377:1990, Part 4).
- ^ Obtained from simple shear box tests for the stress range used in these laboratory model tests.
- ' Obtained from measured values of density during the tank filling.
- " Calculated from the relationship;

  $\phi' = \phi'_{crit} + 0.8\psi$ (after Bolton, 1986) used in the experiments for each of the two different sands, a 'dense' state and a 'loose' state. It was not intended to produce the densest or the loosest states possible for each of the sands, but to obtain the most repeatable dense and loose states in order to provide an adequate variation in properties.

The dense state was produced by tamping the sand in 150-200mm thick layers. Each layer was compacted using a 10 Kg tamper, of base size 200 x 200mm, allowed to fall from a drop height of 150-200mm. Three passes were made over the surface of the sand. Care is required when using this tamping technique as too much pressure and the sand particles start to crush. Another problem with the tamping technique, is the fact that the lower levels of sand receive more compaction as the tank filling proceeds. However, due to the load spreading capacity of the sand, the tamping effects dissipate very quickly and the effect at a short distance below the surface will be very small. The standard procedure, described above, was carried out in the same way for all the dense state tests. Trials were initially conducted using a concrete vibrating poker to obtain a dense state in the sand. However, there were problems when using the poker, particularly with the amount of glass in the tank and also with the poker overheating when placed in the sand. Comparisons were conducted between the tamping technique and the vibrating poker technique and the densities obtained were almost indentical. Since the tamping method was easier to use, this technique was chosen.

The loose state was achieved using a sand raining device placed within the tank, the device being raised up as the tank filled to keep an approximately constant drop height. The design of the sand disperser was based on the requirements of distributing the sand as evenly as possible, to obtain as uniform a density as possible, from a single point of entry of the sand into the tank from the auger. The final pyramid design used for the experiments is shown in Plates 4.17a and b. It took several stages of development to achieve the optimum dispersal of the sand. Scale models were used to test out various designs in order to obtain the best slope, number of sides and hole positions (Plates 4.18a and b). The model tests produced consistently uniform loose samples when compared to the more conventional raining method. This was despite some inevitable mounding of the sand directly below the base holes of the pyramid. Trials of the full scale version also gave a consistent and uniform loose state. It was noted that the 25B sand produced more variable density results due to the difficulty of preventing a certain amount of segregation of the different sized particles. However the percentage variation was small.

4.6 PIPEJACKING TEST PROCEDURE

The experiments simulated closely actual pipejacking procedures. Initial photographs were taken before any movements occurred. The pipe, with the shield located, was then jacked forwards exactly 10mm into the tank. The jacking distance was measured using a vernier measuring arrangement fixed to the guide rails. The reason for the forward jacking distance being fixed at 10mm was the resistance of the sand moving into the shield. The shield opening is slightly larger than the inside diameter of the pipe. This means that the material entering the shield has to be compressed if it is to move back inside the pipe. Increasing the overcut increases this compression factor, particularly in the dense state tests. The sand will tend to form a plug as the pipe is jacked forwards, causing it to behave more and more like a closed shield. This is minimised by reducing the forward jacking distance before excavation takes place. For the pipejacking tests conducted using sand in a dense state, a noticeable increase in force was detected if jacking progressed beyond 10mm for the 0.2 overcut ratio and beyond approximately 30mm for the 0.1 overcut ratio. For the loose state tests much greater distances could be jacked before there was a noticeable increase in force.

At this stage of the test, after the forward jack, another set of photographs was taken. Careful excavation then proceeded at the face using a vacuum cleaner. The suction was kept very low, to make the process more controllable. The excavation was stopped just prior to collapse, i.e. running of the sand into the face, at the crown of the shield. The signs of onset of collapse were gained from experience in the trial tests. More photographs were taken at this stage just in case any relaxation of the sand had occurred during the excavation process. Jacking forwards another 10mm then took place, and the whole procedure was repeated. After each 100mm of jacked movement, the main jack was withdrawn to allow the insertion of a spacing section or a new pipe section. In order to check the effects of relaxation on the sand due to the removal of the jacking force while a new section was added, photographs were taken at this stage and compared with those obtained just prior to the removal of the force. No movements were detected for the tests at lower C/D ratios, but at the higher C/D ratio, where the forces on the pipe were higher, small additional movements were observed as relaxation took place, particularly close to the shield crown. This shows what could happen in practice in more unstable ground conditions.

Photographs were initially taken on the perpendicular plane, position 1, in order to observe the effects of the overcut. After approximately 100mm forward jack (this is dependent on the test) the cameras were moved to position 2 on the longitudinal plane. The cameras were then moved as necessary, to obtain observations of the whole displacement field during the forward jacking part of the test.

The rate of jacking was also investigated, as far as possible, during the test programme. For the main tests a constant rate of 60mm/min was used. However, for parts of several tests, a faster rate of 150mm/min was used, in order to determine the effects of this on the results.

A similar test procedure was adopted for the closed pipejacking tests, the only difference being that no excavation stage was required in these tests, so the photographs were simply taken after each jacking stage. The jacked distance was kept at 10mm, the same as for the open shield pipejacking tests, in order to allow direct comparison of the results.

4.7 PIPEBURSTING TEST PROCEDURE

Before the tank was filled, plaster pipes were fixed to the glass inside the tank, using a tile fixing compound, at a level to ensure that the bursting head, at its maximum expansion, would run along the invert of the plaster pipe. The plaster pipes were positioned up against the inlet seal of the tank to avoid any leakage of the sand. The bursting head was then positioned inside the tank just at the point where the plaster pipe would start to be broken out (Fig. 4.7).

The test procedure, once the tank had been filled, was similar to the closed shield pipejacking tests. The pipe with the bursting head attached, however, is jacked forwards 20mm between photographs in these tests. The cameras were initially set up on the perpendicular plane to capture the lateral bursting displacements throughout the expansion process. The cameras in this plane also captured the displacements as the sand converged onto the installed pipe due to the overburst. The cameras were then moved to the longitudinal plane to capture the sand displacements in this plane. The cameras were not kept in one position, but moved around in the longitudinal plane in order to capture the entire displacement field, which extended well in advance of the bursting operation and also behind the bursting head.

In order to reset the pipebursting tests, careful excavation was required close to the bursting operation. Plate 4.19 shows the plaster pipe during exhumation. The broken pieces of plaster pipe had to be removed completely to avoid contamination of the sand which was required for the subsequent tests. After breaking, the plaster pipe stayed very close to the bursting head and therefore normal excavation could take place until quite close to the burster level. At this stage the vacuum cleaner was used and combined with an archaeological type removal process: all of the broken pieces of plaster pipe, and the sand that was contaminated with smaller pieces of pipe, were completely removed. This meant that the sand did not have to be cleaned after each test, although a small quantity of sand was lost after each test.

4.8 PROGRAMME FOR THE PIPEJACKING TESTS

Numerous preliminary tests were conducted whilst trying to produce a working experiment. Once working satisfactorily, several tests were then conducted as trials to establish the approximate areas of movement in order to position the cameras and maximise the data collected at each point. This was important as there were only three cameras with which to obtain all the sand displacements throughout each test.

Once the trial tests were completed and the appropriate experimental technique had been standardised, the main test programme for the pipejacking tests was begun. Details of the tests conducted are presented in Table 4.2. Several of the tests were duplicated to act as comparisons and to check on the test procedure and the sand displacements observed. The first three tests investigated the effect of increasing C/D ratio on the displacements in a dense Leighton Buzzard sand, using an overcut ratio of 0.1. These tests were then repeated but with the Leighton Buzzard sand in a loose state. The previous six tests were then repeated but using a shield with an overcut ratio of 0.2. For the next twelve tests, the same parameters were investigated using 25B grade sand instead of Leighton Buzzard sand. The test programme thus investigated all the combinations of the various parameters.

To act as a comparison with the tests described above, five additional tests were conducted using a closed pipejacking shield. Table 4.3 gives details of these tests. The first four tests used an overcut ratio of 0.1 and were conducted in Leighton Buzzard sand. Two C/D ratios were used, although one had to be lower than those used in the open shield pipejacking tests, due to the increased forces acting on the closed pipejacking shield. These tests were conducted in both loose and dense states. The final test used an overcut ratio of 0.2 with a dense state Leighton Buzzard sand and a C/D ratio of 2.0. It was expected that another test using a C/D ratio of 5.0 would be conducted but, due to the large extent of the sand displacements observed in the other tests, it was considered that the movements would approach too close to the boundary of the tank with the larger C/D ratio.

In addition to these tests, and to act as a comparison with the open shield pipejacking tests, some tests were tried with no shield. This involved simply pushing the pipe alone into the tank. However, these tests were soon abandoned, as no sensible results could be obtained. The reason for this was that the sand close to the crown of the pipe became very unstable during the forward

Table 4.2 Details of the open shield pipejacking test series

TEST NUMBER	TEST CODE	SAND TYPE	DENSITY STATE	C/D RATIO	t/R RATIO
OPJ1*	4.5dLB0.1	LB	d	4.5	0.1
OPJ2	12.5dLB0.1	LB	d	12.5	0.1
OPJ3*	20.0dLB0.1	LB	d	20.0	0.1
OPJ4*	4.5lLB0.1	LB	l	4.5	0.1
OPJ5	12.5lLB0.1	LB	l	12.5	0.1
OPJ6*	20.0lLB0.1	LB	l	20.0	0.1
OPJ7*	4.5dLB0.2	LB	d	4.5	0.2
OPJ8	12.5dLB0.2	LB	d	12.5	0.2
OPJ9	20.0dLB0.2	LB	d	20.0	0.2
OPJ10*	4.5lLB0.2	LB	l	4.5	0.2
OPJ11	12.5lLB0.2	LB	l	12.5	0.2
OPJ12	20.0lLB0.2	LB	l	20.0	0.2
OPJ13*	4.5d25B0.1	25B	d	4.5	0.1
OPJ14	12.5d25B0.1	25B	d	12.5	0.1
OPJ15	20.0d25B0.1	25B	d	20.0	0.1
OPJ16*	4.5l25B0.1	25B	l	4.5	0.1
OPJ17	12.5l25B0.1	25B	l	12.5	0.1
OPJ18	20.0l25B0.1	25B	l	20.0	0.1
OPJ19	4.5d25B0.2	25B	d	4.5	0.2
OPJ20	12.5d25B0.2	25B	d	12.5	0.2
OPJ21	20.0d25B0.2	25B	d	20.0	0.2
OPJ22	4.5l25B0.2	25B	l	4.5	0.2
OPJ23	12.5l25B0.2	25B	l	12.5	0.2
OPJ24*	20.0l25B0.2	25B	l	20.0	0.2

Notes:

LB	Leighton Buzzard sand
25B	25B grade sand
d	Dense state sand
l	Loose state sand
C	Cover depth
D	Diameter of pipe
t	Overcut value
R	Radius of pipe
*	Indicates tests that were duplicated to compare repeatability of results.

The test code is defined as follows:
Cover depth to diameter ratio (C/D), density state, sand type, overcut ratio (t/R)

Table 4.3 Details of the closed shield pipejacking test series

TEST NUMBER	TEST CODE	SAND TYPE	DENSITY STATE	C/D RATIO	t/R RATIO
CPJ1*	2.0dLB0.1	LB	d	2.0	0.1
CPJ2	2.0lLB0.1	LB	l	2.0	0.1
CPJ3	4.5dLB0.1	LB	d	4.5	0.1
CPJ4*	4.5lLB0.1	LB	l	4.5	0.1
CPJ5	2.0dLB0.2	LB	d	2.0	0.2

Notes: As for Table 4.2

Table 4.4 Details of the pipebursting test series

TEST NUMBER	TEST CODE	SAND TYPE	DENSITY STATE	C/D_o RATIO	D_f/D_o RATIO
PB1*	2.6dLB1.2	LB	d	2.6	1.2
PB2	4.9dLB1.2	LB	d	4.9	1.2
PB3*	2.6lLB1.2	LB	l	2.6	1.2
PB4	4.9lLB1.2	LB	l	4.9	1.2
PB5*	3.8dLB1.7	LB	d	3.8	1.7
PB6	7.0dLB1.7	LB	d	7.0	1.7
PB7	3.8lLB1.7	LB	l	3.8	1.7
PB8	7.0lLB1.7	LB	l	7.0	1.7
PB9*	2.6d25B1.2	25B	d	2.6	1.2
PB10	4.9d25B1.2	25B	d	4.9	1.2
PB11	2.6l25B1.2	25B	l	2.6	1.2
PB12	4.9l25B1.2	25B	l	4.9	1.2
PB13	3.8d25B1.7	25B	d	3.8	1.7
PB14	7.0d25B1.7	25B	d	7.0	1.7
PB15*	3.8l25B1.7	25B	l	3.8	1.7
PB16	7.0l25B1.7	25B	l	7.0	1.7

Notes: As for Table 4.2 except for the following:

D_o Diameter of old pipe
D_f Maximum diameter of burster

The test code is defined as:
Cover depth to diameter ratio (C/D_o), density state, sand type, bursting ratio (D_f/D_o)

jacking. Sand flowed in to the pipe, eliminating any other movements at this position, due to the forward thrusting. This illustrated quite dramatically, the importance of using a shield on the lead pipe, the cutting edge of which must help to provide the support to the sand.

4.9 PROGRAMME FOR THE PIPEBURSTING TESTS

As with the pipejacking tests, several trial tests were conducted initially to standardise the procedure, to gain a 'feel' for how the tests behaved and to investigate the likely extents of the movements to enable the optimum camera positions to be used.

Details of the pipebursting tests conducted are given in Table 4.4. Several tests were duplicated in order to check the consistency of the tests and the displacements obtained. The first two tests were conducted in dense Leighton Buzzard sand using a D_f/D_o ratio of 1.2 (and the 0.169m OD plaster pipe), at two different cover depths (0.4m and 0.8m). Two cover depths were considered satisfactory for obtaining an understanding of the displacements. The C/D_o ratios thus obtained (2.6 and 4.9) were based on typical values from field operations. The scale of the tests can be considered as full scale for the smaller prototype pipebursting operations. For example, the field trial reported by Robins et al (1991), was to replace a 200mm I.D. pipe with a 250mm O.D. pipe at a depth of 1.2m.

The first two tests were repeated, but for the Leighton Buzzard sand in a loose state. These four tests were then repeated for a D_f/D_o ratio of 1.7 (using the 0.125m OD plaster pipe). The cover depths gave C/D_o ratios of 3.8 and 7.0, which combined with the previous tests, represented a good range of typical values from 2.6 to 7.0. These eight tests were repeated using the 25B grade sand. The pipebursting test programme thus incorporated a broad range of different parameters and boundary conditions, which are comparable to field values. This allows almost direct application of the results to common field situations.

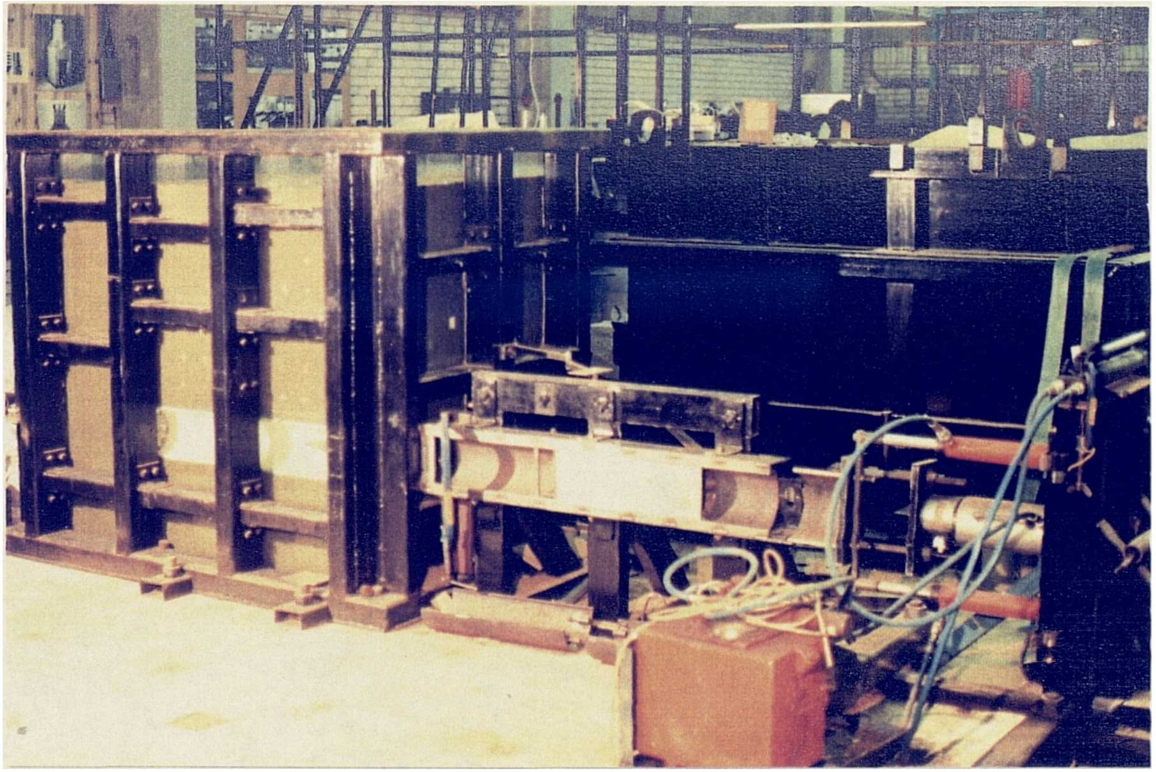

Plate 4.1 General arrangement of laboratory test equipment

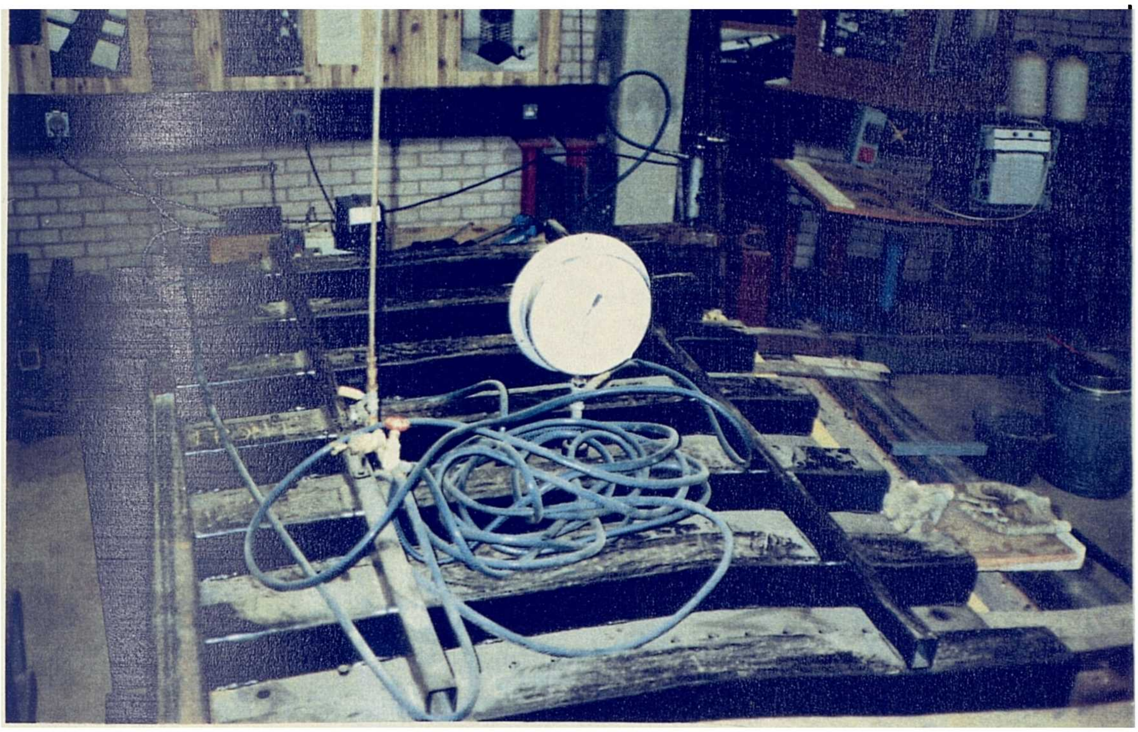

(a) Top view of lid

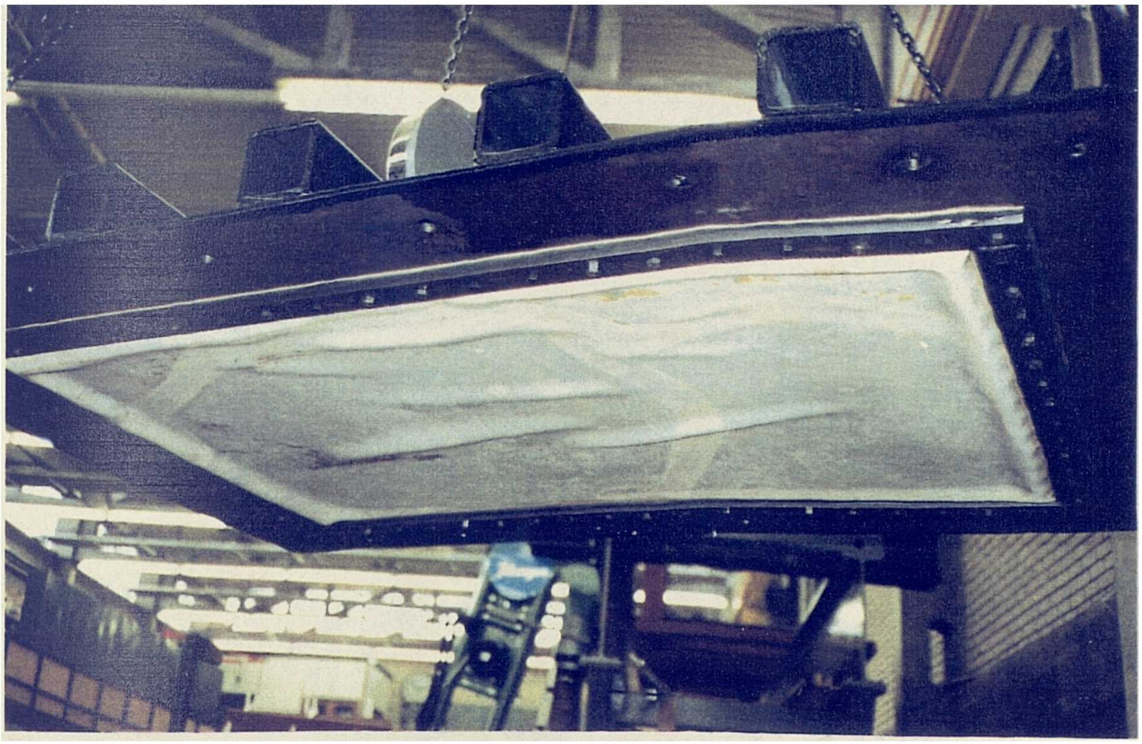

(b) Underside view showing water bag arrangement

Plate 4.2 General arrangement of test tank lid and water bag

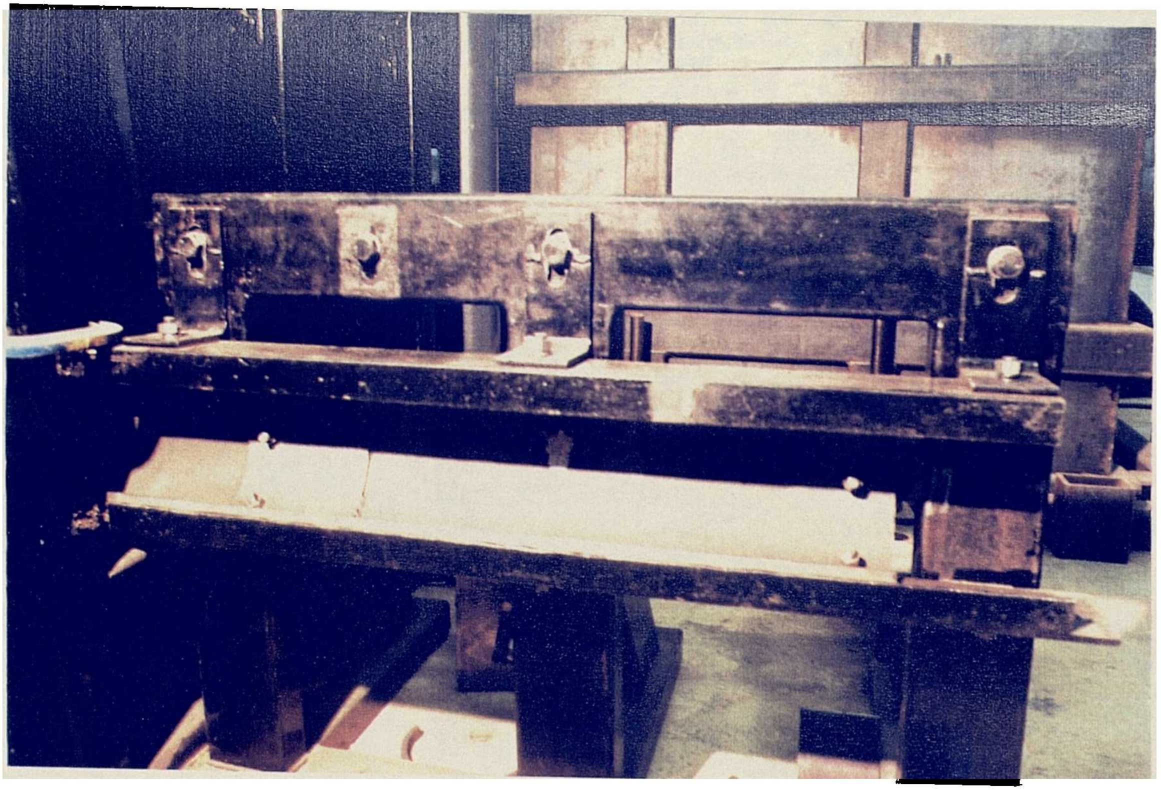

Plate 4.3 Arrangement of the guide rail system

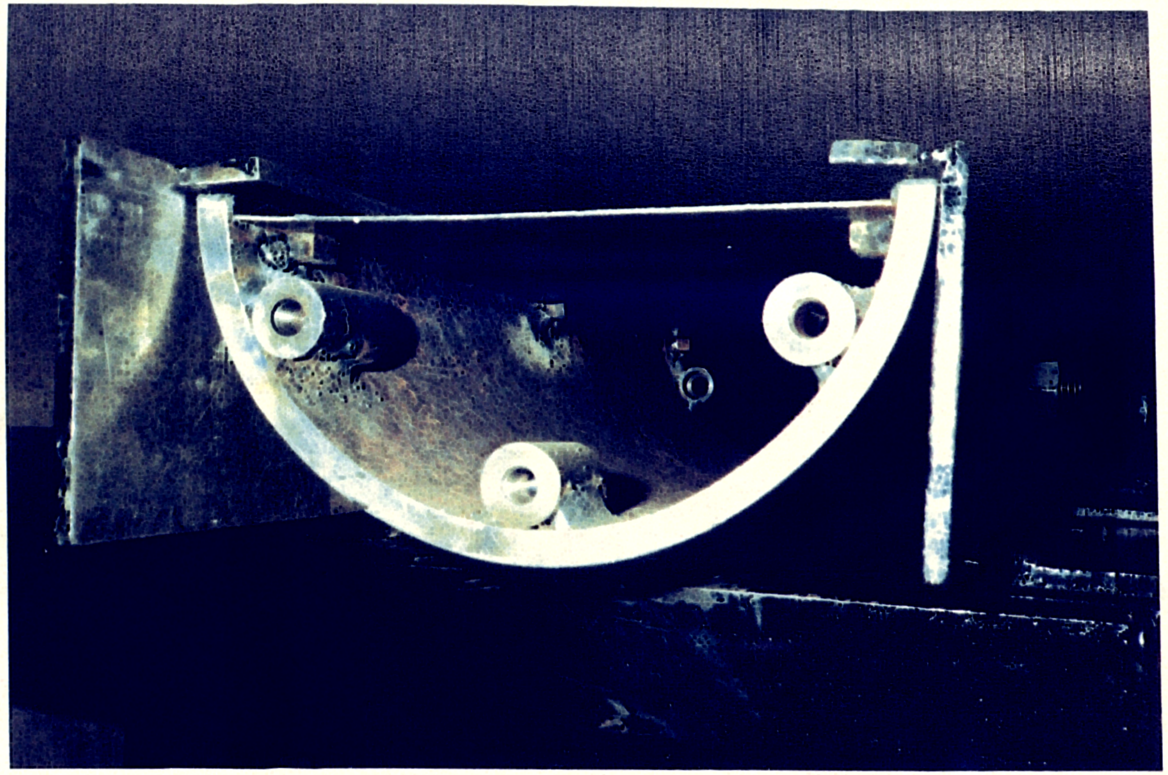

Plate 4.4 Guide system for supporting the semi-circular pipe sections

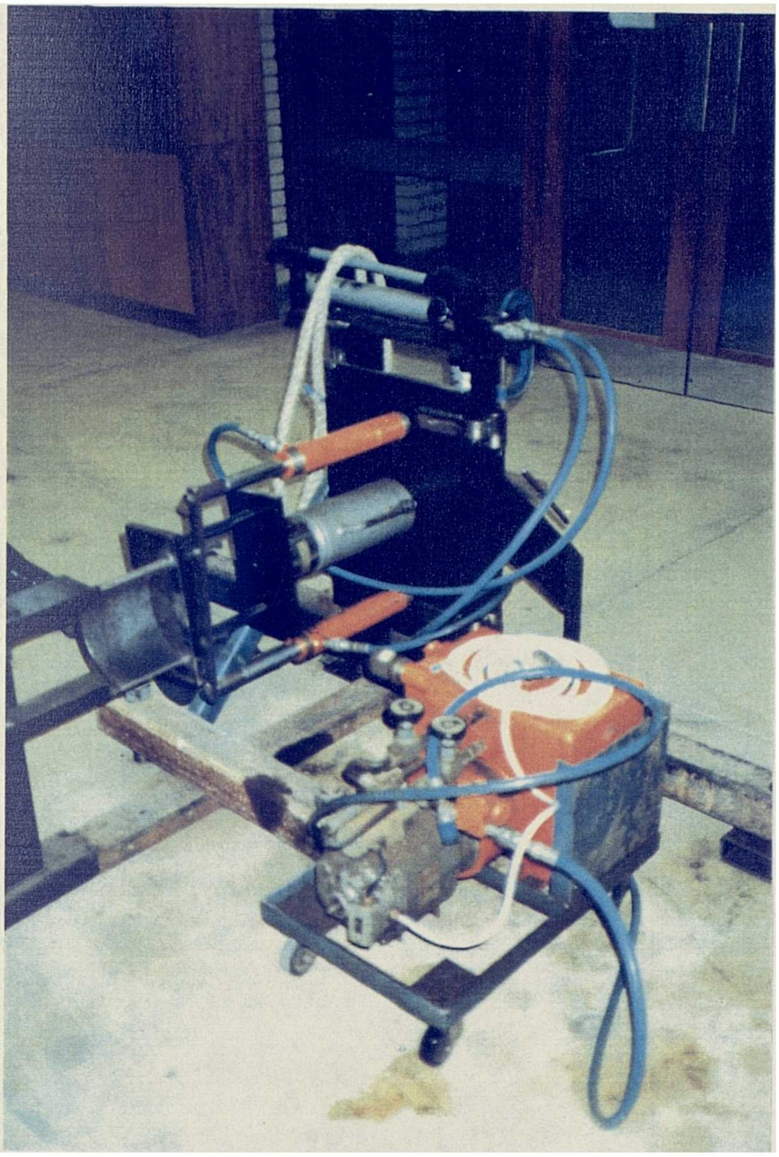

Plate 4.6 Semi-circular pipe sections

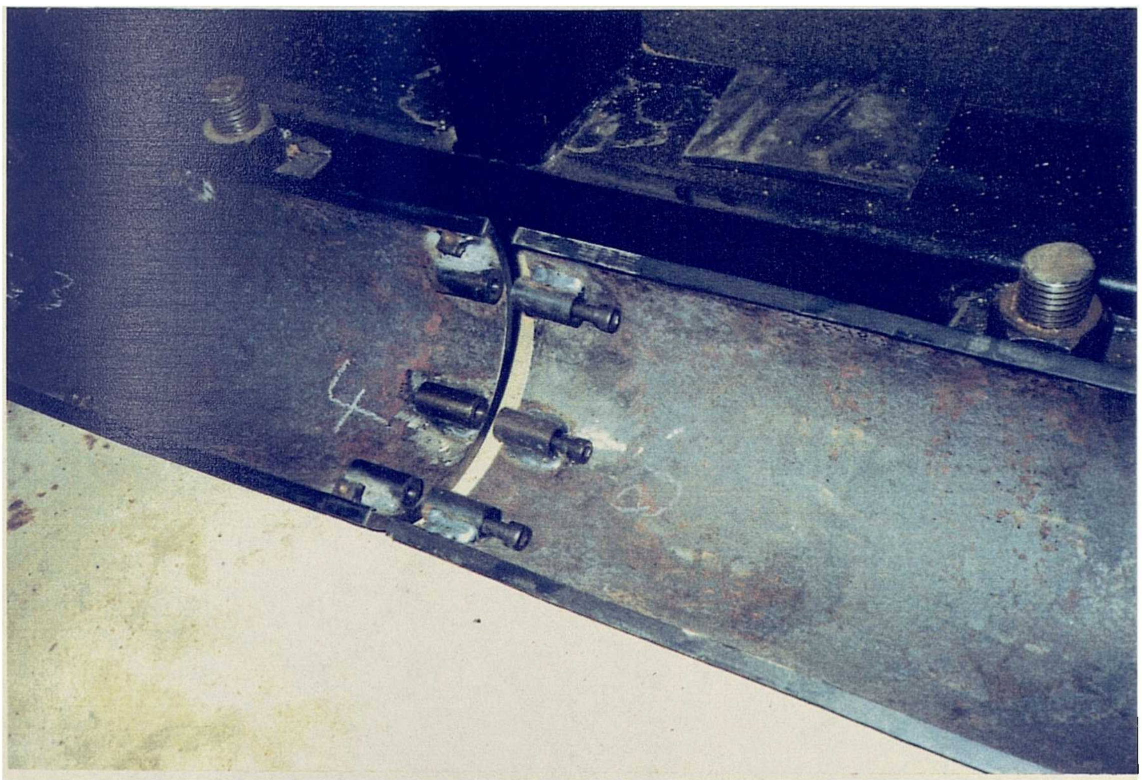

Plate 4.7 Jointing system for pipe sections

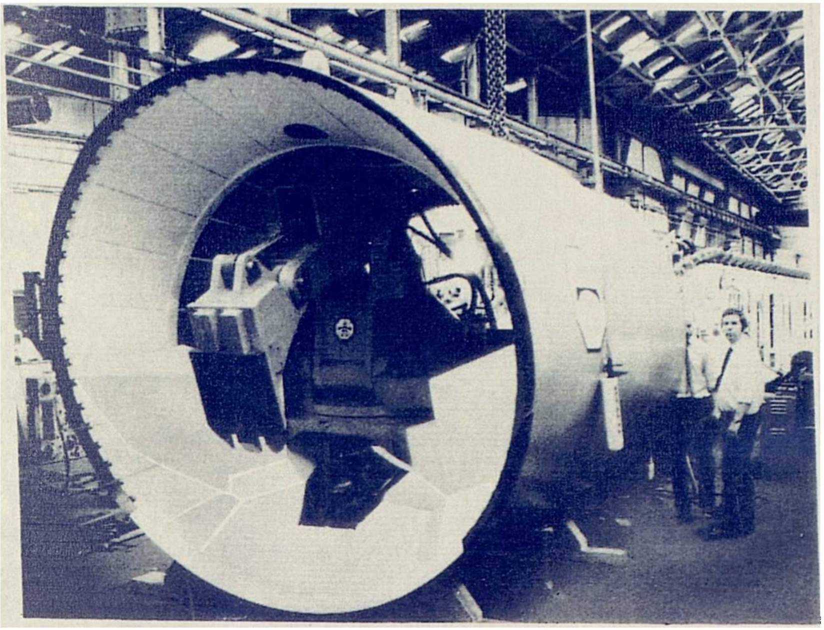

Plate 4.8 Typical prototype pipejacking shield

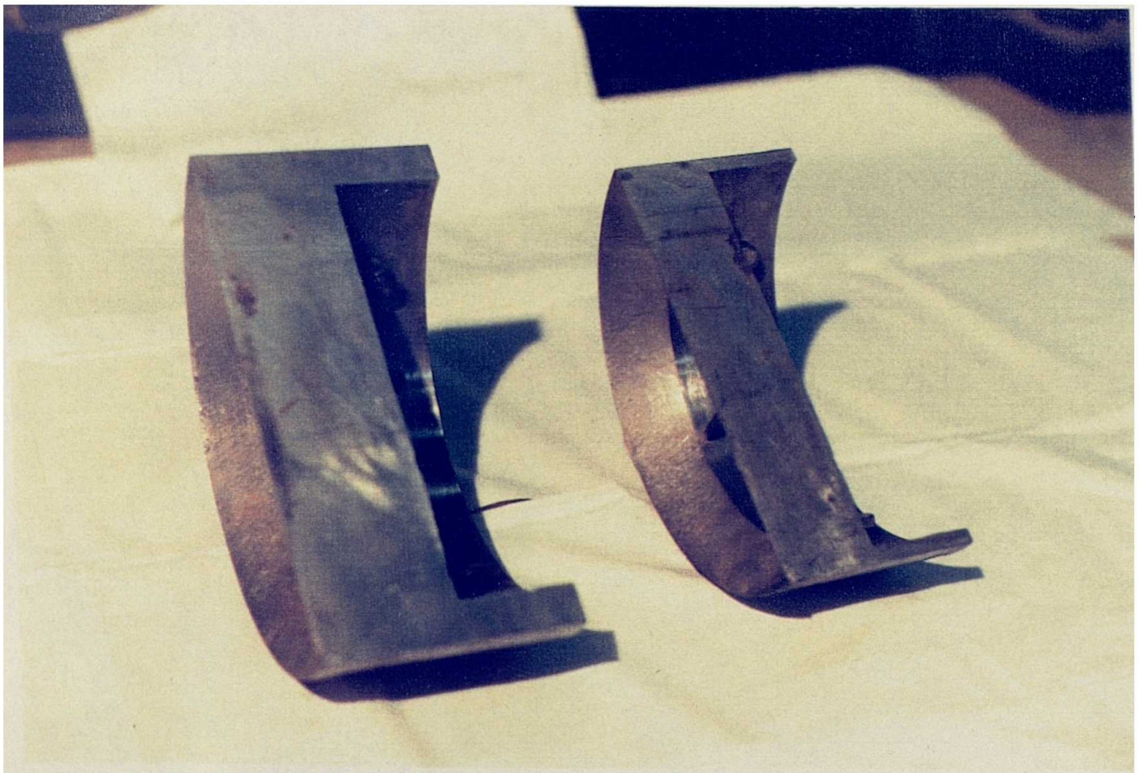

Plate 4.9 Pipejacking shields used during the laboratory tests

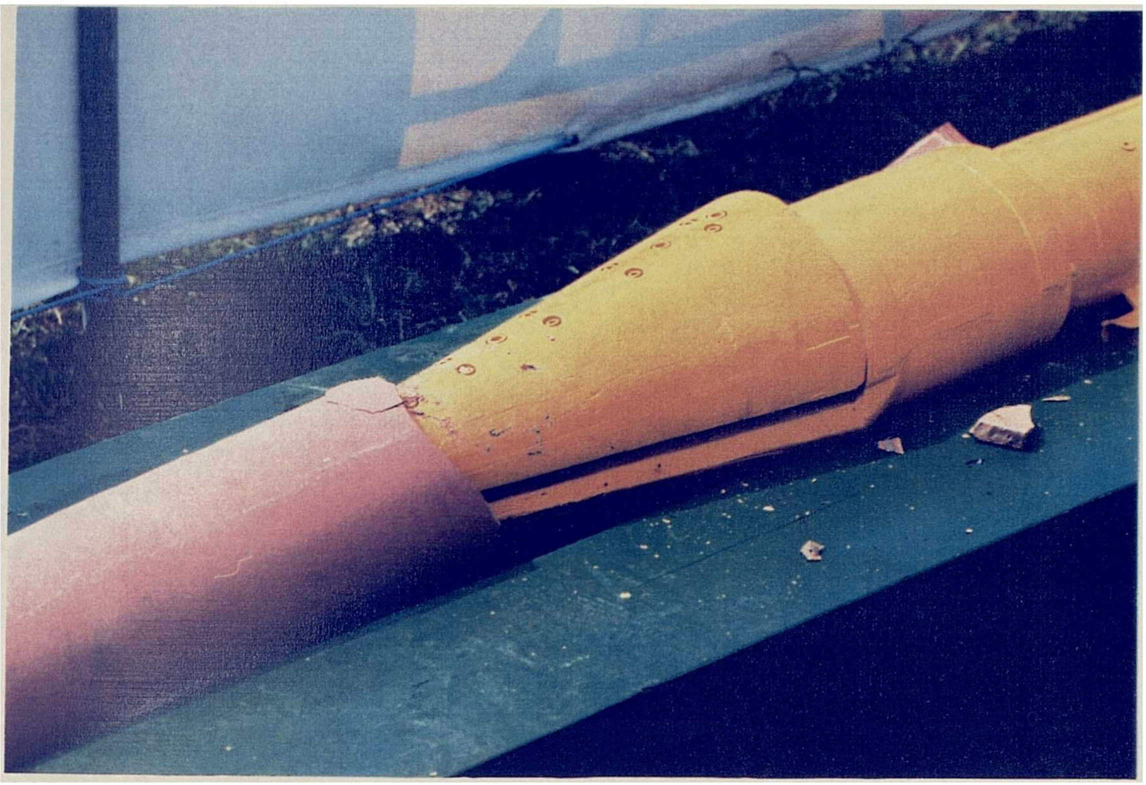

Plate 4.10 Typical prototype pipebursting head

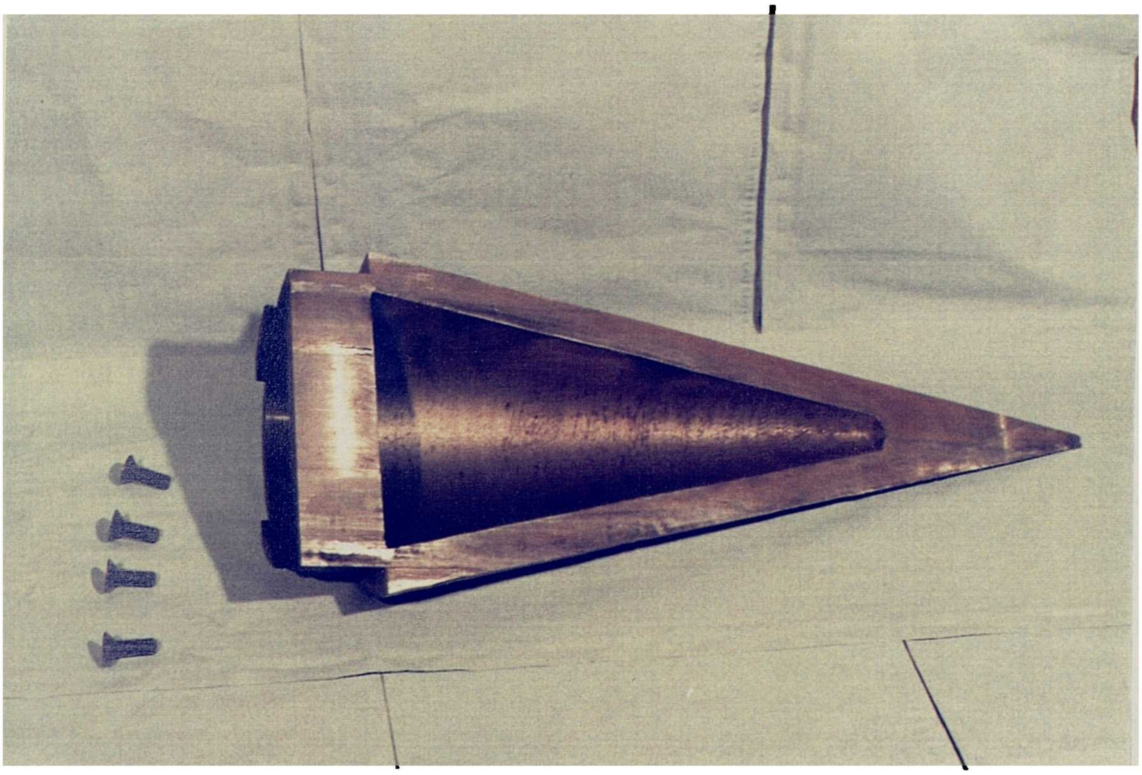

Plate 4.11 Completed pipebursting head use to simulate the expansion type pipebursting operations

Plate 4.12 General arrangement of the equipment used during the filling of the test tank, showing the Floveyor auger

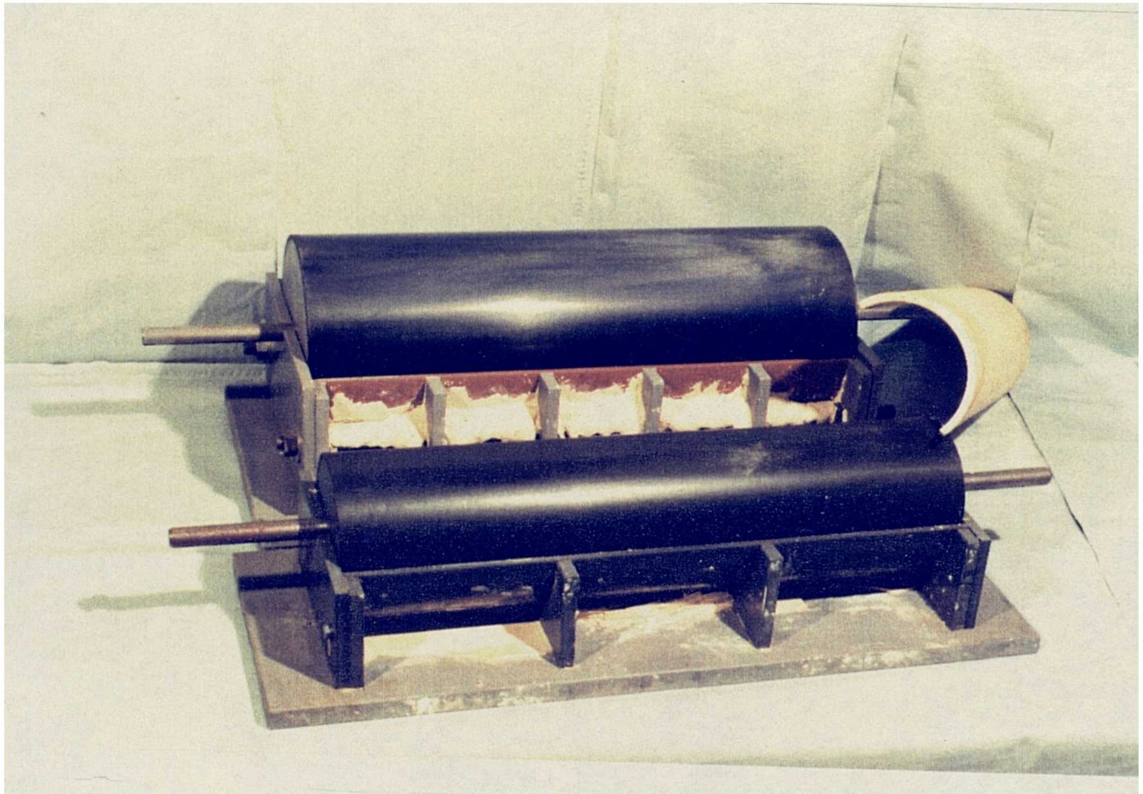

Plate 4.13 Moulds used to construct the plaster pipe sections used to simulate the pipe to be replaced during the pipebursting operation

Plate 4.14 Typical arrangement for the cameras used to record the sand displacements

Plate 4.15 Typical pair of photographs taken during the open shield pipejacking tests

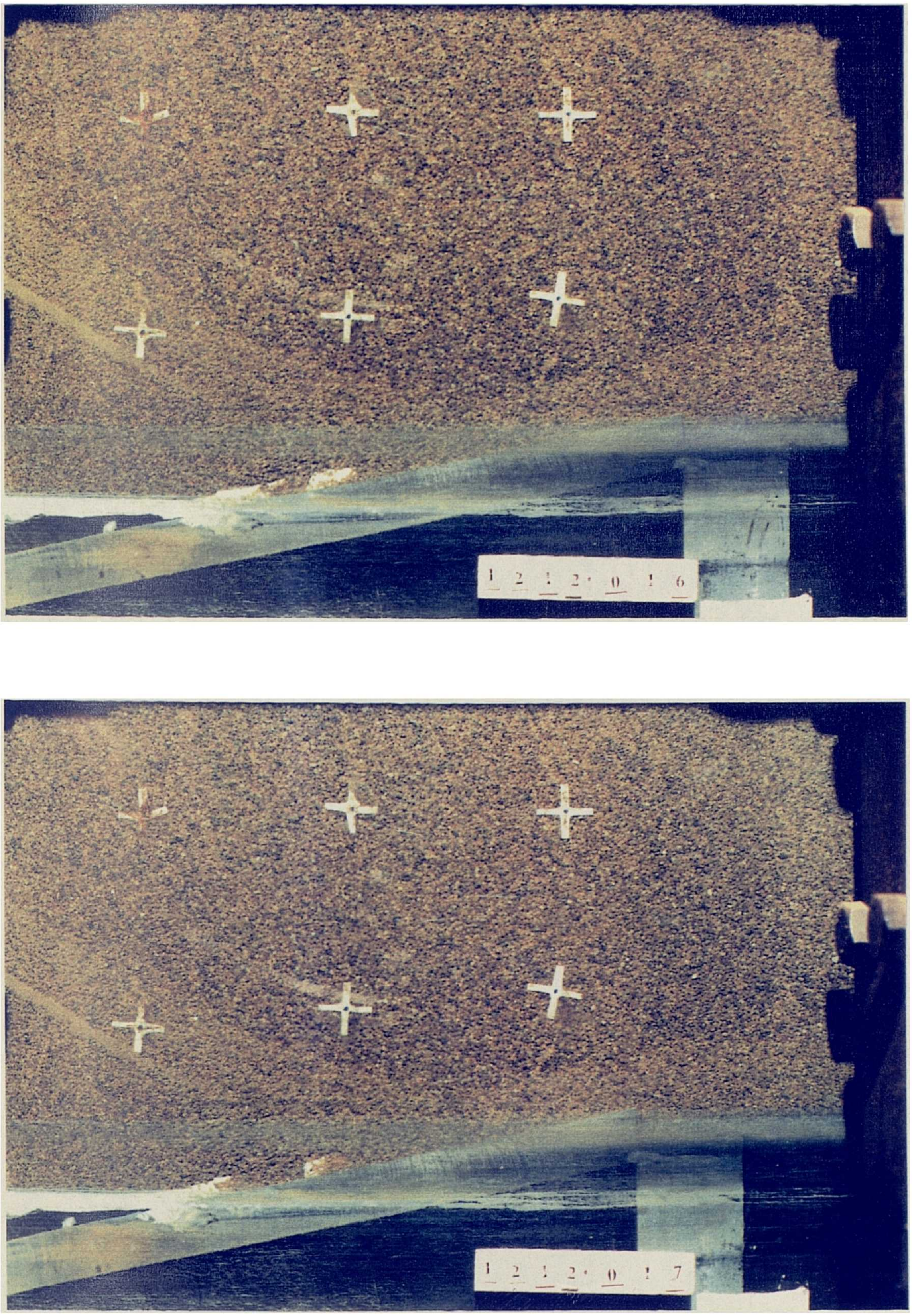

Plate 4.16 Typical pair of photographs taken during the pipebursting tests

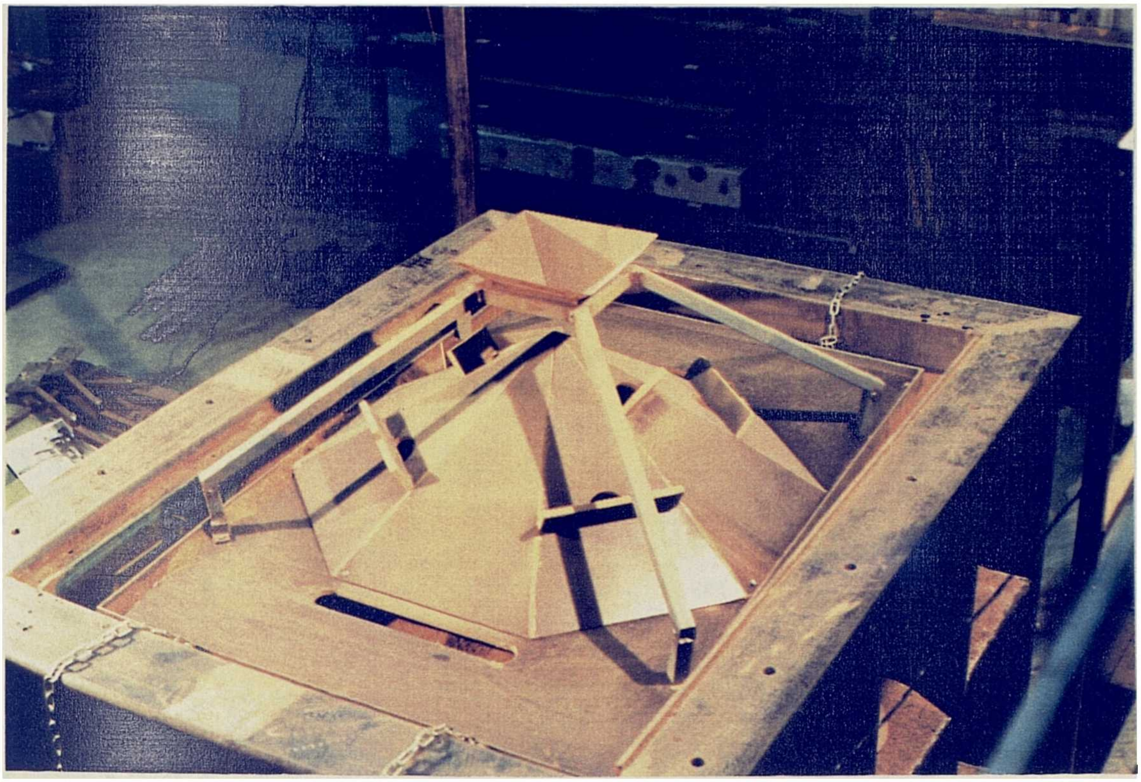

(a) Top view

(b) Underside view

Plate 4.17 Sand dispersal device used for obtaining the loose sand state

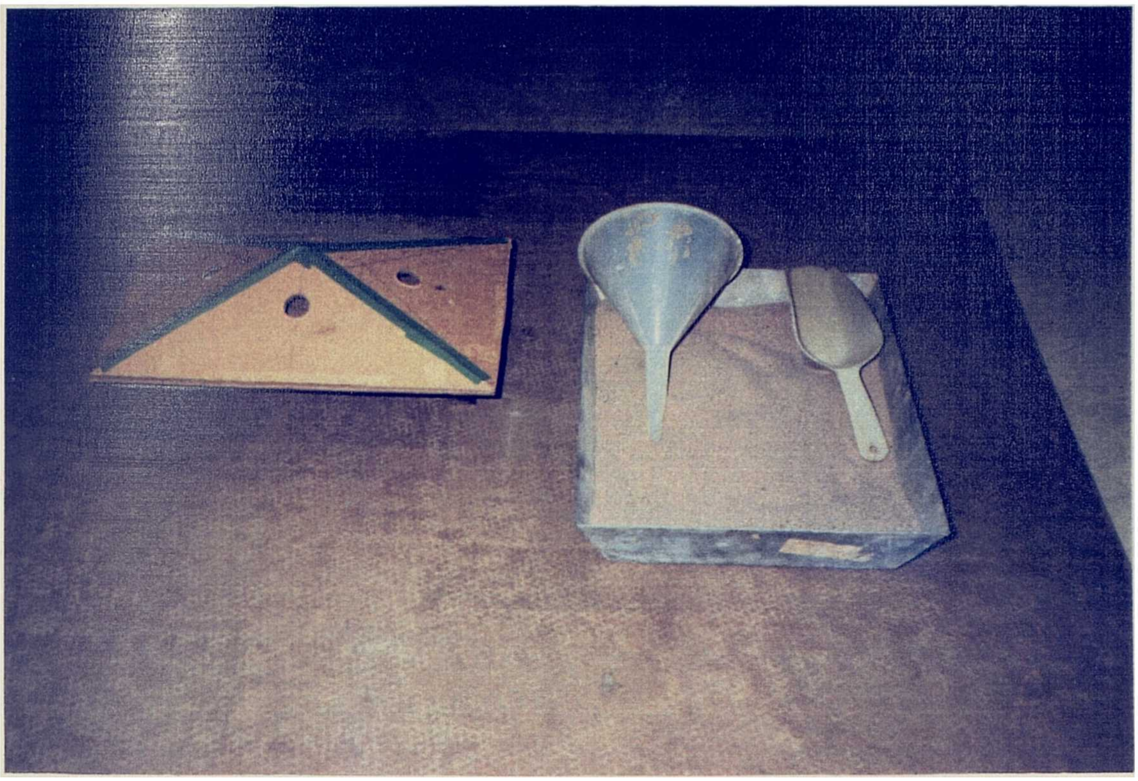

(a) An initial design

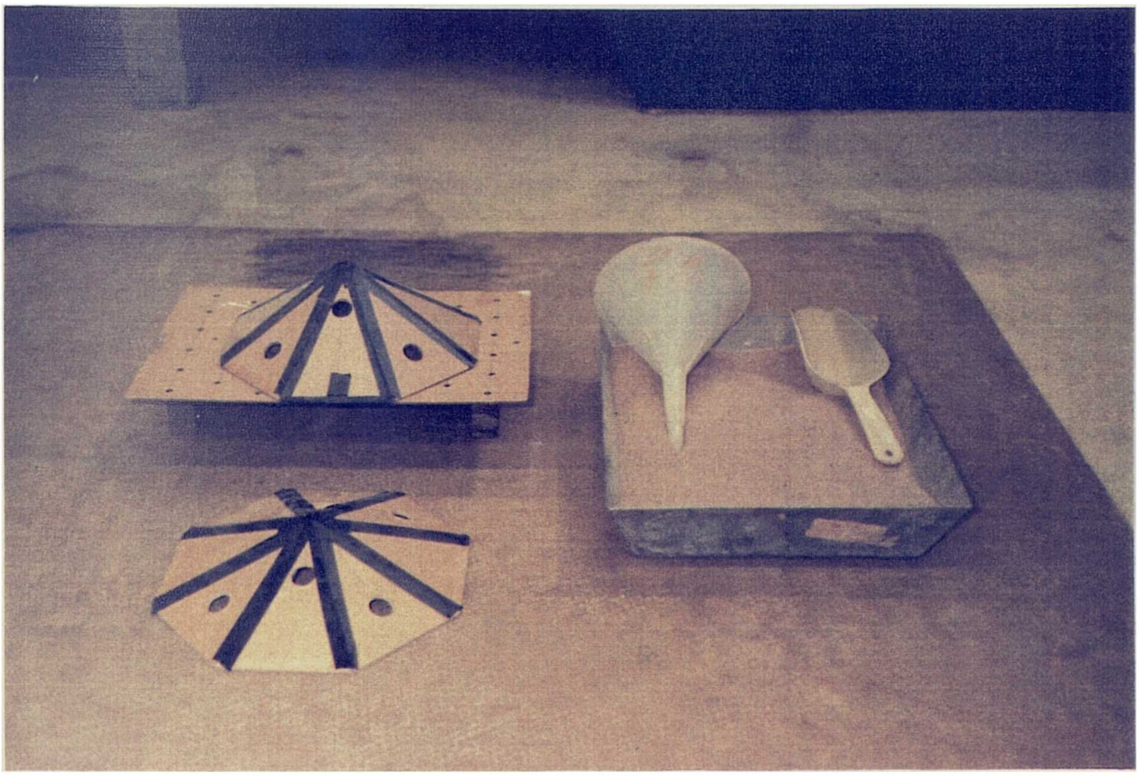

(b) Later designs, with more holes and sides. Different slopes were also investigated

Plate 4.18 Examples of the scale models used to develop the sand dispersal pyramid

Plate 4.19 The broken out plaster pipe during exhumation

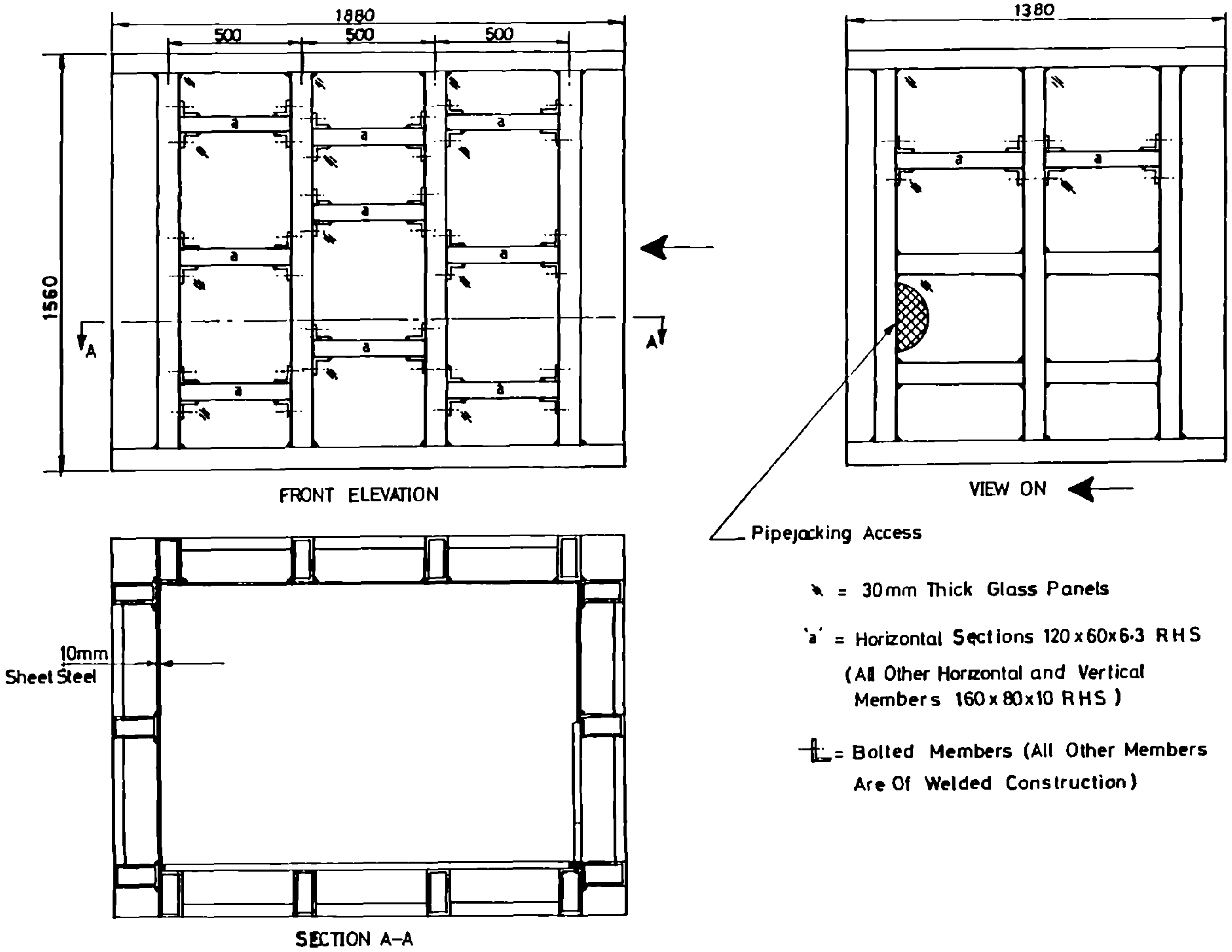

Fig. 4.1 Construction details of the test tank

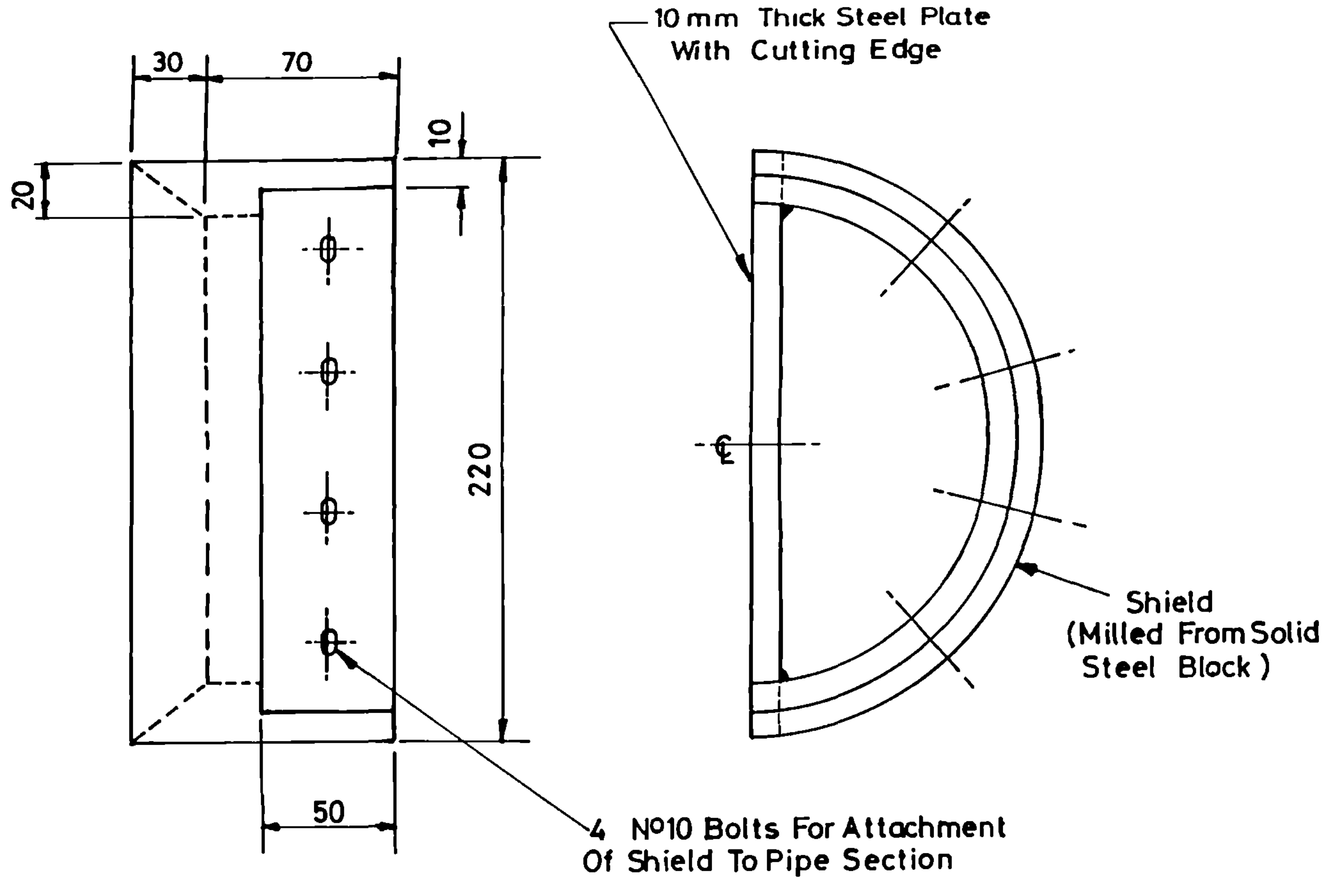

Fig. 4.2 Design for one of the two pipejacking shields (overcut ratio of 0.1)

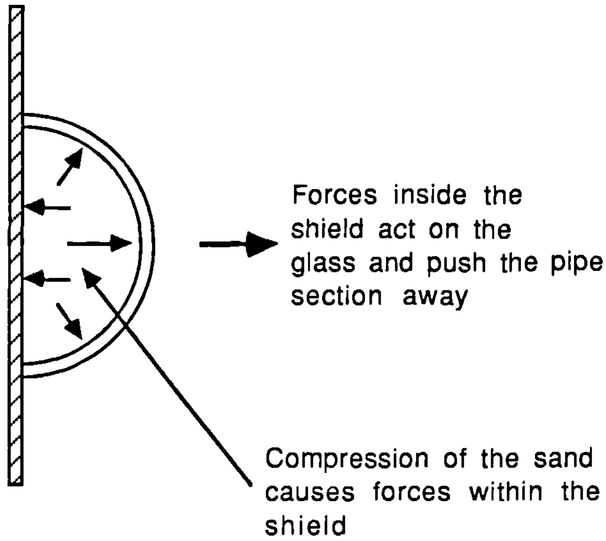

(a) The force of the sand being compressed inside the shield causes a resultant force on the pipe section which pushes it away from the glass

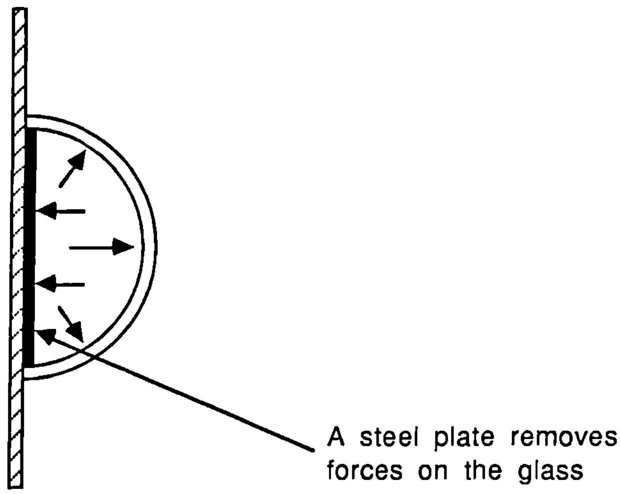

(b) A steel plate fixed to form a 'D' shaped shield alleviates the resultant force on the inside of the shield

Fig. 4.3 The reason why the pipe sections were being pushed away from the glass (a) and the solution (b)

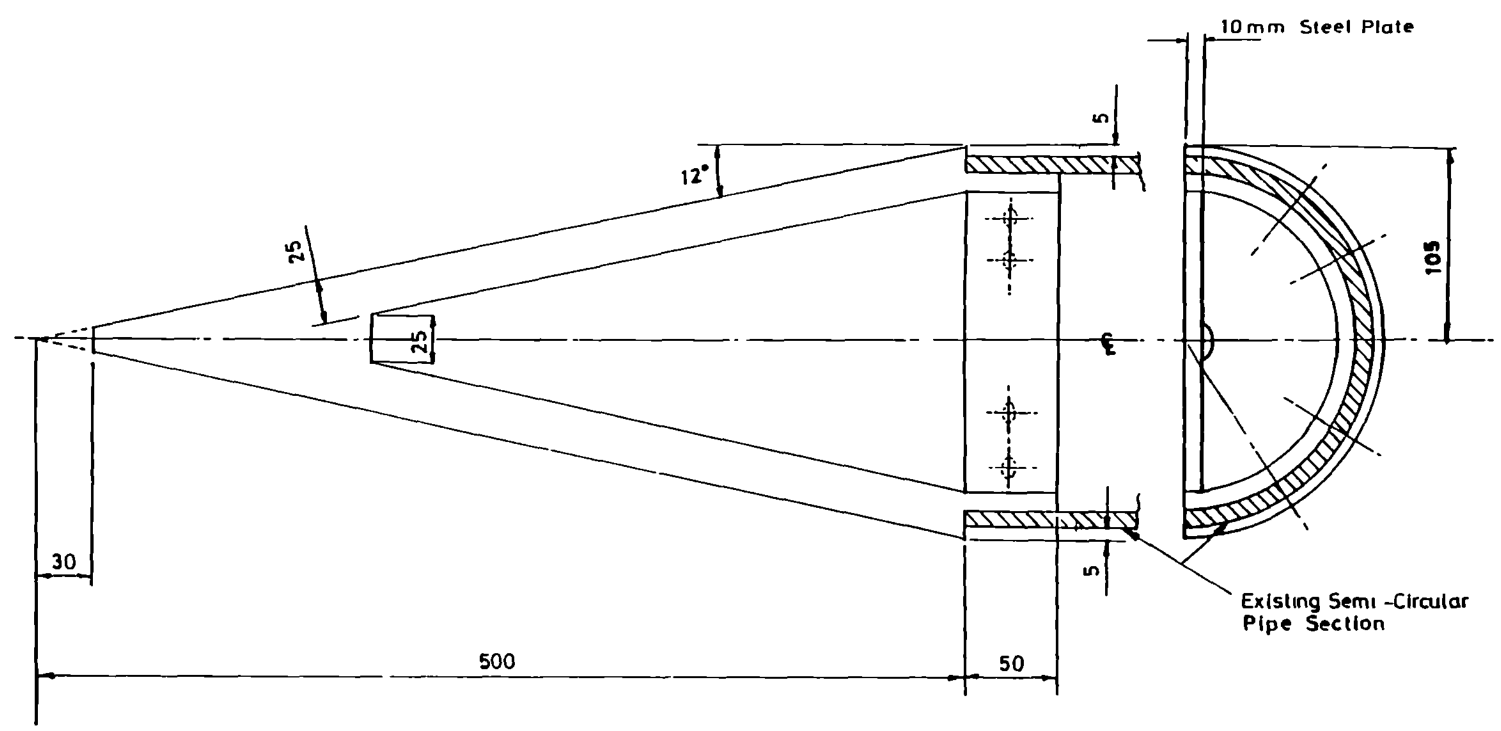

Fig. 4.4 Design for the pipebursting head used in the laboratory tests

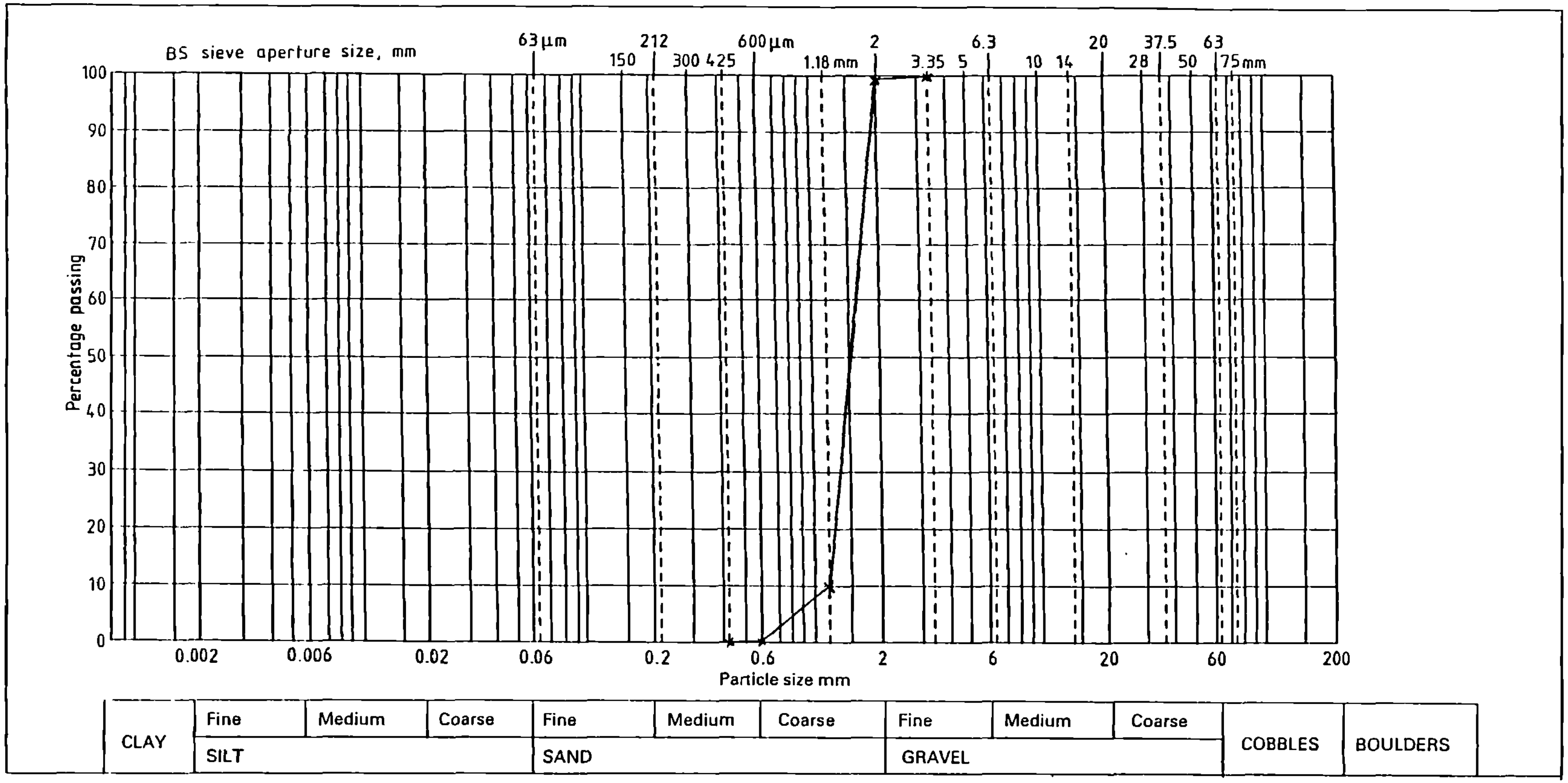

Fig. 4.5 Particle size distribution for the Leighton Buzzard sand

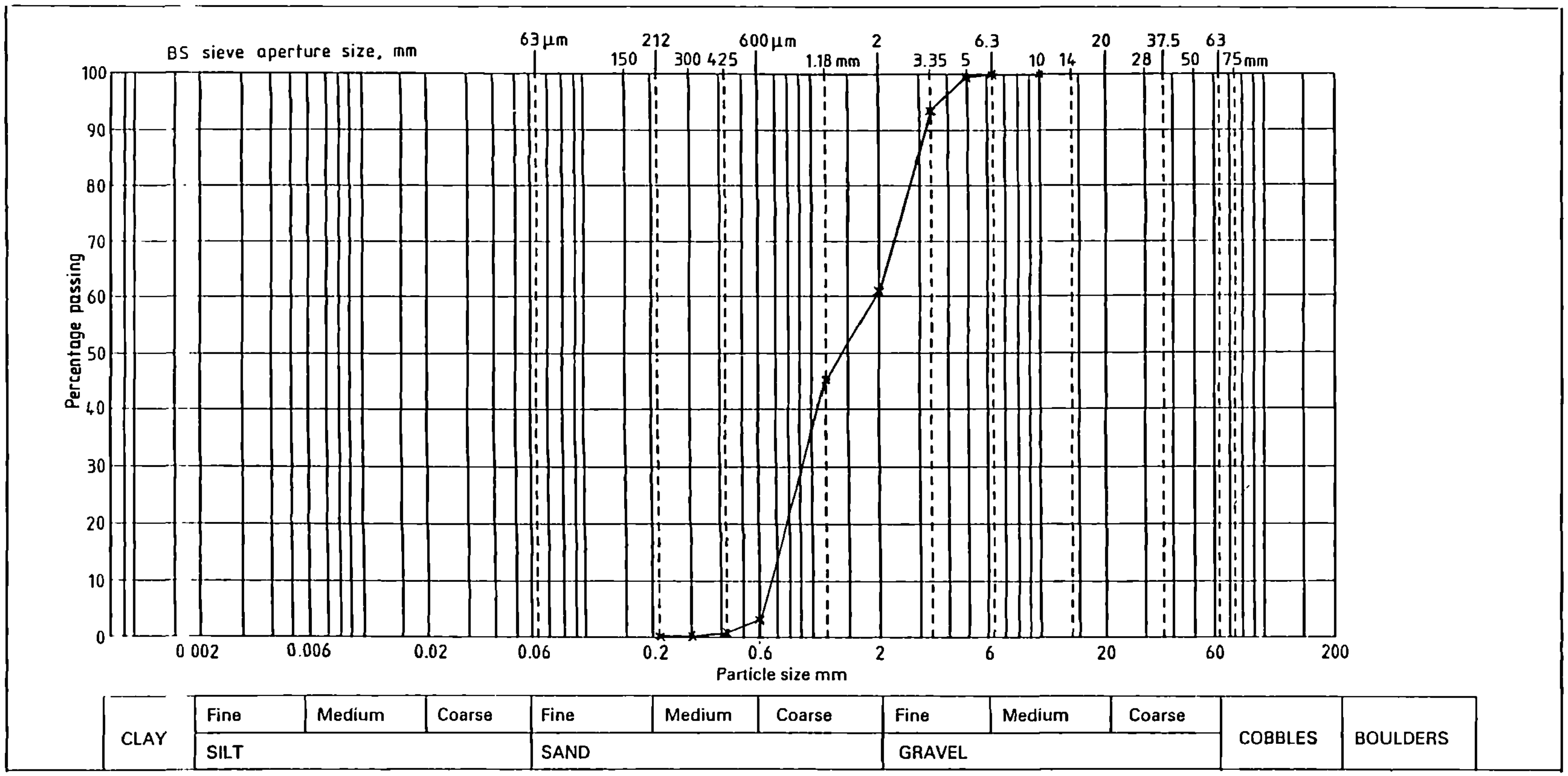

Fig. 4.6 Particle size distribution for the 25B grade sand

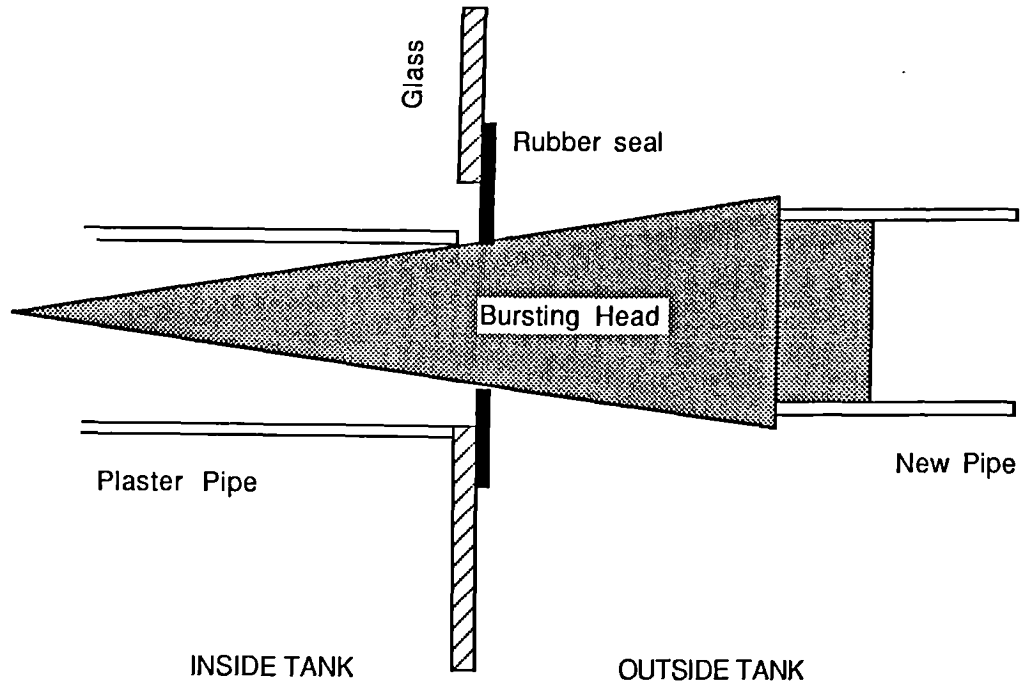

Fig. 4.7 Position of the pipebursting head at the start of each test

CHAPTER FIVE

5 RESULTS OF THE LABORATORY TESTS

5.1 INTRODUCTION

It has been established that various factors influence the ground movements associated with trenchless pipelaying techniques. From these, certain factors were selected which could be investigated under controlled conditions in laboratory experiments. These factors were soil type and density, C/D ratio, overcut ratio (pipejacking tests) and bursting ratio (pipebursting tests). The following presentation of results has the objective of illustrating the effects on the ground movements caused by altering these factors, both their individual effects and their interrelated effects. The movements are presented in both the longitudinal and perpendicular planes. Wherever possible the results are compared with field observations. The discussion then moves to comparing the relationships between the different test series, open shield pipejacking, closed shield pipejacking and the pipebursting tests, and explores the possibilities of interpolating between these test results to extend the scope of the investigation. Practical considerations are also discussed, together with how the results obtained can be interpreted to gauge the effects on adjacent services and structures.

The use of the stereo-photogrammetry technique for data acquisition means that the results are presented as contour plots for both the vertical and horizontal soil displacements. In order to present the large quantity of data, tables of extents of movement regions and magnitudes of the movements are referred to wherever possible. A complete set of the contour plots obtained from the tests are given in Appendix B, as it was impossible to present them all satifactorily within this chapter. The contour and total displacement vector plots are generally only referred to specifically when illustrating particular points. Volumetric strain plots are used to add a further dimension to the analysis for several of the tests and help to give a better understanding of the sand behaviour within, and between, the different areas of observed movement.

In Section 5.5.3, Section 5.10 is referred to when manipulating the data from the pipebursting tests for comparison with pipebursting model test results obtained by Swee and Milligan (1990). It was not thought appropriate to have the information contained in Section 5.10 any earlier in the Chapter as this would have interfered with what is essentially a descriptive section.

5.2 ACCURACY OF THE DISPLACEMENT CONTOUR PLOTS

As the longitudinal plane displacement contour plots only represent the movements for a small proportion of the total operation (20mm forward jack), the first stage of the analysis of the results was to check that these plots represent accurately the movements throughout the total jacking process. This was achieved by tracing the movements of individual particles throughout the whole test, plotting their movements and comparing the actual movements to those predicted from the contour plots.

The paths of two particles have been used in this discussion and compared with those predicted by the contour plots. The particles followed are for pipebursting tests, but similar comparisons were conducted for the two pipejacking test series. One particle was traced during test PB1 and its movements are shown in Fig. 5.1. A comparison between these measured movements and those predicted from the contour plots is made in Table 5.1a. A similar comparison is made for a particle traced during test PB3. Its path is plotted in Fig. 5.2, and Table 5.1b shows the comparison of the values obtained. In both cases the agreement between the contour and actual movements is exceptionally good, which not only validates the contour plots, but also proves the accuracy of the data acquisition procedure.

The movement traces of the particles are quite interesting. If no compression took place above the burster, each particle would theoretically move upwards by 46mm as the burster

Table 5.1 Comparison between observed sand displacements and those predicted by the displacement contour plots for sand particles traced during pipebursting tests

(a) Test PB1 (2.6dLB1.2)

MOVEMENT OF BURSTING HEAD (mm)	ACTUAL MEASURED MOVEMENTS OF SAND PARTICLES (mm)		PREDICTED MOVEMENT FROM DISPLACEMENT CONTOUR PLOTS (mm)	
	Vertical	Horizontal	Vertical	Horizontal
0	0	0	0	0
20	0.5	0.5	1.3	0.7
40	1.2	1.1	1.4	1.0
60	2.0	1.6	2.2	1.7
80	2.7	2.0	2.6	2.2
100	2.9	2.3	2.7	2.2
120	3.1	2.1	3.0	2.2
140	3.5	1.8	3.3	1.9
160	3.6	1.6	3.5	1.7
180	3.6	1.4	3.6	1.4
240	10.0	1.5	10.4	1.8
260	2.8	-0.4	2.6	-0.25
280	1.4	-0.9	1.7	-1.0
300	-0.9	0.4	-0.7	0.5
320	-1.0	0.9	-1.1	0.6
340	-0.9	0.5	-1.0	0.5

Note: The initial position of the sand particle at the start of the test, was 44mm vertically above the plaster pipe and 84mm in advance of the busting unit at the initial break out point of the plaster pipe.

Table 5.1 Comparison between observed sand displacements and those predicted by the displacement contour plots for sand particles traced during pipebursting tests

(b) Test PB3 (2.61LB1.2)

MOVEMENT OF BURSTING HEAD (mm)	ACTUAL MEASURED MOVEMENTS OF SAND PARTICLES (mm)		PREDICTED MOVEMENT FROM DISPLACEMENT CONTOUR PLOTS (mm)	
	Vertical	Horizontal	Vertical	Horizontal
0	0	0	0	0
20	0.5	0.9	0.7	1.1
40	1.0	1.0	1.1	1.2
60	1.4	1.4	1.3	1.5
80	1.6	1.5	1.4	1.7
100	1.7	1.6	1.5	1.7
120	1.8	1.6	1.9	1.6
140	2.0	1.3	2.2	1.5
160	2.7	1.2	2.5	1.2
180	2.2	0.9	2.4	1.0
240	5.3	0.8	5.1	1.1
260	-0.7	-1.5	-0.5	-1.5
280	-2.0	1.1	-2.3	1.0
300	-2.2	1.4	-2.0	1.6
320	-0.6	1.3	-0.5	1.2

Note: The initial position of the sand particle at the start of the test, was 56mm vertically above the plaster pipe and 76mm in advance of the initial break out point of the plaster pipe by the bursting unit.

passed. For the particle in test PB1, the total vertical movement is 37.3mm indicating a low compressibility of the sand above the burster, i.e. it is moving more like a single mass of sand. The angle of the burster adds a horizontal component to the upwards movement. The particle in test PB3, however, only moves upwards by approximately 20mm, indicating considerable compression of the sand above the burster. Both the particles are in similar postions at the start of the bursting operations.

The horizontal movement of the particle in test PB1 reaches a peak just prior to the overburster passing (point 10). The particle then moves backwards slightly, but while still moving upwards. Point 12 onwards marks the stage at which the overburst starts influencing the particle movements, with downward and some forward movement. The particle in test PB3 shows a similar pattern of movement. There is continuing upward and forward movement up to point 10. At this point though, rather than the upward and backwards movement observed in test PB1, there is a downwards and backwards movement, which suggests that the overburst has a quicker influence on the particle movements. Points 11 to 14 show the downward and forward movements as for test PB1, except that the downward magnitude of the movements are greater. As a practical observation, the tracing of the path of the sand particles throughout the pipebursting operation could similarly represent the upperbound movement of a service running perpendicular to the operation at the position of the sand particle.

5.3 THE OPEN SHIELD PIPEJACKING TESTS

The general form of the ground movements, associated with this test series during the jacking part of the operation, is shown in Fig. 5.3. The movement patterns shown in this figure are obtained during the forward jacking stage of the operation with no excavation at the face. The distance jacked, over which these movements were obtained, was 10mm and this is the same for all tests in this test series. Tables 5.2a and b are referred to throughout this discussion section and illustrate trends between

Table 5.2a Observed extents of sand movements for the open shield pipejacking tests, as defined in Fig. 5.3

TEST NUMBER	TEST CODE	EXTENT DIMENSION / PIPE DIAMETER Horizontal Movements A	B	C	D	E	F
OPJ1	4.5dLB0.1	2.18	1.85	0.49	1.10	1.27	0.01
OPJ2	12.5dLB0.1	1.80	1.82	1.02	0.90	1.24	0.15
OPJ3	20.0dLB0.1	1.68	1.80	1.40	0.66	1.26	0.16
OPJ4	4.5lLB0.1	1.86	1.96	0.67	1.37	1.40	0.25
OPJ5	12.5lLB0.1	1.46	1.75	0.94	0.60	1.40	0.24
OPJ6	20.0lLB0.1	1.79	1.73	1.17	0.39	1.26	0.27
OPJ7	4.5dLB0.2	2.60	2.84	1.29	1.06	1.54	0.13
OPJ8	12.5dLB0.2	2.14	2.43	1.36	1.04	1.43	0.18
OPJ9	20.0dLB0.2	2.12	1.87	1.44	0.78	1.24	0.18
OPJ10	4.5lLB0.2	2.74	2.64	0.84	1.43	1.61	0.29
OPJ11	12.5lLB0.2	1.92	2.24	1.47	1.19	1.58	0.25
OPJ12	20.0lLB0.2	1.68	1.61	1.58	0.55	1.37	0.38
OPJ13	4.5d25B0.1	2.30	2.68	0.96	1.10	1.40	0.08
OPJ14	12.5d25B0.1	1.90	2.24	1.16	0.90	1.20	0.12
OPJ15	20.0d25B0.1	1.80	1.96	1.20	0.55	1.10	0.15
OPJ16	4.5l25B0.1	1.75	2.57	0.80	0.90	1.57	0.13
OPJ17	12.5l25B0.1	1.79	2.10	0.90	0.62	1.22	0.21
OPJ18	20.0l25B0.1	1.57	1.69	1.01	0.62	0.87	0.27
OPJ19	4.5d25B0.2	2.76	2.76	0.94	1.10	1.65	015
OPJ20	12.5d25B0.2	2.39	2.43	1.06	0.78	1.61	0.23
OPJ21	20.0d25B0.2	2.08	2.10	1.40	0.00	1.50	0.24
OPJ22	4.5l25B0.2	2.56	2.97	1.41	0.24	1.68	0.18
OPJ23	12.5l25B0.2	2.21	2.14	0.81	0.80	1.51	0.22
OPJ24	20.0l25B0.2	1.86	1.97	1.15	0.70	1.43	0.32

Table 5.2a Observed extents of sand movements for the open shield pipejacking tests, as defined in Fig. 5.3, continued

TEST NUMBER	TEST CODE	EXTENT DIMENSION / PIPE DIAMETER Perpendicular Plane Movements L	M
OPJ1	4.5dLB0.1	2.36	1.10
OPJ3	20.0dLB0.1	1.96	0.96
OPJ4	4.5lLB0.1	S	2.80
OPJ6	20.0lLB0.1	S	2.40
OPJ7	4.5dLB0.2	3.44	1.60
OPJ9	20.0dLB0.2	2.96	1.40
OPJ10	4.5lLB0.2	S	3.40]
OPJ12	20.0lLB0.2	S	2.60
OPJ13	4.5d25B0.1	2.20	0.92
OPJ15	20.0d25B0.1	1.90	0.82
OPJ16	4.5l25B0.1	S	2.16
OPJ18	20.0l25B0.1	S	1.52
OPJ19	4.5d25B0.2	3.20	1.44
OPJ21	20.0d25B0.2	2.82	1.16
OPJ22	4.5l25B0.2	S	2.86
OPJ24	20.0l25B0.2	S	2.24

Note: S - Vertical movements reach surface of sand.

Table 5.2a Observed extents of sand movements for the open shield pipejacking tests, as defined in Fig. 5.3, continued

TEST NUMBER	TEST CODE	EXTENT DIMENSION / PIPE DIAMETER Vertical Movements				
		G	H	I	J	K
OPJ1	4.5dLB0.1	2.57	1.55	2.14	0.50	0.10
OPJ2	12.5dLB0.1	2.27	1.24	1.76	0.57	0.13
OPJ3	20.0dLB0.1	2.19	1.34	1.51	0.63	0.20
OPJ4	4.5lLB0.1	2.60	-	1.86	1.15	0.25
OPJ5	12.5lLB0.1	2.30	-	1.31	0.87	0.31
OPJ6	20.0lLB0.1	2.10	-	1.17	0.84	0.33
OPJ7	4.5dLB0.2	2.91	1.87	2.15	1.09	0.22
OPJ8	12.5dLB0.2	2.55	1.99	1.92	1.22	0.28
OPJ9	20.0dLB0.2	2.29	1.64	1.76	0.64	0.35
OPJ10	4.5lLB0.2	2.98	-	1.92	0.46	0.18
OPJ11	12.5lLB0.2	2.63	-	1.65	0.73	0.24
OPJ12	20.0lLB0.2	2.45	-	1.63	0.73	0.39
OPJ13	4.5d25B0.1	2.65	1.45	1.45	0.95	0.09
OPJ14	12.5d25B0.1	2.10	1.30	1.20	1.00	0.21
OPJ15	20.0d25B0.1	2.25	1.30	1.30	1.15	0.30
OPJ16	4.5l25B0.1	2.64	-	1.51	0.71	0.18
OPJ17	12.5l25B0.1	1.64	-	1.65	1.27	0.21
OPJ18	20.0l25B0.1	1.93	-	1.44	1.59	0.27
OPJ19	4.5d25B0.2	3.22	1.51	2.16	0.99	0.14
OPJ20	12.5d25B0.2	2.60	1.43	1.86	1.15	0.15
OPJ21	20.0d25B0.2	2.55	1.33	1.55	1.31	0.22
OPJ22	4.5l25B0.2	3.00	-	2.07	1.43	0.23
OPJ23	12.5l25B0.2	2.67	-	1.82	1.19	0.24
OPJ24	20.0l25B0.2	2.45	-	1.62	1.09	0.29

Table 5.2b Observed maximum magnitudes for the sand movements during the open shield pipejacking tests, as defined in Fig. 5.3

TEST NUMBER	TEST CODE	MAXIMUM OBSERVED MAGNITUDES OF MOVEMENT (mm) Horizontal Movements 1	2	3 (degrees)	4	5	6
OPJ1	4.5dLB0.1	7.0	2.0	29	-1.0	-	2.5
OPJ2	12.5dLB0.1	6.0	2.0	28	-1.5	-	2.0
OPJ3	20.0dLB0.1	5.5	-	27	-2.0	-	1.0
OPJ4	4.5lLB0.1	8.0	3.0	27	-3.0	-1.0	3.0
OPJ5	12.5lLB0.1	6.0	2.0	36	-2.0	-	4.0
OPJ6	20.0lLB0.1	5.0	1.5	30	-1.5	-1.0	1.5
OPJ7	4.5dLB0.2	7.5	5.0	18	-2.0	-	1.5
OPJ8	12.5dLB0.2	7.0	4.0	21	-1.5	-1.0	2.0
OPJ9	20.0dLB0.2	6.5	3.5	11	-2.0	-1.5	1.5
OPJ10	4.5lLB0.2	8.5	5.5	34	-1.5	-	4.0
OPJ11	12.5lLB0.2	7.5	5.0	33	-1.5	-1.5	2.5
OPJ12	20.0lLB0.2	7.0	4.5	11	-1.5	-2.5	2.5
OPJ13	4.5d25B0.1	6.0	2.5	36	-2.0	-1.0	1.0
OPJ14	12.5d25B0.1	4.0	1.5	34	-1.0	-1.0	2.0
OPJ15	20.0d25B0.1	5.5	1.5	33	-1.5	-1.0	1.0
OPJ16	4.5l25B0.1	9.0	3.5	37	-1.0	-1.5	3.0
OPJ17	12.5l25B0.1	8.0	3.0	39	-2.0	-1.0	2.0
OPJ18	20.0l25B0.1	7.5	2.5	26	-2.0	-	1.5
OPJ19	4.5d25B0.2	7.0	5.0	39	-0.5	-1.5	6.0
OPJ20	12.5d25B0.2	6.5	4.0	30	-1.5	-2.0	2.0
OPJ21	20.0d25B0.2	4.5	4.5	20	-2.5	-2.0	0.5
OPJ22	4.5l25B0.2	9.0	6.5	33	-2.0	-1.5	1.0
OPJ23	12.5l25B0.2	7.5	4.0	27	-1.5	-1.0	2.0
OPJ24	20.0l25B0.2	6.5	5.0	16	-2.0	-	5.0

Table 5.2b Observed maximum magnitudes for the sand movements during the open shield pipejacking tests, as defined in Fig. 5.3, continued

TEST NUMBER	TEST CODE	MAXIMUM OBSERVED MAGNITUDES OF MOVEMENT (mm) Horizontal Movements - Longitudinal Plane 7	8	9	Vertical & Horizontal Movements - Perp. Plane 10*	11^
OPJ1	4.5dLB0.1	1.5	1.5	-2.5	5.0	2.0
OPJ2	12.5dLB0.1	2.0	1.5	-2.0	-	-
OPJ3	20.0dLB0.1	2.5	2.5	-1.5	4.5	2.0
OPJ4	4.5lLB0.1	4.0	-	-3.0	7.2	3.0
OPJ5	12.5lLB0.1	4.0	-	-2.0	-	-
OPJ6	20.0lLB0.1	4.0	-	-2.0	6.3	3.0
OPJ7	4.5dLB0.2	3.0	3.0	-5.0	16.0	2.0
OPJ8	12.5dLB0.2	2.5	2.0	-3.0	-	-
OPJ9	20.0dLB0.2	2.0	3.0	-2.0	15.0	5.0
OPJ10	4.5lLB0.2	4.0	2.5	-4.5	15.5	5.0
OPJ11	12.5lLB0.2	3.0	-	-4.0	-	-
OPJ12	20.0lLB0.2	3.5	-	-2.0	15.0	5.0
OPJ13	4.5d25B0.1	6.0	2.5	-2.0	4.5	2.0
OPJ14	12.5d25B0.1	4.0	2.0	-2.0	-	-
OPJ15	20.0d25B0.1	7.0	2.0	-1.5	4.0	1.5
OPJ16	4.5l25B0.1	3.5	3.0	-3.0	7.0	2.0
OPJ17	12.5l25B0.1	2.0	2.0	-2.0	-	-
OPJ18	20.0l25B0.1	3.0	3.0	-2.0	6.8	2.0
OPJ19	4.5d25B0.2	3.5	4.5	-5.0	14.0	5.0
OPJ20	12.5d25B0.2	4.5	3.0	-5.0	-	-
OPJ21	20.0d25B0.2	1.0	4.0	-3.5	13.0	5.0
OPJ22	4.5l25B0.2	4.0	3.0	-5.0	14.0	5.0
OPJ23	12.5l25B0.2	3.0	2.5	-4.0	-	-
OPJ24	20.0l25B0.2	4.0	5.0	-3.0	13.0	4.0

Notes:
* Vertical movement at 50mm above pipe centreline
^ Maximum observed horizontal movement

the different tests. Table 5.2a gives the extents of the various regions of movement as defined by Fig. 5.3, and Table 5.2b gives the maximum observed magnitudes for particular areas. Not every detail of these tables is discussed, only the more interesting details, although the other values are given for completeness.

5.3.1 Longitudinal Plane Test Results

The discussions in this section refer to Figs. 5.4 to 5.9, which represent the results from six of the tests in this series. Table 5.2a and b can be used to obtain information on the other tests. A complete set of contour plots for this test series is presented in Appendix B. It is interesting that the movements only extend up to approximately three diameters from the shield or pipe, except for the loose state tests above the overcut in which case the movements extend to the surface.

5.3.1.1 Horizontal Movements

In front of the shield, the forward extent of the movements decreases, as does the vertical extent above the crown of the shield (dimensions A and B), as the C/D ratio (cover depth to pipe diameter) increases. This would seem reasonable as the ease with which the sand can be forced forward must reduce as the depth, and hence the mean normal effective stress, increases. The sand consequently finds it easier to move into the shield. The reduction in forward movement in front of the shield, as the C/D ratio increases, is reflected by the reduction in maximum magnitude of the movements, both at the invert and crown of the shield, which also indicates that the sand is being taken up into the shield rather than moving forwards.

The horizontal extent of the movements in front of the shield is generally only slightly less for the loose state tests when compared with the dense state tests, for the same test conditions, although the maximum magnitudes in the loose sands are greater. The similarities in extents must be related to the equlibrium of forces pushing the sand forwards and the forces allowing the sand to enter the shield. For the loose state tests, the sand can move forwards easier due to the greater capacity for compression and this accounts for the larger maximum magnitudes when compared with the dense state tests. However, the loose sand can also move more easily into the shield and pipe, also due to the greater capacity for compression. For the dense state tests, the sand finds it relatively difficult to move forwards due to the density of the material being high. For similar reasons the sand also finds difficulty in moving into the shield due to the compression required. However, due to the forward jacking movement being below that required to form a plug within the shield for the dense state tests between exavations, the sand can more readily move into the shield, and the movements produced are therefore reduced to a level similar to the loose state tests.

The above observations are similarly true for the tests conducted in the 25B grade sand, although due to the slightly greater density than for the Leighton Buzzard sand, the extents are slightly larger. From Table 5.2a it can be seen that the extents in the compression regions are consistently larger by approximately 10%, although this does vary and the extents in regions of dilation are generally similar or less than the corresponding values for the tests in the Leighton Buzzard sand. The maximum magnitudes given in Table 5.2b show a greater variability, although the general trend is for the magnitudes in the 25B grade sand to be larger in regions of compression and smaller in regions of dilation when compared to the Leighton Buzzard sand.

From Table 5.2a the value of dimension K, vertical downwards movement at the shield invert, increases with increasing C/D ratio for all the tests, with the loose state tests producing the greatest increase. Combining this with the reductions in the values of dimensions A and B, suggests that this region of significant movement is moving downwards and inwards towards the shield. This ties in with the observations discussed previously.

There is a distinct shear plane between the positive horizontal and negative horizontal movements extending from the crown of the shield. The angle of this shear plane to the horizontal varies quite considerably from 11° to 39°, although most values lie close to 33°. This angle was measured over a length close to the crown of the shield. It would be expected that the angle would decrease as the C/D ratio increases due to the general reductions in extent of the ground movements in front of the shield, mentioned earlier. It would also be expected that this shear plane is influenced by the angle of the cutting edge of the shield, which is 35^{o}, or to the natural slope of the sand, which is of the same order. There seems to be a pattern that emerges for the shear plane angles as the C/D value increases. The angle appears to be approximately constant as the C/D ratio varies from 4.5 to 12.5 and it then decreases for the C/D ratio of 20. This reduction is quite dramatic for tests OPJ9 and OPJ12, corresponding to an overcut ratio of 0.2 in dense and loose Leighton Buzzard sand respectively, where the reduction in angle is 10^{o} and 22^{o} respectively. Tests OPJ21 and OPJ24 also show a large reduction in the value of the shear angle (10^{o} and 11^{o} respectively). This seems to suggest that the shield size and cover depth have an influence, as also do the local effects around the crown of the shield such as arching. This could possibly be due to the increased dilation at the crown of the shield for higher C/D ratios, which is shown in the volumetric strain plots (Figs. 5.10, 5.11, and 5.12). These plots are dicussed later in this section.

The movements across the top of the shield seem to be quite complex in nature, and do not seem to correspond to any distinct pattern. Studying the contour plots for tests OPJ1, OPJ2,and OPJ3, the movements seem to generate an area of random movement directly above the shield. This area seems to affect the displacement contours and will therefore influence the extents and magnitudes of the movements. The random area is caused because it lies between areas of soil moving in opposite directions. This causes a circular motion effect on the soil which, due to its particulate nature, generates indistinct movements. This area is discussed in greater detail later in this section. It is obvious from the contour plots that the vertical extent of this random area decreases with increased C/D ratio. This seems sensible as the movements show a general reduction in dimension E in Table 5.2a as the C/D ratio increases, due to increased vertical stresses, although tests OPJ1, OPJ2 and OPJ3 seem to remain constant.

The horizontal extent of the movements behind the shield increases with increased C/D values (dimension C). This produces an engulfing effect on the movements at the overcut, shown quite clearly by tests OPJ1 and OPJ2. The extent of the vertical movements at the overcut are dramatically reduced by these horizontal movements over the shield. One test does not appear to follow this pattern, test OPJ22 (Fig. 5.13). This shows the overcut movements swamped by the horizontal movements over the shield at a C/D ratio of 4.5, with only some draw-along movements occurring close to the pipe. Tests OPJ23 and OPJ24, in the same series, show the expected patterns. Further investigation of the photographs, from other stages of test OPJ22, revealed that this was not clearly borne out anywhere else and so could be due to a localised area of non-uniform density, which was a potential problem with the 25B grade sand due to segregation of the particles (Chapter 4, Section 4.6). This does, however, illustrate how quite localised variations within the soil can dramatically influence the ground movements produced.

At the shield overcut, there is apparently not much difference between the loose and dense state tests, with the vertical extent of this area of movements decreasing with an increase in C/D ratio. This is primarily due to the engulfing action of the backward horizontal movements over the shield, mentioned earlier. However, the vertical extents and general boundary to the contours for the loose state tests in this area, are much less well defined, which is indicated by the broken contour lines. There is some movement beyond the extents shown, but the magnitudes are small, and the directions of these movements are such that general patterns are difficult to obtain. The movements therefore do extend upwards further than in the dense state tests, which have a definite cut off. The greater variability of the movements in this area for the loose state tests is illustrated by test OPJ4, which has forward (positive) horizontal movements sandwiched between two areas of backward (negative) horizontal movements. The maximum magnitude of the displacements at the overcut for these horizontal movements is greater for the loose state tests than for the dense state tests. This is presumably because of the reduced effect of the draw-along, and, more importantly, due to the rate of dilation being lower, making the magnitude more detectable.

The horizontal draw-along due to the pipe movements is very similar for all the tests. The draw-along movements extend approximately 6 to 10mm from the pipe or shield surface, the smoother shield surface causing less disturbance. The movements show a random behaviour, which the contour plots illustrate by broken lines. These movements are discussed in the literature review (Section 2.2.1.2), for a set of experiments conducted by Uesugi et al (1988). The random movements in this region, result in gaps and dicontinuities occurring within this shear zone, allowing particles from above to move downwards and fill these gaps. Increasing vertical stresses reduce this shear zone. These tests help to explain some of the observations made in the pipejacking tests, although due to this area being quite small, only general results can be shown.

The maximum magnitude of the horizontal movements at the overcut generally decreases slightly as the C/D ratio increases for both the loose and dense state tests, although some tests show a variable response. The values in the loose tests are slightly larger. These movements are related to the engulfing effects from the backward movements over the shield and are also dependent on the draw-along material, the movement of which has been shown to be quite variable. It would be expected that the draw-along in the loose state tests would be less due to increased compression effects. This means that sand above the shear zone close to the cavity, produced by the shield moving, creating the overcut, can move horizontally and downwards more easily into this cavity.

5.3.1.2 Vertical movement

In front of the shield, both the horizontal and vertical extents of the movement 'bulb' decrease as the C/D ratio increases. This corresponds to the horizontal movements, which show a similar reduction. The increased force required to move the sand upwards towards the surface, as the C/D ratio increases, makes movement into the shield more likely. This is obviously dependent on the difference between the forces acting on the sand, and, as mentioned earlier, the relaxation of the sand that occurs within the shield after excavation is likely to reduce the force required for the sand to move into the shield. This is particularly true for the tests conducted in loose sand. There also seems to be more verticality to the movements in the loose sand. This is possibly due to there only being one measurable 'bulb' of maximum movement in front of the shield for these tests, this being discussed later in the section. The general appearance resulting from the single 'bulb', which is in fact a combination of two 'bulbs', is one of more verticality to the movements.

There are surprisingly similar extents in these tests between the two sized shields. Theoretically the 0.2 overcut ratio, with its larger diameter, should influence a larger mass of sand. However, as mentioned previously, a plug only forms in the shield after a finite jacked movement. This means that up to this point the movements are very similar for both shields, any differences being caused by the larger shield area mobilizing slightly more soil close to the cutting edges.

There are generally two bulbs of movement in front of the shield for the dense state tests, one at the crown and one close to the invert. These must be related to the shield arrangement. The lower bulb is due to the angled cutting section of the shield adding a vertical component to the sand movements (Fig. 5.14). The cutting section at the crown of the shield should produce a downward component in the sand movements. However, due to the general upwards and outwards nature of the surrounding sand displacements, the downward movement must be absorbed by these movements as there is no evidence of any downward movement occurring beyond the shield. A contributing factor to this could be due to the stress relaxation that occurs due to the excavation process, which produces a looser sand state locally at the crown of the shield. The 'bulb' of upwards movement at the crown must therefore be due to some part of the forward movement being deflected upwards. The magnitudes of the movements within this crown 'bulb' are generally less that those at the invert. The higher compressibility of the loose state tests probably explains why tests OPJ4, OPJ5, OPJ6, and OPJ10, OPJ11, OPJ12 do not exhibit the crown movement 'bulb'. The area between the two movement bulbs in front of the shield, where the movements are less, indicates where the sand can be taken into the shield more easily during the forward jacking operation. This corresponds to a similar area on the horizontal movement contour plots.

The area of downward movement at the shield invert is present in all the test results, although of varying size. This indicates a necessity for the release of forces in front of the shield due to the difficulties of upwards movement. The horizontal and vertical extent of this area of movement is governed by a complex interrelationship of C/D ratio, sand density and shield size. The increase in C/D ratio would tend to increase this area, reduction in density would reduce this area, and larger shield size would increase this area. On this basis, it would be expected that test OPJ9, for the Leighton Buzzard sand, and test OPJ21, for the 25B grade sand, would produce the largest extents. However, test OPJ8, for the Leighton Buzzard sand, and test OPJ18 & OPJ22, for the 25B graded sand, show the largest extents. No satisfactory explanation has been found for this observation.

At the shield overcut, the vertical extent of the sand movements for the loose and dense state tests are very different. The dense tests have a finite extent for these movements, which decreases with increasing C/D ratio and increase with larger overcut ratios. The decreasing extent with increasing C/D ratio is to be expected, as the higher stresses increase the effect of dilation and thereby cause a reduction in the extent of the movements. The increasing extent with larger overcut ratios is also expected, simply due to the greater maximum vertical movements possible at the overcut. The loose state tests, however, show no finite extent for the vertical movements, which extend to the soil surface. This would seem reasonable as the dilation rate for a loose sand is small, so the vertical extent of the movements will be large. In the case of the loose state tests, there seems to be a relatively uniform dilation rate for the lower C/D ratios. However, at the C/D ratio of 20 (test OPJ6), there is evidence of a higher dilation rate close to the overcut and then a much more gradual dilation rate extending thereafter to the surface. This would imply that that the sand is moving downwards as a block, i.e. a definite shear failure has occurred within the sand.

Behind the main area of vertical movements, due to the overcut, there are smaller downward vertical movements along the length of the installed pipe, that occur during the jacking. These are also detected in the perpendicular plane movements well after the overcut has passed. These movements occur in all of the tests, although the vertical extents and magnitudes are very variable, The magnitudes tend to be slightly greater for the loose state tests. This variability is indicated on the contour plots by dotted lines. These movements must result from the frictional draw-along of material close to the pipe. The draw-along sand movements are very erratic in nature, as mentioned earlier in this section, and the gaps created allow vertical sand movements to occur above this narrow layer of horizontal movements. The resulting vertical movements are therefore also erratic in nature.

The remaining discussion in this section is of a general nature relating to both the horizontal and vertical contour plots and volumetric strain plots. Between the upward and downward areas of movement directly above the shield there is an area of movement that does not conform to the surrounding areas, bounded by the dotted contour lines. A discussion of this area requires a combination of both the horizontal and vertical contour plots. Fig. 5.15 shows the general ideas behind why this area exists. With reference to Fig. 5.15, sand displacements at **1** are from sand in front of the shield causing upward and backward movements over the shield. The displacements at **2** are due to sand moving towards the overcut. Combining these movements with those at **3**, due to the draw-along effect on the sand caused by the shield, sets up a circular motion within the sand. Due to the particulate nature of the sand within the central area, it is particularly difficult to define any definite magnitudes or directions of movement, which are quite random in nature. The total displacement vector plots (Figs. 5.16 and 5.17) help to provide a more visual appreciation of the movements occurring around this random area over the shield, and also during the forward jacking stage of the open shield pipejacking tests as a whole. There is a definite circular motion of the sand particles around the shield.

Figs. 5.10, 5.11 and 5.12 show the volumetric strain plots for tests OPJ1, OPJ3 and OPJ4 respectively. These can be used to enhance the information obtained from the tests, by allowing relationships to be obtained between the compression and dilation effects occurring within the sand during the jacking process. These effects can be gauged within the different areas of movement and also between these areas.

For the dense state plots, tests OPJ1 and OPJ3, there is an area of compression directly in front of the shield which extends to the limits of the movement. The largest areas of compression are concentrated close to the invert of the shield. The amount of compression decreases horizontally as one moves away from the shield and then increases again to a second maximum before decreasing to zero at the boundary of the movements. This increase in compression could be due to the vertical movements becoming less prominent at that point and allowing the horizontal compression to dominate the volumetric strain values. A zone of dilation develops close to the shield invert as the C/D ratio increases. This is due to the increase in downward spreading of the movements since the sand has greater difficulty in moving upwards where the cover depth is greater.

The area of dilation spreading outwards and upwards from the shield crown would seem to follow the path of the plane observed in the horizontal movement contour plots, between the forward movements in front of the shield and the backward movements over the shield. This area of dilation becomes more prominent at the shield crown for the higher C/D ratio plot, which indicates that there is more stress relaxation occuring at this point during the forward jacking. The compression area over the shield seems to swamp the dilation effects at the overcut as the C/D ratio increases. This increase in volumetric compression corresponds to a reduction in downward movements, and therefore dilation, at the overcut. The dilation areas behind the shield are similar for both tests.

Bringing in test OPJ4, a loose state test, enables the effects of sand density to be incorporated into the volumetric strain developments. It can be seen that the basic areas of volumetric strain are very similar, although the dilation area at the invert of the shield has already developed for this lower C/D ratio test. The dilation close to the crown of the shield still develops, although the compression directly at the crown, corresponding to the cutting edge of the shield, is high. Test OPJ4 does show the expected low dilation areas spreading upwards from the overcut. The addition of the results from test OPJ4 allows the approximate prediction of any of the open shield pipejacking volumetric strain plots, certainly with regard to areas of compression or dilation, and even to some extent the magnitudes.

During some of the tests the rate of jacking was varied in accordance with the test procedure outlined in Chapter 4, Section 4.7. The effect of the rate of jacking on the extents and magnitudes of the sand movements was recorded. The results for the higher jacking rate are presented in Table 5.3 and the dimensions correspond to those in Table 5.2a and b and Fig. 5.3. Only values for some of the dimensions in Fig. 5.3 are given and values recorded only if a difference is observed from the slow jacking rate results. It can be seen from the results that there was little or no effect on the extents for the loose state tests in front of the shield, and the observed magnitudes are also the same for these tests. The dense state tests, in comparison, show a small increase in extents in front of the shield both vertically and horizontally. This slight increase is also borne out in the observed magnitudes. This difference must be due to the reduced time available for the sand to move into the shield. For the loose state tests, this is obviously not detectably significant for this increase in jacking rate and must be due to the density of the sand allowing it to move into the shield with the same ease. For the dense state tests, however, the rate of jacking does have an effect, obviously causing the sand to behave more like a plug in the shield opening. For the movements at the overcut, the increased rate of jacking does seem to have an effect on the sand movements in both the loose and dense state tests. The maximum observed vertical displacement at the overcut in both density states is increased, and for the dense state tests this has led to an increase in vertical extent of the movements. The maximum horizontal movements at the overcut are however reduced. This must therefore mean that the increased jacking rate affects the

Table 5.3 Extents and magnitudes observed for increased jacking rate (compare to Table 5.2) - indicates values where there was no detectable change

TEST NUMBER	TEST CODE	EXTENT DIMENSION / PIPE DIAMETER			
		A	B	G	H
OPJ1	4.5dLB0.1	2.30	1.90	2.65	1.60
OPJ2	12.5dLB0.1	1.95	1.89	2.35	1.30
OPJ3	20.0dLB0.1	1.75	1.85	2.25	1.35
OPJ4	4.5lLB0.1	-	-	-	-
OPJ5	12.5lLB0.1	-	-	-	-
OPJ6	20.0lLB0.1	-	-	-	-

TEST NUMBER	TEST CODE	MAXIMUM OBSERVED MAGNITUDES OF MOVEMENT (mm)			
		1	2	6	9
OPJ1	4.5dLB0.1	7.5	2.0	2.0	-4.0
OPJ2	12.5dLB0.1	7.0	2.0	1.0	-3.0
OPJ3	20.0dLB0.1	6.0	-	0.5	-2.5
OPJ4	4.5lLB0.1	-	-	2.0	-5.0
OPJ5	12.5lLB0.1	-	-	3.0	-3.5
OPJ6	20.0lLB0.1	-	-	1.0	-3.0

draw-along of sand close to the pipe, seemingly reducing it. This allows more sand to move downwards into the cavity left by the overcut.

5.3.2 Perpendicular Plane Test Results

Figs. 5.18, 5.19, 5.20 and 5.21 show the results in the perpendicular plane due, to the overcut, for four tests from the open pipejacking test series. Table 5.2a and b should also be used as a reference, as this gives magnitudes and extents for all of the tests in this series. Results were only obtained from the tests with C/D ratios of 4.5 and 20.0, as this was considered adequate to investigate the trends involved with the sand movements.

5.3.2.1 Vertical movements

Substantial movements were restricted to sand contained within an area immediately above the pipe, with only very small movements to the sides and none below. These movements extend vertically upwards to a finite distance in the dense state tests, and to the surface in the loose state tests. This difference occurs due to the higher dilation rate in the dense state tests compared with that for the loose state, and also the ability of arching effects to develop within the dense sand at the tunnel shoulders. The effect is similar to the trapdoor tests conducted by Terzarghi (1943) and Steensen-Bach and Steenfelt (1991), which are described in Chapter 2. In the dense state tests, the extent decreases with increasing C/D ratio, corresponding to an increase in theeffectof dilation caused by the higher stresses. There is also a decrease in lateral extent of the movements with an increase in C/D ratio. Dilation in the loose state tests seems to be much more uniform than for the dense sand. This is probably due to local variations in sand density altering the dilation rate, which is more noticeable for the higher rates in the dense state tests. The maximum magnitudes of the vertical movements are the same for both the dense and loose state tests, and are much larger than those observed in the longitudinal plane. This is because at the perpendicular plane of observation there is no draw-along of material caused by the forward movement of the pipe. The measured sand movements are therefore solely due to the shield overcut. This is also evident from the vertical extents of these movements, which are greater in the perpendicular plane. Smaller lateral extents would also be expected if the draw-along effects were occurring.

Table 5.4 shows the vertical surface settlements observed during test OPJ4 (10mm) and test OPJ10 (20mm). Comparison of these profiles with the generally accepted error function curve is difficult due to the necessity for knowing the trough width parameter, i. If, however, it is assumed that the distance at which the movements become zero is 2.5i (standard trough width), an i value can be estimated. The settlements predicted by the error function curve can thus be estimated and these are also shown in Table 5.4. It appears that the settlement profiles in the loose sand tests do correspond to an error funtion curve quite well, which does not tie in with some of the field observations (Hansmire, 1976). However, it could be that the error function curve can be forced to fit more or less any values reasonably well depending on the i value chosen, as shown by O'Reilly and New (1982) with their formula for trough width parameter in cohesionless/cohesive soils. The field discrepancies could be due to poor choice of the i value. Ryley et al (1980) fit the error function curve to the settlement data for a tunnel constructed in cohesionless soil (Fig.2.35) with considerable success.

5.3.2.2 Horizontal movements

The contour plots for these movements consist of an 'ear shaped bulb' emerging from the side of the pipe between the crown and the springing, which reaches the surface for the loose state tests. This indicates that the horizontal movements increase close to the pipe and that these movements also increase close to the surface, due to the funnelling effects causing spreading. The movement contours seem more vertical for the dense state tests than the loose, which seem to start closer to the pipe springings and thereby cause an increase in lateral extent. The loose state tests also induce a greater magnitude of sand movement. The

Table 5.4 Surface settlement values caused by the pipejacking shield overcut compared to predicted values using the error function curve

LATERAL EXTENT OF SURFACE SETTLEMENTS (mm)	VERTICAL SETTLEMENT (mm) TEST OPJ4 L	T	TEST OPJ10 L	T
0	0.90	0.90	2.10	2.10
100	0.75	0.77	1.80	1.97
200	0.55	0.55	1.40	1.63
300	0.40	0.29	1.00	1.20
400	0.20	0.12	0.80	0.76
500	0.00	0.00	0.55	0.43
600	-	-	0.25	0.21
700	-	-	0.00	0.10

L - Laboratory test results

T - Theoretical prediction using the error function curve extent of these movements coincide with that for the vertical movements.

A comparison of these results with those obtained by other researchers is given below. The comparison is made on the basis of the total displacement vector plots produced from the vertical and horizontal contour plots (Figs. 5.22 and 5.23). These show a high vertical component to the movement with only a slight horizontal component close to the pipe springing level. The results obtained by Potts (1976), which were discussed in the literature review and presented in Fig. 2.41, show a close resemblance to the results presented in this thesis. The narrow funnelling action during propagation of movements, common to the behaviour of cohesionless materials, is repeated, especially for the loose state tests. The effect of dilation on the propagation of movements is indicated by the extent of the dense state test movements only just reaching the surface. Also noticeable is the lack of movements below the tunnel springing for both the loose and dense state tests. Potts reduced the internal pressure to induce collapse, whereas for the pipejacking tests in this thesis the overcut produced an instantaneous variation from full support to none, which could account for some differences close to the tunnel. The results of Cording et al (1976), also described in the literature review, produce similar findings (Fig. 2.47), although they do appear to show more movement below the pipe springings. Their results do show the concentrated lateral extent of the subsurface movements, whereas the lateral extent of the movements increases considerably as the sand surface is approached. Any further or more detailed comparison between these sets of data is of questionable value due to the wide difference in boundary parameters used in the tests.

The problem with the data from Potts (1976) tests, when comparing them with the pipejacking results, is that although conducted at different cover depths and densities, they had no cut off to the movements (i.e. there was no boundary to restrict the movements). Therefore it is difficult to investigate the effects of different overcut ratios with this technique. There is also the problem that Potts' work is wholly static, i.e. there is no influence from something moving within the soil as in the pipejacking tests, in which the pipe was being jacked forwards. This must have a effect on the movements observed. The tests conducted by Cording et al (1976) did have a definite boundary to the movements, due to the use of an inner pipe, and therefore should provide a better comparison. However, the problem with these results is the limited number of test results presented. Although the cover depth, the density of the sand and the overcut value are increased between the tests, only three test results are presented and with so many variables being changed between each test, no comparisons can be made between the tests. The pipejacking test results described in this thesis combine both of the above researchers work, to both reinforce and extend the ground movement data in this plane caused by the overcut ratio. From the movements observed at the overcut it is also possible to infer movements due to the total ground losses occuring for the whole operation, including face losses, by representing these losses as an equivalent overcut value (see Section 5.8.2).

5.3.3 Open Shield Pipejacking, Excavation and Face Collapse

All of the preceding results in the longitudinal plane have been based on the forward jacking part of the pipejacking operation. Excavation has been considered implicit in these results, as some sand is taken up into the shield and pipe during the jacking process and this can be considered as 'excavated' ground. As discussed in Chapter 3, Section 3.4, the excavation process is very difficult to model in any other way than that used, in order to obtain repeatablility whilst keeping the simulation simple. However, for the open face pipejacking tests excavation was required between the jacking stages of the test, in order to stop the sand simply plugging the shield and pipe opening.

As mentioned previously, the excavation process involved a careful suction technique to remove the small quantity of sand entering the shield after each forward jack. This technique proved successful without causing any detectable ground movements or collapse of the face. It was, however, thought interesting to investigate briefly the effect of over-excavation and the resulting ground movements produced. This was achieved by sucking out 'too much' sand and causing a 'run' of sand into the shield. Several of these induced collapses were investigated for different sand densities and C/D ratios. All the runs emanated from the crown of the shield, which is sensible, as this is the most unstable part of the face. Fig. 5.24 shows the extents of the sand movements in the dense state tests with C/D ratios of 4.5 and 12.5 and for the loose state tests with C/D ratios of 4.5 and 12.5. Only boundaries to the movements can be obtained rather than displacement contours, because of the large movements occurring and the 'disappearance' of sand particles. Thus only displacements close to the boundaries of the movements could be measured, and these would be of limited value. In each case the sand run continues until equilibrium is re-established. For the dense state tests, high dilation rates and arching effects between the sand mass in front of the shield and that over the shield, particularly for the higher C/D ratio, must be helping to contain the movements into a concentrated 'bulb'. For the loose state tests, due to the dilation rates being much lower, the sand movements continue up to the surface, although these movements become quite small especially for the higher C/D ratio. A comparison of these results can be made with the results obtained by Chambon and König (1991) investigating collapse in three-dimensional model tests conducted in a sandy soil. Similar patterns of movements are obtained for these tests as shown in Fig. 2.50, with a narrow concentrated 'bulb' of movements extending upwards. The collapse movements extend more uniformly from the crown to the invert level of the shield than observed in the pipejacking tests, due to the uniform reduction in face pressure rather than a localised induced failure. The results for the C/D ratio of 2 seem to extend upwards slightly more than the test with the C/D ratio of 1, although the lateral extent is slightly less. This is different from the pipejacking tests, which show a definite reduction in vertical extent with increased C/D ratios. Although this suggests an apparent increase in the effect of dilation and arching, theory would suggest otherwise. No satisfactory explanation can be offered for these observations except that there could be a different ground loss occurring at collapse, which is very difficult to accurately repeat between tests.

Fig. 2.46a and b show the collapse patterns for three-dimensional model tests in soft clay conducted by Mair (1979). The tests investigated the effects of tunnel geometry on the collapse pressure at different C/D ratios. The figures produced from these tests are not very clear, but comparing the tests with a P/D ratio of zero, for the tests conducted in sand, shows that the lateral extents are much greater in the soft clay.

Heuer (1976) conducted field studies of cases in which catastrophic collapse has occurred during soft ground tunnelling operations. Collapses in various soil types are presented and seem to show similar patterns of results to those shown above. However, the figures presented in this paper are schematic and a more detailed comparison is impossible.

5.4 THE CLOSED SHIELD PIPEJACKING TESTS

All the movements presented for this test series are in the longitudinal plane, as the movement patterns in the perpendicular plane at the overcut were identical to the open shield test results. Reference should be made to Table 5.5a and b, which gives comparative values for the extents and maximum magnitudes of the movements for each of the tests in this series. Figs. 5.25 to 5.29 show the horizontal and vertical displacement contour plots used in this discussion. The general patterns of movements obtained from these tests are obviously similar in many respects to the open shield pipejacking tests results described in Section 5.2. The main difference is that the sand moved by the shield has nowhere to go: it does not have a chance to enter the shield. This means that all the forward motion of the shield is transmitted into the sand particles, leading to movements extending further both horizontally and vertically than for the open pipejacking tests. Total displacement plots are shown in Figs. 5.30 and 5.31, for tests CPJ1 and CPJ2 respectively. These help to present, in a visual way, the points raised in the following discussion. They particularly show the large horizontal movements in front of the shield. These figures also highlight the much greater upward

Table 5.5a Observed extents of sand movements for the closed shield pipejacking tests, as defined in Fig. 5.3

TEST NUMBER	TEST CODE	EXTENT DIMENSION / PIPE DIAMETER Horizontal Movements			
		A	C	D	F
CPJ1	2.0dLB0.1	3.12	1.00	0.70	0.16
CPJ2	2.01LB0.1	3.56	0.46	S	0.28
CPJ3	4.5dLB0.1	4.70	1.20	0.98	0.34
CPJ4	4.51LB0.1	3.44	0.44	S	0.26
CPJ5	2.0dLB0.2	4.22	1.04	S	0.24

TEST NUMBER	TEST CODE	EXTENT DIMENSION / PIPE DIAMETER Vertical Movements			
		H	I	J	K
CPJ1	2.0dLB0.1	1.36	3.26X	1.90	0.22
CPJ2	2.01LB0.1	S	2.64X	1.70	0.32
CPJ3	4.5dLB0.1	1.20	6.10X	2.10	0.36
CPJ4	4.51LB0.1	S	3.38	1.74	0.16
CPJ5	2.0dLB0.2	S	4.96	2.36	0.36

X - Total surface extent of upward movements

Table 5.5b Observed maximum magnitudes for the sand movements during the closed shield pipejacking tests, as defined in Fig. 5.3

TEST NUMBER	TEST CODE	MAXIMUM OBSERVED MAGNITUDES OF MOVEMENT (mm)				
		3 (degrees)	4	6	8	9
CPJ1	2.0dLB0.1	76	-1.5	3.0	6.0	-3.0
CPJ2	2.0lLB0.1	57	-1.0	4.0	3.0	-5.0
CPJ3	4.5dLB0.1	82	-1.0	2.5	4.0	-2.5
CPJ4	4.5lLB0.1	51	-3.0	3.0	2.0	-4.0
CPJ5	2.0dLB0.2	72	-2.5	4.0	6.0	-6.0

movements in the dense state test CPJ1, when compared with the loose state test CPJ2. Test CPJ2 although showing greater horizontal extents for the movements in front of the shield, shows that the magnitude of the movements reduces quicker than for test CPJ1. The funnelling effects caused by the overcut in test CPJ2 are also evident from Fig. 5.31.

The effect of increased rate of jacking was also investigated for the closed shield pipejacking test. As expected, however, the movements in front of the shield were not affected by this increased rate in either extent or magnitude. The only detectable differences in sand movements were observed at the shield overcut and these corresponded to those observed in the open shield pipejacking tests, with increased vertical displacements for faster jacking rates.

5.4.1 Vertical movements

There is a small amount of upwards movement directly in front of the shield, although movement at this point is predominantly horizontal as would be expected. These upwards movements increase in magnitude, away from the the shield until a maximum value is achieved, whereafter the vertical movement decreases both horizontally away from the shield and upwards towards the sand surface. The maximum vertical movement for test CPJ5 (t/R=0.2) is no greater than for test CPJ1 (t/R=0.1), being 6mm, although the maximum movement is further away from the pipejack and therefore the maximum surface movement for test CPJ5 is greater. The downwards movements, close to the invert of the shield are more prominent in the closed shield tests than for the open shield tests, as expected, due to the greater quantity of sand having to move forwards. The complex relationships between depth and density, mentioned for the open pipejacking tests in this area, still prevail. This means that no distinct relationships can be obtained for this area of movement. The movements in this region for test CPJ5 are greater due to the greater shield size, than for tests CPJ1 to CPJ4 (for all of which t/R=0.1).

For test CPJ1 the horizontal extents tend to indicate a relatively direct path for the movements to the sand surface, whereas for test CPJ3, with a greater C/D ratio, a much more forwards and then upwards pattern of movement is produced. Test CPJ5, with the greater overcut ratio, exhibits a larger horizontal extent with a greater amount of mobilised sand being pushed forwards.

For the loose state tests, the vertical movements in front of the shield still show the increasing then decreasing pattern that is displayed by the dense state tests. However, the higher compression that occurs in the loose sand causes the movements to reduce much more rapidly such that, in the case of CPJ4, the movements do not reach the surface.

The vertical movements over the top of the shield and at the overcut are similar in general form to the open shield pipejacking tests, as expected, due to the arrangement being essentially the same except for the closed/open shield. The vertical movements emanating from the front of the shield in the dense state tests, tend to extend back behind the front of the shield, as did the movements for the open pipejacking tests. The backwards extent of these movements increases as the C/D ratio increases. This would be expected to continue as the C/D ratio increases still further and it becomes increasingly difficult for the sand to move upwards, so is forced to move over the shield. Similar observations were made for the loose state tests (CPJ2 and CPJ4). The greater magnitude and extent of downwards movements in these tests can clearly be seen to be squeezed backwards across the shield as the C/D increases, due to the larger bulb of upwards movements emanating from the front of the shield.

At the overcut, the dense state tests with an overcut ratio of 0.1 show a finite extent for the movements and that the extent reduces with increasing C/D ratio as for the open pipejacking tests. For test CPJ5 the vertical movements at the overcut just reach the sand surface, due to the greater magnitude of vertical movement caused by the larger overcut. The loose state tests show the vertical movements extending to the surface and dominating the movements over the shield. The maximum magnitude of the displacements at the overcut appears to decrease with increase in

C/D ratio, for both the dense and loose state tests. This value is only really dependent on the draw-along effects, so it must be that the increased C/D ratio is influencing these draw-along effects, which in turn are affecting the vertical movements at the overcut.

5.4.2 Horizontal movements

The horizontal extent of the movements directly in front of the shield increases with increasing C/D ratio, and verifies the ideas presented in the vertical movement section concerning the increasing force required for the sand to move upwards. Increasing overcut ratio also increases the horizontal extent of the movements, due to the greater area of mobilised sand in front of the shield attempts to form a deeper shear plane within the sand. The loose state tests seem to produce similar or greater horizontal extents, as in the case of test CPJ1 and test CPJ2, even with the compressibility of the sand being greater in the loose state tests. This implies that the sand in the loose state tests finds it easier to move horizontally, whereas in the dense state tests the movements are forced to the surface more quickly. When the movements reach the sand surface they tend to spread. Obviously the pattern of the movements directly in front of the face of the shield is initially almost entirely horizontal, as expected. The movements then reduce up towards the sand surface and then increase again slightly at the surface, due to the spreading effect mentioned above.

The shear plane, that lies between the forward movements in front of the shield and the backwards movements over the shield, is much more vertical than for the open shield pipejacking tests. The angles, measured to the horizontal close to the crown of the shield, range from 51^{o} to 82^{o}, compared with approximately 33^{o} for the open shield pipejacking tests. This implies that the cutting edge of the open pipejacking shield does influence the angle of this plane. The dense state tests produce a noticeably higher angle (72^{o}-82^{o}) compared with the loose state tests, which have angles of 51^{o} and 57^{o}. This suggests that there is more upwards and backwards movement over the shield for the loose state tests.

The movements over the top of the shield extend to the surface for all the tests. For the dense state tests, the movements close to the shield are related to the shield overcut, whereas further away they are caused by the spreading effect of the movements in front of the shield. Test CPJ5 has the greatest backwards horizontal movement close to the shield, due to the influence of the larger overcut value. The loose tests show some dependence on the movements in front of the shield, although most is due to the overcut movements which are much more dominant in the loose state tests. The area of random movement, found directly above the shield for all the open pipejacking tests, only occurs in these tests for the higher C/D ratio, in both the loose and dense state tests. This is attributed to the greater backwards movement over the shield wiping out any random motion over the shield.

The horizontal movements at the overcut for test CPJ1 are forced backwards and somewhat limited by the movements across the top of the shield. This does not appear to take place for the higher C/D ratio in test CPJ3. Again this is probably related to the lack of the random area of movements directly above the shield, as mentioned above. The forward movements at the overcut in test CPJ5 are not significantly influenced by the movements over the shield, with the forward movements extending to the surface.

5.5 THE PIPEBURSTING TESTS

5.5.1 Longitudinal Plane Results

The movements presented in this section are based on the bursting head moving forwards a distance of 20mm. Therefore, as with the pipejacking tests, these represent only a 'snapshot' of the movements that would occur as the total bursting head passed. This 20mm forward jacking distance means that a maximum of 4mm of upwards movement can occur immediately adjacent to the bursting head, due to its angle of 12^{o}.

The general form of the movements observed during the pipebursting tests are shown in Fig. 5.32. Table 5.6a and b presents the extents and maximum magnitudes of movements obtained from the contour plots for each of the pipebursting tests. Reference should be made to Figs. 5.33 to 5.36, which show the displacement contour plots obtained from the tests conducted in the Leighton Buzzard Sand for the upsizing (D_f/D_o) ratio of 1.2. Appendix B contains the complete set of results obtained from this test series. Figs. 5.37 and 5.38 should also be referred to, as these show the vector displacement plots for tests PB1 and PB3 respectively and help to illustrate more visually the points being discussed in the following section.

5.5.1.1 Vertical movements in the dense state tests.

The movements are shown in Figs. 5.33a and 5.34a. As expected, there is a high proportion of upwards movement above the bursting head. These movements disperse as they move towards the surface, spreading forwards well ahead of the burst position and backwards behind the overburst. The angle of the shear plane, between the upwards movements over the burster and the downwards movements due to the overburst, to the vertical, varies from -16^o to 18^{o*}(Table 5.6b), i.e. the plane varies from in front of the overburst to behind it. This seems to depend on the C/D_o ratio, for the lower C/D_o ratio tests the plane is behind the overburst whereas for the higher C/D_o ratio test it is in advance of the overburst. This must be due to the sand finding it easier to spread with the lower C/D_o ratio. The maximum 4mm displacement drops to 1.8mm at the sand surface for test PB1, and to 1.0mm for test PB2, which is not quite a 50% reduction for a doubling of the C/D ratio.

The downward movements at the overburst extend a finite distance above it. The maximum magnitudes are the same, although the extent is less for test PB1. Consideration of the dilation rates alone, however, would suggest that the extent should be greater when compared with PB2 (which has a higher C/D_o ratio and thus a greater mean normal effective stress at this point). This discrepancy in the extents is attributed to the

*for the Leighton Buzzard sand and from -27^o to 34^o for the 25B grade sand

Table 5.6a Observed extents of sand movements for the pipebursting tests, as defined in Fig. 5.32

TEST NUMBER	TEST CODE	EXTENT DIMENSION (mm) Vertical Movements A	B	C	K
PB1	2.6dLB1.2	680	160	140	-
PB2	4.9dLB1.2	940	200	220	-
PB3	2.6lLB1.2	112	S	-160	380
PB4	4.9lLB1.2	224	S	-312	480
PB5	3.8dLB1.7	1020	152	144	-
PB6	7.0dLB1.7	1172	192	190	-
PB7	3.8lLB1.7	115	S	-220	380
PB8	7.0lLB1.7	428*	S	-192	480
PB9	2.6d25B1.2	640	100	156	-
PB10	4.9d25B1.2	748	160	80	-
PB11	2.6l25B1.2	192	S	136	308
PB12	4.9l25B1.2	312*	S	136	384
PB13	3.8d25B1.7	800	160	80	-
PB14	7.0d25B1.7	1000	160	116	-
PB15	3.8l25B1.7	400	S	136	304
PB16	7.0l25B1.7	460*	S	140	400

Notes:

* - Extent measurement not taken at surface.

S - Vertical movements reach surface of sand.

K - Surface extent if vertical movements caused by the overburst, reach the surface.

Table 5.6a Observed extents of sand movements for the pipebursting tests, as defined in Fig. 5.32, continued

TEST NUMBER	TEST CODE	EXTENT DIMENSION (mm) Horizontal Movements D	E	F	G
PB1	2.6dLB1.2	368	332	88	104
PB2	4.9dLB1.2	600	348	188	252
PB3	2.6lLB1.2	132	100	S	68
PB4	4.9lLB1.2	288*	268	S	80
PB5	3.8dLB1.7	688	336	80	160
PB6	7.0dLB1.7	860	336	268	100
PB7	3.8lLB1.7	112	172	S	28
PB8	7.0lLB1.7	540*	212	S	100
PB9	2.6d25B1.2	388	216	96	136
PB10	4.9d25B1.2	488	276	116	172
PB11	2.6l25B1.2	172	112	S	138
PB12	4.9l25B1.2	360*	240	S	136
PB13	3.8d25B1.7	548	252	96	68
PB14	7.0d25B1.7	700	148	132	172
PB15	3.8l25B1.7	428	180	S	120
PB16	7.0l25B1.7	460*	280	S	122

Table 5.6a Observed extents of sand movements for the pipebursting tests, as defined in Fig. 5.32, continued

TEST NUMBER	TEST CODE	EXTENT DIMENSION (mm) Perpendicular Plane Movements H	I	J
PB1	2.6dLB1.2	S	380	560
PB2	4.9dLB1.2	S	288	850
PB3	2.6lLB1.2	S	200	360
PB4	4.9lLB1.2	620	272	288
PB5	3.8dLB1.7	S	220	600
PB6	7.0dLB1.7	S[x]	272[x]	648[x]
PB7	3.8lLB1.7	S	252	380
PB8	7.0lLB1.7	544	232	328[*]
PB9	2.6d25B1.2	S[+]	-	420[+]
PB10	4.9d25B1.2	S	328	960[^]
PB11	2.6l25B1.2	S	220	428
PB12	4.9l25B1.2	740	296	344
PB13	3.8d25B1.7	S[x]	248[x]	628[x]
PB14	7.0d25B1.7	S[x]	304[x]	688[x]
PB15	3.8l25B1.7	S	276	468
PB16	7.0l25B1.7	696	256	340[*]

Notes:

S - Vertical movement reach surface of sand.
+ - Movements close to start of bursting operation.
x - Movement midway through bursting operation - full expansion movements too great for tank.
^ - This extent could be affected by edge effects from tank.

Table 5.6b Observed maximum magnitudes for the sand movements during the pipebursting tests, as defined in Fig. 5.32

TEST NUMBER	TEST CODE	MAXIMUM OBSERVED MAGNITUDES OF MOVEMENT (mm)				
		1	2	3	4	5
PB1	2.6dLB1.2	1.8	-1.5	2.0	-2.0	2.0
PB2	4.9dLB1.2	1.0	-1.5	3.0	-1.5	1.5
PB3	2.6lLB1.2	0.6	-2.5	2.0	-1.5	1.5
PB4	4.9lLB1.2	-	-2.0	2.0	-1.0	2.0
PB5	3.8dLB1.7	2.1	-1.5	2.0	-2.0	2.0
PB6	7.0dLB1.7	0.8	-1.5	3.0	-1.5	1.5
PB7	3.8lLB1.7	0.3	-2.5	2.0	-1.5	1.5
PB8	7.0lLB1.7	-	-2.0	2.0	-1.0	2.0
PB9	2.6d25B1.2	2.0	-1.5	2.5	-2.5	1.5
PB10	4.9d25B1.2	1.3	-1.5	3.0	-1.5	1.5
PB11	2.6l25B1.2	0.8	-2.0	2.5	-1.5	1.5
PB12	4.9d25B1.2	-	-2.0	2.0	-1.0	2.0
PB13	3.8d25B1.7	2.1	-1.5	2.5	-1.5	2.0
PB14	7.0d25B1.7	1.1	-1.5	2.5	-1.5	1.5
PB15	3.8l25B1.7	0.8	-2.0	2.0	-1.5	1.5
PB16	7.0l25B1.7	-	-2.0	2.5	-1.0	1.5

Table 5.6b Observed maximum magnitudes for the sand movements during the pipebursting tests, as defined in Fig. 5.32, continued

TEST NUMBER	TEST CODE	OBSERVED ANGLE OF SHEAR PLANES (Degrees)	
		6	7
PB1	2.6dLB1.2	14	-11
PB2	4.9dLB1.2	27	18
PB3	2.6lLB1.2	32	21
PB4	4.9lLB1.2	45	18
PB5	3.8dLB1.7	27	-16
PB6	7.0dLB1.7	32	18
PB7	3.8lLB1.7	24	22
PB8	7.0lLB1.7	55	18
PB9	2.6d25B1.2	18	-27
PB10	4.9d25B1.2	27	10
PB11	2.6l25B1.2	34	34
PB12	4.9l25B1.2	27	8
PB13	3.8d25B1.7	30	18
PB14	7.0d25B1.7	34	27
PB15	3.8l25B1.7	18	31
PB16	7.0l25B1.7	34	14

Note: Negative angles indicate plane is behind overburst.

increased engulfing effect of the upwards movements above the burster in test PB1.

5.5.1.2 Vertical movements in the loose state tests.

The movements are shown in Figs. 5.35a and 5.36a. The vertical movements for the loose state tests give a different pattern compared with the dense state tests. The upwards movements directly above the burster are similar, except the compression of the sand in these tests is greater and therefore the movements attenuate quicker. This reduces the maximum vertical movement at the surface to 0.6mm for test PB3 (one third of the value for the equivalent dense state test) and the movements stop short of the surface in test PB4. The spread of these movements is small for both test PB3 and PB4 and in fact appears to reduce for test PB4. There is a shear plane between the upwards movements close to the burster and the downwards movement caused by the overburst, as before. This plane varies from 18^{o} to 22^{o} to the vertical for the tests in the Leighton Buzzard sand. For these loose state tests there is therefore, a consistent pattern for the angle of this shear plane. The angle is greater for tests PB3 and PB7 (with the lower C/D_o ratio), the angles being 21^{o} and 22^{o} respectively, and this drops to 18^{o} for both tests for the higher C/D_o ratio, i.e. the plane becomes more vertical. This must be due to the increased verticality of the movements caused by the increased distance to the surface. Also, due to the higher stresses, there is a reduction in the extent of the downward movements at the overburst, which reduces the forward encroachment of these movements. This is similarly true for the tests conducted in the 25B grade sand, although the difference in angle is much greater. The angle of the planes in tests PB11 and PB15 are 34^{o} and 31^{o} respectively, and these drop in tests PB12 and PB14, with the higher C/D_o ratio, to 8^{o} and 14^{o} respectively.

The downward movements are dominant in these loose state tests. The movements extend to the surface and spread laterally, making the funnelling effect of the sand quite obvious.

5.5.1.3 Horizontal movements in the dense state tests

The movements are presented in Figs. 5.33b and 5.34b. One area to note is just in front of the point where the old pipe is broken out. The horizontal movements here extend well in advance of this point and the extent increases for the higher C/D ratio presumably due to the greater forces restricting upwards movement. The horizontal movements increase close to the surface as the movements spread. The shear plane, separating the forward movements from the backward movements over and behind the overburst, varies from 14^{o} to 27^{o} to the vertical in tests PB1 and PB2 respectively. Increasing the C/D_o ratio increases this angle, i.e. it becomes less vertical, and this is borne out by the results from other dense state tests in the Leighton Buzzard sand and also in the corresponding test in the 25B grade sand. This variation in angle indicates an increase in upwards and backwards movement at the overburst with increasing C/D_o ratio.

As expected, the total surface extent (dimensions D and E in Table 5.6a), is the same as for the vertical movements (dimension A in Table 5.6a). The forward horizontal movements at the overburst are engulfed by increasing backwards movements caused by the burster at the lower C/D ratio, and this reduces the vertical extent of these movements.

5.5.1.4 Horizontal movements in the loose state tests

The movements are presented in Figs. 5.35b and 5.36b. The horizontal movements in these tests are split into three distinct regions, all of which reach the surface for the lower C/D ratio. The forward horizontal movements over the burster extend slightly in advance of the burster head. The extent of the movements is reduced when compared with the dense state tests. For the angle of the shear plane, between the forward and backward movements at the overburst, a similar pattern emerges as for the dense state tests, with an increasing angle (i.e. becoming less vertical) for an increasing C/D_o ratio. This is consistent throughout all the loose state tests. The angles are larger than those observed in the dense state tests, due to the increased horizontal and vertical movements at (or influence of) the overburst.

The two regions of seemingly opposing movements over and behind the overburst, form the horizontal components to the funnelling movements for the overburst. The total displacement vector plot for test PB3 (Fig. 5.38) shows this funnelling effect at the overburst quite clearly. If this is compared to the total displacement vector plot for test PB1 (Fig. 5.37), a dense state test, the upwards movements are more dominant and there is only a small amount of downwards movement at the overburst.

5.5.2 General Points Concerning the Longitudinal Plane Pipebursting Test Results

In addition to Figs. 5.33 to 5.36, Figs. 5.39 to 5.42 for tests using a D_f/D_o ratio of 1.7 in Leighton Buzzard sand should also be considered. The main difference between the higher and lower D_f/D_o ratio tests is the extent of the movements in front of, and directly above, the burster head. The movements close to the overburst are very similar in both test series, which is to be expected, as nothing in this area has been changed between the two tests. The extents of the vertical and horizontal movements were expected to increase, due to the greater area of the burster exposed to the sand at any given moment. The implications for services or structures of the larger extents of the movements are discussed in Section 5.10.2. Due to the larger length of plaster pipe being broken out in the higher D_f/D_o ratio tests there was an increased instability and more uneven break out. This caused areas of leakage along the length of pipe being broken out, particularly close to the tip of the bursting head. This is clearly shown in Figs. 5.39 and 5.41 (for tests PB5 and PB7) on both the horizontal and vertical contour plots. The movements in the affected areas are still in the correct direction, either upward or forward, but they are reduced due to the soil entering the plaster pipe. This problem was particularly evident in the more unstable loose state tests at lower C/D_o ratios.

Comparison of the tests conducted in Leighton Buzzard sand with those in the 25B grade sand shows that the results are very similar. However, the magnitudes of the movements at the surface above the burster are generally greater for the 25B grade sand due to its slightly greater density. This allows less compression to occur due to the more restricted particle movement, because of the better grading. At the overburst this situation is obviously reversed with the 25B grade sand producing lesser movements and extents due to higher dilation rates.

The dense state tests provide the upperbound to the movements directly over the bursting head, i.e. in the compression area. The loose state tests, however, provide the upperbound to the movements at the overburst. The tests in the loose and dense states therefore produce two different potential movement profiles for any adjacent services or structures. This is discussed further in Section 5.10. This difference in movements patterns is shown quite clearly by the total displacement vector plots, Figs. 5.37 and 5.38. The dense state test shows predominantly upwards movements over the burster, which spread up towards the surface in advance and behind the bursting unit. The extent of the upwards movement behind the bursting unit for the dense state test is due to there being less restriction on these movements provided by the small extent of the downward movements at the overburst. In contrast, with the loose state test, although still exhibiting the upward movements over the burster, the upwards movements reduce in magnitude more rapidly and the forward spreading is somewhat reduced. The downward movements, caused by the overburst, dominate the movement patterns in the loose state test, encroaching in advance of the overburst and thereby reducing the backwards spreading of the upward movements. The concentrated funnelling effect caused by the overburst is quite evident.

In order to understand the relationships between the areas of compression and dilation during the pipebursting operation, volumetric strain plots can be produced from the horizontal and vertical displacement contour plots. Two volumetric strain plots are presented in Figs. 5.43 and 5.44, for tests PB1 and PB3 respectively. Some of the main features of these plots are discussed below. Reference should also be made to Figs. 5.33 and 5.35, which show the displacement contour plots for these tests.

Considering test PB1, there is a region of dilation which follows the path of the zero contour between the forward and backward movements at the overburst. The dilation region just behind the overburst, is due to the downward vertical movements caused by the overburst. The other dilation region, in advance of the bursting operation, must be due to the relative movements between an area of purely horizontal movement and an area of combined vertical and horizontal movement. The dilation at the ground surface is due to the spreading effects caused by the surface. There is a region of relatively high compression, just above the region of dilation at the overburst, caused by backwards movements over the overburst. There is always compression at the extents of the movements within the sand due to the movements reducing to zero.

Considering test PB3, there is a compression region directly over the overburst due to the backward and upward movements, and the forward and downward movements, coming together. There is dilation to the right of this caused by the vertically downward movements (settlement behind the overburst) extending up to the surface. The dilation over the burster follows the plane of zero movement in both the horizontal and vertical displacement plots. The compression region on the left is due to the vertically upward displacements dominating the movements. Dilation at the surface is due to both the spreading of the sand, caused by heave, and also the junction between this and the funnelling effects of the settlement movements. The compression region close to the surface over the overburst must be due to the opposing horizontal movements caused by the funnelling effects, this being greater than the dilation due to the downward movement of the sand. As for test PB1, there is compression close to the extents of the movements as they reduce to zero. Both the volumetric strain plots presented here show the quite complex volume changes that occur within the sand during the bursting operation, which are dependent on the relative magnitudes and directions of the displacements. It indicates that the bursting process has a significant effect on the ground and its resultant properties, and also on the longitudinal strains generated within adjacent services running both parallel and perpendicular to the pipebursting operation.

An interesting point to note is that, due to the compression region above the burster, the sand in this area in the loose state tests would be expected to become progressively denser as the test proceeded. By the time the overburst reaches any point throughout the pipebursting operation, the sand is in a denser state than before the bursting, therefore the dilation rate would be expected to be higher and thus the movements at the overburst less, (if it were possible to compare them to the movements that would have been caused when the sand was at its original density). It is difficult to assess this effect as the compression always occurs. However, there is still a large difference in the movements between the loose and dense state tests, therefore the effect seems to be small. Presumably at higher C/D values the effect would be greater.

It was noticed during the tests that directly above the burster the broken out pieces of plaster pipe stay close to it. However, these pieces of plaster pipe are irregular in both shape and size and move erratically as the burster moves forwards, which enables gaps to form between them. The sand is thus able to move downwards to fill these gaps causing some erratic sand movements in this region, illustrated in Fig. 5.45. The higher the C/D value the smaller the pieces of pipe become, causing more sand to move downwards into the increasing number of gaps. The effects are greatest in the loose state tests, although the effects do not seem to affect the overall movements since they are very localised.

The effect of increased rate of forward jacking was also investigated for these pipebursting tests. The actual extents and magnitudes of the sand movements over the burster were not detectably different for the higher rate of jacking when compared with the lower rate. However, the pipebursting operation became more unstable, i.e. the breaking out of the plaster pipe was more erratic and irregular, particularly for the smaller diameter pipe. This led to increased sand leakage and 'runs' of sand into the plaster pipe, which in several cases caused the test to be stopped completely due to the blockage caused. This increased instability obviously affected the sand movements quite significantly, the loose state tests being affected more. In several tests the upwards movements over the burster were totally obscured by the downwards movements due to leakage, and settlement was observed at the sand surface. Due to the large magnitudes of movements involved with these sand 'runs' it is difficult to obtain reliable movement contours (similar to the movements observed during the face collapse in the open shield pipejacking tests). An indication only of the effects is therefore shown in Fig. 5.46, for test PB7. The effects on the movements at the overburst, due to the increased rate of jacking are less obvious in these tests compared with the pipejacking tests. This is probably due to the smaller size of the overburst used in comparison to the overcut values. Although differences were detected in certain tests, they were very small and could have been due to the natural variability of the sand density within the test.

5.5.3 Perpendicular Plane Results

For these results, reference should be made to Table 5.6a and b and Figs. 5.47 to 5.52.

The results in the perpendicular plane were obtained at various stages throughout the pipebursting operation, although generally either early on in the bursting or near to full expansion. For test PB1 two results were obtained, one close to the start of the bursting process and one near to full expansion for a 20mm forward jacking distance, i.e. a 4mm expansion (Figs. 5.47 and 5.48). The results for the early stage show areas of movements that are greatly reduced when compared with those close to full expansion. At the early stage, the amount of plaster pipe broken out is small and directly above the burster head. This means that the movements generated are predominantly vertical and concentrated into a narrow area. Comparison of the maximum magnitude for the movements above the burster shows these are only slightly less for the early stage of the burst, compared with the full expansion stage for the same jacked distance of 20mm. This slight discrepancy is due to the slightly increased depth to the maximum induced movement at the earlier stage of the burst. Due to the reduced lateral extents of the movements at the early stage of the bursting operation compared to the latter stage for the same jacking distance, yet with only a slight difference in maximum vertical magnitude at the surface, the early stage of bursting could produce greater maximum differential movements in the soil and therefore in services running perpendicular to the bursting operation. However, due to the summation of movements as the bursting progresses, the total movements need to be considered, rather than just the last 4mm of expansion, in order to gauge the total effects on services. This is discussed in Section 5.10.

The results obtained for full expansion for test PB1 (Fig. 5.49), which are the total movements throughout the bursting process, show that some sand is disturbed below the pipe springings. However, this is not as great as might have been expected due to the fact that the bursting unit only gradually breaks out the plaster pipe, therefore the sand in this region will have only been disturbed towards the end of the expansion process. This produces some radial movements, although, due to the close proximity of the sand surface, the movements are predominantly above the pipe springings. Due to the gradual breaking out of the plaster pipe and the highly vertical nature of the movements, the extents of the movements are not that much greater than those observed in Fig. 5.47, for the last 4mm of expansion, although the magnitudes are obviously much greater for the full expansion. Comparing these extents to the those obtained in test PB2 (Fig. 5.50), using a larger C/D ratio, more movement is observed below the pipe springings due to the sand finding it more difficult to move upwards. However, due to the higher stresses in the sand, (because of the greater depth), the compression rate is increased and this tends to reduce the extents of the movements. There is also a much more definite shear plane for the vertical movements in test PB1 compared to test PB2.

Tests PB3 and PB4 (Figs. 5.51 and 5.52) are loose state tests and the results shown are for movements at full expansion. These show a considerable reduction in extents and higher compression rates (from the contour spacings) when compared with the dense state tests. The movements reach the surface in test PB3, but stop a finite distance above the burster in test PB4. The extent of the radial movements in test PB4 is greater than for test PB3, illustrating that the influence of the surface is reducing.

Fig. 5.47c shows the total displacement vector plot for the dense state test PB1, close to the start of the expansion process, and this clearly shows the concentrated vertical nature of the sand displacements. Figs. 5.49c and 5.51c show the total displacement vector plots for a dense state test, PB1, and a loose state test, PB3, at full expansion of the burster. The results for the loose state sand illustrates the more rapid decrease in magnitudes both above and below the pipe springing level, and also the reduced extents of these movements. The spreading effect due to the surface is evident in both plots.

The lower compression rates for the dense state tests indicate a much more 'block-like' movement of the sand above the burster when compared with the loose state tests. If the sand above the burster were a rigidly cemented material it would shear along two planes due to the bursting process, and a solid block of material would move upwards, with the movements close to the burster being the same as those at the surface (i.e. no compression). The findings of Robins et al (1990) indicate a zone of higher compression close to the burster (up to 300mm) and then a mass movement of the soil above. This localised higher compression zone could have been due to the influence of the pneumatic bursting unit used in the trial, vibrating the soil and locally affecting the density. The block movement of the sand above this region is rather difficult to believe as some compression must occur in the sand since it is not totally rigid. For the pipebursting tests shown in this thesis, the dense state sand is not a rigid block and therefore some compression does take place, the rate of which does reduce towards the surface. In test PB2, the 40mm-30mm vertical movements contours are spaced at 260mm, whereas the 30mm-20mm contours are spaced at 320mm. The vertical movements produce a very definite shear plane and close to this it would be expected that large amounts of dilation, due to both the vertical movements and the lateral
would occur,

movements as the sand collapes sideways. Fig. 5.53 illustrates this point.

As expected, due to its slightly higher density, the results for the 25B grade sand produced larger extents and higher magnitudes of movement compared with the Leighton Buzzard sand. The results, apart for this, are very similar for both sands. Areas of local variation in density are more noticable in the 25B grade sand tests.

The horizontal contour plots in the perpendicular plane show a similar pattern of movement to the pipejacking test results at the overcut, but with the direction of the movements reversed. There is an 'ear shaped bulb' emerging from the pipe shoulders. The magnitude of these movements reduces as they move further from the pipe and then increase slightly close to the sand surface, due to the spreading effect. The horizontal movements decrease rapidly from a relatively uniform maximum value distributed around the side of the burst, the extent of which is dependent on the amount of old pipe being broken out at this stage. The rate of reduction and extent of the horizontal movements is dependent on the cover depth and the density of the sand. For tests PB1 and PB3 the extents and magnitudes of the movements are very similar, indicating that the density has only a minor effect compared to the surface influence. The lateral extent at the surface is slightly reduced for test PB3. For tests PB2 and PB4 the density seems to have more influence, with the lateral extent due to the burster being slightly greater in the dense state tests and the vertical extent of the movements reaching the surface. In the loose state test, the vertical extent of the movements stops well short of the surface. The 'ear shaped bulb' in the loose state test seems to be directed more upwards, although the movements are reducing more rapidly than in the dense state test. It is interesting to note that for both the loose and dense state tests, the increase in cover depth does not appear to greatly increase the lateral extent of the movements close to the burster, even though the sand must find it more difficult to move upwards. This may be only manifested at higher cover depths, or it could be that the higher stresses within the sand cause a higher compression rate in this area.

If the centreline values for the vertical movement contour plots on the perpendicular plane are compared with the longitudinal plane results, which are all produced for a 20mm forward jacking distance, there are disrepancies in the results (Fig. 5.33, 5.47 and 5.48). Near the start of the bursting operation the movements compare well, but near to full expansion the influence of the overburst in the longitudinal plane significantly alters the expected movements, which are those shown by the perpendicular plane plots. There is also the effect of the horizontal component of the sand movements due to the angle of the burster. These are not detected in the perpendicular plane as the movements are two dimensional. In the longitudinal plane the horizontal movements are most noticeable in advance of the bursting operation. This is a similar situation to the pipejacking tests, in which the draw-along effects significantly reduced the overcut movements in the longitudinal plane, but not in the perpendicular plane which recorded the theoretical maximum movements. This is a problem with conducting these types of tests. Similar problems must have been experienced in the tests conducted by Swee and Milligan (1990), although no mention is made of this. However, if the vertical movements in advance of the burster unit are summed in the longitudinal plane (Fig. 5.33a and Table 5.8), the total magnitude is 12.0mm, (as the longitudinal plane displacement contour plots only represent 20mm of forward jacking movement, summation is required to obtain the total magnitudes. This is described further in Section 5.10). If this displacement is added to that obtained from the perpendicular plane (Fig. 5.49), which is 21mm, then a total maximum vertical displacement (i.e. full expansion) of 33mm is achieved. This implies that 2.5mm of vertical movement caused is by the spreading of the sand behind the overburst, since the total vertical movement at the centreline of the burst was 35.5mm. This calculation illustrates that the movements observed in the perpendicular plane do represent the movements that occur over the bursting unit during the test. A similar comparison can be made for all other tests, with the same result. A second example is given in this discussion for test PB2. The vertical movements in advance of the bursting unit (Fig. 5.34a and Table 5.8) total 8.0mm. The total movement over the bursting unit from the perpendicular plane (Fig. 5.50a) is 10.5mm, which gives a total of 18.5mm. The movements behind the overburst (Fig. 5.34a) total 1.1mm, giving an overall total of 19.5mm. This compares very well with that observed purely from the longitudinal plane (19.3mm). This is discussed further in Section 5.10.2.

As shown from the literature review in Chapter 2, there are very few data with which comparison of these pipebursting results can be made. However, the following discussion compares the perpendicular plane pipebursting results with those described by Swee and Milligan (1990), also based on model tests conducted in dense Leighton Buzzard 14/25 sand. Reference will be made to Figs. 2.14a and 2.15 from the literature review. Due to the limited data, only the surface movements in the perpendicular plane will be compared.

Comparison between these two test series is difficult and certain considerations need to addressed. In the model tests described by Swee and Milligan, the pipebursting unit is allowed to move vertically upwards as it is moved forwards, whereas in the tests described herein this is assumed to have already occurred and the pipebursting unit runs along the invert of the old pipe. In addition the boundary conditions for the two test series are not exactly the same and there are insufficient data to determine how much affect the variation in boundary conditions will have on the results.

Tests PB1 and PB2 will be used for the comparison as these most closely match the Swee and Milligan (Oxford) model test conditions, with C/D_o values of 2.6 and 4.9 respectively. However the D_f/D_o ratio in the Oxford tests was 2.2 compared with model tests PB1 and PB2, in which D_f/D_o is 1.2. From Table 5.8 described in Section 5.10, the maximum vertical movements at the surface throughout the pipebursting operation (δ_v) for tests PB1 and PB2 are 35.5mm and 19.3mm respectively. The maximum possible vertical movement due to the expansion process in these tests is 46.0mm (i.e. twice the radial expansion value R_f). This is because the bursting unit during the tests is moving along the invert of the old pipe. Thus $\delta_v/R_f=35.5/23.0=1.54$ for test PB1, and for test PB2 $\delta_v/R_f=19.3/23.0=0.83$. From Swee and Milligan's results (Fig.2.15), for the test with C/D_o=2.5, δ_v/R_f=1.4, which is in good agreement with the pipebursting test results reported herein. Similarly, for the Oxford test having a C/D_o=5, δ_v/R_f=0.9, this again compares very closely to the result shown above for the Loughborough pipebursting tests. These results are shown in Fig. 5.54 and this graph can be used to predict maximum vertical movements for other test conditions.

Comparison of the lateral extents of the surface movements caused by the bursting operation in these two model test series is more difficult. Using Figs. 5.49 and 5.50, the lateral extents for tests PB1 and PB2 are 550mm and 850mm respectively and these correspond to X/D_o values of 3.0 and 4.5 respectively. In comparison, Fig. 2.15 (after Swee and Milligan, 1990) gives considerably higher X/D_o values of approximately 5.7 and 6.0 for the corresponding tests. This difference could be attributed to a number of reasons. The effect of the upwards movement of the burster itself in the Oxford tests could contribute to the increased spread, or it could be that the normalisation of the lateral surface extent using D_o might not be valid. If a comparison is made of the ratios of the extents for the Loughborough pipebursting tests (850/550=1.54) and for the Oxford model tests (150/100=1.50), they are found to be quite close. This shows that the extents are increasing in similar proportions for the same increase in C/D_o ratio. A comparison of the surface heave profiles is given in Figs. 5.55a and b. A description of how these were obtained for the Loughborough pipebursting tests is given in Section 5.10. In order to compare the lateral extents, and believing that normalisation with respect to D_o is invalid in this case due to the differences between the tests of the D_f/D_o ratio, the values are normalised using the ratio of cover depths between the two model tests. For the Oxford tests the cover depths are 62.5mm and 125mm respectively, whereas for test PB1 and PB2 with cover depths of 400mm and 800mm respectively. The ratios are thus 62.5/400 and 125/800 giving a value of 0.156 for both tests. Using this ratio to calculate the profiles, it can be seen that the profiles are quite different for the two tests with the data for the Loughborough tests dropping much more quickly away from the centreline than those for the Oxford tests. This indicates that the

Oxford tests had a greater density thereby reducing the compression rate and producing a much more 'block' like movement in the displaced soil. The discrepancies could also be due to the differences in D_f/D_o ratio between the tests. The effects of the gradual breaking out of the plaster pipe during the expansion process could also account for these differences. As mentioned earlier, this does lead to a reduction of the movements around the pipe particularly at, and below, the pipe springing level, which are only broken out later on in the expansion process such that the full expansion value is not experienced.

5.6 COMPARISON BETWEEN THE OPEN SHIELD PIPEJACKING TESTS AND THE CLOSED SHIELD PIPEJACKING TESTS

5.6.1 Dense State Test

Figs.5.4 and 5.27 and Tables 5.2 and 5.6 should be refered to when reading this section.

5.6.1.1 Vertical movements

It is clear from examination of the above figures and tables that the vertical upward movements in front of the shield are dramatically reduced for the open shield. Both the vertical and horizontal extents of the upward movement for the open shield are approximately 50% of that for the closed shield test. The downward movements at the shield invert are also reduced.

The vertical movements for the open shield tests are more localised into two areas close to the shield, one near to the invert of the shield and one at the shield crown. The closed shield tests shows a more uniform spread of movements. As mentioned in Section 5.3.1, the cutting edge in the open shield is the only position in the face where a solid thrust is provided to the sand, and due to the angled nature of this cutting edge, a vertical component of movement is induced into the sand.

The only difference, of a physical nature, between the open shield and the closed shield tests is the shield itself, and therefore the differences observed in the resulting sand movements must be solely due to this. This is clearly shown by the downward movements at the overcut, which are the same for both sets of tests. The vertical movements are very similar in both magnitude and extent, although due to the larger backwards spread of the upward movements in front of the closed shield, the extent of the downward movement is slightly reduced.

5.6.1.2 Horizontal movements

The horizontal movements exhibit a similar reduction in extent to the vertical movements in front of the shield in the open shield tests. The horizontal extent is approximately 60% that of the equivalent closed shield test and its vertical extent is only about 30%. The maximum magnitude of the movements in front of the open shield (8mm at the invert) is only slightly less than for the closed shield test (10mm uniform). However, the concentrated nature of this maximum value in the open shield test means that there is less mobilising effect on the sand. The contours for the closed shield test seem to extend horizontally at the same angle as those for the open shield contours at the invert and only become more vertical when the open shield contours end.

The shear plane between the forward and backward movements in front of, and across the top of, the shield is almost vertical for the closed shield, but much shallower in the case of the open shield (approximately 33^{o}). This is attributed to the much greater upward movement of sand in the closed shield tests increasing the angle of this plane. The arrangement of the shield therefore seems to have an influence on the angle of this plane. The angle of the plane could also be influenced by the stresses within the soil and the angle of shearing resistance of the soil. It is difficult to investigate this further with the available data.

The backward movement across the top of the shield is also reduced in extent for the open shield tests compared with the closed shield tests, although the maximum magnitude of these movements has the same value of 1mm. The forward movements at the shield overcut are very similar in both extent and magnitude for the two sets of tests. This shows that for this arrangement the shield type has little effect on the movements, although this should be investigated for further C/D ratios.

As highlighted in Section 5.4, the area of random movement directly above the shield that is present for all the open pipejacking tests, is only present for the higher C/D ratio closed pipejacking tests. For the open shield pipejacking tests the random area decreases with higher C/D ratios, which is to be expected due to the higher vertical stresses forcing the backward movements closer to the shield. The difference in the closed shield pipejacking tests could be because, at the lower C/D ratio, much more draw-along of material can occur due to the lower stresses, thus wiping out the random area (or at least making it less obvious).

5.6.2 Loose State Test

Figs. 5.7 and 5.28 and Tables 5.2 and 5.6 should be refered to when reading this section.

5.6.2.1 Vertical movements

There is a reduction in extent of the movements in front of the open shield compared with the closed shield, however the difference is not as large as for the dense state tests, being approximately 60% for both the horizontal and vertical extents. The maximum magnitude is larger for the open shield test (4mm) compared with that using the closed shield (2mm). This is due to the cutting edge of the open shield, as mentioned previously, producing an upward component to the movements. The vertical movements at the overcut seem to be similar in magnitude and extent for both tests.

5.6.2.2 Horizontal movements

The biggest differences between these plots are the movements over the shield and at the overcut. The extents for the open shield are reduced and there are differences in the movement patterns. It appears that the forward movements at the overcut for the open shield, are not as dominant as they are for the closed shield, with the backward movements over the open shield suppressing the forward movement at the overcut. There seems to be a better definition of the movements at the overcut for the closed pipejacking tests, with the funnelling effect more visible, and the movements are clearly shown reaching the sand surface. As before a similar pattern is shown in front of the shields, with the concentrated movements occuring for the open shield due to the cutting edge.

5.7 COMPARISON BETWEEN THE PIPEBURSTING TESTS AND THE CLOSED SHIELD PIPEJACKING TESTS

Reference is made to Figs. 5.25 to 5.28 for the closed shield pipejacking test results, and Fig. 5.39 to 5.42 for the pipebursting tests results. For the dense state tests, there is a definite relationship between the pipebursting test results and the closed shield pipejacking test results. This is not suprising as the main superficial difference between the tests, for the movements in front of the shield, is the angle of the face of the shield. The movements above the dotted line in Fig. 5.56, which compares the horizontal movements for pipebursting test PB5 and closed shield pipjacking test CPJ1, are very similar in terms of both extents and magnitudes.

It must be remembered, however, there are certain differences between these tests. Firstly, the shield for the pipejacking tests is 100mm long between the face and the overcut, whereas the pipebursting head has an instantaneous change from the burster face to the overburst value. The shield length for the closed pipejacking tests seems to have the effect of extending the horizontal movements over the shield, and also to cause the area of random movement to develop directly above the shield, when compared with the pipebursting tests. Secondly, the pipeburster is jacked forwards 20mm, as opposed to 10mm for the pipejacking tests. From the movements recorded this seems to mean that 10mm jacking movement in the closed shield pipejacking tests is equivalent to 20mm jacking movement in the pipebursting tests, for the test arrangement in the dense state tests used. Thirdly, the closed shield pipejacking tests have a 10mm overcut value, whereas the pipebursting tests have a 5mm overburst value.

Consideration of the loose state tests also appears to show close similarities in both magnitudes and extents for both the horizontal and vertical displacements (Figs. 5.26 and 5.41, and Figs. 5.28 and 5.42). The only differences are that there is a larger vertical extent of the movements above the burster and that the overcut/overburst movements are slightly different in magnitude and extent, which is to be expected as the overcut is twice that of the overburst used. In addition, the movements due to the overcut in the pipejacking tests are offset to the right, due to the shield length. These differences are basically due to the reasons mentioned previously. The results for both the dense and loose state tests consistently tie in for the two test series. The pipebursting tests using $D_f/D_o=1.7$ have been used for comparison, as these give a fuller picture of the pipebursting movements and therefore relate better to the closed shield pipejacking tests.

5.8 INTERPOLATION ANALYSIS

5.8.1 Interpolation Between the Open Shield Pipejacking Tests

Interpolation provides a means of obtaining the likely movements (magnitudes and extents) from a partially supported face during pipejacking, i.e. between the two extremes of full support and no support, or between degrees of over-pressurisation of the face. Here only the open shield pipejacking tests are looked at.

There are many interpolations that can be conducted, for all the magnitudes and extents of movements, in order to obtain a full description of the results for a pipejacking arrangement lying between the ranges of the tests conducted. Tables 5.2 shows the important values of magnitudes and extents, and interpolation can clearly be conducted between any of these. However, for an initial feel for the likely movements, examination of some are probably more beneficial than others. As examples, dimensions A and G, in

Table 5.2a, will be used to illustrate the interpolation process. Interpolation can be conducted from different perspectives, depending on the information required. Graphical plots are the easiest manual way of conducting the interpolation. Two graphs are plotted for each of the dimensions A and G and are shown in Figs. 5.57a and b. Fig. 5.57a shows the influence of shield size (overcut ratio), and Fig. 5.57b shows the same data, but with the emphasis on the cover depth (C/D ratio). These figures show the value of both A and G increasing with increasing overcut ratio and decreasing as the C/D ratio increases. Linear relationships have been assumed between the data points, as any other relationship cannot be justified with the small ranges of the data and the limited data points.

Similar information can be obtained for each of the other values in Table 5.2. It must be remembered with any interpolation, and particularly extrapolation, of the data that full understanding of the relationships assumed and the boundary conditions is necessary. For example the onset of a plug of soil forming within the shield for larger shield sizes may invalidate any extrapolation above an overcut ratio of 0.2.

In the perpendicular plane relationships can also be obtained. Fig. 5.58a shows the relationship between the overcut value and the maximum surface settlement for the loose state tests for different cover depths. Fig. 5.58b shows the relationship between cover depth and the maximum surface settlement for different overcut values. These two figures can be tested using the results obtained from the model tests of Cording et al (1976). Comparison in the perpendicular plane is possible as both tests record the effects due to overcut alone since no draw-along effects are incorporated into the results. The data required from two of these tests is given in Table 5.7a and b. Using Fig. 5.58b and considering test 1, maximum values for the surface settlement (7.4mm and14.8mm) can be obtained for a cover depth of 285mm for each of the overcut values (t=10mm and t=20mm respectively). Plotting these values onto an extended version of Fig. 5.58a (Fig.5.58c) allows the value of the maximum surface settlement to be obtained as 3.2mm, for an extrapolated overcut value of 4.4mm. This compares reasonably with the 3.0mm actually measured. A similar analysis can be conducted for test 2, with the result that the maximum surface settlement predicted is 3.7mm. This compares with 3.3mm actually measured. There is a greater error in this case due to the fact that the density in this test is higher than test 1 and therefore the sand movements will be less due to a greater dilation rate.

Using Figs. 5.58a and b, prediction of the maximum surface settlement above a full scale tunnelling operation can be attempted. The data for this example is given in Table 5.7c. Using Fig. 5.55a first in this case, due to the much greater cover depth, a value for the overcut is required. The data give the volume loss measured during construction. This can only be converted into an equivalent overcut value by using the error function profile and the relationship obtained by O'Reilly and New (1982) for the trough width parameter, i, in cohesionless soil given in the literature review (equation 2.4). To obtain an i value at the tunnel crown, the value of H is taken as 0.5D. This gives an i value of 0.46m. Using the relationship for the O'Reilly and New method the volume loss, Vs, is given by $Vs= 2\pi.i.W$, where W is the equivalent overcut value. In this case W=243mm. Using this in Fig. 5.58a (t=W), the maximum surface settlements for both the cover depths (C=1m and C=4m) can be obtained (27.8mm and 27.5mm respectively). If these are plotted onto an extended version of Fig. 5.58b (Fig. 5.5d) and the line extrapolated, a value of maximum surface settlement of 27.1mm can be obtained, which compares quite favourably to the measured value of 21.5mm. The main problem with this technique is that volume loss is generally used as the basis of settlement prediction. The only way of relating this to an equivalent overcut value is by the assumption of the error function curve. This curve is very dependent on the trough width parameter, i, which is calculated on the basis of a formula derived by O'Reilly and New (1982) from very few field data. Combining this with the fact that the field situation is very variable makes prediction very difficult. This variability is shown by comparison of the observed maximum surface settlement from the above example with an example having similar parameters by Peck (1969). In this case Z=10.4m, D=5.3m and V_L=1.9%, which resulted in an observed W_{max}=85mm, nearly four times as great.

Table 5.7 Data for model tests conducted by Cording et al (1976) and data from a tunnel construction reported by Boden and McCaul (1974)

	(a) TEST1	(b) TEST2
D (mm)	146.0	143.0
Z (mm)	356.0	432.0
C (mm)	283.0	361.0
t (mm)	4.4	5.6
W_{max} (mm) (at sand surface)	3.0	3.3
Relative Density (%)	35	65

(c) Tunnelling data

D (m)	4.15	
Z (m)	10.0	
C (m)	7.93	
V_{loss} (%)	2.0	($0.27 m^3/m$)
W_{max} (mm) (at ground surface)	21.5	
Slurry (bentonite) shield construction in sandy gravel		

5.8.2 Interpolation Between the Closed Shield Pipejacking Tests

This tests series was limited to five tests since these were primarily conducted as a comparison for the open shield pipejacking tests, rather than a complete test series in its own right. However, it has been shown that these tests are able to provide a link between the pipejacking test results and those obtained from the pipebursting tests.

As they stand, these tests can provide an insight into the effects of overpressuring the face and increasing the C/D ratio. Interpolation can be conducted between all the values of magnitudes and extents in Table 5.5. Fig. 5.59 shows one example of the graphical interpolation between C/D ratio and extent A from the table, which is the length of ground surface affected by the movements. As before, care needs to be taken over the boundary conditions. In the example given, extrapolation in theory can be conducted for values of C/D ratio greater than 4.5, however it would be expected that the extent A will probably decrease eventually, rather than continuing to increase.

The single test for the shield with the overcut ratio of 0.2, provides the possibility of extending the interpolation to other sized shields. However as the C/D ratio for this test was only 2.5, which does not relate directly to the open pipejacking tests, the movements can only be inferred. The reason for not conducting these closed pipejacking tests for higher C/D ratios has been discussed earlier in Section 4.9.

5.8.3 Interpolation Between the Open Shield Pipejacking Tests and the Closed Shield Pipejacking Tests

Interpolation between these tests in a numerical sense is difficult, as only two tests from each series can be directly related, due to the difficulties of conducting closed shield pipejacking tests at higher C/D ratios. Tests OPJ1 and OPJ2, using the open shield, relate to tests CPJ3 and CPJ4 respectively, which use the closed shield. These are able to give an idea of the effects of the shield on the ground movements in different densities of sand and it is possible to interpolate between the magnitudes and extents for varying degrees of face support. Fig. 5.60 illustrates this in graphical form for the horizontal extent of the movements directly in front of the shield and an overcut ratio of 0.1. The relationships for different densities are almost parallel indicating a very uniform increase in extents with increasing degree of face support.

5.8.4 Interpolation Between the Pipebursting Tests

As for the open shield pipejacking tests, numerous interpolations can be made between the various magnitudes and extents for the tests, which are shown in Table 5.6. Fig. 5.61a shows the graphical interpolation between different D_f/D_o ratios and the observed surface extent for the vertical movements. As shown, the effect of different C/D ratios and density can be incorporated into the graph. It is important to realise the boundary conditions for this graph. There is a lower bound value of D_f/D_o ratio that cannot be passed. This relates to the fact that the internal diameter of the old pipe is very close to the pipeburster tip during breaking out. In the tests the vertical distance from the pipe invert to the tip of the burster is 125mm, if the internal diameter of the old pipe is less than this the pipeburster will not fit into the old pipe. There is also an upper bound value when the maximum diameter of the burster and the internal diameter of the old pipe are almost the same, i.e. a size for size replacement: if the old pipe were any larger the burster would fit inside the pipe and not be able to break it out.

A second graph (Fig. 5.61b) shows the relationship between the maximum magnitude of the vertical surface movements obtained from the longitudinal plane plots for test PB1 and PB2, against cover depth for the dense state tests. To attempt extrapolation of this graph for higher cover depths the pipebursting field trial results described by Rogers et al (1990), Table 2.1 in the literature review, will be used. This trial was conducted in a stiff clay soil, which can be considered similar in behaviour to a dense state sand. The cover depth is taken as 1.1m and an assumed maximum expansion at the burster level of

90mm is used. From Fig. 5.61b, these data give a maximum surface movement of 10.0mm. This is the movement for an expansion of 46mm at the burster level (the amount of expansion usedin the pipe bursting tests). The value of maximum surface movement can be factored up to correspond to the 90mm expansion very simply, as shown below:

$$10.0 \times \frac{90}{46} = 19.6\text{mm}$$

The recorded maximum surface movement in Table 2.1 was 19mm, which shows an excellent agreement to that predicted using the extrapolated and factored value from Fig. 5.61b. The lateral extent of the surface movements observed in the trial during the pipebursting operation is approximately 1.3-1.5m. From Fig. 5.61c, a graph showing the surface extents observed in the laboratory tests against the cover depth, the predicted lateral extent of the surface movements in the field trial is 1.1m, which is quite close to the observed value of 1.4m.

A second example of the use of Fig. 5.61b is given by prediction of the full scale laboratory trial results described in Robins et al (1990). This used a dense sand and a cover depth of 1.0m. The maximum expansion at the burster level was 90mm. From Fig. 5.61b, the maximum surface movement for a 46mm expansion at burster level is 12.0mm. Therefore, for full expansion the surface movement is shown below:

$$12.0 \times \frac{90}{46} = 23.5\text{mm}$$

From the laboratory trial data, the maximum observed surface movement was approximately 25mm, which again shows a very good correlation. Although these results are not conclusive proof of the quality of the laboratory test results, due to the limited comparative data available, the results are encouraging.

5.8.5 Interpolation Between the Closed Shield Pipejacking Tests and the Pipebursting Tests

As mentioned previously, there are definite similarities between these two test series. Interpolation can thus be conducted to establish the effects of different face angles on the sand movements. The graphical plots shown in Figs. 5.62a and b show the relationships between the angle of the face and the maximum vertical and horizontal movements, respectively, observed during the tests and normalised with respect to the maximum jacking distance. These are given as examples, although other relationships can obviously be established. The pipeburster used in these tests had an angle to the horizontal of 12^{o}, and the closed pipejacking shield, therefore, has an angle to the horizontal of 90^{o}. Different cover depths and densities have also been shown on this graph. A good indication of the movements between the different tests can be obtained from this method. The graph in Fig. 5.62a shows the values of maximum vertical movement for a buster angle of 12^{o} and 90^{o} and assumed relationships between these points shown by the dotted lines. It is expected that the movements would increase to a maximum at some angle that would induce the largest vertical movements into the soil, and then decrease to the values at 90^{o}, as these should be minimum values.

It should be noted that the smaller D_f/D_o ratio is used for interpolation between these tests as these seem to give results that are more compatible with those of the closed shield pipejacking test results. The closed pipejacking tests were conducted using different overcut ratios and these results can be used to help predict the movements for different overburst values for the pipebursting tests, due to there being such close similarity of the observed movements.

5.9 DISCUSSION OF THE PRACTICAL IMPLICATIONS OF THE GROUND MOVEMENT RESULTS OBSERVED DURING THE PIPEJACKING TESTS

The movements presented and discussed in the previous sections for the pipejacking tests are due to the jacking stage of the pipejacking operation. The excavation stage provides a very variable situation which would be difficult to model consistently. As mentioned previously, the excavation used in the tests provided a means of removing the sand without causing any detectable ground movements. The use of microtunnelling machines means that, in theory, the forward jacking and the excavation should be carried out simultaneously, thus avoiding some of the thrusting movements observed in the model tests. However, careful control is required in order to match these processes exactly and whilst maintaining the face support. As reported by DeMoor and Taylor (1991) and others, overpressurising the face causes forward movements in the soil and heave effects at the surface. This could be considered similar to the closed pipejacking tests, which allow no material to enter the shield. Even the open shield, although the face is unsupported, does move an area of sand in front of the shield forwards, mainly due to the shield itself. The difference here is that some sand can enter the shield, i.e. there is some simulated excavation. An idea of the amount of simulated excavation taking place during the forward jacking stage of the open shield pipejacking tests can be obtained by looking at the forward movements in front of the shield. Taking test OPJ4 (Fig. 5.7), the maximum movements at the crown bulb and the invert bulb are 2mm and 7mm respectively, and the minimum value is 1.5mm towards the centre of the face. If the maximum forward jacking distance of 10mm is taken away from each forward jacking movement this gives an idea of the relative movement of sand into the the shield and hence an idea of the amount of 'excavated' sand. This is shown in Fig. 5.63. It can be seen that the sand mainly enters the shield above the springing level which is the path of least resistance.

As explained in Section 4.2.8, the shields had to be exaggerated in size in order to obtain observable sand displacements at the overcut. However, by simple extrapolation of the movements obtained for the 0.2 and 0.1 overcut shields, a good approximation of smaller overcut ratios can be obtained. It can be seen from Fig. 5.64 that these become less than 1mm below an overcut ratio of 0.05, for the dense and loose state tests. Bentonite slurry injected around the pipe to reduce friction with the soil during jacking will also help to reduce the magnitude, and therefore the extents of the ground movements caused by the overcut. The general pattern of movements will however be the same and thus bentonite injection can be considered as an effective reduction in the overcut ratio. Extrapolation can therefore be carried out to establish the likely movements for an appropriate reduction in overcut ratio. Using bentonite must also influence the draw-along effects on the soil close to the pipe, presumably reducing them. As this draw-along effect reduces the observed movements at the overcut in the laboratory tests, some judgement has to be made as to the effect of the bentonite on these movements in the field situation.

5.10 THE EFFECTS ON ADJACENT STRUCTURES AND SERVICES OF THE OBSERVED GROUND MOVEMENTS

5.10.1 Introduction

There is an important practical reason for obtaining the movement patterns associated with various trenchless techniques described in the previous sections, since they allow the effects on adjacent services and structures to be gauged. Some have been outlined within the previous discussions, for example in the discussion of the pipebursting tests in the perpendicular plane. Several examples are given in this section illustrating how the soil movements can be used to estimate pipe/structure movement using the presented plots. Initially the pipebursting test results are considered followed by the pipejacking tests, with the longitudinal plane results considered before those obtained from the perpendicular plane.

It must be remembered that the pipejacking shields are exaggerated versions of the prototype and therefore the results cannot be directly related to the field situation. The results therefore require extrapolation to reduce (or increase) the effects caused by the larger shield and the overcut, as mentioned in Section 5.9. These tests are only scale models of most prototype pipejacking operations, although microtunnelling operations, a subsection of pipejacking, do operate down to diameters used in the model tests. This means that generally the extents and magnitudes need scaling up, depending on the relative size of the shield and the forward jacking distance used.

As the longitudinal plots are only 'snap-shots' of the movements that occur during a whole pipejacking/pipebursting cycle (i.e. representing either 20mm or 10mm jacked movement), the complete movement picture is obtained by the summation of a number of the same contour plots offset by 10mm or 20mm, depending on the forward jacking distance used. This process is illustrated in the following section.

5.10.2 Application of the Test Results

Tests PB1 to PB4 (Figs. 5.33 to 5.36) of the pipebursting series are used initially to illustrate the movements on a pipeline/road pavement running directly above pipebursting operations in the longitudunal plane. Tests PB1 and PB3 are for the road pavement, and tests PB2 and PB4 are for a pipeline at mid depth above the burster. Tables 5.58a and b give the magnitudes of the vertical and horizontal movements obtained from the displacement contour plots for each of these tests at 20mm intervals along either the pipeline or road pavement, and summed totals are given at 100mm intervals. This is for a 'snap-shot' of the movements, but each point on the pipeline will show this amount of movement during the passage of the burster. This means that a summation of the movements in advance of a particular point will indicate the total movement that point has experienced at that stage of the pipebursting operation.

The significance of the larger D_f/D_o ratio is the increased total displacements that occur during the passage of the bursting

Table 5.8a Horizontal and vertical displacements obtained from the displacement contour plots at 20mm intervals along the sand surface for tests PB1 (2.6dLB1.2), PB2 (4.9dLB1.2) & PB3 (2.6lLB1.2)

VERTICAL MOVEMENTS

POINT NUMBER	DISTANCE ALONG SURFACE BETWEEN POINTS (mm) 20	40	60	80	100	SUM
1	0.00	0.10	0.20	0.30	0.40	1.00
2	0.60	0.65	0.75	0.80	0.90	4.70
3	1.05	1.10	1.20	1.30	1.40	10.75
4	1.45	1.55	1.60	1.70	1.75	18.80
5	1.80	1.80	1.70	1.60	1.60	27.30
6	1.40	1.35	1.25	1.15	1.00	33.45
7	0.80	0.60	0.40	0.20	0.00	35.45

HORIZONTAL MOVEMENTS

POINT NUMBER	DISTANCE ALONG SURFACE BETWEEN POINTS (mm) 20	40	60	80	100	SUM
1	0	0.25	0.50	0.70	1.00	2.45
2	1.05	1.10	1.15	1.20	1.20	8.15
3	1.10	1.05	1.05	1.00	0.80	13.15
4	0.60	0.40	0.25	0.10	-0.10	14.40
5	-0.40	-0.60	-0.75	-0.80	-1.00	10.85
6	-1.00	-1.00	-1.00	-1.00	-1.00	5.85
7	-1.00	-1.00	-0.90	-0.60	-0.45	1.90
8	-0.25	0.00	0.00	0.00	0.00	1.65

Table 5.8a Horizontal and vertical displacements obtained from the displacement contour plots at 20mm intervals along the sand surface for tests PB1 (2.6dLB1.2), PB2 (4.9dLB1.2) & PB3 (2.6lLB1.2), continued

VERTICAL MOVEMENTS

POINT NUMBER	DISTANCE ALONG SURFACE BETWEEN POINTS (mm) 20	40	60	80	100	SUM
1	0.03	0.05	0.10	0.11	0.13	0.42
2	0.20	0.25	0.26	0.29	0.30	1.72
3	0.35	0.37	0.38	0.40	0.42	3.64
4	0.45	0.46	0.47	0.49	0.50	6.01
5	0.60	0.70	0.75	0.80	0.90	9.76
6	0.95	1.00	1.00	0.95	0.90	14.56
7	0.80	0.70	0.55	0.50	0.45	17.56
8	0.35	0.30	0.25	0.22	0.20	18.88
9	0.18	0.15	0.13	0.11	0.10	19.22
10	0.05	0.03	0.00	0.00	0.00	19.30

HORIZONTAL MOVEMENTS

POINT NUMBER	DISTANCE ALONG SURFACE BETWEEN POINTS (mm) 20	40	60	80	100	SUM
1	0.15	0.26	0.35	0.60	0.80	2.16
2	1.10	1.20	1.35	1.50	1.50	8.81
3	1.50	1.50	1.50	1.50	1.50	16.31
4	1.50	1.50	1.50	1.50	1.40	23.71
5	1.35	1.25	1.10	1.00	0.80	29.21
6	0.50	0.30	0.20	0.15	0.00	30.36
7	-0.05	-0.10	-0.20	-0.25	-0.30	29.46
8	-0.40	-0.50	-0.50	-0.50	-0.50	27.06
9	-0.50	-0.50	-0.50	-0.35	-0.25	24.96
10	-0.15	0.00	0.00	0.00	0.00	24.81

Table 5.8a Horizontal and vertical displacements obtained from the displacement contour plots at 20mm intervals along the sand surface for tests PB1 (2.6dLB1.2), PB2 (4.9dLB1.2) & PB3 (2.6lLB1.2), continued

VERTICAL MOVEMENTS

POINT NUMBER	DISTANCE ALONG SURFACE BETWEEN POINTS (mm) 20	40	60	80	100	SUM
1	0.00	0.25	0.50	0.60	0.55	1.90
2	0.25	0.00	-0.15	-0.25	-0.30	1.45
3	-0.50	-0.55	-0.75	-0.90	-1.00	-2.25
4	-1.05	-1.10	-1.05	-1.00	-0.90	-7.35
5	-0.70	-0.55	-0.40	-0.25	-0.10	-9.35
6	0.00	0.00	0.00	0.00	0.00	-9.35

HORIZONTAL MOVEMENTS

POINT NUMBER	DISTANCE ALONG SURFACE BETWEEN POINTS (mm) 20	40	60	80	100	SUM
1	0.40	0.50	0.50	0.50	0.50	2.40
2	0.25	-0.10	-0.25	-0.50	-0.75	1.05
3	-1.00	-1.00	-1.00	-1.00	-0.75	-3.70
4	0.00	0.50	1.00	1.00	1.00	-0.20
5	1.00	1.00	0.75	0.65	0.40	3.60
6	0.25	0.00	0.00	0.00	0.00	3.85

Table 5.8b Horizontal and vertical displacements obtained from the displacement contour plots at 20mm intervals at mid-depth through the sand for tests PB2 (4.9dLB1.2) and PB4 (4.9lLB1.2)

VERTICAL MOVEMENTS

POINT NUMBER	DISTANCE BEWTEEN POINTS AT MID-DEPTH BELOW SURFACE (mm) 20	40	60	80	100	SUM
1	0.00	0.00	0.10	0.20	0.35	0.65
2	0.65	0.90	1.40	1.90	2.05	7.55
3	2.10	2.20	2.20	2.20	2.30	18.55
4	2.40	2.50	2.40	2.50	2.60	30.95
5	2.60	2.60	2.50	2.60	2.40	43.65
6	2.30	2.20	2.20	2.05	1.50	53.90
7	1.0	0.45	0.20	0.00	0.00	55.55

HORIZONTAL MOVEMENTS

POINT NUMBER	DISTANCE BEWTEEN POINTS AT MID-DEPTH BELOW SURFACE (mm) 20	40	60	80	100	SUM
1	0.05	0.10	0.15	0.20	0.25	0.75
2	0.30	0.30	0.35	0.35	0.40	2.45
3	0.45	0.55	0.55	0.50	0.45	4.95]
4	0.45	0.40	0.35	0.30	0.30	6.75
5	0.25	0.20	0.15	0.10	0.00	7.45
6	-0.15	-0.20	-0.30	-0.45	-0.50	5.85
7	-0.50	-0.20	-0.30	-0.25	-0.10	4.50

Table 5.8b Horizontal and vertical displacements obtained from the displacement contour plots at 20mm intervals at mid-depth through the sand for tests PB2 (4.9dLB1.2) and PB4 (4.9lLB1.2), continued

VERTICAL MOVEMENTS

POINT NUMBER	DISTANCE BEWTEEN POINTS AT MID-DEPTH BELOW SURFACE (mm) 20	40	60	80	100	SUM
1	0.00	0.00	0.10	0.20	0.30	0.60
2	0.40	0.50	0.50	0.50	0.50	3.00
3	0.40	0.35	0.25	0.10	0.00	4.10
4	-0.10	-0.20	-0.30	-0.40	-0.60	2.50
5	-0.65	-0.70	-0.75	-0.70	-0.60	-0.9
6	-0.50	-0.40	-0.30	-0.20	-0.15	-2.45
7	-0.05	0.00	0.00	0.00	0.00	-2.50

HORIZONTAL MOVEMENTS

POINT NUMBER	DISTANCE BEWTEEN POINTS AT MID-DEPTH BELOW SURFACE (mm) 20	40	60	80	100	SUM
1	0.00	0.00	0.00	0.00	0.00	0.00
2	0.00	0.00	0.05	0.10	0.10	0.25
3	0.10	0.05	0.05	0.00	-0.10	0.35
4	-0.15	-0.25	-0.30	-0.40	-0.25	-1.00
5	-0.20	-0.10	0.10	0.25	0.30	-0.65
6	0.40	0.40	0.30	0.20	0.10	0.75

unit. Instead of 46mm maximum total upwards movement (calculated from the difference between the maximum burster diameter and the internal diameter of the plaster pipe, 210mm-164mm), there is 91mm (210mm-119mm) for these tests. This means that a sand particle initially close to the breakout point over the burster in the longitudinal plane will have moved vertically upwards a greater distance by the time the burster has passed. The increase in extent of the movements, due to the greater area of pipe being broken out, means that a greater length of service or road pavement, running parallel to the bursting operation, is affected by the soil movements at any one time. For the 20mm forward jack used in these tests the magnitudes of the movements are very similar for the different D_f/D_o ratios (for example Figs. 5.33 and 5.39). However, due to the larger extents of the movements, the total maximum movements from the summation process will be considerably larger.

The dense state tests show a large amount of heave movement developing with only a small amount of settlement as the overburst passes. The loose tests, however, show only a small amount of heave movement and a high degree of settlement at the overburst. These different modes of movement will exert different stress and strain regimes on the pipe or road pavement. From the total horizontal and vertical movements for the whole burst, curvature, stresses and strains can be calculated along the length of a service or road pavement above the burster. As an initial analysis, these can be calculated assuming that the service/road moves exactly as the ground, i.e. they have the same stiffness. Realistically, however, the service/pavement would have a much greater stiffness and therefore the induced curvature, stresses and strains would be less. This assumption therefore produces the worst case. To incorporate different stiffnesses requires a stress analysis method, as shown in Fig. 2.61 in the literature review. Other factors can also influence the behaviour of services, such as jointing and connections, and it is therefore a complex relationship. This has been investigated thoroughly by Attewell et al (1986). It is beyond the purpose of this discussion to go into this subject, since the aim here is to provide guidance on how to obtain the ground movement data from the presented results. The calculated curvatures (Appendix D shows the formulae used) based on the surface movements during test PB1 and PB3 are shown in Table 5.9. These simply provide a comparative indication of the curvatures caused by the vertical movements, however they do illustrate the general procedure. A more rigorous analysis can obviously be conducted if required. It can be seen that the curvature for the dense state test changes from compression at the surface to tension, with the maximum value of cuvature being in the tension region close to the maximum displacement. This value is approximately twice that for the maximum value of curvature in the compression region. For the loose state test, the compression at the surface changes quickly into a tension state, and then alternates between compression and tension during the operation before regaining a compression state just before the displacements stabilize. The maximum value of curvature occurs in the third compression region, and is 67% larger than the maximum curvature during the dense state test, indicating that the loose state test provides the more critical condition for surface curvature. A more detailed investigation involving the determination of stresses and strains, for both the vertical and horizontal movements, would be required to make any conclusion as to which condition will produce the most critical situation overall. Although the stresses within the ground, caused by the jacking process, are transmitted over much greater distances than the detectable soil displacements and can impose forces on services or structures, the most likely cause of failure is from differential movements within the service or structure that arise from the soil displacements within that area.

A similar procedure to that above can be carried out to determine the total movements throughout the jacking process for the open shield pipejacking tests and the closed shield pipejacking tests in the longitudinal plane. The main difference between these tests and the pipebursting tests is that the jacking distance between measurements is 10mm rather than 20mm. Table 5.10a illustrates the vertical movements obtained for tests CPJ1, CPJ2 and CPJ3 of the closed shield pipejacking test series, for points 100mm apart. Summation of the movements shows that the total

Table 5.9 Curvatures induced into a service and road pavement, assuming they have the same stiffness as the soil, due to vertical ground displacements in tests PB1 (2.6dLB1.2) and PB3 (2.6lLB1.2)

POINT NUMBER	SUMMED VERTICAL MOVEMENTS (mm)	CURVATURE (m^{-1})
0	0.00	0.20
1	1.00	0.27
2	4.70	0.24
3	10.75	0.20
4	18.80	0.05
5	27.30	-0.24
6	33.45	-0.42
7	35.45	-0.20
8	35.45	0.00

POINT NUMBER	SUMMED VERTICAL MOVEMENTS (mm)	CURVATURE (m^{-1})
0	0.00	0.38
1	1.90	-0.24
2	1.45	-0.33
3	-2.25	0.36
4	-2.35	-0.69
5	-9.35	0.70
6	-9.35	0.00

Table 5.10a Vertical displacements obtained from the displacement contour plots at 10mm intervals, summed at 100mm intervals,along the surface of the sand for test CPJ1 (2.0dLB0.1), CPJ2 (2.0lLB0.1) & CPJ3 (4.5dLB0.1)

POINT NUMBER	DISTANCE ALONG SURFACE BETWEEN POINTS (mm)										TOTAL
	10	20	30	40	50	60	70	80	90	100	
1	0.00	0.05	0.08	0.10	0.20	0.20	0.25	0.25	0.30	0.35	1.68
2	0.40	0.45	0.50	0.55	0.60	0.65	0.70	0.70	0.75	0.80	7.78
3	0.90	0.90	0.95	1.00	1.15	1.30	1.40	1.60	1.70	1.90	20.58
4	1.95	2.00	2.10	2.20	2.30	2.45	2.60	2.70	2.80	3.00	44.68
5	3.00	3.00	3.00	3.00	3.00	3.00	3.00	2.80	2.60	2.10	73.18
6	2.00	1.95	1.80	1.70	1.50	1.30	1.20	1.00	0.95	0.80	87.38
7	0.75	0.70	0.55	0.50	0.40	0.30	0.20	0.15	0.10	0.00	91.03

Table 5.10a Vertical displacements obtained from the displacement contour plots at 10mm intervals, summed at 100mm intervals,along the surface of the sand for test CPJ1 (2.0dLB0.1), CPJ2 (2.0lLB0.1) & CPJ3 (4.5dLB0.1), continued

POINT NUMBER	DISTANCE ALONG SURFACE BETWEEN POINTS (mm) 10	20	30	40	50	60	70	80	90	100	TOTAL
1	0.00	0.00	0.00	0.00	0.00	0.05	0.08	0.10	0.13	0.15	0.51
2	0.20	0.20	0.25	0.30	0.35	0.38	0.40	0.43	0.45	0.50	3.97
3	0.52	0.54	0.58	0.60	0.62	0.65	0.68	0.70	0.73	0.75	10.34
4	0.80	0.80	0.82	0.85	0.88	0.90	0.92	0.95	0.98	1.00	19.24
5	1.00	1.00	1.00	1.00	1.00	1.00	1.00	1.00	1.00	0.95	29.19
6	0.90	0.85	0.80	0.70	0.60	0.50	0.40	0.20	0.00	-0.10	34.04
7	-0.15	-0.20	-0.30	-0.40	-0.50	-0.55	-0.65	-0.75	-0.80	-0.95	28.79
8	-1.00	-1.00	-1.00	-1.00	-1.00	-1.00	-1.00	-1.00	-1.00	-1.00	18.79
9	-1.00	-1.00	-1.00	-1.00	-0.95	-0.90	-0.85	-0.80	-0.75	-0.70	9.84
10	-0.65	-0.60	-0.55	-0.40	-0.35	-0.30	-0.20	-0.10	0.00	0.00	6.69

Table 5.10a Vertical displacements obtained from the displacement contour plots at 10mm intervals, summed at 100mm intervals,along the surface of the sand for test CPJ1 (2.0dLB0.1), CPJ2 (2.0lLB0.1) & CPJ3 (4.5dLB0.1), continued

POINT NUMBER	DISTANCE ALONG SURFACE BETWEEN POINTS (mm) 10	20	30	40	50	60	70	80	90	100	TOTAL
1	0.00	0.05	0.06	0.08	0.10	0.12	0.15	0.18	0.20	0.10	1.04
2	0.13	0.15	0.20	0.22	0.25	0.28	0.30	0.31	0.32	0.33	3.53
3	0.35	0.38	0.40	0.42	0.40	0.42	0.44	0.46	0.47	0.48	7.75
4	0.50	0.50	0.52	0.53	0.55	0.58	0.60.	0.61	0.63	0.65	13.42
5	0.68	0.70	0.72	0.73	0.75	0.76	0.77	0.78	0.79	0.80	20.90
6	0.85	0.88	0.90	0.92	0.95	0.98	1.00	1.00	1.00	1.00	30.38
7	1.00	1.00	1.00	1.00	1.00	1.00	1.00	1.00	1.00	1.00	40.38
8	0.95	0.92	0.90	0.88	0.85	0.82	0.80	0.78	0.75	0.75	48.78
9	0.72	0.70	0.68	0.65	0.62	0.60	0.57	0.54	0.52	0.50	54.88
10	0.47	0.45	0.42	0.40	0.38	0.36	0.34	0.33	0.32	0.30	58.65
11	0.30	0.29	0.28	0.26	0.24	0.22	0.20	0.19	0.18	0.18	60.99
12	0.15	0.12	0.10	0.09	0.08	0.07	0.06	0.05	0.04	0.04	61.79
13	0.03	0.01	0.00	0.00	0.00	0.00	0.00	0.00	0.00	0.00	61.83

Table 5.10b Curvature values for positions at 100mm intervals due to the vertical sand displacements over the pipejacking tests given in Table 5.7a

CPJ1 (2.0dLB0.1)

POINT NUMBER	SUMMED VERTICAL MOVEMENTS (mm)	CURVATURE (m^{-1})
0	0.00	0.34
1	1.68	0.44
2	7.78	0.67
3	20.58	1.13
4	44.68	0.44
5	73.18	-1.43
6	87.38	-1.06
7	90.03	-0.37
8	90.03	0.00

CPJ2 (2.0lLB0.1)

POINT NUMBER	SUMMED VERTICAL MOVEMENTS (mm)	CURVATURE (m^{-1})
0	0.00	0.10
1	0.51	0.20
2	3.97	0.30
3	10.34	0.25
4	19.24	0.11
5	29.19	-0.51
6	34.04	-1.00
7	28.79	-0.48
8	18.79	0.11
9	9.84	0.58
10	6.69	0.32
11	6.69	0.00

vertical movement for test CPJ1 is 91mm. For test CPJ2, there is 34mm upwards and 27.3mm downwards, giving a residual upwards movement of only 6.7mm. Test CPJ3 gives a total vertical movement of 62mm, which compared with test CPJ1 indicates that an approximate doubling of the C/D ratio produces a reduction of one third in the vertical movements. The dense state tests (tests CPJ1 and CPJ3) show only upwards movement at the surface due to the installation of the pipe, whereas the loose state test (test CPJ2) shows both upwards and downwards movement at the surface. As for the pipebursting operations, this will impose different stress and strain regimes on structures or services and possibly greater differential movements in the loose state tests at the inflection point. The curvature values caused by these movements for points 100mm apart, for tests CPJ1 and CPJ2, are presented in Table 5.10b, the same assumptions on relative stiffness being made as for the pipebursting tests. The results for the dense state test indicate an initial compression region at the surface which changes to a tension region. The maximum curvature occurs in the tension region, although this is only slightly greater than the maximum compression curvature. For the loose state test, the curvature changes from initially compression at the surface to a region of tension and then back to a region of compression. The maximum curvature occurs in the tension region and this is approximately double the value for the maximum curvature in the compression region. In these examples the dense state test produces the maximum curvature at the surface.

The open shield pipejacking tests show very localised movements, with these only generally extending two diameters from the pipe and shield, except in the loose state tests at the overcut. The movements likely to occur in a service at a greater distance than two diameters from the installation, due to the forward jacking part of the operation, are negligible. Comparison between the open and closed shield tests does illustrate the effect on the ground movements, and therefore adjacent services, due to increasing over-pressurisation of the face or variations in equilibrium between the excavation and forward jacking processes.

The longitudinal plane movements only give the sand movements along the centreline of the installation process. Although these represent the maximum vertical movements, they may not be the maximum movements induced into the service or structure. It could be that a service offset from the centreline could experience resultant magnitudes, from horizontal and vertical movements, that are greater than those at the centreline. However, having investigated this using some of the plots, the horizontal movements do not become significant until a certain distance away from the centreline, by which time the vertical movements have reduced considerably and thus the resultant magnitude is less than the vertical movements at the centreline.

For a service running perpendicular to the line of the pipebursting operation, a similar procedure is followed as for the parallel service. The maximum movements of the service, which will occur at the burster centreline, can be obtained from the longitudinal plane contour plots. The perpendicular plane plots provide an indication of the longitudinal curvature of the service.

The curvatures for the sand surface profiles for both extreme stages of the burst, close to the start and at full expansion, are shown in Table 5.11. Although the extents are smaller early on in the bursting process, possibly giving a more critical maximum to zero differential movement, the much greater magnitudes at the later stage of the burst, over only a slightly greater extent, gives the greatest curvatures and greatest potential damage to services. It should be noted that these were obtained purely from the perpendicular displacement plots and therefore do not take into account the additional vertical movements in advance of the bursting unit or well behind the overburst, which as explained previously can only be obtained from the longitudinal plane movements. However, as also shown earlier, these perpendicular plane movements do fit in very well with the longitudinal plane movements directly over the burster unit. It is therefore proposed that the longitudinal plane movement results are used to obtain the movements at the centreline throughout the pipebursting operation, and thereafter the perpendicular plane results are used to predict the lateral extent and lateral horizontal movements, which cannot be

Table 5.11 Curvature values for positions 100mm apart, calculated from the vertical displacement above test PB1 (2.6dLB1.2) in the perpendicular plane (Fig. 5.47a and 5.49a)

Close to the start of the bursting operation

DISTANCE FROM PIPE CENTRELINE (mm)	SUMMED VERTICAL MOVEMENTS (mm)	CURVATURE (m^{-1})
0	1.7	-0.04
100	1.5	-0.02
200	1.1	-0.02
300	0.5	0.01
400	0.0	0.01
500	0.0	0.00

At full expansion

DISTANCE FROM PIPE CENTRELINE (mm)	SUMMED VERTICAL MOVEMENTS (mm)	CURVATURE (m^{-1})
0	21.0	-0.60
100	18.0	-0.10
200	15.0	0.10
300	12.0	-0.10
400	8.0	0.00
500	4.0	0.10
600	0.0	0.00
700	0.0	0.00

obtained in the longitudinal plane. The perpendicular plane can also be used to relate the longitudinal vertical movements to those away from the centreline.

For the pipejacking tests, as mentioned in Section 5.3.2, the perpendicular plane movements due to the overcut provide the worst case movements as these are not affected by the draw-along effects close to the pipe. Using the longitudinal plane results, and comparing these to the maximum perpendicular plane results at the centreline, provides an indication of the magnitude of the over-estimation which can be factored down if required. In addition to the vertical movements, the perpendicular plane does give an indication of the lateral extents and likely horizontal movements caused by the overcut. The curvatures, and stress and strain regimes in pipelines or road pavements running perpendicular to the line of the pipejack can be calculated, based on the worst case or the factored down movements to tie in with the longitudinal plane results. The factoring down can be done by using the results from the tests for both overcut ratios and extrapolating these by the desired amount. This is based on the maximum magnitude of the vertical movement at the overcut observed in the longitudinal plane.

In order to help tie in the movements observed for the perpendicular and longitudinal planes, and to extend these to a more three dimensional intepretation, allowing the effects on road pavements and surface structures to be investigated, surface movements were obtained for certain tests. These were measured during two closed pipejacking tests and two pipebursting tests in dense Leighton Buzzard sand, i.e. the tests where the subsurface movements reached the surface, the surface of the sand being firm due to the density, and not in the 25B grade sand which due to the irregular particle sizes, gave inaccurate results. The results were obtained as described in Chapter 4 Section 4.3, by vertical measurements taken onto ball bearings accurately positioned on a grid arrangement at the sand surface or by using dial gauges. The results obtained tied in favourably with those measured at the glass faces and provide a good indication of the surface extents. The results for four of the tests are shown in Figs. 5.65a and b and 5.66a and b. The two results for the closed pipejacking tests show that the larger C/D test produces the larger surface extent of movements but that the magnitudes being much smaller, as expected. A similar result would have been expected for the pipebursting tests, however the small magnitudes at the surface for the higher C/D ratio test produced smaller extents. In terms of lateral extent from the centreline, the higher C/D ratio tests produced a much quicker decrease in movements in front of, and behind, the maximum movement. The lower C/D ratio tests produced a much more uniform spread of movements. These results are for just one section of the jacking process and summation of the surface movement plots offset by either 10mm or 20mm to each other, will create the full description for the whole operation (as for the longitudinal plane contour plots).

5.10.3 Illustrative Example

In order to better illustrate the use of the ground movement data presented in this thesis, and the process of obtaining the movements, an example is given below. This does duplicate some of the examples given previously in this chapter, but it is considered that this example helps to draw together all the different parts of the process. The example uses the results of test PB1 of the pipebursting test series. Figs. 5.31 and 5.49a and Table 5.8a are referenced. The example assumes that it is required to know the surface movements caused by the complete passage of the pipeburster.

From the longitudinal plane displacement contour plots, the surface vertical and horizontal movements are obtained throughout the full passage of the pipeburster for points 100mm apart (Table 5.8a). Using the summed values, i.e. the total displacement at each point, the surface profile shown in Fig. 5.67a can be obtained. This indicates a maximum vertical movement of 35.5mm, which occurs at the maximum expansion of the pipeburster as it passes beneath.

To obtain the movements in the perpendicular plane, the maximum vertical displacement at the centreline is applied to Fig. 5.49a. The surface movements away from the centreline are then obtained by factoring this maximum according to the ratios of the original movements to the original maximum movement. For example, the vertical movement at a distance 100mm from the centreline is 35.5x(18.0/21.0)=30.4mm. This is repeated across the surface. The lateral extent of the movements is assumed to be approximately constant. This gives a total surface profile in the perpendicular plane for the full passage of the pipeburster as shown in Fig. 5.67b. The horizontal movements are obtained directly from the full expansion plot (Fig. 5.49b).

5.11 CONCLUDING DISCUSSION

In this chapter are presented the results from three separate test programmes: open shield pipejacking, closed shield pipejacking and pipebursting. Each set of results has initially been discussed individually, highlighting interesting and relevant features of the data in both the longitudinal and perpendicular planes, with regard to the various factors being investigated. Wherever possible, results from other sources have been used to compare with the laboratory data, although these are very limited. After the discussions on the individual test programmes, there are sections comparing the results between these programmes. This highlighted certain similarities which could be used to extend and enhance the results. Interpolation between the test data has been shown to provide a powerful technique to extend the results. This is important for the pipejacking tests, which used exaggerated shield sizes and overcut ratios in order to obtain observable sand movements, however, extrapolation allows the movements caused by much smaller overcut ratios to be predicted. Practical implications, and the effects on adjacent services and structures caused by the ground movements obtained from the tests, are also discussed and examples are given of how the results can be used for prediction purposes.

As shown, the direct application of the test results to field data, or to make predictions of ground movements, is not straightforward and many factors need to be considered. It is important to fully understand the limitations of the results presented in this chapter in order that they can be used beneficially. This is particularly true for the perpendicular plane results, which for both the pipebursting and pipejacking tests have been shown to differ from those expected from the longitudinal plane movements. However, knowing how and why the movements differ does allow the use of these results for prediction purposes.

Presenting the sand movements in the way used in this thesis does give the opportunity to investigate movement patterns throughout the trenchless pipelaying operation. This allows not only the final, or maximum, movements to be known, but also how these movements develop during the operation and how the various regions of movements interact. This is important when conducting a more fundamental investigation, such as was required in this case, and helps one to gain a better understanding of the effects of certain parameters on the ground movements. It also allows scope for application of the results to a wider range of conditions than would otherwise be possible.

Although the test results presented in this chapter are for dry sands, many of the results can be applied to cohesive soils. For example, above a pipebursting operation dense state sands will behave in a similar way in compression to overconsolidated clay soils. The loose state sands in compression will also perhaps behave in a similar way to relatively compressible clay soils, although it should be remembered that undrained disturbance of saturated clays will result in no volume change, subsequent movements occurring as a result of porewater pressure dissipation. At the overcut, during a pipejacking operation, soft alluvial soils will behave in a similar manner to loose state sand, although the similarity for dilating soils is less accurate. There obviously are differences in behaviour due to the particulate nature of sands. However, as long as the differences are understood, sensible and quite accurate predictions can be made about the likely displacements occuring in cohesive soils. This is difficult to prove as the data available for displacements around trenchless pipelaying operations are very limited. However, the example given in Section 5.8.4, which made a prediction of the maximum surface movement above a pipebursting operation in stiff clay and which produced excellent agreement with that observed, shows, in an albeit limited way, that this extension to the results is valid.

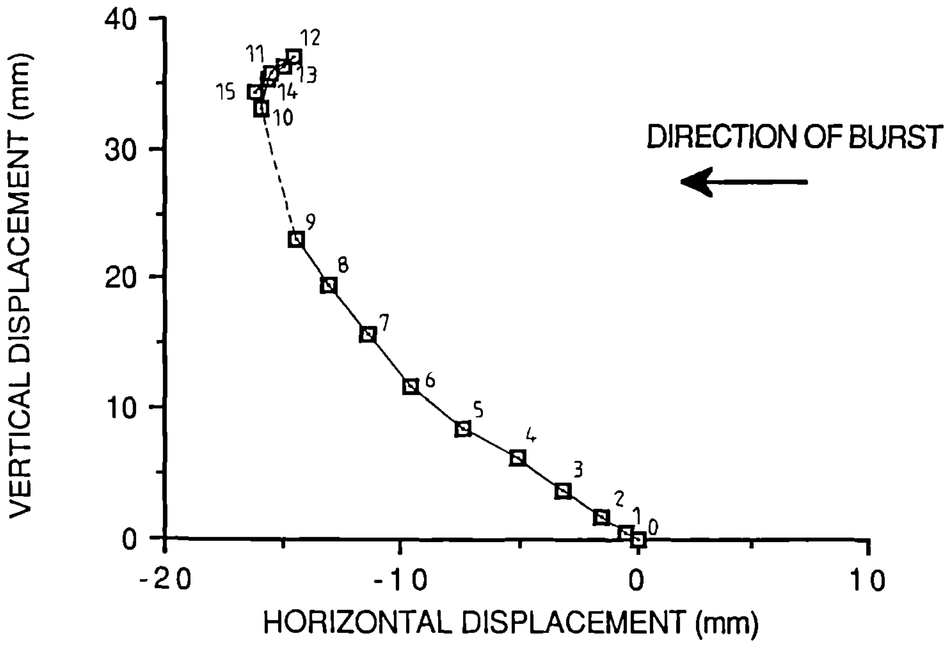

Fig. 5.1 Displacements of a sand particle traced during test PB1 (2.6dLB1.2)

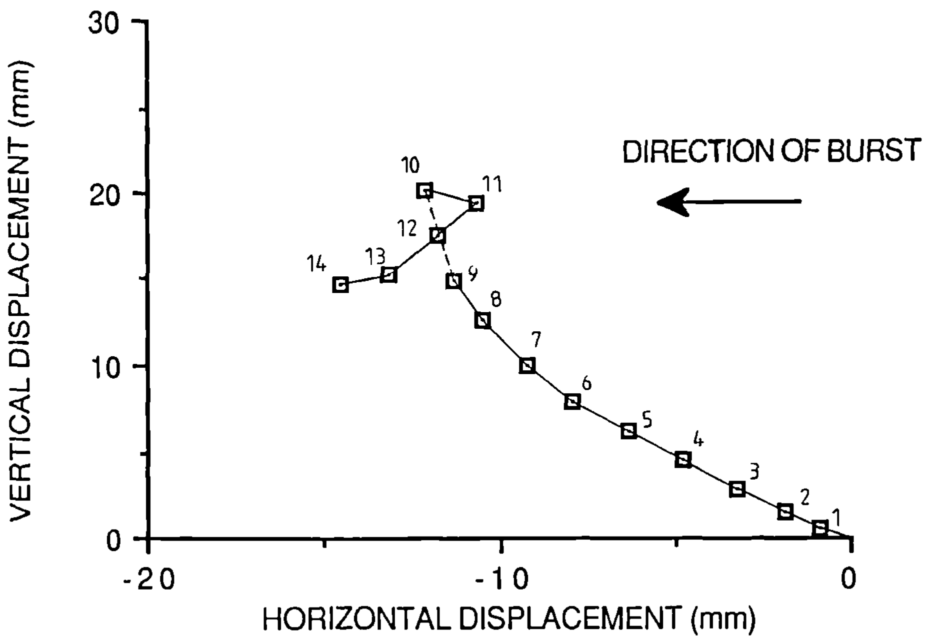

Fig. 5.2 Displacements of a sand particle traced during test PB3 (2.61LB1.2)

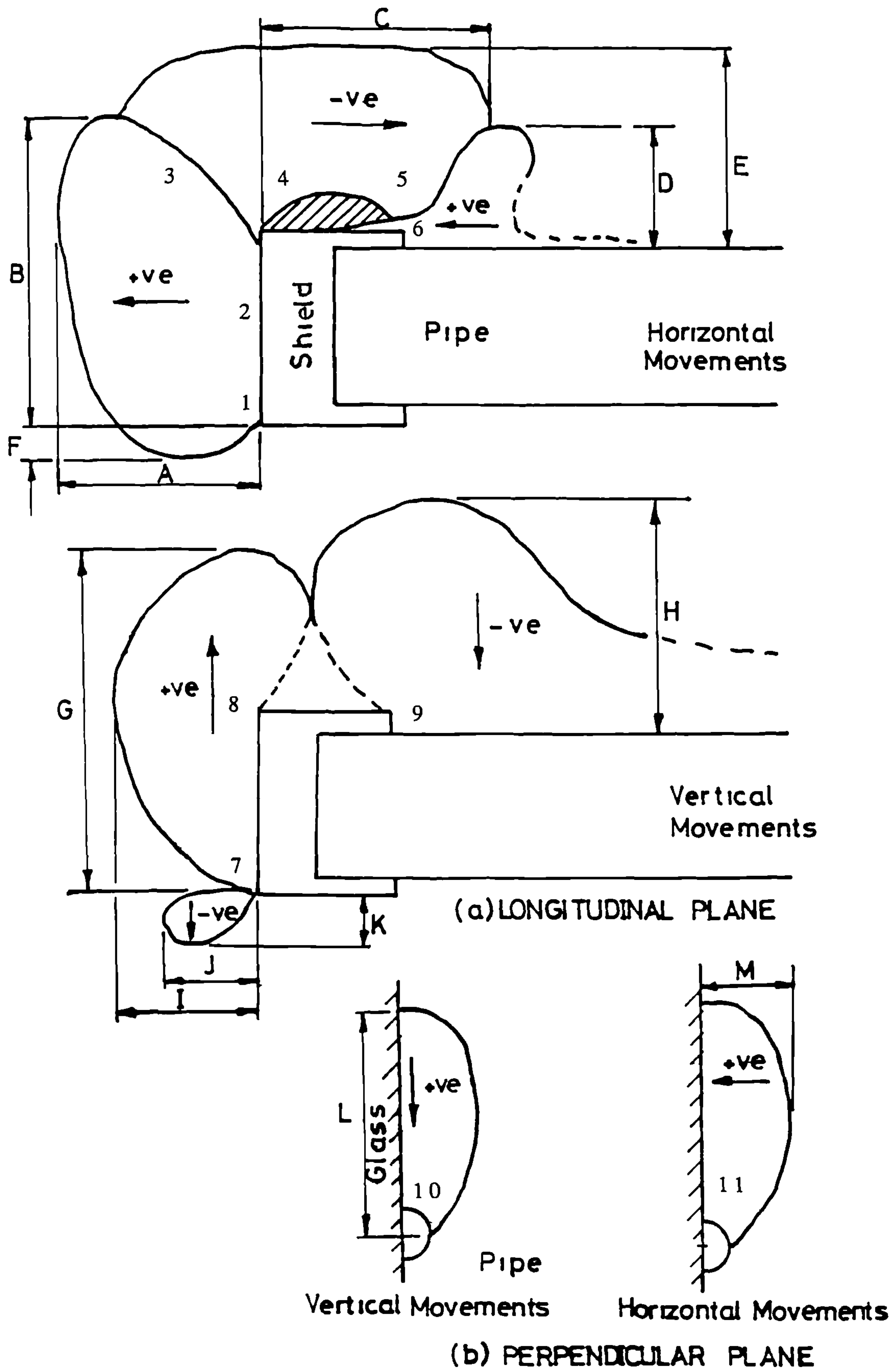

Fig. 5.3 General form of the ground movements associated with the forward jacking stage of the open shield pipejacking tests

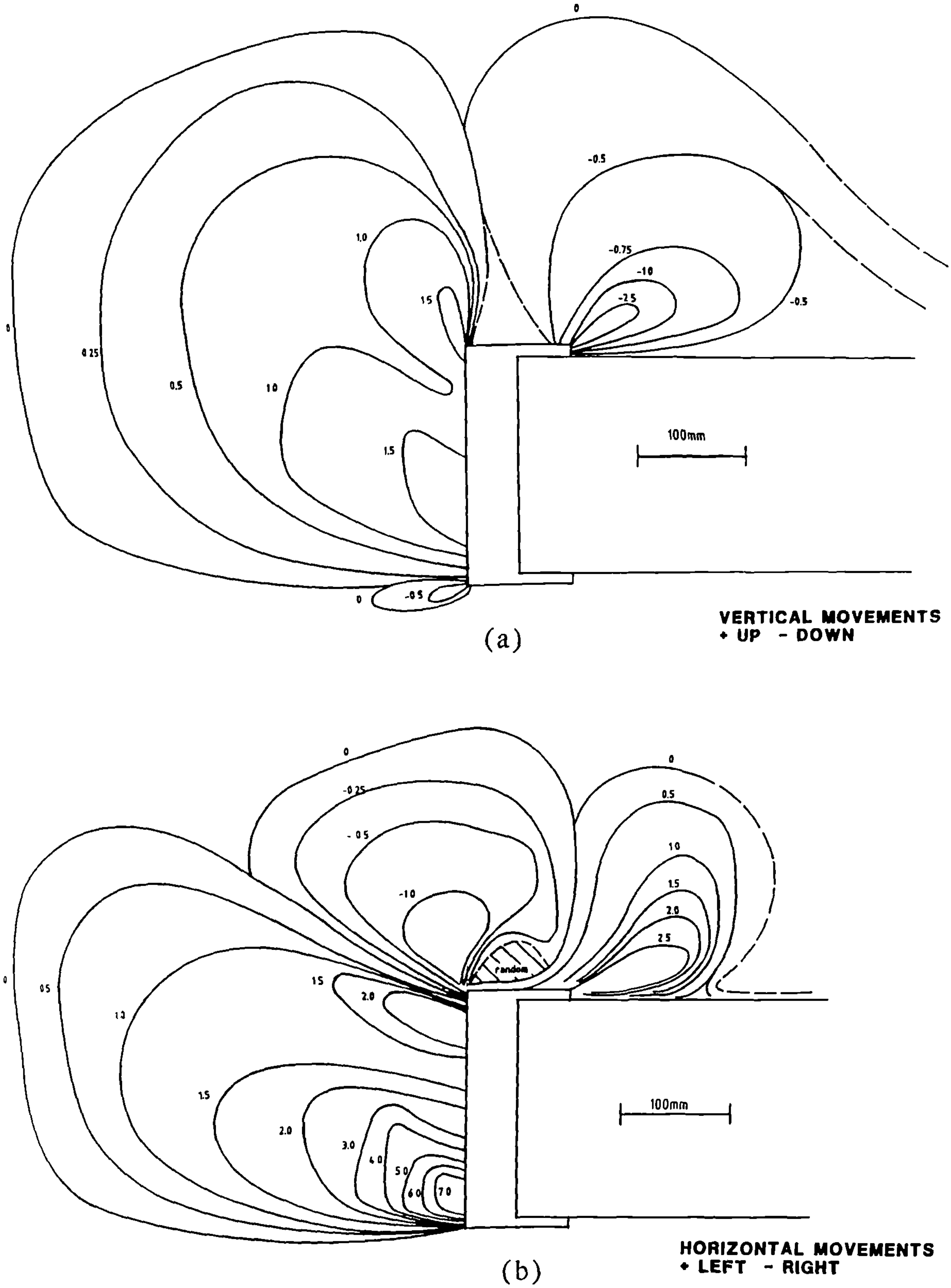

Fig. 5.4 Displacement contour plots for test OPJ1 (4.5dLB0.1)

(10mm forward jacking distance, contours in mm)

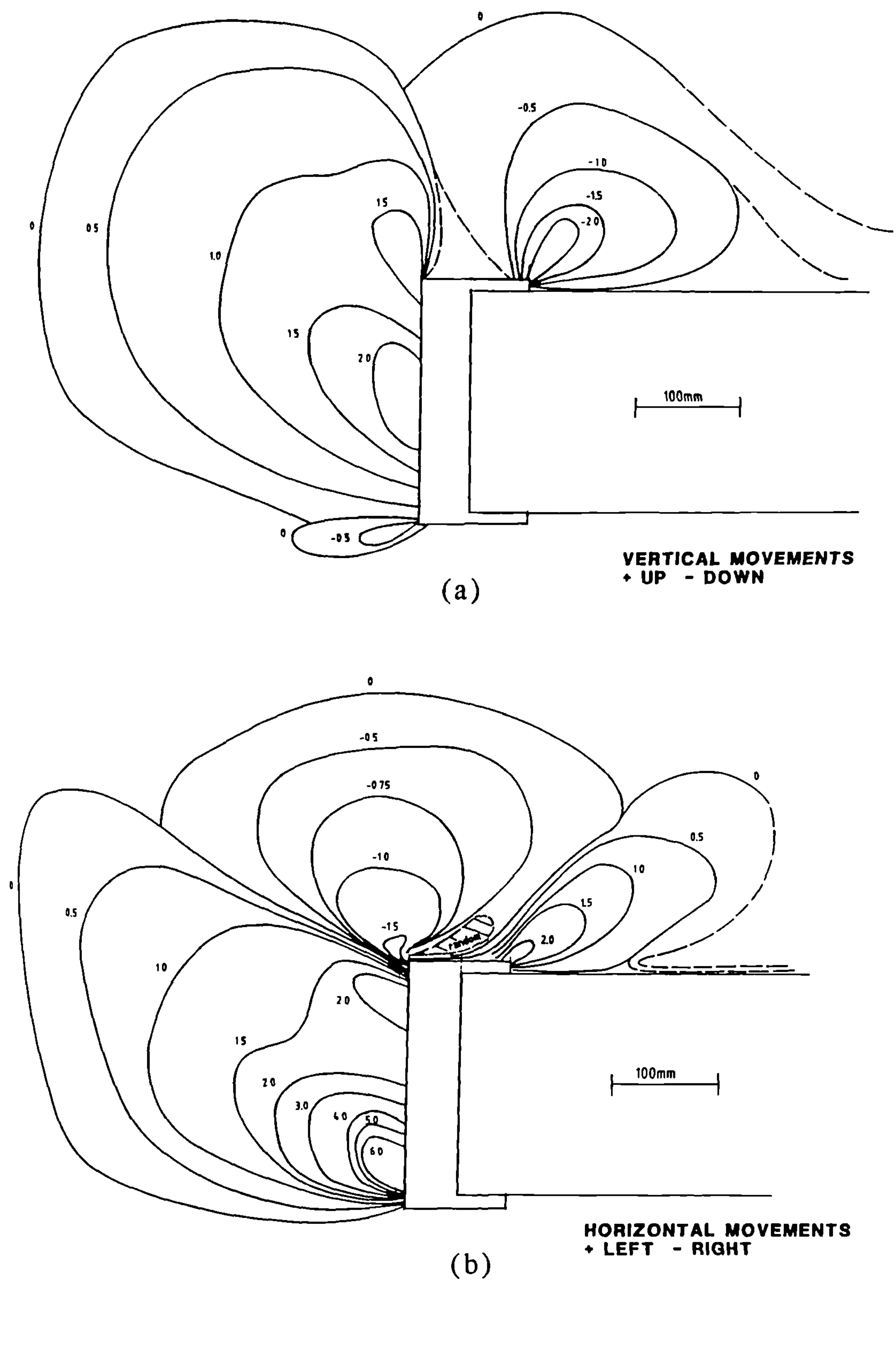

Fig. 5.5 Displacement contour plots for test OPJ2 (12.5dLB0.1)

(10mm forward jacking distance, contours in mm)

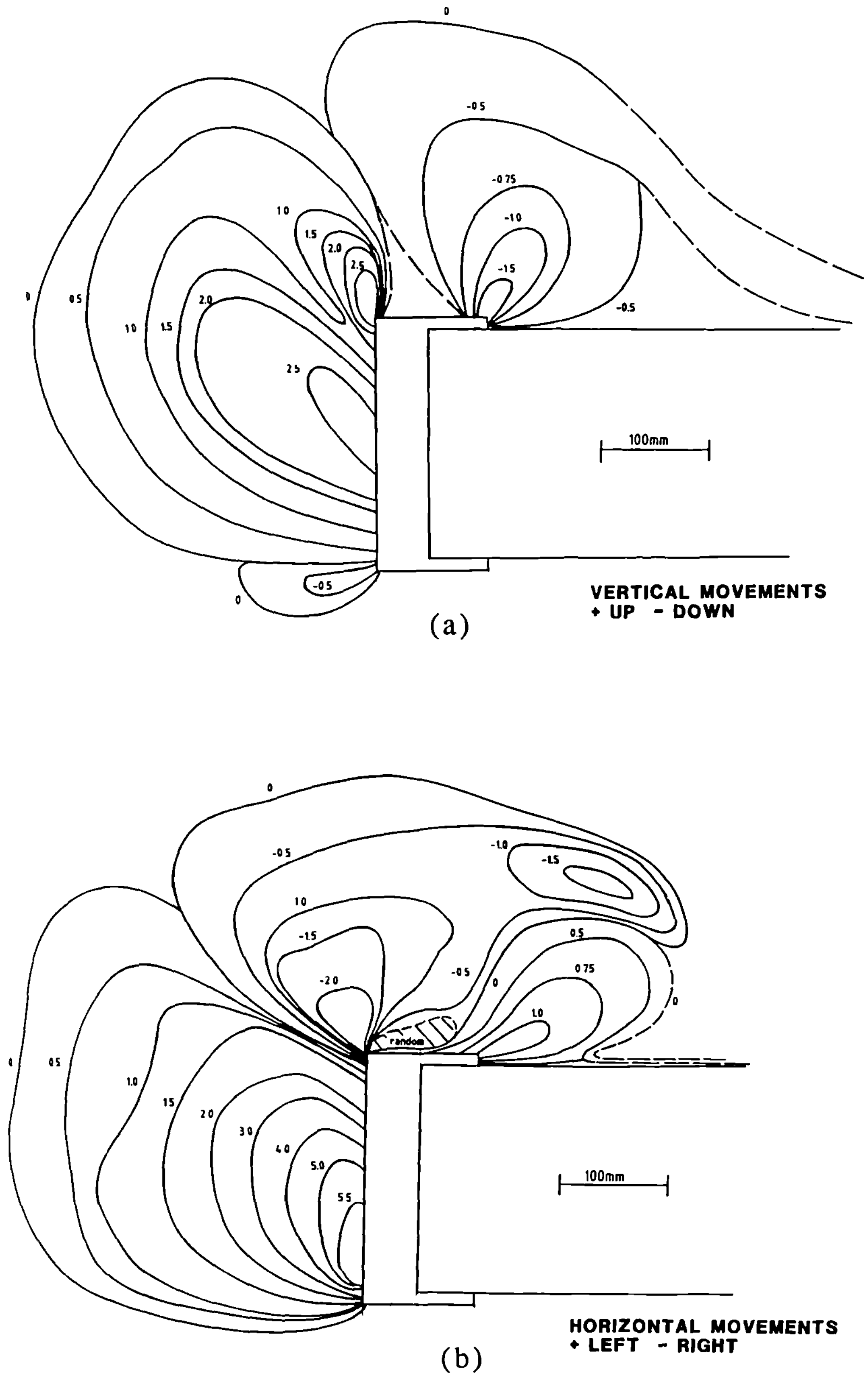

Fig. 5.6 Displacement contour plots for test OPJ3 (20.0dLB0.1) (10mm forward jacking distance, contours in mm)

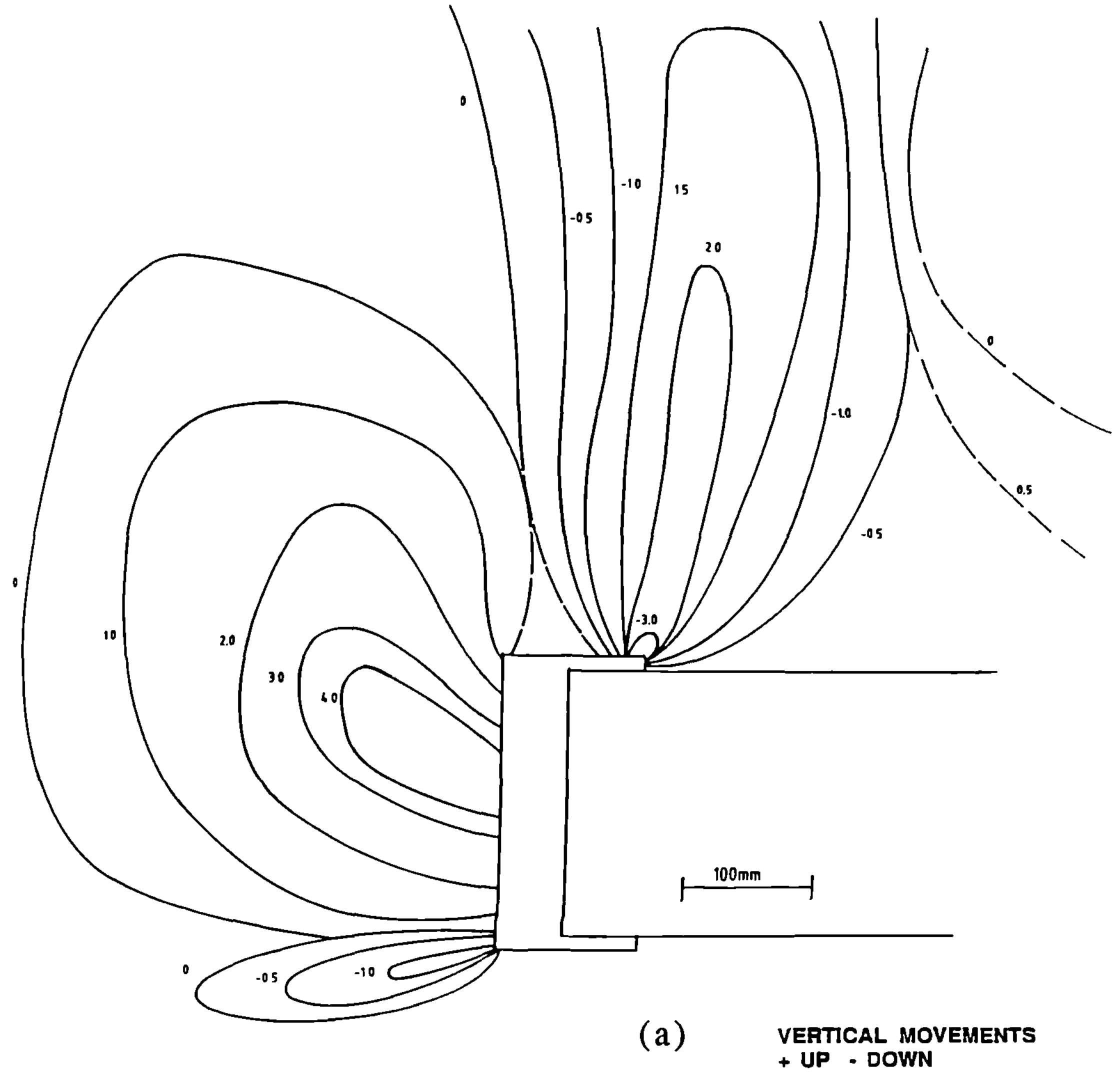

Fig. 5.7 Displacement contour plots for test OPJ4 (4.5lLB0.1)

(10mm forward jacking distance, contours in mm)

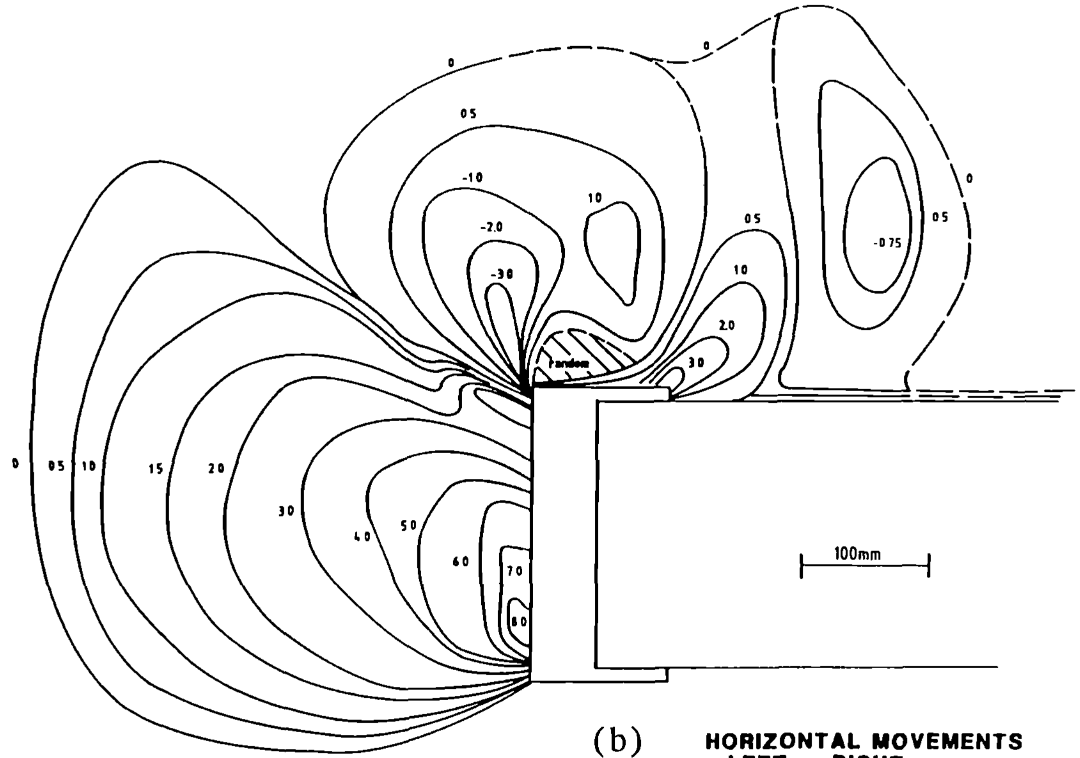

(b) **HORIZONTAL MOVEMENTS**
+ LEFT - RIGHT

Fig. 5.7 Displacement contour plots for test OPJ4 (4.5ILB0.1) continued

(10mm forward jacking distance, contours in mm)

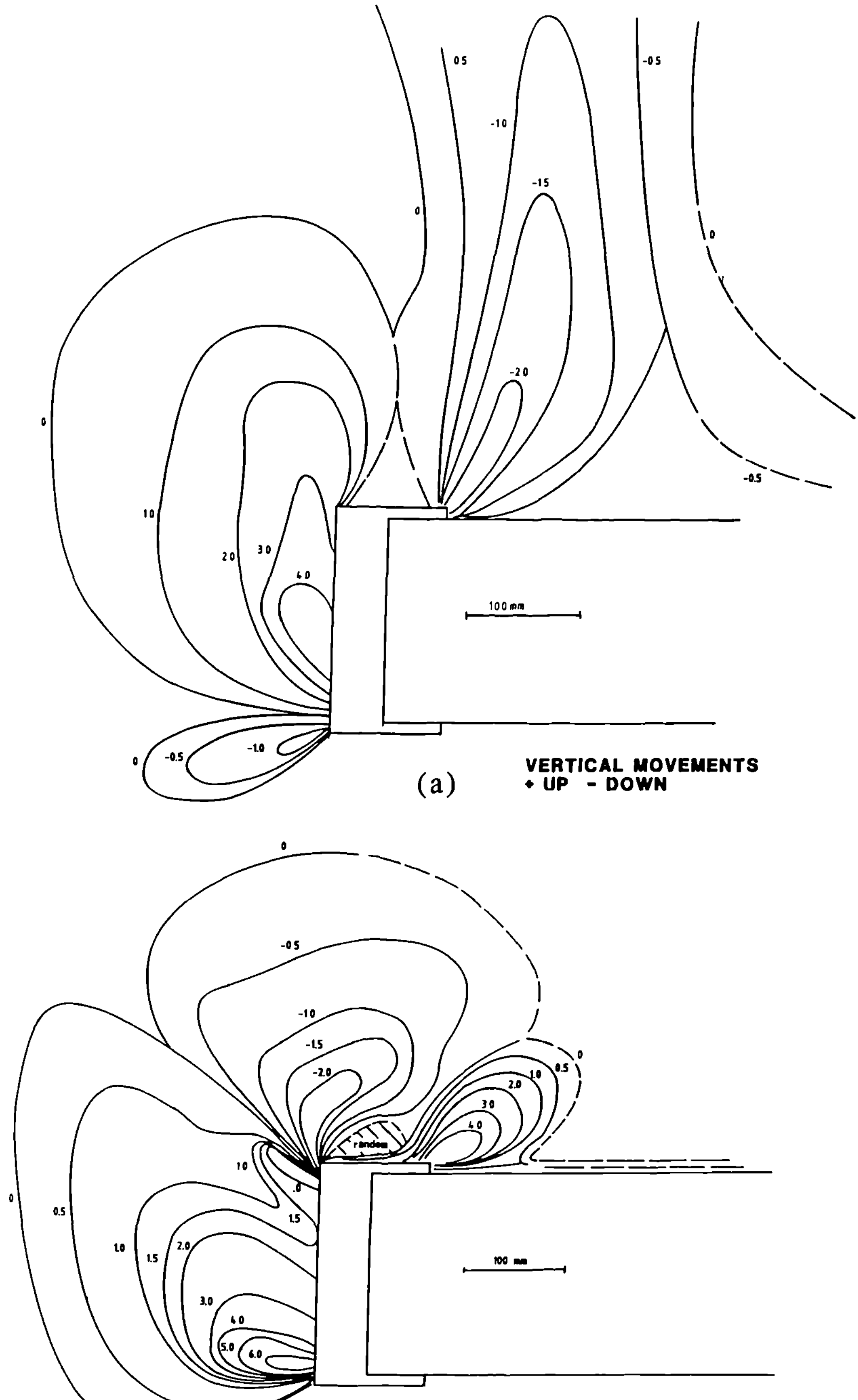

Fig. 5.8 Displacement contour plots for test OPJ5 (12.5ILB0.1)

(10mm forward jacking distance, contours in mm)

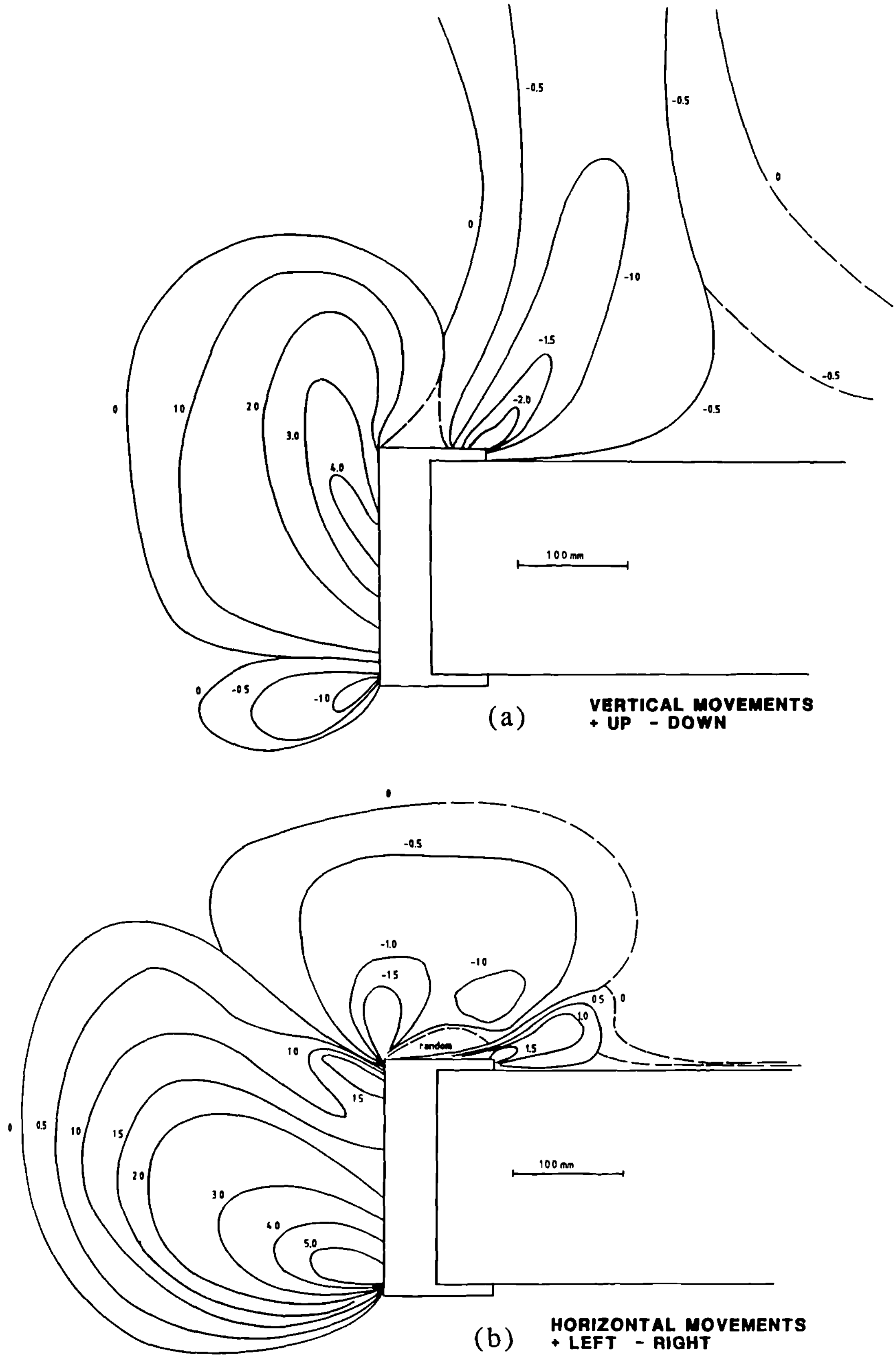

Fig. 5.9 Displacement contour plots for test OPJ6 (20.01LB0.1)

(10mm forward jacking distance, contours in mm)

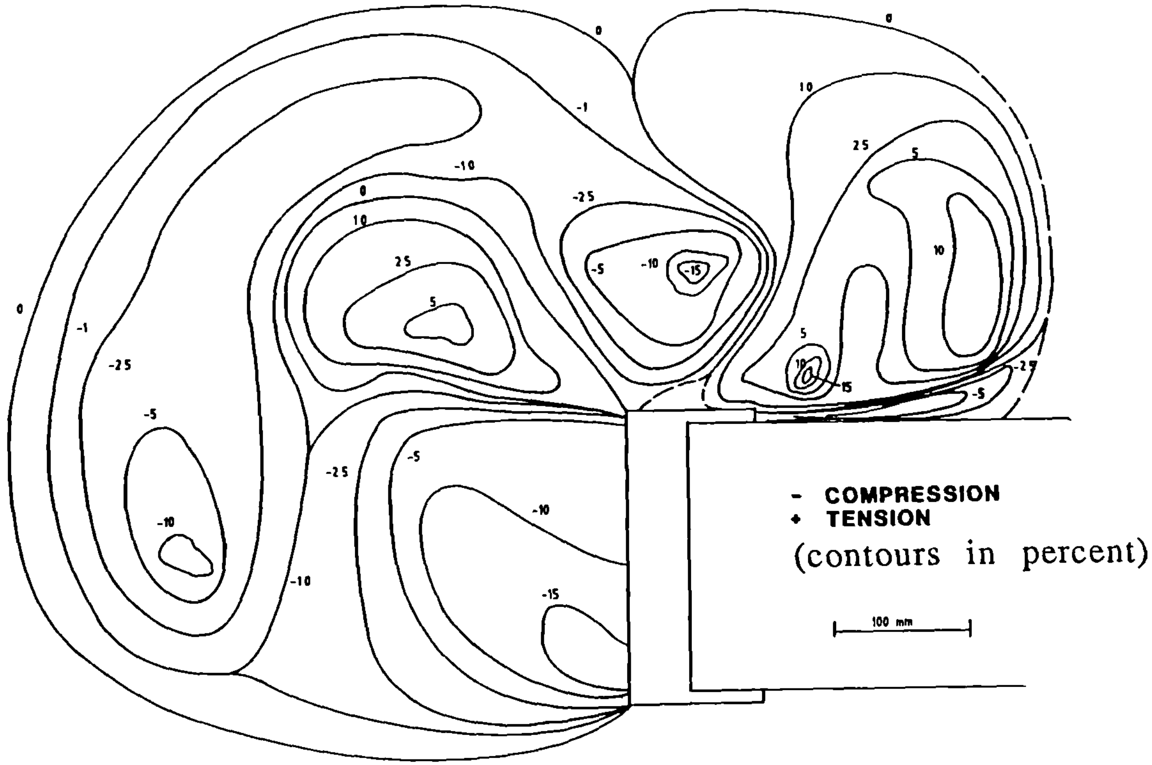

Fig. 5.10 Volumetric strain plot for test OPJ1 (4.5dLB0.1)

(10mm forward jacking distance)

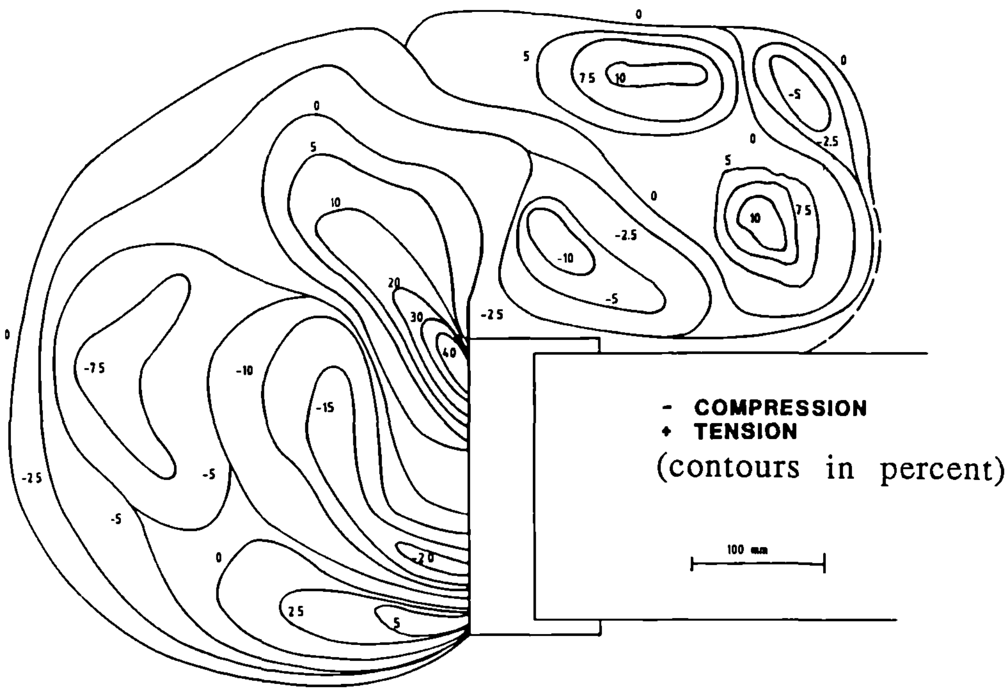

Fig. 5.11 Volumetric strain plot for test OPJ3 (20.0dLB0.1)

(10mm forward jacking distance)

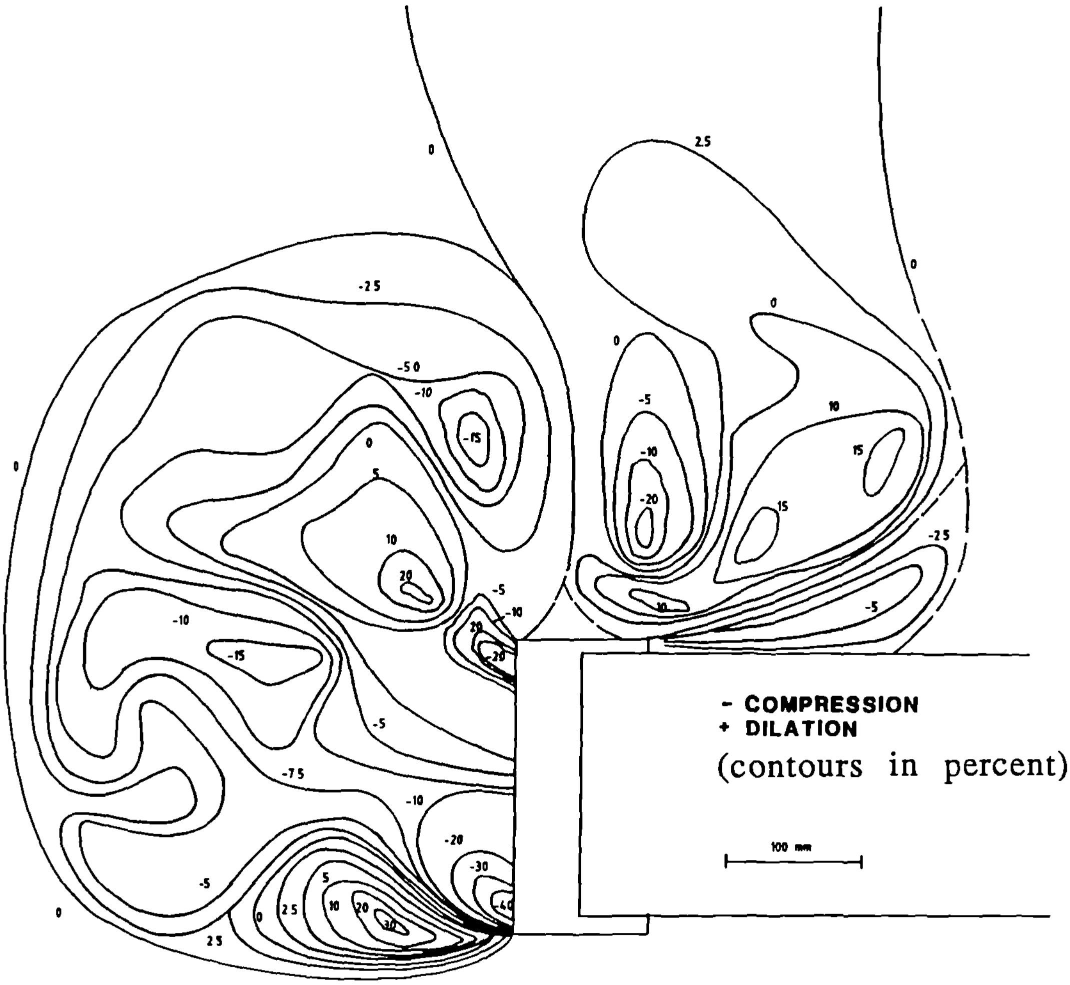

Fig. 5.12 Volumetric strain plot for test OPJ4 (4.5lLB0.1)

(10mm forward jacking distance)

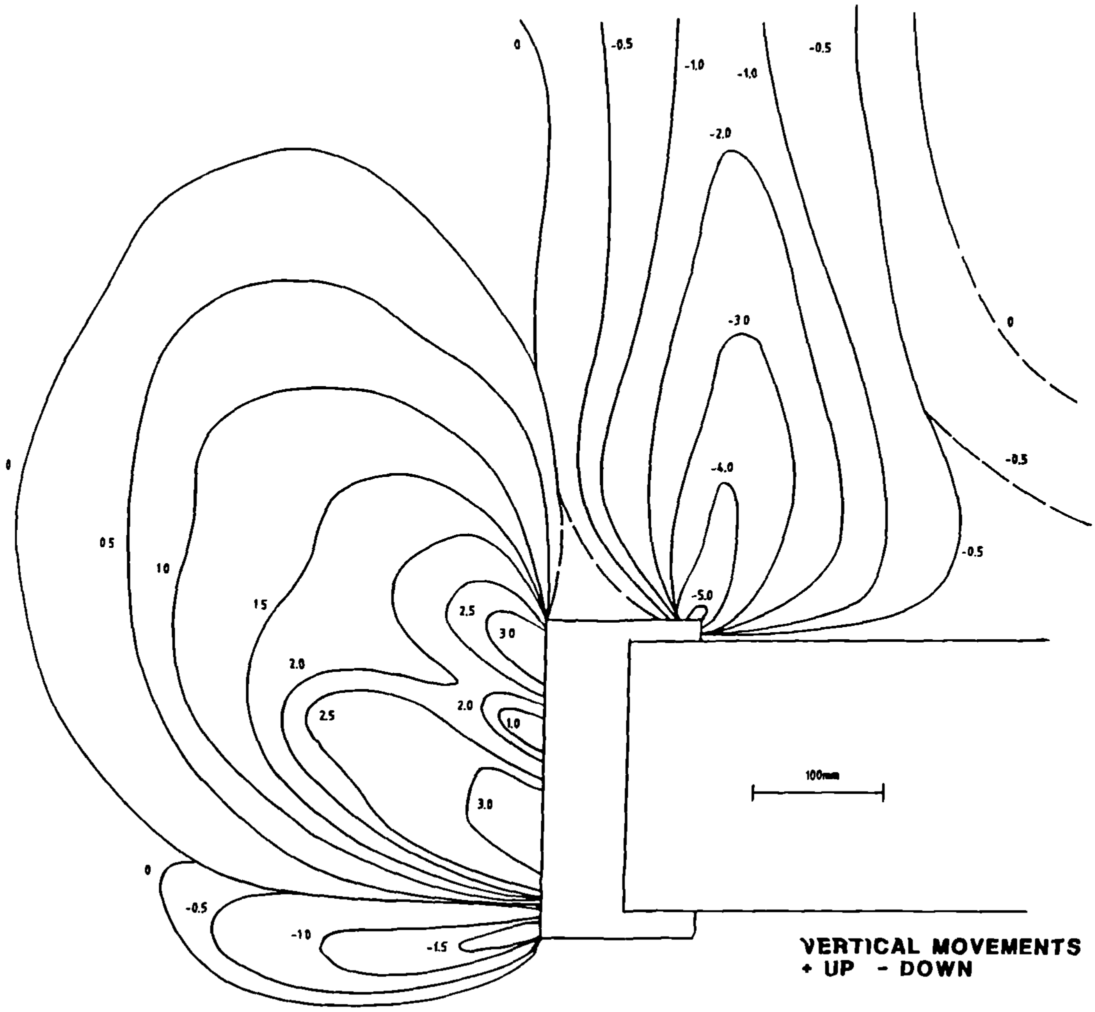

(a)

Fig. 5.13 Displacement contour plots for test OPJ22 (4.5125B0.2)
(10mm forward jacking distance, contours in mm)

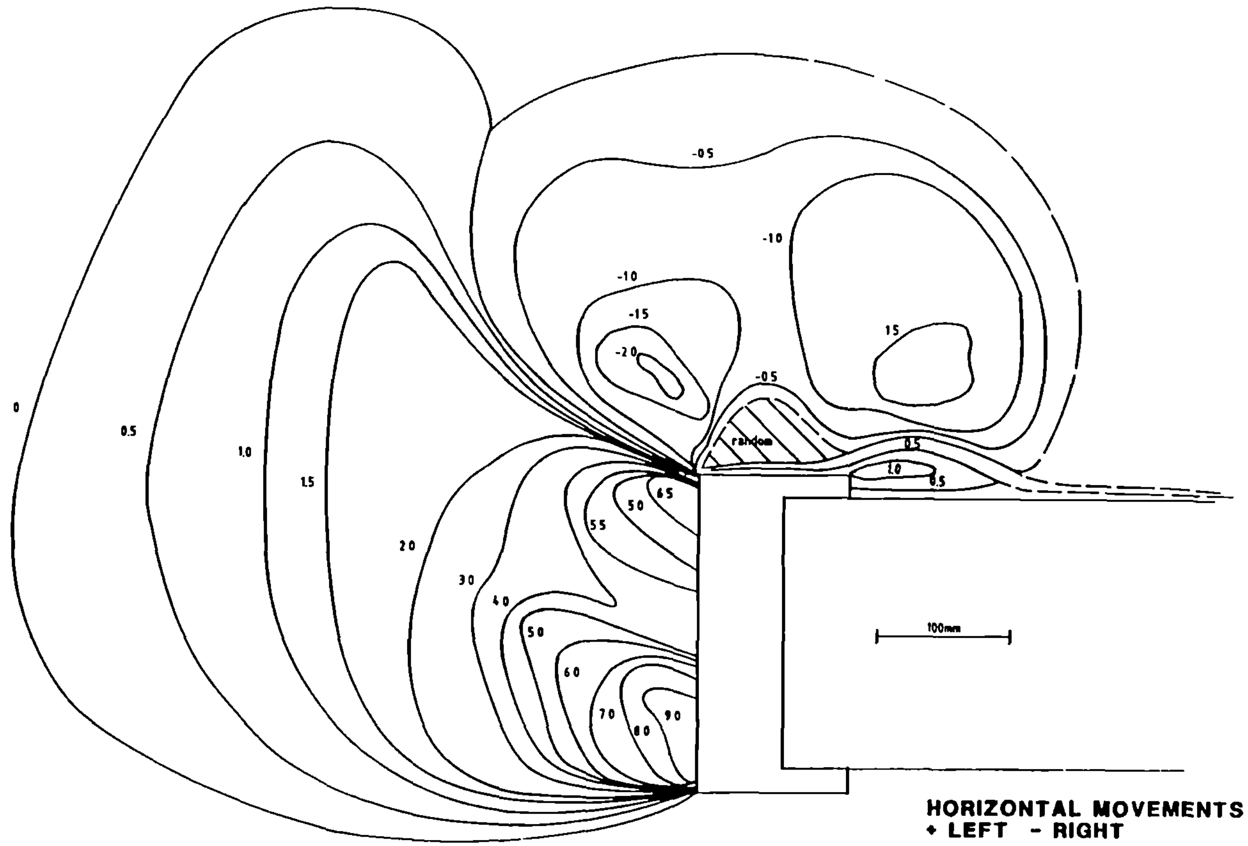

(b)

Fig. 5.13 Displacement contour plots for test OPJ22 (4.5125B0.2) continued

(10mm forward jacking distance, contours in mm)

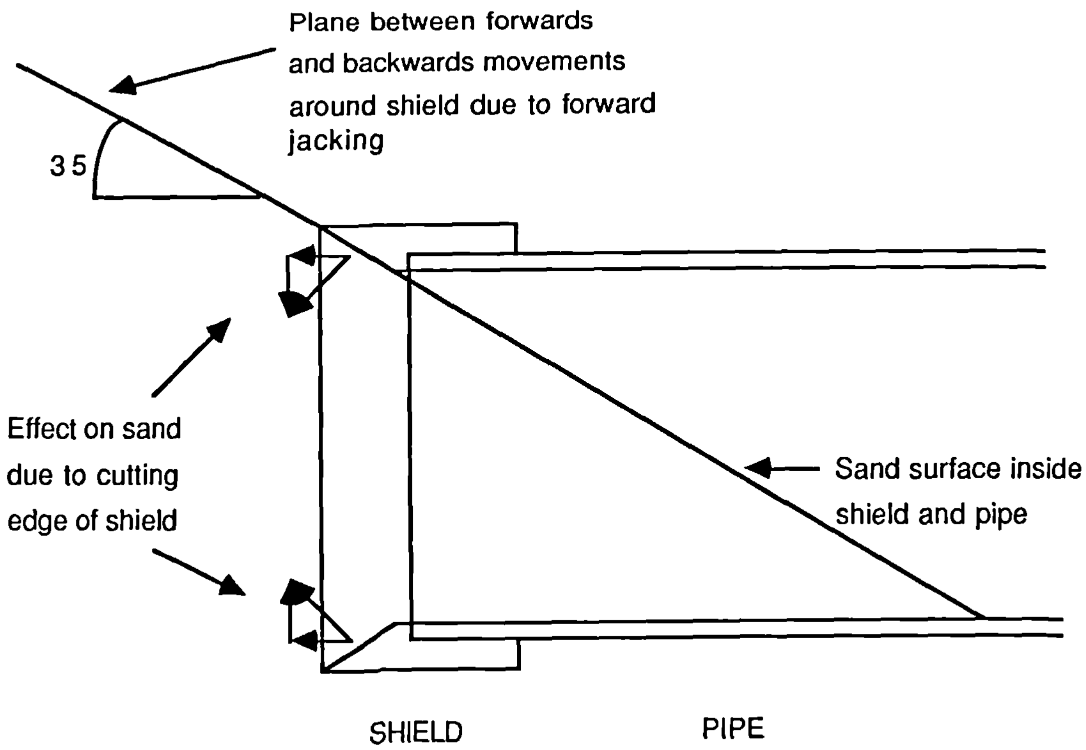

Fig. 5.14 The effect of the pipejacking shield on the sand movements

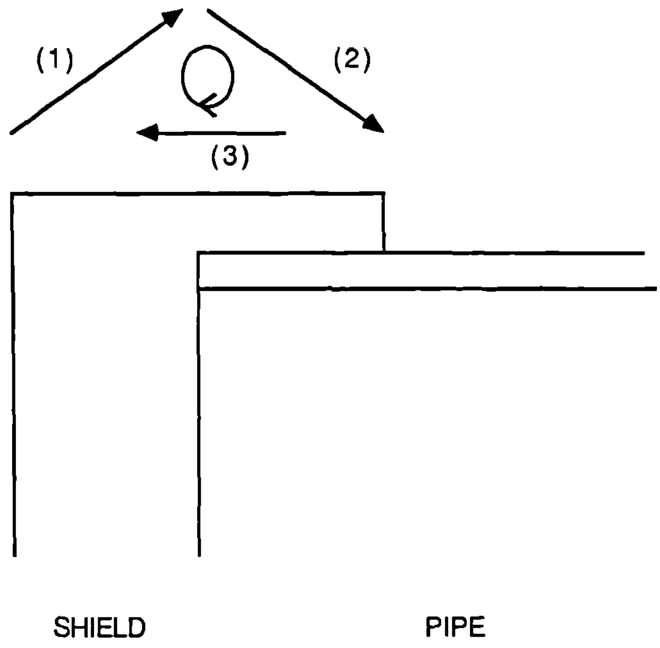

(1) Upwards and backwards movement
from in front of the shield

(2) Downwards and backwards movement
caused by the influence of the overcut

(3) Forwards movement caused by draw-along
of material

Fig. 5.15 Development of the area of random sand movements directly above the pipejacking shield

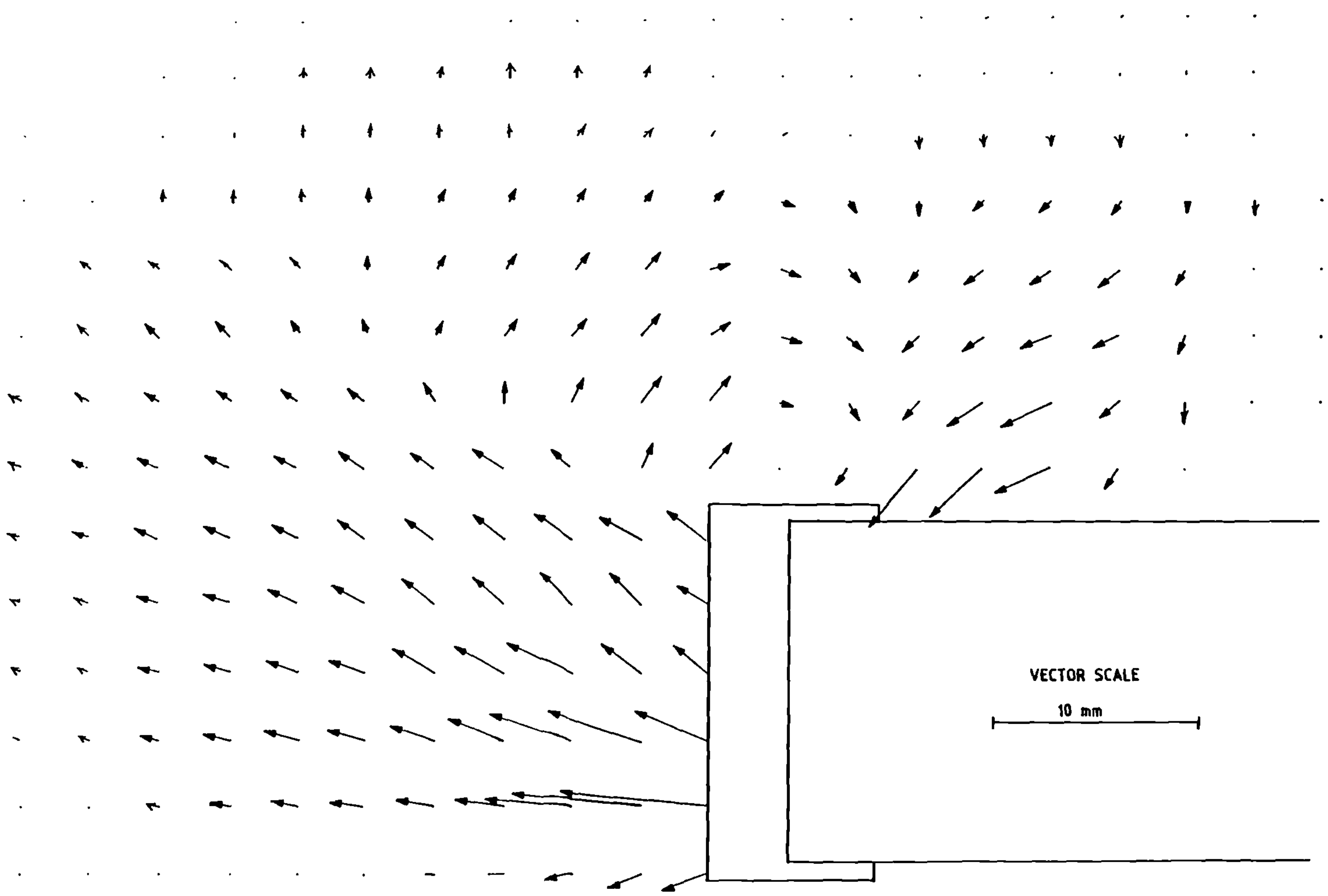

Fig. 5.16 Total displacement vector plot for test OPJ1 (4.5dLB0.1)

(10mm forward jacking distance)

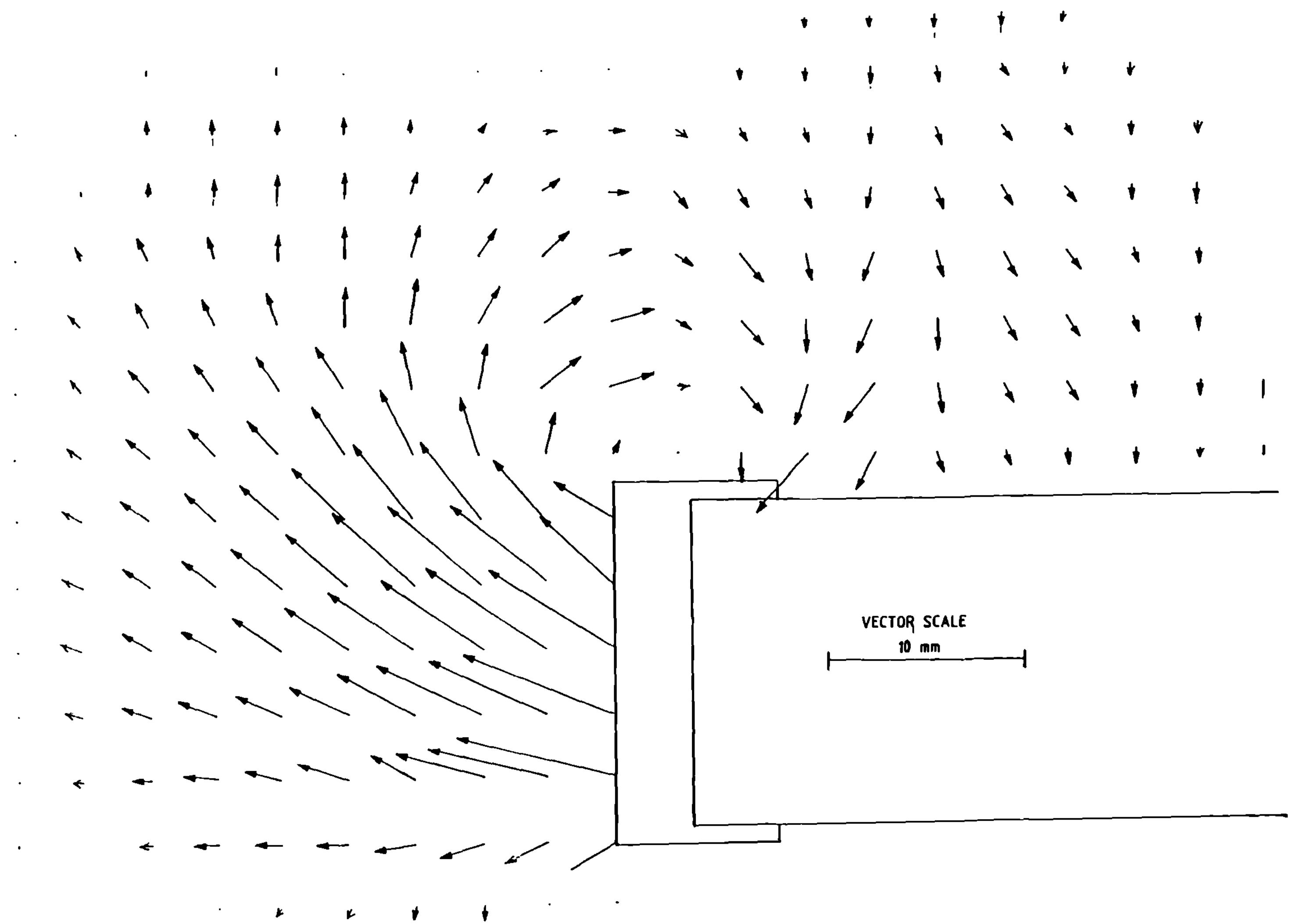

Fig. 5.17 Total displacement vector plot for test OPJ4 (4.5lLB0.1)

(10mm forward jacking distance)

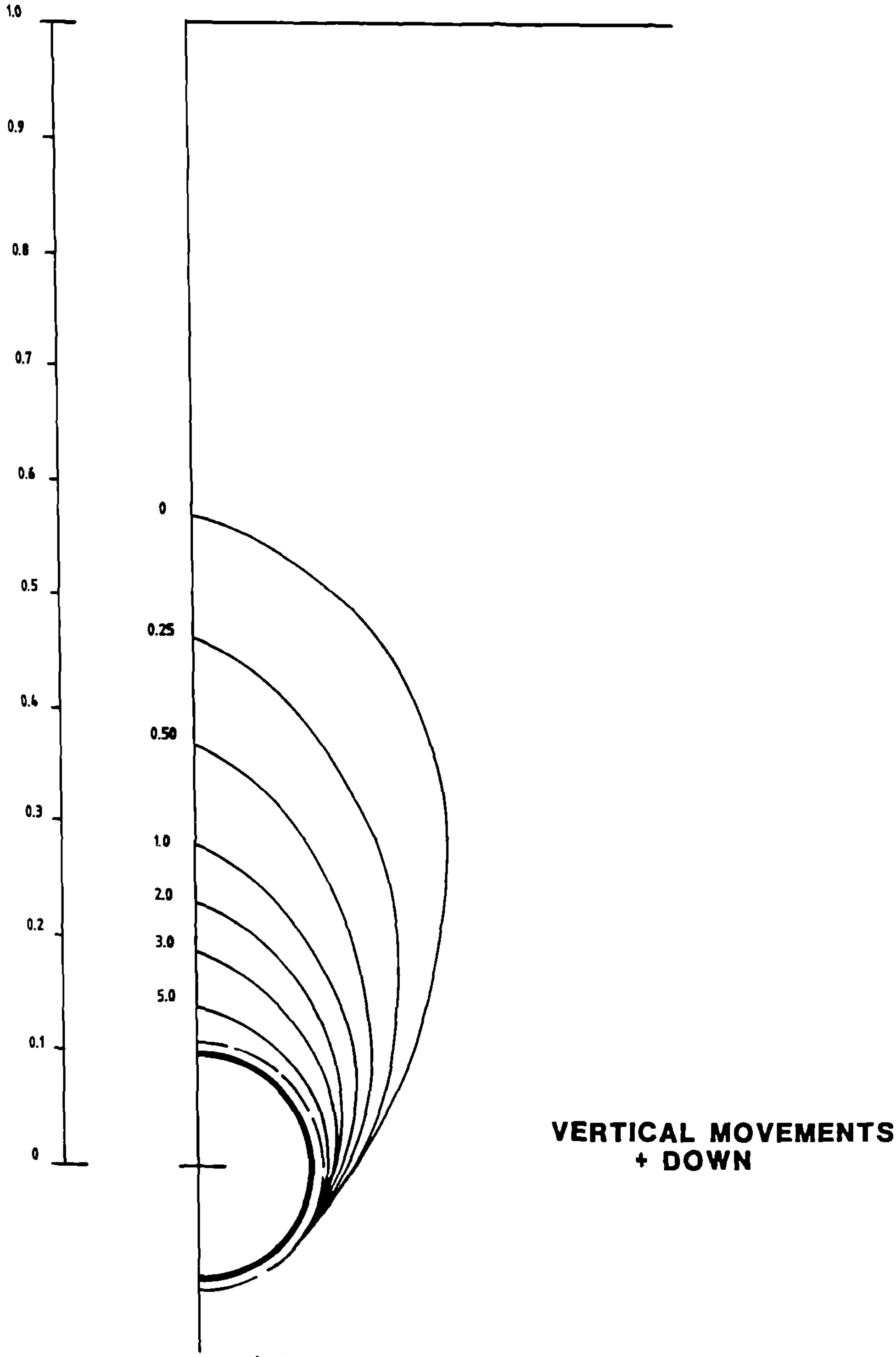

(a)

Fig. 5.18 Displacement contour plots in the perpendicular plane due to the pipejacking shield overcut for test OPJ1 (4.5dLB0.1)

(contours in mm)

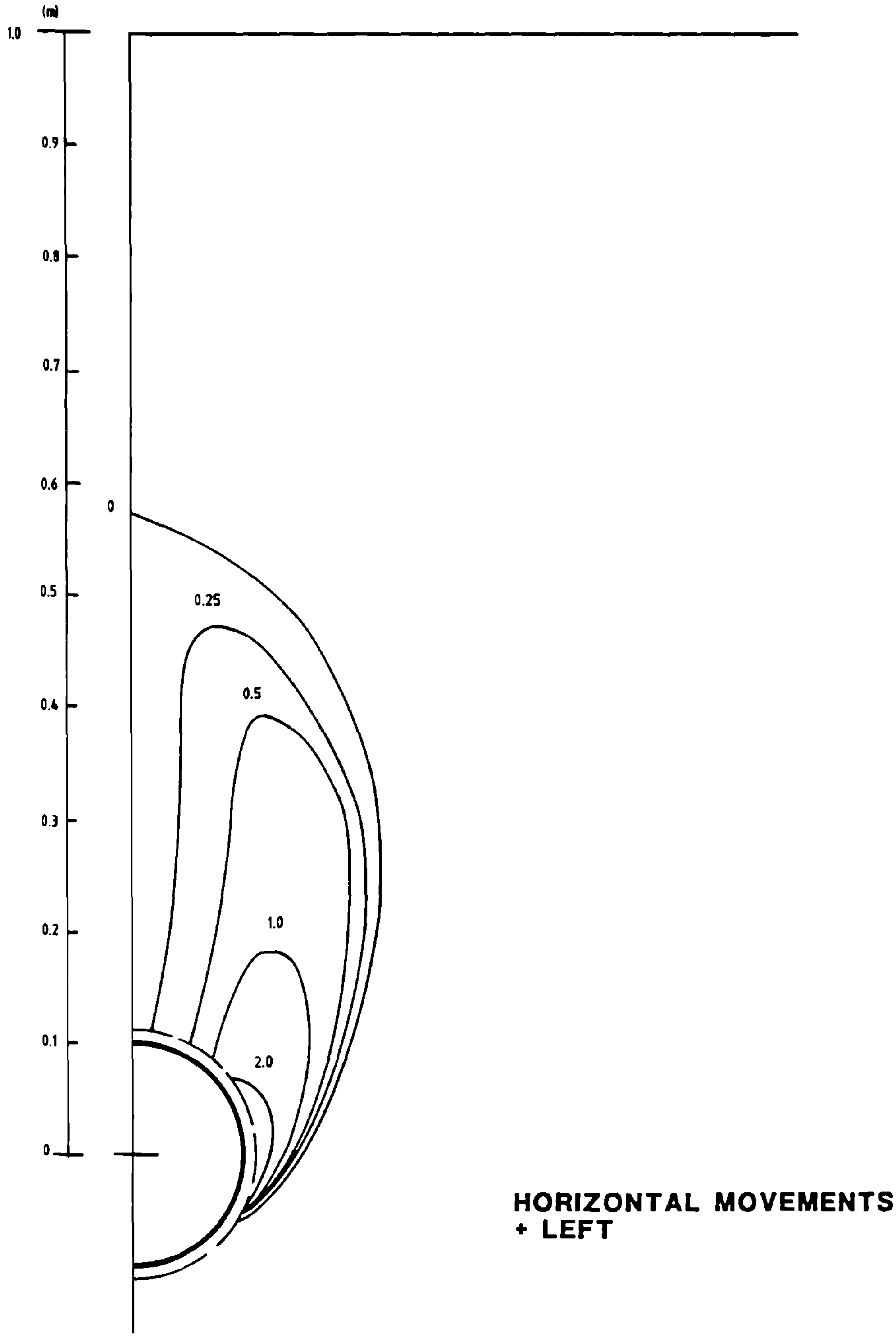

(b)

Fig. 5.18 Displacement contour plots in the perpendicular plane due to the pipejacking shield overcut for test OPJ1 (4.5dLB0.1), continued

(contours in mm)

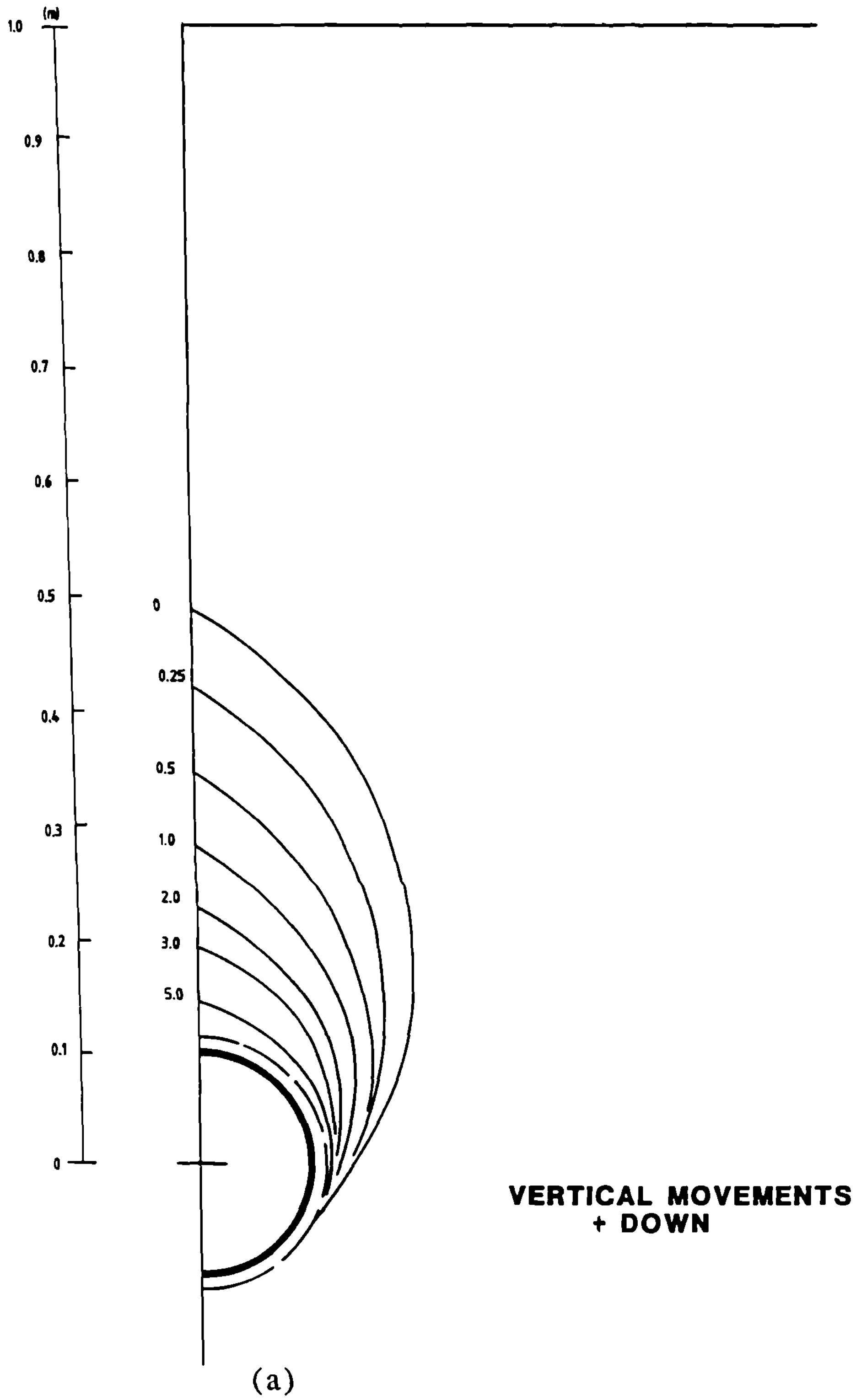

(a)

Fig. 5.19 Displacement contour plots in the perpendicular plane due to the pipejacking shield overcut for test OPJ3 (20.0dLB0.1)

(contours in mm)

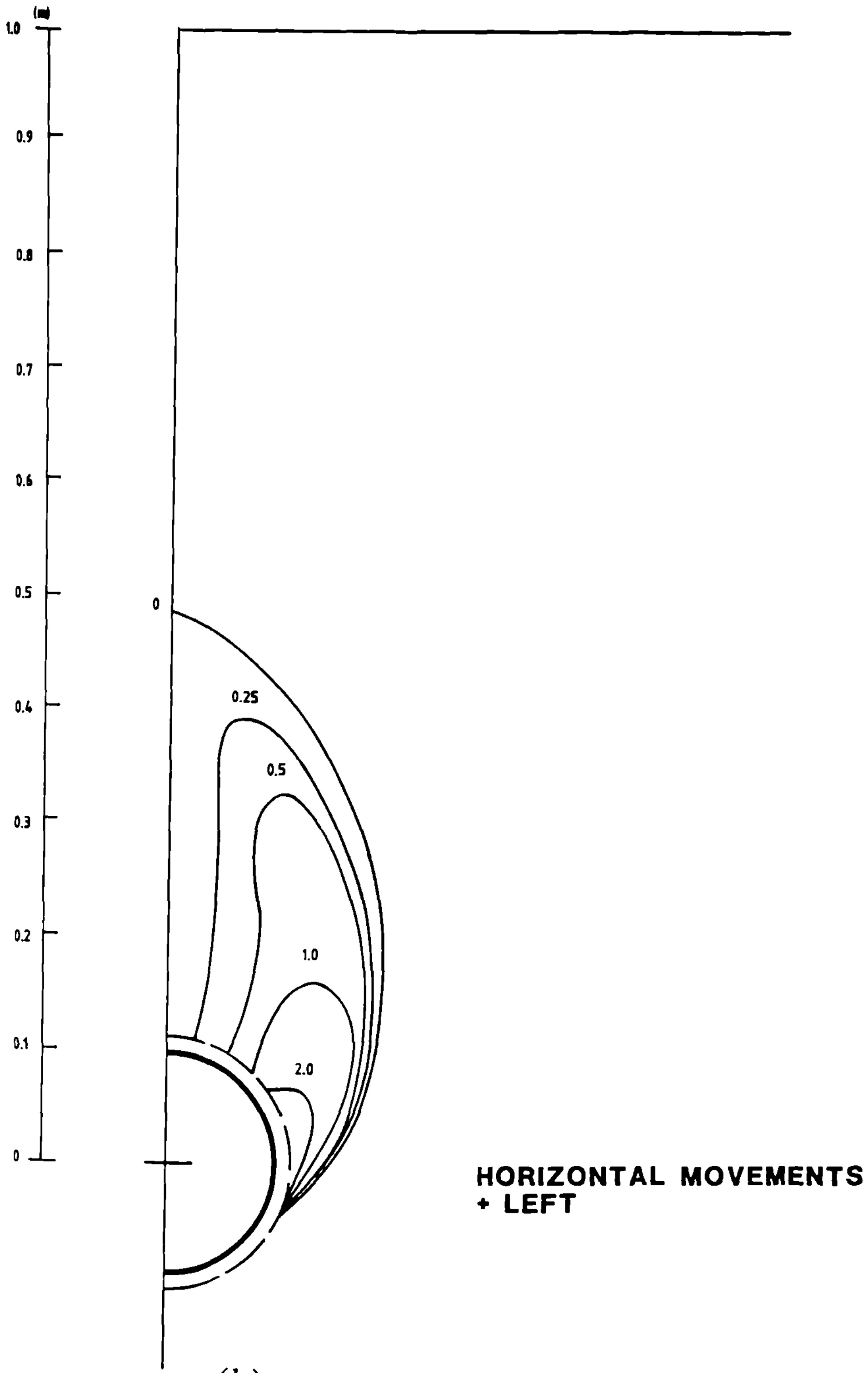

(b)

Fig. 5.19 Displacement contour plots in the perpendicular plane due to the pipejacking shield overcut for test OPJ3 (20.0dLB0.1), continued

(contours in mm)

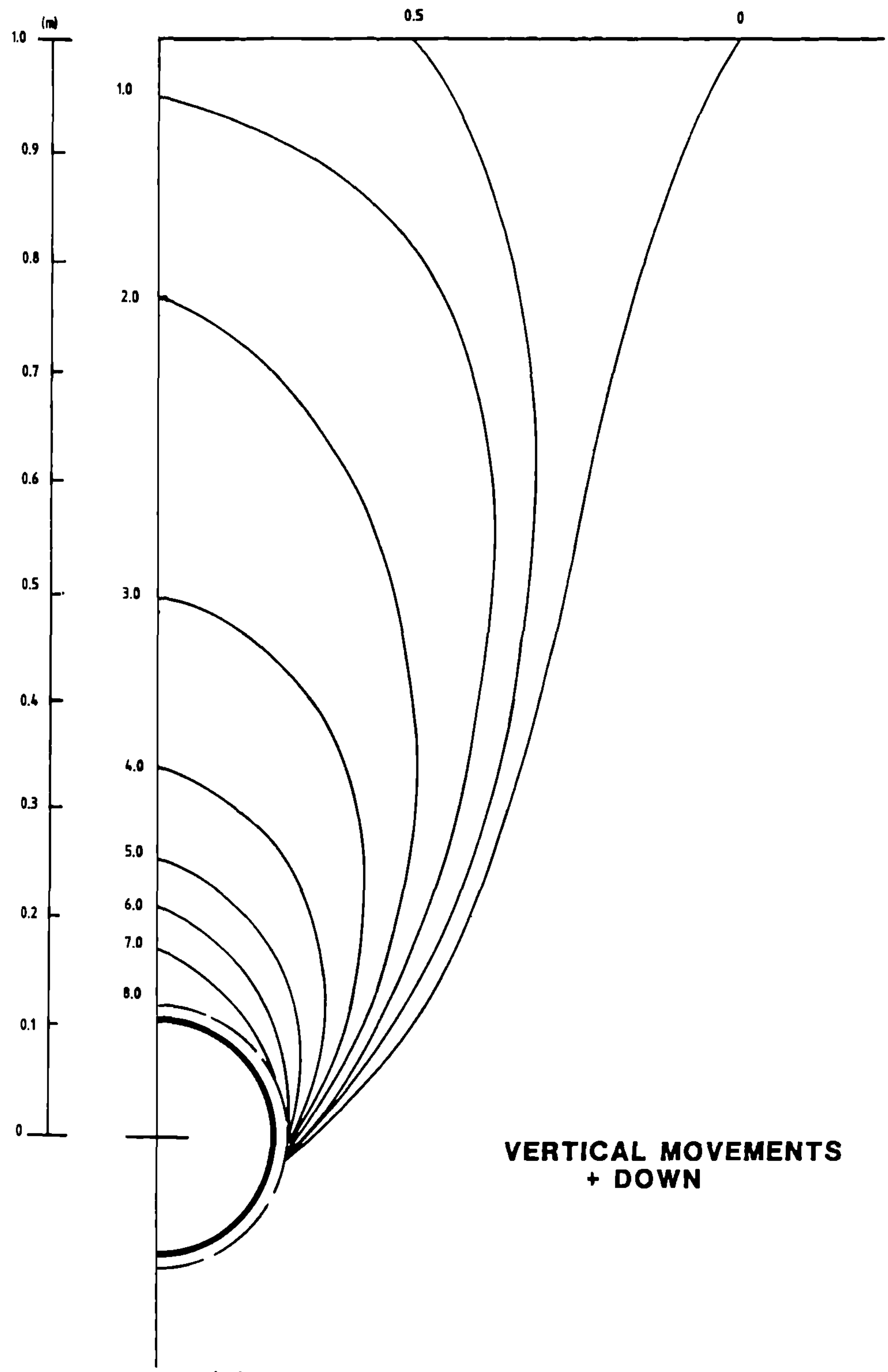

(a)

Fig. 5.20 Displacement contour plots in the perpendicular plane due to the pipejacking shield overcut for test OPJ4 (4.5ILB0.1)

(contours in mm)

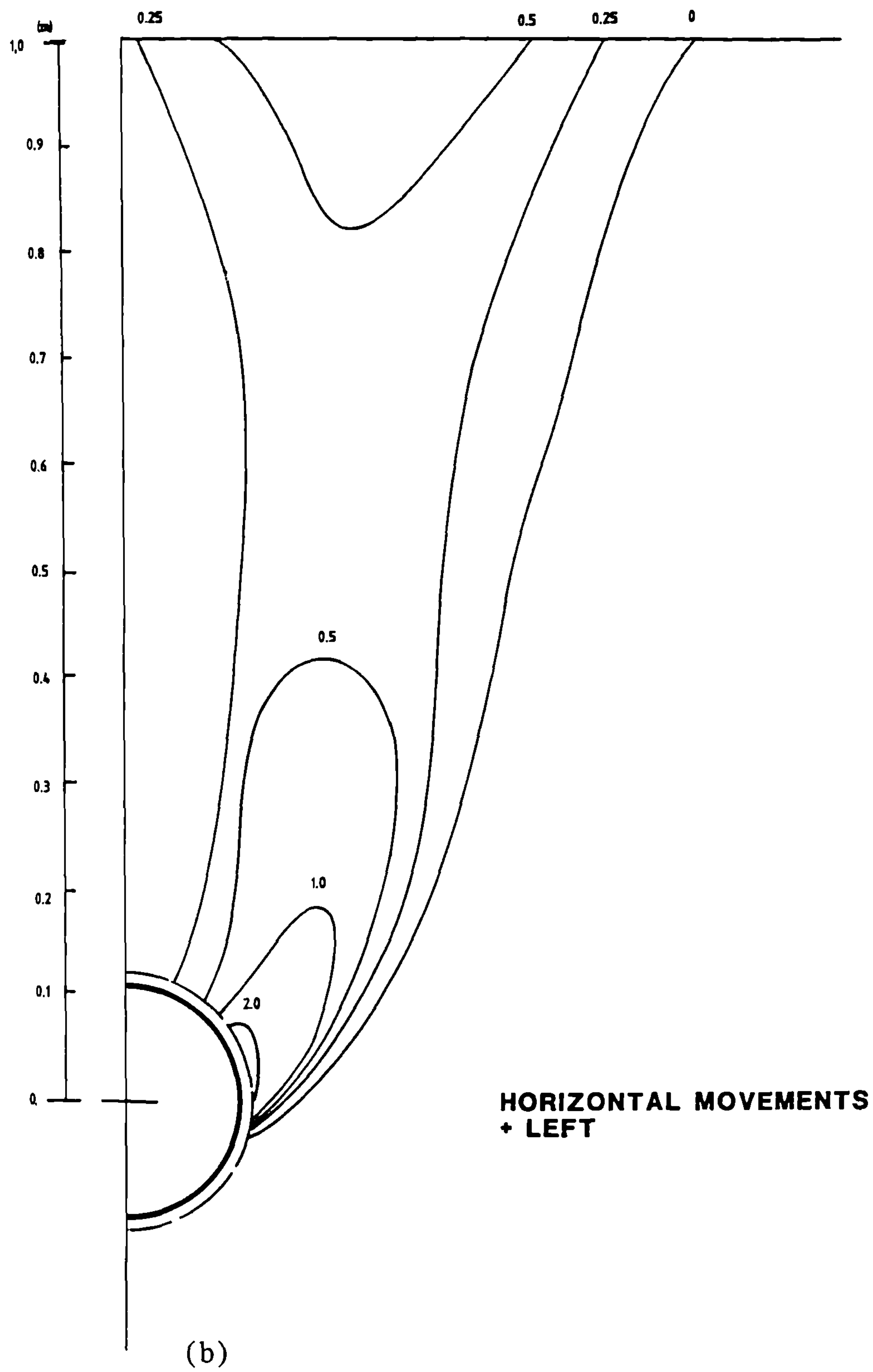

(b)

Fig. 5.20 Displacement contour plots in the perpendicular plane due to the pipejacking shield overcut for test OPJ4 (4.51LB0.1), continued

(contours in mm)

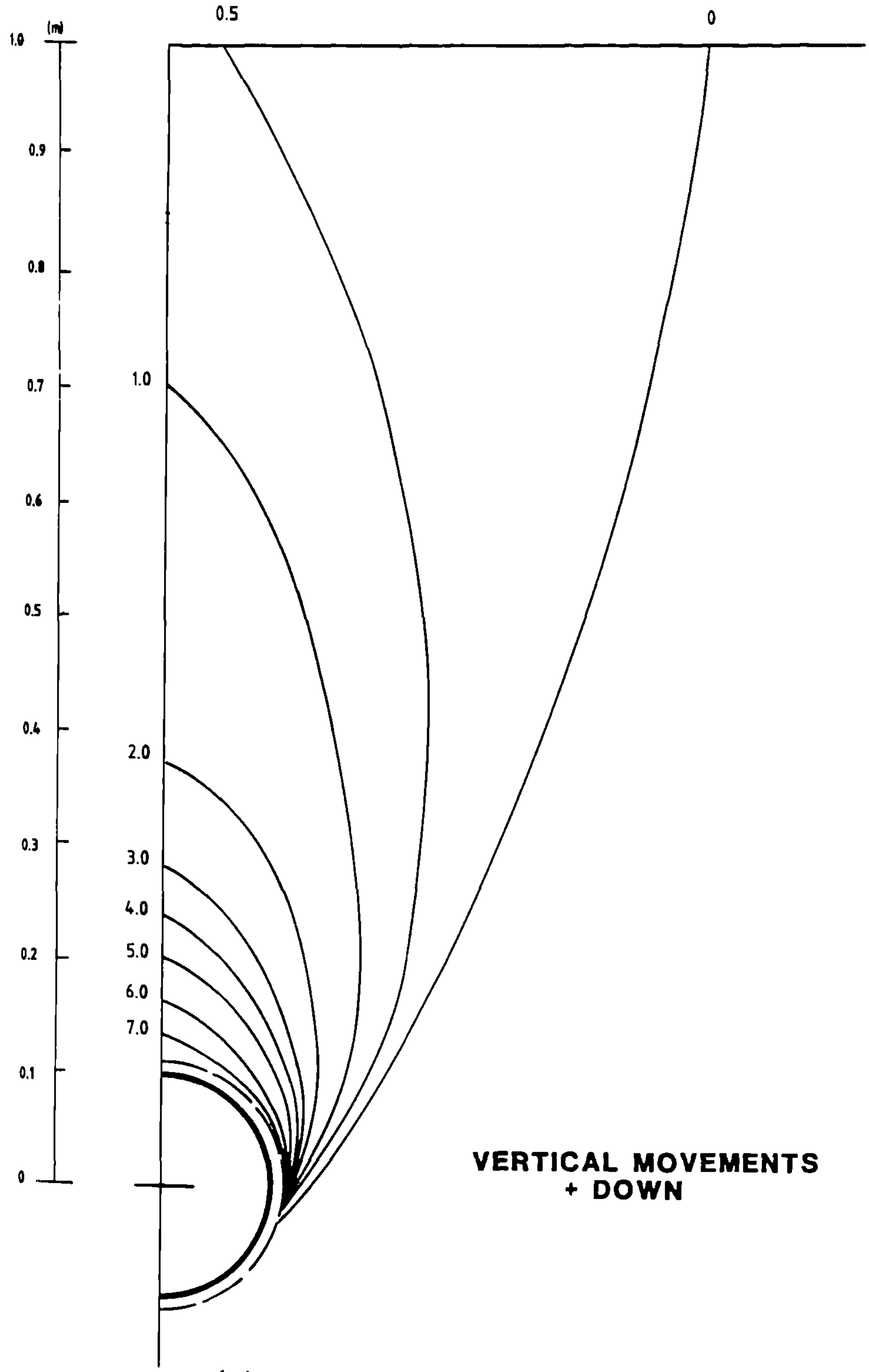

(a)

Fig. 5.21 Displacement contour plots in the perpendicular plane due to the pipejacking shield overcut for test OPJ6 (20.0ILB0.1)

(contours in mm)

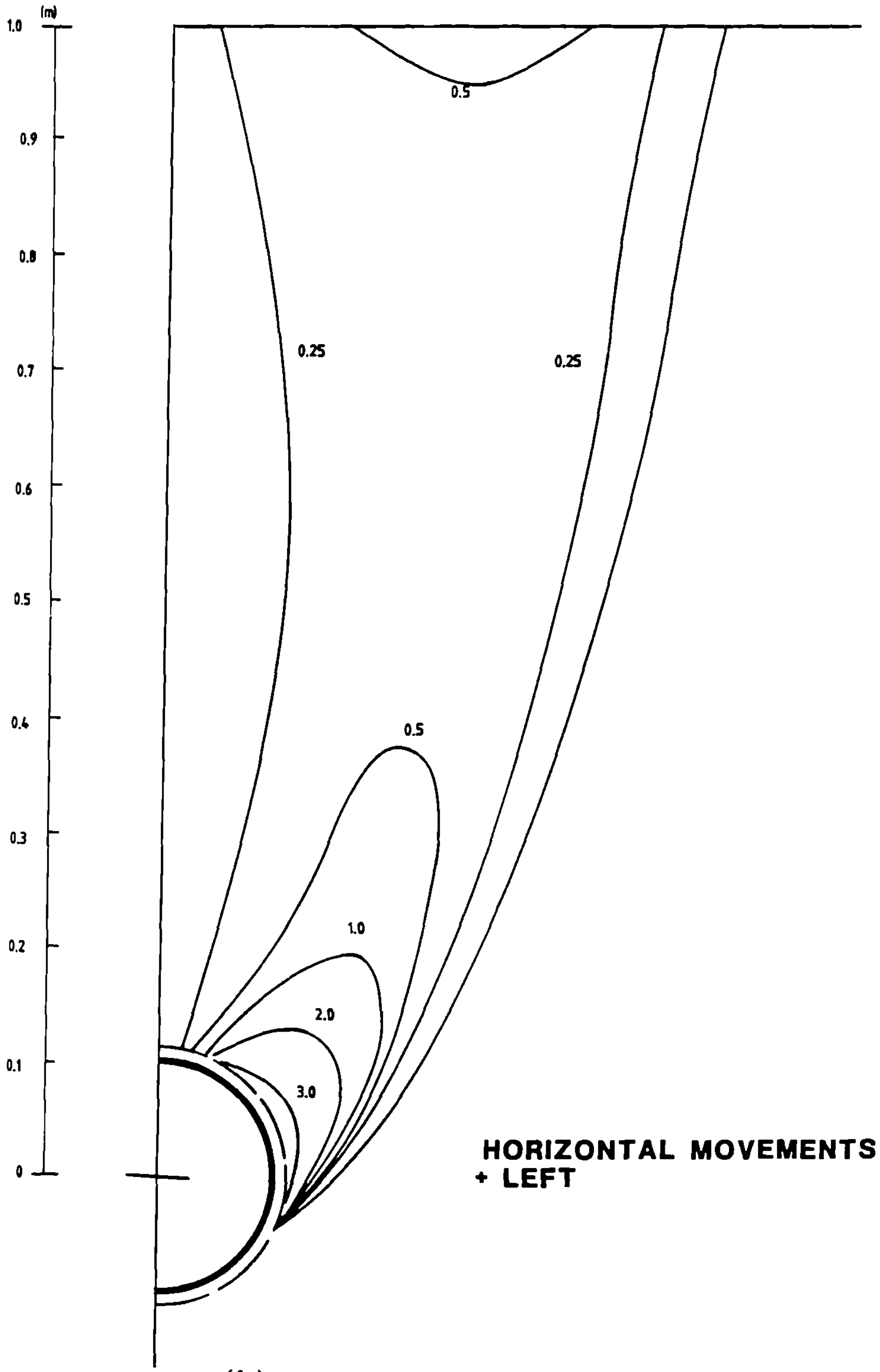

(b)

Fig. 5.21 Displacement contour plots in the perpendicular plane due to the pipejacking shield overcut for test OPJ6 (20.0lLB0.1), continued

(contours in mm)

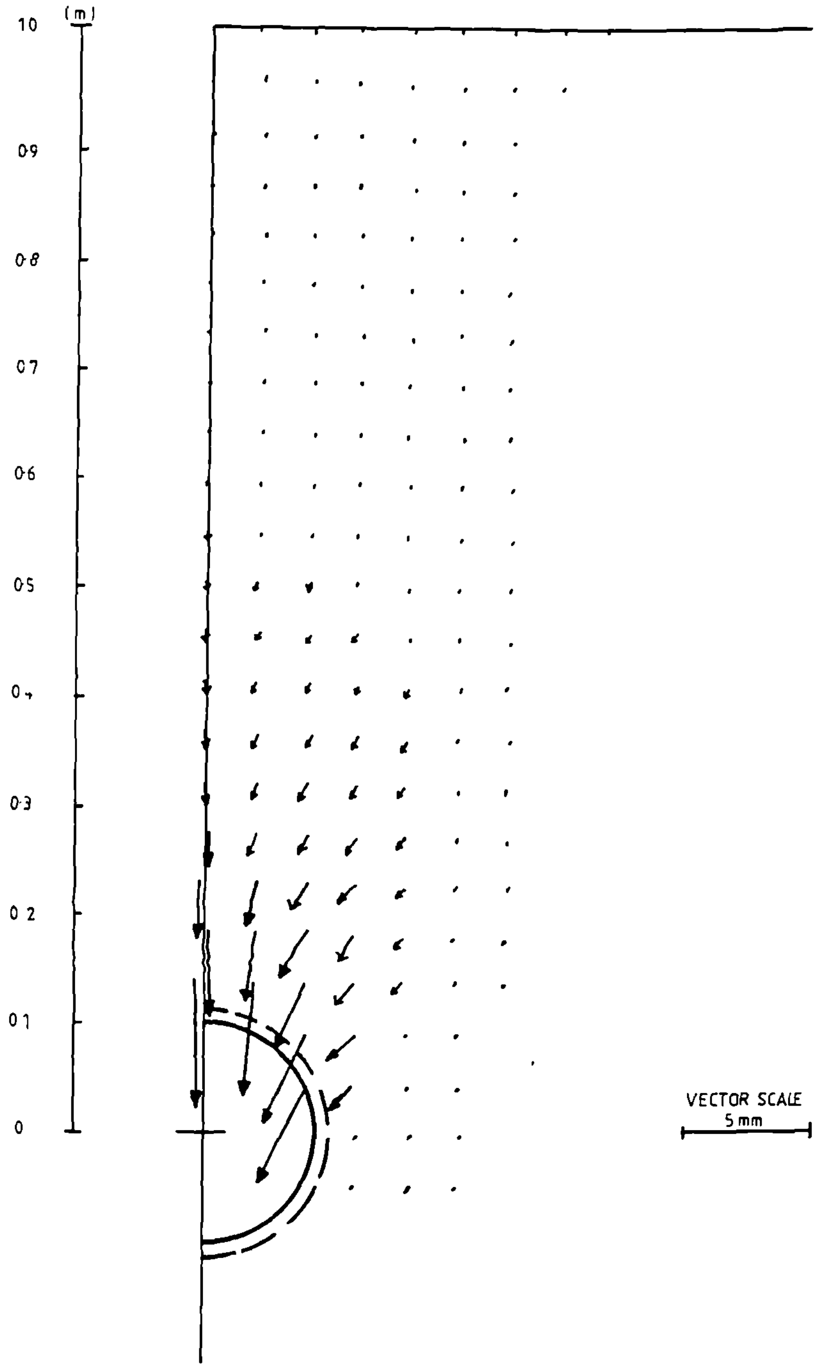

Fig. 5.22 Total displacement vector plot in the perpendicular plane caused by the pipejacking shield overcut for test OPJ1 (4.5dLB0.1)

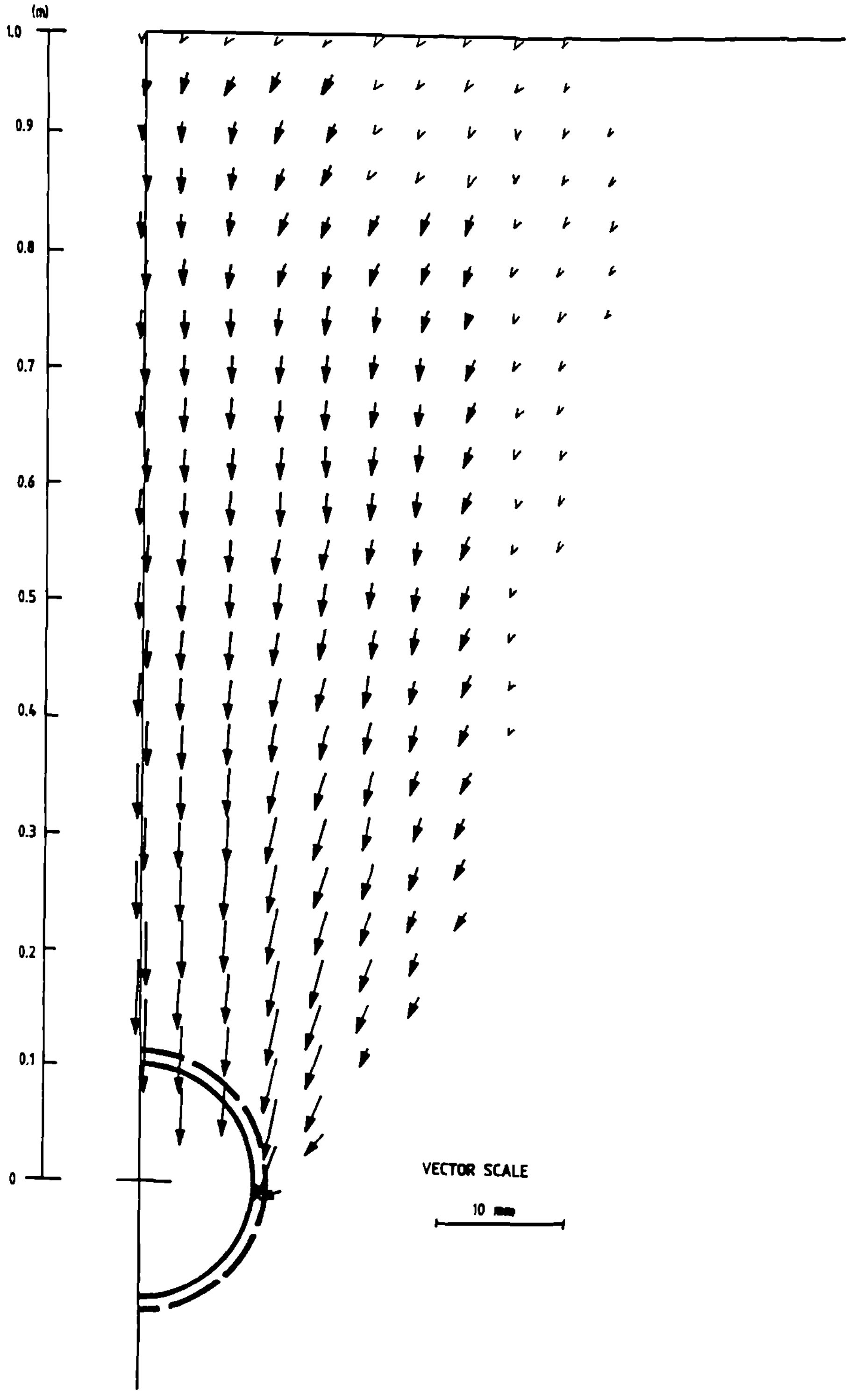

Fig. 5.23 Total displacement vector plot in the perpendicular plane caused by the pipejacking shield overcut for test OPJ4 (4.5ILB0.1)

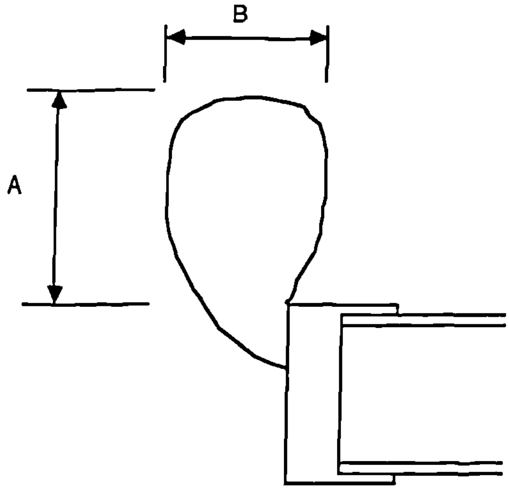

	C/D=4.5	C/D= 2[illegible]
A	500	200
B	200	100
C	400	350
D	150	100

(Dimensions in mm)

(a) Tests OPJ1 (4.5dLB0.1) and OPJ3 (20.0dLB0.1)

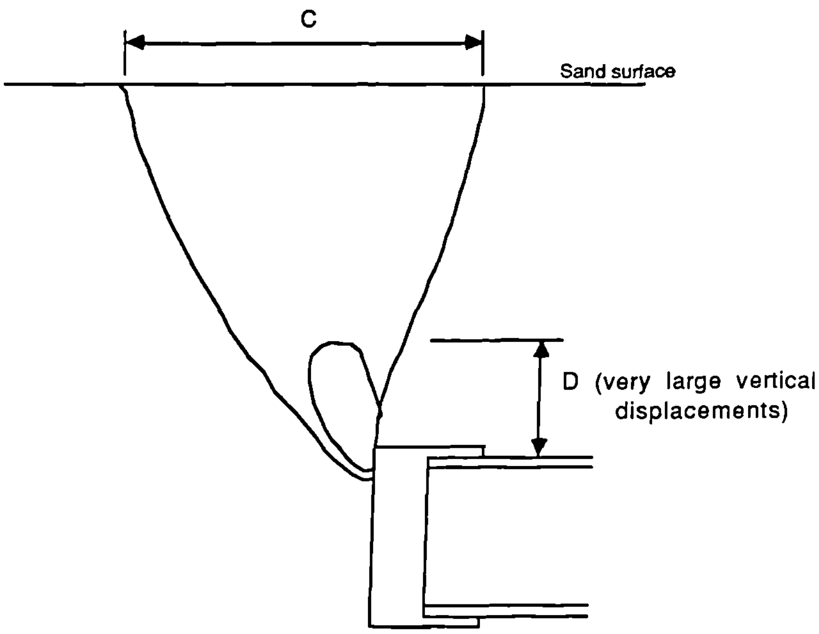

(b) Tests OPJ4 (4.5lLB0.1) and OPJ6 (20.0lLB0.1)

Fig. 5.24 Extents of movements due to face loss

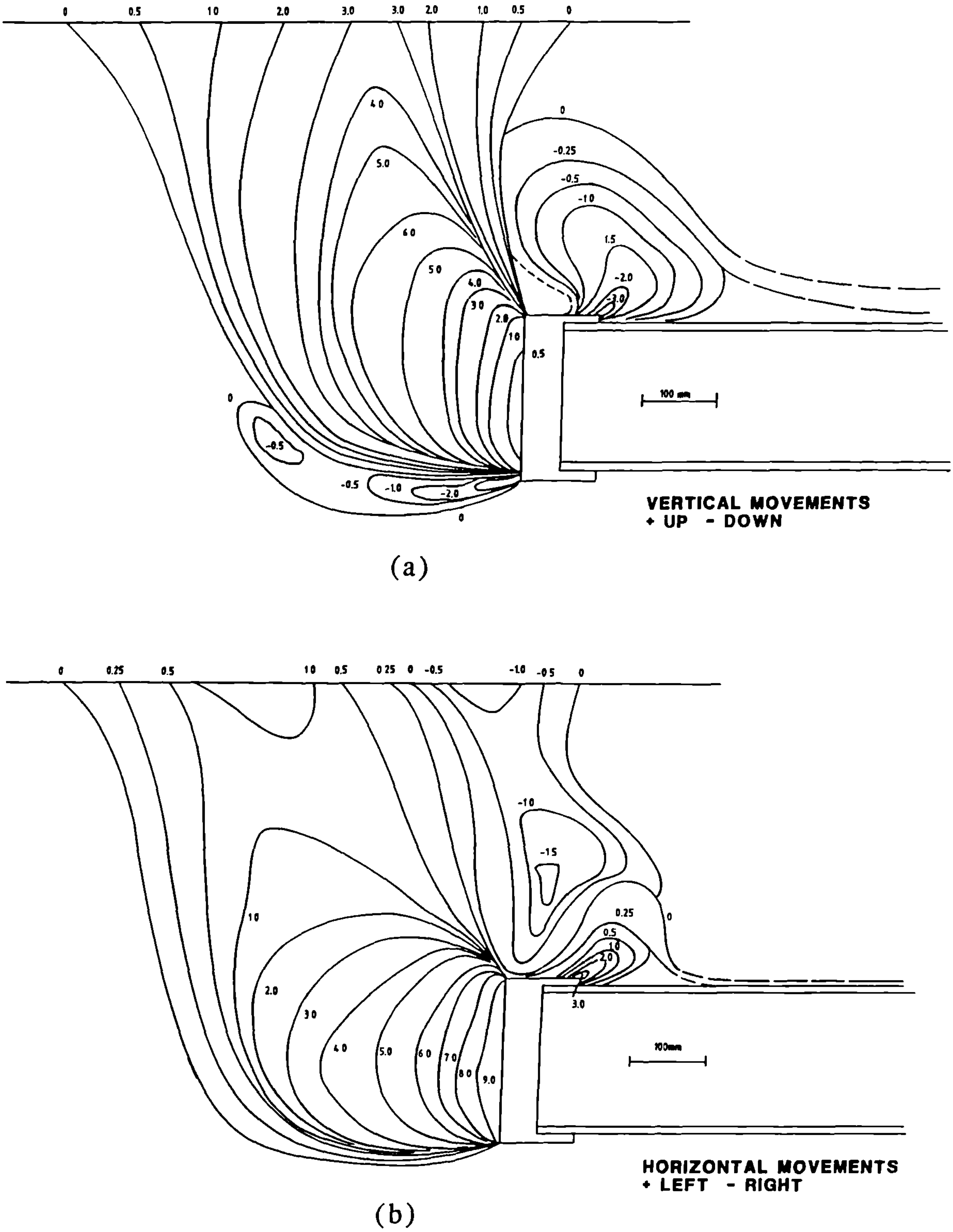

Fig. 5.25 Displacement contour plots for test CPJ1 (2.0dLB0.1)

(10mm jacking distance, contours in mm)

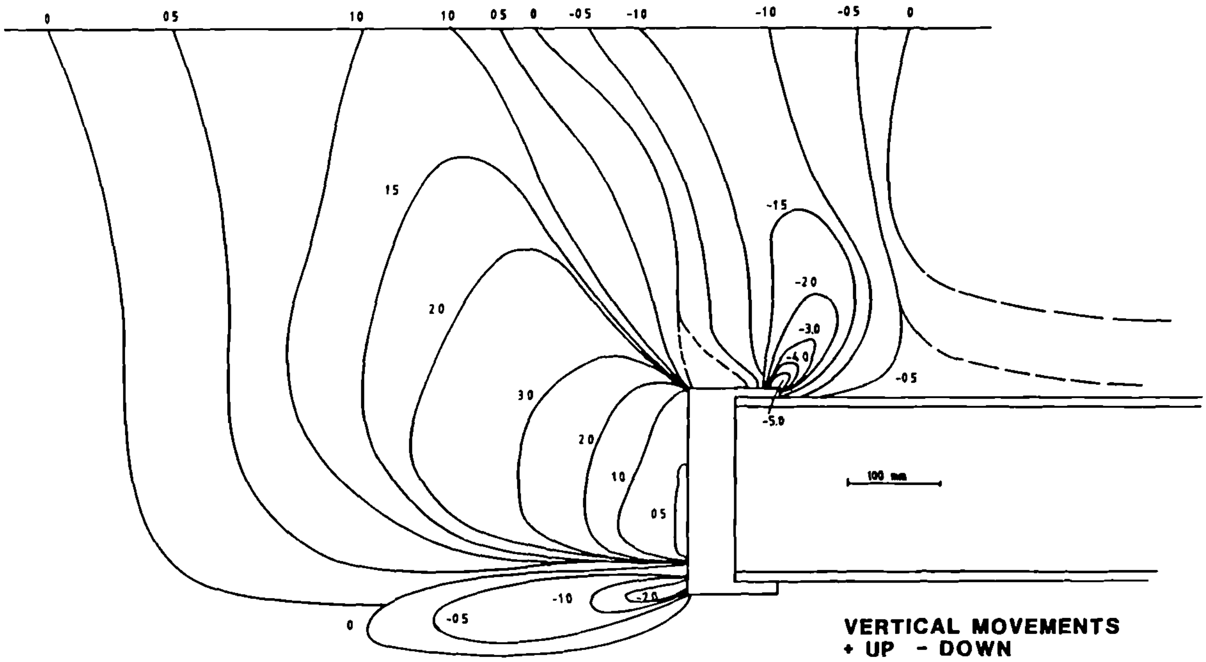

(a)

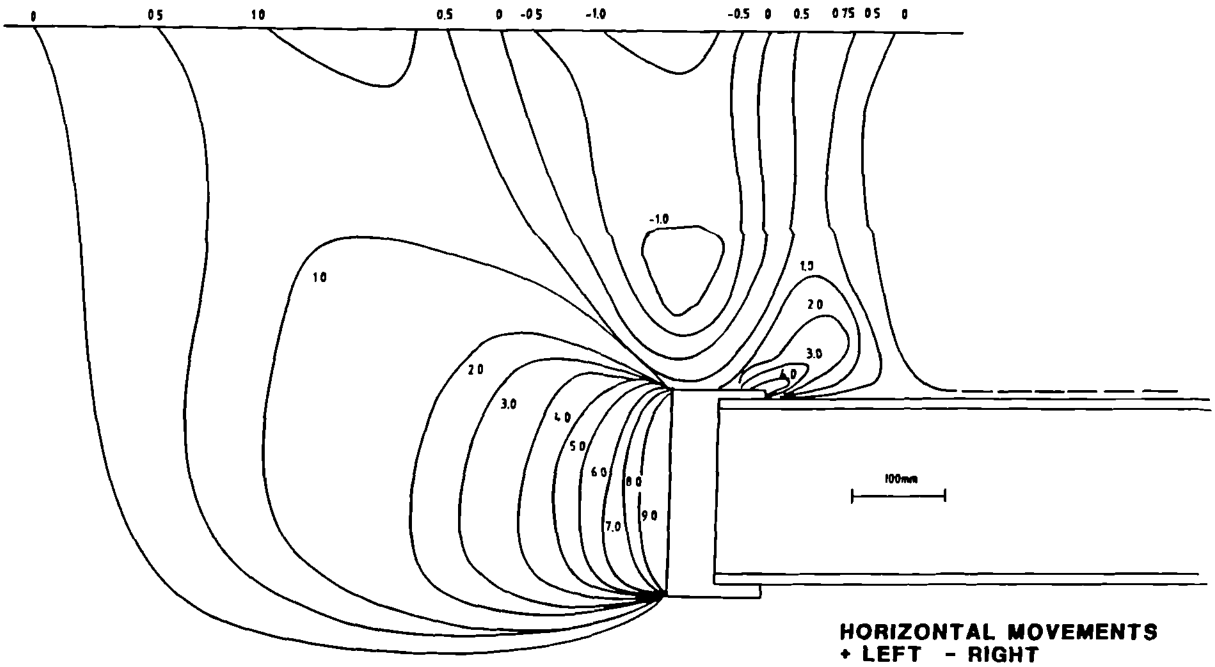

(b)

Fig. 5.26 Displacement contour plots for test CPJ2 (2.0ILB0.1)

(10mm jacking distance, contours in mm)

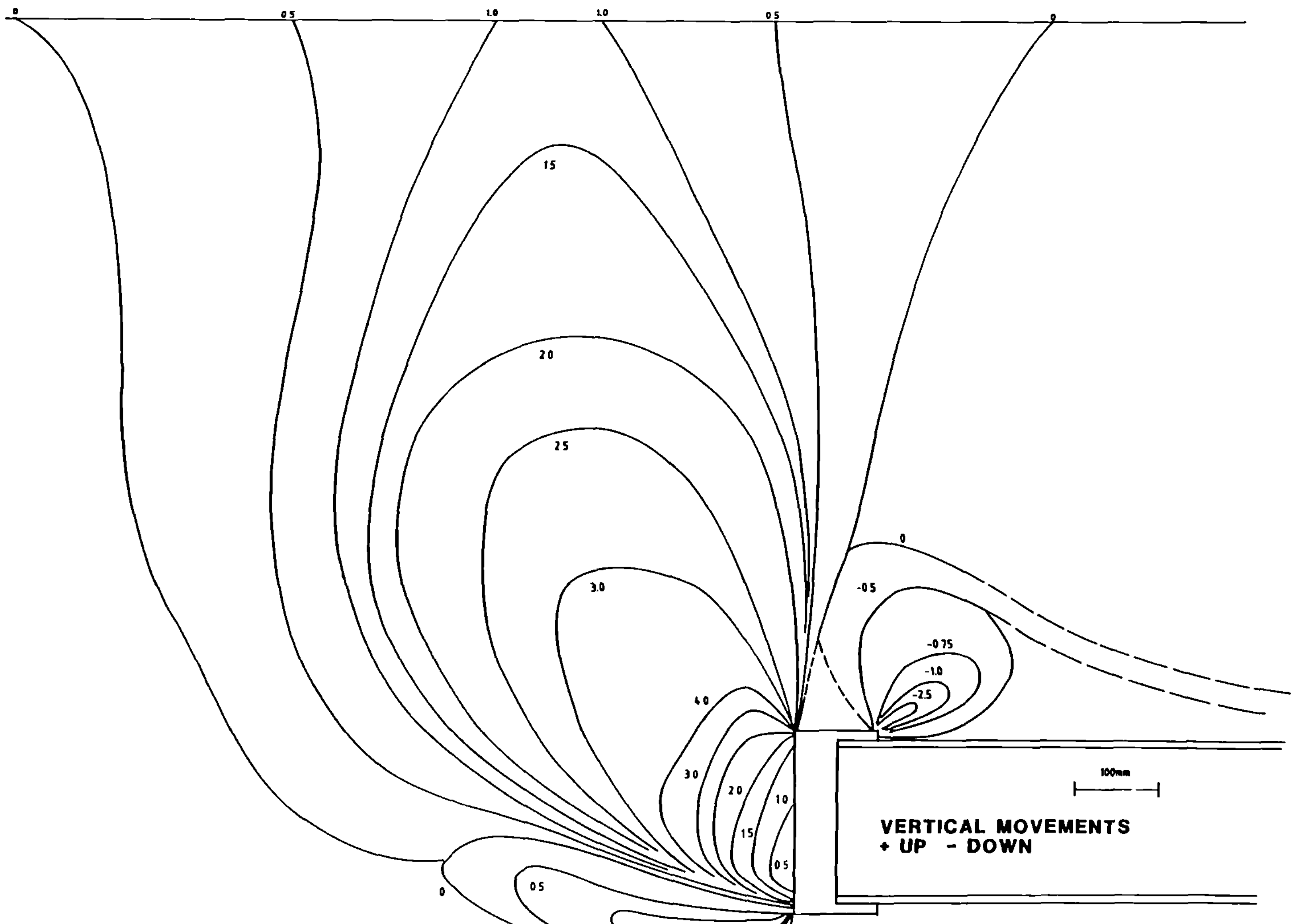

(a)

Fig. 5.27 Displacement contour plots for test CPJ3 (4.5dLB0.1)
(10mm jacking distance, contours in mm)

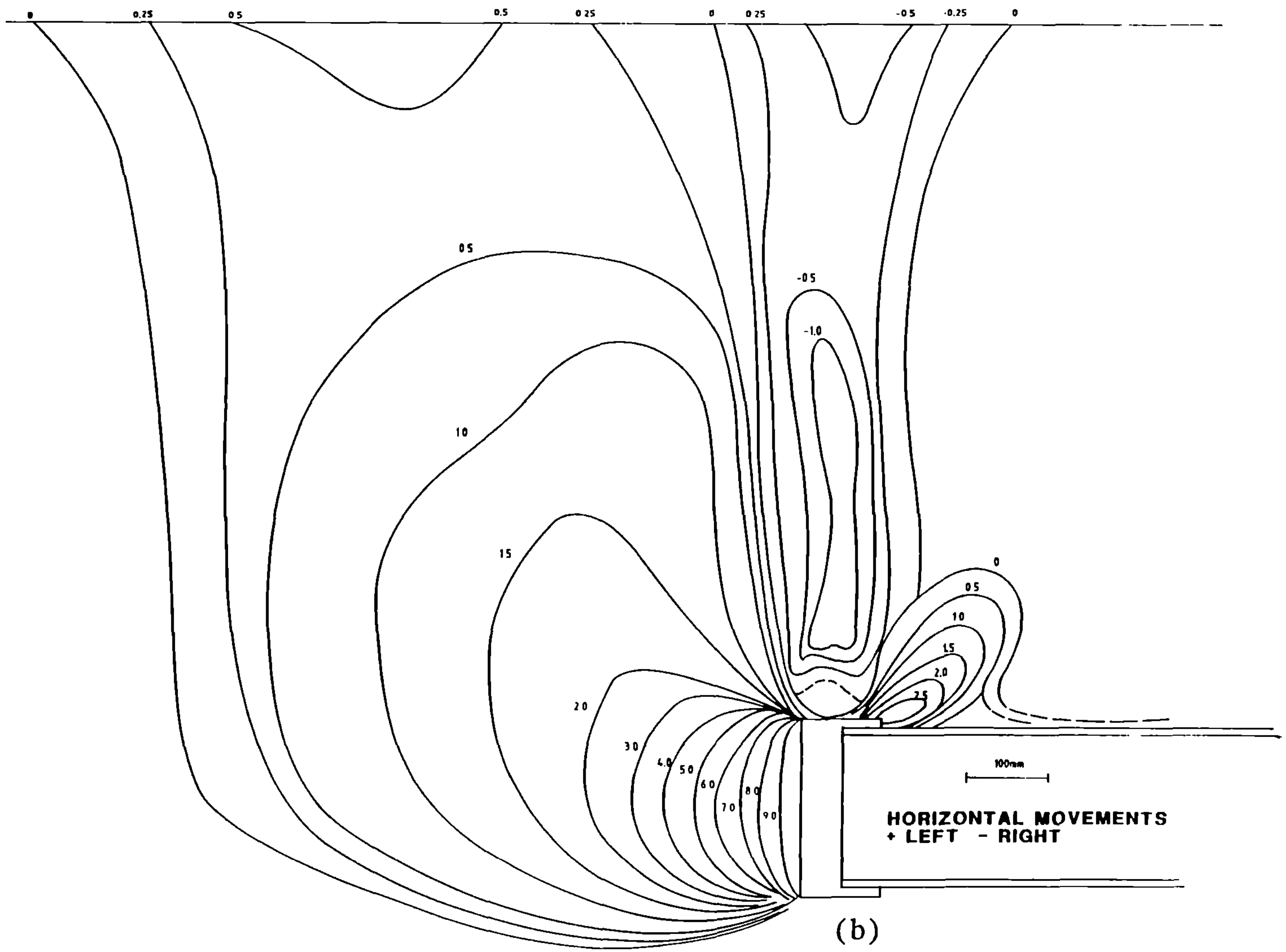

(b)

Fig. 5.27 Displacement contour plots for test CPJ3 (4.5dLB0.1) continued

(10mm jacking distance, contours in mm)

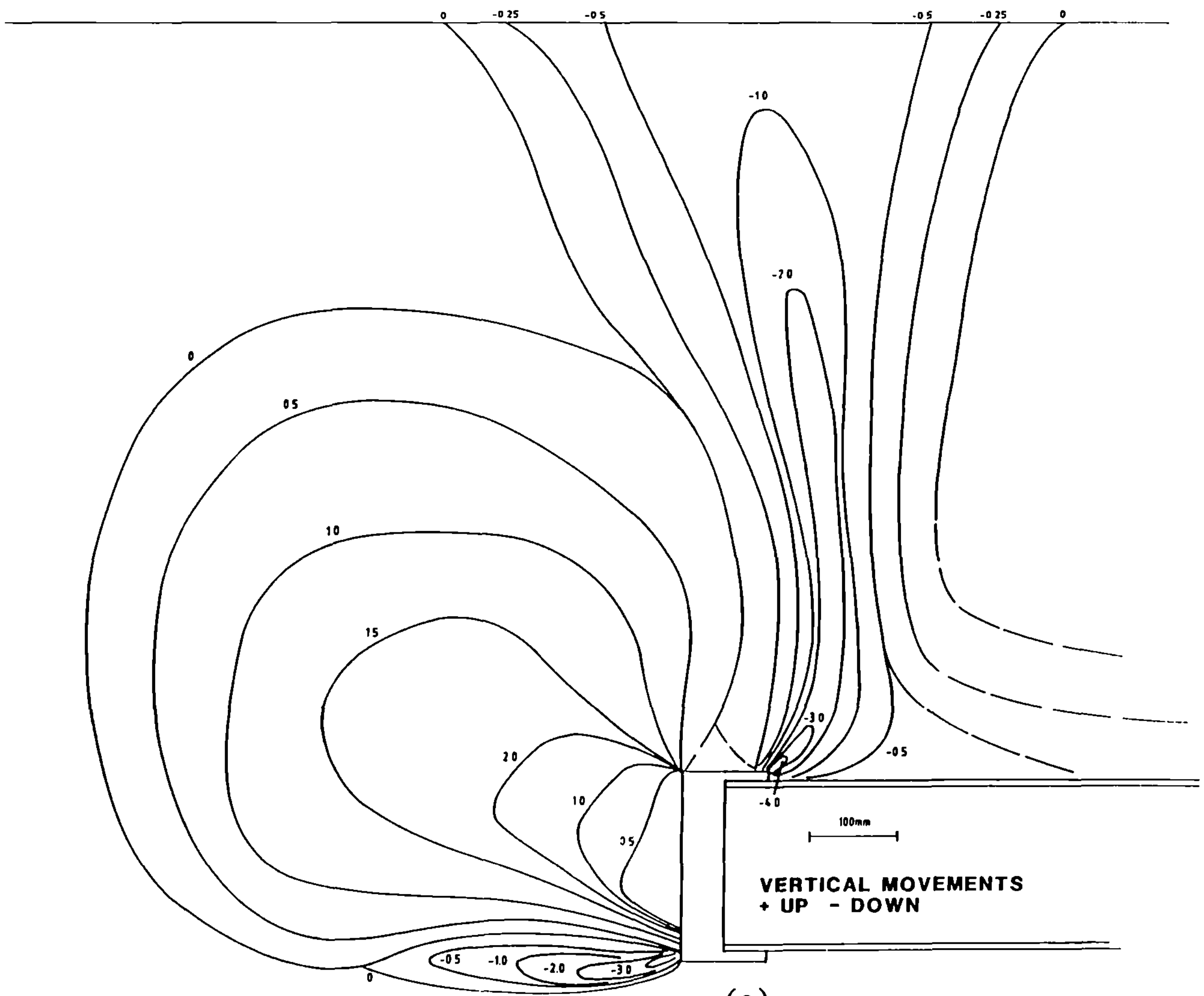

(a)

Fig. 5.28 Displacement contour plots for test CPJ4 (4.5lLB0.1)
(10mm jacking distance, contours in mm)

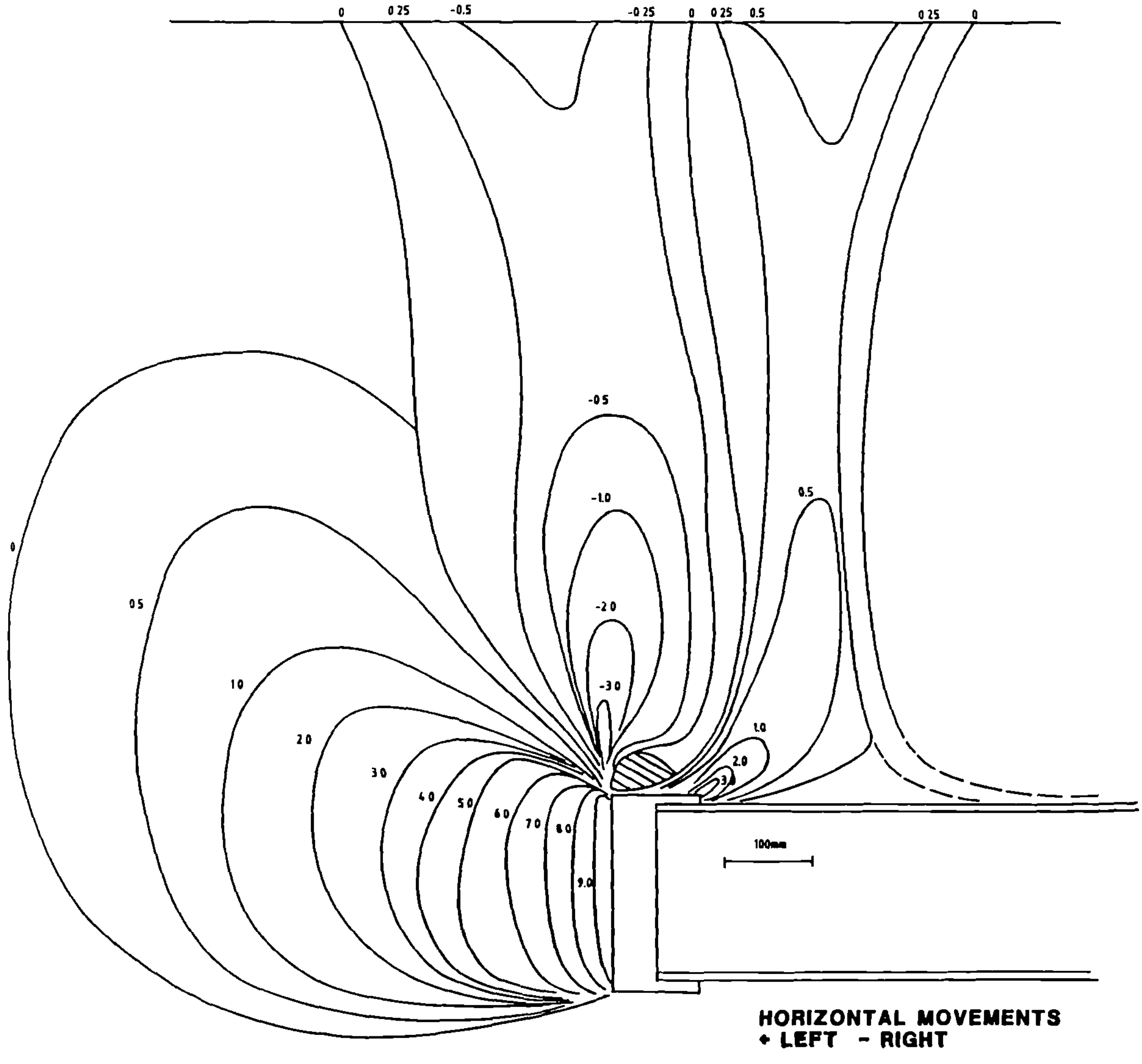

(b)

Fig. 5.28 Displacement contour plots for test CPJ4 (4.5ILB0.1) continued

(10mm jacking distance, contours in mm)

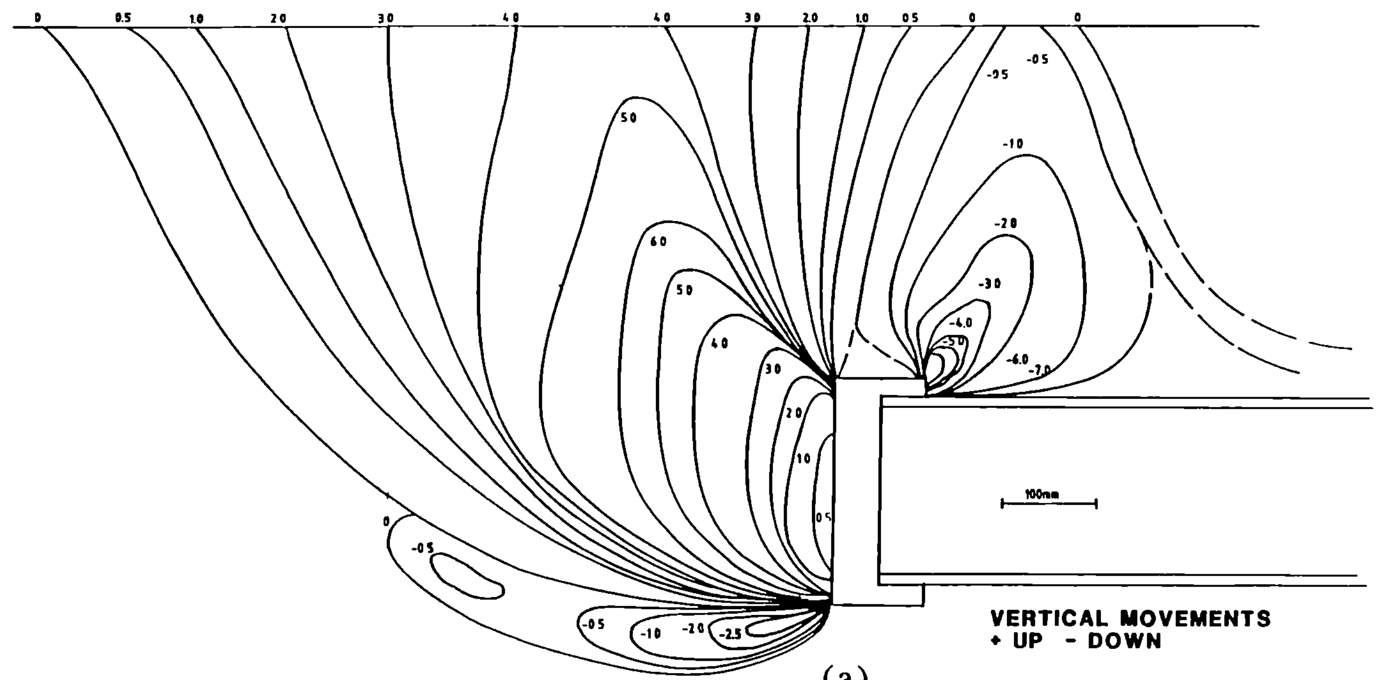

(a)

Fig. 5.29 Displacement contour plots for test CPJ5 (2.0dLB0.2) (10mm jacking distance, contours in mm)

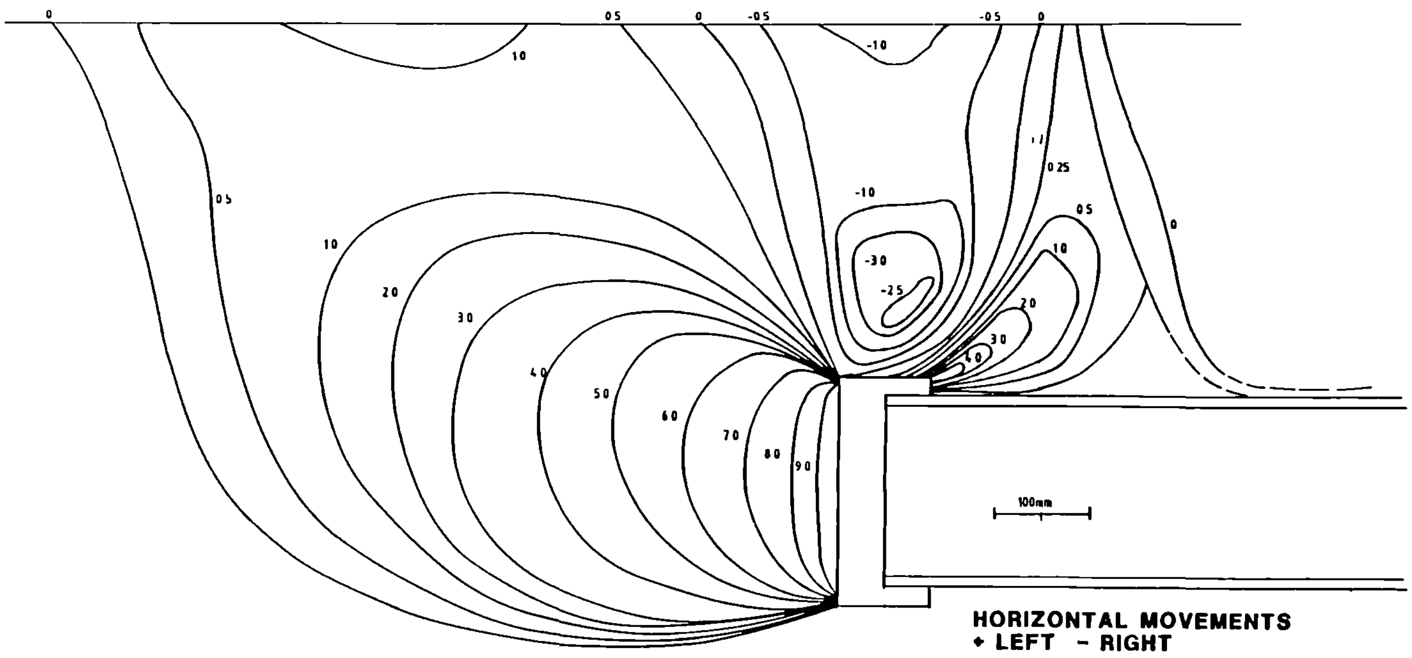

(b)

Fig. 5.29 Displacement contour plots for test CPJ5 (2.0dLB0.2) continued

(10mm jacking distance, contours in mm)

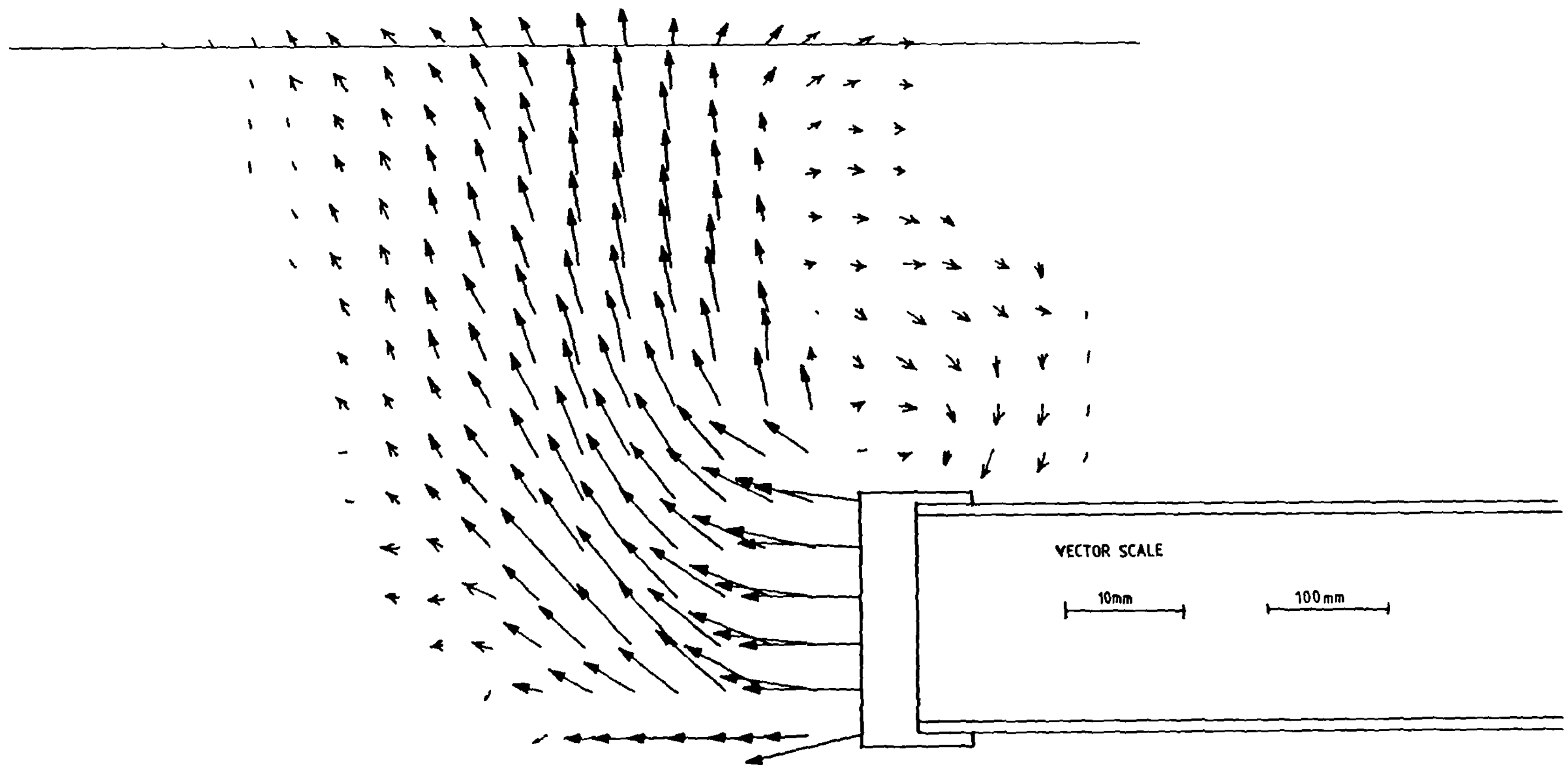

Fig. 5.30 Total displacement vector plot for test CPJ1 (2.0dLB0.1)

(10mm jacking distance)

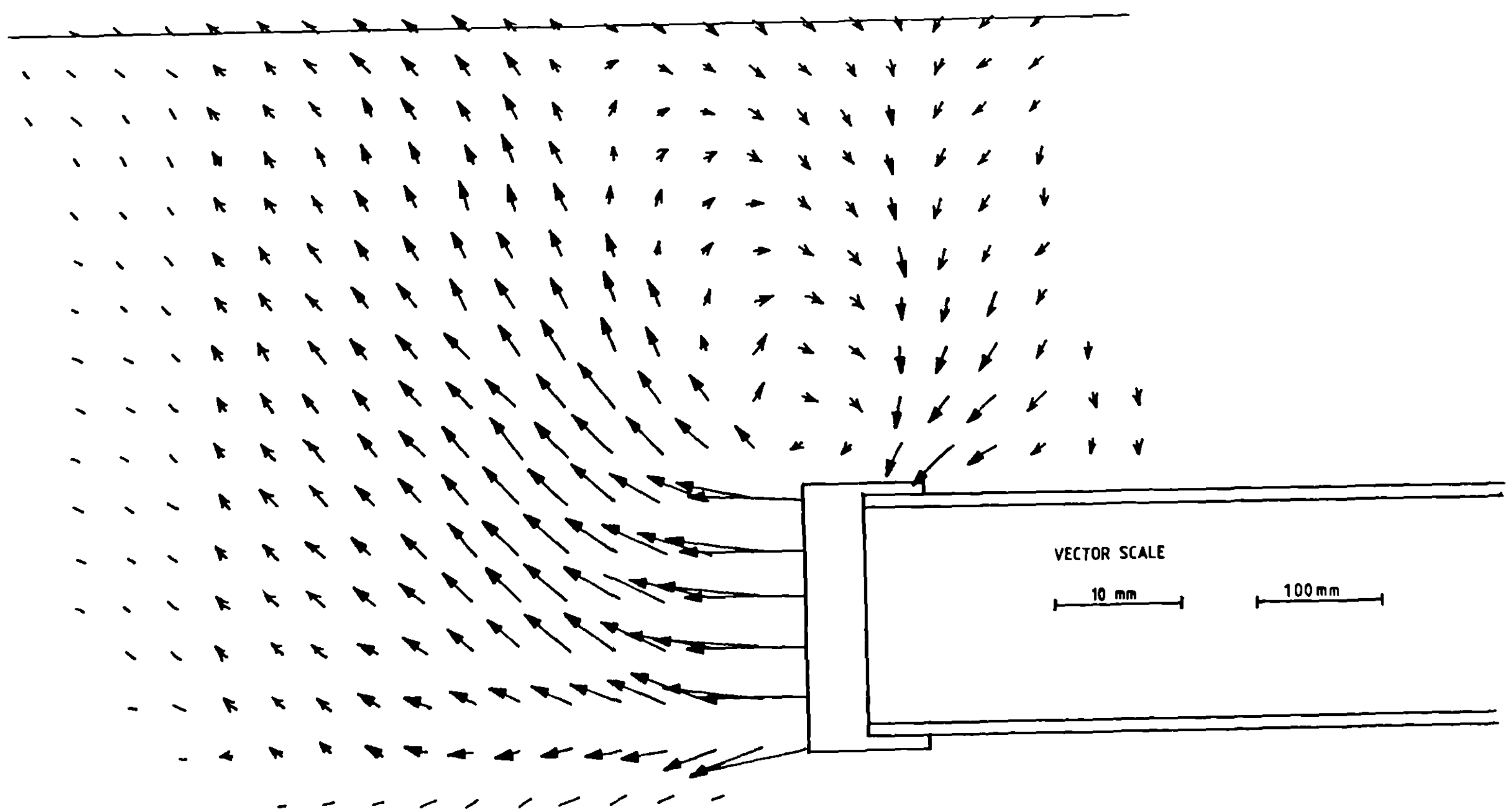

Fig. 5.31 Total displacement vector plot for test CPJ2 (2.0lLB0.1)

(10mm jacking distance)

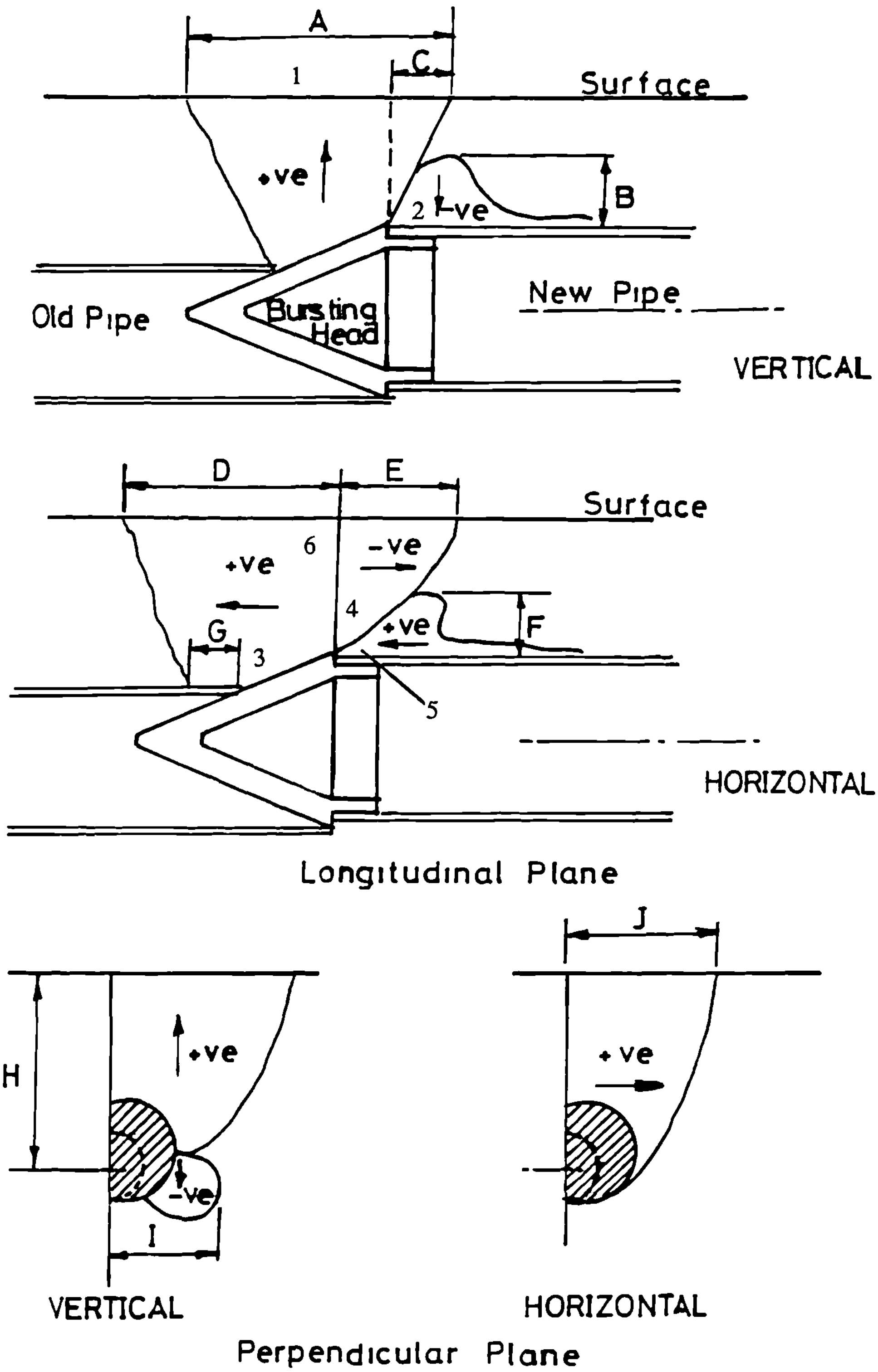

Fig. 5.32 General form of the ground movements associated with the pipebursting tests

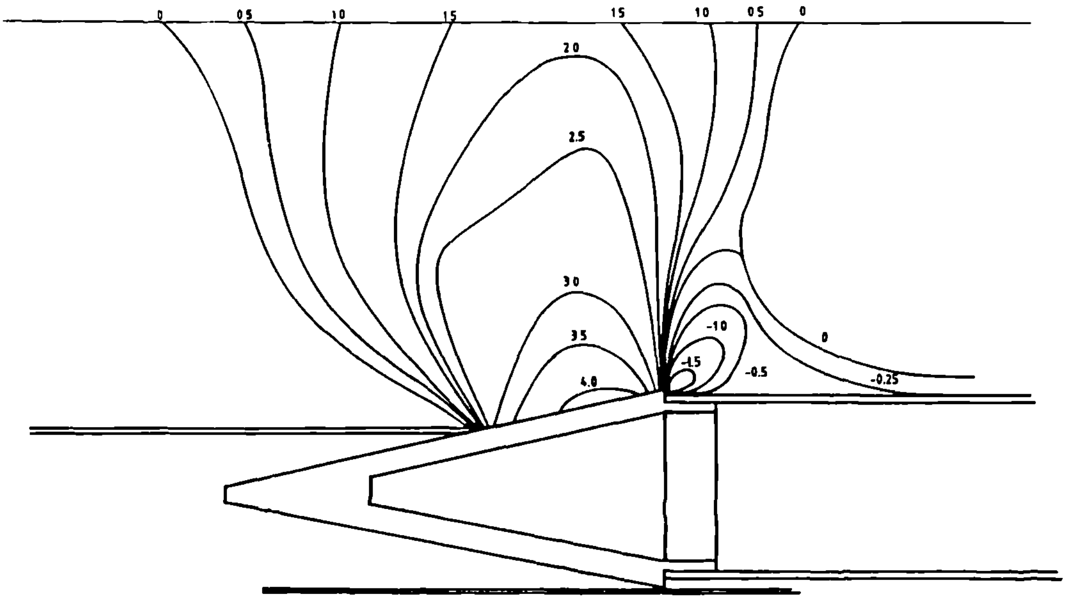

(a) VERTICAL MOVEMENTS
+ UP - DOWN

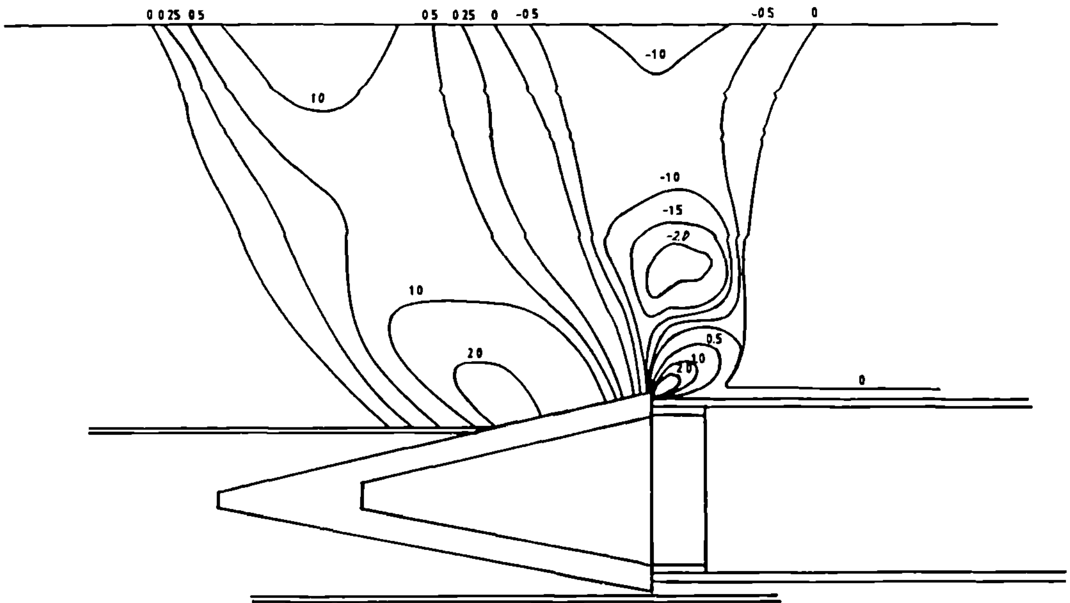

(b) HORIZONTAL MOVEMENTS
+ LEFT - RIGHT

Fig. 5.33 Displacement contour plots for test PB1 (2.6dLB1.2)

(20mm jacking distance, contours in mm)

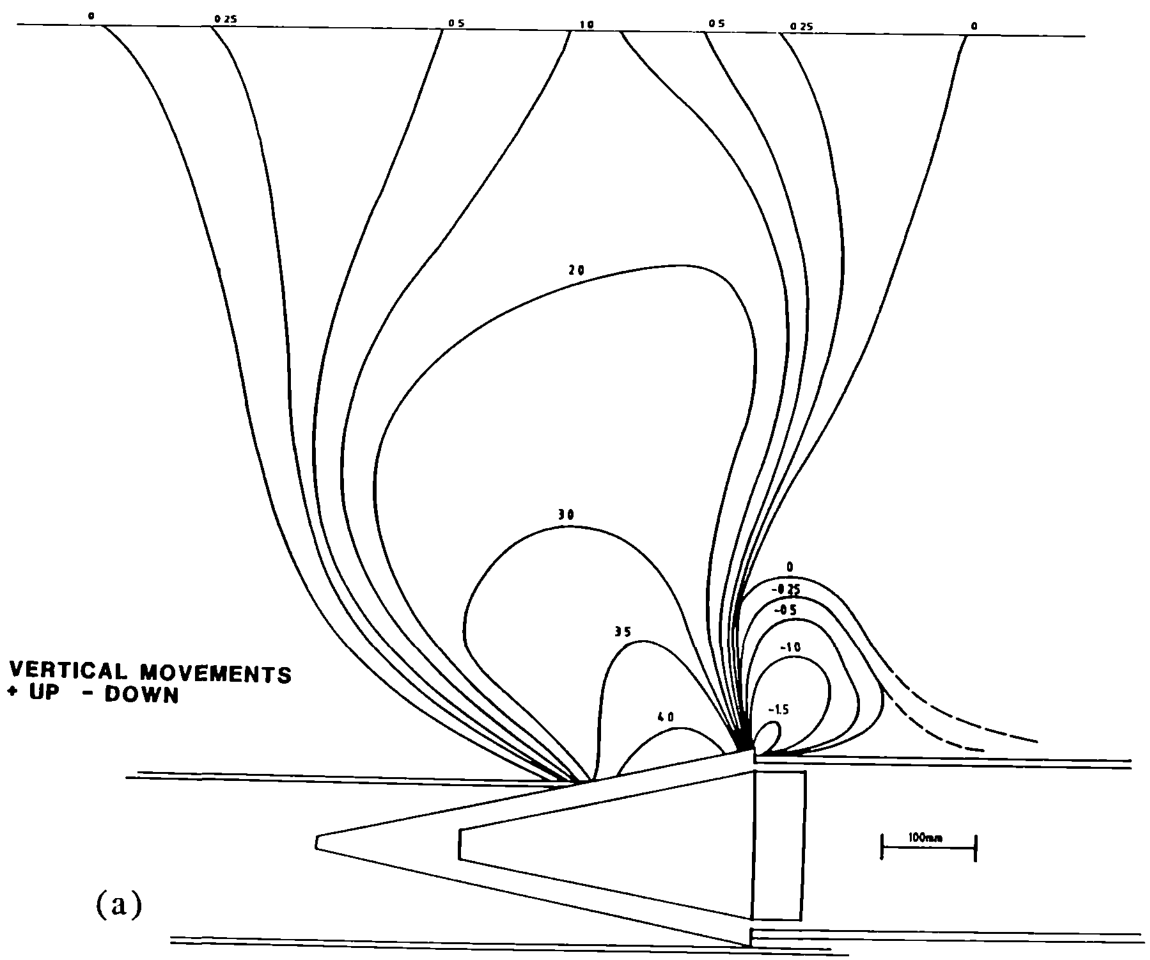

Fig. 5.34 Displacement contour plots for test PB2 (4.9dLB1.2)

(20mm jacking distance, contours in mm)

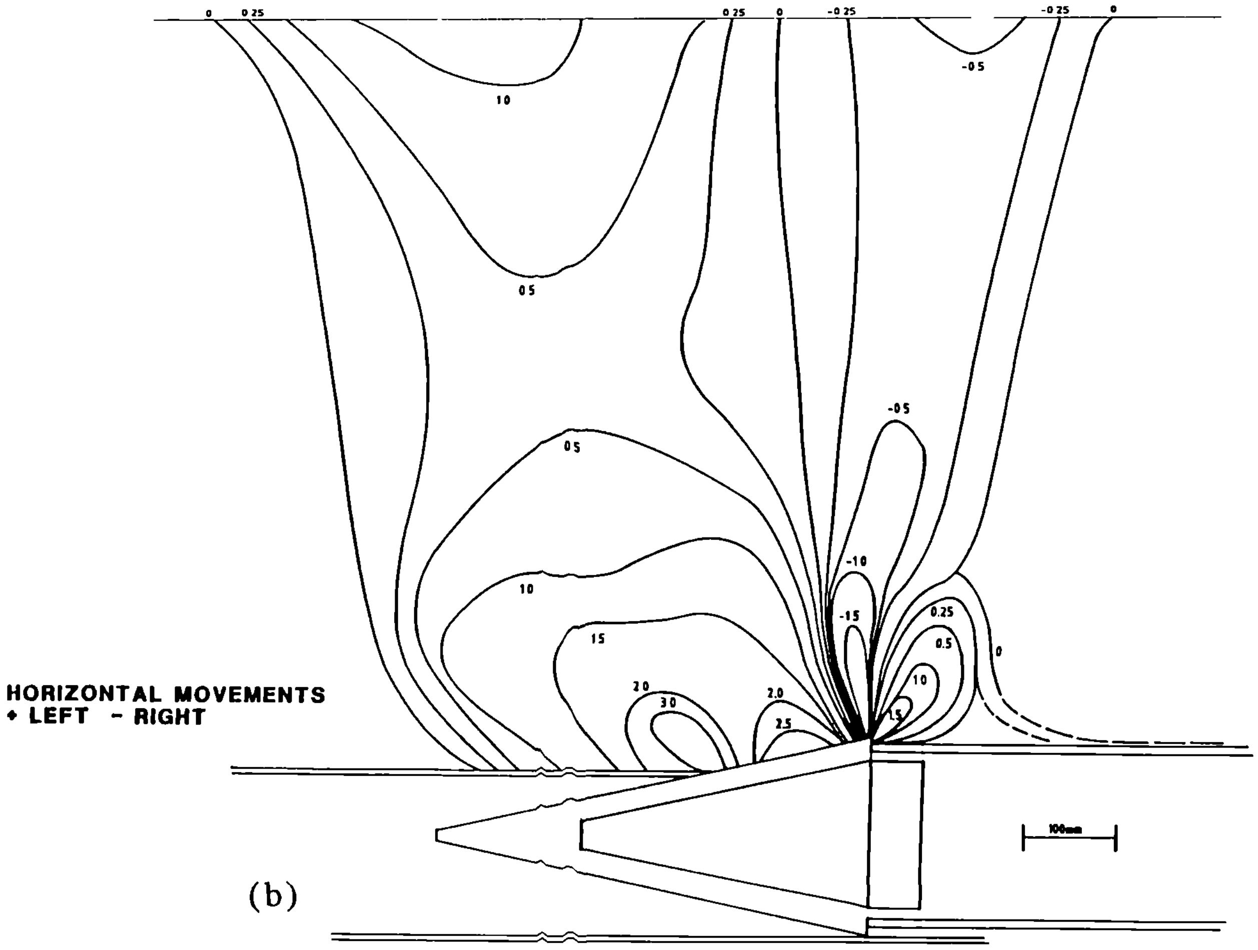

(b)

Fig. 5.34 Displacement contour plots for test PB2 (4.9dLB1.2) continued

(20mm jacking distance, contours in mm)

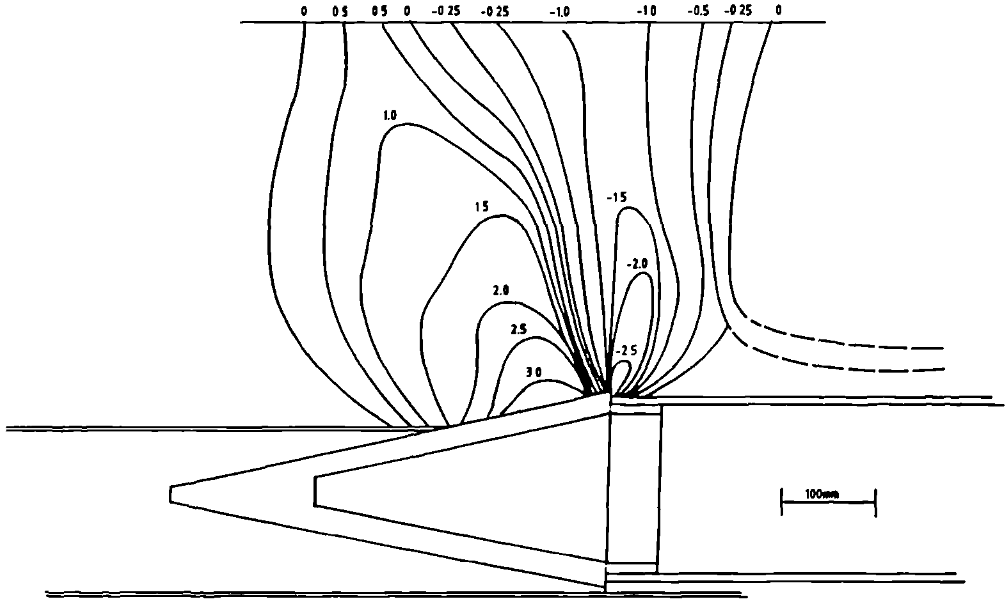

(a) VERTICAL MOVEMENTS
+ UP - DOWN

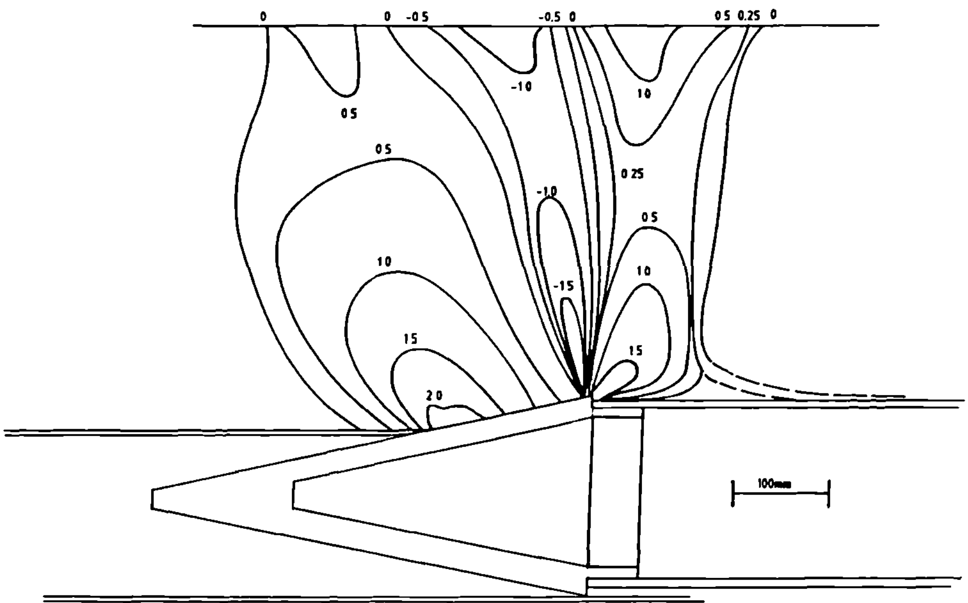

(b) HORIZONTAL MOVEMENTS
+ LEFT - RIGHT

Fig. 5.35 Displacement contour plots for test PB3 (2.6lLB1.2)

(20mm jacking distance, contours in mm)

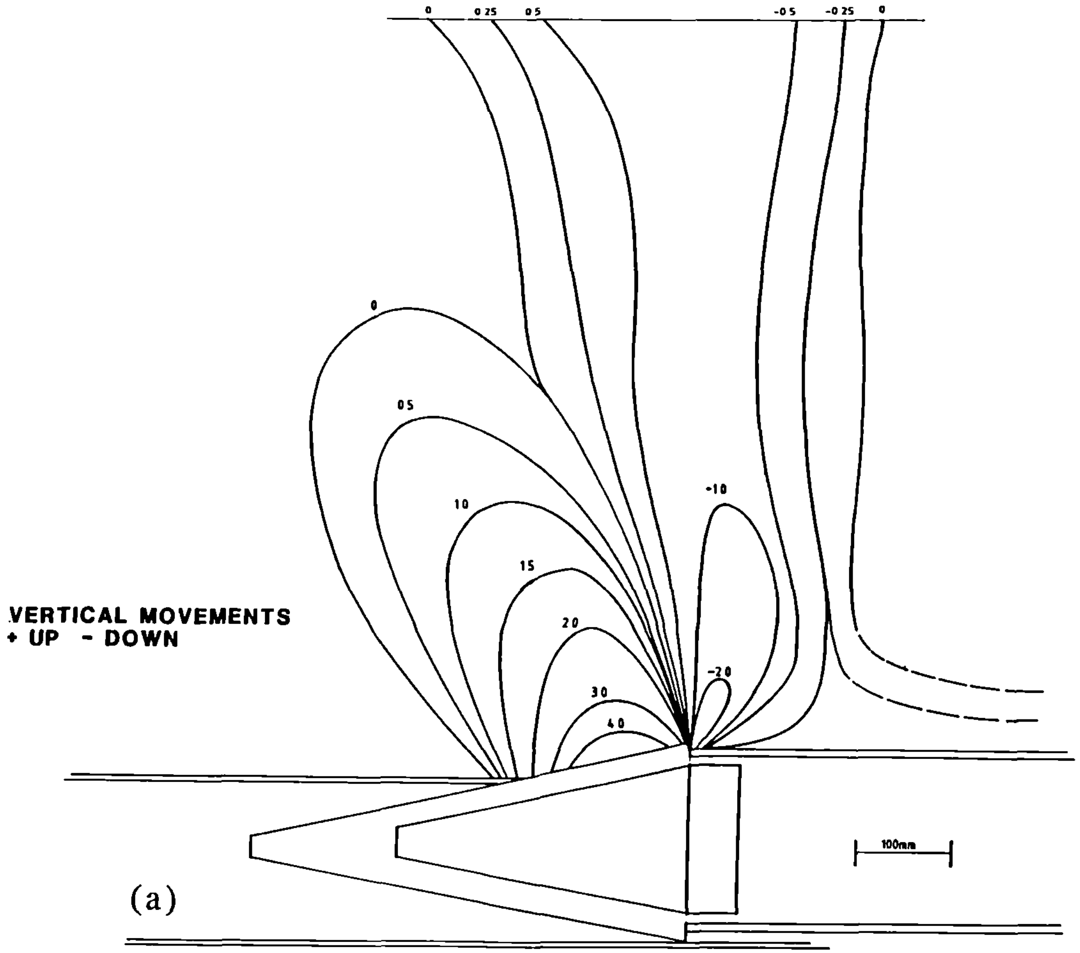

Fig. 5.36 Displacement contour plots for test PB4 (4.9ILB1.2)
(20mm jacking distance, contours in mm)

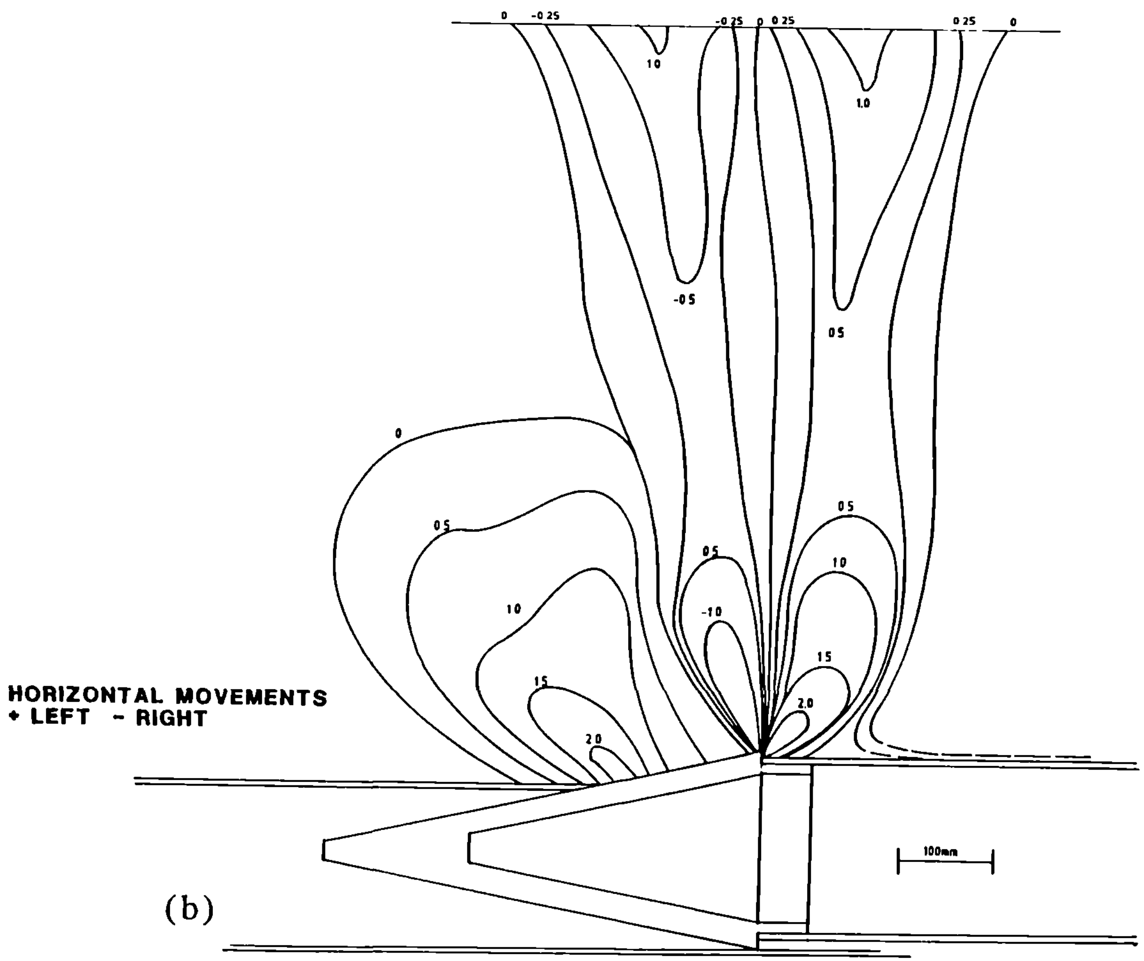

(b)

Fig. 5.36 Displacement contour plots for test PB4 (4.9ILB1.2) continued

(20mm jacking distance, contours in mm)

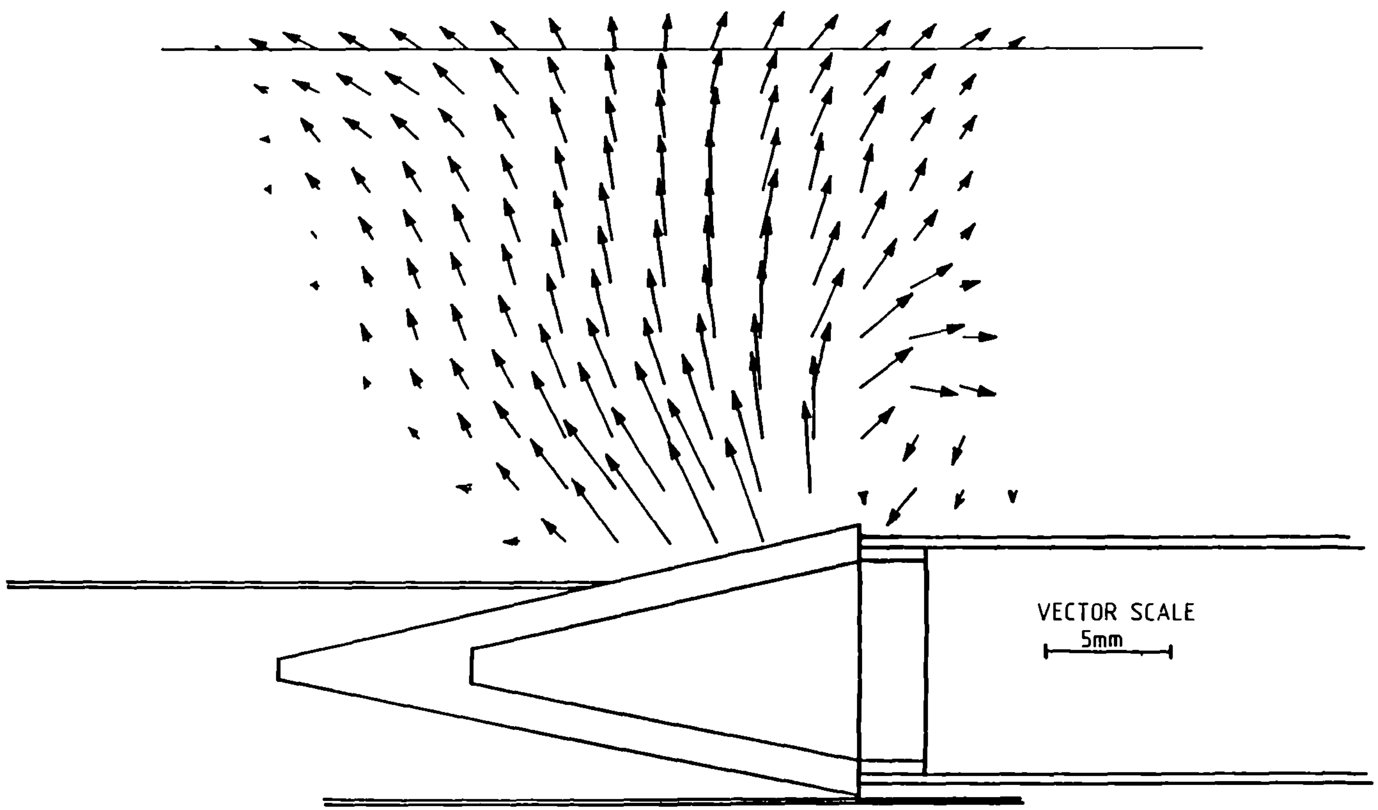

Fig. 5.37 Total displacement vector plot for test PB1 (2.6dLB1.2)

(20mm jacking distance)

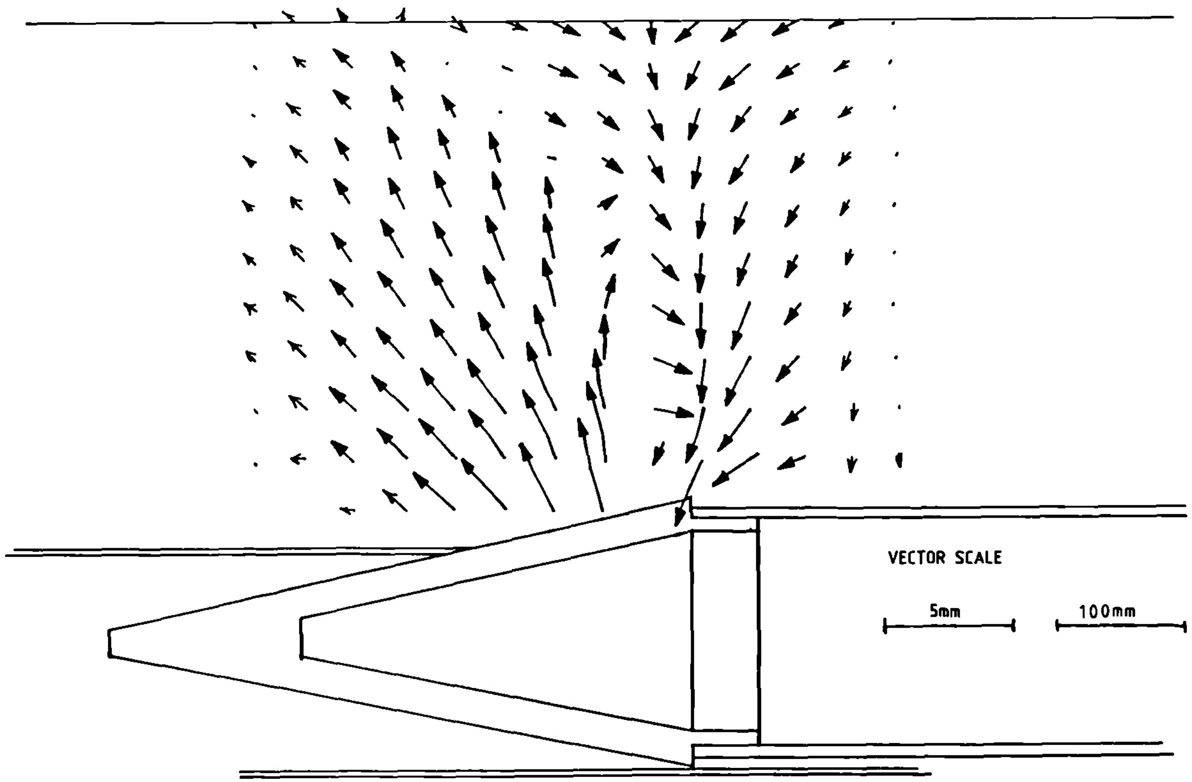

Fig. 5.38 Total displacement vector plot for test PB3 (2.6lLB1.2)

(20mm jacking distance)

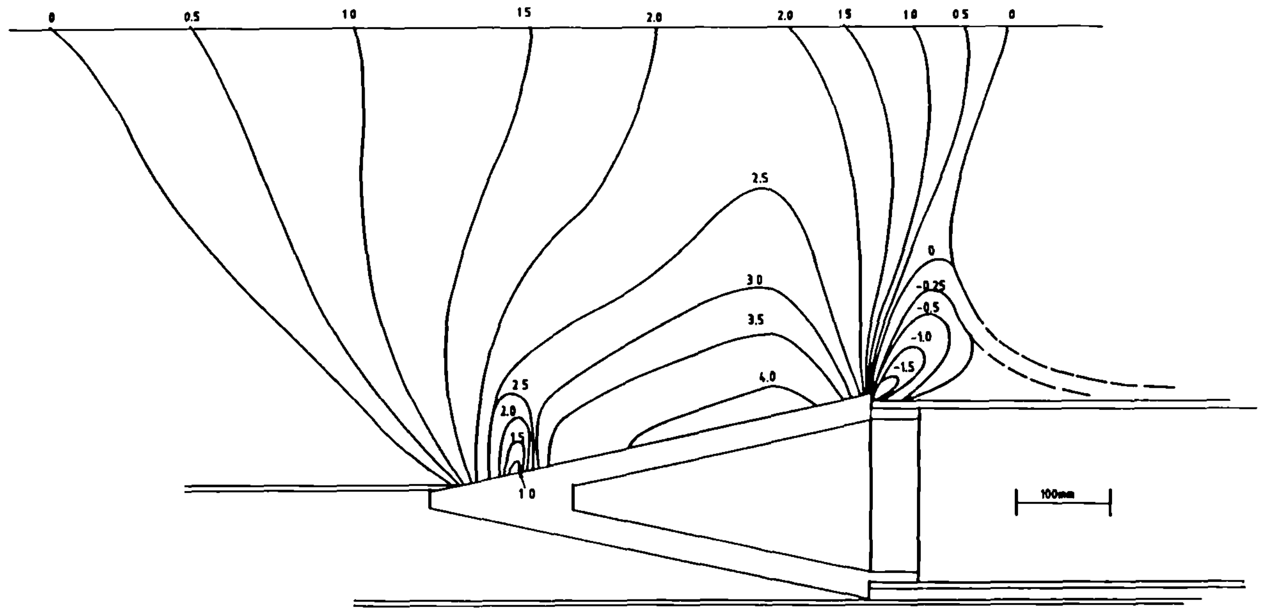

(a) VERTICAL MOVEMENTS
+ UP - DOWN

Fig. 5.39 Displacement contour plots for test PB5 (3.8dLB1.7)
(20mm jacking distance, contours in mm)

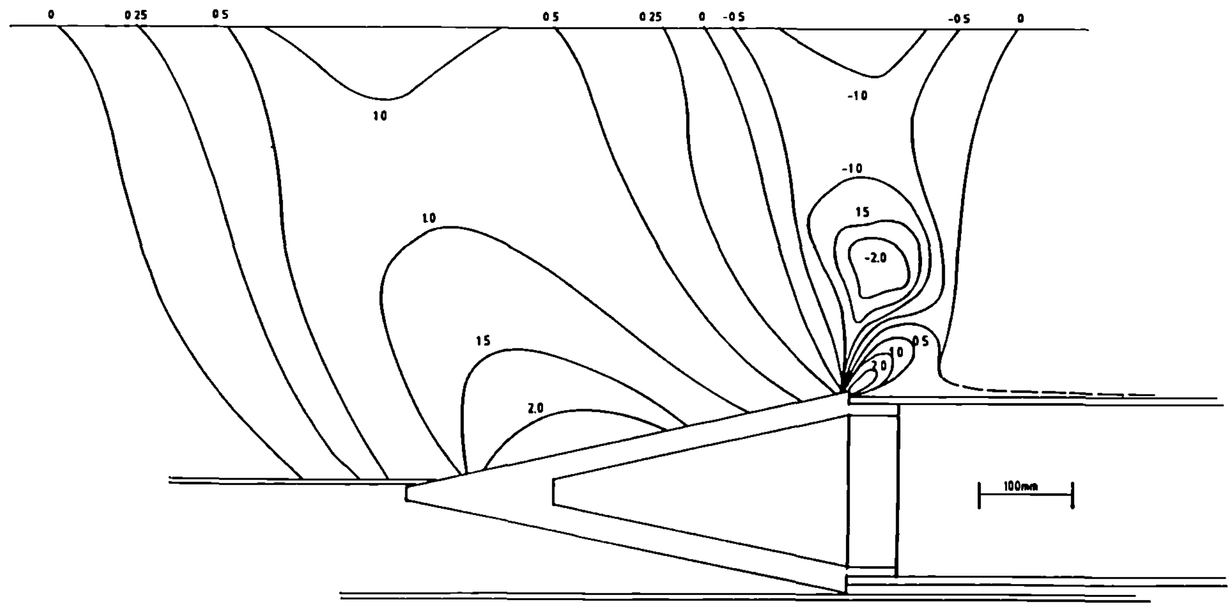

(b) HORIZONTAL MOVEMENTS
+ LEFT - RIGHT

Fig. 5.39 Displacement contour plots for test PB5 (3.8dLB1.7) continued

(20mm jacking distance, contours in mm)

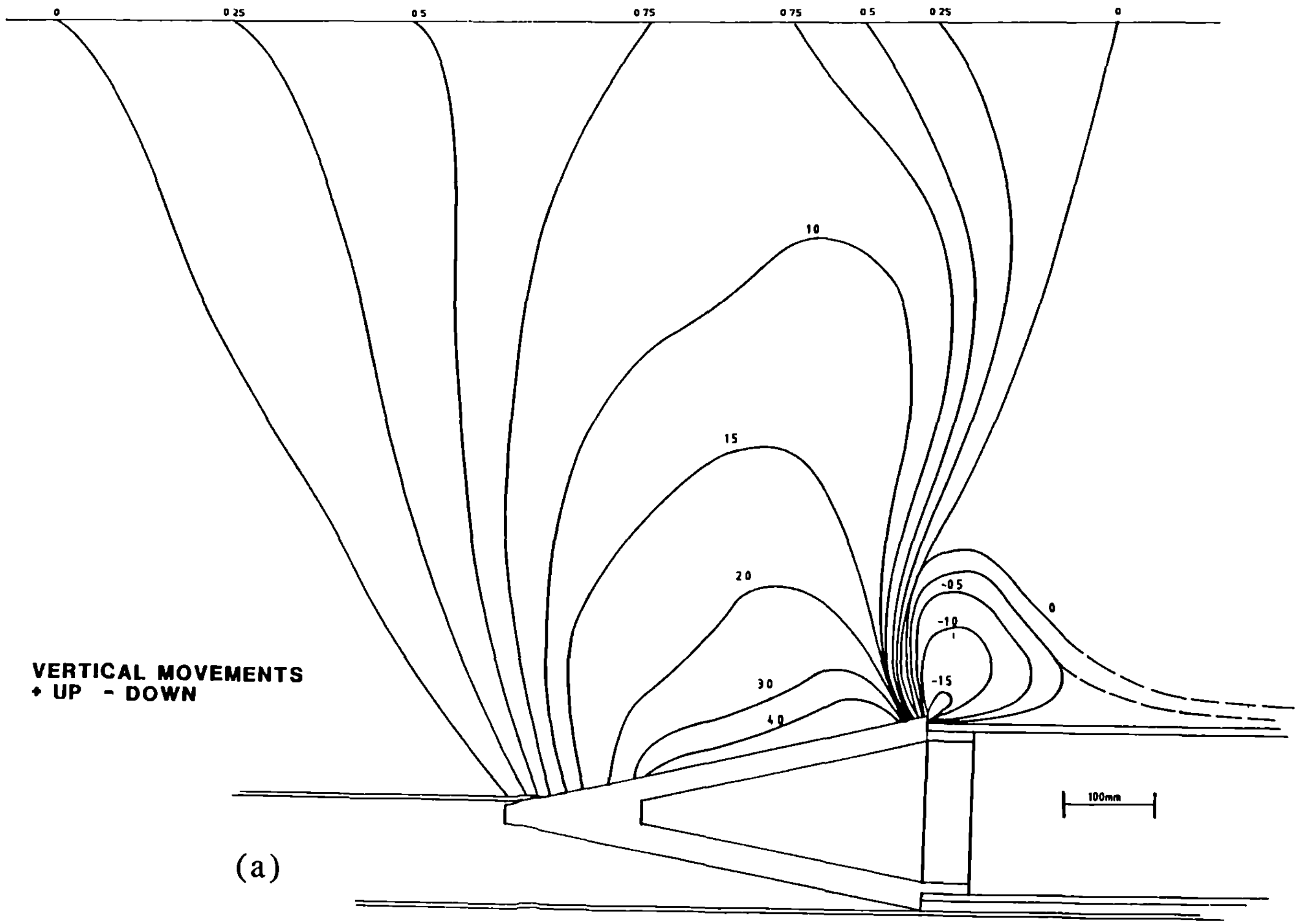

Fig. 5.40 Displacement contour plots for test PB6 (7.0dLB1.7)
(20mm jacking distance, contours in mm)

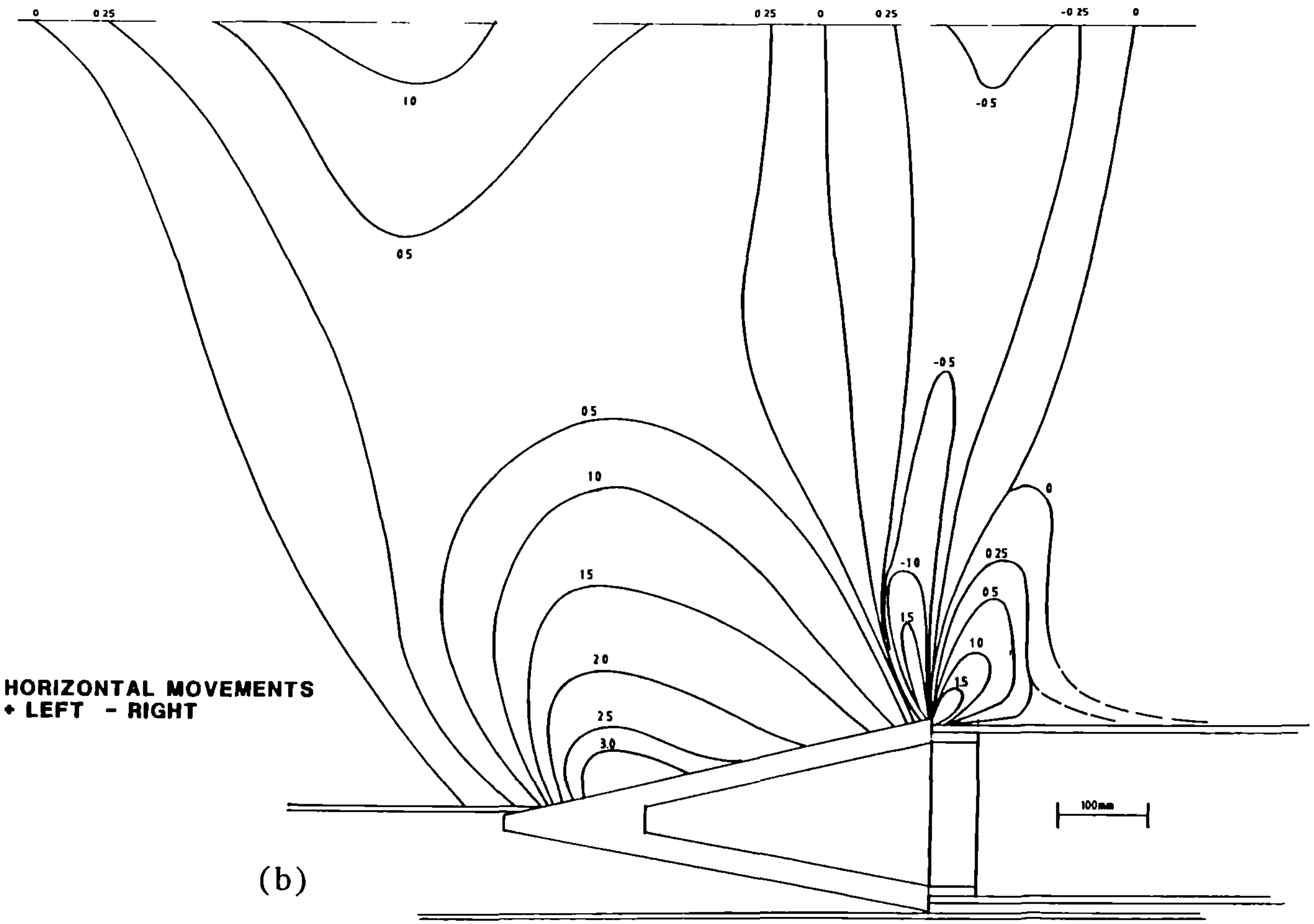

(b)

Fig. 5.40 Displacement contour plots for test PB6 (7.0dLB1.7) continued

(20mm jacking distance, contours in mm)

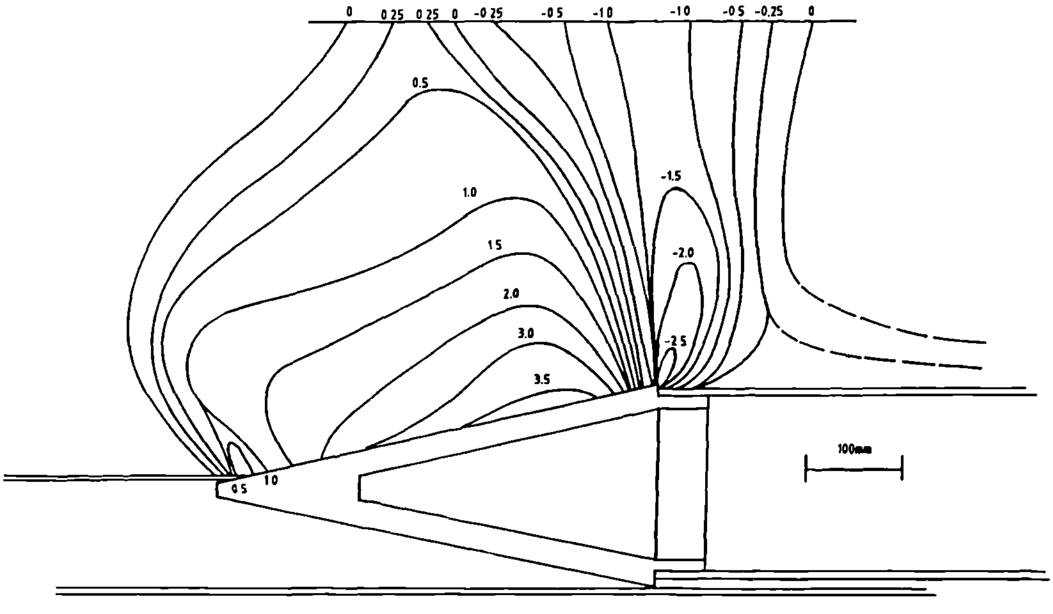

(a)

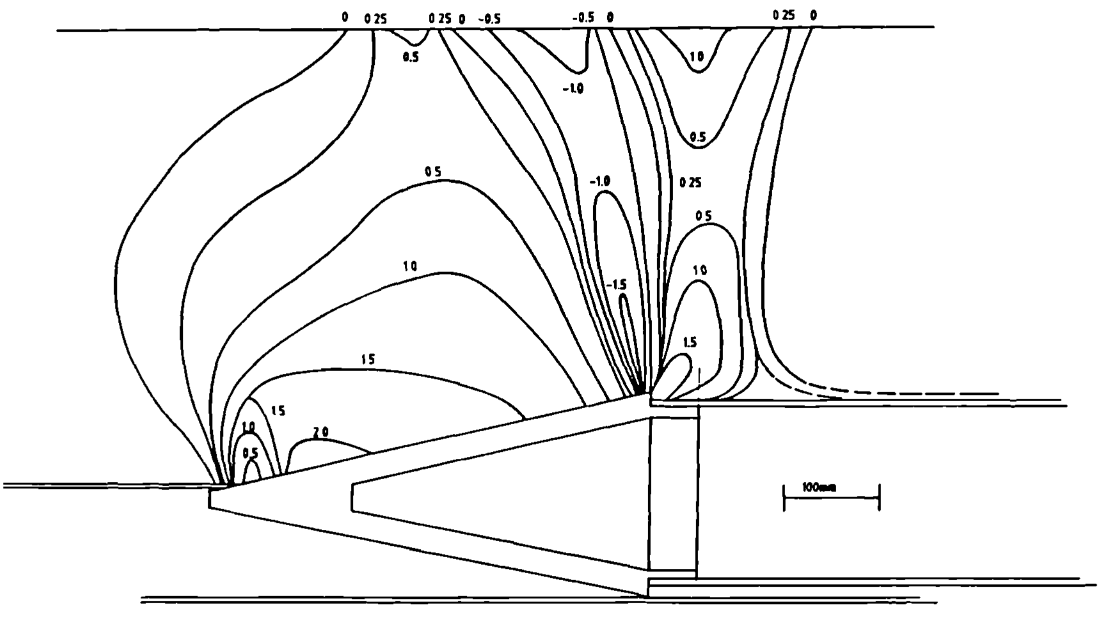

(b)

Fig. 5.41 Displacement contour plots for test PB7 (3.8ILB1.7)

(20mm jacking distance, contours in mm)

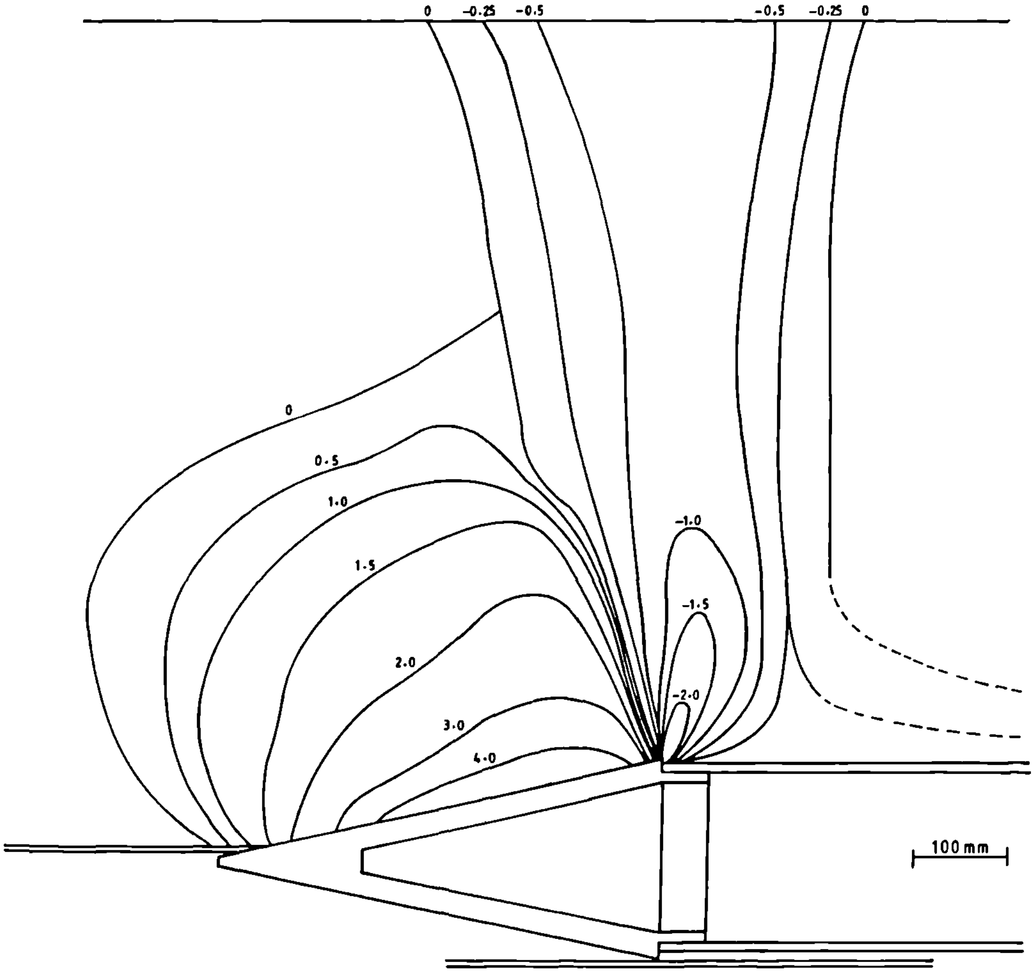

(a)

VERTICAL MOVEMENTS
+ UP - DOWN

Fig. 5.42 Displacement contour plots for test PB8 (7.0ILB1.7) (20mm jacking distance, contours in mm)

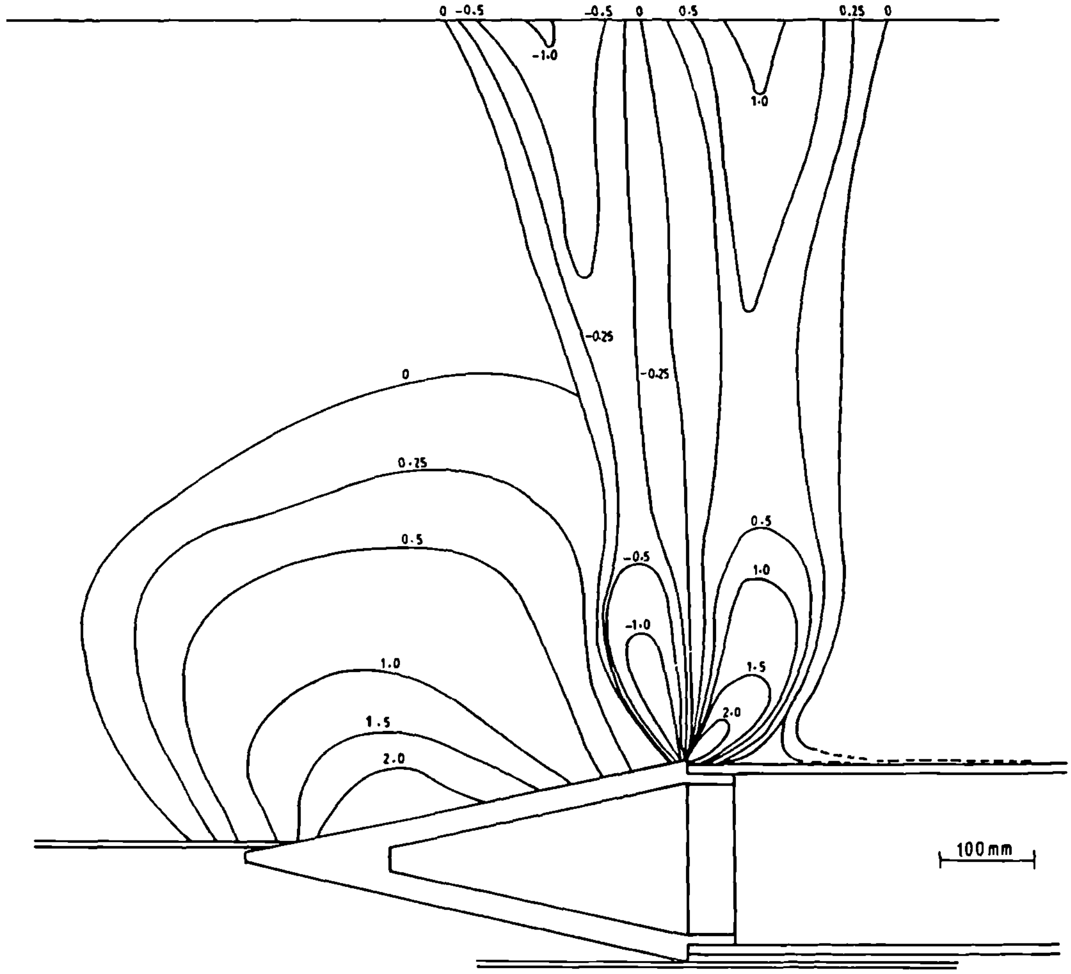

(b)

HORIZONTAL MOVEMENTS
+ LEFT - RIGHT

Fig. 5.42 Displacement contour plots for test PB8 (7.01LB1.7) continued

(20mm jacking distance, contours in mm)

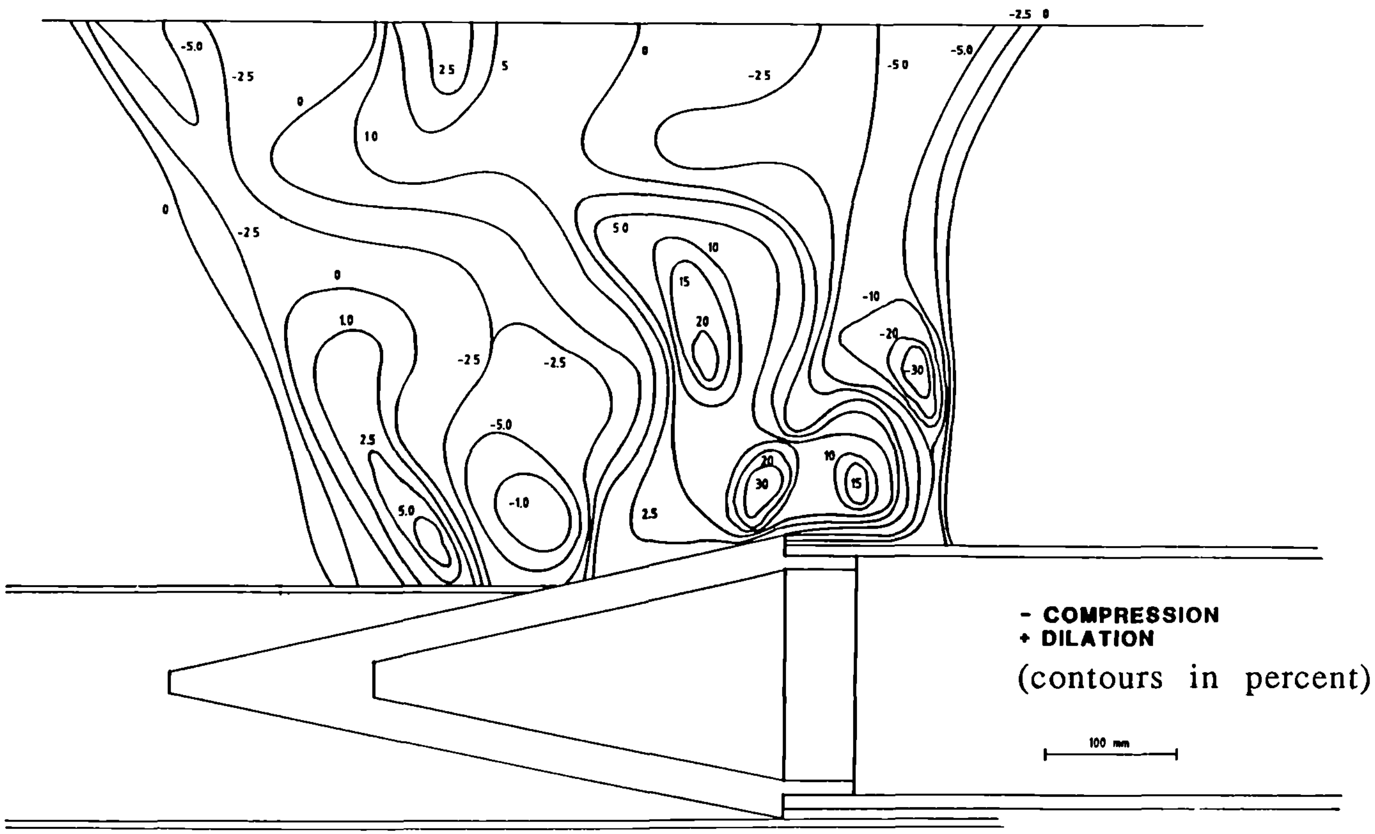

Fig. 5.43 Volumetric strain plot for test PB1 (2.6dLB1.2)

(20mm jacking distance)

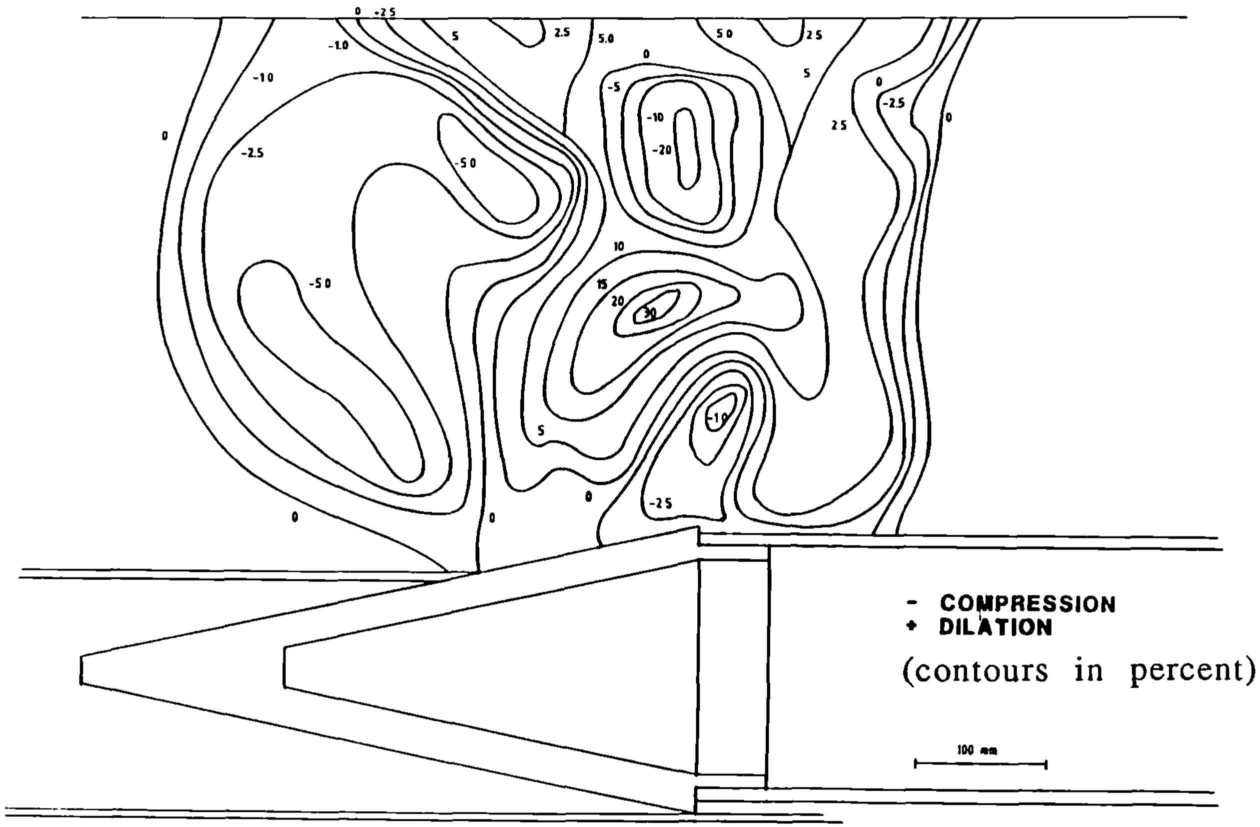

Fig. 5.44 Volumetric strain plot for test PB3 (2.6lLB1.2)

(20mm jacking distance)

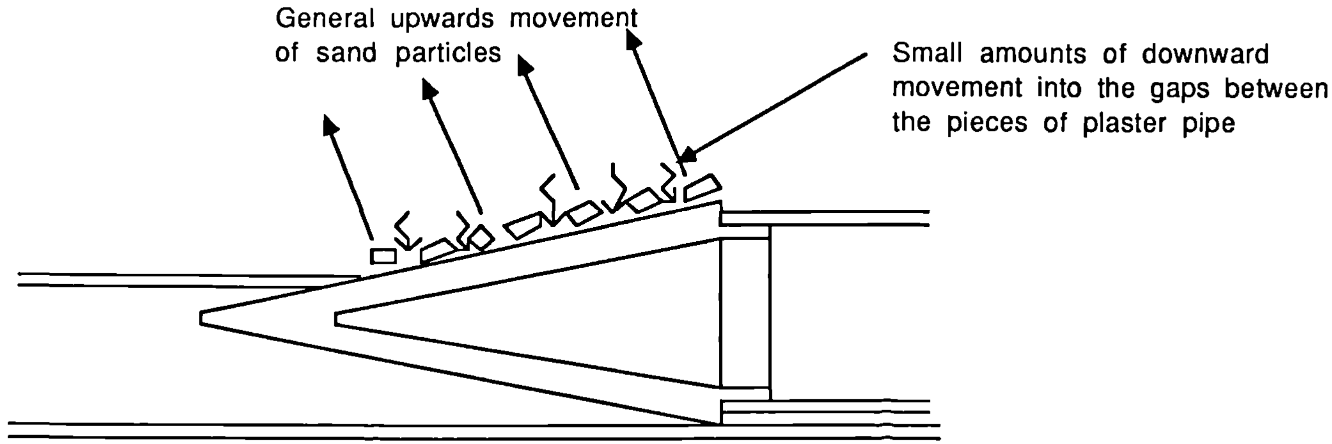

Fig. 5.45 Random downwards movements caused by the movement of pieces of broken plaster pipe close to the pipeburster

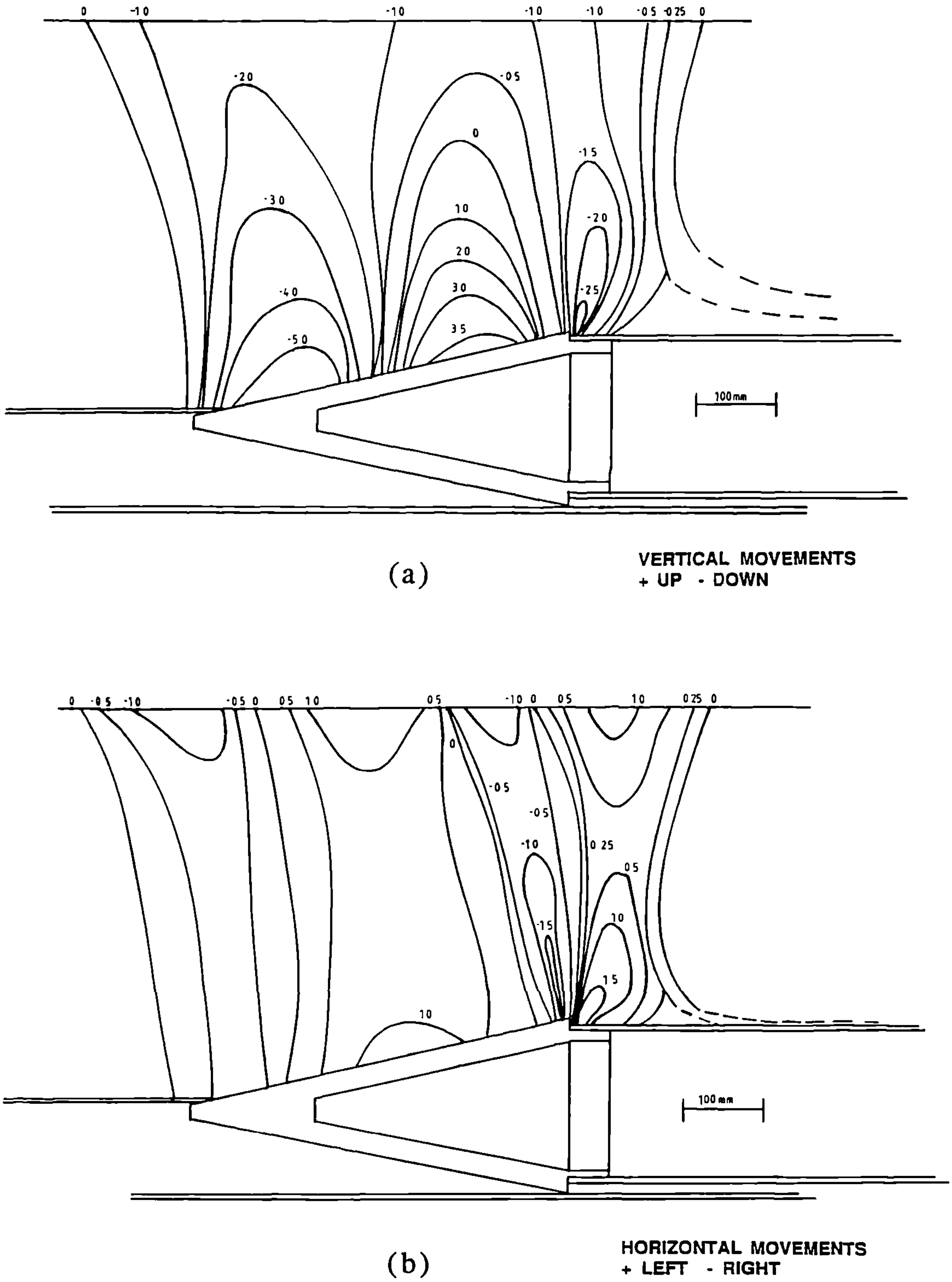

Fig. 5.46 Indication of the effects of sand leakage during pipebursting for test PB7 (3.81LB1.7)

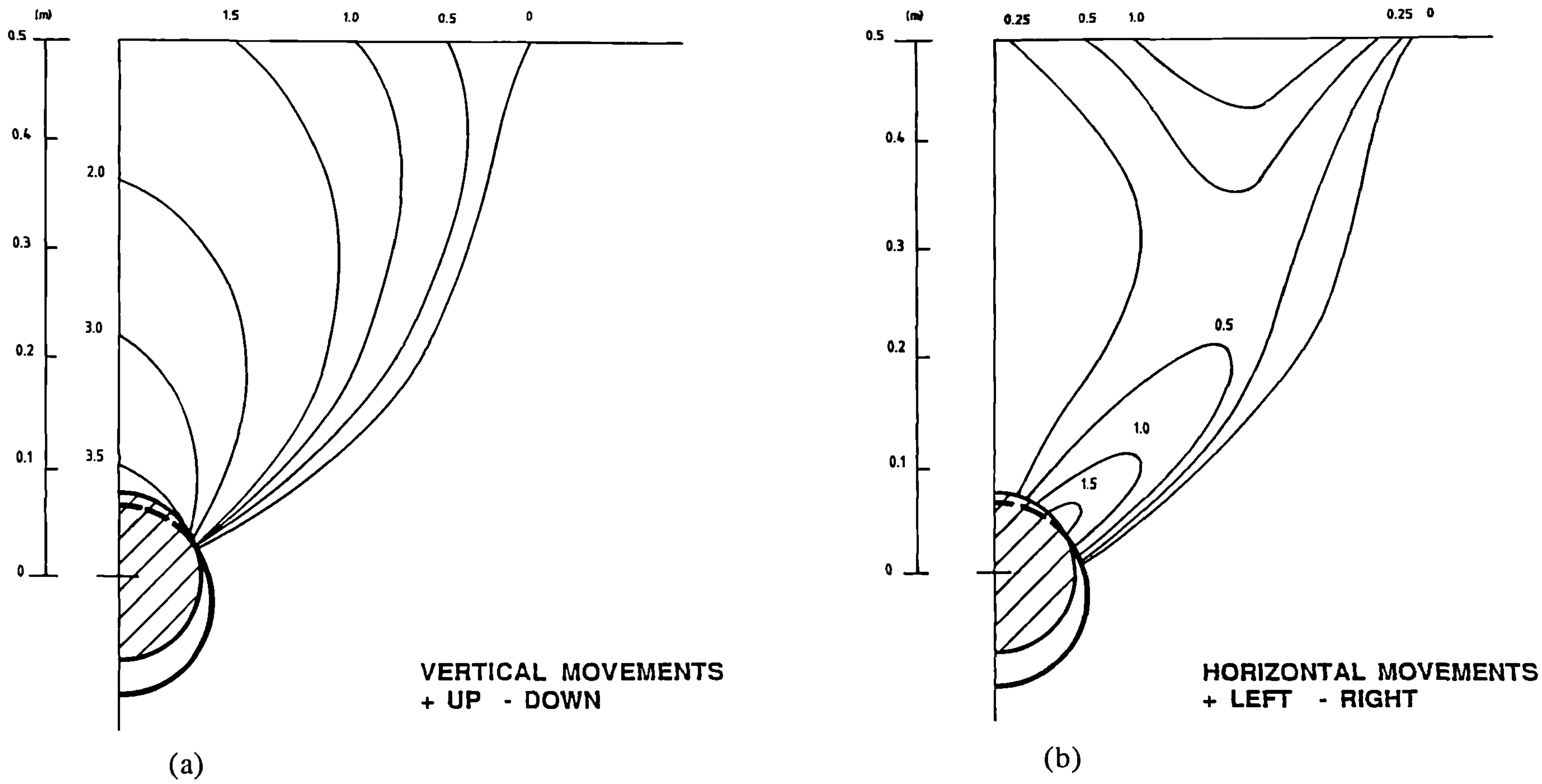

Fig. 5.47 Displacement contour plots in the perpendicular plane for test PB1 (2.6dLB1.2) close to the start of expansion for a 20mm forward jack

(contours in mm)

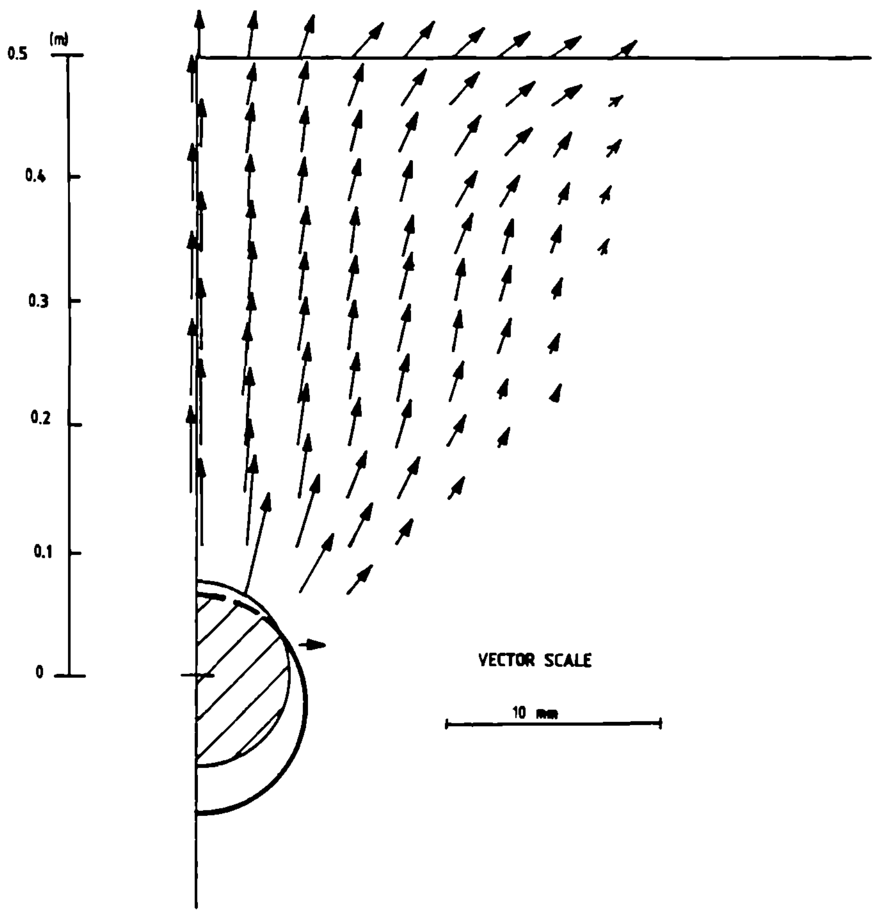

Fig. 5.47c Total displacement vector plot for test PB1 (2.6dLB1.2) close to the start of expansion for a 20mm forward jack

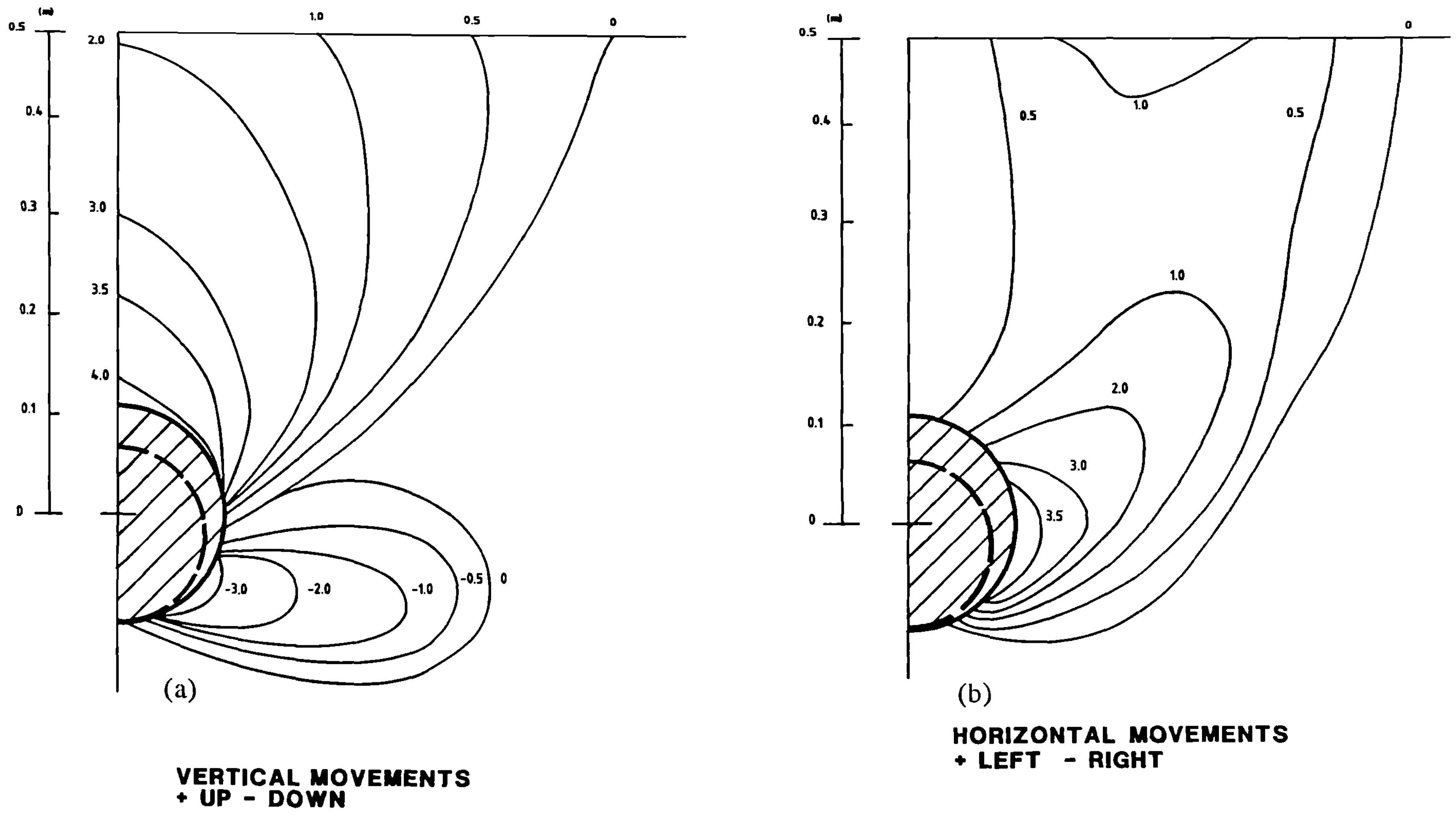

Fig. 5.48 Displacement contour plots in the perpendicular plane for test PB1 (2.6dLB1.2) close to full expansion for a 20mm forward jack

(contours in mm)

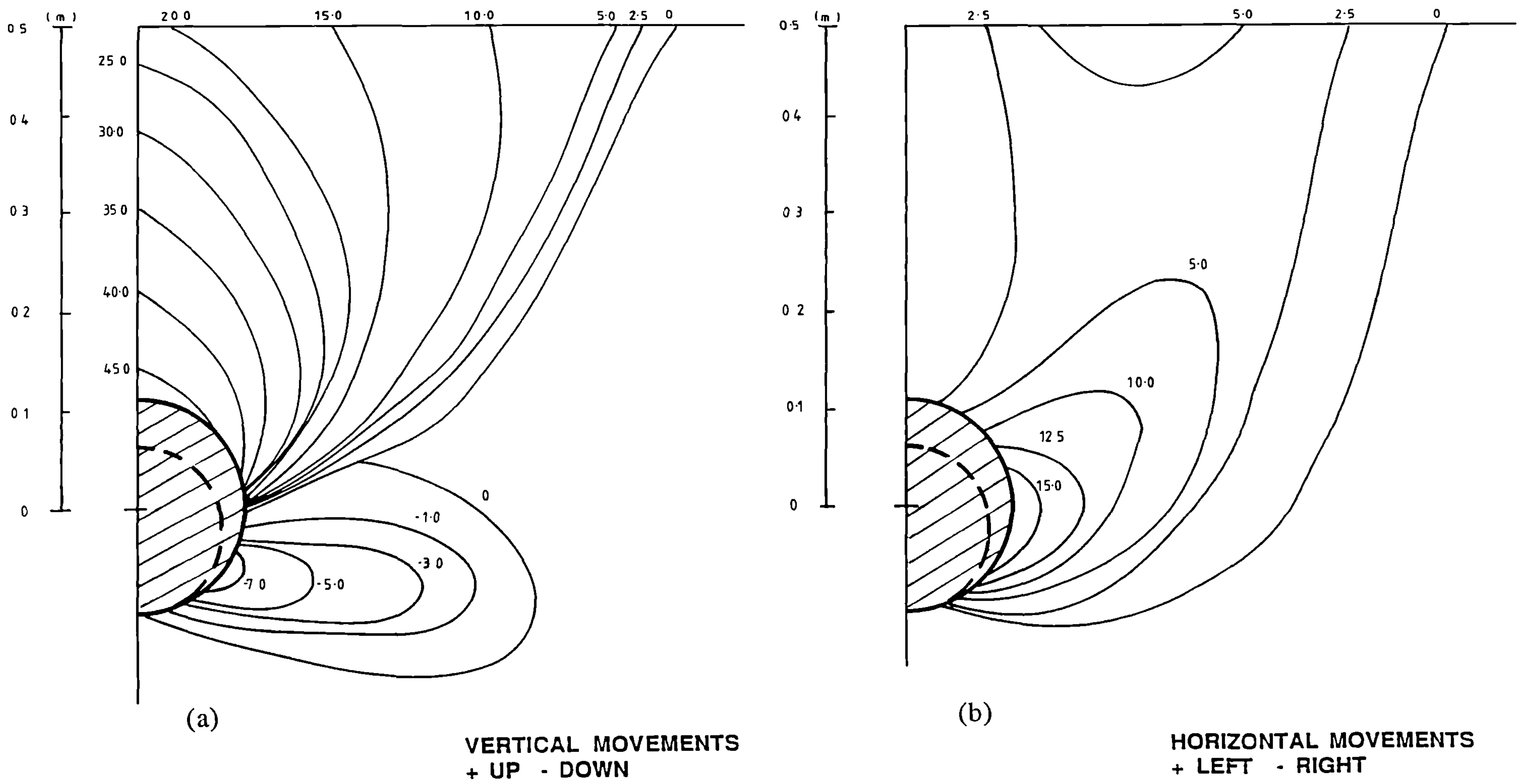

Fig. 5.49 Displacement contour plots in the perpendicular plane for test PB1 (2.6dLB1.2) at full expansion

(contours in mm)

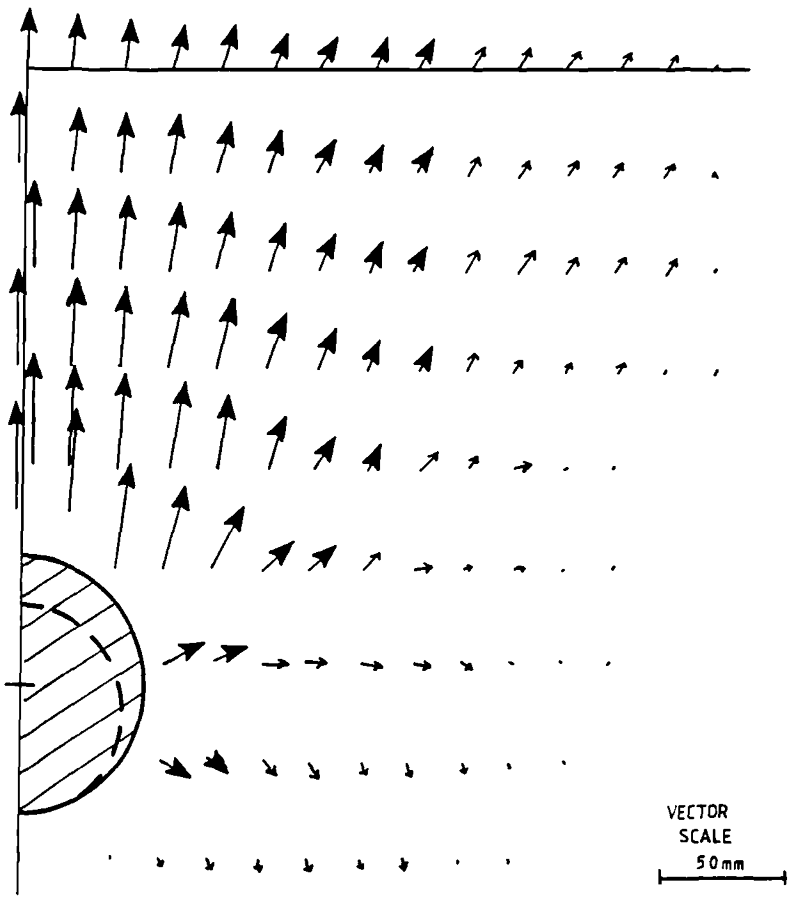

Fig. 5.49c Total displacement vector plot for test PB1 (2.6dLB1.2) at full expansion

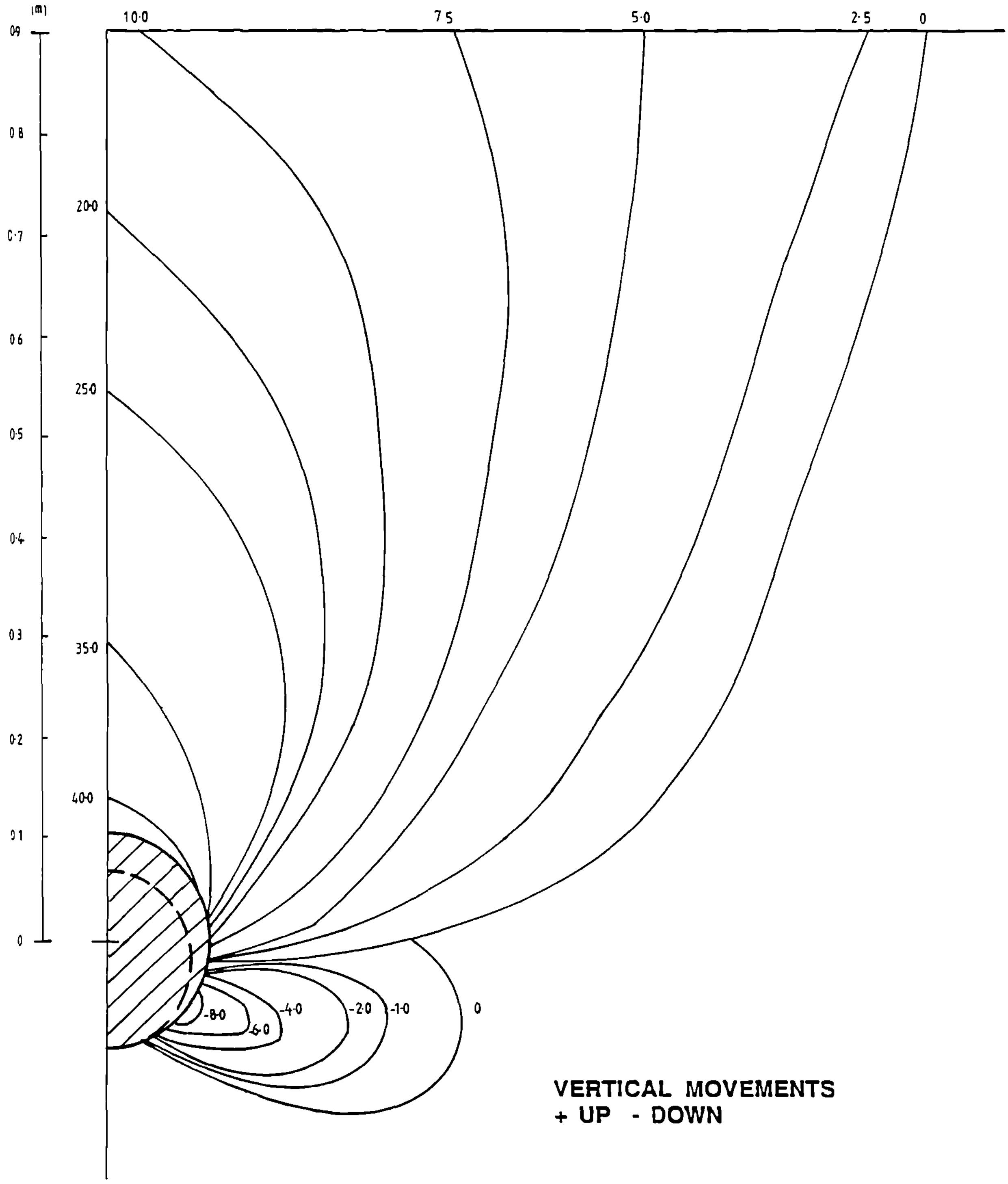

(a)

Fig. 5.50 Displacement contour plots in the perpendicular plane for test PB2 (4.9dLB1.2) at full expansion

(contours in mm)

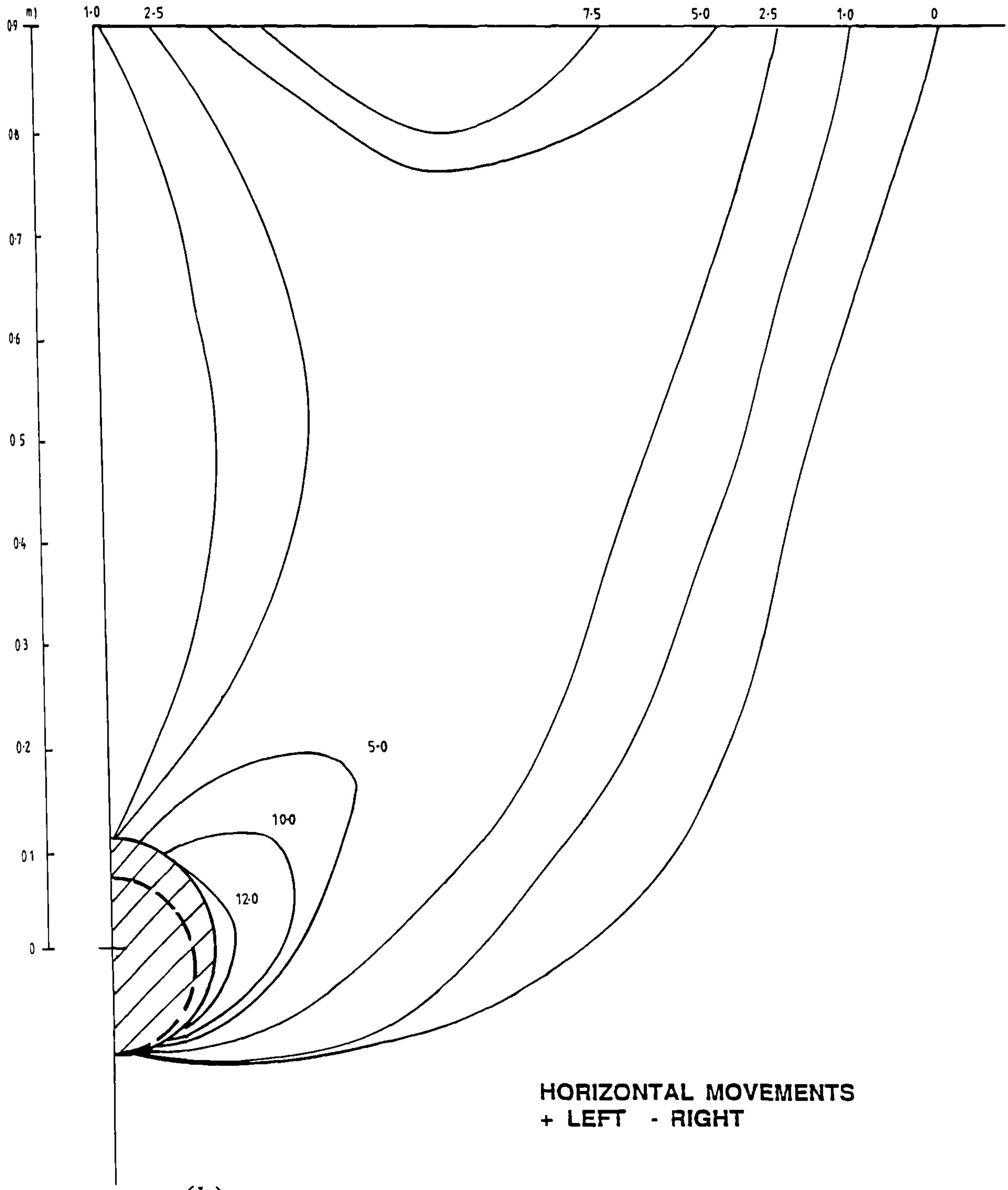

(b)

Fig. 5.50 Displacement contour plots in the perpendicular plane for test PB2 (4.9dLB1.2) at full expansion continued

(contours in mm)

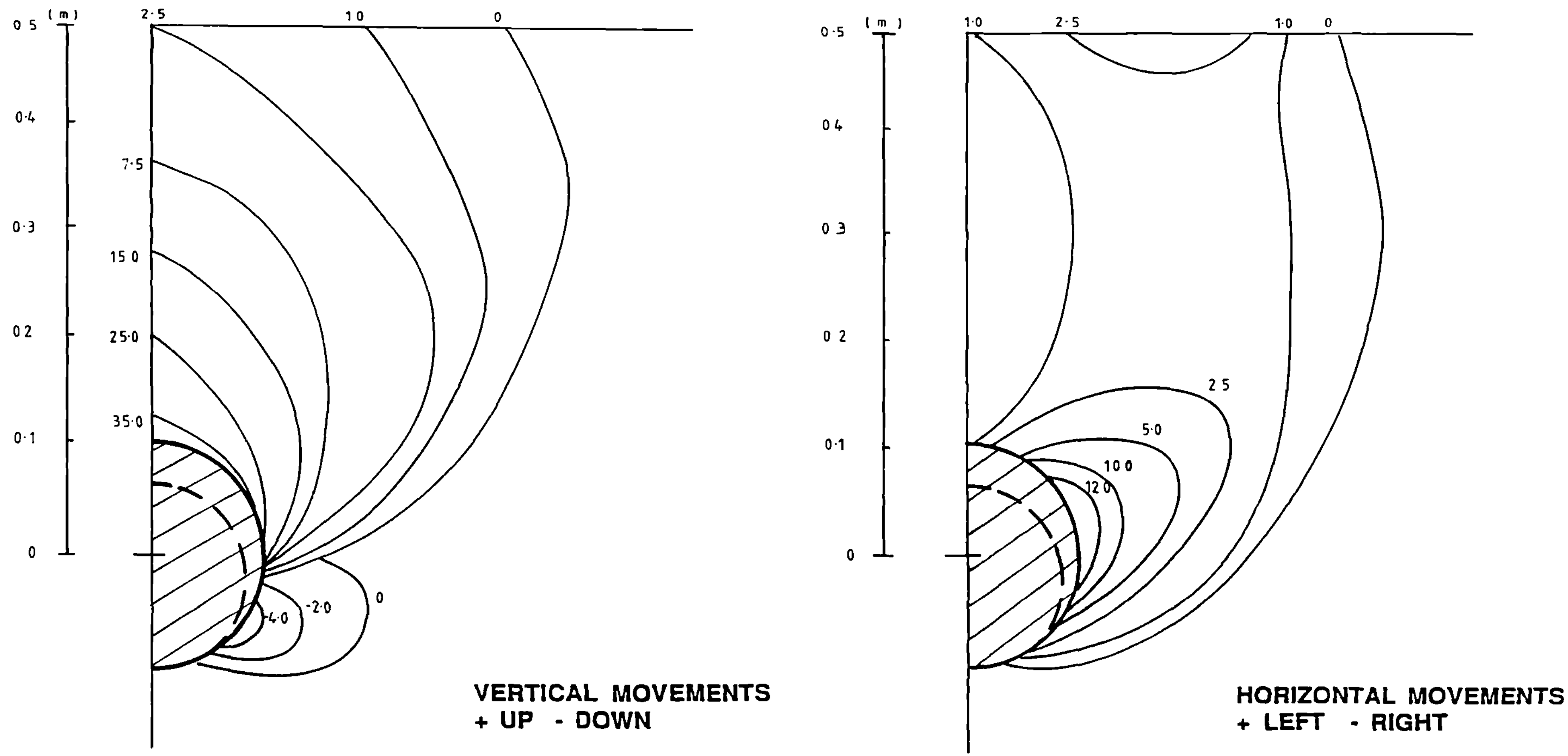

(a) (b)

Fig. 5.51 Displacement contour plots in the perpendicular plane for test PB3 (2.6lLB1.2) at full expansion

(contours in mm)

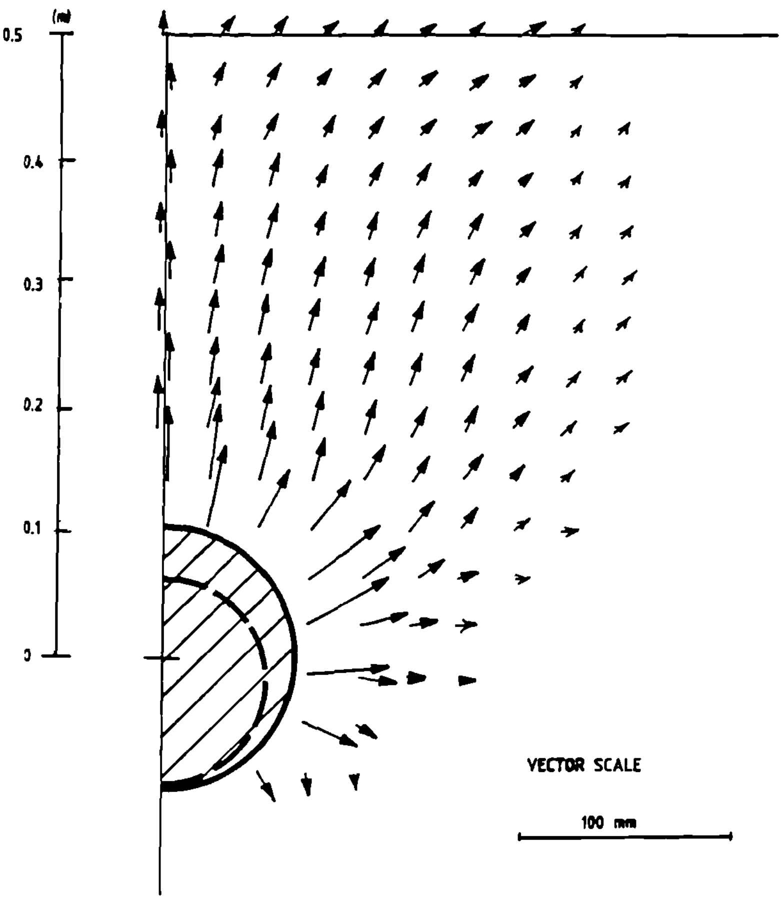

Fig. 5.51c Total displacement vector plot for test PB3 (2.61LB1.2) at full expansion

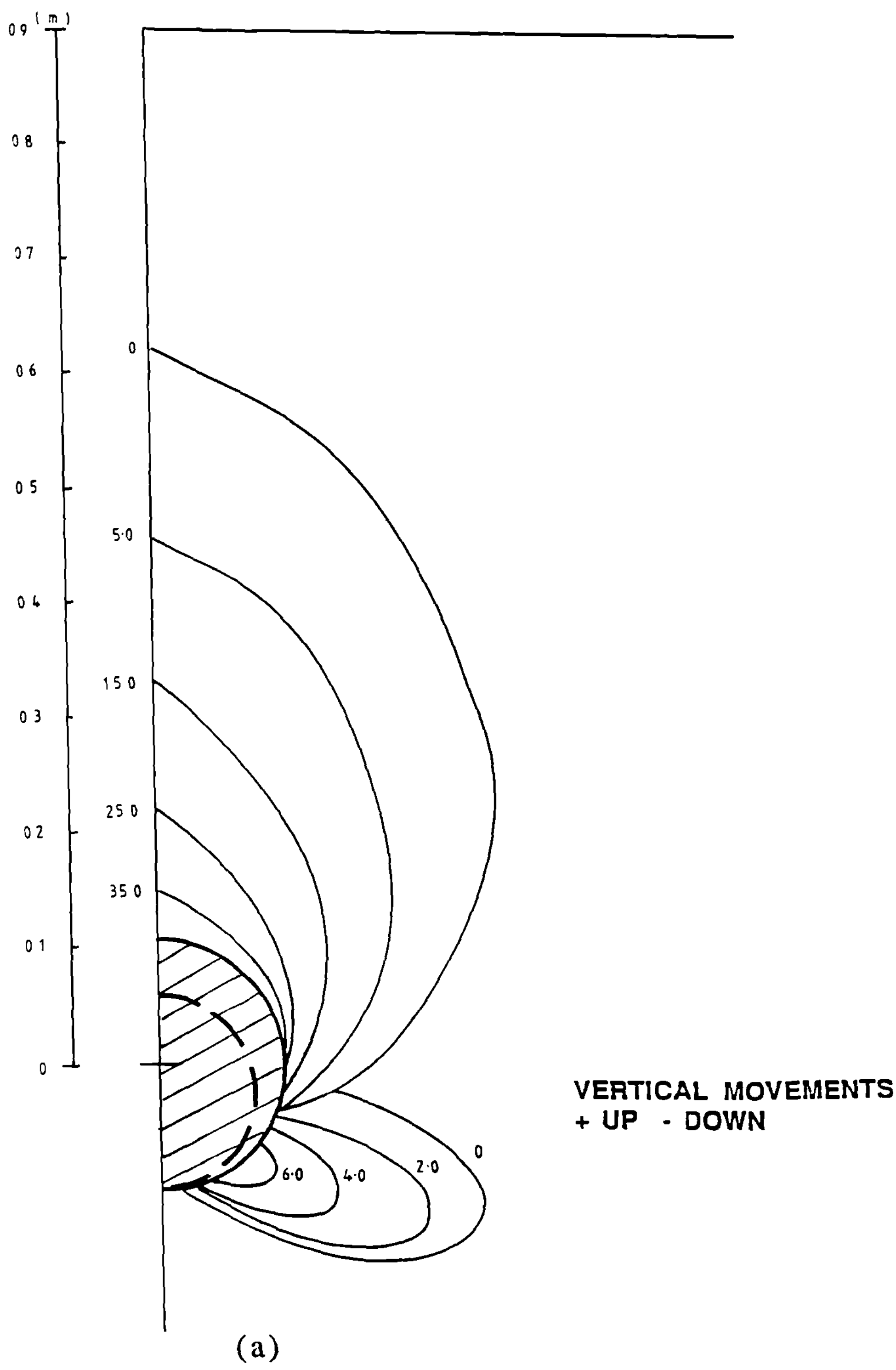

Fig. 5.52 Displacement contour plots in the perpendicular plane for test PB4 (4.9ILB1.2) at full expansion

(contours in mm)

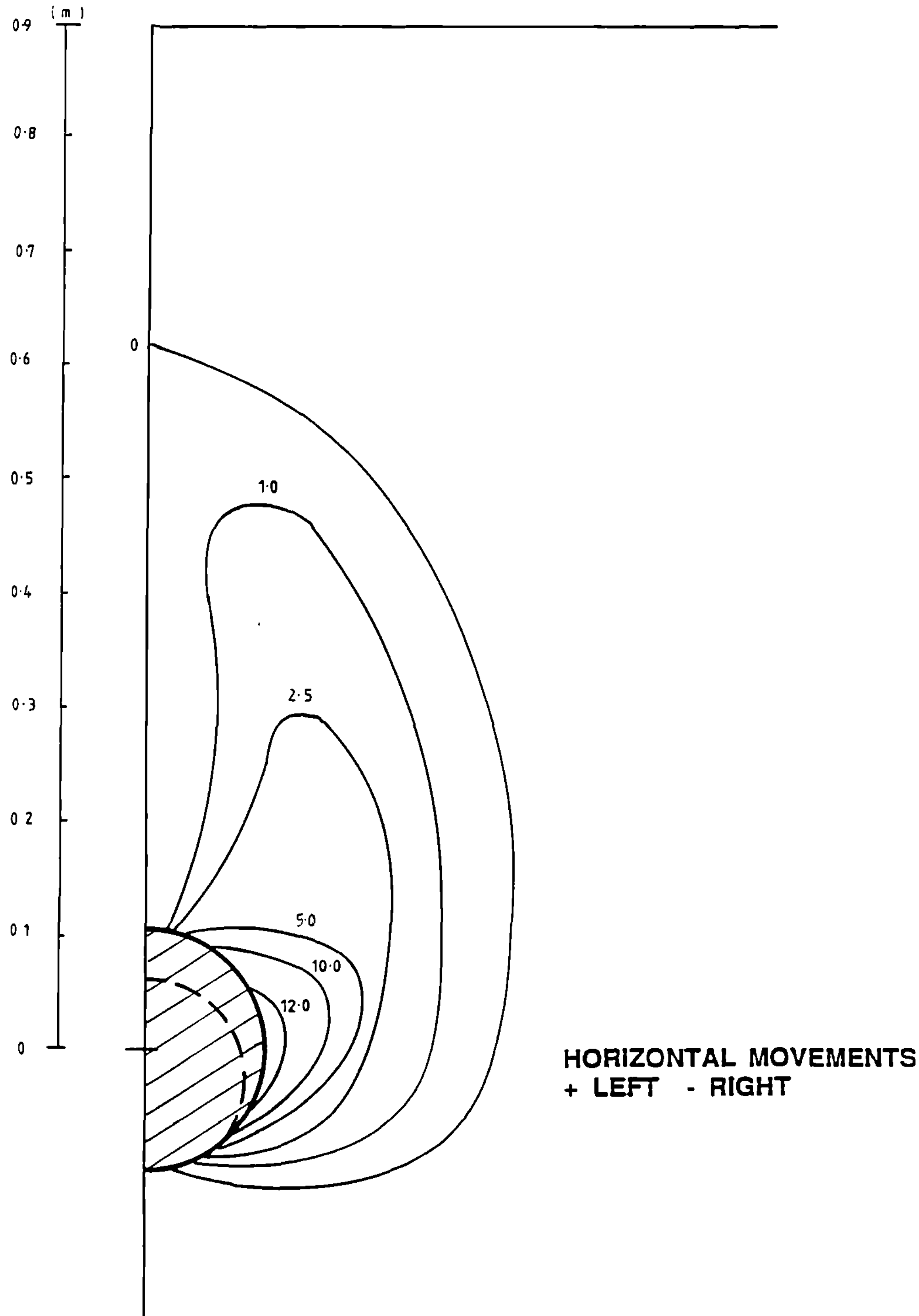

(b)

Fig. 5.52 Displacement contour plots in the perpendicular plane for test PB4 (4.9lLB1.2) at full expansion continued

(contours in mm)

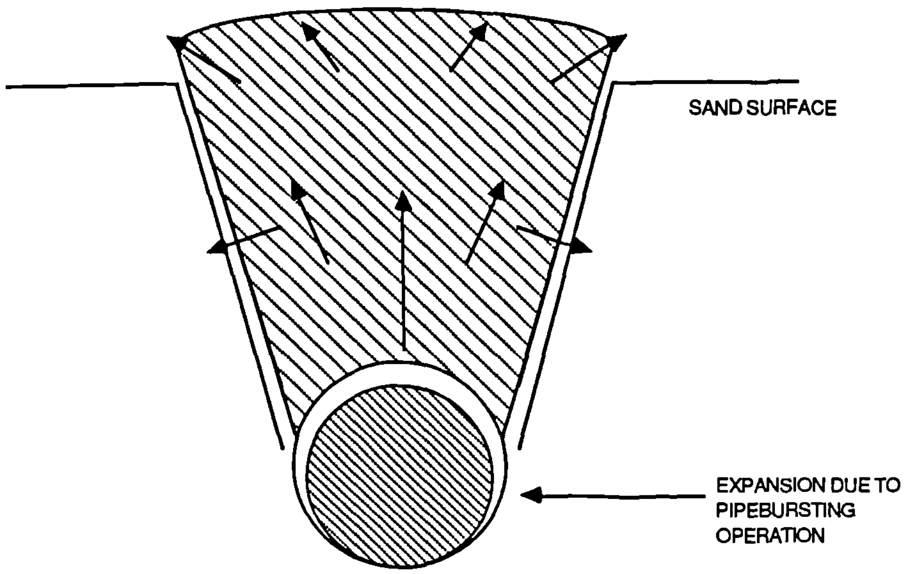

Fig. 5.53 Effects of the upwards bursting action on the soil close to the shear planes

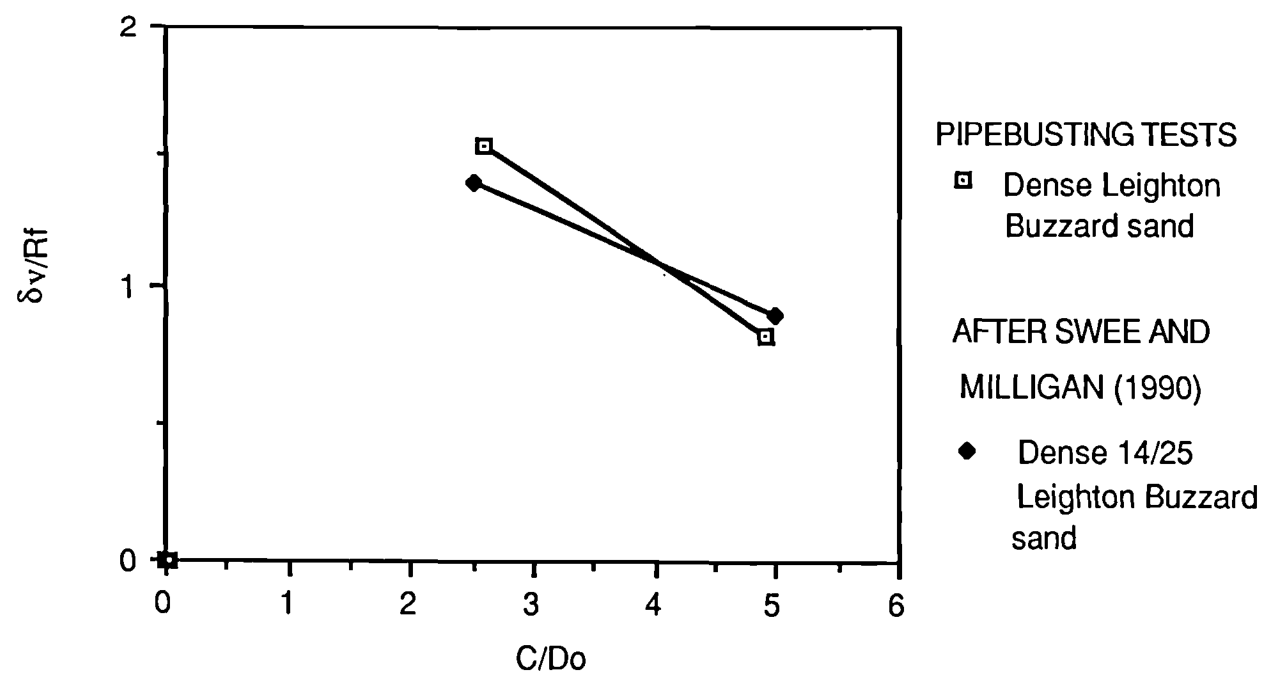

Fig. 5.54 Graph showing the relationship between C/D_o (Cover depth/old pipe diameter) and δ_v/R_f (maximum surface heave/maximum radial expansion)

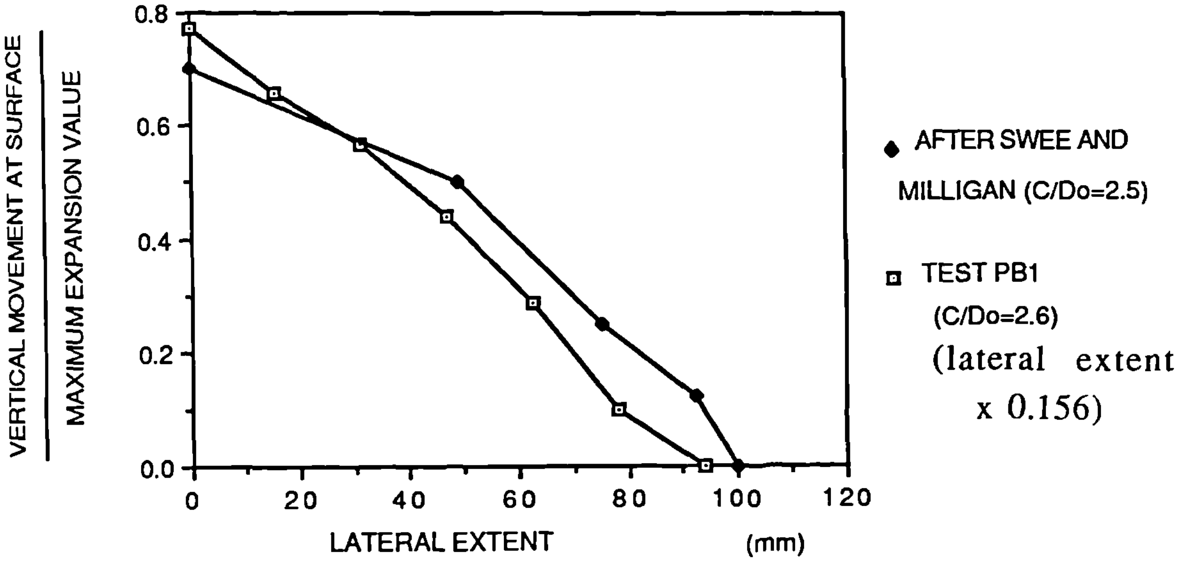

Fig. 5.55a Comparison of surface heave profiles obtained test PB1 (2.6dLB1.2) and the Swee and Milligan (1990) model test with C/D_O=2.5

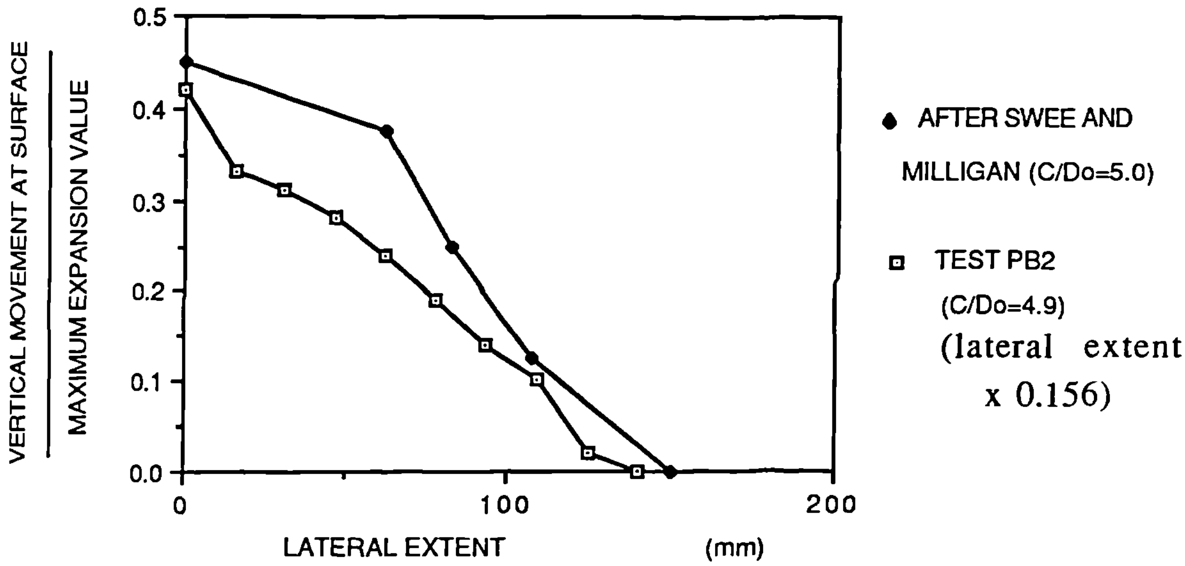

Fig. 5.55b Comparison of surface heave profiles obtained test PB2 (4,91LB1.2) and the Swee and Milligan (1990) model test with C/D_O=5.0

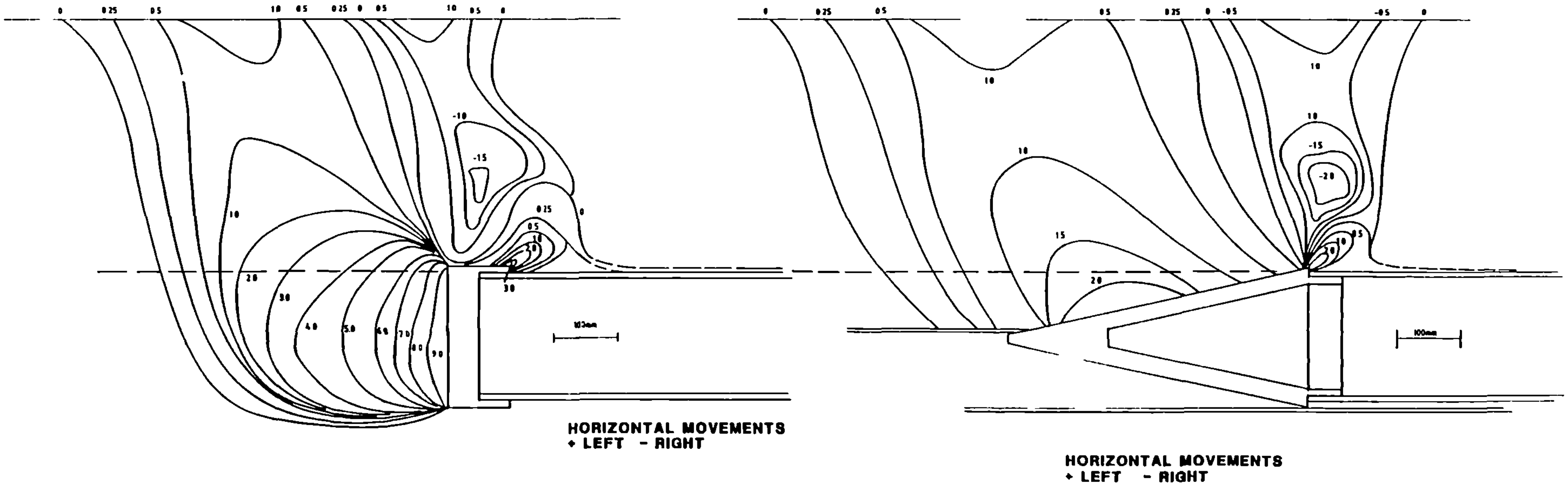

Fig. 5.56 Comparison of the vertical displacement contour plots for test PB5 (3.8dLB1.7) and CPJ1 (2.0dLB0.1)

(contours in mm)

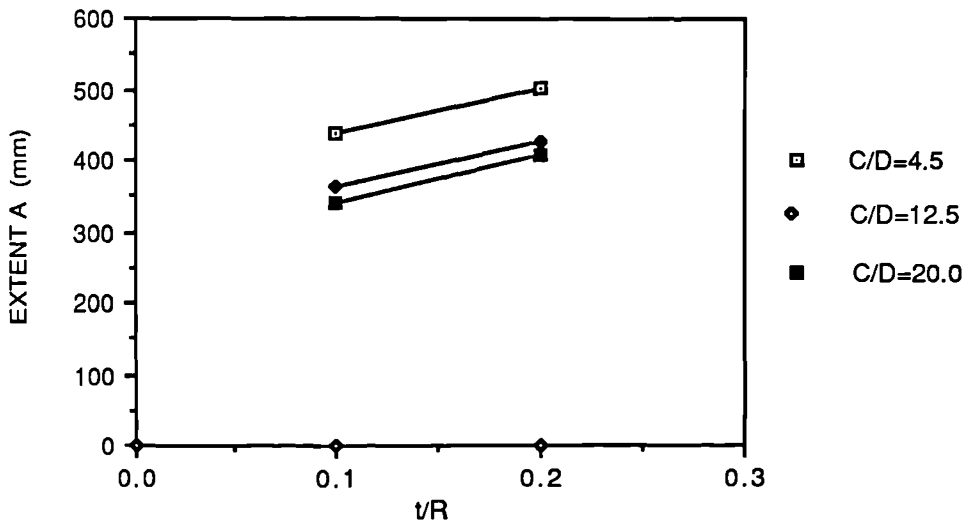

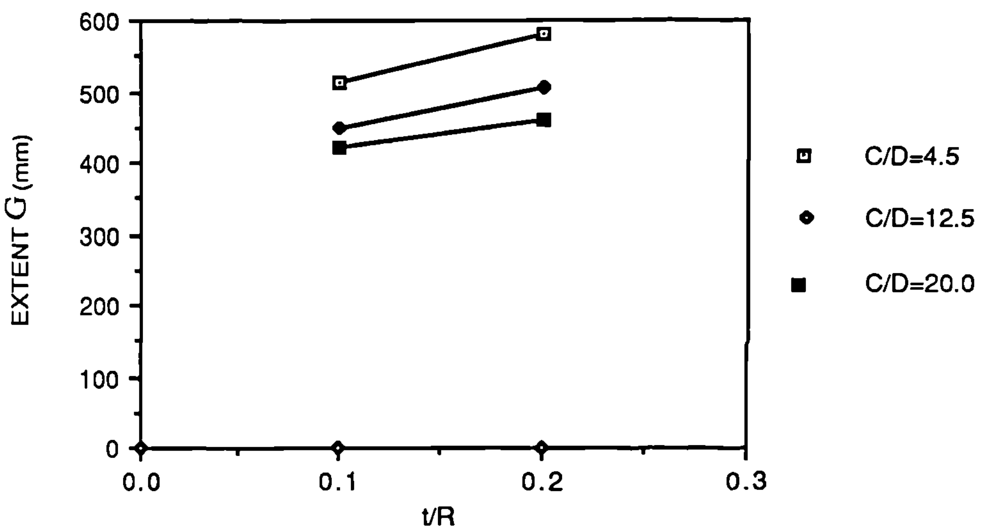

Fig. 5.57a Graphs showing the relationships between dimensions A and G and overcut ratio for different C/D ratios

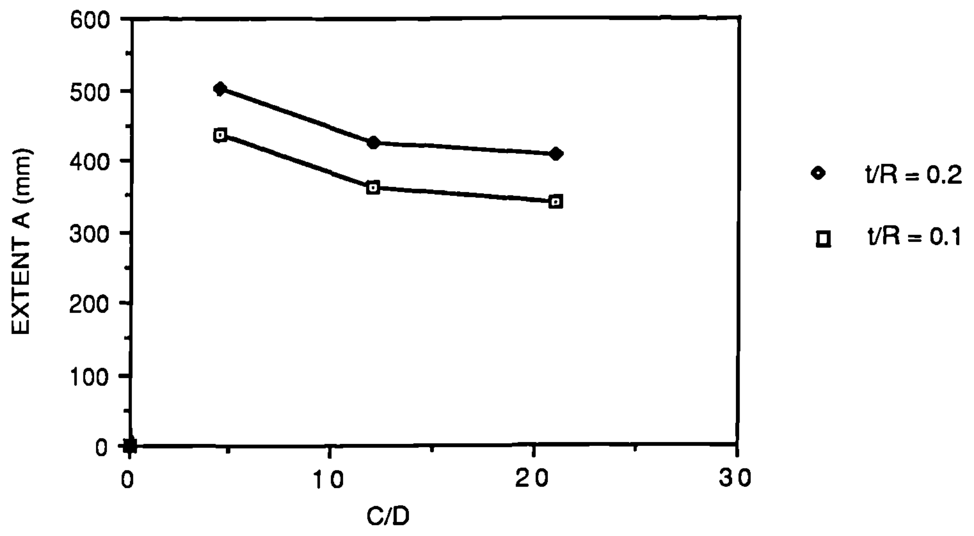

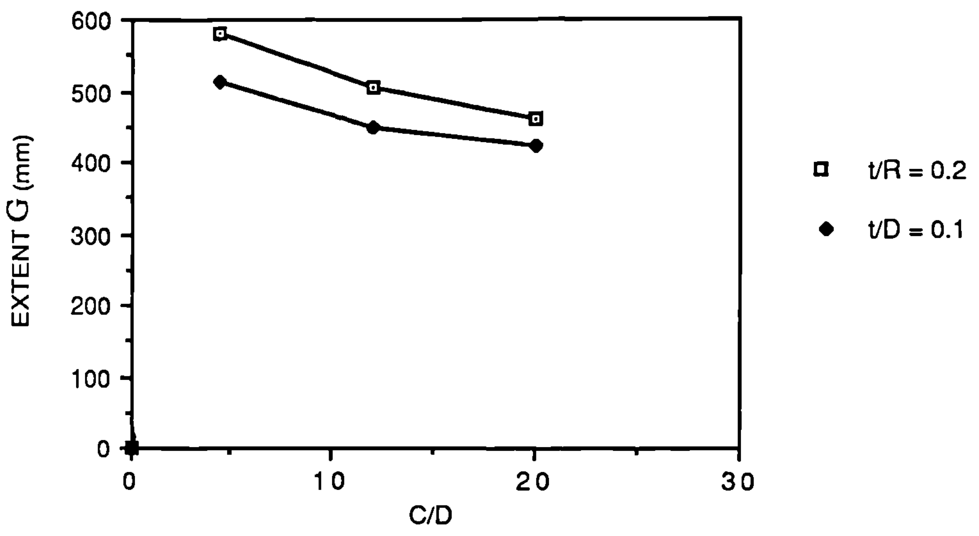

Fig. 5.57b Graphs showing the relationships between dimensions A and G and different C/D ratios for different overcut ratios

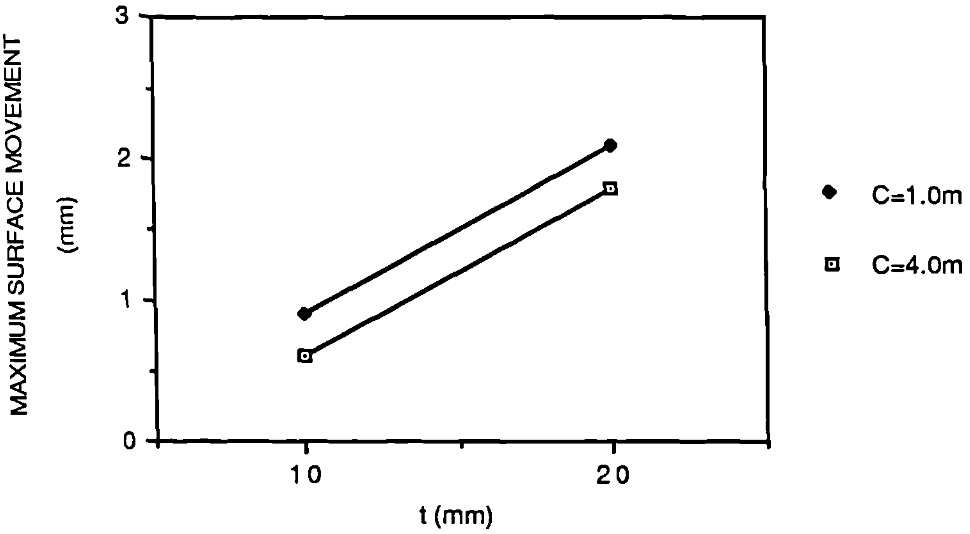

Fig. 5.58a Graph showing the relationship between overcut value and the maximum surface settlement for loose state pipejacking tests

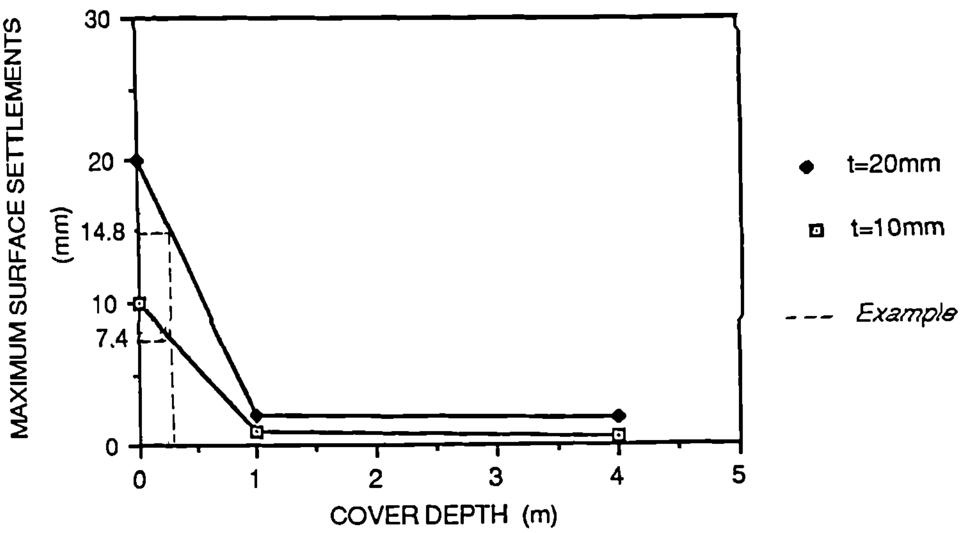

Fig. 5.58b Graph showing the relationship between the cover depth and the maximum surface settlement for the loose state pipejacking tests for different overcut values

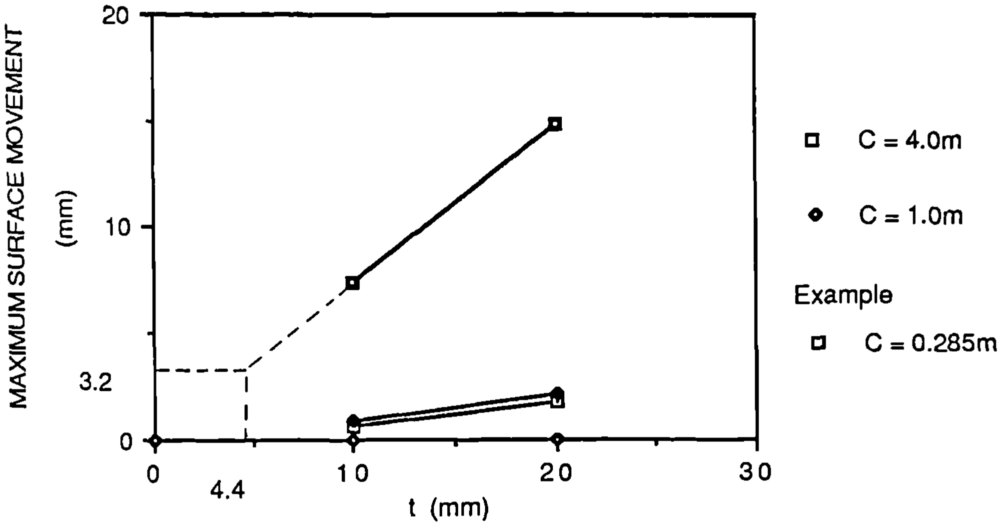

Fig. 5.58c Extended version of Fig. 5.58a which allows example data to be shown

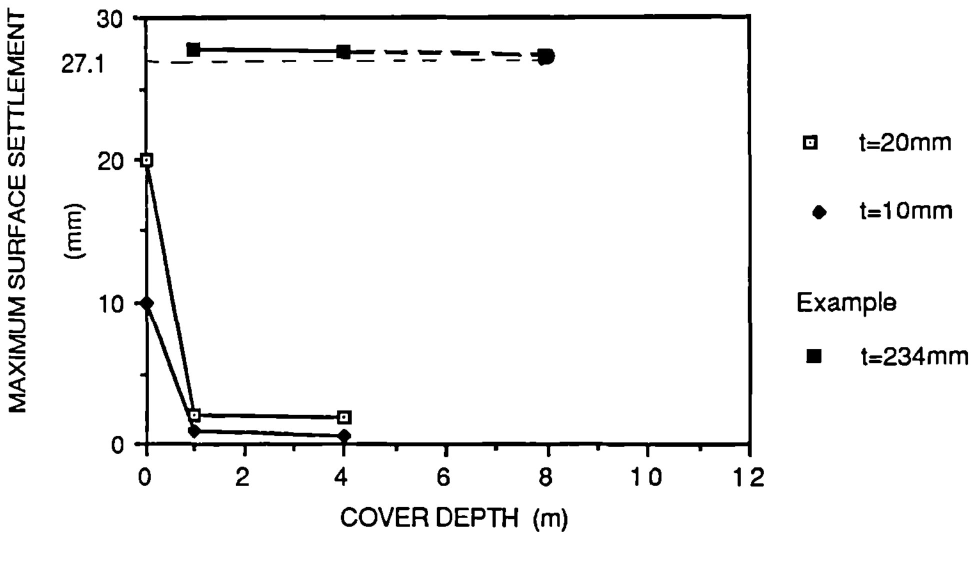

Fig. 5.58d Extended version of Fig. 5.58b which allows example data to be shown

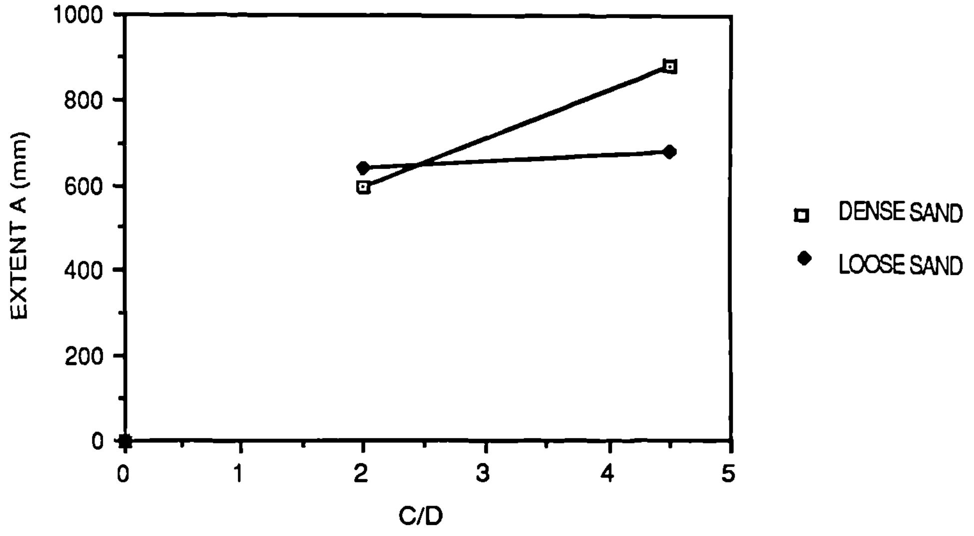

Fig. 5.59 Graph showing the relationship between C/D ratio and dimension A from Table 5.4

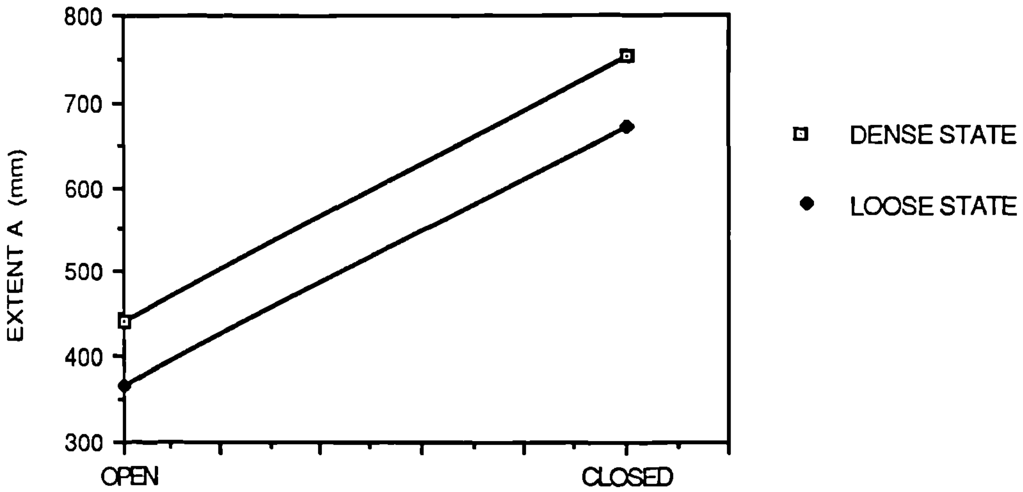

Fig. 5.60 Graph showing the relationship between horizontal extent in front of the shield and degree of support at the face (overcut ratio = 0.1)

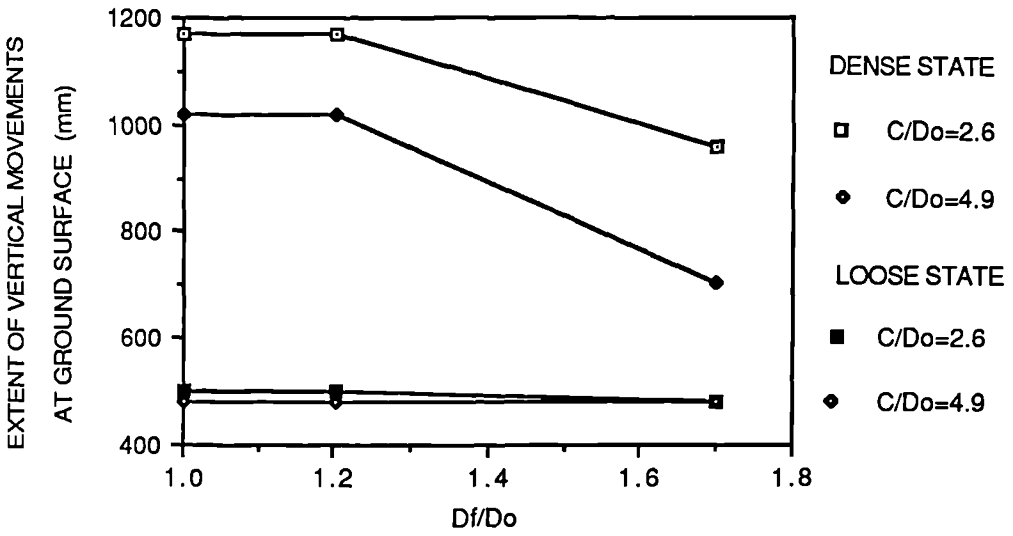

Fig. 5.61a Graph showing the the relationship between observed surface extent from the vertical movements and the D_f/D_o ratio for different densities and C/D ratios

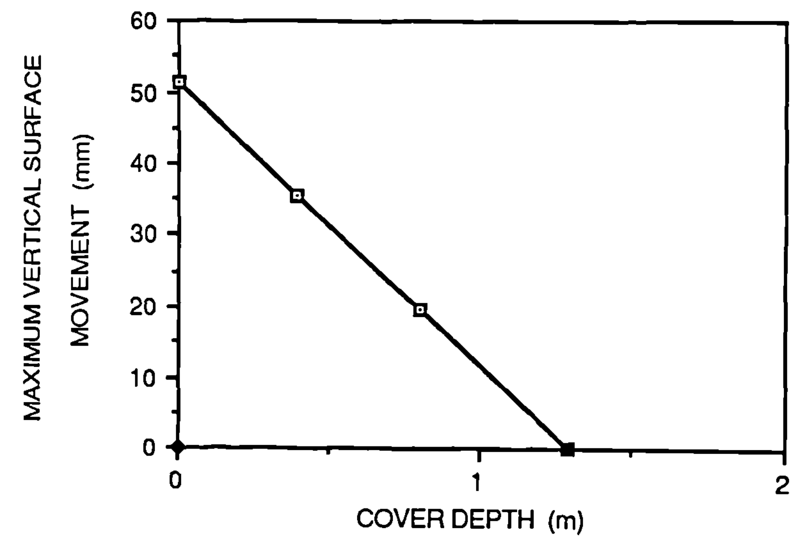

Fig. 5.61b Graph showing the relationship between maximum magnitude of the surface movements and cover depth, for the dense state tests

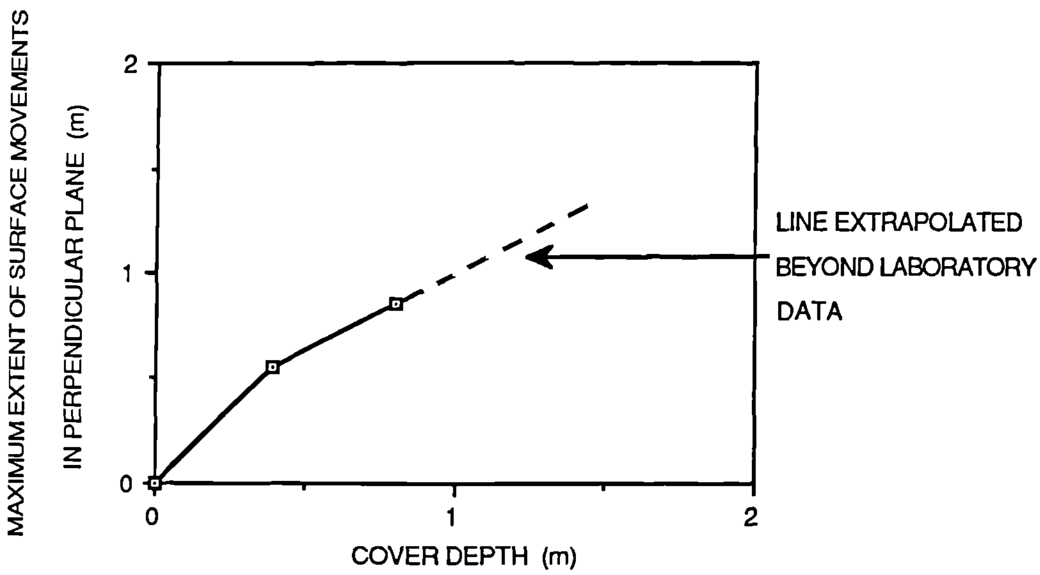

Fig. 5.61c Graph showing the relationship between observed surface extent of the movements and cover depth

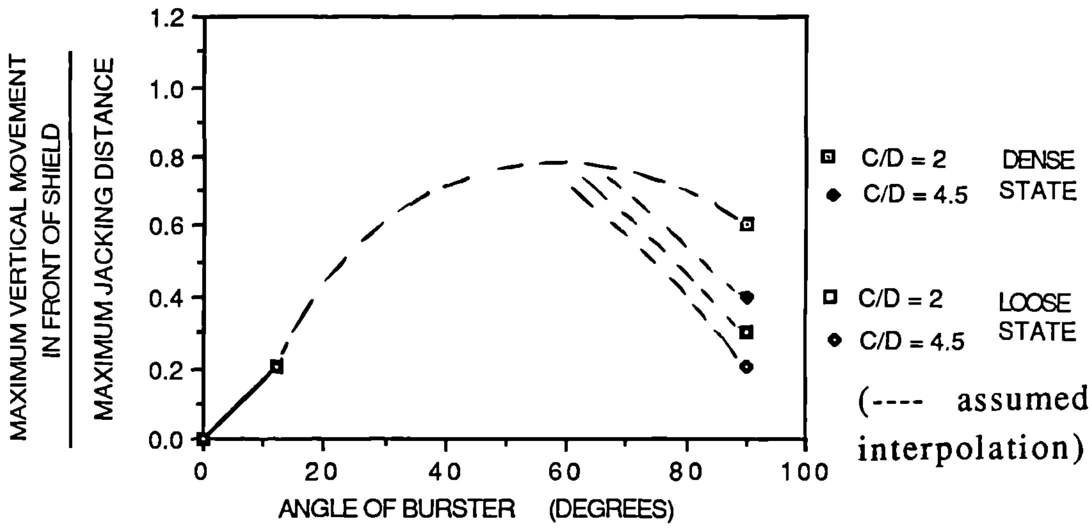

Fig. 5.62a Graph showing the relationship between angle of the bursting face to the horizontal and the maximum vertical movements

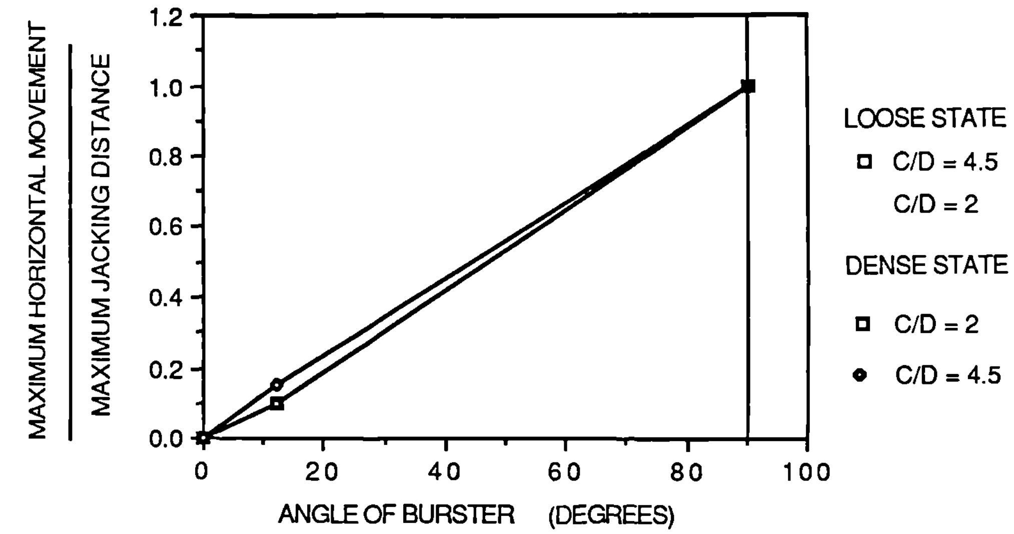

Fig. 5.62b Graph showing the relationship between angle of the bursting face and maximum horizontal movements

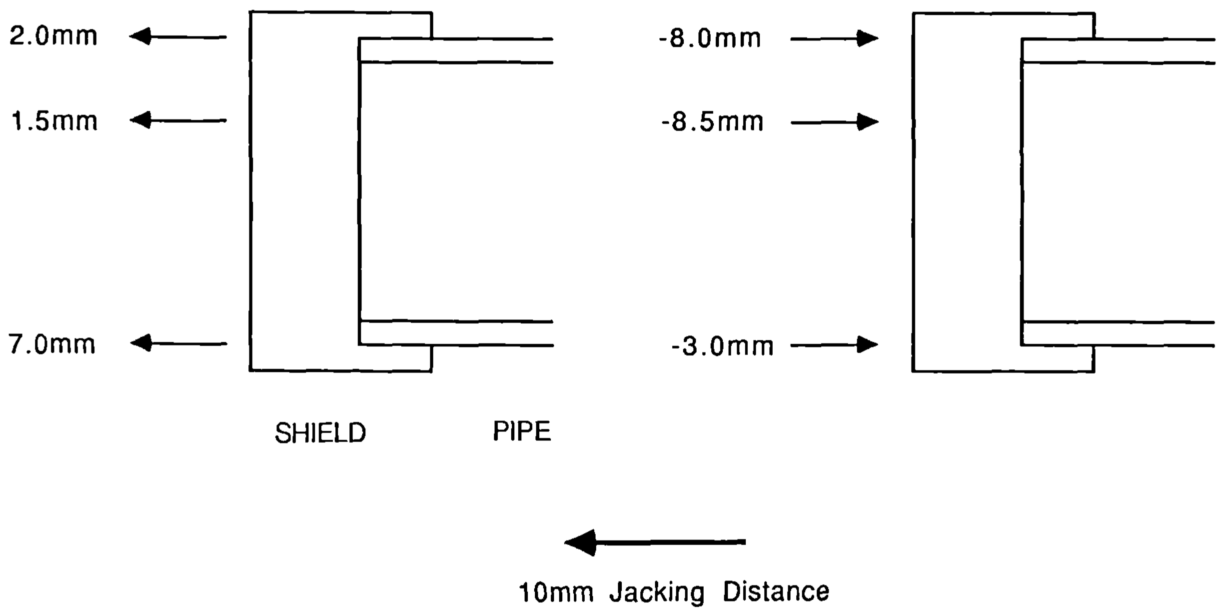

Fig. 5.63 Example illustrating the relative movement into the open pipejacking shield during the jacking operation for test OPJ4 (4.5ILB0.1), (simulated excavation)

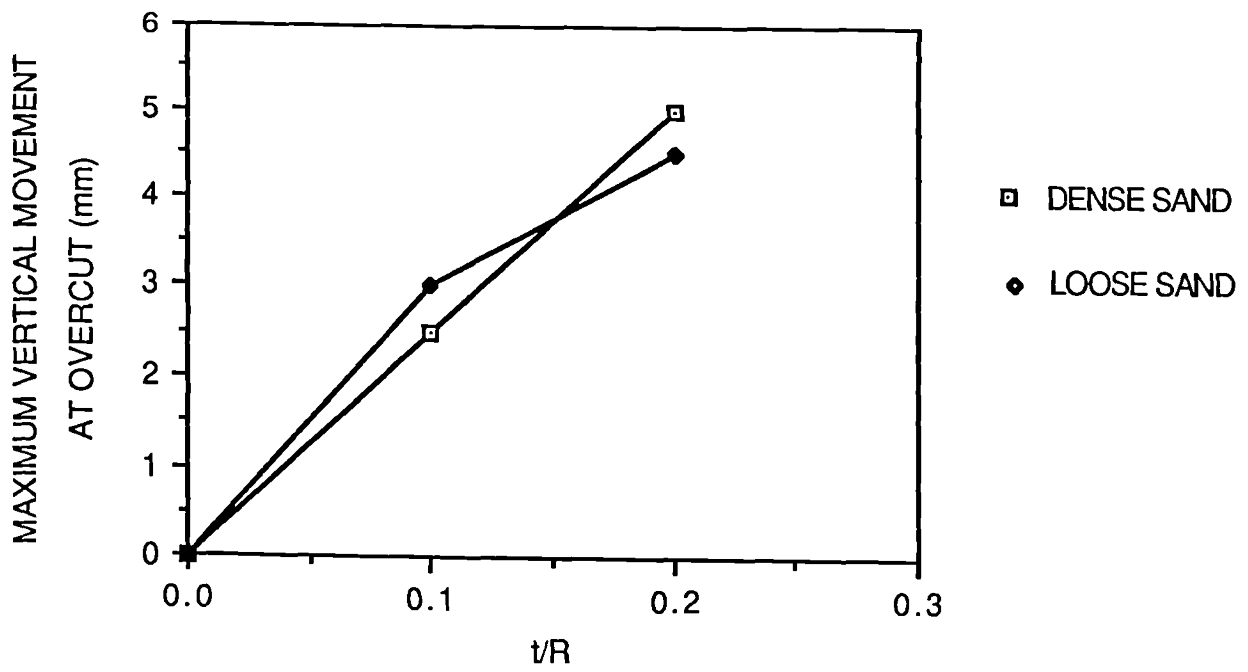

Fig. 5.64 Graph showing the relationship between maximum vertical movement at the overcut and overcut ratio

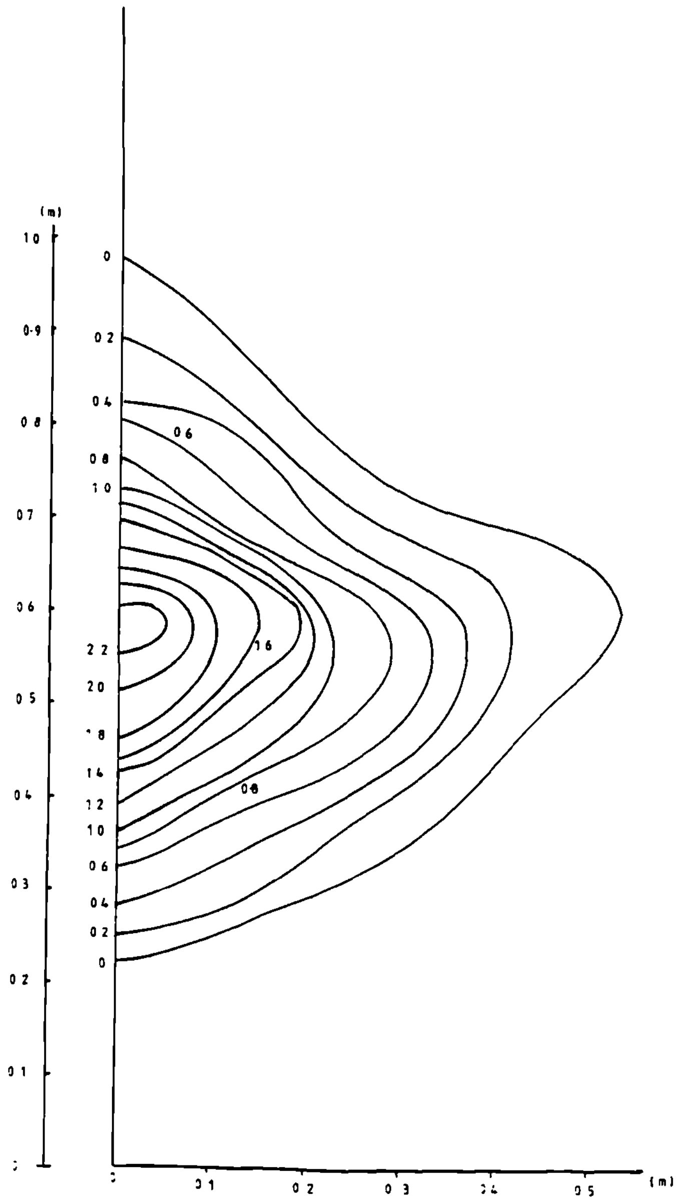

(a) Test CPJ1 (2.0dLB0.1)

(10mm jacking distance, contours in mm)

Fig. 5.65 Vertical surface displacements

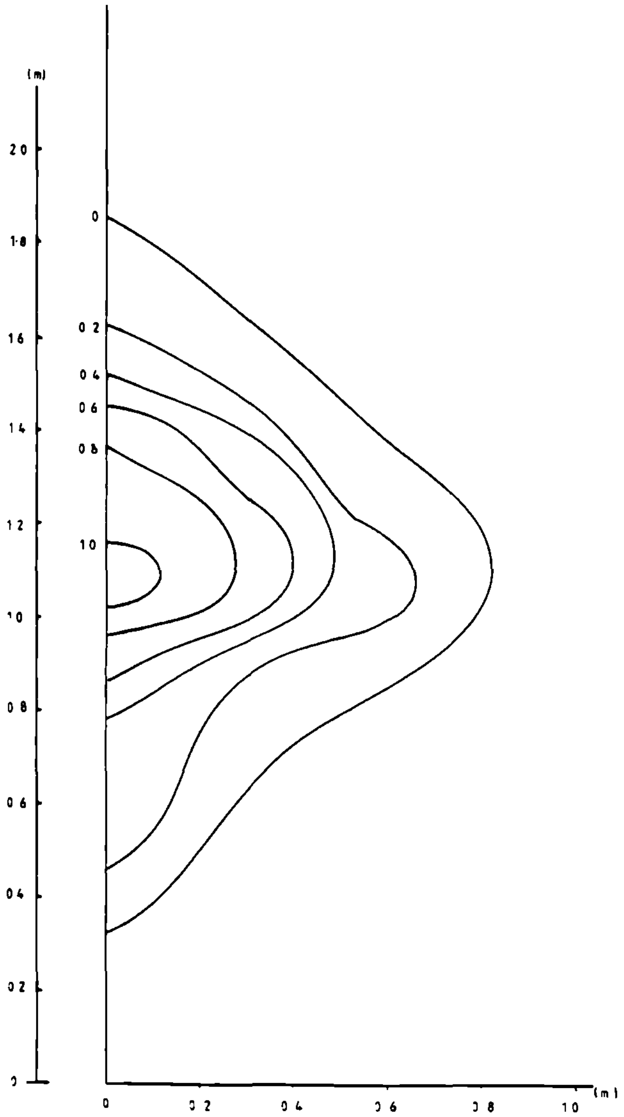

(b) Test CPJ3 (4.5dLB0.1)

(10mm jacking distance, contours in mm)

Fig. 5.65 Vertical surface displacements continued

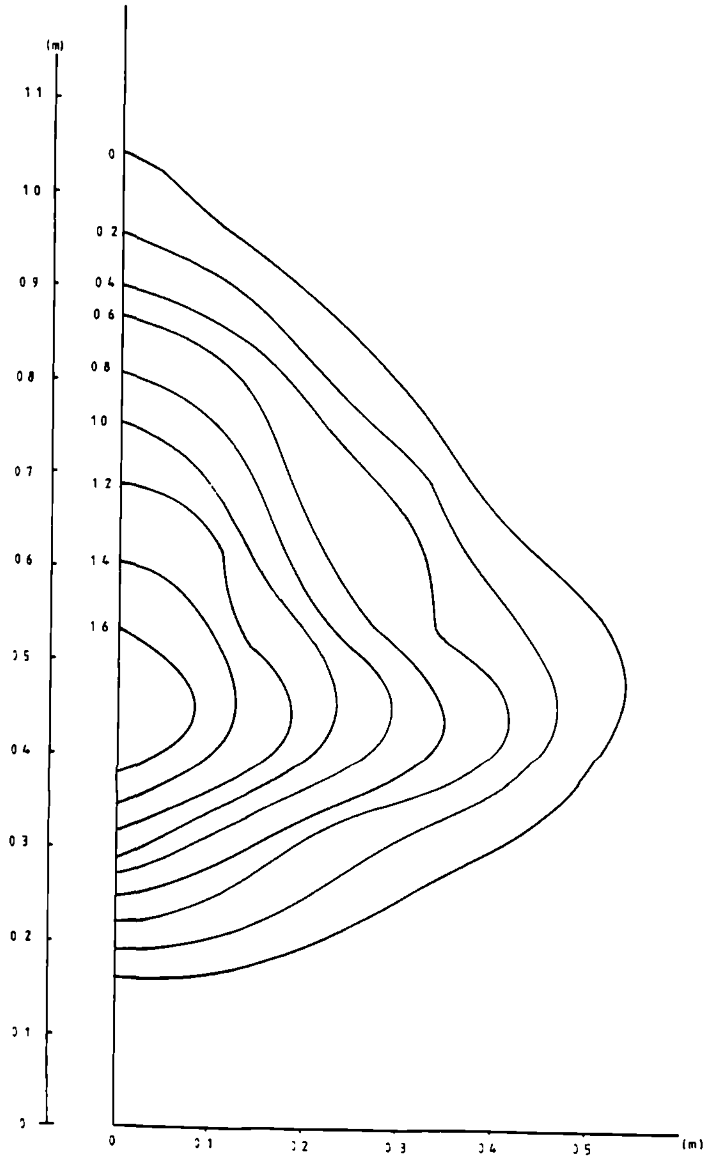

(a) Test PB1 (2.6dLB1.2)

(20mm jacking distance, contours in mm)

Fig. 5.66 Vertical surface displacements

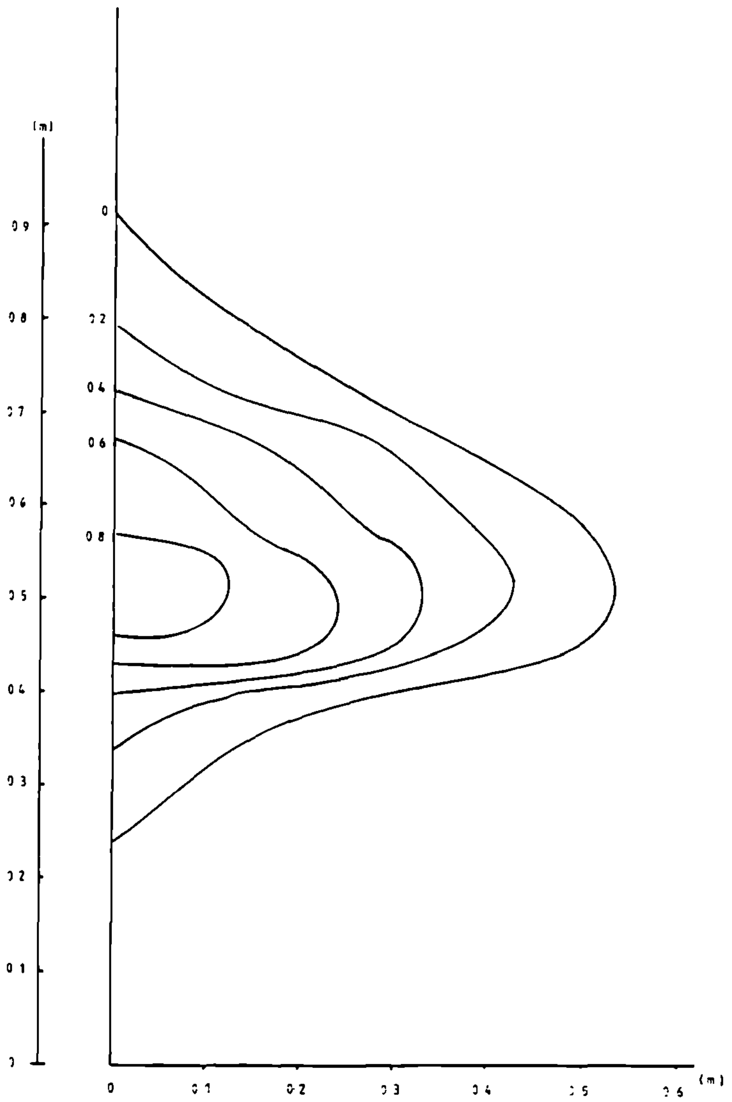

(b) Test PB2 (4.9dLB1.2)

(20mm jacking distance, contours in mm)

Fig. 5.66 Vertical surface displacements continued

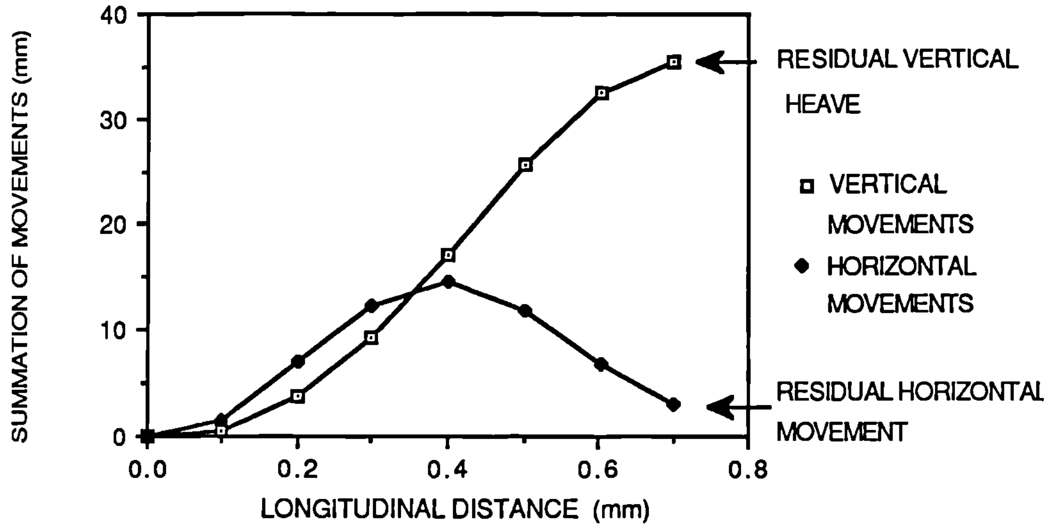

(a) Longitudinal plane

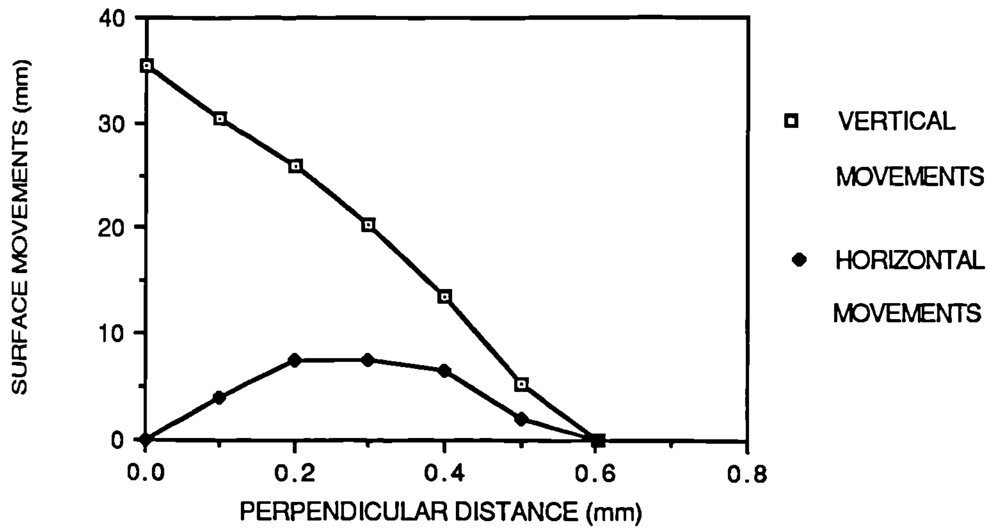

(b) .Perpendicular plane

Fig 5.67 Total surface displacements for test PB1 (2.6dLB1.2) at 100mm intervals

CHAPTER SIX

6 THEORETICAL MODELLING

6.1 INTRODUCTION

As highlighted in the literature review in Chapter 2, Sections 2.2.1.3 and 2.2.2.3, there has been very little work specifically conducted on the theoretical modelling of ground movements around trenchless pipelaying operations. Convergent techniques can be considered similar in certain respects to soft ground tunnelling operations and therefore the analyses developed for tunnels could be applied to both. More work appears to have been conducted into expansive techniques, with the work of O'Rourke (1985) and Swee and Milligan (1990). However, the methods outlined in these papers are not complete analyses and the Swee and Milligan (1990) method only predicts the lateral extents of the movements in sands. O'Rourke's analysis is based on a cavity expansion method, but assumes a deep pipebursting operation as the effects of the ground surface are not taken into account. British Gas is known to be developing finite element models for pipebursting, but none of this work has been published, although it is mentioned briefly in a general report by Herbert and Leach (1990).

Trenchless pipelaying techniques are generally used for much smaller scale operations than full scale tunnelling techniques, and thus the costs involved are proportionately lower. The cost of a full finite element analysis, even today with powerful computers, is high, particularly for a 'one-off' analysis. Relatively complex numerical modelling would be required to simulate accurately the pipejacking procedure. It is therefore less attractive, and generally not financially viable, for these smaller jobs. What is actually required is a theoretical model that can be applied quickly and easily to any situation and that will provide a good idea of the ground movements that are likely to occur during the operation. If these initial predicted movements look like being a problem, more complex analyses can then be conducted.

This chapter investigates two simple closed form solutions for the modelling of trenchless pipelaying operations that have the potential to provide the simple analysis method required. The first is based on the error function curve representing the surface settlement profile and is only discussed briefly. The second is investigated more thoroughly and is based on fluid flow theory.

6.2 ERROR FUNCTION ANALYSIS

A simple technique for use with soft ground tunnelling is proposed by O'Reilly and New (1982). The technique, which is described in Chapter 2, Section 2.3.3.7, is based on the error function curve as representing the surface settlement profile. The analysis cannot take into account different soils, although the lateral extent of the surface settlement profile can be adjusted for non-cohesive and cohesive soils, based on equations 2.3 and 2.4 in Chapter 2. These equations, however, were derived from limited large scale soft ground tunnelling data and this results in relatively limited ranges for their use. Straight application of this method to smaller scale operations or laboratory model tests is therefore not possible and when tried gave nonsensical results.

There are two options available if this analysis is to be applied to trenchless pipelaying operations or the laboratory tests. The first is to derive new equations for the trough width parameter (i), based on field data from trenchless operations, but this is very limited and therefore this option is not possible at the present time. Alternatively, the operation to be analysed can be scaled up to suit the ranges for the original i value formulae. This involves mutiplying each of the parameters, such as pipe depth, pipe diameter and overcut, by a suitable arbitrary factor that brings the pipe depth within the ranges for which the i value formulae were derived. An example is presented in Fig. 6.1 for one of the open shield pipejacking tests (test OPJ4) in the perpendicular plane at the overcut. The test conditions are shown together with the scaled up values used as the input for the analysis. Table 6.1 shows some of the results obtained, which have been scaled down. These are compared with the laboratory

Table 6.1 Comparison between the observed sand displacements and those predicted by the error function analysis

OPJ4 (4.5dLB0.1)

COORDINATE (from pipe axis) (m)	LABORATORY TEST RESULT (mm)		THEORETICAL ANALYSIS RESULT (mm)	
	V	H	V	H
Centreline above pipe axis				
0.20	6.00	0.00	6.50	0.00
0.30	4.30	0.00	3.60	0.00
0.40	3.50	0.00	2.50	0.00
0.50	2.90	0.00	1.90	0.00
0.60	2.50	0.00	1.58	0.00
0.70	2.10	0.00	1.33	0.00
0.80	1.60	0.00	1.10	0.00
0.90	1.10	0.00	1.00	0.00
1.00	0.85	0.00	0.90	0.00
0.1,0.0	6.00	0.80	0.00	0.00
0.1,0.2	3.70	0.35	1.10	0.35
0.2,0.1	2.70	0.80	0.00	0.00
0.3,0.4	0.95	0.25	0.10	0.05
0.3,0.6	0.70	0.30	0.30	0.10
Surface values (from centreline)				
0.0	0.85	0.00	0.90	0.00
0.1	0.70	0.50	0.80	0.70
0.2	0.50	0.50	0.66	0.55
0.3	0.35	0.50	0.50	0.20
0.4	0.20	0.40	0.30	0.10
0.5	0.05	0.10	0.10	0.05
0.6	0.00	0.00	0.00	0.00

Note: Positive values indicate vertical movements are downwards and horizontal movements are to the left.

tests results. The centreline values seem to compare very favourably to those observed in the laboratory model tests, giving an excellent correlation from close to the pipe right through to the surface movements. The movements away from the centreline however, are not predicted well by this analysis. This is due to the analysis not being able to model movements below the crown of the pipe and also due to the concentrated nature of the predicted movements close to the pipe. Comparison of the surface settlements reveals a very good agreement, with the lateral extent of the movements being very accurately predicted. In summary, for this example it has been shown that the centreline and surface sand movements are quite well predicted by the analysis, however the subsurface movements away from the centreline are poorly predicted. The problem with this analysis for modelling the laboratory tests is that the dense state tests cannot be modelled satisfactorily, due to the high dilation rates associated with this material.

A second example is presented in Fig. 6.2, which shows the results of the analysis of test PB1 of the pipebursting laboratory tests. As with the previous example, the input data had to be scaled up to fit in with the i value ranges. Table 6.2 compares the predicted and observed sand displacements (after being scaled down). It it immediately obvious, that the predicted centreline movements correlate quite well, although the predicted values do initially reduce more quickly above the burster. The surface movements are predicted quite closely over the first 400mm from the pipe centreline, even in the case of the horizontal movements. Further away from the centreline the error function model over-estimates the movements and the lateral extent of the surface heave profile. The predicted subsurface movements are good for the vertical values, but the horizontal movements are greatly over-estimated. The overall indication from these, and other examples not presented here, is that the analysis technique offers a good prediction of the dense state pipebursting laboratory test results.

Thus for the pipejacking analysis only loose state tests can be adequately modelled by the error function technique because of dilation effects in dense sand. In contrast, for the pipebursting

Table 6.2 Comparison between the observed sand displacements and those predicted by the error function analysis

PB1 (2.6dLB1.2)

COORDINATE (from pipe axis) (m)	LABORATORY TEST RESULT (mm)		THEORETICAL ANALYSIS RESULT (mm)	
	V	H	V	H
Centreline above pipe axis				
0.15	44.0	0.00	38.60	0.00
0.20	42.0	0.00	34.30	0.00
0.30	35.0	0.00	28.20	0.00
0.40	29.0	0.00	23.90	0.00
0.50	21.0	0.00	20.70	0.00
0.1,0.1	39.0	8.00	35.50	35.50
0.2,0.2	22.5	5.00	20.40	20.40
0.3,0.3	12.5	4.00	12.80	12.80
Surface values (from centreline)				
0.0	21.00	0.00	20.80	0.00
0.1	18.00	3.00	19.75	3.95
0.2	15.00	5.00	17.10	6.85
0.3	12.00	5.00	13.50	8.00
0.4	8.00	4.00	9.70	7.00
0.5	4.00	1.50	6.30	6.30
0.6	0.00	0.00	3.80	4.50
0.7	0.00	0.00	2.00	2.50
0.8	0.00	0.00	1.00	1.00
0.9	0.00	0.00	0.40	0.50
1.0	0.00	0.00	0.00	0.00

Note: Positive values indicate vertical movements are upwards and horizontal movements are to the right.

tests, only dense state tests can be modelled due to the high compression rate for the loose state sand. A further problem with this analysis is its inability to model anything other than the two-dimensional perpendicular plane displacements.

Applying this analysis to the pipebursting field trial data, presented by Chapman and Rogers (1991), produces the results shown in Fig. 6.3, in which a comparison is made for several of the measured soil displacements. The predicted and observed soil movements for this case show an excellent correlation, with the possible exception of point E. Although the measured displacements are limited, their good correlation with the predicted movments indicates that for this case, the O'Reilly and New analysis provides a good predictive method. The stiff clay soil around the field trial, which was relatively incompressible, suits the analysis very well.

6.3 FLUID FLOW THEORY ANALYSIS

6.3.1 Description and Development

One of the most interesting closed form solutions described in the literature review, in Chapter 2, Section 2.3.3.7, is based on incompressible fluid flow theory. Sagaseta (1987) outlines this method in general terms and then describes its use for more specific applications, such as soft ground tunnelling. Sagaseta's method actually combines a fluid analysis approach with elastic solutions in order to allow the ground surface effect to be taken into account. The fluid approach alone only allows deep problems to be analysed where surface boundary effects can be ignored.

The general approach suggested by Sagaseta is shown in Fig. 6.4 for volume loss at a finite depth. The steps involved in the analysis shown in this figure are described below:

Step1 The effect of the soil surface is neglected and the strains are computed as though the sink was in an infinite medium.

Step 2 The strain calculated in Step 1 will produce some stresses at the free surface, thus violating the stress free condition. These stresses can be partially cancelled by considering a virtual source, a negative mirror image of the actual sink with respect to the soil surface. This will produce opposite normal stresses and the same shear stresses as the actual sink. The strains due to the image are added to those calculated in Step 1.

Step 3 The remaining shear stresses at the surface are then evaluated and subsequently removed. The resulting strains are again added to those obtained from Steps 1 and 2.

The fluid mechanism approach is no longer applicable to Step 3 and a different approach, using solid mechanism methods, is used. The method involves:

a) Evaluation of the strain at the surface by differentiation of the displacement field obtained in Steps 1 and 2.

b) From these strains, the corresponding surface stresses are calculated.

c) Finally the strain field, in a half-space subjected to a system equal and opposite to those calculated in b), is determined. Sagaseta derives equations for the soft ground tunnelling situation for both the surface and subsurface ground movements. These equations, together with the derivation, are given in Appendix C, Section C.1.2.

Rogers & O'Reilly (1990) adapted these equations to allow application to pipejacking based on Fig. 6.5, for movements caused in the plane perpendicular to the pipe centreline. This adaptation uses a uniformly distributed ground loss based on the overcut. The derivation of these equations from the original equations is given in Appendix C, Section C.2, the derived equations being:

$$-W_x = R.\delta R.x\left[\frac{1}{r_1{}^2} - \frac{1}{r_2{}^2}\right] \tag{6.1}$$

$$-W_y = R.\delta R\left[\frac{y}{r_1{}^2} + \frac{2(Z-y)}{r_2{}^2}\right] \tag{6.2}$$

where $r_1 = (x^2 + y^2)^{1/2}$ and $r_2 = (x^2 + (2Z - y)^2)^{1/2}$

The equations for the additional displacements, i.e. for Step 3, are as follows:

$$-W_x = \frac{2.R.\delta R.x}{r_2^2}\left[1 - \frac{2(Z-y)(2Z-y)}{r_2^2}\right] \qquad (6.3)$$

$$W_y = \frac{2.R.\delta R.(Z-y)}{r_2^2}\left[1 - \frac{2x^2}{r_2^2}\right] \qquad (6.4)$$

In order to improve the lateral spread of the results and to concentrate the ground movements above the tunnel, Rogers and O'Reilly (1991) propose a variable ground loss around the tunnel and considered this ground loss to include all the volume losses due to the tunnelling operation (Fig. 6.6b). This is justified by the fact that during the pipejacking operation, the installed pipes will not tend to stay in the centre of the excavated cavity, but will settle and run along the invert of this cavity. This modification improved the prediction of ground movement extent, although it still gave a relatively large lateral extent to the movements. A further restriction on the ground loss that improves the extent of movement greatly, is to vary the volume loss from zero at the springings to a maximum value at the crown (Fig. 6.6c). Although this representation of the ground losses is not necessarily realistic of the prototype situation, in situations where sands predominate above the pipe it is a reasonable assumption, as there is very little movement below the springing level.

The next stage of the model's development, was to try to model the conditions in the laboratory tests. This involved modelling sands, knowing that dilation and compression dominate the properties of these soils. This meant that some sort of dilation and compression effect had to be incorporated into the model in order to give it any realistic chance of modelling the laboratory situation. Sagaseta (1987) indicates how compressibility could possibly be incorporated into the model, although no examples are given of its use. Sagaseta (1987) does, however, show how these ideas can influence the lateral extent of the surface settlement profile above a tunnel. Sagaseta (1987) presents equation 6.5, which is shown to be applicable to displacements caused around expanding cavities.

$$W_r(r) = k\,\frac{a}{n}\left[\frac{a}{r}\right]^{\alpha} \qquad (6.5)$$

Equation 6.6 shows the basic equation used in the fluid flow analysis:

$$W_r(r) = \frac{a}{n}\left[\frac{a}{r}\right]^{n-1} \qquad (6.6)$$

This equation demonstrates that the incompressible flow model is one particular solution of equation 6.5, when k=1 and α=n-1. Sagaseta (1987) suggests the following relationships for α in equation 6.5, in order to take into account compressibility and dilation. (The α power factor reduces or increases the rate at which the displacements vary as one moves away from the sink.) For a sink in a dense soil or a source in a loose soil,

$$\alpha = \frac{(n-1)}{\alpha_a} \qquad (6.7)$$

For a sink in a loose soil or a source in a dense soil,

$$\alpha = (n-1)\,\alpha_a \qquad (6.8)$$

where $\alpha_a = (1-\sin\psi')/(1+\sin\psi')$ and ψ' is the angle of dilatancy of the soil. This means that with n=2 and $\psi'=0$, the analysis is the same as the original incompressible flow model. This is explained further in Appendix C, Section C.4.

Applying these modifications to the general analysis is straightforward for Steps 1 and 2, but very difficult for Step 3, due to the complex integrations involved. Sagaseta (1991) sugests, however, that a good approximation can be obtained by ignoring the Step 3 calculations, i.e. the additional surface stresses. This is particularly applicable as one moves deeper away from the ground surface and these stresses become less significant. It was therefore decided to try the analysis without Step 3. This was compared with one in which Step 3 was included, i.e. for the incompressible case ($\alpha=1$). The differences were found to be very small for an example using parameters related to those in the laboratory model tests, although the differences did increase towards the surface. The results are shown in Table 6.3. The incorporation of these ideas into the analysis is described in Appendix C. The equations derived are used in all the subsequent analyses, unless specifically stated otherwise. These modifications make the analysis much more powerful and versatile.

The following sections outline the models developed for predicting ground movements associated with trenchless pipelaying techniques, specifically for comparison with the laboratory test results. Four models are presented, two for pipejacking and two for pipebursting operations, one being for the perpendicular plane and the other for the longitudinal plane in each case.

The following analyses are all based on the laboratory model tests using the Leighton Buzzard sand described in this thesis. The dilation angles for the density states used in laboratory tests were calculated from the shearing angles at peak and at critical states, given in Table 4.1. For the loose state analyses the dilation angle is taken as 6^{o}, and for the dense state analyses the dilation angle is taken as 17.5^{o}.

6.3.2 Pipejacking Tests - Perpendicular Plane

This model is very similar to the original pipejacking model developed by Rogers and O'Reilly (1990). The model does, however, incorporate the variable ground loss distribution of maximum ground loss at the crown and zero at the springing level (Fig. 6.6c). As mentioned previously, this representation of the ground loss distribution may not be realistic in field situations, with the ground loss distribution shown in Fig. 6.6b being perhaps more appropriate. However, for the prediction of the sand displacements in the laboratory tests, which are primarily investigating the effects of the shield overcut, the more restricted

Table 6.3 Comparison between the analyses; one taking into account the additional surface stresses and one without the additional surface stresses

VERTICAL MOVEMENTS						
Distance above pipe axis (m)	Distance from centreline of pipe (m)					
	0.0		0.2		0.4	
	1	2	1	2	1	2
0.3	8.2	8.2	6.3	6.1	2.1	2.3
0.4	6.9	6.5	5.9	5.5	2.4	2.7
0.6	4.4	4.9	4.0	4.4	2.7	3.0
0.8	3.6	4.3	3.5	4.1	2.9	3.3
1.0	4.0	4.2	3.9	4.0	3.4	3.5

HORIZONTAL MOVEMENTS						
Distance above pipe axis (m)	Distance from centreline of pipe (m)					
	0.0		0.2		0.4	
	1	2	1	2	1	2
0.3	0.0	0.0	2.7	2.9	2.1	2.4
0.4	0.0	0.0	1.8	1.8	2.0	1.9
0.6	0.0	0.0	0.9	0.8	1.4	1.1
0.8	0.0	0.0	0.6	0.3	1.0	0.5
1.0	0.0	0.0	0.5	0.0	0.9	0.0

Note: 1 indicates analysis with Step 3
2 indicates analysis without Step 3

ground loss provides the best approximation for the concentrated funnelling effects observed. This model also includes the modifications to the fluid flow theory which model dilatancy and compressibility.

Two examples are presented to illustrate the use of the model developed, with the predicted sand displacements being compared with the laboratory test results. Figs. 6.7a and b show the predicted displacement patterns, with certain of the model test results for specific points given as a comparison in Table 6.4. It can clearly be seen that both the loose and dense states are modelled well. This indicates that the adjustments to the model, to incorporate dilatency, are surprisingly good considering the approximate and relative unsophistication of the analysis. It should be noted, however, that the lateral extent of the predicted vertical movements is too great, particularly for the loose state example. Due to the simplifications made to the analysis to incoporate dilation, i.e. the removal of Step 3, the surface horizontal movements are not predicted in the analysis. As mentioned previously, it is always a problem with simplified analyses, such as this fluid flow model, that the soil is not modelled very accurately and therefore inaccuracies in the results are inevitable. Although the examples given are for a C/D ratio of 4.5 and an overcut ratio of 0.1, other values can be modelled with similarly good results.

6.3.3 Pipejacking Tests - Longitudinal Plane

Modelling the longitudinal plane of the pipejacking tests with the fluid flow model developed is far more complex. It was therefore decided initially to only model the ground movements caused by the overcut. The key to successful longitudinal modelling concerns the position of the sink, to which the sand is assumed to move. The sink is the point at which the volume loss is occurring, in this case the sink is the formation of a cavity by the forward movement of the shield. The sand is therefore assumed to move radially into this cavity area. Fig. 6.8 shows the general philosophy behind the analysis. The sink is considered to have two positions (this is because to use the fluid flow analysis

Table 6.4 Comparison of observed soil displacements with those predicted by the fluid flow analysis for tests OPJ1 and OPJ4

OPJ1 (4.5dLB0.1)

COORDINATE (from pipe axis) (m)	LABORATORY TEST RESULT (mm)		THEORETICAL ANALYSIS RESULT (mm)	
	V	H	V	H
Centreline above pipe axis				
0.15	4.50	0.00	4.70	0.00
0.20	2.80	0.00	2.30	0.00
0.25	1.60	0.00	1.30	0.00
0.30	0.90	0.00	0.90	0.00
0.35	0.60	0.00	0.60	0.00
0.40	0.43	0.00	0.40	0.00
0.45	0.30	0.00	0.30	0.00
0.50	0.17	0.00	0.26	0.00
0.55	0.05	0.00	0.20	0.00
0.60	0.00	0.00	0.15	0.00
0.65	0.00	0.00	0.10	0.00
0.70	0.00	0.00	0.00	0.00
0.1,0.0	3.80	1.50	2.00	2.00
0.1,0.2	0.45	0.50	1.30	0.64

Note: Positive values indicate vertical movements are downwards and horizontal movements are to the left.

Table 6.4 Comparison of observed soil displacements with those predicted by the fluid flow analysis for tests OPJ1 and OPJ4, continued

OPJ4 (4.5ILB0.1)

COORDINATE (from pipe axis) (m)	LABORATORY TEST RESULT (mm)		THEORETICAL ANALYSIS RESULT (mm)	
	V	H	V	H
Centreline above pipe axis				
0.15	7.20	0.00	6.50	0.00
0.20	6.00	0.00	4.40	0.00
0.25	4.90	0.00	3.30	0.00
0.30	4.30	0.00	2.60	0.00
0.35	3.90	0.00	2.10	0.00
0.40	3.50	0.00	1.80	0.00
0.45	3.10	0.00	1.60	0.00
0.50	2.90	0.00	1.40	0.00
0.60	2.50	0.00	1.15	0.00
0.70	2.10	0.00	1.00	0.00
0.80	1.60	0.00	0.90	0.00
0.90	1.10	0.00	0.87	0.00
1.00	0.85	0.00	0.85	0.00
0.1,0.0	6.00	0.80	4.50	2.00
0.1,0.2	3.70	0.35	3.00	1.40
0.2,0.1	2.70	0.80	1.20	0.70
0.3,0.4	0.95	0.25	0.90	0.50
0.3,0.6	0.70	0.30	0.80	0.25
Surface values (from centreline)				
0.0	0.85	0.00	0.85	0.00
0.1	0.70	0.50	0.83	0.00
0.2	0.50	0.50	0.80	0.00
0.3	0.35	0.50	0.73	0.00
0.4	0.20	0.40	0.65	0.00
0.5	0.05	0.10	0.57	0.00
0.6	0.00	0.00	0.41	0.00
0.7	0.00	0.00	0.30	0.00
0.8	0.00	0.00	0.20	0.00
0.9	0.00	0.00	0.10	0.00
1.0	0.00	0.00	0.00	0.00

Note: Positive values indicate vertical movements are downwards and horizontal movements are to the left.

the movements of the soil must be directed to a single point. As the cavity has a finite length it is not posible to direct the movements to a single point (sink) and therefore this is approximated by having two sinks one at either end of the cavity and conducting separate analysises on each): the first of these sinks occurs at the junction between the pipe and the shield and represents the point at which maximum collapse occurs immediately after the shield has passed (ie. immediately after jacking), and the second occurs at the same position before jacking. Calculation using sinks at each of these positions predicts the movements in areas 1 and 2 respectively. Summation and averaging of the movements takes place where overlap occurs for these two analyses (area 3). This means that two separate analyses are conducted for this model. In the analysis, R (Fig. 6.5) is equal to t (the magnitude of the overcut) and δR is equal to the variable t' that occurs due to the nature of the volume loss. Thus a particle at point P, will have a value of $\delta R = t'$. The volume loss in this analysis is considered as area 4, i.e. the cavity left after the forward jacking has taken place.

The calculation of δR for each of the two separate analyses, from points 1 and 2, is the next consideration. For analysis 1, if the actual volume area is traced out, δR would begin as t for points directly over the overcut and then increase to $(t^2 + J^2)$ as the angle increased from the vertical, where J is the forward jacking distance. δR would then decrease to J as the angle to the vertical reached 90^o. The initial increase of δR was thought unlikely to occur in practice and it was decided to make δR a constant t value in this region. The area where δR decreased from $(t^2 + J^2)$ to J was also thought to be unrealistic as δR would be expected to decrease to zero as the angle to the vertical approached 90^o. It was therefore decided to make δR in this region vary linearly from t to zero. This leads to δR remaining at a constant value of t until an angle of $\tan^{-1}(J/t)$ to the vertical, and then decreasing from t to zero linearly up to an angle of 90^o to the vertical. For similar reasons to those mentioned above, for the analysis from position 2, δR is taken as a constant t throughout.

The predicted displacement patterns for two separate analyses are given in Figs. 6.9a and b. The comparative movements from the laboratory tests are given for specific positions in Table 6.5, which compares the predicted and measured movement values. It can be seen that the values above the overcut are modelled quite well and that the values away from this position are not so well predicted, this latter discrepancy appearing to be worse for the loose state test (OPJ4 in Table 6.5b). It must be remembered that the model presented here only models the overcut and does not attempt to take into account the influences of other areas of movement, such as those over the shield due to the face movements and those effects caused by material being drawn along close to the pipe. It can be seen however, that although not specifically modelled, the draw-along effects, which tend to reduce the movements at the overcut in the model tests, seem to be implicit in the theoretical modelling process since the displacements are much less than 10mm (the overcut value used in these tests).

6.3.4 Pipebursting Tests - Perpendicular Plane

The model for predicting the sand movements in this plane is similar to the one developed for the pipejacking tests in the perpendicular plane, except that the sink is changed to a source, thus reversing the direction of the movements. In addition to this, the model allows the prediction of the movement patterns throughout the bursting process as the bursting head breaks out more and more of the old pipe. This idea is shown in Fig. 6.10, in which it can be seen that the amount of expansion can be specified, allowing investigation of the soil movements throughout the busting process. The analysis uses a variable burst value of zero at the burster invert and a maximum value at the burster crown. This helps the analysis to take into account the effects of the ground surface tending to attract more of the movement at shallow depths and assumes the bursting head is moving along the invert of the old pipe. The calculation of the soil movements is conducted in series of specified steps, i.e. 4mm expansion for each step to match the pipebursting laboratory tests. The movements for each expansion step are summed to produce the overall movements. The analysis is conducted in steps in order that the

Table 6.5 Comparison between the predicted displacements, using the fluid flow analysis, and those observed in the laboratory tests, for test OPJ1 and OPJ4

OPJ1 (4.5dLB0.1)

COORDINATE (from outside of pipe at overcut) (m)	LABORATORY TEST RESULT (mm)		THEORETICAL ANALYSIS RESULT (mm)	
	V	H	V	H
Directly above overcut				
0.025	2.50	1.50	2.80	1.10
0.050	0.80	0.50	1.20	0.20
0.075	0.70	0.40	0.70	0.10
0.100	0.60	0.20	0.50	0.05
0.150	0.55	0.10	0.30	0.00
0.200	0.40	0.00	0.20	0.00
0.250	0.20	0.00	0.15	0.00
0.300	0.10	0.00	0.10	0.00
0.350	0.00	0.00	0.05	0.00
0.05,0.05	-1.50	1.50	-1.20	1.20
0.1,0.1	-0.70	1.30	-0.40	0.40
-0.05,0.15	-0.20	-0.30	-0.20	-0.20
0.15,0.2	-0.30	0.00	-0.20	0.15

Note: Positive values indicate vertical movements are downwards and horizontal movements are to the left.

Table 6.5 Comparison between the predicted displacements, using the fluid flow analysis, and those observed in the laboratory tests, for test OPJ1 and OPJ4, continued

OPJ4 (4.5ILB0.1)

COORDINATE (from outside of pipe at overcut) (m)	LABORATORY TEST RESULT (mm)		THEORETICAL ANALYSIS RESULT (mm)	
	V	H	V	H
Directly above overcut				
0.025	3.10	3.00	3.50	3.00
0.050	2.40	0.90	3.00	0.90
0.100	2.00	-0.30	2.60	-0.30
0.150	1.80	-0.20	2.10	-0.15
0.200	1.75	-0.10	1.90	-0.10
0.250	1.60	-0.05	1.50	-0.05
0.300	1.50	0.00	1.30	0.00
0.350	1.40	0.00	1.20	0.00
0.400	1.30	0.00	1.20	0.00
0.45	1.20	0.00	1.10	0.00
0.50	1.10	0.00	1.05	0.00
0.05,0.05	-2.00	1.80	-3.30	3.00
0.1,0.1	-1.30	0.00	-2.00	1.10
0.15,0.2	-1.00	-0.60	-1.60	0.90
-0.05,0.15	-0.80	-0.80	-1.20	-0.90

Note: Positive values indicate vertical movements are downwards and horizontal movements are to the left.

effects of gradual break out of the original pipe can be simulated. This is important as points on the burster during expansion that are within the old pipe, i.e. not exposed to the surrounding soil, do not transmit movements into the soil. The total induced movements in the soil surrounding the burster are therefore not neccesarily equal to the total expansion value of the burster during the pipebursting operation.

Three examples of the use of this model are presented in this section. The first two relate to the same test (pipebursting test PB1), but at different stages of the expansion process. The first is close to the start of the bursting operation and is for a maximum expansion of 4mm. The second example is close to the end of the bursting operation and uses a maximum expansion of 46mm. The third example is for the same test arrangement, but with a loose state sand close to the end of the bursting operation and uses a maximum expansion of 46mm (pipebursting test PB3). The results obtained from the analyses are presented in Figs. 6.11a, b and c, which show the predicted displacement patterns and some comparative results from the laboratory tests. These can be compared with the total displacement vector plots for the corresponding tests given in Figs. 5.44c, 5.46c and 5.48c respectively. Certain values for both the predicted and measured displacements are given in Table 6.6. The results show relatively good agreement in all cases for both the centreline and subsurface values, although it must be noted that the lateral extents of the predicted movements are overestimated, particularly for the examples close to full expansion where there is consistently double the extent. As mentioned in the literature review in Chapter 2, Rogers and O'Reilly (1991) and Chapman and Rogers (1991) used this analysis, although without the dilation/compression capabilities, for predicting the movements around two full scale trials, one in the laboratory and one in the field. The results shown in Figs. 2.17 and 2.18 respectively show similarly good agreement with observed values. The lateral extents do seem to be overestimated by this analysis technique as a result of it not attempting to model the soil properties *per se*, and therefore not predicting failure planes within the soil mass.

Table 6.6 Comparison between the observed displacements in laboratory pipebursting tests and those predicted using the fluid flow analysis in the perpendicular plane

(a) Test PB1, close to start of bursting operation (20mm jacking distance)

COORDINATE (from pipe axis) (m)	LABORATORY TEST RESULT (mm)		THEORETICAL ANALYSIS RESULT (mm)	
	V	H	V	H
Centreline above pipe axis				
0.10	3.50	0.00	3.42	0.00
0.15	3.30	0.00	2.70	0.00
0.20	3.10	0.00	2.30	0.00
0.30	2.50	0.00	1.90	0.00
0.40	1.90	0.00	1.70	0.00
0.50	1.75	0.00	1.65	0.00
0.1,0.1	2.10	1.00	1.80	1.30
0.2,0.2	1.45	0.55	1.10	0.80
0.3,0.3	0.50	0.13	0.70	0.30
Surface values (from centreline)				
0.00	1.75	0.00	1.65	0.00
0.10	1.50	0.60	1.60	0.00
0.20	1.10	1.00	1.40	0.00
0.30	0.50	1.00	1.00	0.00
0.40	0.00	0.00	0.60	0.00
0.50	0.00	0.00	0.40	0.00
0.60	0.00	0.00	0.20	0.00
0.70	0.00	0.00	0.10	0.00
0.80	0.00	0.00	0.00	0.00

Note: Positive values indicate vertical movements are upwards and horizontal movements are to the right.

Table 6.6 Comparison between the observed displacements in laboratory pipebursting tests and those predicted using the fluid flow analysis in the perpendicular plane, continued

(b) Test PB1, total movements at the end of the bursting operation

COORDINATE (from pipe axis) (m)	LABORATORY TEST RESULT (mm)		THEORETICAL ANALYSIS RESULT (mm)	
	V	H	V	H
Centreline above pipe axis				
0.15	44.00	0.00	40.90	0.00
0.20	41.50	0.00	32.60	0.00
0.25	38.00	0.00	27.80	0.00
0.30	35.00	0.00	24.90	0.00
0.35	32.00	0.00	22.90	0.00
0.40	28.00	0.00	21.80	0.00
0.45	24.00	0.00	21.10	0.00
0.50	21.00	0.00	20.90	0.00
0.1,0.1	40.00	7.50	30.10	15.00
0.2,0.2	20.00	5.00	15.50	9.30
0.3,0.3	13.00	4.00	12.10	5.00
0.0,0.2	-0.80	12.00	-1.50	10.50
-0.1,0.2	-3.50	1.00	-4.20	1.50
Surface values (from centreline)				
0.0	21.00	0.00	20.90	0.00
0.1	18.00	3.00	19.00	0.00
0.2	15.00	5.00	17.10	0.00
0.3	12.00	5.00	13.90	0.00
0.4	8.00	5.00	10.90	0.00
0.5	4.00	2.00	8.50	0.00
0.6	0.00	0.00	5.60	0.00
0.7	0.00	0.00	3.20	0.00
0.8	0.00	0.00	2.10	0.00
0.9	0.00	0.00	1.30	0.00
1.0	0.00	0.00	0.00	0.00

Note: Positive values indicate vertical movements are upwards and horizontal movements are to the right.

Table 6.6 Comparison between the observed displacements in laboratory pipebursting tests and those predicted using the fluid flow analysis in the perpendicular plane, continued

(c) Test PB3, total movements at the end of the bursting operation

COORDINATE (from pipe axis) (m)	LABORATORY TEST RESULT (mm)		THEORETICAL ANALYSIS RESULT (mm)	
	V	H	V	H
Centreline values above pipe axis				
0.15	32.00	0.00	32.00	0.00
0.20	25.00	0.00	15.00	0.00
0.25	18.00	0.00	8.50	0.00
0.30	13.00	0.00	5.50	0.00
0.35	9.00	0.00	4.00	0.00
0.40	6.50	0.00	3.10	0.00
0.45	3.50	0.00	2.70	0.00
0.50	2.50	0.00	2.60	0.00
0.1,0.1	23.00	8.00	21.00	12.00
0.2,0.2	6.00	2.00	4.00	3.00
0.3,0.3	1.00	1.00	1.40	1.00
-0.05,0.1	-4.00	5.00	-2.50	3.50
Surface values (from centreline)				
0.0	2.50	0.00	2.60	0.00
0.1	1.75	2.50	2.30	0.00
0.2	1.00	2.50	1.80	0.00
0.3	0.30	1.00	1.20	0.00
0.4	0.00	0.00	0.80	0.00
0.5	0.00	0.00	0.45	0.00
0.6	0.00	0.00	0.30	0.00
0.7	0.00	0.00	0.10	0.00
0.8	0.00	0.00	0.00	0.00

Note: Positive values indicate vertical movements are upwards and horizontal movements are to the right.

6.3.5 Pipebursting Tests - Longitudinal Plane

The analysis developed for predicting the ground movements associated with pipebursting in the longitudinal plane, is quite comprehensive. It is able to model both the upwards movements directly over the burster and also the effects of the overburst. It is also capable of modelling the interaction of these two areas of movement. Draw-along effects are not modelled, although as for the pipejacking analysis in the longitudinal plane, the model nevertheless appears to predict the movements at the overburst quite well. The model uses two separate analyses for the two areas of movement, one over the burster and one at the overburst, which are then combined to give the full displacement pattern. The development of the analysis is shown in Fig. 6.12.

The first problem when trying to model the movements over the burster head are that they are spread along a finite length rather than a point source, which is a requirement when using the fluid flow model. However, as shown, a simulation of movement along a length can be made using a point source at the centre of the pipe/burster interface (position 1 on Fig. 6.12). Using R as the radius of an imaginary pipe and a δR value which varies from zero at the springing of the imaginary pipe to a maximum value at the crown, the movements generated simulate those observed in the laboratory tests (i.e. there is not a uniform movement above the bursting head due to the horizontal movement effects; instead the vertical movements tend to decrease towards the latest part of the old pipe to be broken out). The movements generated by the fluid flow analysis which are within the area occupied by the bursting head are taken as zero.

The prediction of the movements at the overburst (position 2 in Fig. 6.12) uses exactly the same model as that developed for prediction of the overcut movements during the pipejacking tests (Fig. 6.8). Area 3 in Fig. 6.12 is where overlap occurs between the movements generated by the two analyses. The movements in this area are summed together. As the movements from analysis 1 are predominantly upward and those from analysis 2 are predominantly downward, combining the two helps to develop the circular pattern of movements observed in the actual model tests above the overburst.

Two examples are presented to demonstrate the application of the above analysis to the pipebursting laboratory test results. Figs 6.13 and 6.14 show the displacement patterns obtained for a dense state analysis and a loose state analysis respectively, with a C/D ratio of 1.2 and a 20mm forward jacking distance. These can be compared with those observed in the corresponding physical model tests PB1 and PB3 (Figs. 5.35 and 5.36). Tables 6.7a and b present a direct comparison between the predicted and observed sand displacements. Generally the results for both the patterns of movements and the magnitudes of the movements can be seen to compare very favourably. However, as for the other models, no prediction of the horizontal surface movements is made. The surface extents seem to be predicted relatively well using this analysis, as are the directions and magnitudes of the subsurface movements.

6.4 GENERAL DISCUSSION OF THE ANALYSIS TECHNIQUES AND FUTURE DEVELOPMENTS

It is quite clear from the results presented in the previous sections that the fluid flow analysis technique is versatile and relatively simple to apply to a wide range of situations. It is also shown to be surprisingly good at predicting the displacements of both loose and dense state sand observed during the laboratory test simulations of both pipejacking and pipebursting operations. The real power of the technique is the ability to summate flows from any number of sinks or sources in order to simulate a particular situation that may be quite complex.

The prediction of the lateral extent of the movements in the perpendicular plane for a pipebursting operation in sand, presented by Swee and Milligan (1990), could be incorporated into the pipebursting analysis presented in Section 6.3.4. As shown, the lateral extent of the predicted sand displacements is too great using the fluid flow analysis. Thus a potential method of overcoming this problem is to apply the shear plane cut-off

Table 6.7 Comparison between observed displacements with those predicted by the fluid flow analysis for pipebursting tests in the longitudinal plane

(a) Test PB1 (2.6dLB1.2)

COORDINATE (m)	LABORATORY TEST RESULT (mm)		THEORETICAL ANALYSIS RESULT (mm)	
	V	H	V	H
Taken from maximum point on burster				
0.05,0.0	3.80	1.00	3.60	1.30
0.0,0.05	1.75	-0.50	2.55	-0.30
0.05,0.05	3.40	0.20	3.10	0.50
0.1,0.1	3.00	0.40	2.80	0.60
0.2,0.2	2.40	0.50	2.00	0.40
0.3,0.4	1.20	1.00	1.30	0.20
0.2,0.3	1.80	0.40	1.60	0.20
-0.05,0.05	-1.00	0.50	-0.60	0.50
-0.05,0.1	-0.30	-1.60	-0.25	-1.00
Surface values				
-0.15	0.00	0.00	0.00	0.00
-0.10	0.50	-0.60	0.00	0.00
-0.05	1.10	-1.00	0.00	0.00
0.00	1.30	-1.00	1.90	0.00
0.05	1.60	-1.00	1.80	0.00
0.10	1.80	-0.75	1.80	0.00
0.15	1.70	-0.20	1.70	0.00
0.20	1.60	0.25	1.60	0.00
0.25	1.40	0.70	1.50	0.00
0.30	1.30	1.00	1.40	0.00
0.35	0.90	1.00	1.10	0.00
0.40	0.70	1.00	1.00	0.00
0.45	0.40	1.00	0.70	0.00
0.50	0.20	0.50	0.50	0.00
0.55	0.00	0.00	0.30	0.00

Note: Positive values indicate vertical movements are upwards and horizontal movements are to the left.

Table 6.7 Comparison between observed displacements with those predicted by the fluid flow analysis for pipebursting tests in the longitudinal plane, continued

(b) Test PB3 (2.61LB1.2)

COORDINATE (m)	LABORATORY TEST RESULT (mm) V	H	THEORETICAL ANALYSIS RESULT (mm) V	H
Taken from maximum point on burster				
0.05,0	3.10	0.70	3.20	1.40
0.0,0.05	-2.00	-0.50	-1.40	-0.60
0.05,0.05	2.50	0.30	2.00	0.10
0.1,0.1	1.90	0.50	1.10	0.20
0.2,0.2	1.30	0.70	1.10	0.30
0.3,0.4	0.50	0.50	0.50	0.00
0.2,0.3	0.80	0.30	0.85	0.10
-0.05,0.05	-1.50	1.30	-1.30	1.00
-0.05,0.1	-1.75	1.20	-1.00	0.40
-0.05,0.2	-1.00	0.40	-0.80	0.20
Surface values				
-0.20	0.00	0.00	-0.40	0.00
-0.15	-0.10	0.50	-0.50	0.00
-0.10	-0.50	0.90	-0.60	0.00
-0.05	-0.80	1.00	-0.70	0.00
0.00	-1.00	1.00	-0.60	0.00
0.05	-1.00	-0.50	-0.60	0.00
0.10	-0.75	-1.00	-0.05	0.00
0.15	-0.35	-1.00	-0.40	0.00
0.20	-0.13	-0.30	-0.10	0.00
0.25	0.50	0.40	0.40	0.00
0.30	0.50	0.50	0.30	0.00
0.35	0.00	0.00	0.10	0.00

Note: Positive values indicate vertical movements are upwards and horizontal movements are to the left.

suggested by these researchers, based on the dilation angle of the sand. This would fit in quite well with the fluid flow analysis, which already requires the dilation angle to be input. The main problem with a straight addition of the cut-off, is that the surface movements would suddenly drop to zero at the cut-off point (Fig. 6.15a). This could, however, be overcome in turn by smoothing of the surface movements or by assuming a simple triangular surface profile as an approximation (Leach and Reed, 1987). These possibilities are shown in Fig. 6.15b.

If the dilation angle is not known for the soil, the fluid flow analysis can always be used by assuming an incompressible soil and using a dilation angle of zero (ψ=0).

The fluid flow analysis at this stage is a two-dimensional modelling technique requiring separate models to be used in two planes. However, Sagaseta (1987) did outline how three-dimensional displacements could be predicted, by incorporating a three-dimensional sink or source. The mathematics do become quite complex for this situation, and it would be expected that further simplifications would be required in the analysis in order to keep the three-dimensional technique simple. This would need careful assessment to see whether sensible, and accurate, results would be obtained. It would also need to be assessed whether the extra effort would yield much additional information and significantly improve the analysis.

Two simple closed form solutions have been described in this chapter. The major advantage of these analysis techniques is the fact that they require only very limited details of the insitu soil parameters. The O'Reilly and New method uses none, only requiring the nature of the soil to be input, either cohesive or non-cohesive. The fluid flow method also requires no soil parameters for the simplest incompressible analysis (ψ=0), although if the dilation angle is known for the soil the analysis can be significantly improved. The main problem with other theoretical modelling, and especially numerical modelling, such as that using finite elements, is their reliance on detailed soil parameters, which are often difficult to obtain and the accuracy of which greatly influence the final results. The analysis technique in the first place is by no means necessarily accurate, due to the approximate nature of the constitutive soil models used in the analysis. Inaccuracy in the soil parameters and constitutive models only compound the errors and inaccuracies in the physical simulation of the operation being analysed. Other researchers mentioned in the literature review have shown that the effects of these compounded errors can be significant and, therefore, for application to certain operations such as tunnelling, careful use is required.

Until the numerical analysis techniques are improved and made more user friendly, to allow quick and simple application to a particular problem, then the simple analysis techniques such as those shown in this chapter will be of value. At the very least they will always be able to provide a close first predictive analysis and allow a good indication of the likely soil displacements for a particular operation. As long as the limitations of the analysis technique are fully appreciated, which is the case with any theoretical modelling technique, then it has been shown that quite accurate results can be obtained. To further test the analysis techniques described in this Chapter more field data on ground movements obtained during trenchless operations are required. The development of the analysis technique based on the fluid flow theory is still continuing and it is hoped that several ideas still to be incorporated into the analysis will overcome some of the problems with the present analysis.

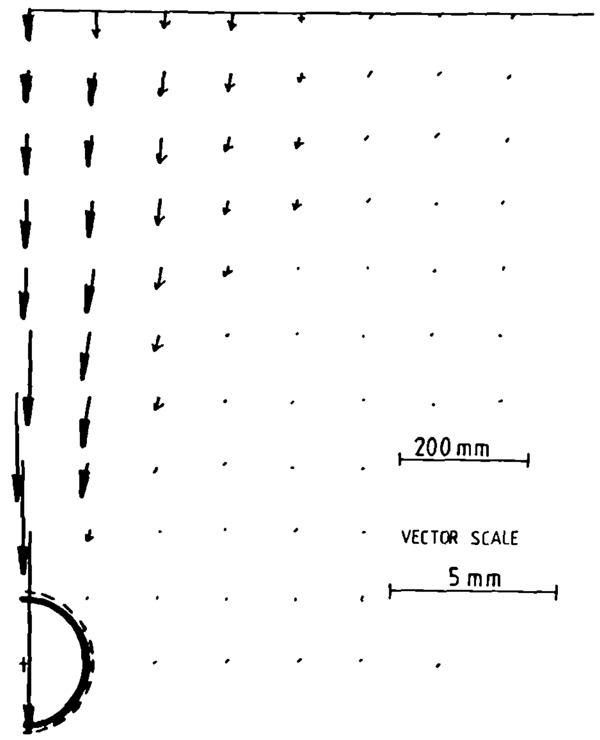

Input Parameters	Actual Data	Scaled Up Data For Analysis
Z	1.0m	5.0m
D	0.2m	1.0m
t	10mm	50mm
Soil Type	N.C.	N.C.

Fig. 6.1 Application of the error function analysis to test OPJ1

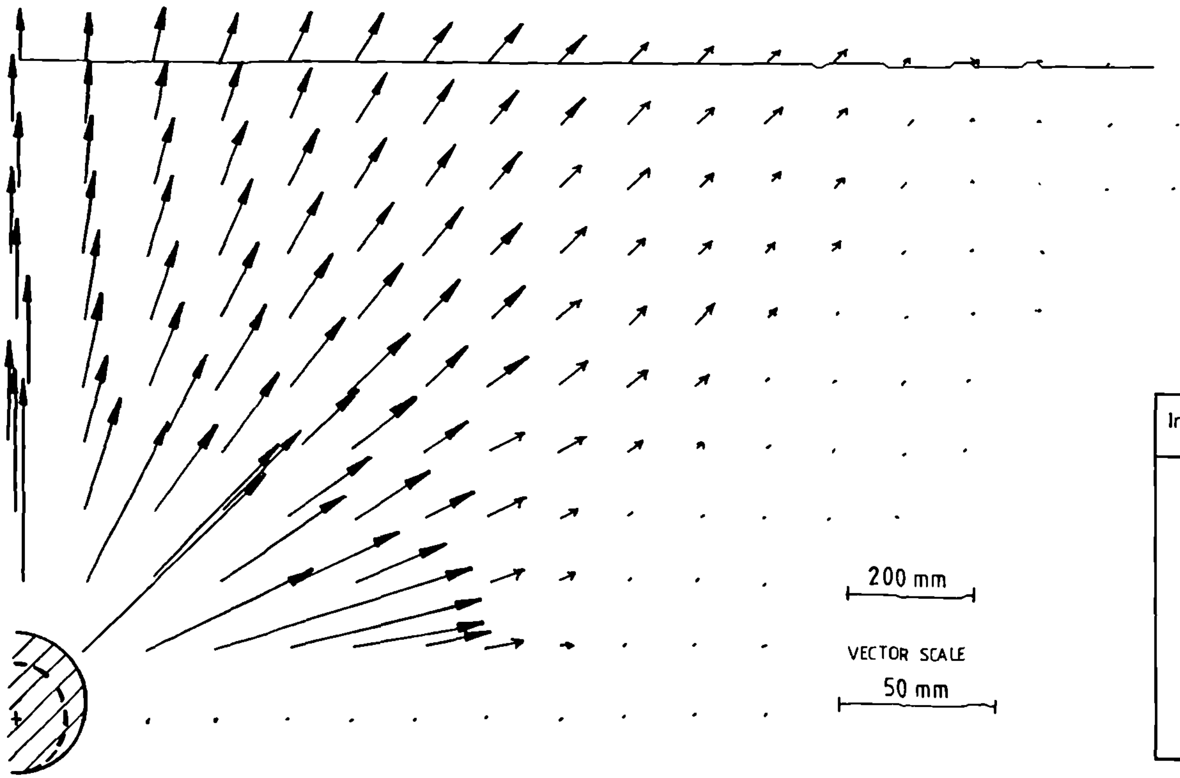

Input Parameters	Actual Data	Scaled Up Data For Analysis
Z	0.5m	5.0m
Do	0.169m	1.69m
Rf	46mm	460mm
Soil Type	N.C.	C.

Fig. 6.2 Application of the error function analysis to test PB1 (2.6dLB1.2)

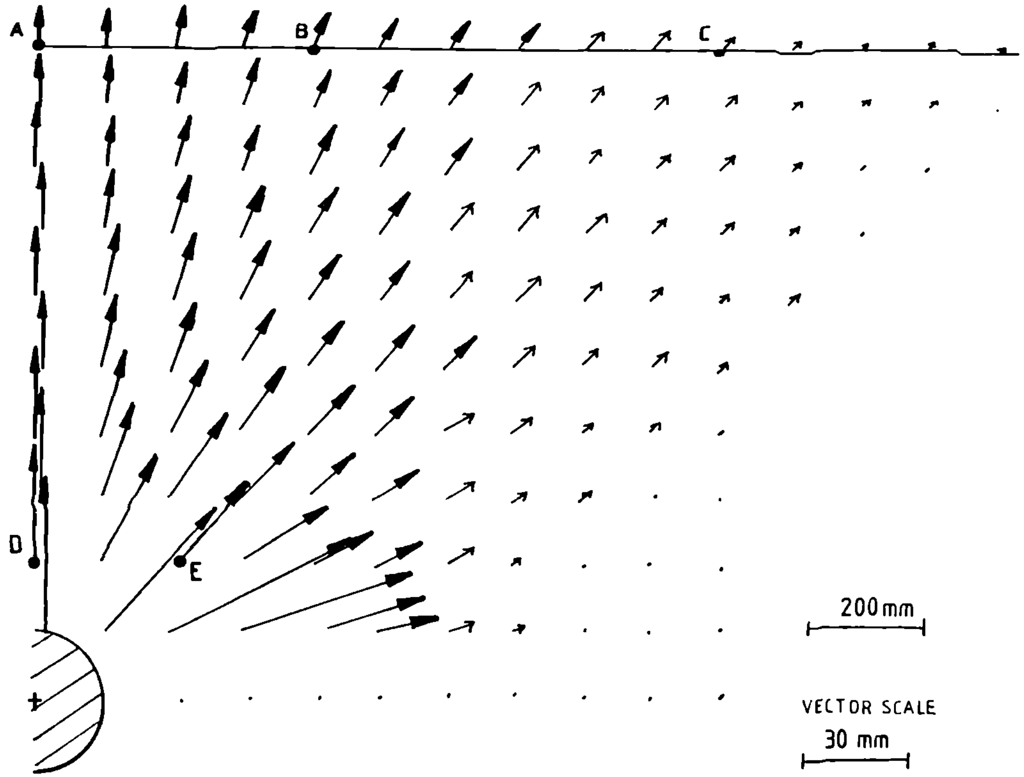

Input Parameters	Actual Data	Scaled Up Data For Analysis
Z	1.2m	6.0m
Do	0.2m	1.0m
Rf	90mm	450mm
Soil Type	C.	C.

POINT	ACTUAL	ANALYSIS
A	19	16
B	12	13
C	1	3
D	33	34
E	13	28

Fig. 6.3 Comparison between the observed ground displacements and those predicted by the error function analysis

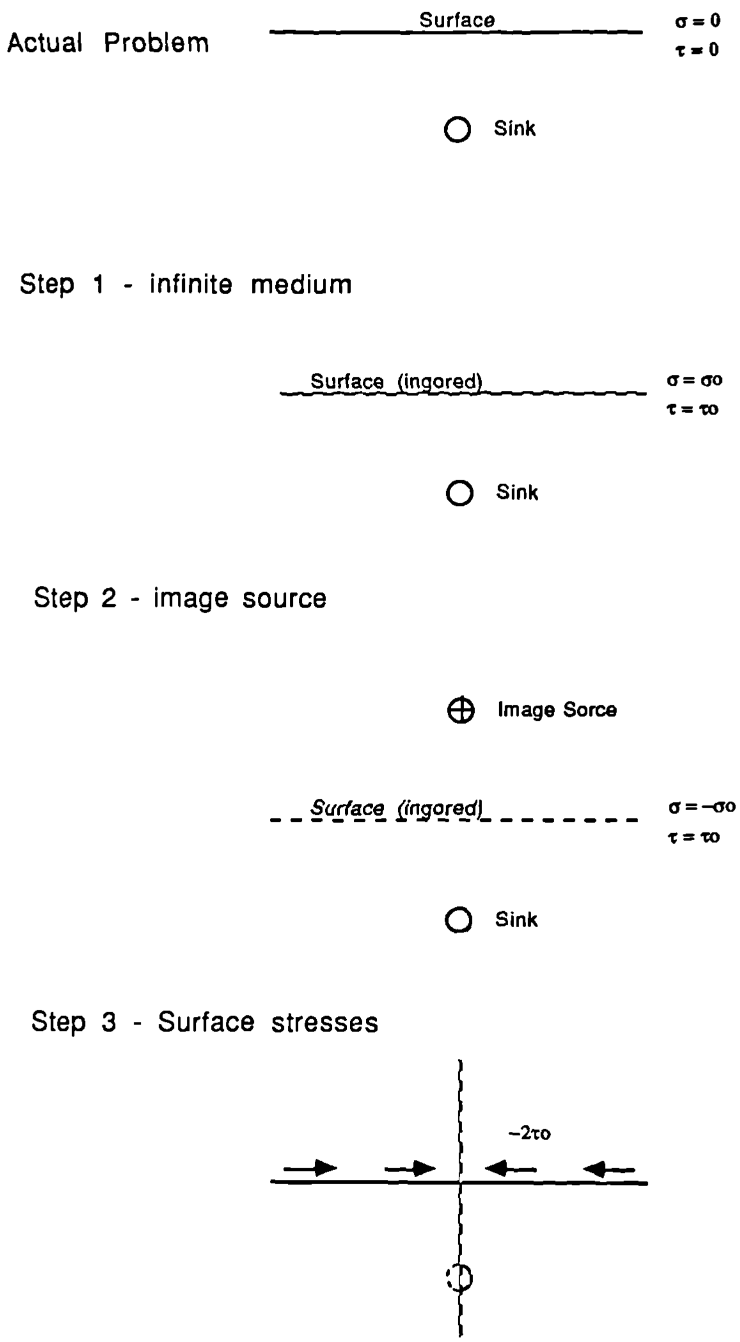

Fig. 6.4 General approach for application of the fluid flow analysis to the situation of a volume loss at a finite depth (after Sageseta (1987))

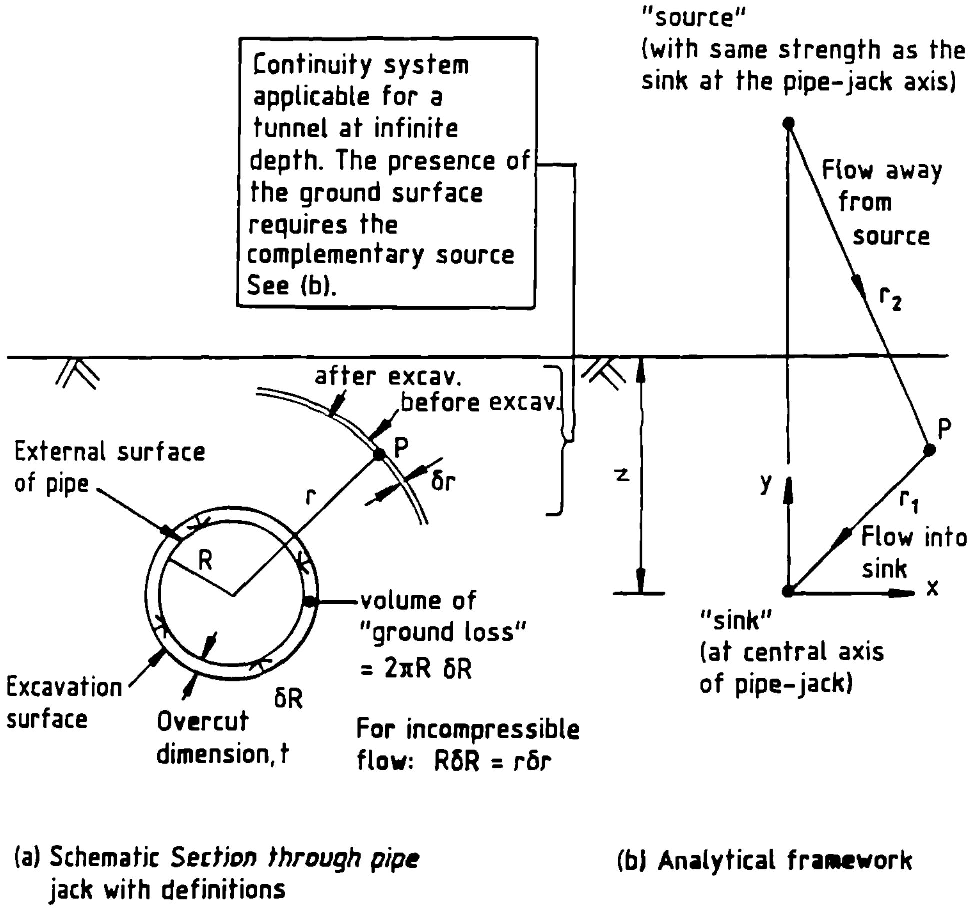

Fig. 6.5 Application of the fluid flow method to pipejacking operations (after Rogers & O'Reilly (1990))

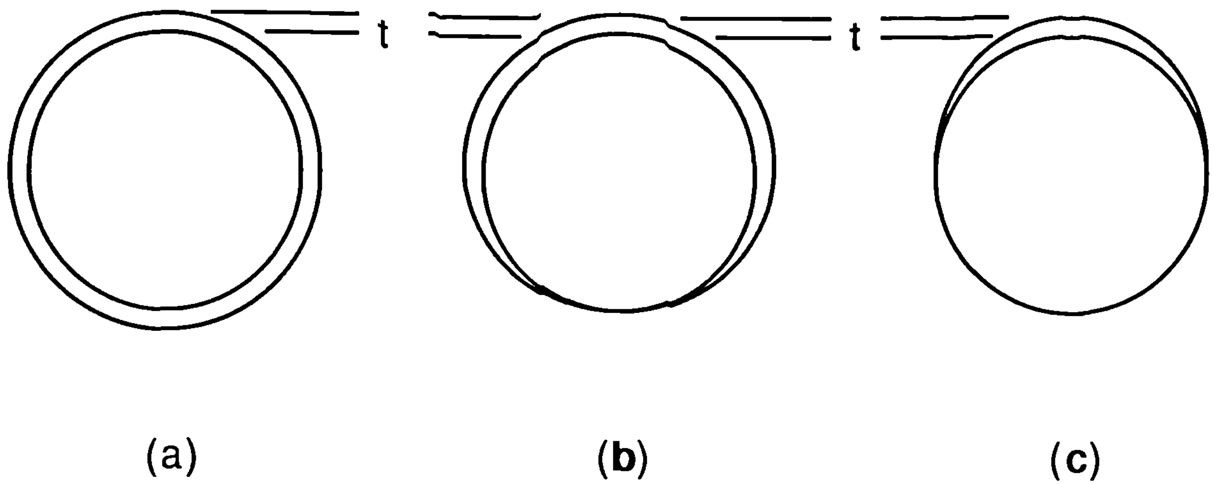

(a) Uniform

(b) Variable 1 — Zero at the pipe invert and maximum at the pipe crown

(c) Variable 2 — Zero at the pipe springings and maximum at the pipe crown

Fig. 6.6 Distribution of ground loss around the pipejack

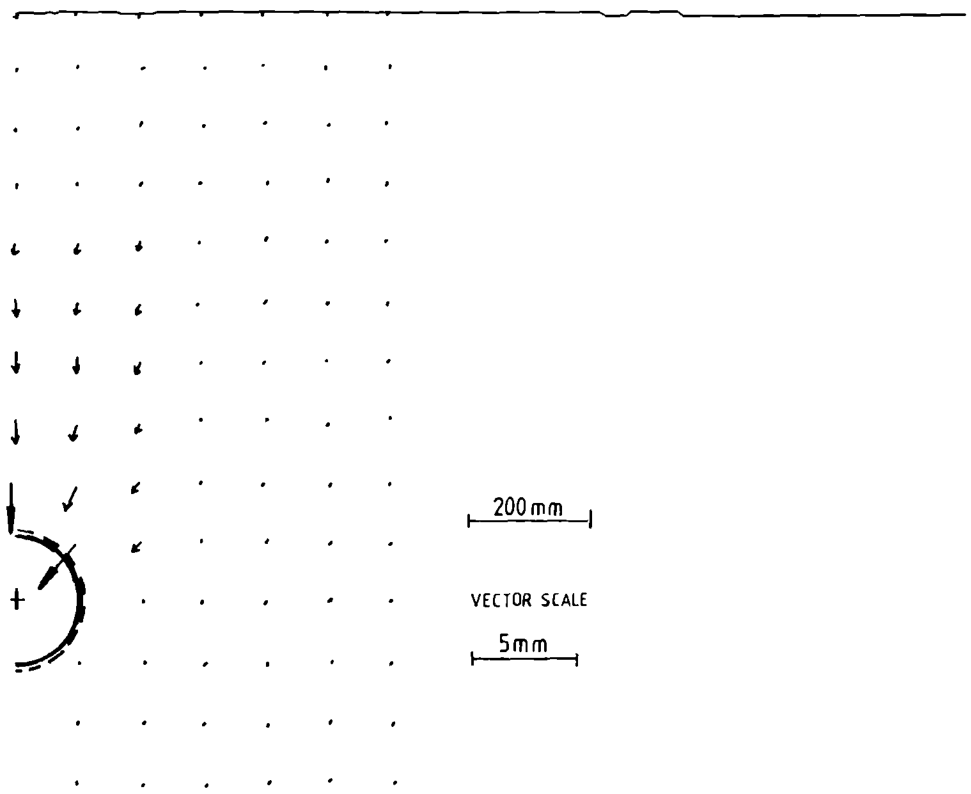

Input Parameters	Test OPJ1 Data
Z	1.0m
D	0.2m
t	10mm
Soil Density	d
Dilation Angle	17.5

(a) OPJ1 Dense state test

Fig. 6.7 Predicted vector displacements for two pipejacking laboratory tests

OPJ1 (4.5dLB0.1)

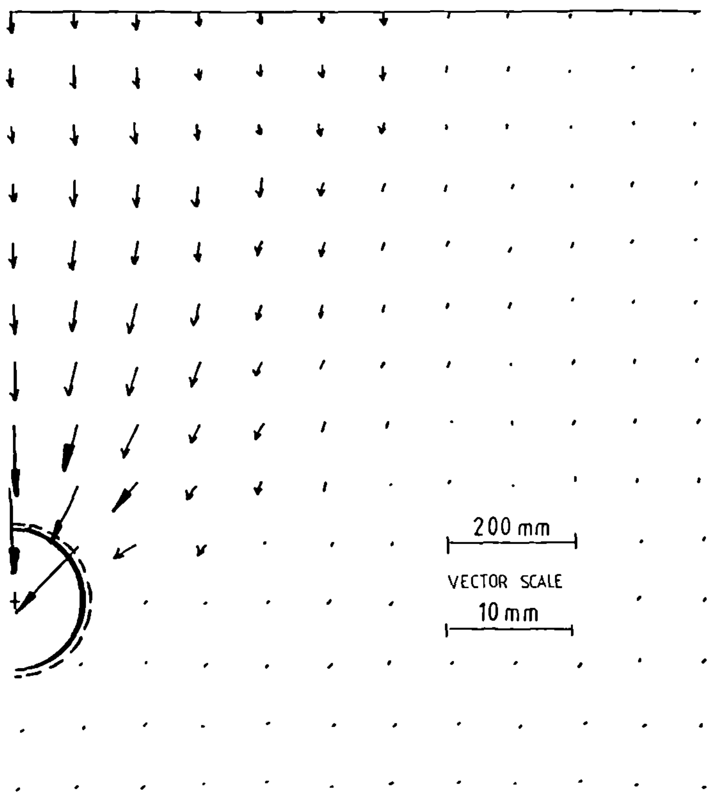

Input Parameters	Test OPJ4 Data
Z	1.0 m
D	0.2 m
t	10 mm
Soil Density	l
Dilation Angle	6

(b) OPJ4 Loose state test

Fig. 6.7 Predicted vector displacements for two pipejacking laboratory tests, continued

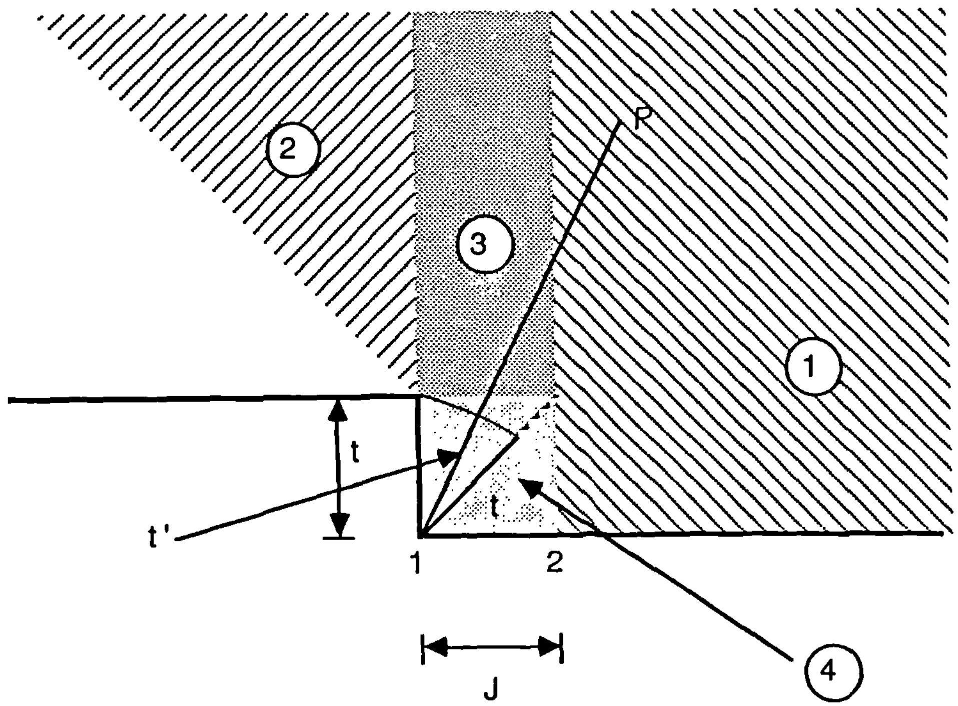

Fig. 6.8 General idea behind pipejacking model in the longitudinal plane at the overcut using the fluid flow analysis

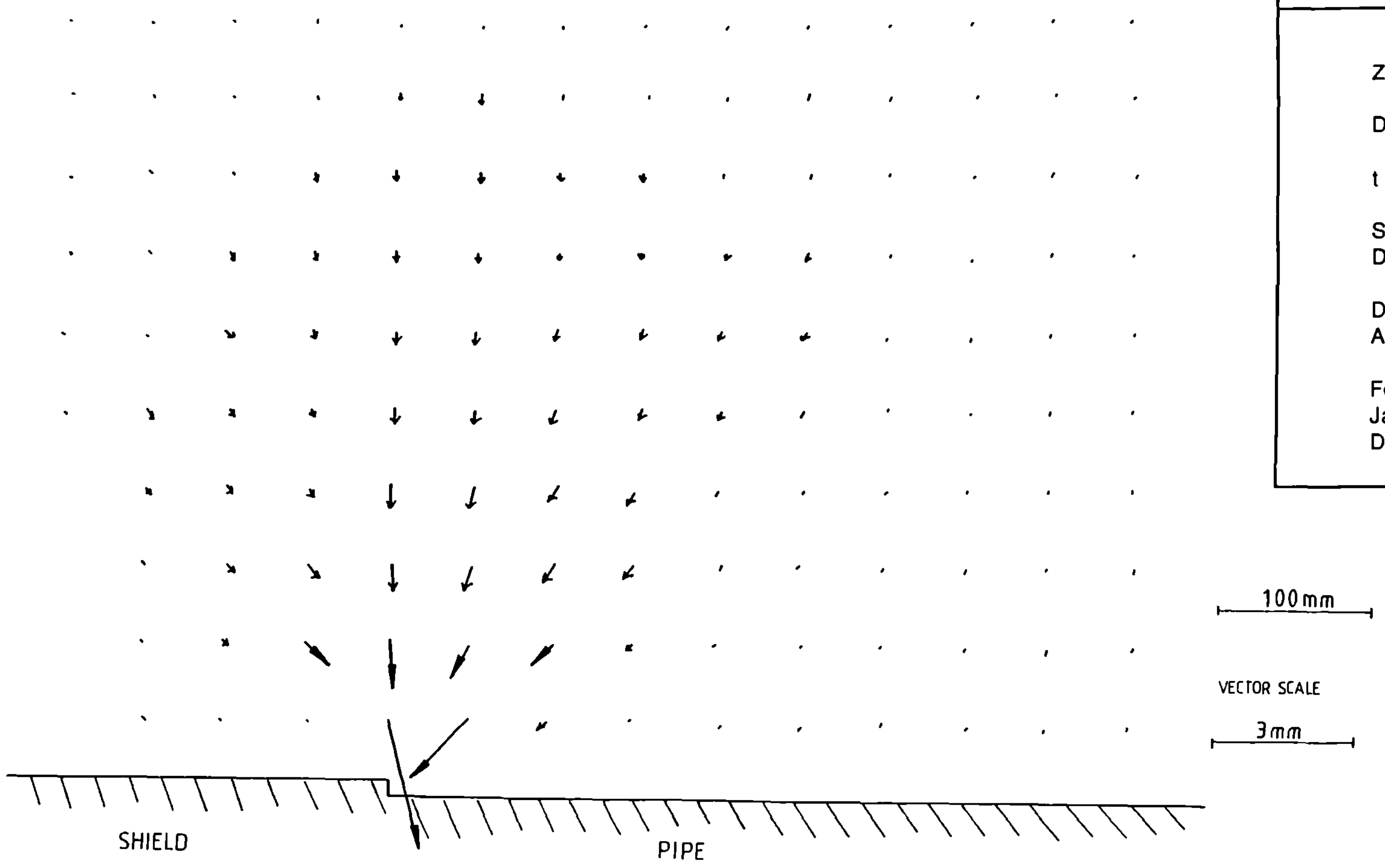

Input Parameters	Test OPJ1 Data
Z	1.0m
D	0.2m
t	10mm
Soil Density	d
Dilation Angle	17.5
Forward Jacking Distance	10mm

(a) OPJ1 Dense state test

Fig. 6.9 Predicted displacement vectors using the fluid flow analysis for two pipejacking tests in the longitudinal plane at the overcut

Input Parameters	Test OPJ4 Data
Z	1.0m
D	0.2m
t	10mm
Soil Density	I
Dilation Angle	6
Forward Jacking Distance	10mm

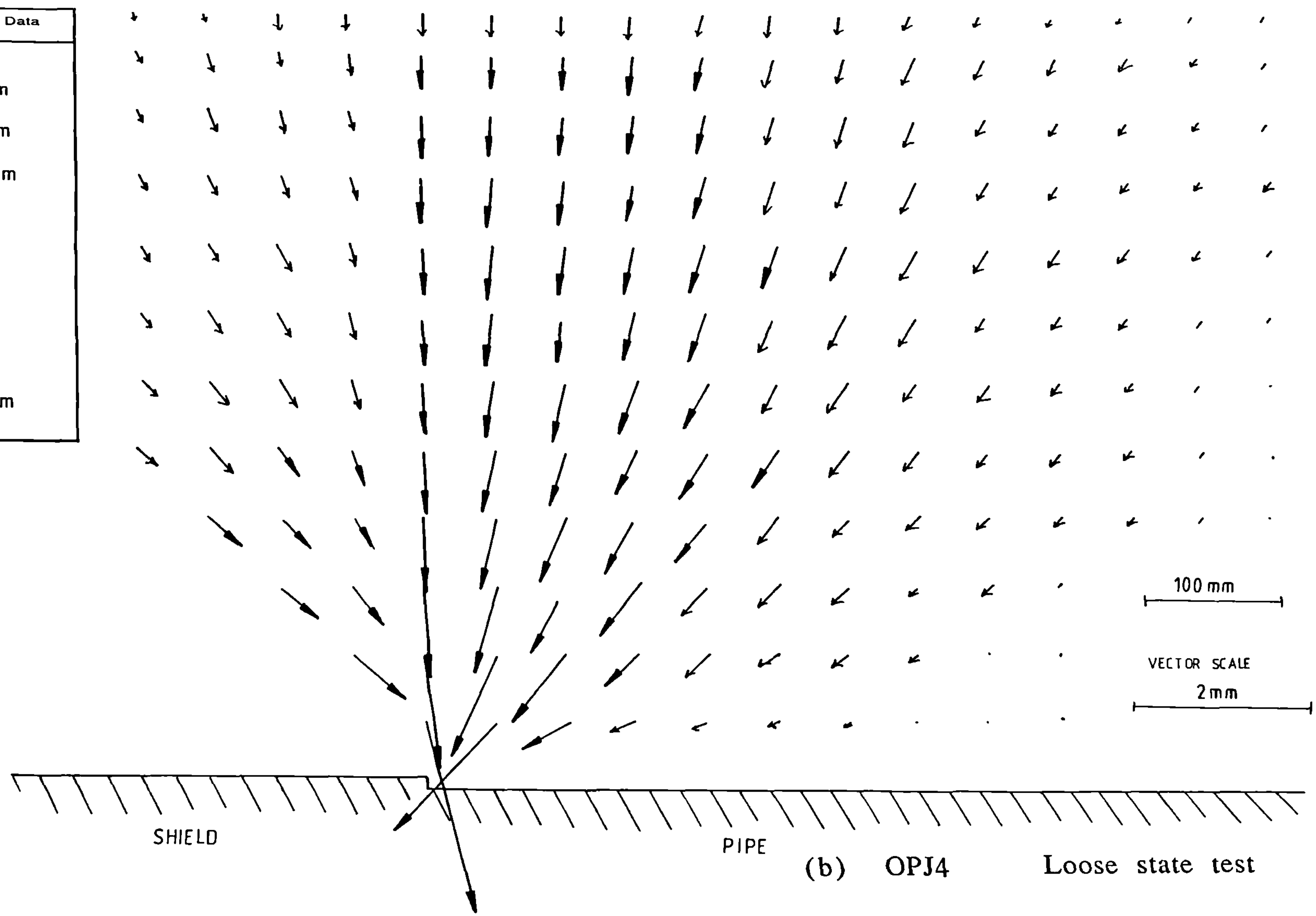

(b) OPJ4 Loose state test

Fig. 6.9 Predicted displacement vectors using the fluid flow analysis for two pipejacking tests in the longitudinal plane at the overcut, continued

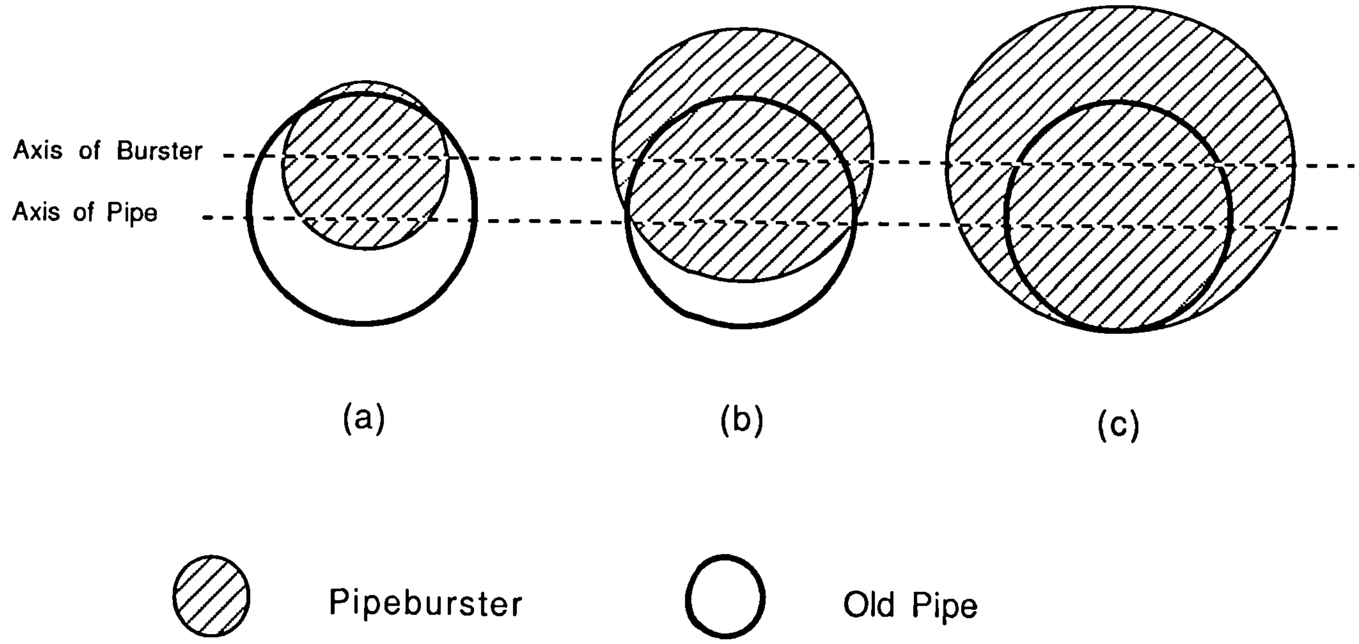

Fig. 6.10 Gradual breaking out of the old pipe is simulated in the analysis

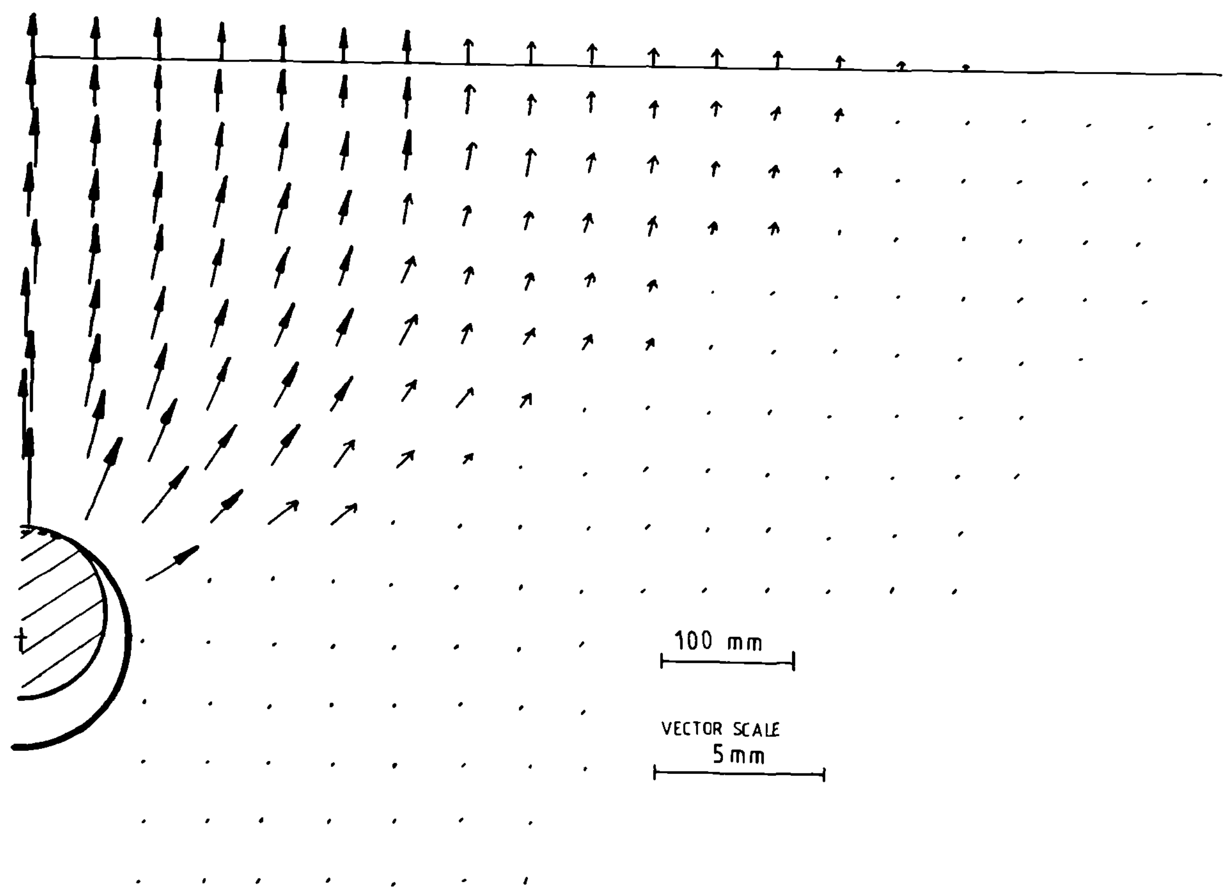

Input Parameters	Test PB1 Data Start of Burst
Z	0.52m
Do	0.169m
Df	0.21m
Rf	4mm
Soil Density	d
Dilation Angle	17.5

(a) PB1 (Close to start of expansion)

Fig. 6.11 Predicted displacement vectors using the fluid flow analysis for pipebursting tests in the perpendicular plane

PB1 (2.6dLB1.2)

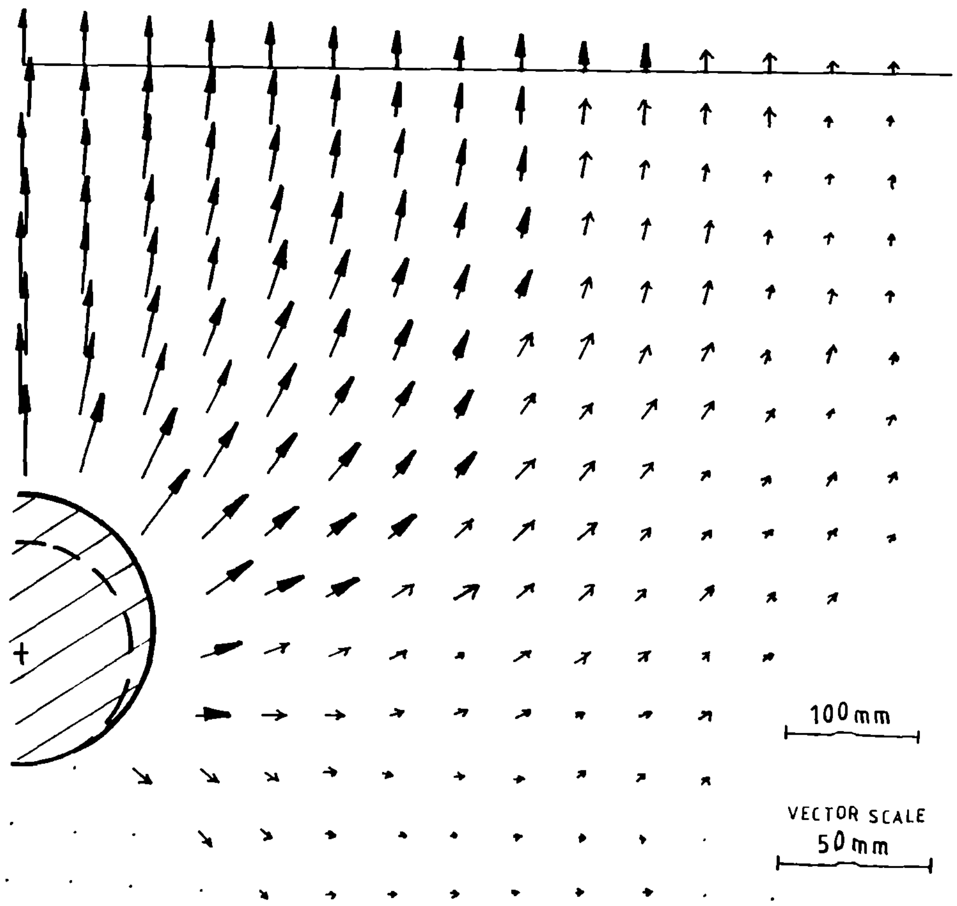

Input Parameters	Test PB1 Data End of Burst
Z	0.52m
Do	0.169m
Df	0.21m
Rf	46mm (4mm Stages)
Soil Density	d
Dilation Angle	17.5

(b) PB1 (At full expansion)

Fig. 6.11 Predicted displacement vectors using the fluid flow analysis for pipebursting tests in the perpendicular plane, continued

PB1 (2.6dLB1.2)

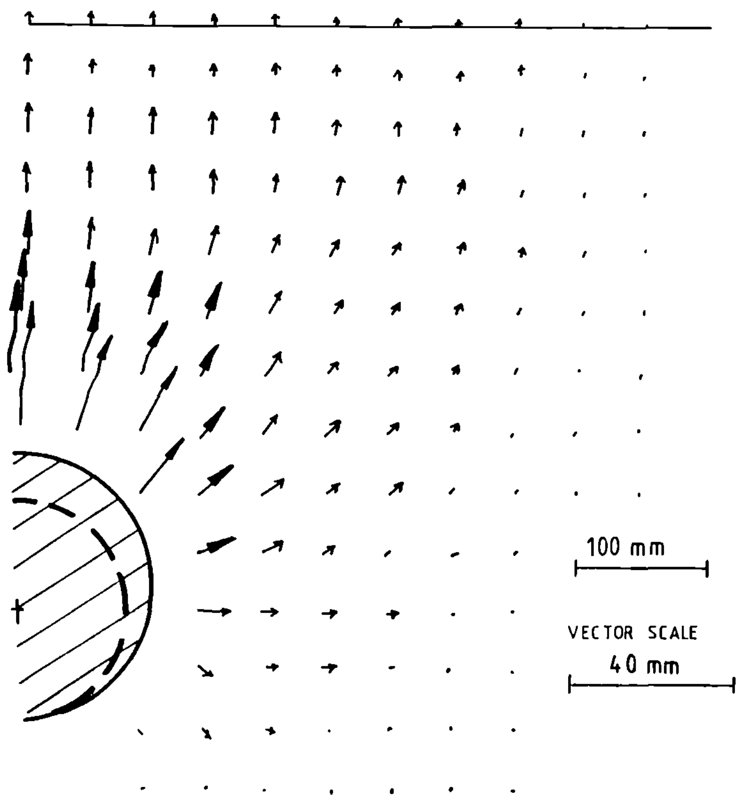

Input Parameters	Test PB3 Data End of Burst
Z	0.52m
Do	0.169m
Df	0.21m
Rf	46mm (4mm Stages)
Soil Density	I
Dilation Angle	6

(c) PB3 (At full expansion)

Fig. 6.11 Predicted displacement vectors using the fluid flow analysis for pipebursting tests in the perpendicular plane, continued

PB3 (2.61LB1.2)

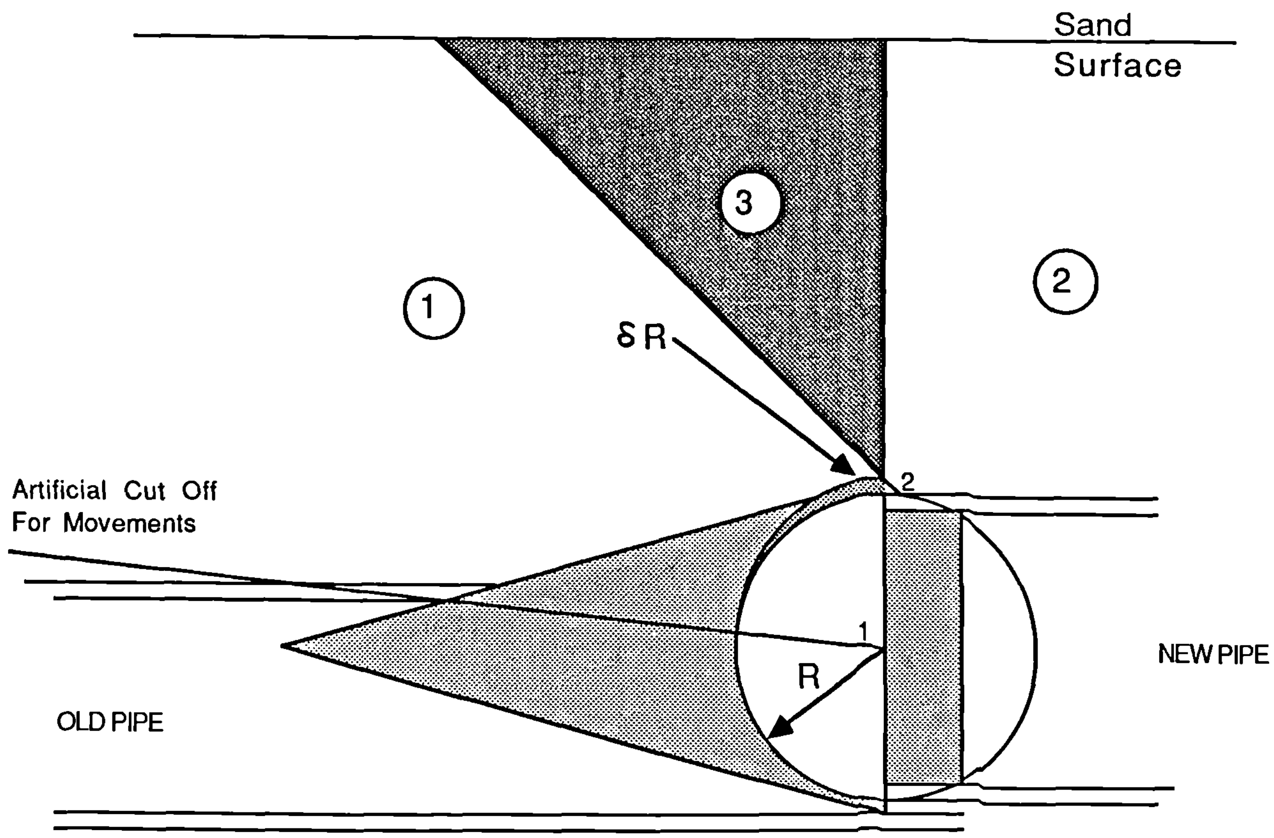

Fig. 6.12 General ideas behind the development of the fluid flow analysis for the prediction of displacements for pipebursting tests in the longitudinal plane

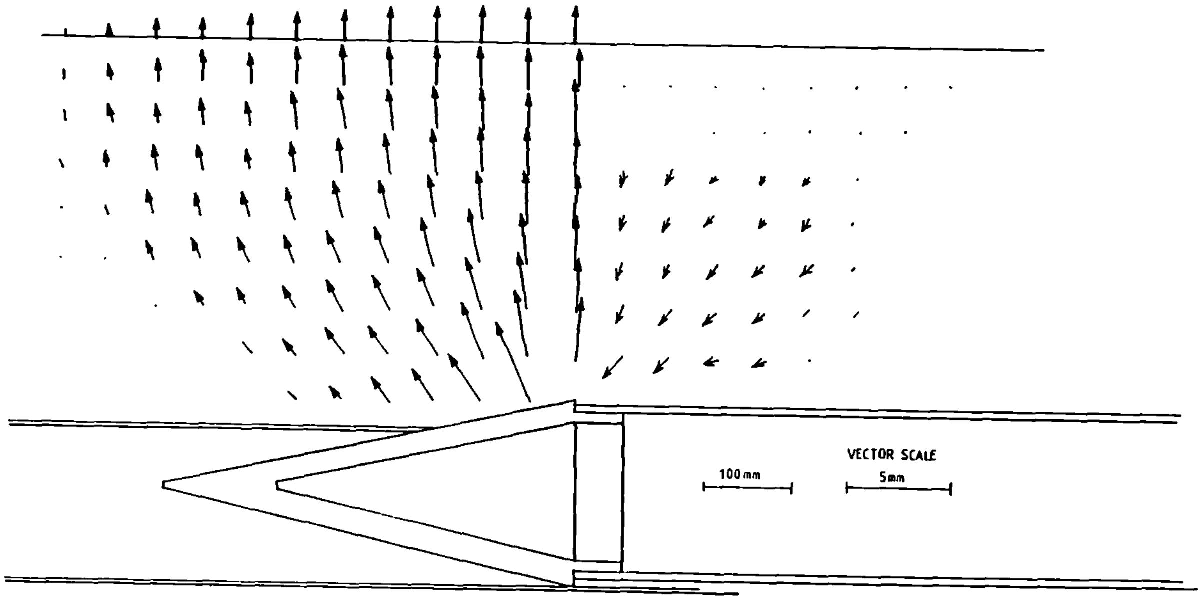

Input Parameters	Test PB1 Data End of Burst
Z	0.52 m
Do	0.169 m
Df	0.21 m
Angle of Burster	12
Forward Jacked Distance	20 mm
Soil Density	d
Dilation Angle	17.5

Fig. 6.13 Predicted displacement vectors using the fluid flow analysis for test PB1 (dense state test)

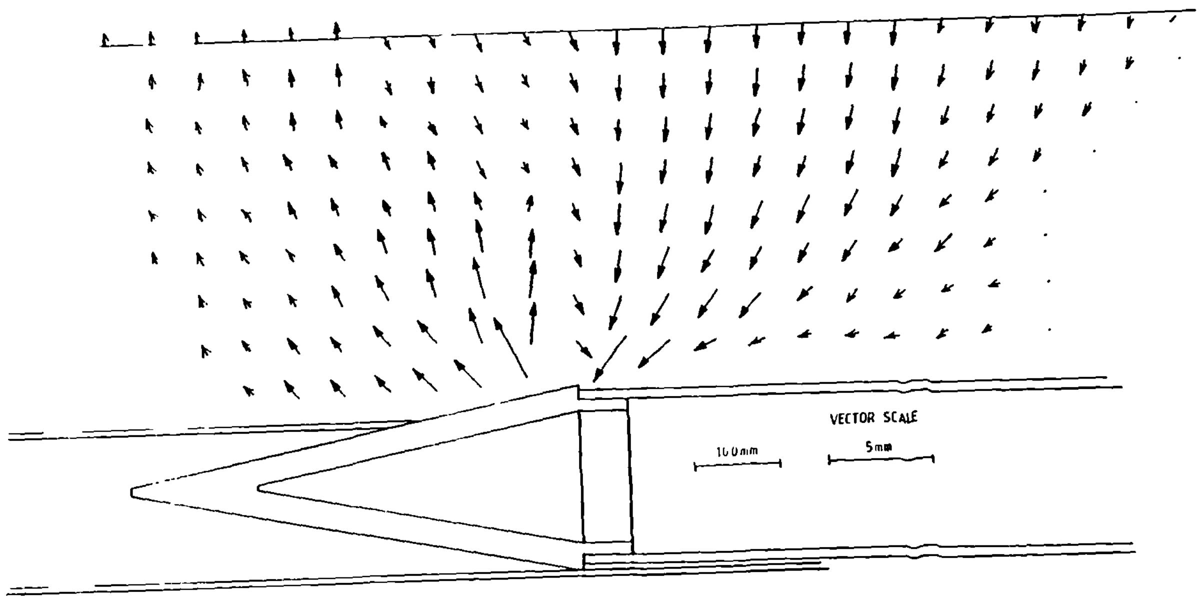

Input Parameters	Test PB1 Data End of Burst
Z	0.52m
Do	0.169m
Df	0.21m
Angle of Burster	12
Forward Jacked Distance	20mm
Soil Density	1
Dilation Angle	6

Fig. 6.14 Predicted displacement vectors using the fluid flow analysis for test PB3 (loose state test)

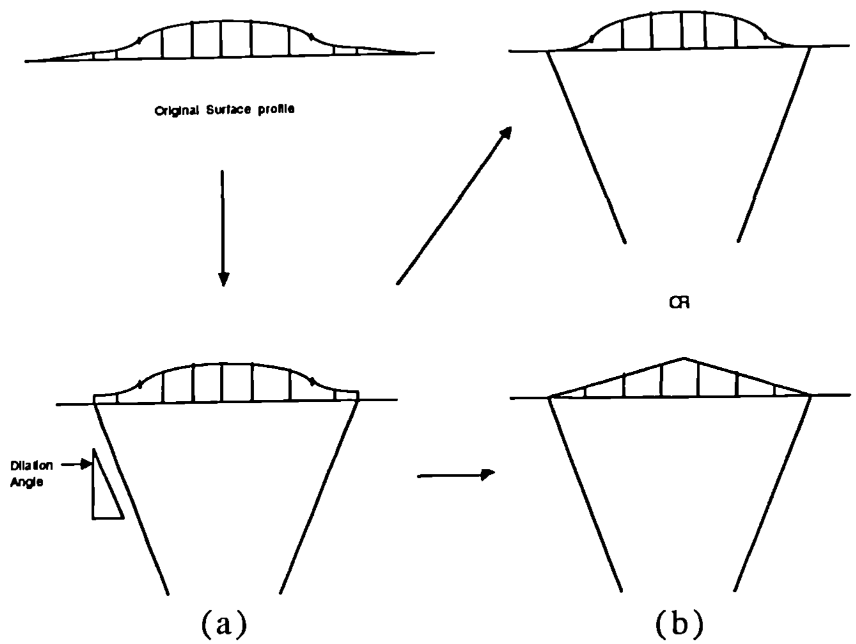

Fig. 6.15 Application of the ground movement zone based on the soil dilation angle (Swee & Milligan (1990)) during a pipebursting operation combined with the fluid flow analysis.

CHAPTER SEVEN

7 CONCLUSIONS AND RECOMMENDATIONS FOR FUTURE RESEARCH

7.1 GROUND MOVEMENTS ASSOCIATED WITH TRENCHLESS PIPELAYING TECHNIQUES

A thorough review of the literature was conducted and the need for a fundamental experimental investigation of the ground movements associated with trenchless pipelaying techniques was established. A major plane strain test facility has been developed together with appropriate modelling techniques to simulate both pipejacking and pipebursting operations. Chapter 3 and 4 have shown the considerations necessary to produce these facilities and the problems encountered. The simulation of prototype situations is not a simple task and it was found that the less complicated the simulation made (i.e. not trying to model every small detail of the prototype), the more usable and more definitive the results were. Preliminary theoretical modelling work was also undertaken, investigating the use of simple closed form solutions for predictive analysis.

The results of the laboratory tests revealed how the ground movements are influenced by all of the factors investigated, including cover depth, overcut ratio and sand type and density, and how these factors interacted with each other to alter the movement patterns produced during trenchless operations. A large proportion of this work is of a very visual nature and the interpretation of the results is largely descriptive. Wherever possible, however, the results have been used to predict ground movements obtained from other sources, with promising results. The data from other sources are very limited and it is often difficult to make simple comparisons due to many differences in parameters and/or boundary conditions. The way the results from the laboratory model tests are presented in this thesis allows investigation of the soil movements throughout the trenchless operation, rather than simply giving the resultant movements at the end. This is important as it is necessary to obtain as much information as possible, at this stage of the investigations into trenchless pipelaying operations, in order to give a more fundamental appreciation of the ground movements being caused.

The displacements observed during the forward jacking stage of the open shield pipejacking tests showed a distinct circular motion in front of, and over, the shield, and at the overcut, which caused a random area of movements to develop directly over the shield. The effect of increasing cover depth was to reduce the extents of the movements in all areas around the pipejacking operation, particularly in front of the shield. The higher stresses at the increased cover depth caused more sand to be forced into the open shield. At the overcut the higher stresses increase the arching effects within the sand, and also increases the effect of dilation in the dense state sands, causing reduced extents of the movements.

The shield has an important effect on the ground movements ahead of the pipejacking operation during the forward jacking stage. The open shield produces localised areas of contact with the soil and therefore localised maximum magnitudes of movement, whereas the closed shield (over-pressurised face) affects a greater area of soil and produces considerably greater extents of movements for the same forward jacking distance. The three test programmes (open and closed shield pipejacking and pipebursting) provide an overall picture of the effects of different face/shield arrangements. The closed shield test provides a link with the pipebursting tests and allows the effects on the ground movements of different burster angles to be predicted.

The pipebursting tests showed a high degree of upward sand movements directly over the burster as expected, and these spread in advance of the bursting operation. The extents of these movements were very dependent on the density of the sand and the cover depth, this being related to the amount of compression occurring in the sand. The sand close to the maximum expansion of the bursting unit spread backwards and tended to produce circular movement patterns at the overburst. The density of the sand had a large influence on the movements at the overburst, the loose state sand having the greatest affect and causing downwards movements that spread in advance of the overburst affecting the upwards movements directly over the busting unit.

The practical implications of the sand movements observed during the laboratory tests are presented in terms of the effects on adjacent services and structures. For the open shield pipejacking tests the effects are concentrated within approximately two-three pipe diameters of the operation, during the forward jacking stage. The loose state test movements do extend to the surface at the overcut due to the low dilation rate, although the movements are small farther than approximately four pipe diameters away from the operation. The movements associated with the pipebursting tests are very dependent on the density of the sand. The dense state tests produce the upperbound to the movements over the burster and loose state tests the upperbound to the movements at the overburst. This produces quite different curvature profiles in services running above the bursting operation. The effect of different bursting ratios (i.e. the ratio of the burster diameter to the old pipe diameter), also has an important effect on both the extents and magnitudes of the soil movements in the longitudinal and perpendicular planes to the line of the pipebursting operation. For larger bursting ratios more of the old pipe is being broken out at any moment during the operation and more of the bursting unit is exposed to the surrounding soil. This means that more soil is affected by the bursting unit and due to the greater expansion associated with a larger bursting ratio, larger movements are experienced by the soil. This has important implications for services (and structures), lying both parallel and transverse to the pipebursting operation as a greater length is affected by the soil movements and larger movements are experienced, possibly inducing potentially damaging differential movements.

Interpolation analysis in the form of graphical plots, provided an excellent way of expanding the information gained from the tests to help predict likely movement patterns caused by different combinations of the factors investigated in the laboratory tests. If the limitations of the results are understood, careful extrapolation can also be conducted with many of the factors, for example overcut ratio, to expand the range of the results still further. The link between the test results provided by the open shield pipejacking tests, the closed shield pipejacking tests and the pipebursting tests is very useful for ground movement prediction purposes. However, it must be remembered that the pipejacking tests are small scale compared to the prototype operations, although microtunnelling techniques are used down to this size, whereas the pipebursting tests are on the lower bound of the prototype operations. The improved understanding of the ground movements and the mechanisms of ground movement associated with trenchless techniques, gained though the test progammes described in the thesis, will provide a valuable basis on which to develop these techniques. It will also allow greater confidence and understanding of the effects changes in design will have on the surrounding ground.

The theoretical modelling of the laboratory results and field data, by two closed form solutions using an error function analysis and a fluid flow analysis respectively, produced good correlations between predicted and measured movements. The error function analysis is, however, restricted to the perpendicular plane and to certain types of soil, depending on the constant volume assumption. The fluid flow analysis is shown to be more versatile and has been applied to both the perpendicular and longitudinal planes for the pipejacking and pipebursting operations. The incorporation of dilation/compressibility effects into the fluid flow analysis meant that modelling the laboratory tests could also be conducted with remarkably accurate results for the densities and sand types used. There are problems with this anlaysis, for instance the over-estimation of the lateral extents of the movements particularly in the perpendicular plane, although further developments could improve this situation.

7.2 RECOMMENDATIONS FOR FUTURE WORK

The test programmes described in this thesis provide a comprehensive investigation of ground movements associated with trenchless pipelaying techniques. However, the data obtained from the tests have not been presented here in the most convenient form for practical use, simply due to the nature of this report. What is really required is for all of the data to be placed into a computer database system, which would enable both instant access to the laboratory test data and also permit interpolation and extrapolation of the results. This should be tied in with the theoretical analysis techniques and field data so that predictions of the ground movements can be made based on all the available data at one time. The system would allow the user to input the available information about the technique to be used and the site conditions. The computer system would then search the data and produce three sets of results concerning the ground movements. The first results would be based on the theoretical modelling, the second on the laboratory modelling data and the third on any field data produced under similar conditions. This will give the user information that can be used to make a judgement on the likely ground movements for the particular trenchless technique and site being considered.

The lack of field data is a fundamental barrier to the understanding of the ground movements associated with trenchless pipelaying techniques. Such data are required to provide comparisons with the laboratory results, and thereby to give more confidence when relating them to field situations and also expand the general information on these techniques. Controlled field trials in well defined ground conditions, or full scale laboratory tests, would help to enhance the available information considerably. Field data would also help the development and further testing of the theoretical models described in this thesis.

REFERENCES

Asquith J., Birkett M. and Reynard B., (1989), *Pipebursting in Yorkshire - A case study*, Proceedings of the Fourth International Conference on Trenchless Construction for Utilities, NO-DIG '89, Paper 5.3.

Atkinson J.H. and Bransby P.L., (1978), *The mechanics of soils :- An introduction to critical state soil mechanics*, University Series in Engineering, McGraw-Hill, 1978.

*1

Atkinson J.H. and Mair R.J., (1981), *Soil mechanics aspects of soft ground tunnelling*, Ground Engineering Serial, July 1981.

Atkinson J.H., and Potts D.M., (1977a), *Stability of a shallow circular tunnel in cohesionless soil*, Geotechnique 27, No. 2, pp 203-215.

Atkinson J.H. and Potts D.M., (1977b), *Subsidence above shallow tunnels in soft ground*, Journal of Geotechnical Engineering Division, ASCE, Vol. 103, GT4, pp 307-325.

Attewell P.B., (1978), *Ground movements caused by tunnelling in soil*, Proceedings for the International Conference on Large Ground Movements and Structures, Pentech Press, pp 812-948.

Attewell P.B., (1988), *An overview of site investigation and long-term tunnelling-induced settlement in soil*, Engineering Geology of Underground Movement, Proceedings of the 23rd Annual Conference of the Engineering Group of the Geotechnical Society, Nottingham, pp 55-61.

Attewell P.B. and Boden J.B., (1971), *Development of stability ratios for tunnels driven in clay*, Tunnels and Tunnelling Serial, May/June 1971, pp 195-198.

Attewell P.B., Farmer I.W. and Glossop N.H., (1978), *Ground deformation caused by tunnelling in a silty alluvial clay*, Ground Engineering Serial, November 1978, pp 32-41.

Attewell P.B., Yeates J. and Selby A.R., (1986), *Soil movements induced by tunnelling and their effects on pipelines and structures*, Blackie, 1986.

Attewell P.B. and Woodman J.P., (1982), *Predicting the Dynamics of Ground Settlement and its Derivatives caused by Tunnelling in Soil*, Ground Engineering Serial, Vol. 15, No. 8, pp 13-36.

Barratt D.A. and Tyler R.G., (1976), *Measurements of Ground Movements & Lining Behaviour on the London Underground at Regents Park*, Transport & Road Research Laboratory (TRRL) Laboratory Report No. 684.

Boden J.B. and McCaul, (1974), *Measurement of ground movements during a bentonite tunnelling experiment*, Transport & Road Research Laboratory (TRRL) Laboratory Report No. 653.

Bolton M.D., (1986), *The strength and dilatancy of sands*, Geotechnique 36, No. 1, pp 65-78.

British Standards Institute, (1990), *Methods of tests for soils for Civil Engineering purposes*, BS1377, 1990.

Broms B.B. and Bennermark H., (1967), *Stability of clay at vertical openings*, Journal of the Soil Mechanics Foundation Division, ASCE, 93, No. SM1, pp 71-94.

Burland J.B. and Wroth C.P., (1975), *Settlement of buildings and associated damage*, Building Reasearch Establishment (B.R.E.), Current Paper CP33/75.

Butterfield R., Harkness R.M. and Andrawes K.Z., (1970), *A stereo-photogrammetric method for measuring displacement fields*, Geotechnique 20, No. 3, pp 308-314.

Cairncross A.M., (1973), *Deformations around model tunnels in stiff clay*, PhD Thesis, Cambridge University.

Chambon P. and Konig D., (1991), *Face stability of shallow tunnels in granular soils*, Proceedings of the International Conference Centrifuge '91, Pub. A.A. Balkema, Rotterdam, pp 99-105.

Chapman D.N. and Rogers C.D.F., (1991), *Ground movements associated with trenchless pipelaying operations*, Proceedings of the Fourth International Conference on Ground Movements and Structures, Cardiff July 1991, Edited by J. D. Geddes, Pub. Pentech Press, pp 91-107.

Clarkson T.E. and Ropkins J.W.T., (1977), *Pipejacking applied to large structures*, Proceedings of the Institution of Civil Engineers, Vol. 62, Part 1, November 1977 , pp 539-561.

Clough G.W. and Leca E., (1989), *With focus on the use of finite element methods for soft ground tunnelling,* Proceedings of the Conference on Tunnels et Micro-Tunnels en Terrain Meuble du Chantier a la Theorie, Paris 1989, pp 531-573.

Clough G.W. and Schmidt B., (1977), Design and performance of excavations and tunnels in soft clay, State-of-the-Art Report, Proceedings of the International Symposium on Soft Clay, Bangkok, 1977.

Clough G.W., Shirasuma T. and Finno R.J., (1985), *Finite element analysis of advanced shield tunnelling*, Proceedings of the Fifth International Conference on Numerical Methods in Geomechanics, Vol. 2, pp 1167-1174.

Cole M., (1986), *2.1m diameter pipejack at Greenwich*, Pipejacking Conference 1986, International Press Centre, London, October 1986.

Cording E.J., Hansmire W.H., MacPherson W.H., Lenzini P.A. and Vonderohe A.P., (1976), *Displacements around tunnels in soil*, Report prepared by the University of Illinois for U.S. Department of Transportation, Report No. DOT-TST76T-22.

Davis E.H., (1968), *Theories of soil plasticity and the failure of soil masses*, Soil Mechanics: Selected Topics, Edited by I.K. Lee, Pub. Butterworth, pp 341-380.

Davis E.H., Gunn M.J., Mair R.J. and Senevirane H.N., (1980), *The stability of shallow tunnels and underground openings in cohesive material*, Geotechnique, 30, No.4, 1980, pp 397-416.

De Moor E.K. and Taylor R.N., (1989), *Field studies of a shallow tunnel in very soft ground at Tilbury*, Report of the research conducted under SERC Research Contract No. GR/E/43256, Geotechnical Engineering Research Centre Report GE/89/22.

De Moor E.K. and Taylor R.N., (1991), *Ground response to construction of a sewer tunnel in very soft ground*, Proceedings of the Sixth International Symposium Tunnelling '91, London, April 1991, Institution of Mining & Metallurgy, Elsevier Applied Science, pp 43-54.

Eisenstein Z., El-Nahhas F. and Thomson S., (1981), *Strain field around a tunnel in stiff soil*, Proceedings of the Tenth International Conference on Soil Mechanics and Foundation Engineering, Stockholm 1981, Vol. 1, Session 2 : Tunnelling in Soils, pp 283-288.

El-Nahhas F., (1980), *The behaviour of tunnels in stiff soil*, PhD Thesis, The University of Alberta.

Gibson R.E. and Anderson W.F., (1961), *In-situ measurement of soil properties with the pressure-meter*, Civil Engineering and Public Works Review, No. 56, 658, 1961, pp 615-618.

Glossop N.H., (1977), *Soil Deformations caused by Soft Ground Tunnelling*, PhD Thesis, Durham University.

Hansmire W.H., (1975), *Field measurements of ground displacements about a tunnel in soil*, PhD Thesis, University of Illinois.

Herbert R. and Leach G., (1990), *Damage control procedures for distribution mains*, Presented at the 56th Autumn Meeting of the Institution of Gas Engineers, London, November 1990, IGE Communication No. 1437, Report No. E748.

Heurer R.E., (1976), *Catastrophic ground loss in soft ground tunnels*, Proceedings to the Rapid Excavation and Tunnelling Conference, Las Vegas, June 1976, pp 265-290.

Howe M. and Hunter P., (1985), *Trenchless mainlaying within British Gas*, Proceedings of the First International Conference on Trenchless Construction for Utilities, NO-DIG '85, April 1985, pp 43-50.

Howland A.F., (1980), *The Prediction of the Settlement Above Soft Ground Tunnels by considering the Groundwater Response with the Aid of Flow Net Constructions*, Proceedings of the Second International Conference on Ground Movements & Structures, Edited by Geddes J.D., Pub. Pentech Press, pp 345-378.

Hurrell M.R., (1984), *The empirical prediction of long-term surface settlements above shield-driven tunnels in soil*, Proceedings of the Third International Conference on Ground Movements & Structures, Cardiff, July 1984, Edited by Geddes J.D., Pub. Pentech Press, London, pp 161-170.

Iliffe A. and Spedding A., (1990), *Bursting update - case study of U.K.'s largest moling contract*, Proceedings of the 5th International Conference on Trenchless Construction for Utilities, NO-DIG'90, Rotterdam, Paper D2.

Lanz B., (1973), *Pipe Jacking*, Tunnels and Tunnelling, Vol. 5, March 1973, pp165-174.

Leach G. and Reed K., (1989), *Observations and Assessment of the Disturbance caused by Displacement Methods of Trenchless Construction*, Proceedings for the Fourth International Conference on Trenchless Construction for Utilities, London, NO-DIG '89, Paper 2.4.

Litwiniszyn J., (1956), *Application of the equations of stochastic processes to the mechanics of loose bodies*, Archiwum Mechaniki Stosowanej, Warsaw, Poland, Vol. 8, No. 4, pp 393-411.

Mair R.J., (1979), *Centrifugal modelling of tunnel construction in soft clay*, PhD Thesis, Cambridge University.

Mair R.J., (1992), *Recent developments in geotechnical research: Application to tunnels and deep excavations*, Institution of Civil Engineers, Unwin Memorial Lecture 1992, March 1992, (to be published).

Martos F., (1958), *Concerning an approximate equation of the subsidence trough and its true factor*, Proceedings of the International Strata Control Congress, Leipzig, 1958, pp 191-205.

McCaul C., (1978), *Settlements caused by tunnelling in weak ground at Stockton-on-Tees*, Department of the Environment & Department of Transport, TRRL Report SR383.

McCaul C. and O'Reilly M.P., (1987), *Ground movement caused by compressed air tunnelling in boulder clay*, Tunnels & Tunnelling, June 1987, pp 37-42.

Microtunnelling, (1987), *Pipebursting*, Microtunnelling Serial, Spring 1987, pp 20-29.

New B.M. and O'Reilly M.P., (1991), *Tunnelling induced ground movements: predicting their magnitudes and effects*, Proceedings of the Fourth International Conference on Ground Movements and Strucures, Cardiff, July 1991, Edited by J. D. Geddes, Pub. Pentech Press, pp 671-697.

Noden W.R., (1987), *Effects of moling on trafic and road structure during a sewer renovation contract in Oxford*, Proceedings of the Second International Conference on Trenchless Construction for Utilities, NO-DIG '87, Paper 5.4.

Norgrove W.B., Cooper I. and Attewell P.B., (1979), *Site investigation procedures adopted for the Northumbrian Water Authorities Tynside Sewerage Scheme, with special reference to settlement prediction when tunnelling through urban areas*, Proceeding of the Conference Tunnelling '79, Edited by M.J. Jones, Institution of Mining and Metallurgy, London, pp 79-104.

O'Reilly M.P., Mair R.J. and Aidermen G.H., (1991), *Long term settlements over tunnels : an eleven year study at Grimsby*, Proceedings of the Sixth International Symposium Tunnelling '91, Institution of Mining and Metallurgy,London, April 1991, Pub. Elsevier Applied Science, pp 55-64.

O'Reilly M.P. and New B.M., (1982), *Settlements above tunnels in the United Kingdom - their magnitude and prediction*, Proceedings of the Conference Tunnelling '82, Institution of Mining and Metallurgy, London, Edited by M.J. Jones, pp 173-181.

O'Reilly M.P. and Rogers C.D.F., (1990), *Ground movements asociated with pipejacking and trenching*, Proceedings of the Fifth International Conference on Trenchless Construction for Utilities, NO-DIG'90, Paper B1.

O'Rourke T.D., (1985), *Ground movements caused by trenchless construction*, Proceedings of the First International Conference on Trenchless Construction for Utilites, NO-DIG '85, April 1985, London, pp 51-63.

Orr T.L.L., (1976), *The behaviour of lined and unlined model tunnels in stiff clays*, PhD Thesis, Cambridge University.

Owen R.C., (1984), *Observations of the Effects of Shallow Tunnels on Buried Services*, British Gas Publication.

Peck R.B., (1969), *Deep excavations and tunnelling in soft ground*, Proceedings of the Seventh International Conference on Soil Mechanics & Foundation Engineering, State-of-the-Art Volume, Mexico City, 1969, pp 225-290.

Pipe Jacking Asociation (1984), *Case Histories in Pipe Jacking.*

Polshin D.E. and Tokar R.A., (1957), *Maximum allowable non-uniform settlement of structures*, Proceedings of the Fourth International Conference on Soil Mechanics & Foundation Engineering, London, Vol. 1, pp 402-405.

Poole A.G., Roosbrook R.B. and Reynolds J.H., (1985), *Replacement of small-diameter pipes by pipe bursting*, Proceedings of the First International Conference on Trenchless Construction for Utilities, NO-DIG '85, April 1985, London, pp 147-159.

Potts D.M., (1976), *Behaviour of lined and unlined tunnels in sand*, PhD Thesis, Cambridge University.

Poulos H.G. and Davis E.H., (1980), *Pile foundation analysis and design*, Pub. John Wiley & Sons.

Reed K., (1987), *The application of moling techniques in the water industry*, Proceedings of the Second International Conference on Trenchless Construction for Utilities, NO-DIG '87, London, Paper 2.2.

Robins P.J., Rogers C.D.F. and Scott A.M., (1990), *Design and development of ductile iron pipes for use with pipe bursting*, Proceedings of the Conference Pipeline Management '90, London, pp 4.1-4.13.

Rogers C.D.F., O'Reilly M..P. and Atkin R., (1989), *Pipe jacking beneath Burnham-on-Sea : A case history*, Proceedings of the Second International Conference on Foundations & Tunnels '89, Pub. Engineering Technics Press, pp 51-56.

Rogers C.D.F. and O'Reilly M.P., (1991), *Ground movements associated with pipe installation and tunnelling*, Proceedings of the Tenth European Conference on Soil Mechanics and Foundation Engineering, Florence, May 1991, Pub. A.A. Balkema, Rotterdam, Vol. 2, pp 907-910.

Rogers C.D.F., Robins P.J. and Scott A.M., (1991), *Field performance of a new ductile iron pipe for use with pipe bursting*, Proceedings of the Seventh International Conference on Trenchless Construction for Utilities, NO-DIG '91, Hamburg, October 1991, pp 663-670.

Romo M.P. and Diaz M.C., (1981), *Face stability and ground settlements in shield tunnelling*, Proceedings of the Tenth International Conference on Soil Mechanics & Foundations Engineering, Stockholm, 1981, Vol. 1, Session 2 : Tunnelling in Soils, Pub. A.A. Balkema, Rotterdam, pp 357-360.

Ryley M.D., Johnson P.E., O'Reilly M.P. and Barratt D.A., (1980), *Measurements of ground movements around three tunnels in loose cohesionless soil*, Department of Transport, Transport and Road Reasearch Laboratory (TRRL) Laboratory Report No. 938.

Sagaseta C., (1987), *Analysis of undrained soil deformation due to ground loss*, Geotechnique 37, No.3, pp 301-320.

Sagaseta C., (1991), *Personal Communication.*

Schmidt B., (1969), *Settlements and ground movements associated with tunnelling in soil,* PhD Thesis, University of Illinois.

Selby A.R., (1987), *Some variables in the calculation of the effects upon floor slabs of tunnelling-induced settlements*, Proceedings of the First International Conference on Foundations & Tunnels, March 1987, Edited by M.C. Forde, pp 15-19.

Selby A.R. and Attewell P.B., (1989), *Estimation of ground movements and their effects caused by tunnelling in compressible soils,* Proceedings of the Conference on Foundations & Tunnelling, London, 1989, pp 323-330.

Seneviratne H.N., (1979), *Deformations and pore pressure around model tunnels in soft clay,* PhD Thesis, Cambridge University 1979.

Skempton A.W. and McDonald D.H., (1956), *Allowable settlements of buildings,* Proceedings of the Institution of Civil Engineers, Vol. 5, Part 3, 1956, pp 727-768.

Smith I.A.A., (1972), *Stress and strain in a sand mass adjacent to a model wall,* PhD Thesis, Cambridge University.

*2

Steensen-Bach J.O. and Steenfelt J.S., (1991), *Subsidence due to shield tunnelling in sand*, Proceedings to the Tenth European Conference on Soil Mechanics & Foundation Engineering, Florence, Vol II, A.A. Balkema, Rotterdam, pp 863-868.

Stein D., Mollers K. and Bielecki R., (1989), *Microtunnelling - installation and renewal of non-mansize supply and sewerage lines by the trenchless construction method*, Pub. Ernst & Sohn, Berlin.

Stroud M.A., (1971), *Sand at low stress levels in the simple shear apparatus*, PhD Thesis, Cambridge University.

Swee J.K.L. and Milligan G.W.E., (1990), *Pipebursting - model tests*, Proceedings of the International Conference NO-DIG '90 OSAKA, Japan, Paper H3.

Sweet A.L. and Bogdanoff J.L., (1965), *Stochastic model for predicting subsidence*, Journal of the Engineering Mechanics Division, ASCE, April 1965, EM2, pp 21-45.
*3
Terzarghi K., (1943), *Theoretical soil mechanics*, Chapman and Hall.

Uesugi, Kishida H. and Tsubakihara Y., (1988), *Behaviour of sand particles in sand-steel friction*, Proceedings of the Japanese Society of Soil Mechanics and Foundation Engneering, Soils and Foundations, Vol 28, 1, March 1988, pp 107-118.

UMIST (Sewer Rehabilitation Research Group), Green C. and Wood J., (1987), *Current Research into the social costs of sewerage systems*, Proceedings of the Second International Conference on Trenchless Construction for Utilities, NO-DIG '87, London, Paper 5.3.

Underground, (1986), *Focus on Pipebursting*, Underground Serial, July 1986, pp 18-23.
*4
Vesic A., (1972), *Expansion of cavities in an infinte soil mass*, Journal of the Soil Mechanics & Foundations Division, ASCE, 98 SM3, March 1972, pp 265-290.

Wahls H.E., (1981), *Tolerable settlement of buildings*, Journal of the Geotechnical Engineering Division, ASCE, VOl. 107, pp 1489-1504.

Ward W.H. and Pender M.J., (1981), *Tunnelling in soft ground - general report (session 2)*, Proceedings of the Tenth International Conference on Soil Mechanics & Foundation Engineering, Stockholm, Pub. A.A. Balkema, Rotterdam, Vol. 4, pp 261-275.
*5

Wong R.C.K. and Kaiser P.K., (1986), *Ground behaviour near soft ground tunnels*, Proceedings of the International Congress on Large Underground Openings, Florence, Italy, Vol. 1, pp 942-951.

Wong R.C.K. and Kaiser P.K., (1987), *Prediction of ground movements above shallow tunnels*, Proceedings of the International Symposium on Prediction and Performance in Geotechnical Engineering, Pub. A.A. Balkema, Rotterdam, pp 329-343.

Wong R.C.K. and Kaiser P.K., (1991), *Performance assessment of tunnels in cohesionless soils*, Journal of Geotechnical Engineering, American Society of Civil Engineers, Vol. 117, 12, December 1991, pp 1880-1901.

Wong K.W. and Vonderohe A.P., (1978), *Photogrammetric measurement of displacements around tunnels in sandy soils*, Proceedings of the American Society of Photogrammetry, 44th Annual Meeting, Washington D.C., 1978, pp 373-388.

*1

Atkinson J.H., Brown E.T. and Potts D.M., (1975), *Collapse of shallow unlined tunnels in dense sand*, Tunnels and Tunnelling, May 1975, pp 81-87.

*2

Sokolowski V.V., (1960), *States of soil media*, Pub. Butterworth, London.

*3

Taylor R.N., (1984), *Ground movements associated with tunnels and trenches*, PhD Thesis, University of Cambridge.

*4

Vafaeian M., (1991), *Analysis of soil behaviour during excavation of shallow tunnel*, Journal of the South East Asian Geotechnical Society - Ground Engineering, Vol. 22, No. 2, December 1991, pp 257-267.

*5

Winkler E, (1867), *Die lehre von elastizitat und festigkeit,* (On elastisity and flexibility), Prague.

BIBLIOGRAPHY

Atkinson J.H., Brown E.T. and Potts M., (1975), *Collapse of shallow unlined tunnels in dense sand*, Tunnels and Tunnelling Serial, May 1975, Part 7, No. 3, pp 81,84 & 87.

Balasubamaniam K., (1989), *Singapore's experience in trenchless technology and its potential for use in developing countries*, World Water 1989, Pub. Thomas Telford, pp 53-63.

Broms B.B. and Shirlaw J.N., (1989), *Settlement caused by earth pressure shields in Singapore*, Proceedings of the Conference Tunnels et Micro-tunnels en Terain Meuble du Chantier a la Theorie, Paris, 1989, pp 209-219.

Craig R.N., (1983), *Pipejacking: a state-of-the-art review*, CIRIA Technical Note 112.

Cuniberti J.S., (1989), *Tunnels without settlement*, Proceedings of the Conference Tunnels et Micro-tunnels en Terain Meuble du Chantier a la Theorie, Paris, 1989, pp 64-70.

Glossop N.H. and Farmer I.W., (1979), *Settlement associated with removal of compressed air pressure during tunnelling in alluvial clay*, Geotechnique 29, No. 1, pp 67-72.

Ghaboussi J., Ranken R.E. and Karshenas M., (1979), *Analysis of subsidence over soft ground tunnels*, Proceedings of the International Conference on the Evaluation and Prediction of Subsidence, 1979, Pensacola Beach USA, pp 182-196.

Hanafy E.A. and Emery J.J., (1980), *Advancing face simulation of tunnel excavation and lining replacement*, Proceedings of the Second International Conference on Ground Movement and Structures, Cardiff 1980, Edited by J.D. Geddes, Pub. Pentech Press, pp 377-394.

Kawamoto T. and Okuzono K., (1977), *Analysis of ground surface settlement due to shallow shield tunnels,* International Journal for Numerical and Analytical Methods in Geomechanics, Vol. 1, 1977, pp 271-281.

Kimura T. and Mair R.J., (1981), *Centrifugal testing of model tunnels in soft clay,* Proceedings of the Tenth International Conference on Soil Mechanics and Foundation Engineering, Stockholm, 1981, Vol. 1, Session 2, pp 319-322.

Leblais Y. and Bochon A., (1991), *Villejust tunnel: slurry shield effects on soil and lining behaviour and comments on monitoring requirements,* Proceedings of the Sixth International Symposium Tunnelling '91, April 1991, Institution of Mining and Metallurgy, London, Pub. Elsevier Applied Science, pp 65-77.

Mair R.J., Gunn M.J. and O'Reilly M.P., (1981), *Ground movements around shallow tunnels in soft clay,* Proceedings of the Tenth International Conference on Soil Mechanics and Foundation Engineering, Stockholm, 1981, Vol. 1, Session 2, pp 323-328.

O'Reilly M.P., Ryley M.D., Barratt D.A. and Johnson P.E., (1980), *Comparison of settlements resulting from three methods of tunneling in loose cohesionless soil,* Proceedings of the Second International Conference on Ground Movement and Structures, Cardiff 1980, Edited by J.D. Geddes, Pub. Pentech Press, pp 359-376.

Sagaseta C., (1988), *Author's reply to Schmidt B. (1988),* Geotechnique 38, No.2, pp 647-649.

Schmidt C., (1988), *Discussion of 'analysis of undrained soil deformation due to ground loss' by Sagaseta C., (1987),* Geotechnique 38, No.2, pp 647-649.

Schmidt B., (1974), *Prediction of settlements due to tunnelling in soil: three case histories,* Proceedings of the International

Conference on Rapid Excavation and Tunnelling, San Fransisco, USA, 1974, Vol. 2, Edited by H.C. Pattison & E. D'Appdonia, pp 1179-1200.

Washbourne J., (1984), *Slurry lubrication for jacked tunnel linings*, Civil Engineering Technology Serial, February 1984, pp 7-9.

Yeates J., (1984), *The response of buried pipelines to ground movements caused by tunnelling in soil*, Proceedings of the Third International Conference on Ground Movements and Structures, Cardiff, Edited by J.D. Geddes, Pub. Pentech Press, pp 129-144.

APPENDIX A

APPENDIX A ERROR IN SAND PARTICLE MEASUREMENT DUE TO GLASS REFRACTION

The derivation and the use of the formulae used to calculate the likely error in the measurement of the sand particle movements due to refraction are given below.

From Fig. A.1 the following relationships can be obtained.

$$\tan \alpha_1 = x_1/z \qquad (A.1)$$
$$\tan \alpha_2 = x_2/z \qquad (A.2)$$
$$\tan \alpha_1 = y_1/(t+z) \qquad (A.3)$$
$$\tan \alpha_2 = y_2/(t+z) \qquad (A.4)$$

$$\sin \beta_1 = \sin \alpha_1 / M \qquad (A.5)$$
$$\sin \beta_2 = \sin \alpha_2 / M \qquad (A.6)$$

$$\tan \beta_1 = (y_1 - x_1)/t - d_1/t \qquad (A.7)$$
$$\tan \beta_2 = (y_2 - x_2)/t - d_2/t \qquad (A.8)$$

where M is the refractive index of glass. The error in the observed sand particle measurement, W, is equal to $(d_2 - d_1)$, therefore taking equation A.7 from A.8 and rearranging gives:

$$(d_2 - d_1) = (y_2 - x_2) - (y_1 - x_1) - (\tan \beta_2 - \tan \beta_1).t \qquad (A.9)$$

Using typical values for the photographs used in this project, an example is given below using the above equations.

Values:	x_1 = 50mm)	15mm maximum sand particle
	x_2 = 65mm)	movement with 50mm being close to the edge of the photographs
	M = 1.4	(refractive index of toughened glass)
	t = 30mm	
	z = 400mm	

From equations A.1 and A.2, $\alpha_1 = 7.1^o$ and $\alpha_2 = 9.2^o$ respectively.

From equations A.3 and A.4, $y_1 = 53.6$mm and $y_2 = 69.6$mm respectively, which gives an observed sand particle movement of $(y_1 - y_2) = 15.8$mm, which is in error by $(d_2 - d_1)$.

Equations A.5 and A.6 give β_1 and β_2 values of 5.1^o and 6.6^o respectively.

This gives an error in the sand particle measurement, from equation A.9, of **0.2**mm. The percentage error on the actual sand movement for the worst conditions is:

$$(0.3/(16.1-0.3)).100 = \mathbf{1.3\%}$$

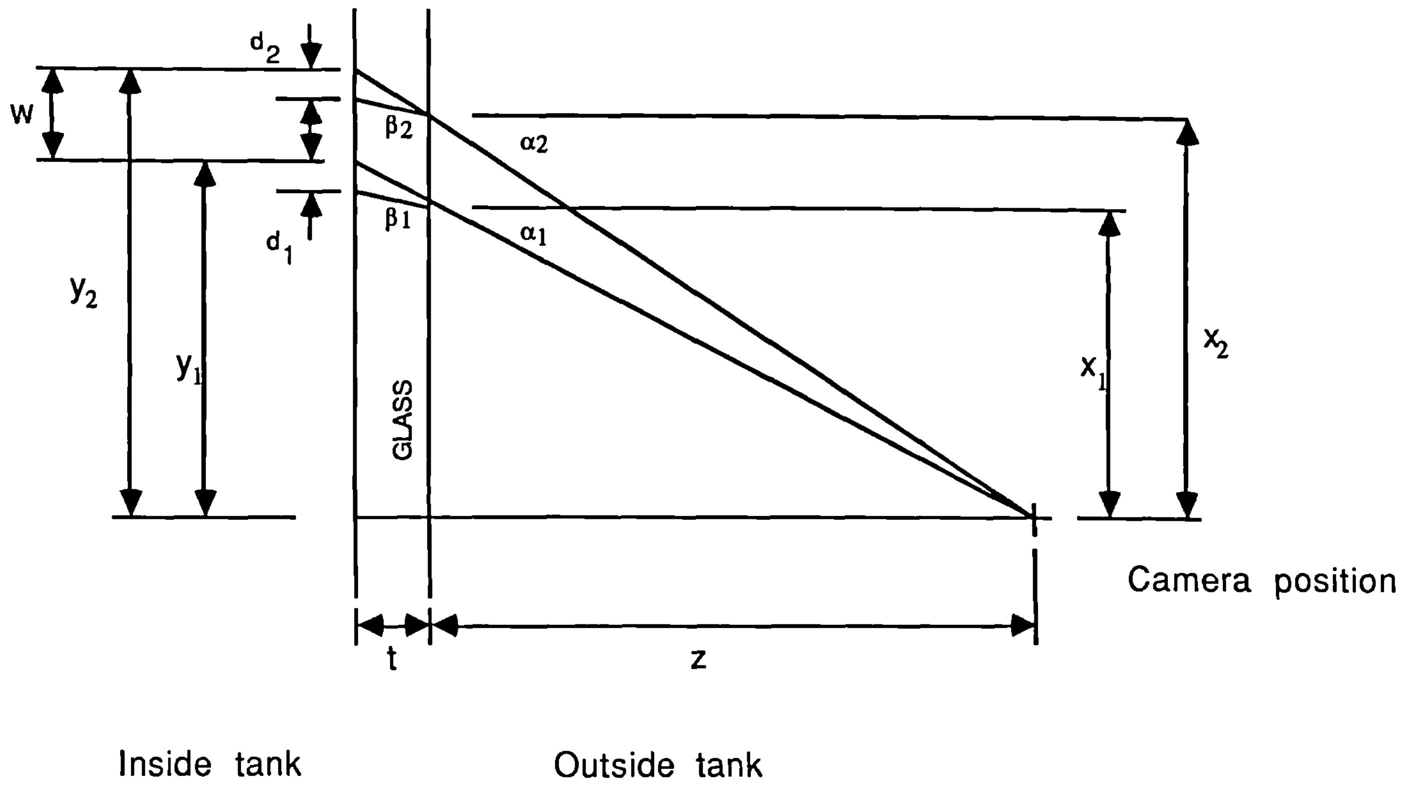

Fig. A.1 Schematic representation of the error in particle movements due to glass refraction

APPENDIX B

APPENDIX B LABORATORY TEST RESULTS

B.1 OPEN SHIELD PIPEJACKING TESTS - LONGITUDINAL PLANE RESULTS

The following figures show the horizontal and vertical displacement contour plots for all the open shield pipejacking tests in the longitudinal plane (24 tests). The contours are in millimetres and represent the movements in the sand caused by a 10mm forward jack of the shield and pipe. Test codes are given to aid comparison between results. The test code is defined as: Cover depth to diameter ratio (C/D), density state of sand, sand type, overcut ratio (t/R).

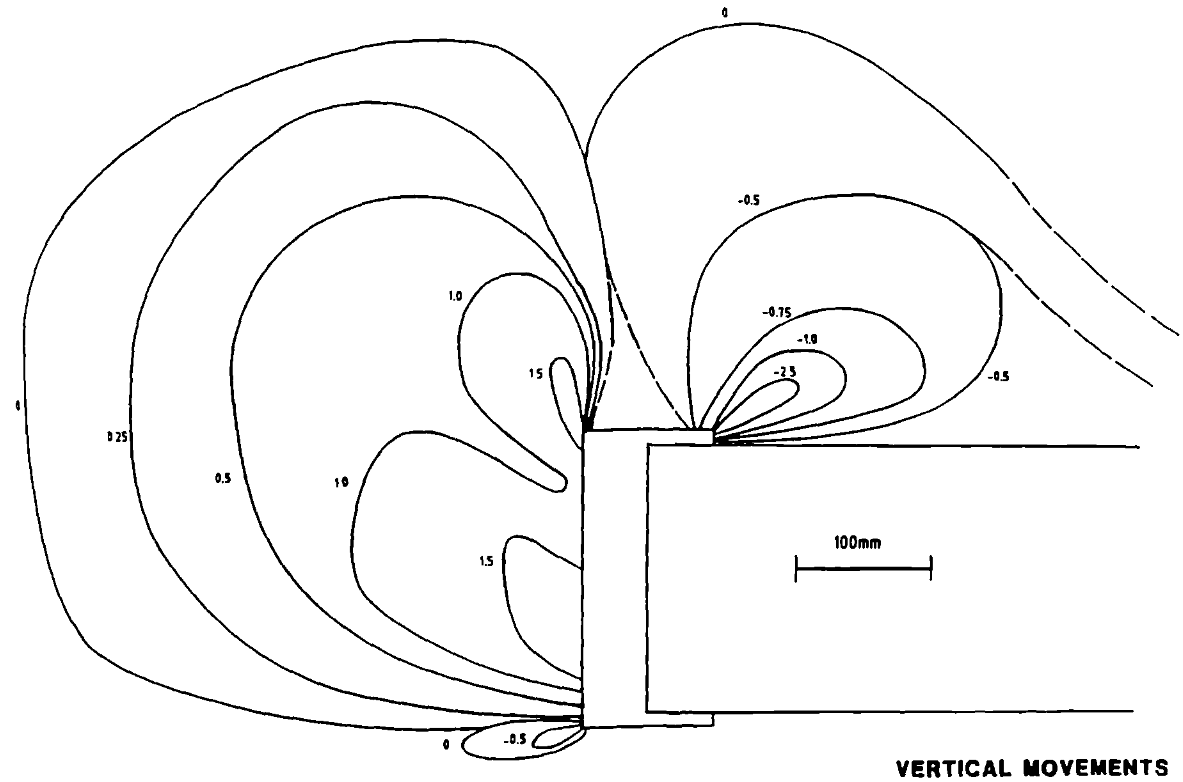

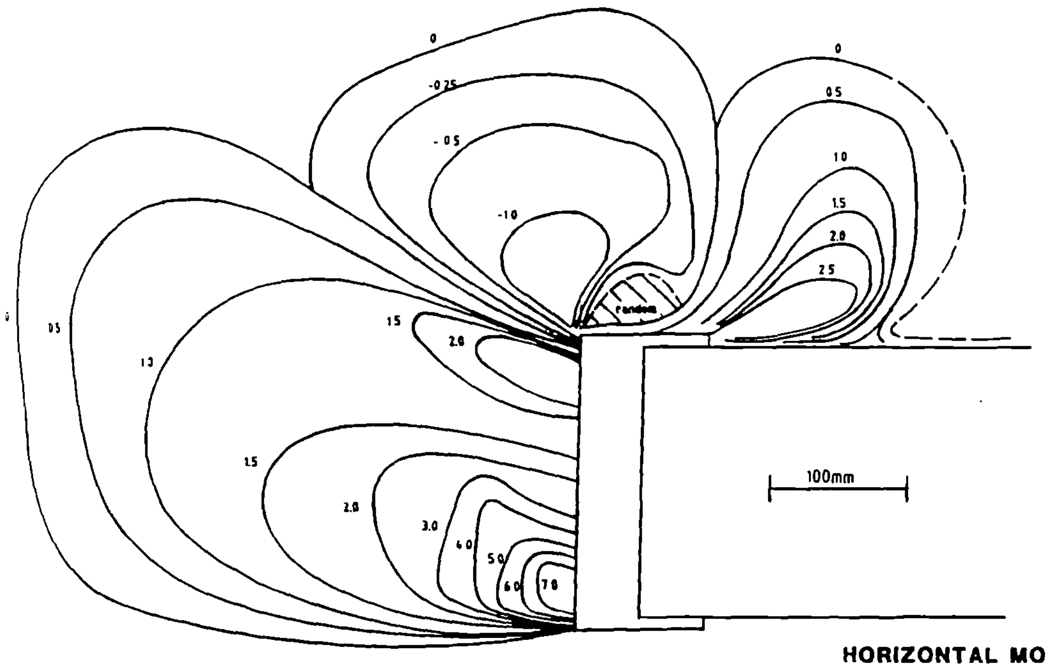

TEST OPJ1

4.5dLB0.1

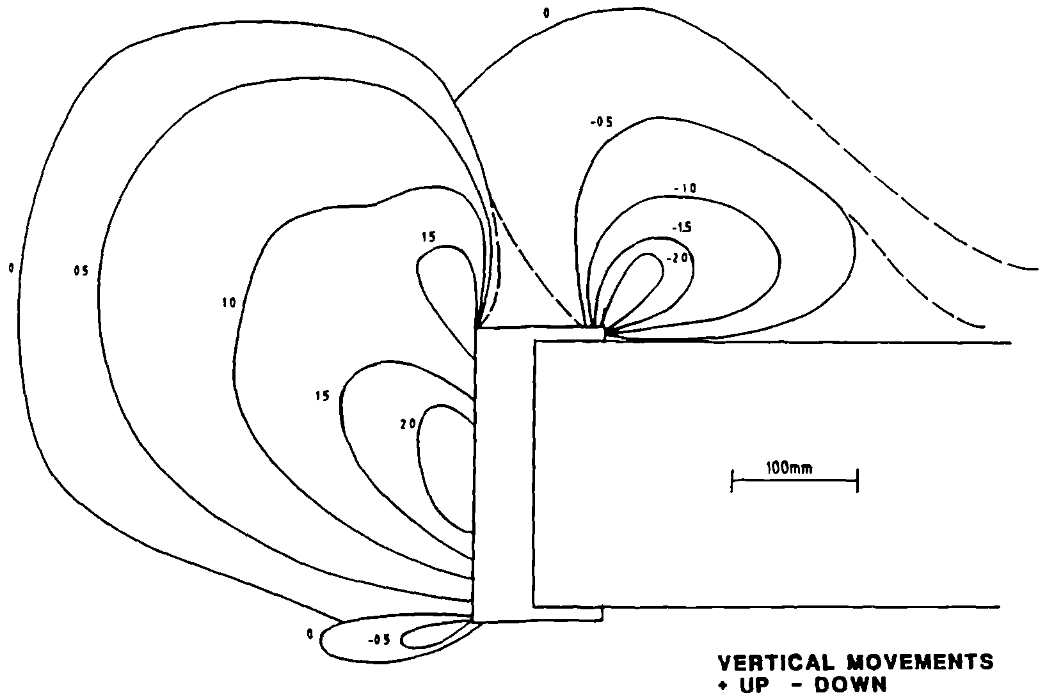

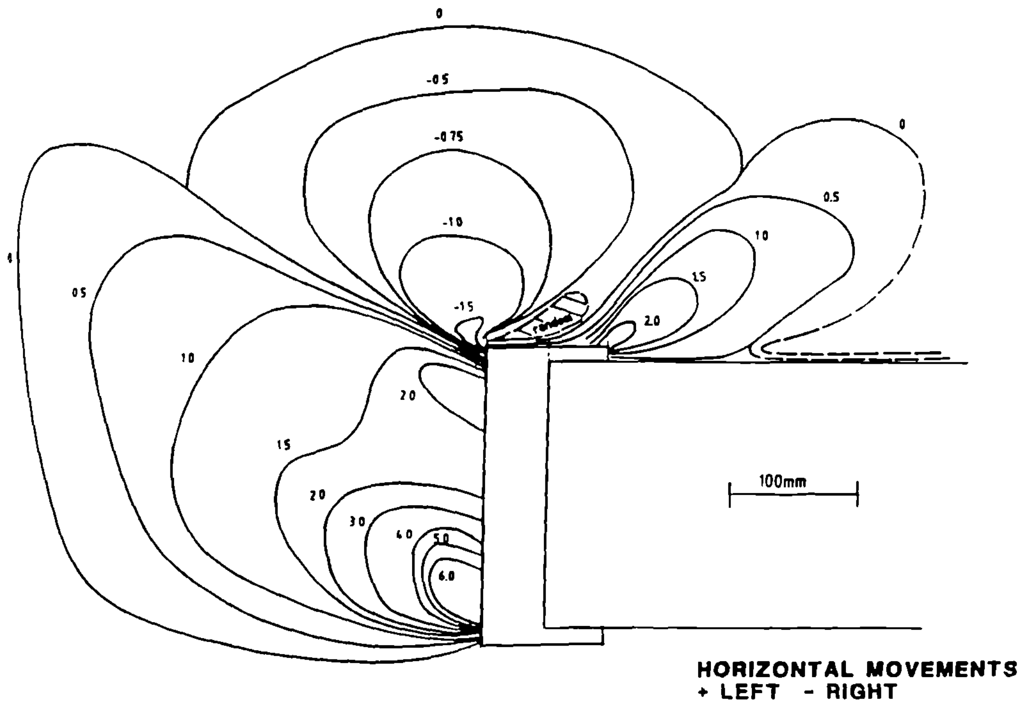

TEST OPJ2

12.5dLB0.1

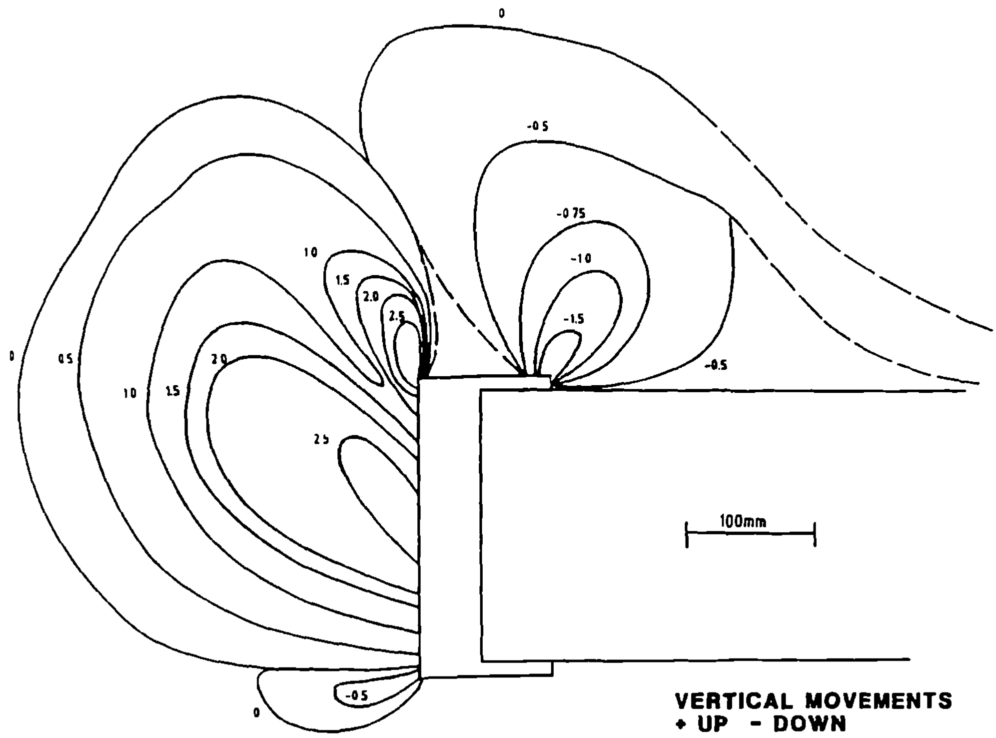

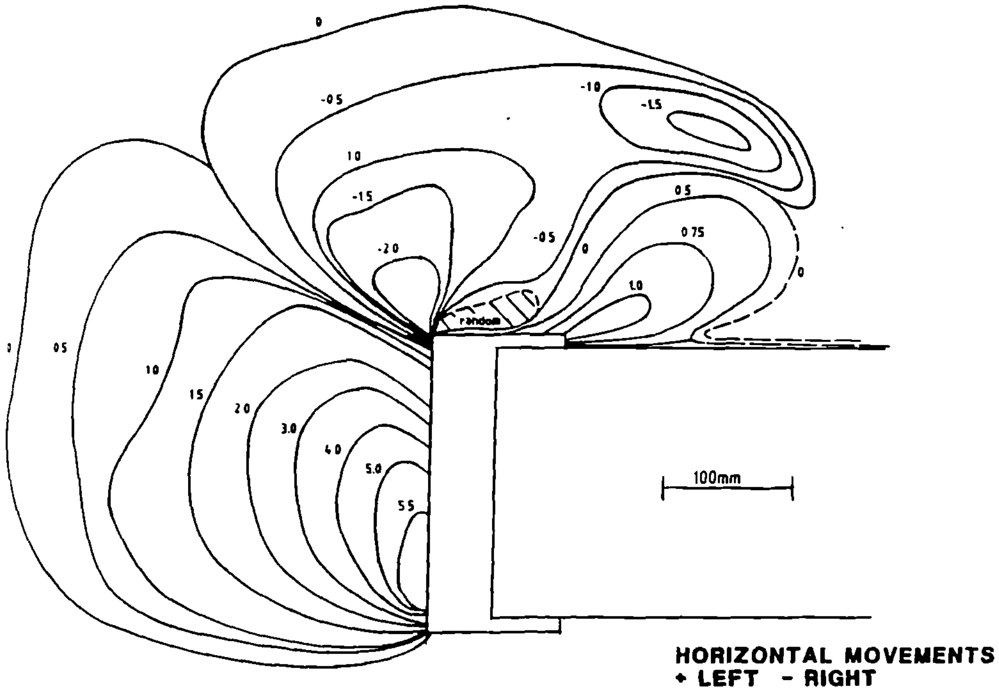

TEST OPJ3

20.0dLB0.1

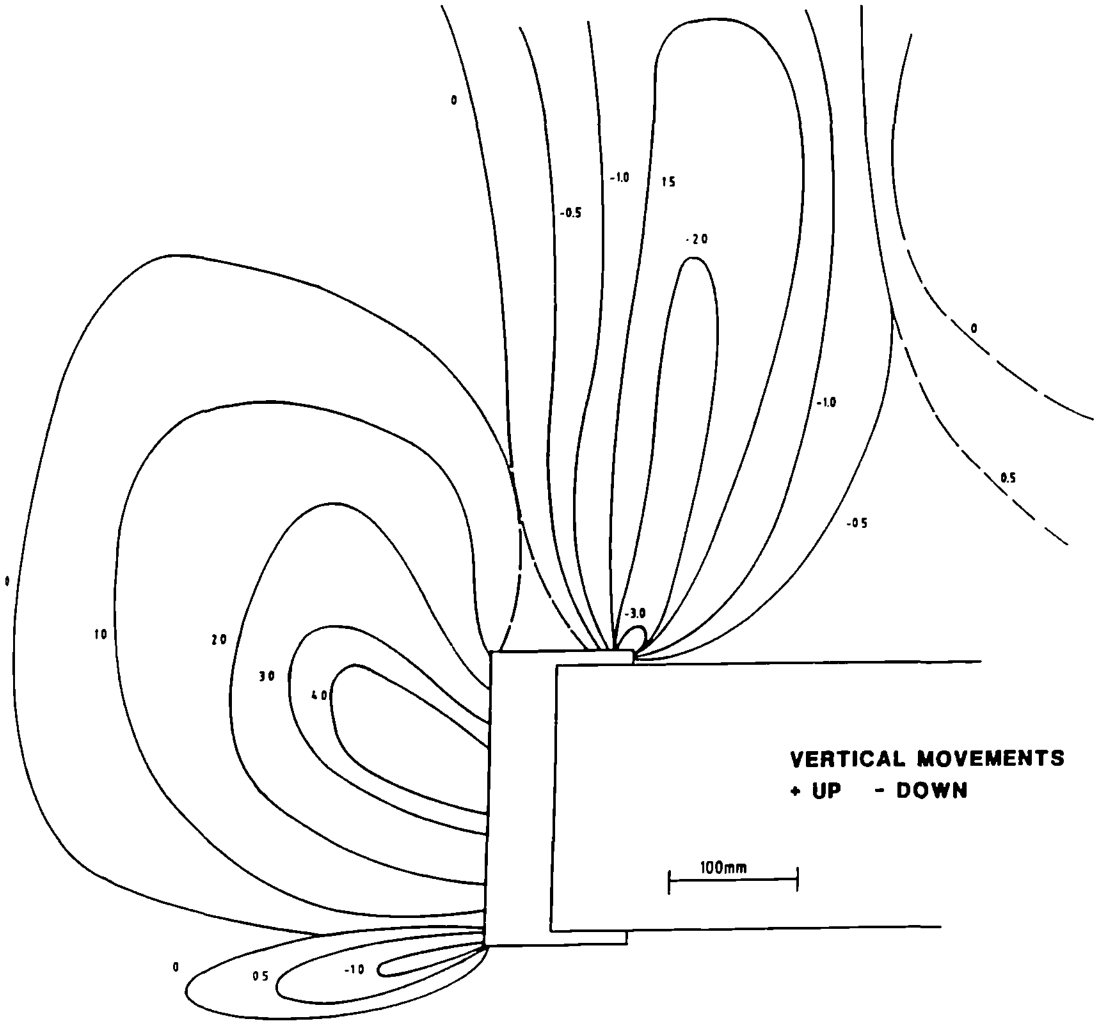

TEST OPJ4

4.5ILB0.1

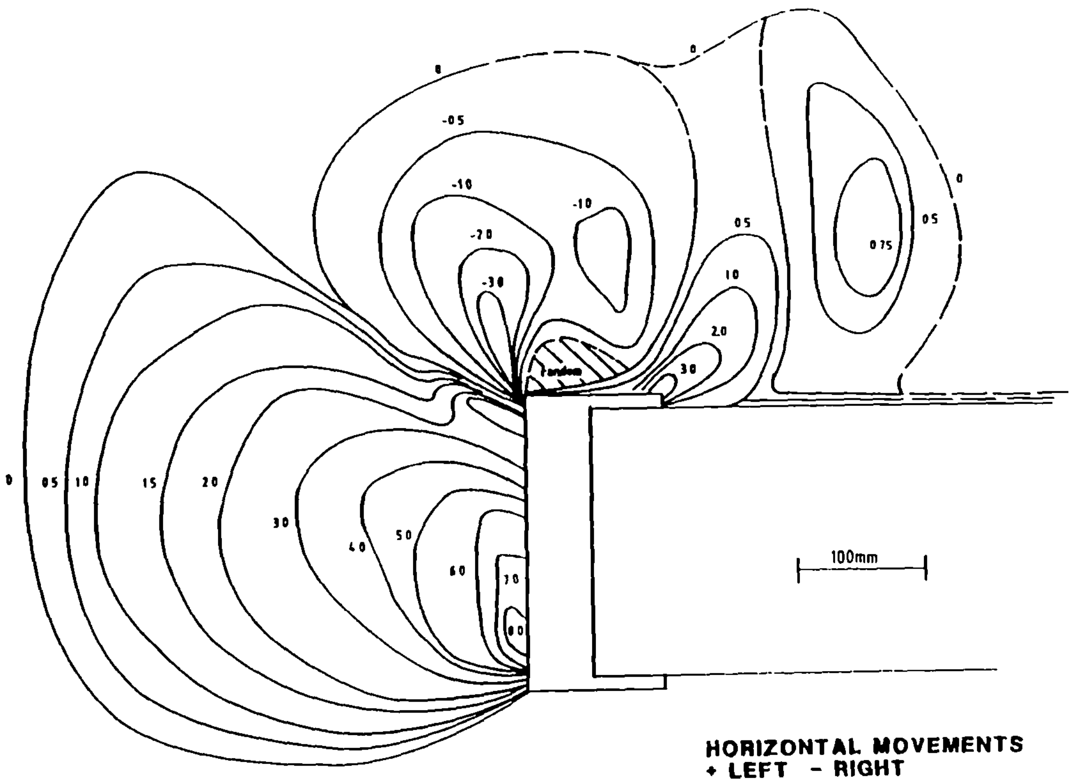

TEST OPJ4

4.5ILB0.1

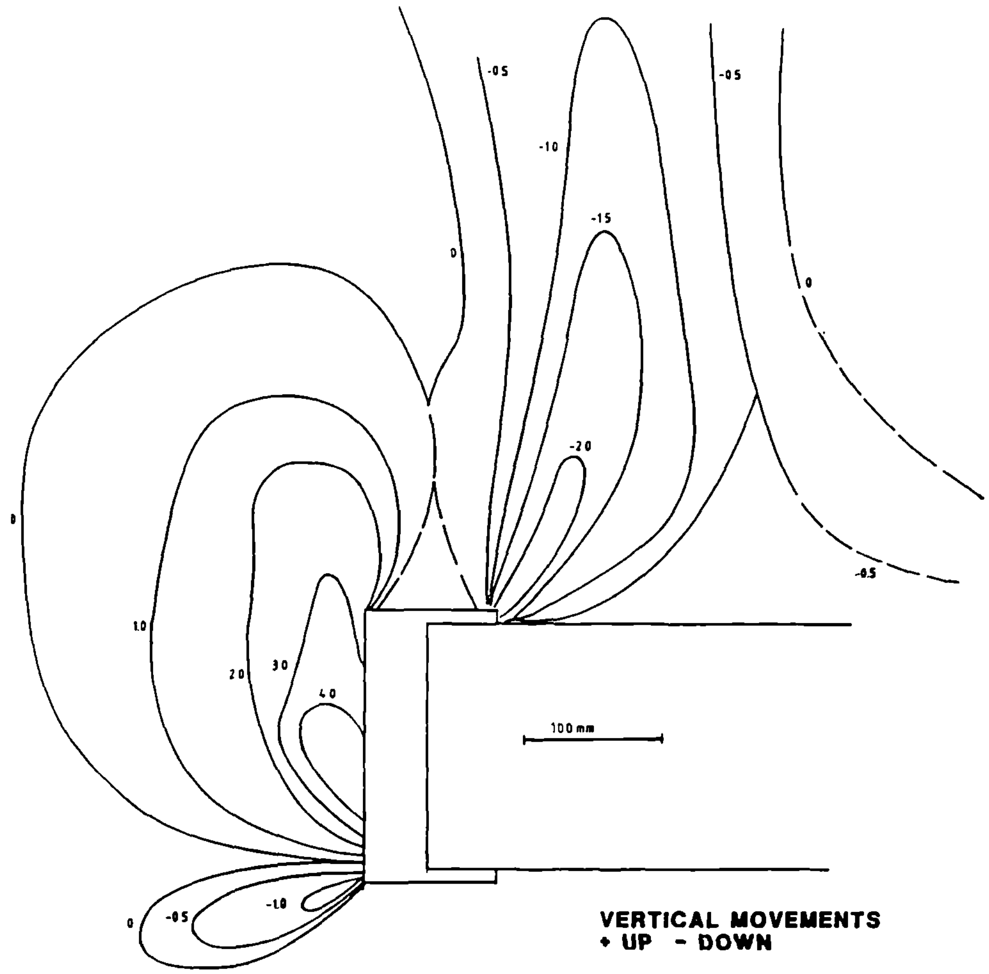

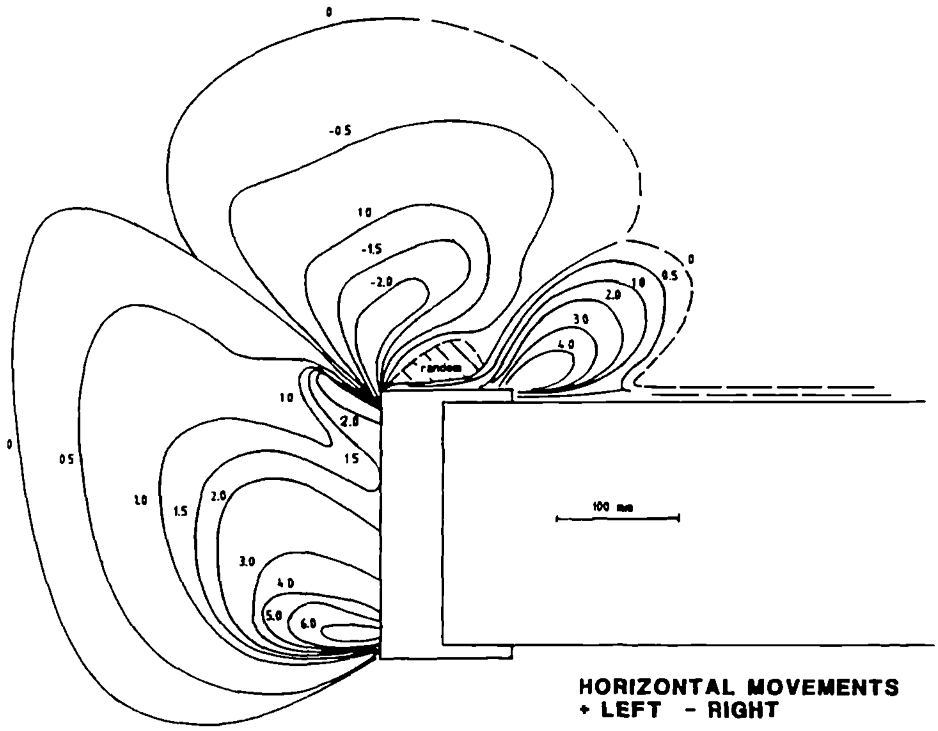

TEST OPJ5

12.5lLB0.1

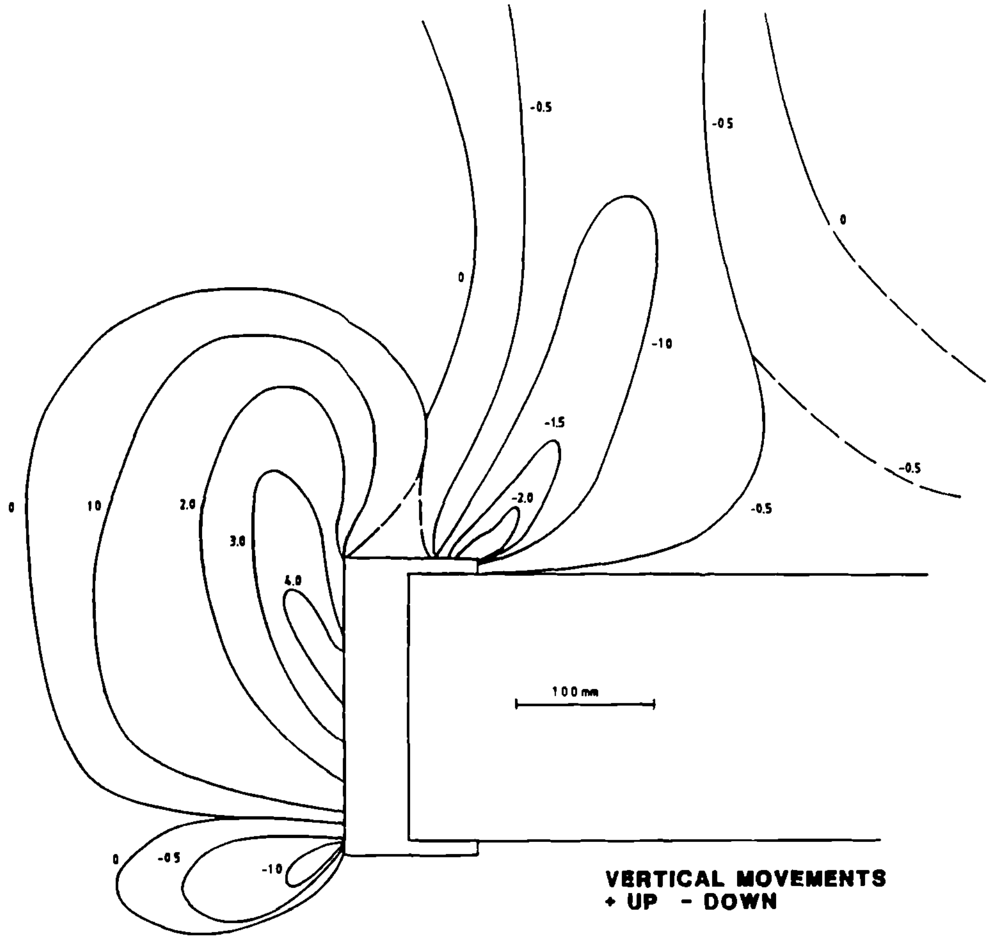

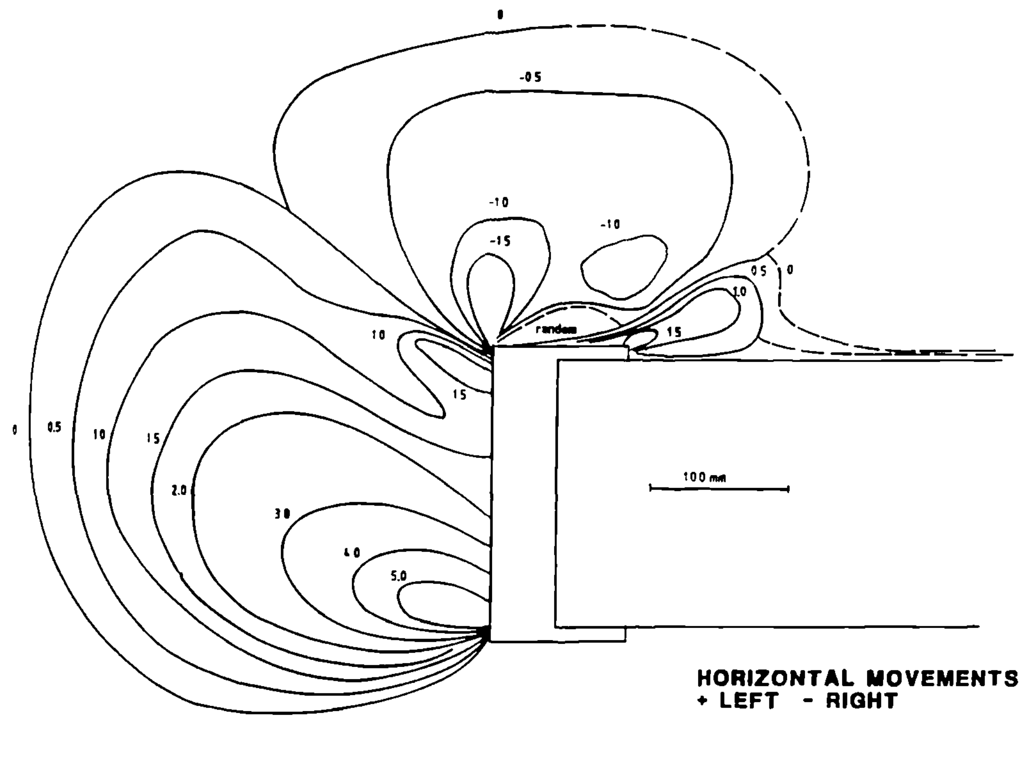

TEST OPJ6
20.01LB0.1

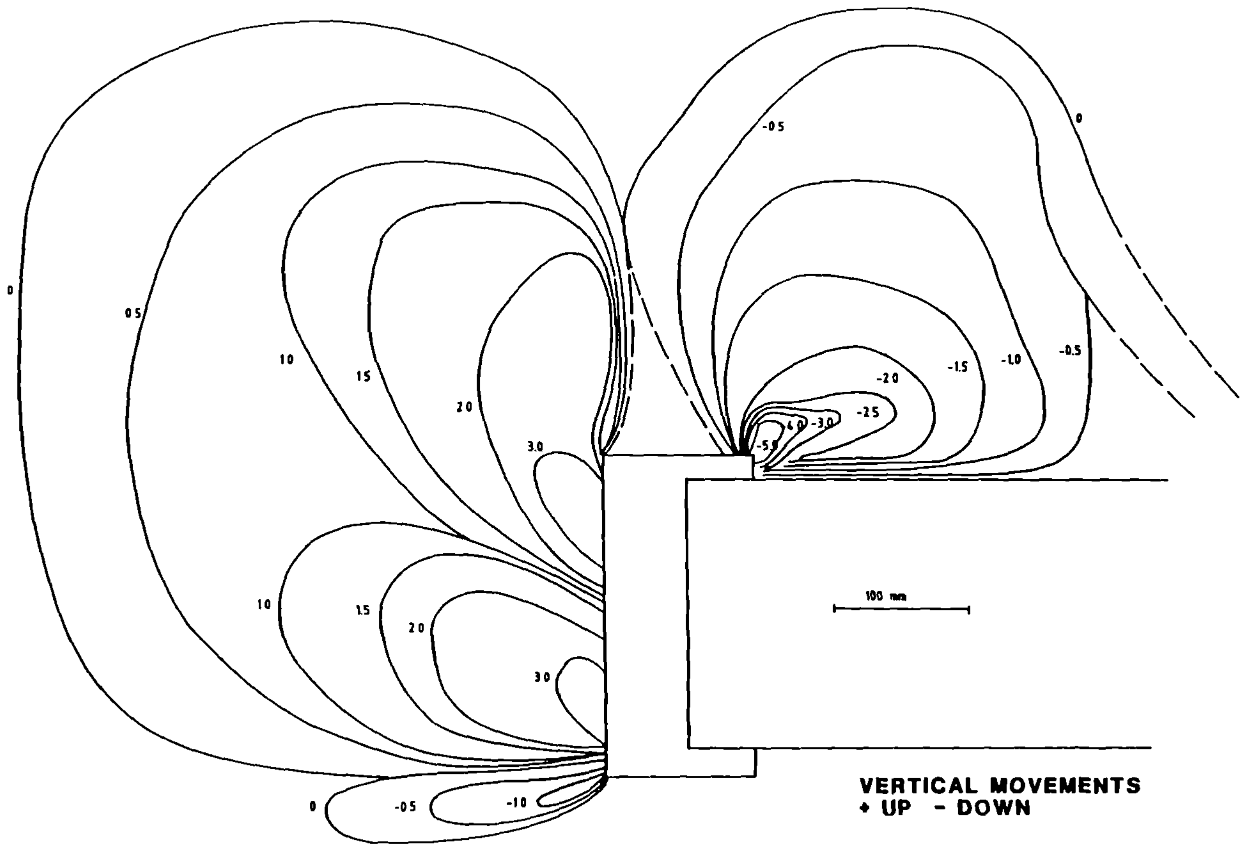

TEST OPJ7

4.5dLB0.2

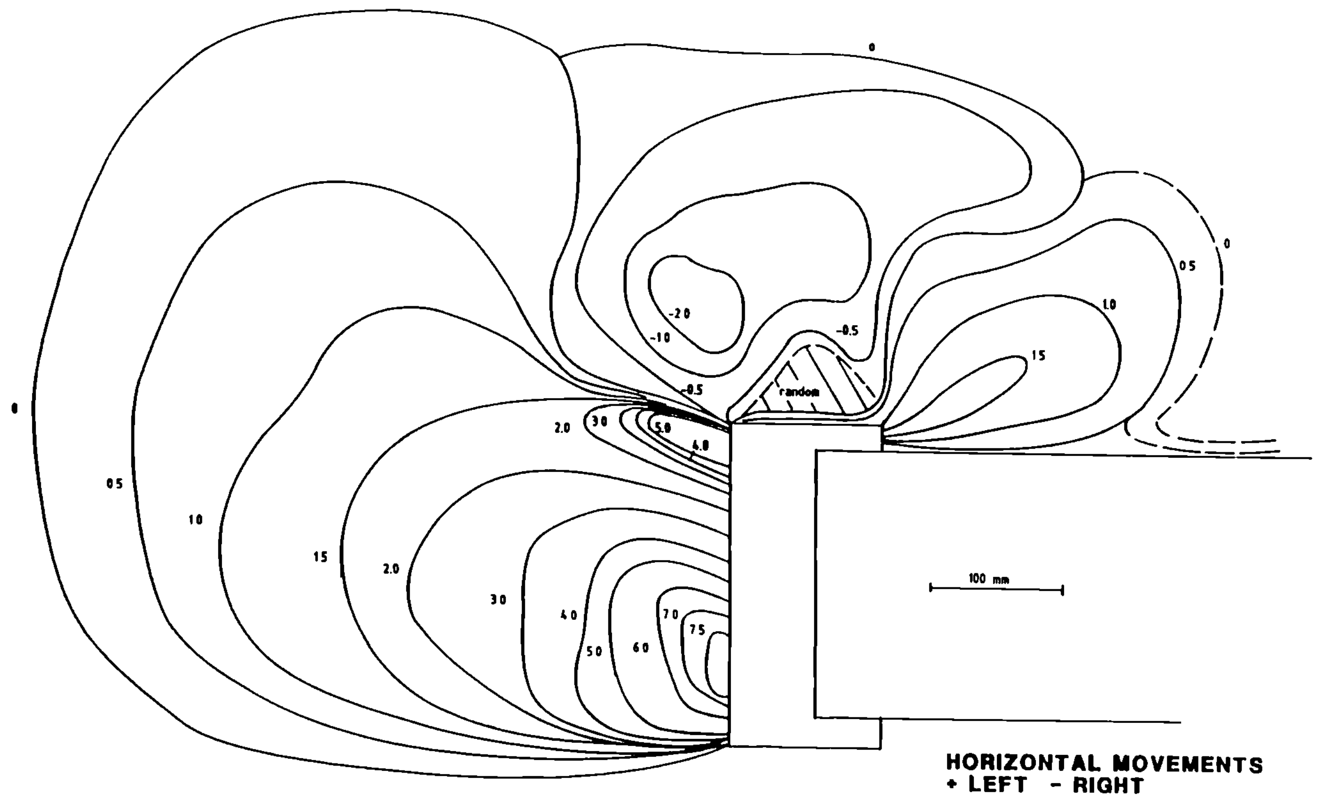

TEST OPJ7
4.5dLB0.2

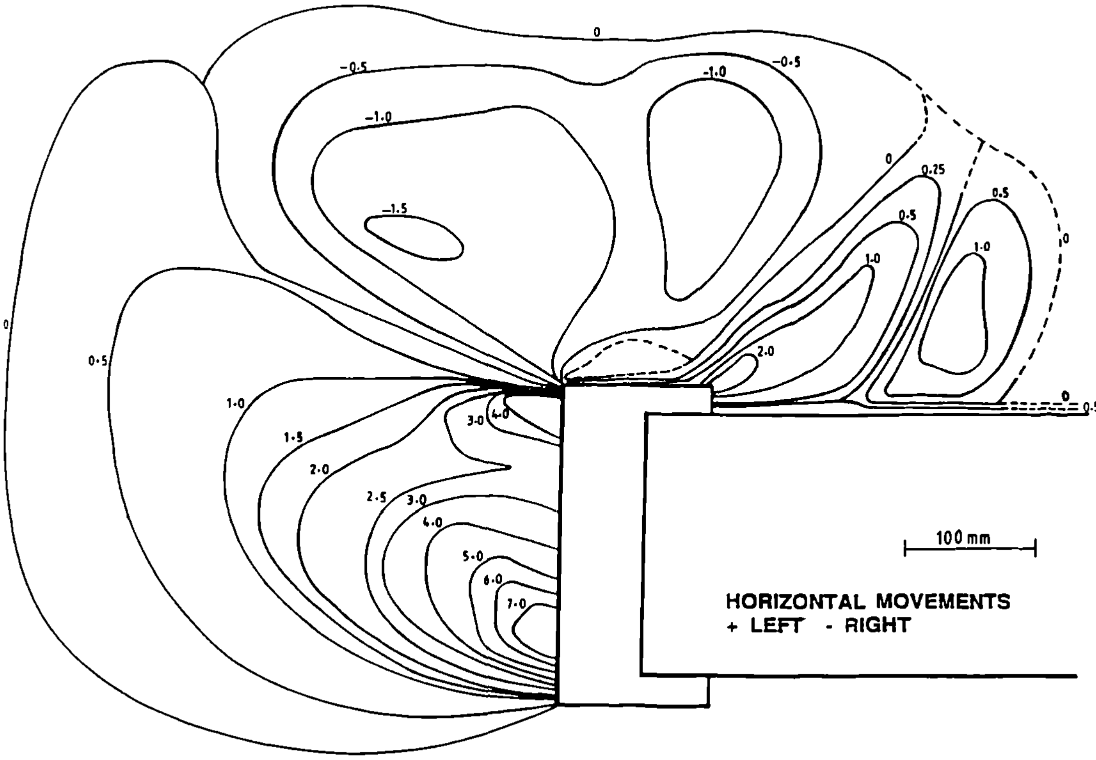

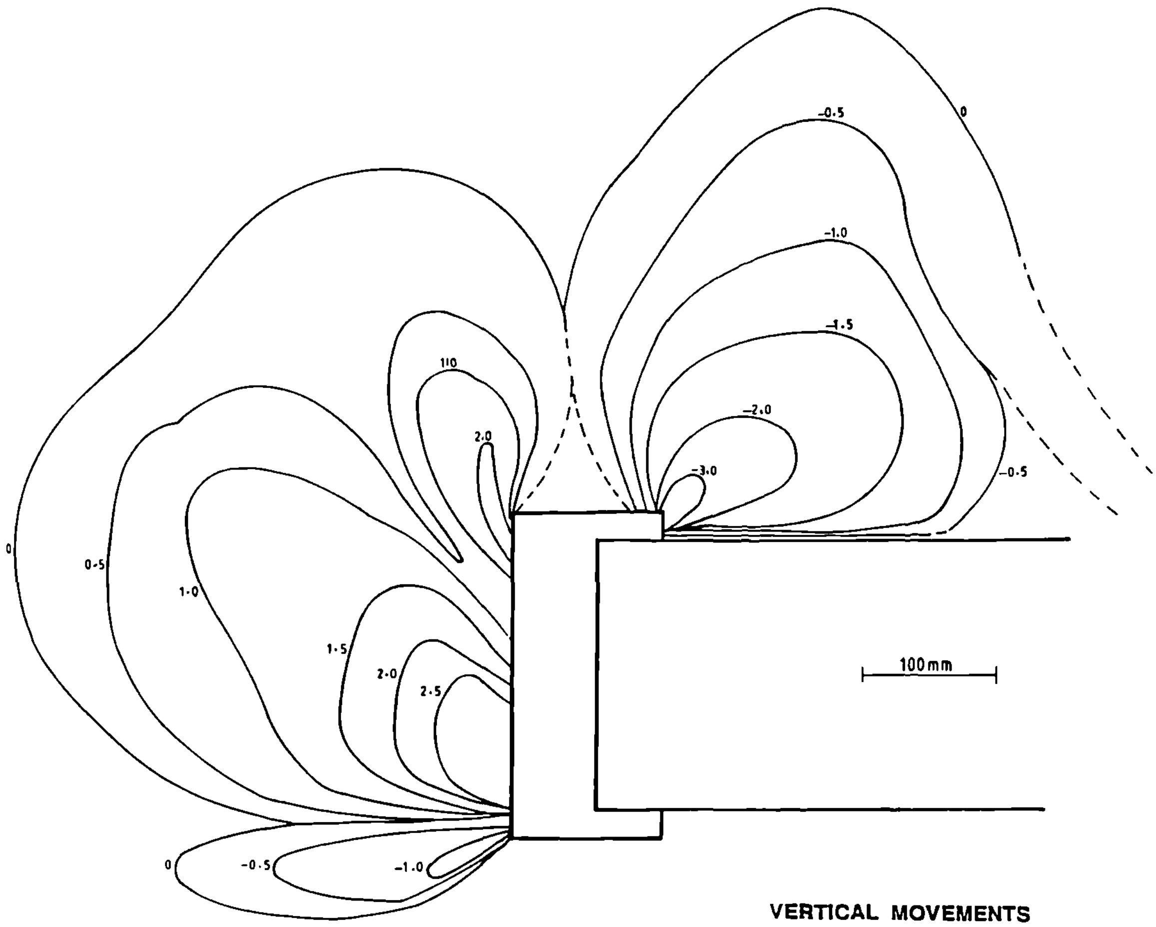

TEST OPJ8

12.5dLB0.2

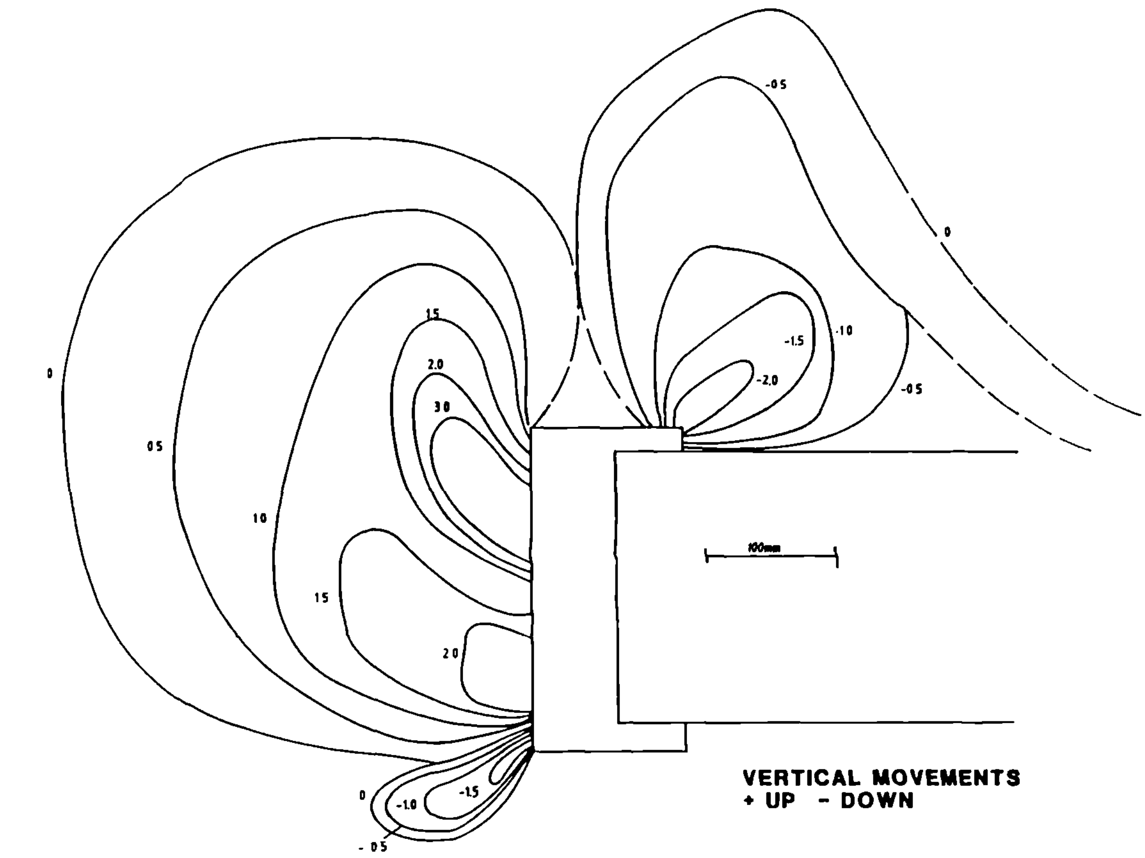

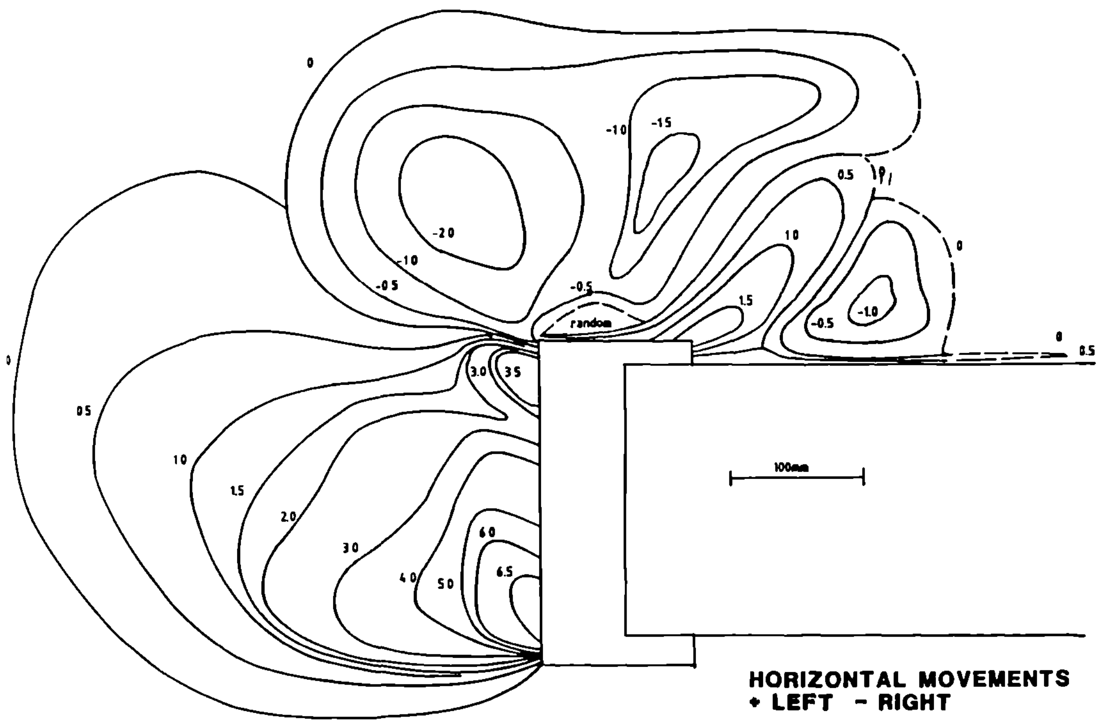

TEST OPJ9
20.0dLB0.2

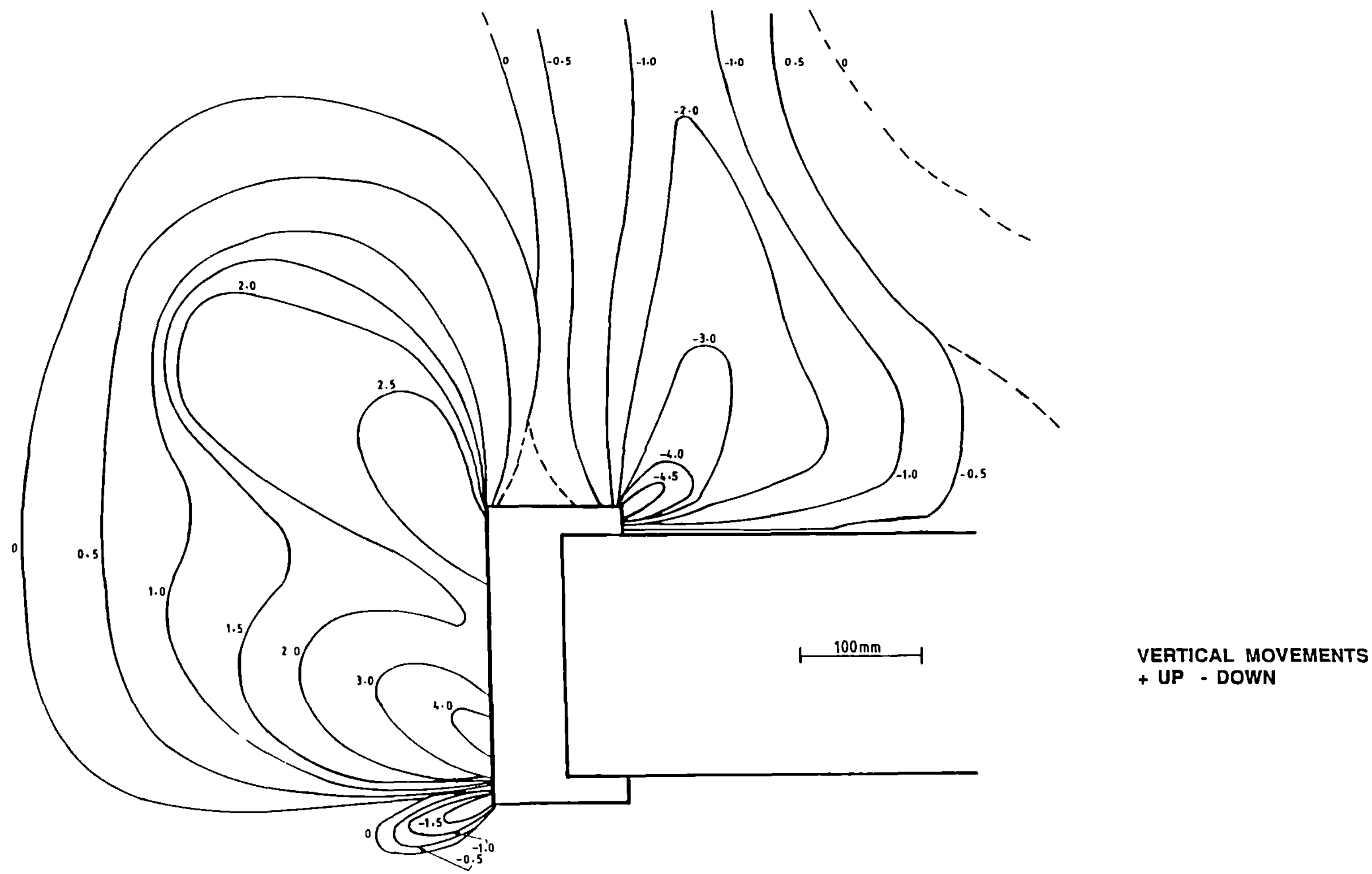

TEST OPJ10
4.5ILB0.2

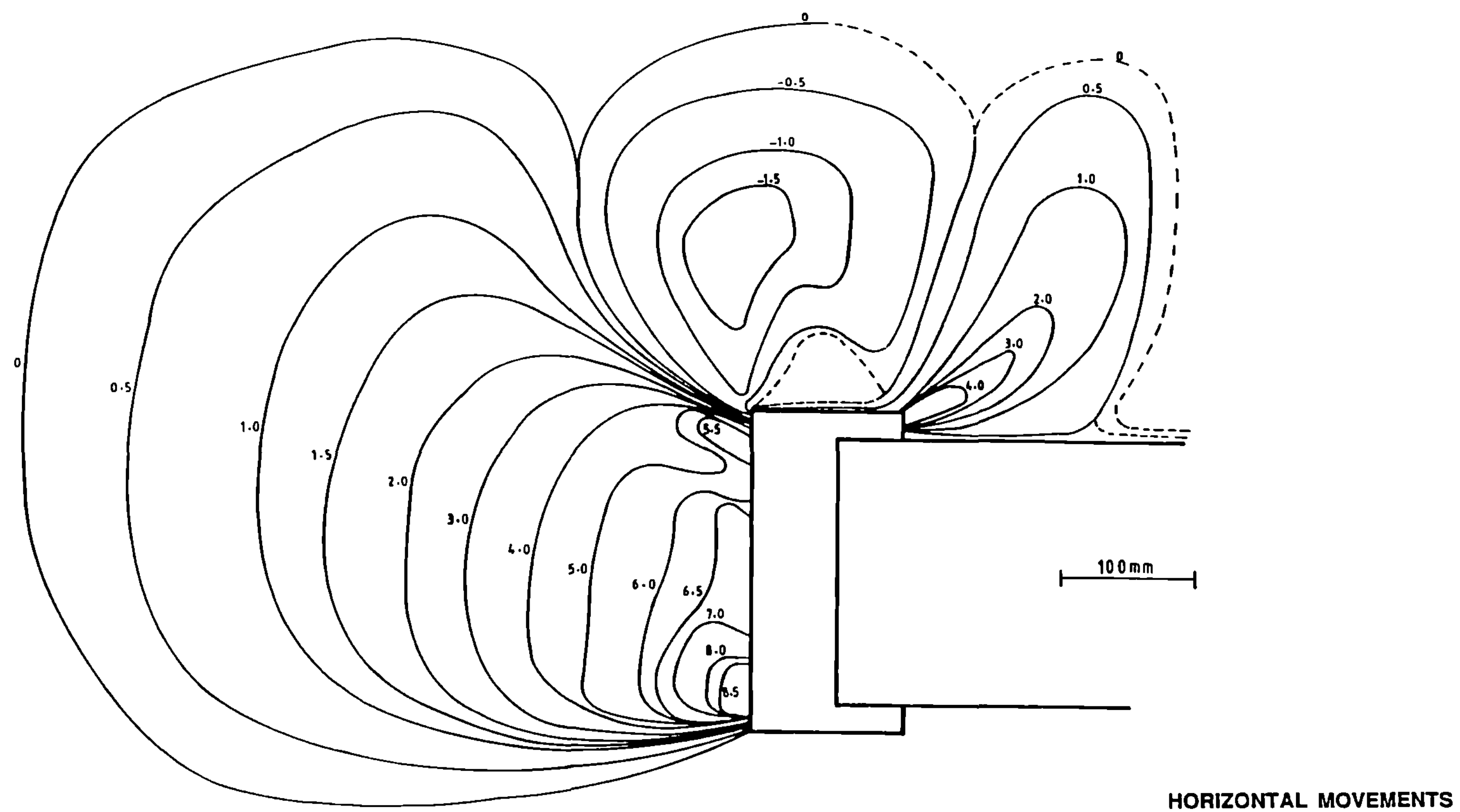

TEST OPJ10
4.5ILB0.2

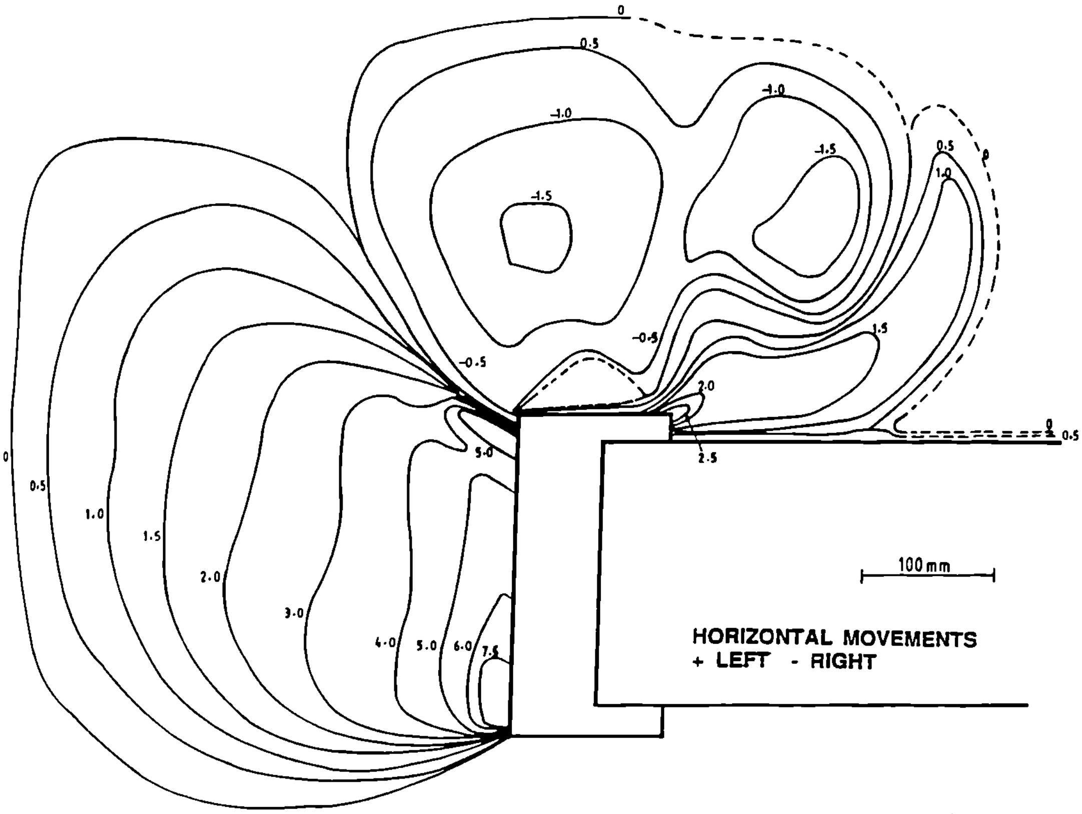

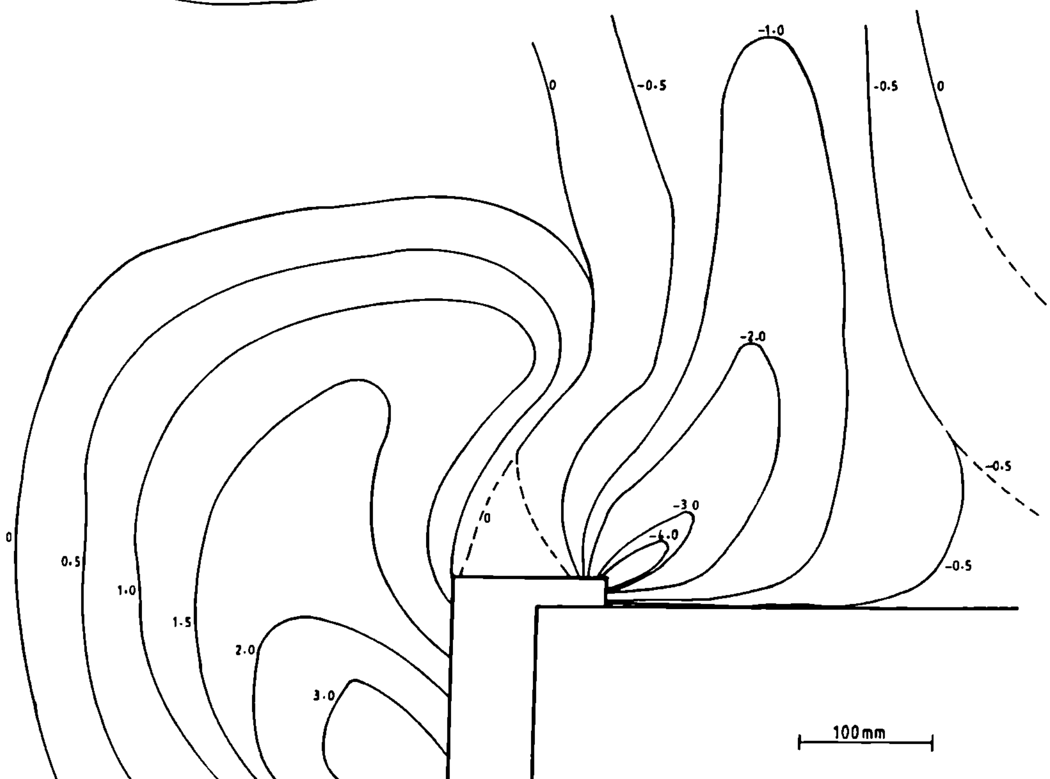

TEST OPJ11

12.5ILB0.2

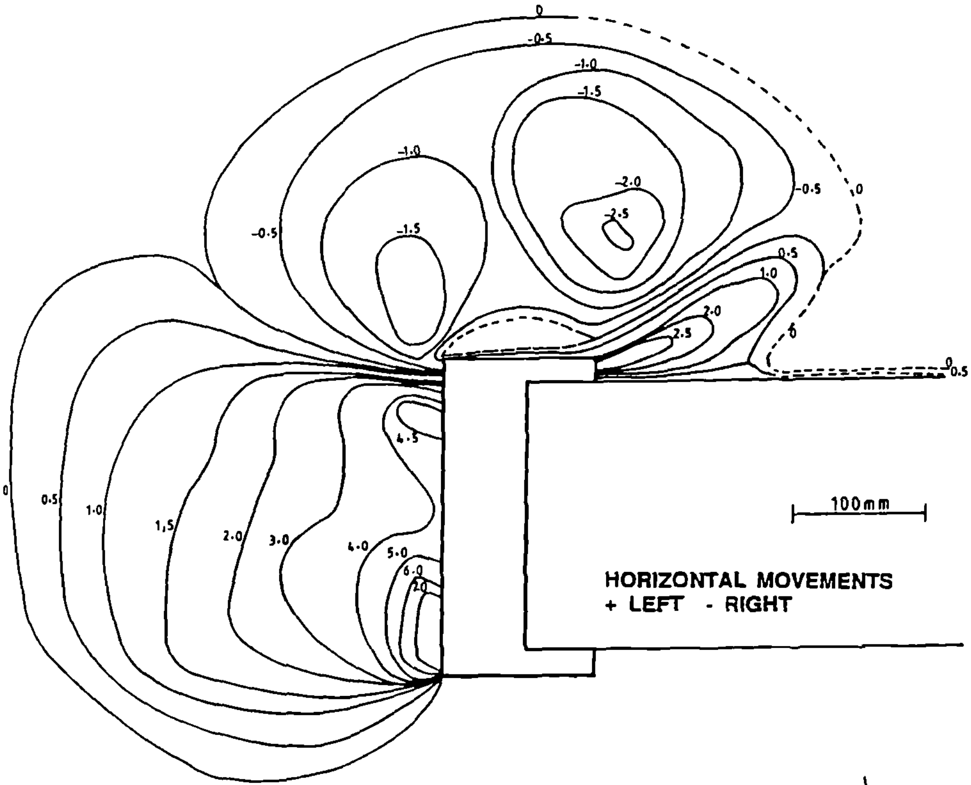

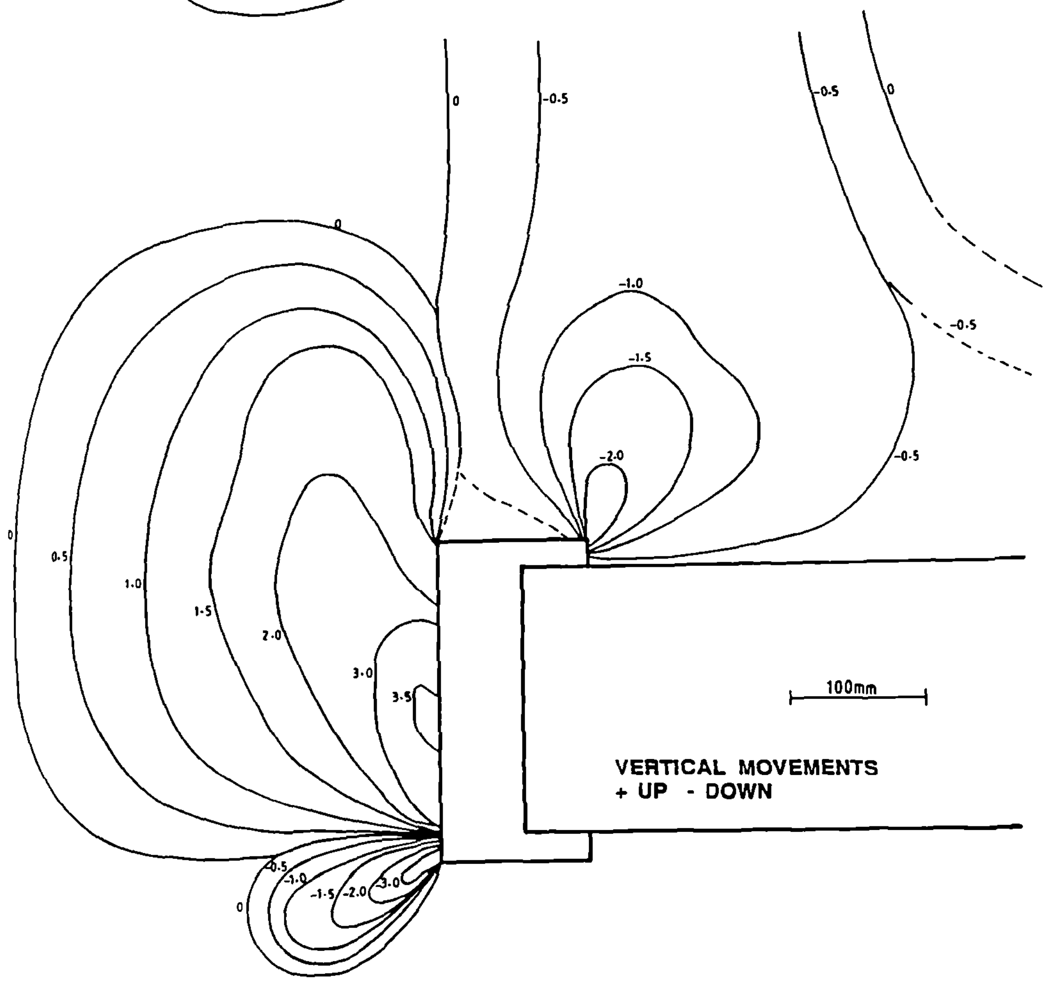

TEST OPJ12

20.0lLB0.2

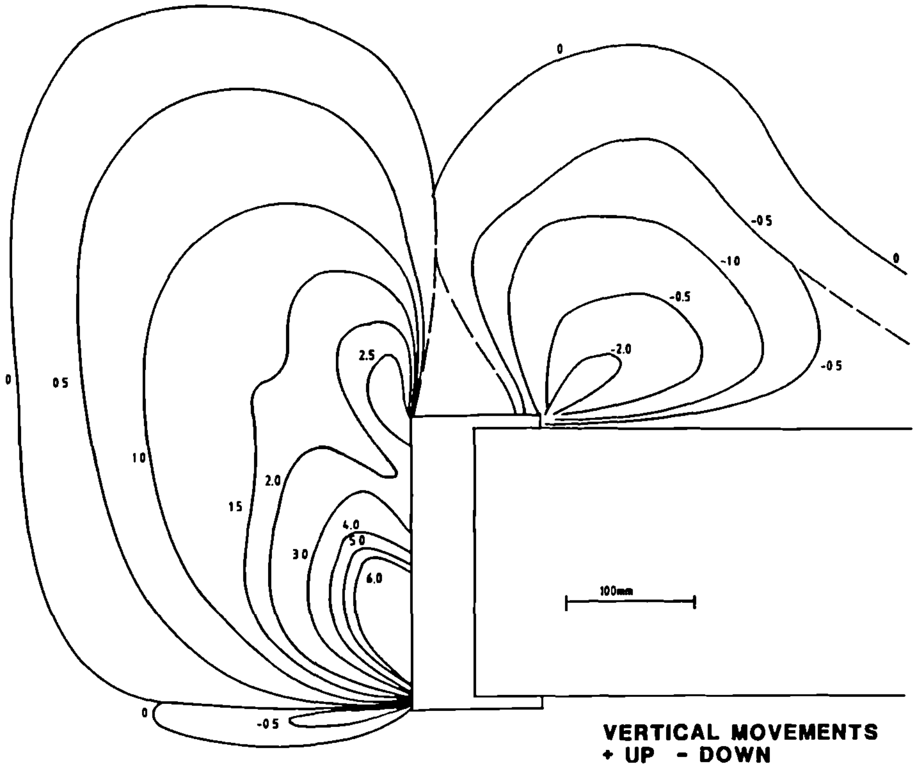

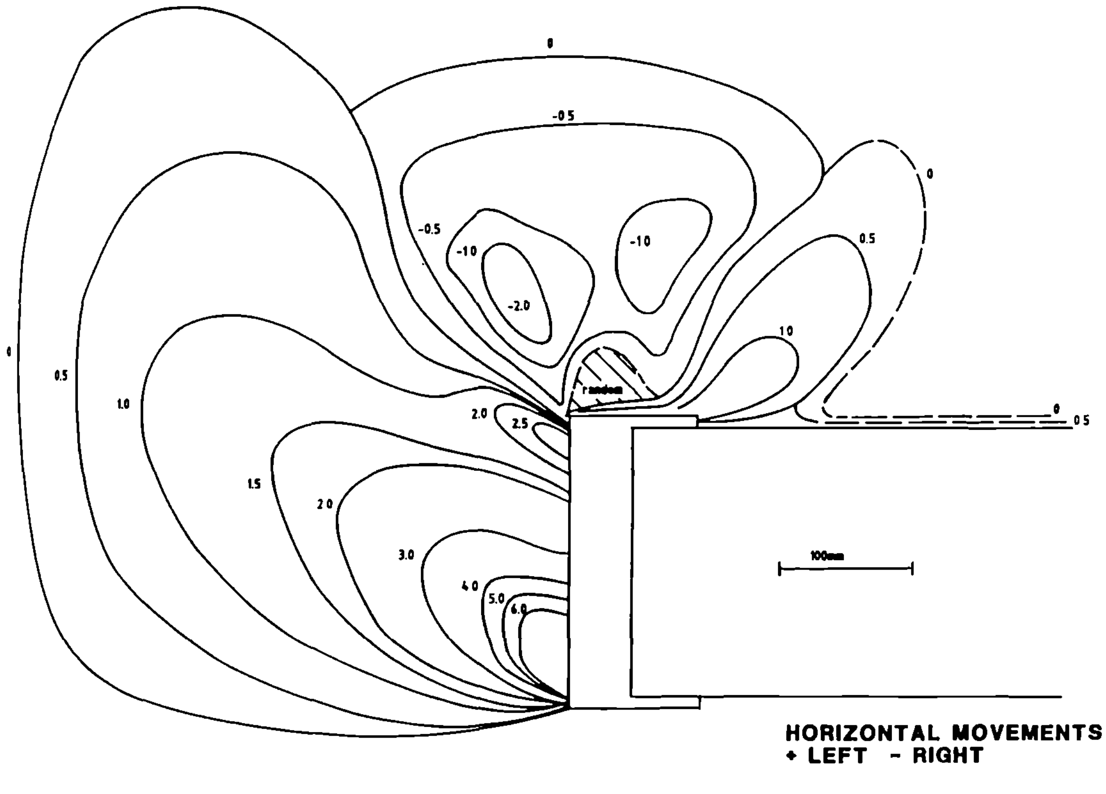

TEST OPJ13

4.5d25B0.1

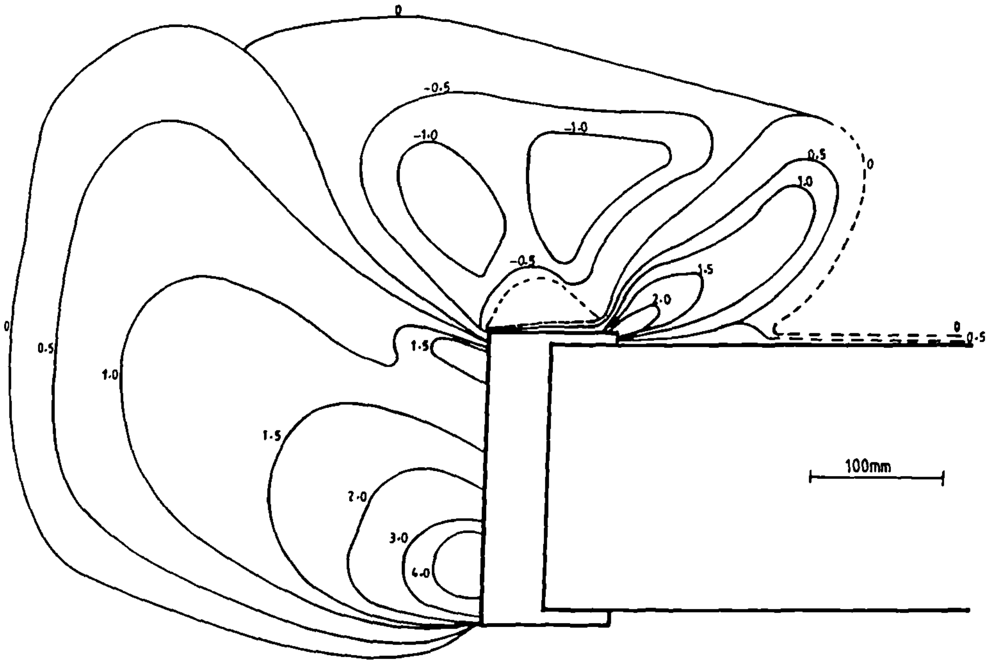

HORIZONTAL MOVEMENTS
+ LEFT - RIGHT

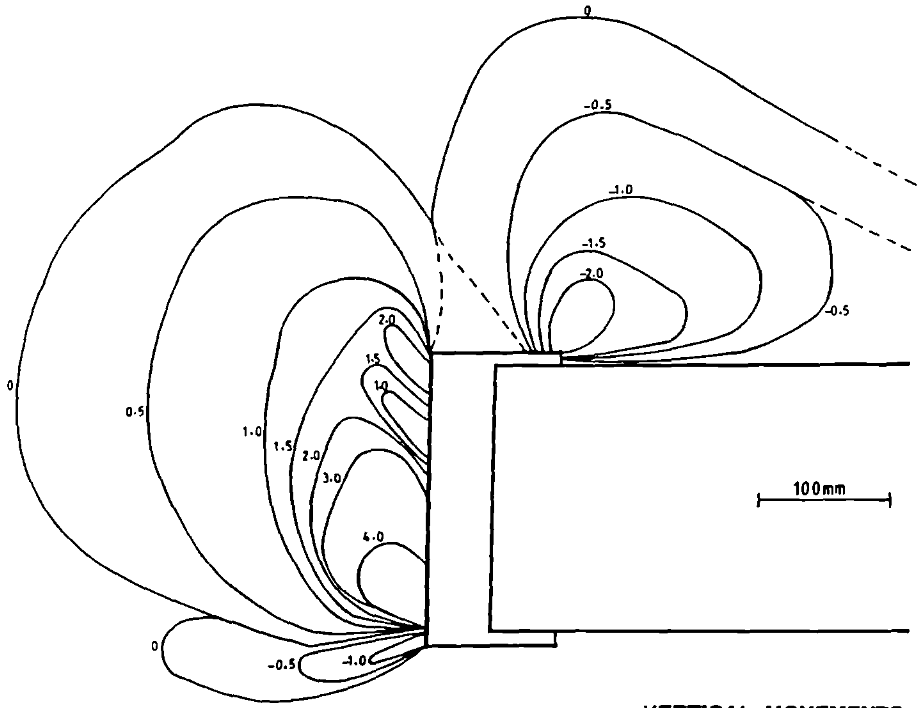

VERTICAL MOVEMENTS
+ UP - DOWN

TEST OPJ14

12.5d25B0.1

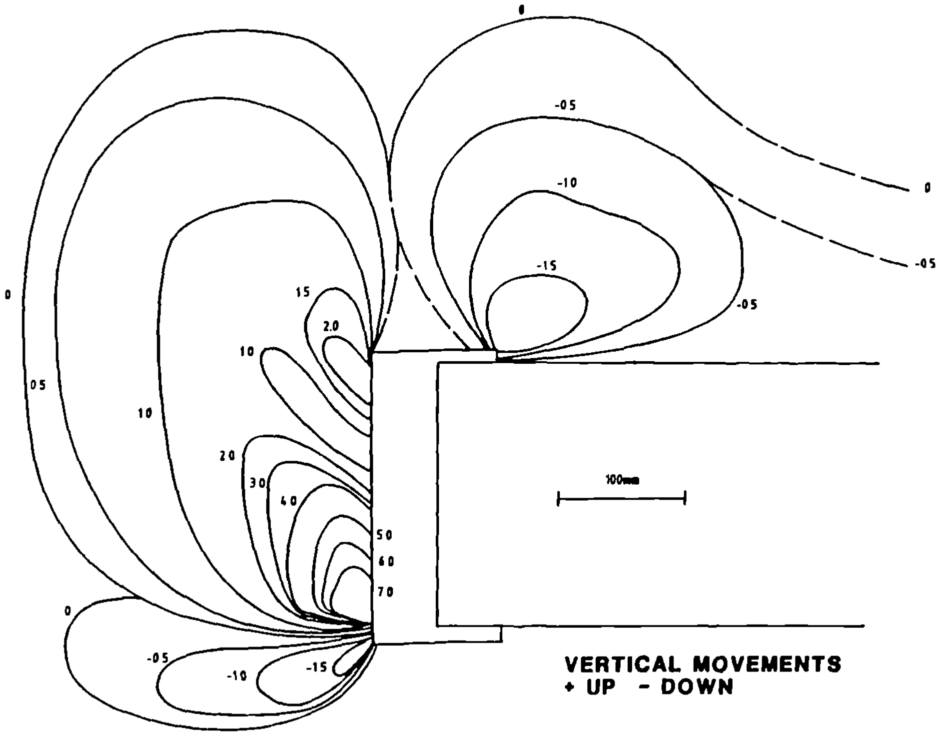

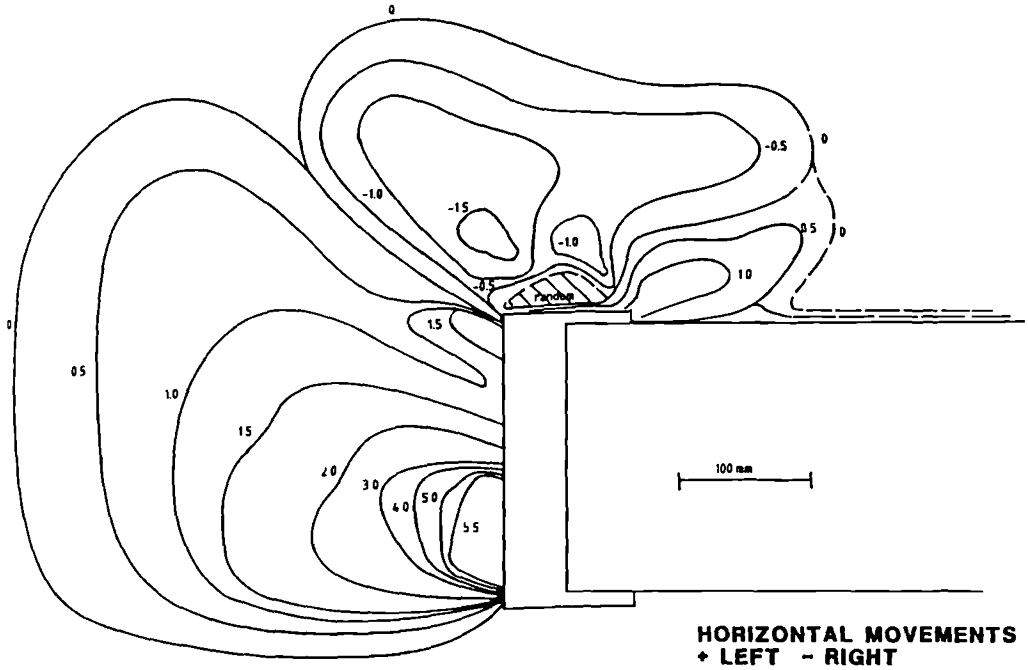

TEST OPJ15

20.0d25B0.1

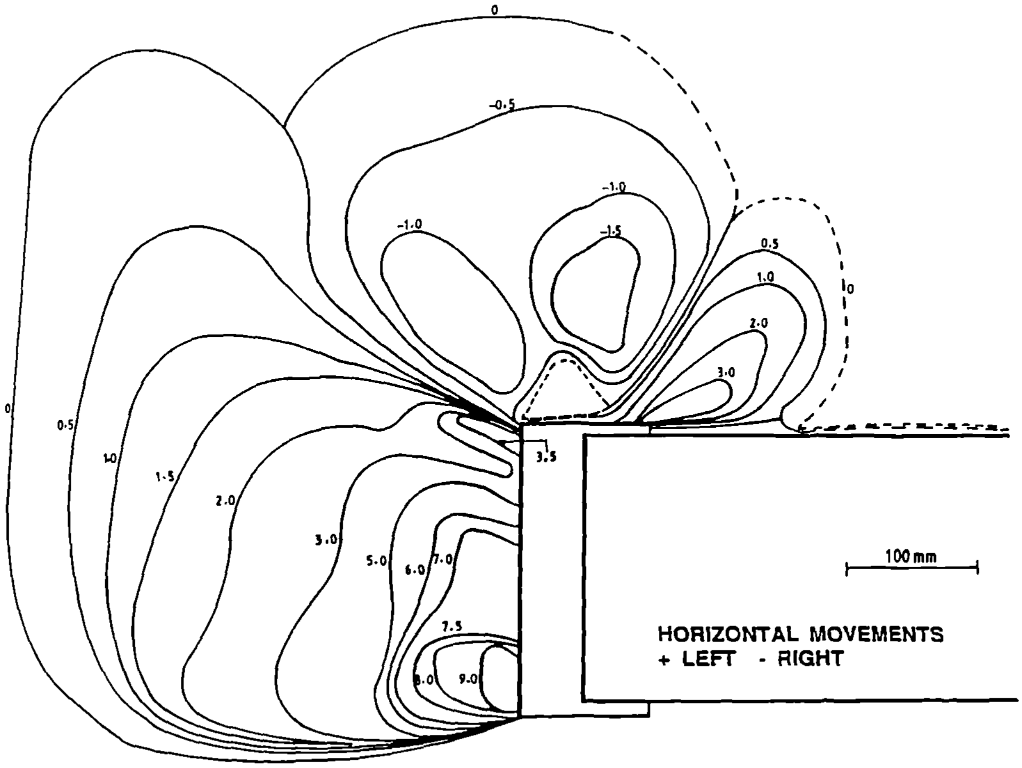

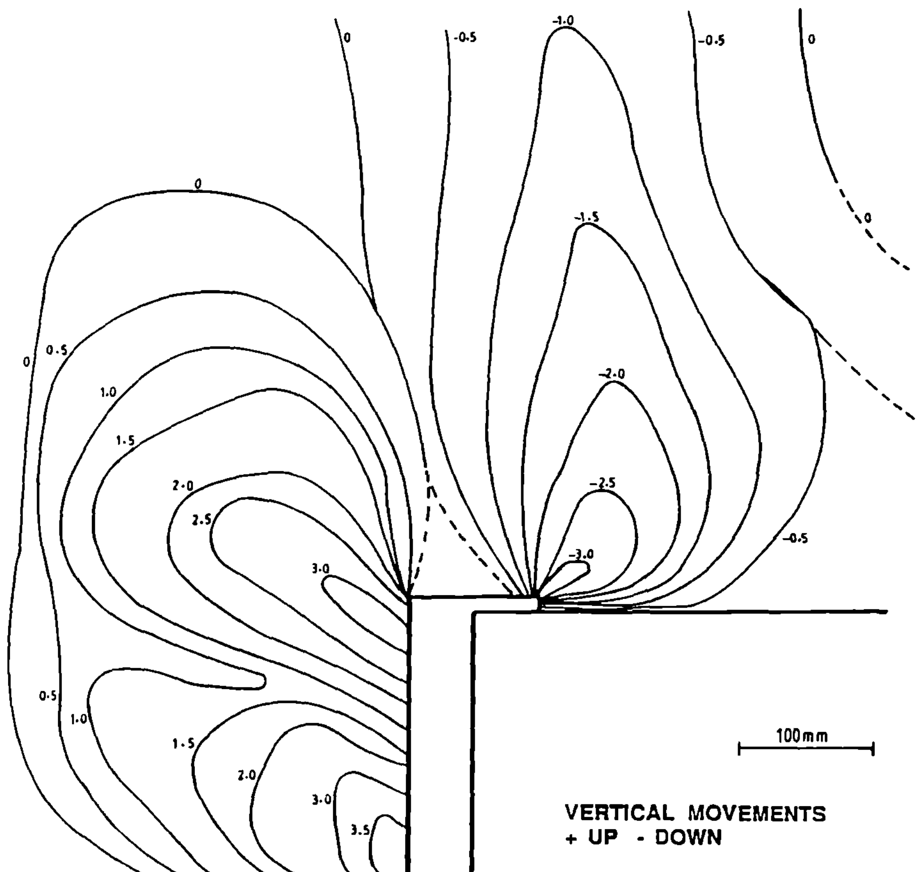

TEST OPJ16

4.5125B0.1

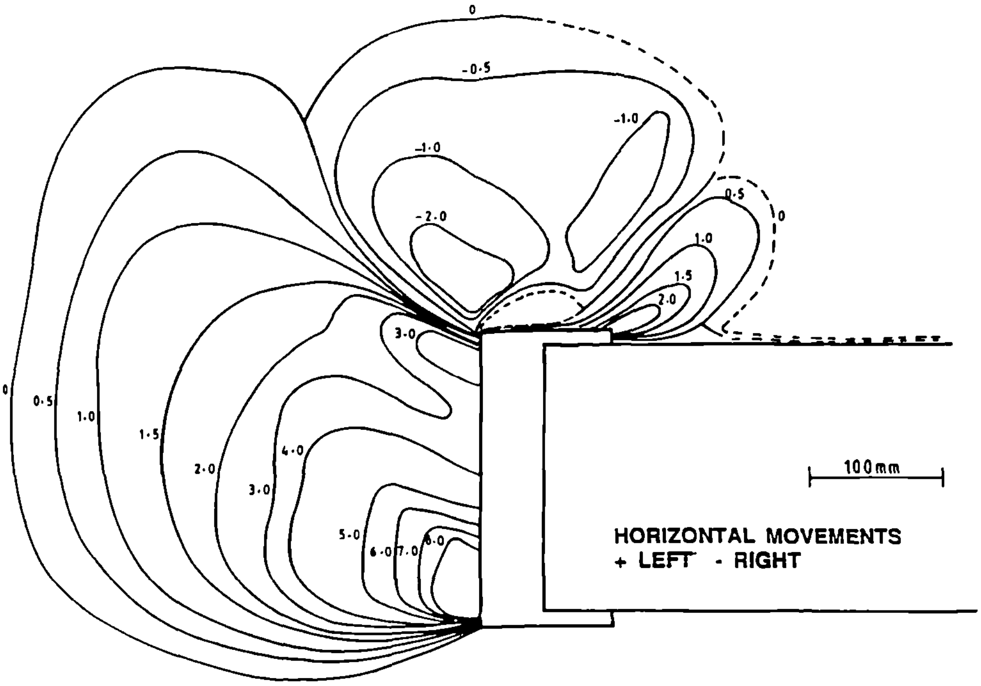

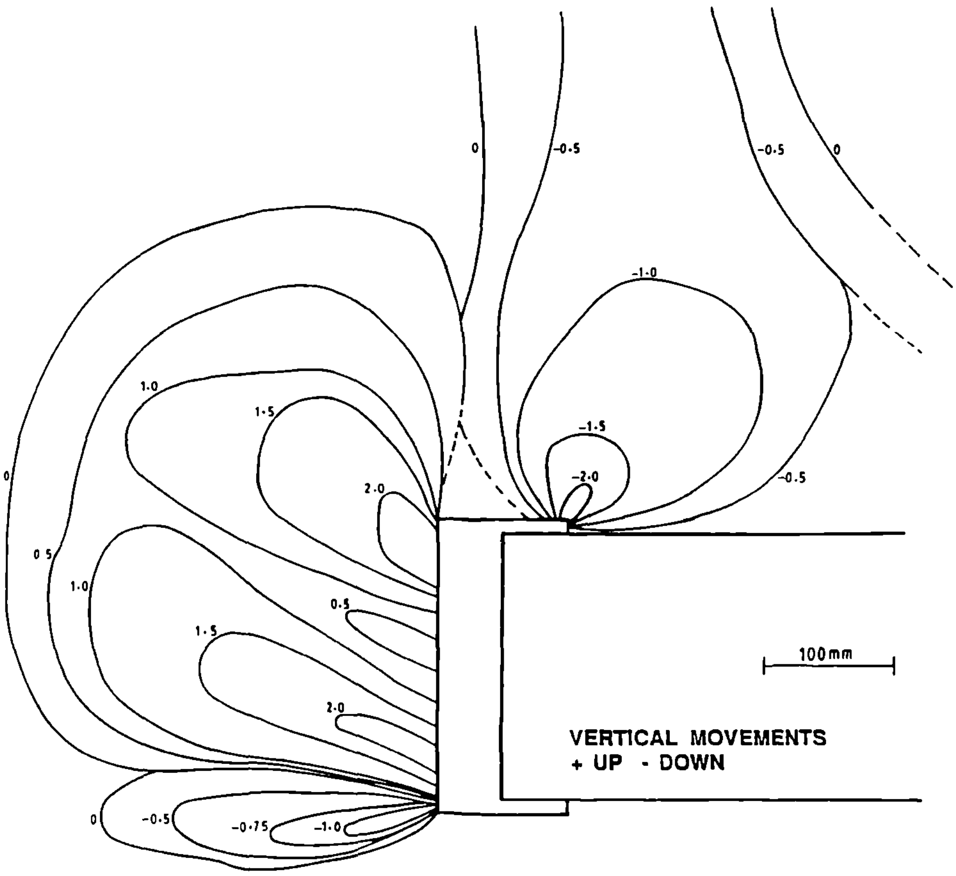

TEST OPJ17

12.5125B0.1

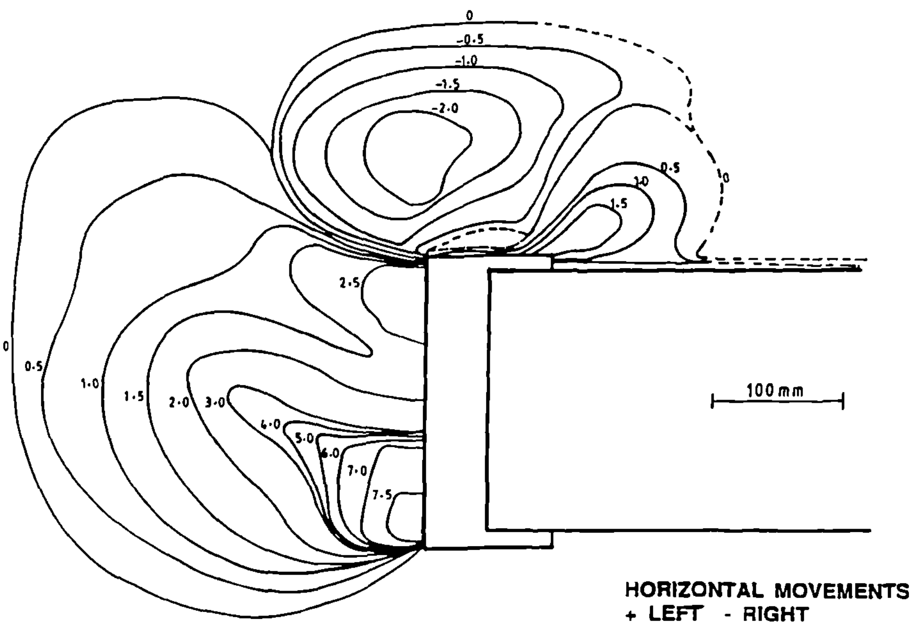

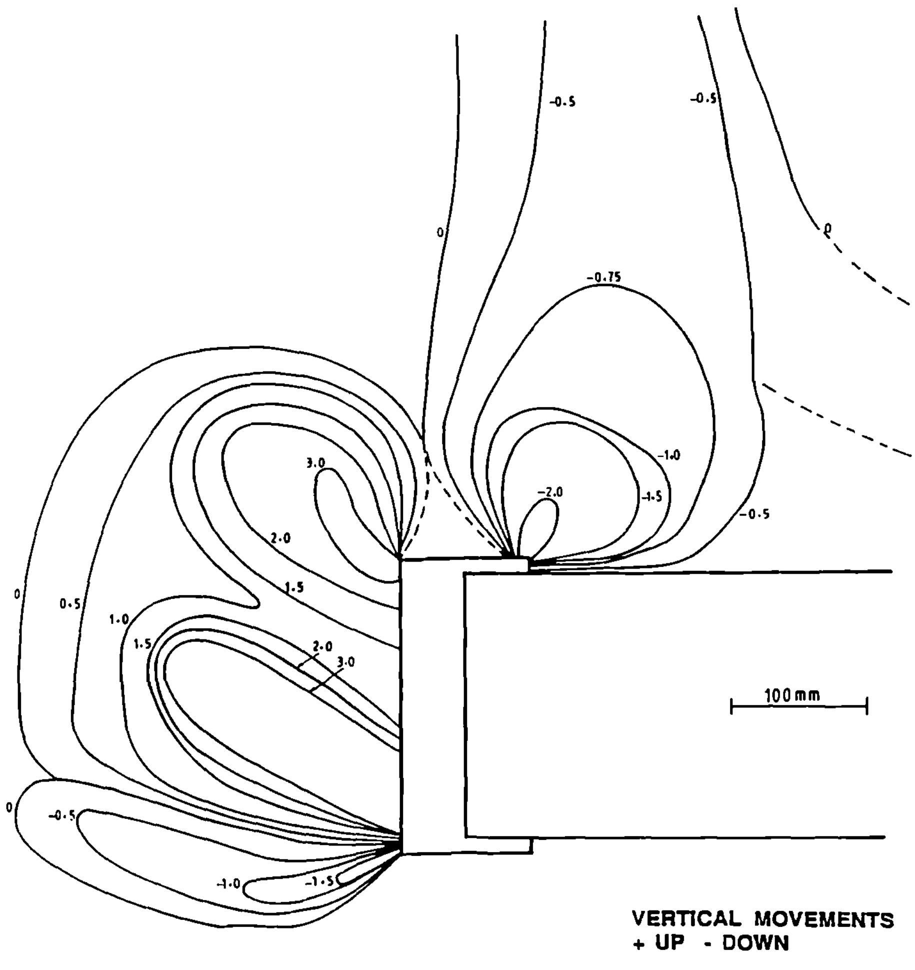

TEST OPJ18

20.0125B0.1

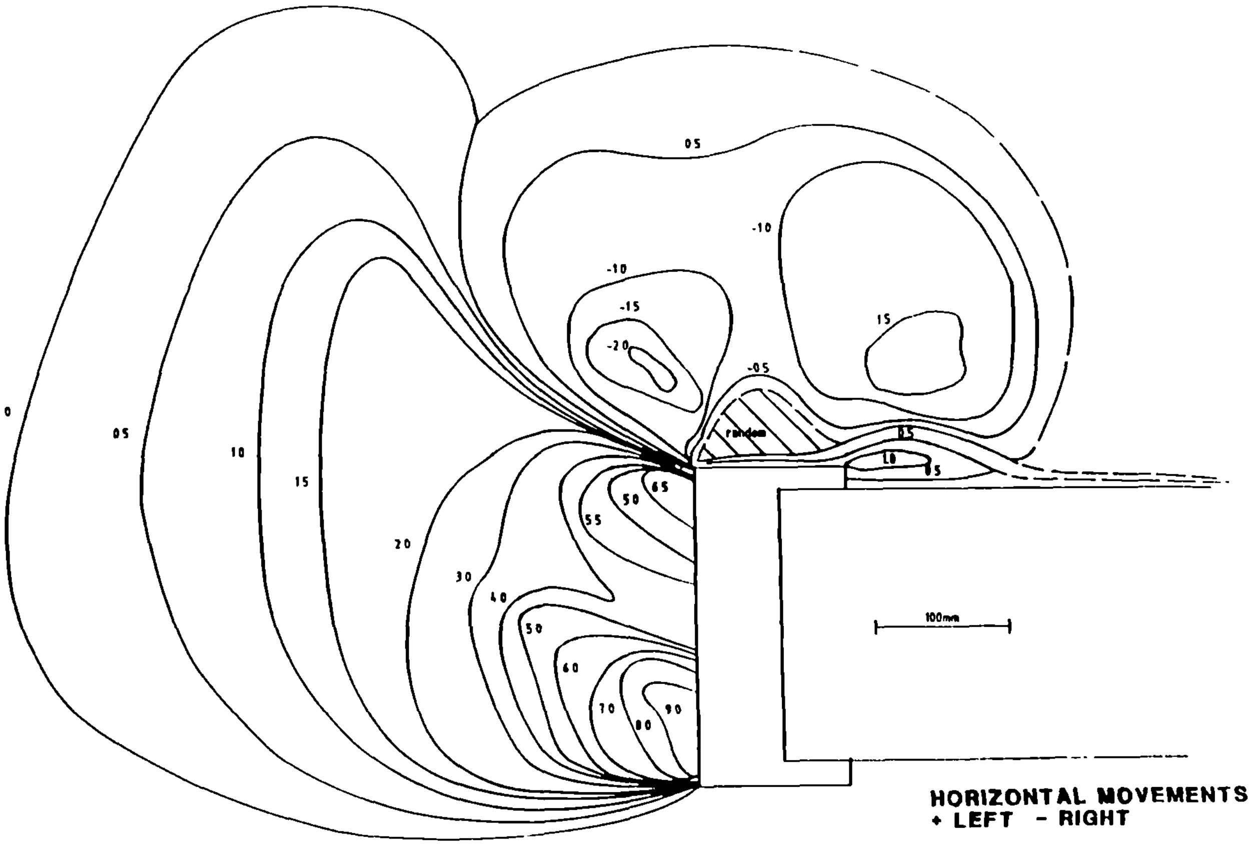

TEST OPJ19

4.5d25B0.2

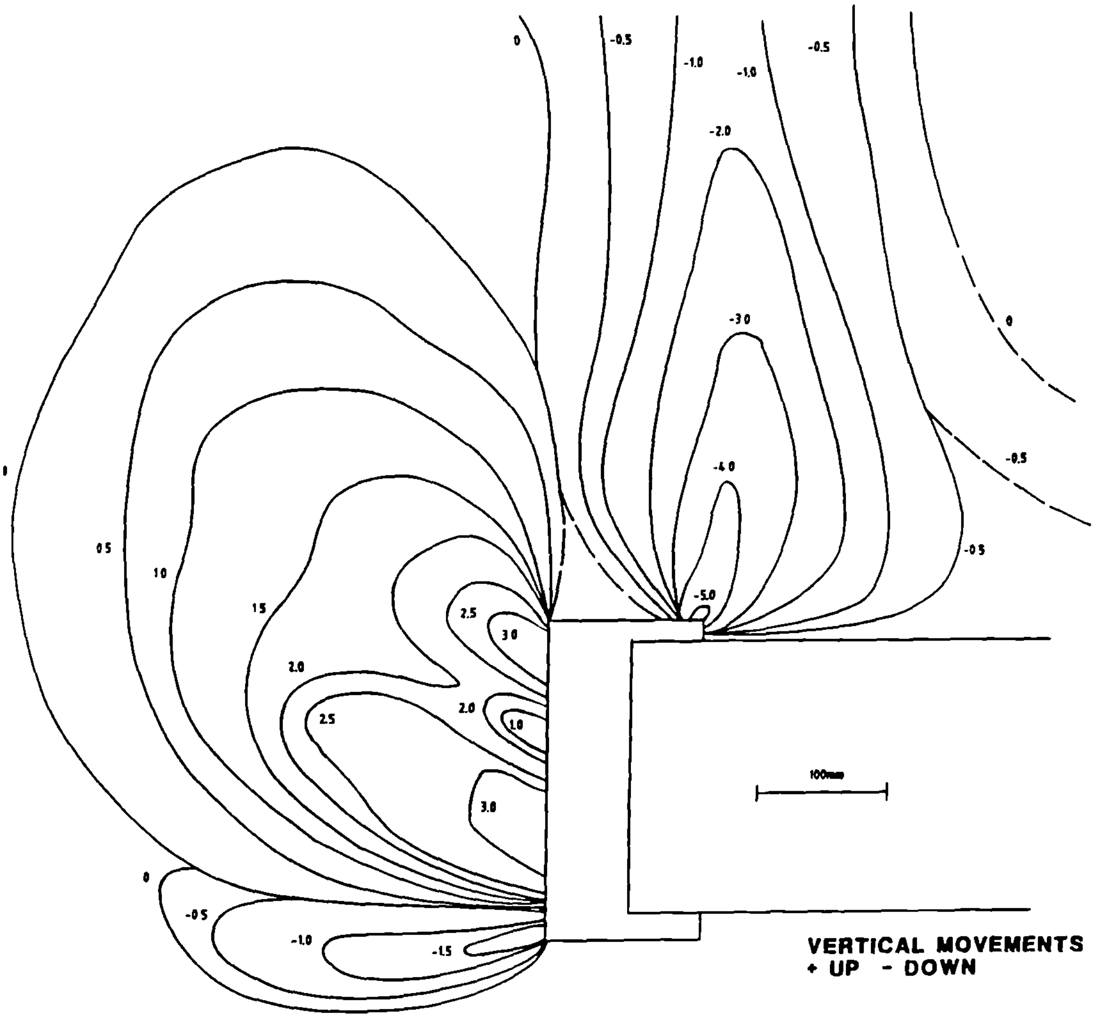

TEST OPJ19

4.5d25B0.2

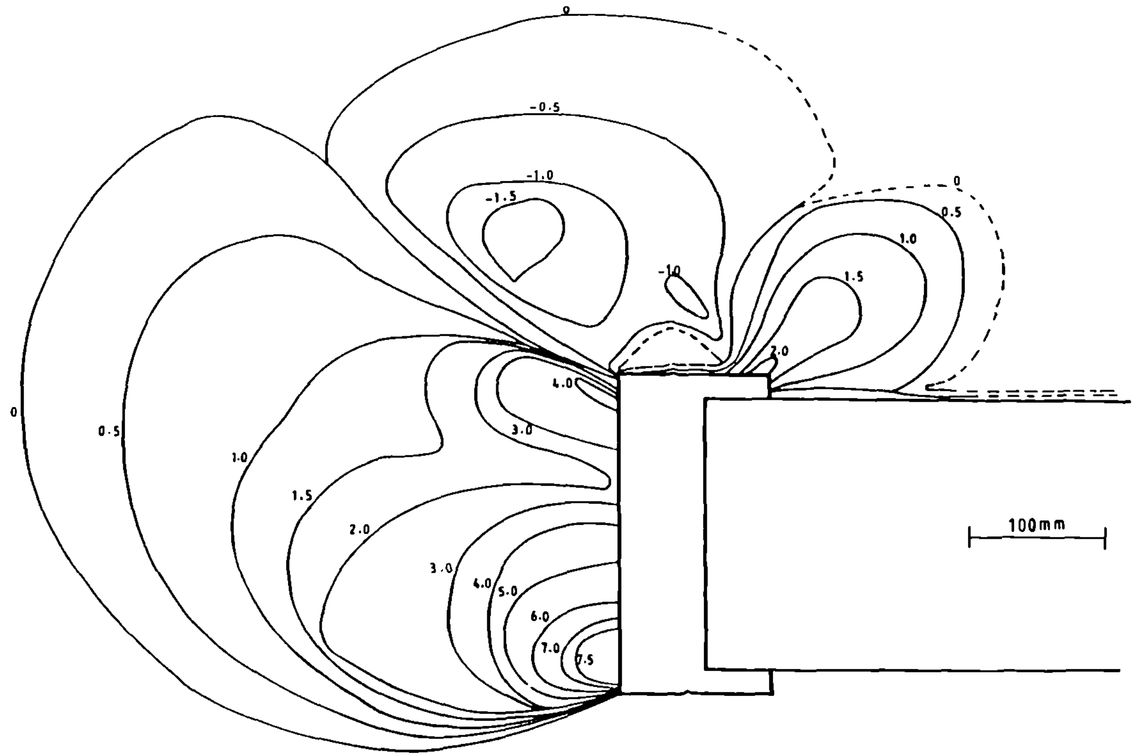

HORIZONTAL MOVEMENTS
+ LEFT - RIGHT

TEST OPJ20

12.5d25B0.2

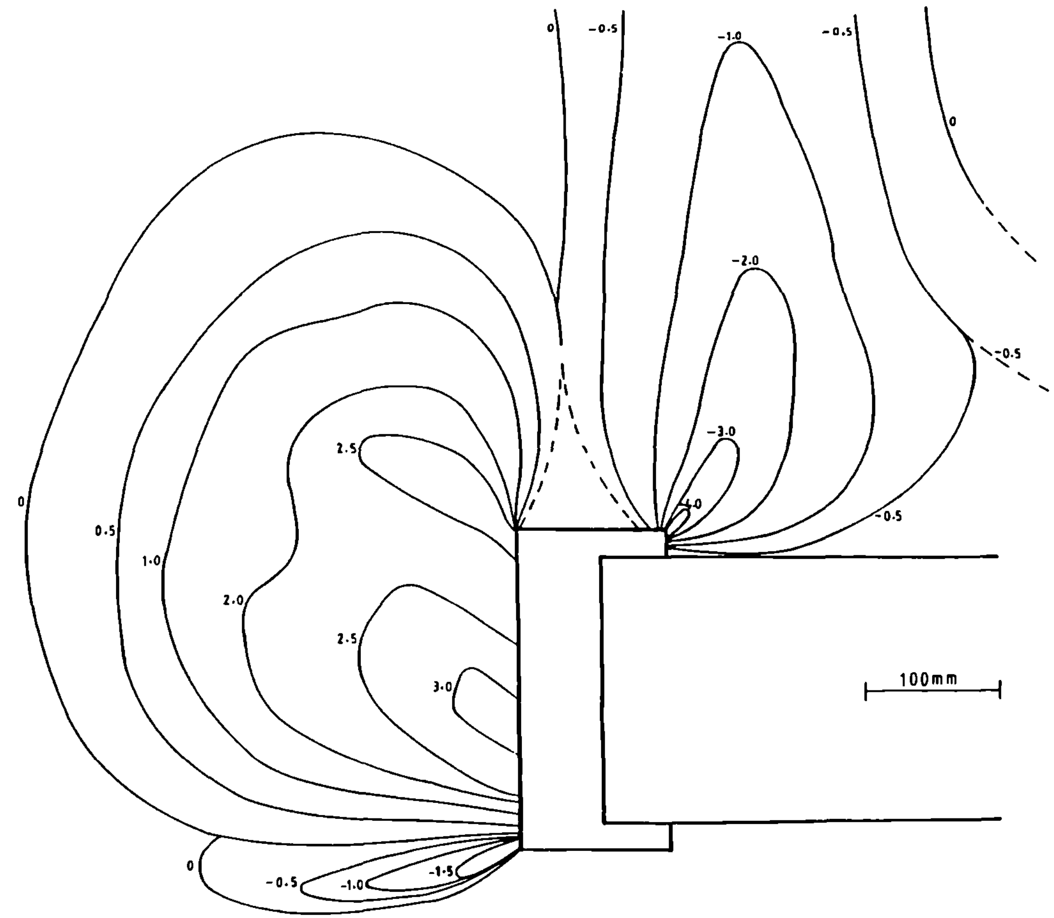

VERTICAL MOVEMENTS
+ UP - DOWN

TEST OPJ20
12.5d25B0.2

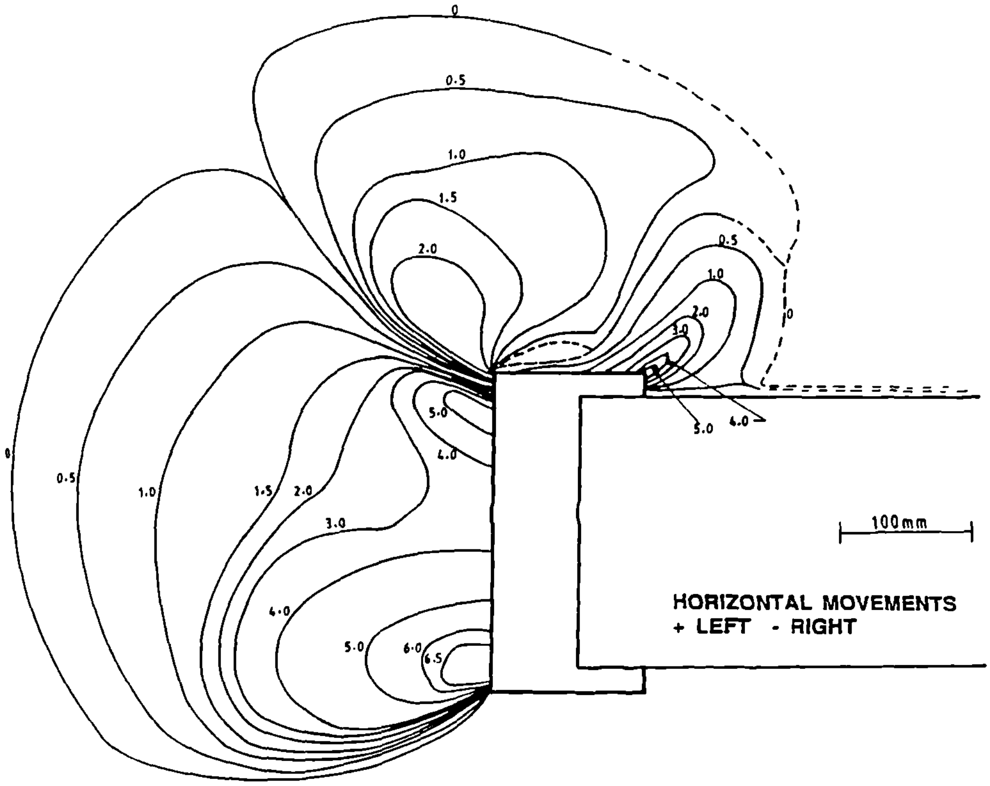

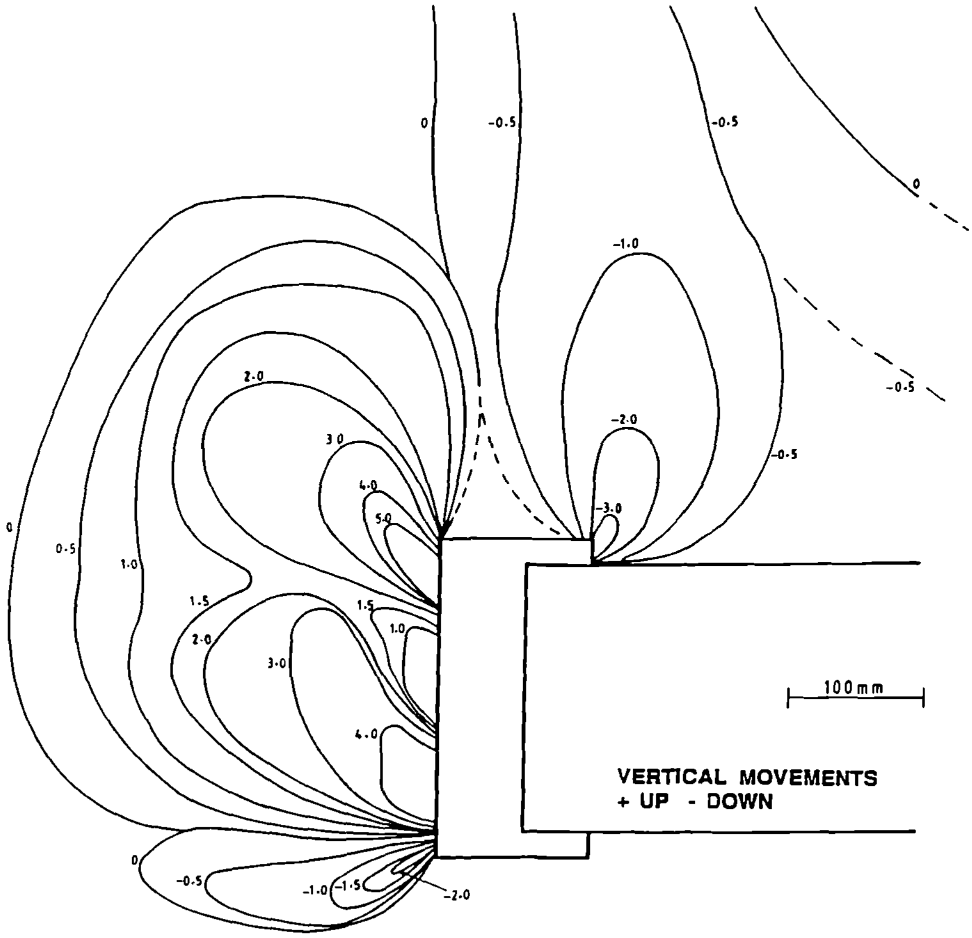

TEST OPJ21

20.0d25B0.2

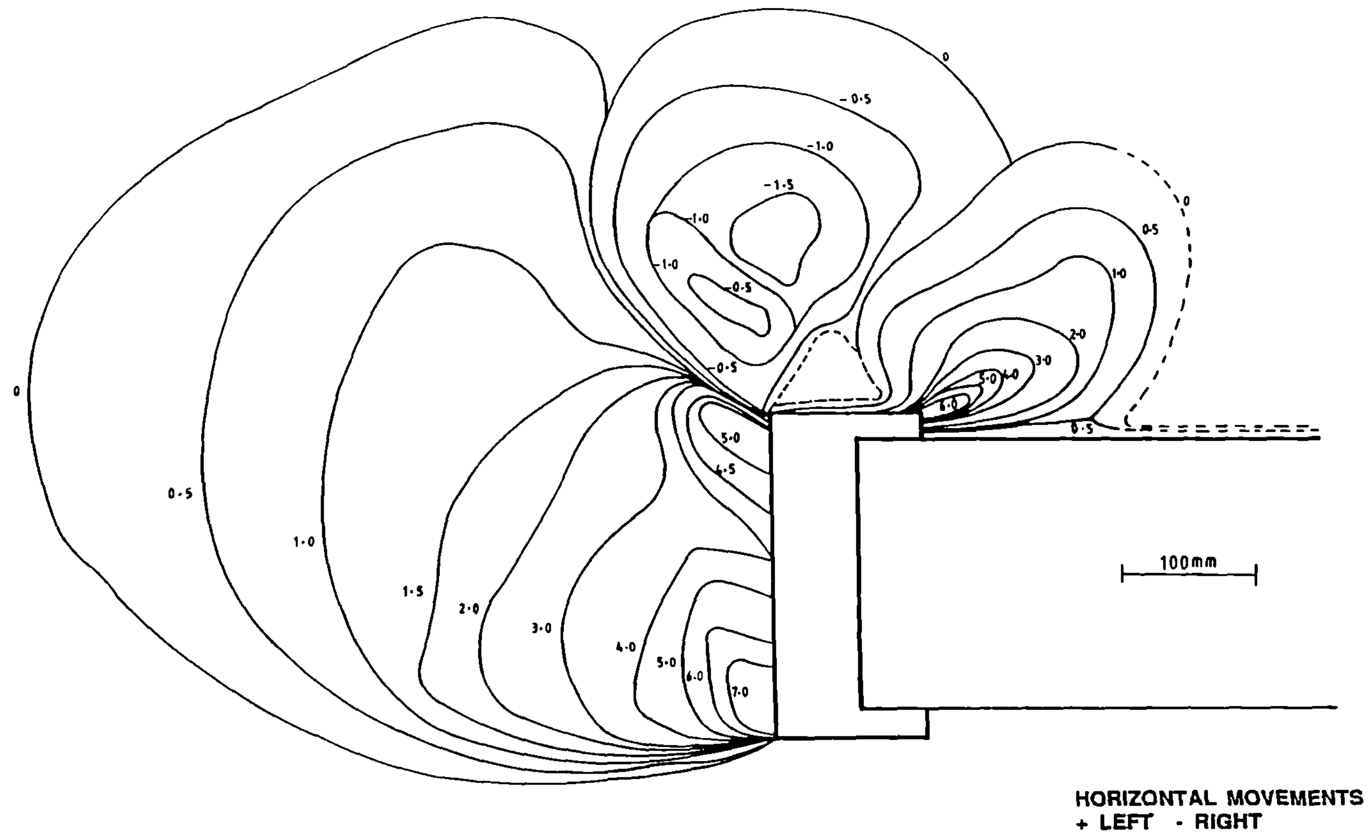

TEST OPJ22

4.5125B0.2

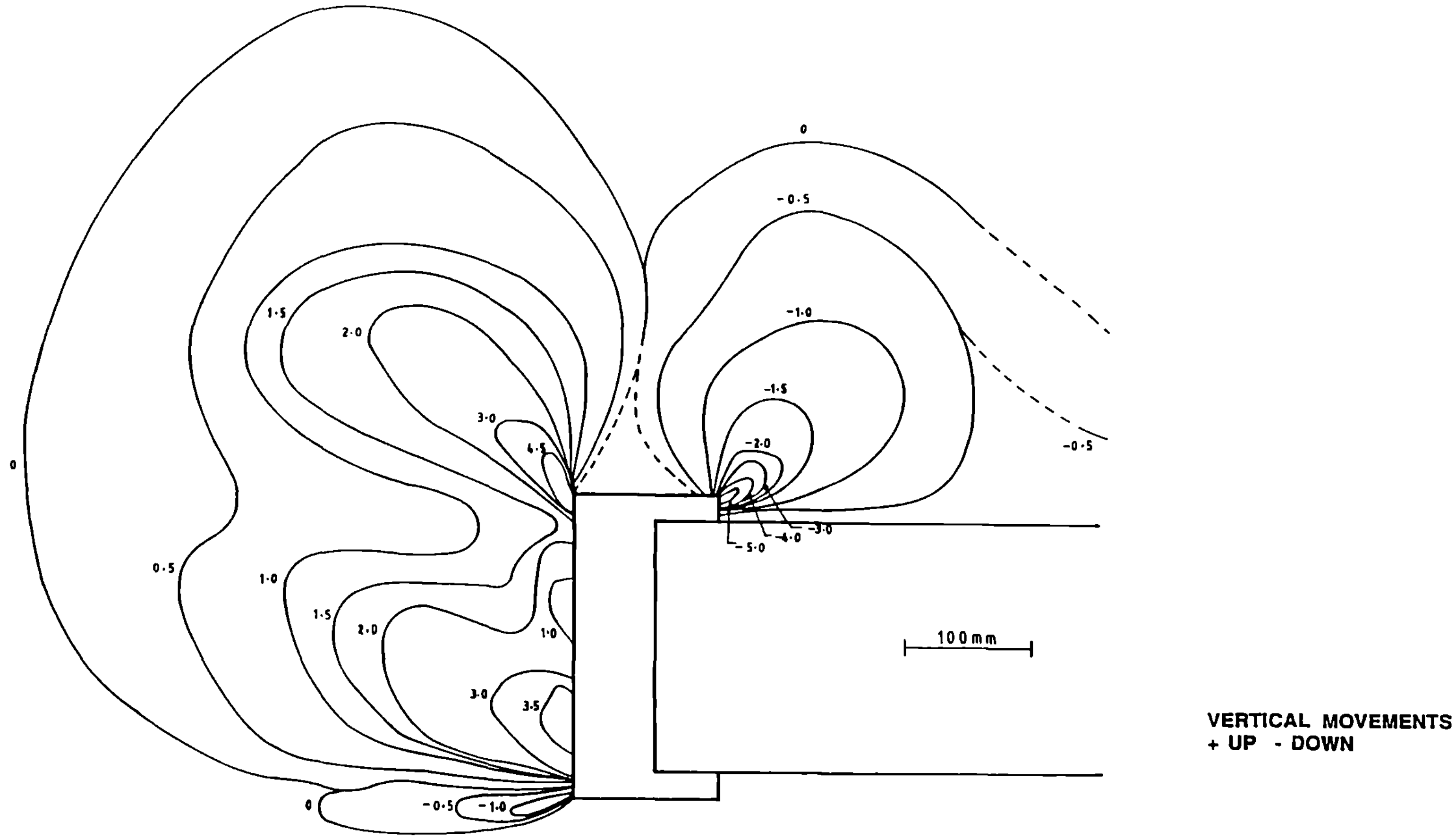

TEST OPJ22
4.5125B0.2

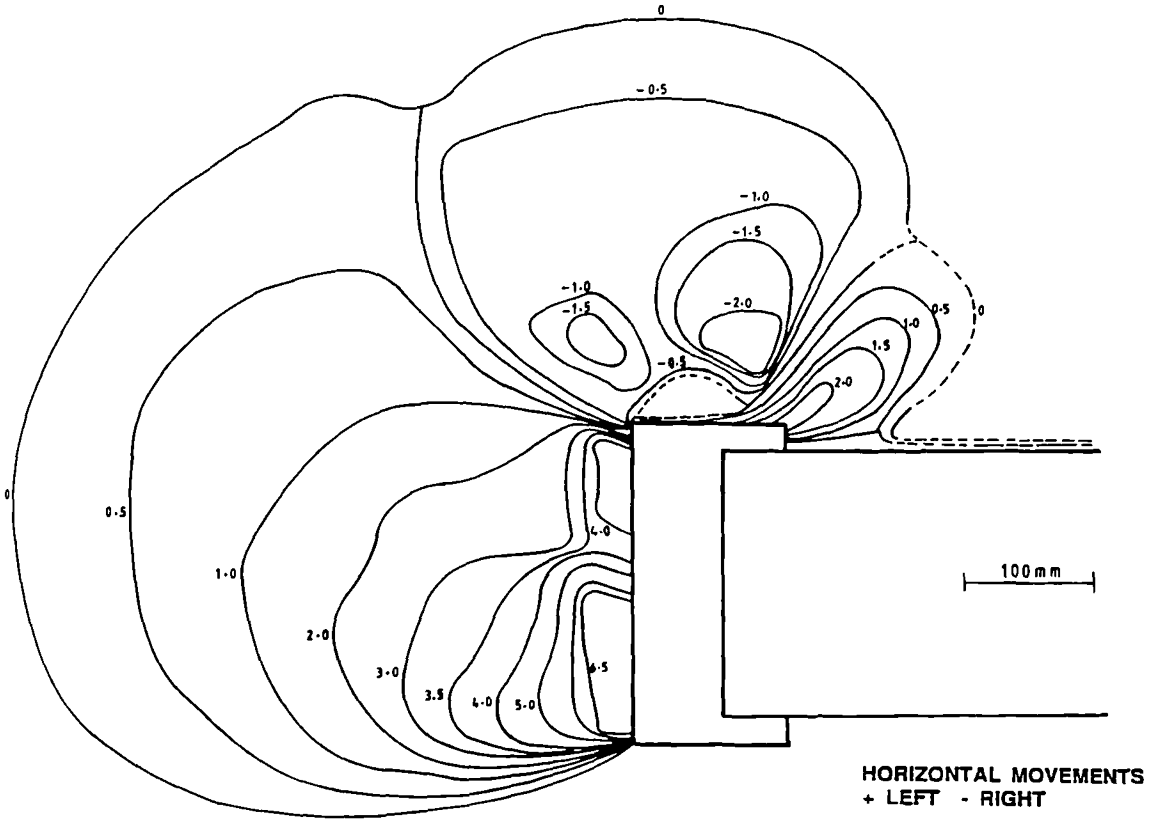

HORIZONTAL MOVEMENTS
+ LEFT - RIGHT

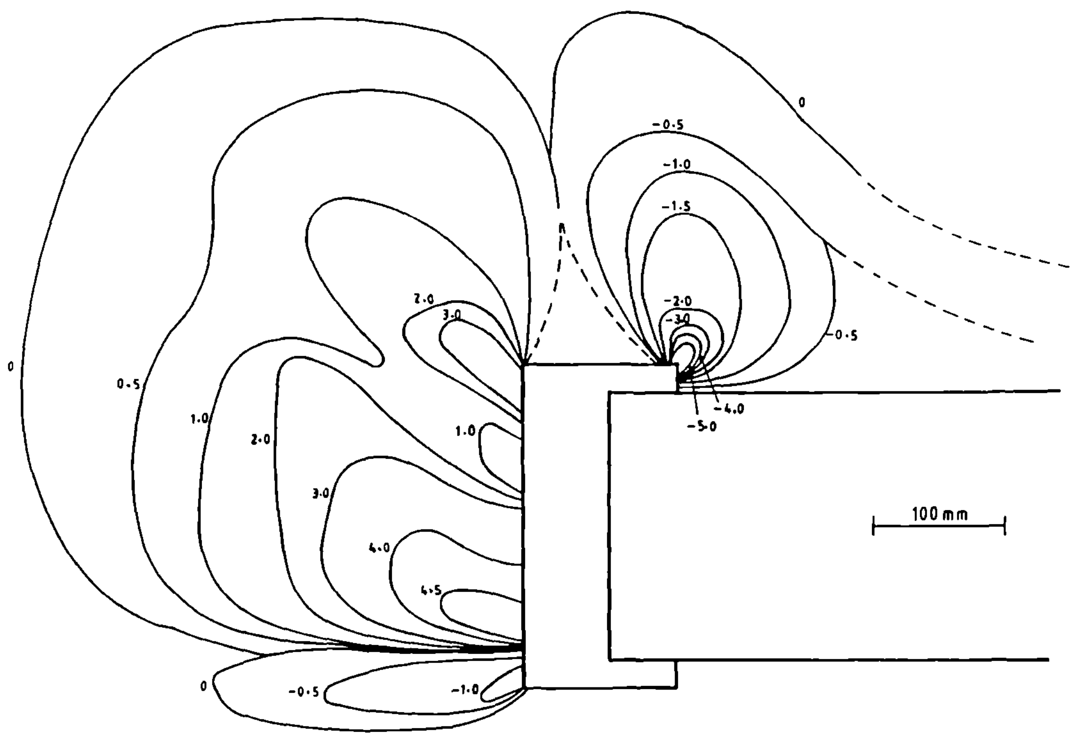

VERTICAL MOVEMENTS
+ UP - DOWN

TEST OPJ23
12.5125B0.2

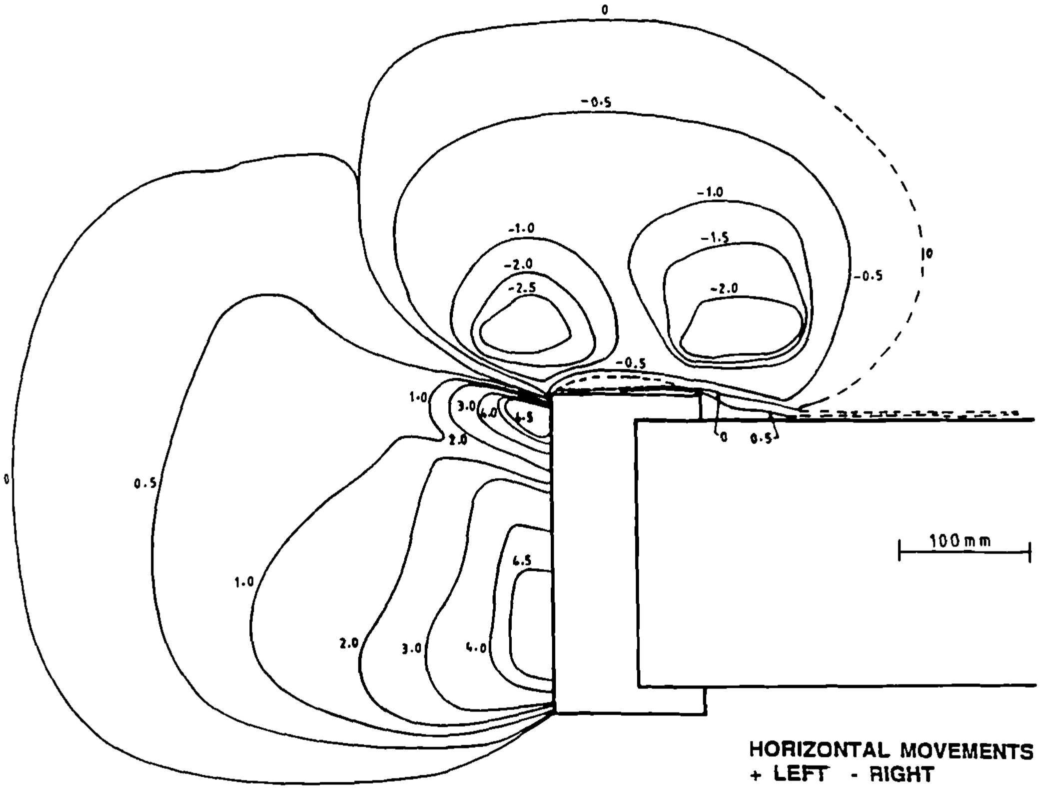

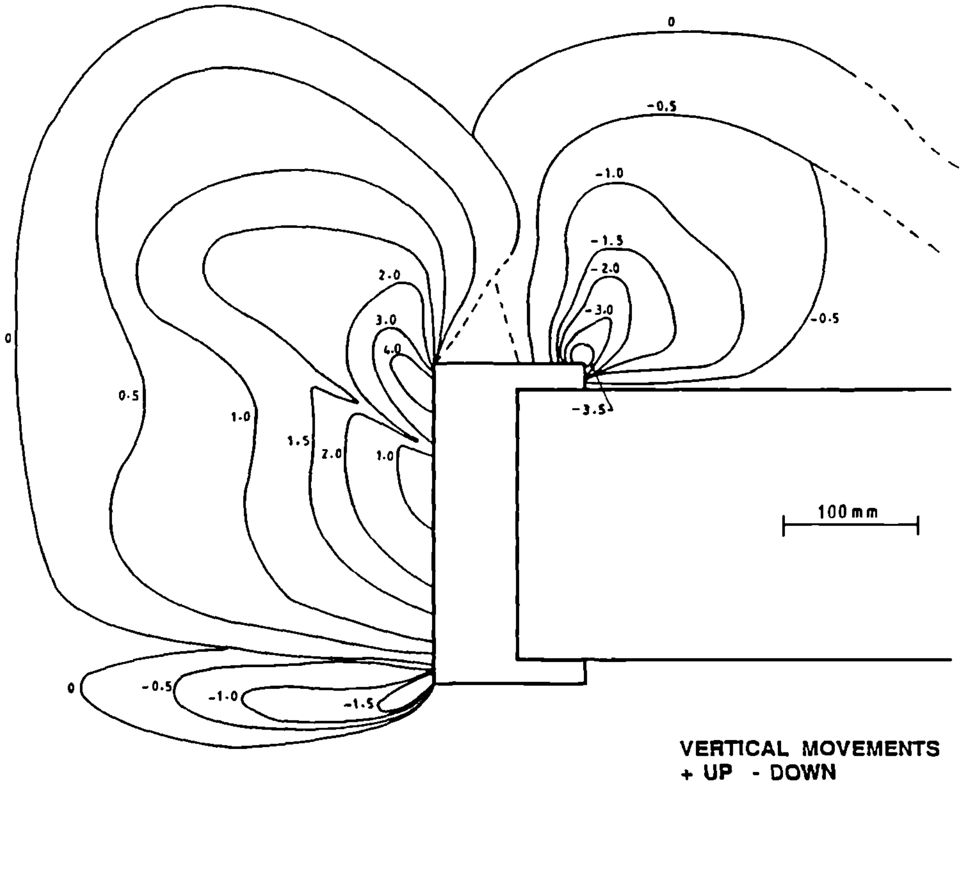

TEST OPJ24
20.0125B0.2

B.2 OPEN SHIELD PIPEJACKING TESTS - PERPENDICULAR PLANE RESULTS

The following figures show the horizontal and vertical displacement contour plots for the open shield pipejacking tests in the perpendicular plane. The movements were only observed for the tests with C/D ratios of 4.5 and 20. The contours are in millimetres and represent the movements in the sand caused as the overcut on the pipejacking shield passed the plane of observation. Test codes are given to aid comparison between results. The test code is defined as: Cover depth to diameter ratio (C/D), density state of sand, sand type, overcut ratio (t/R).

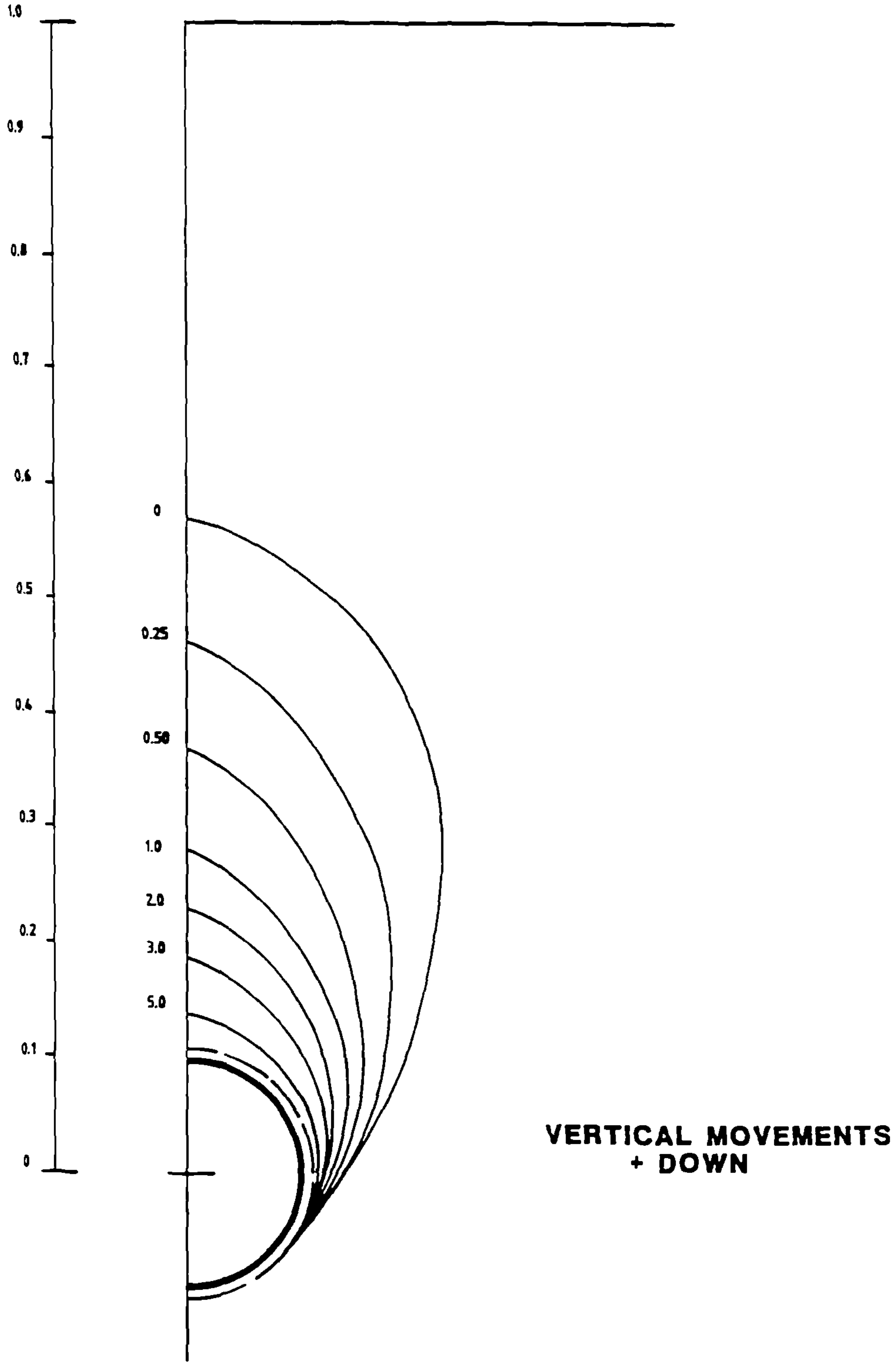

TEST OPJ1

4.5dLB0.1

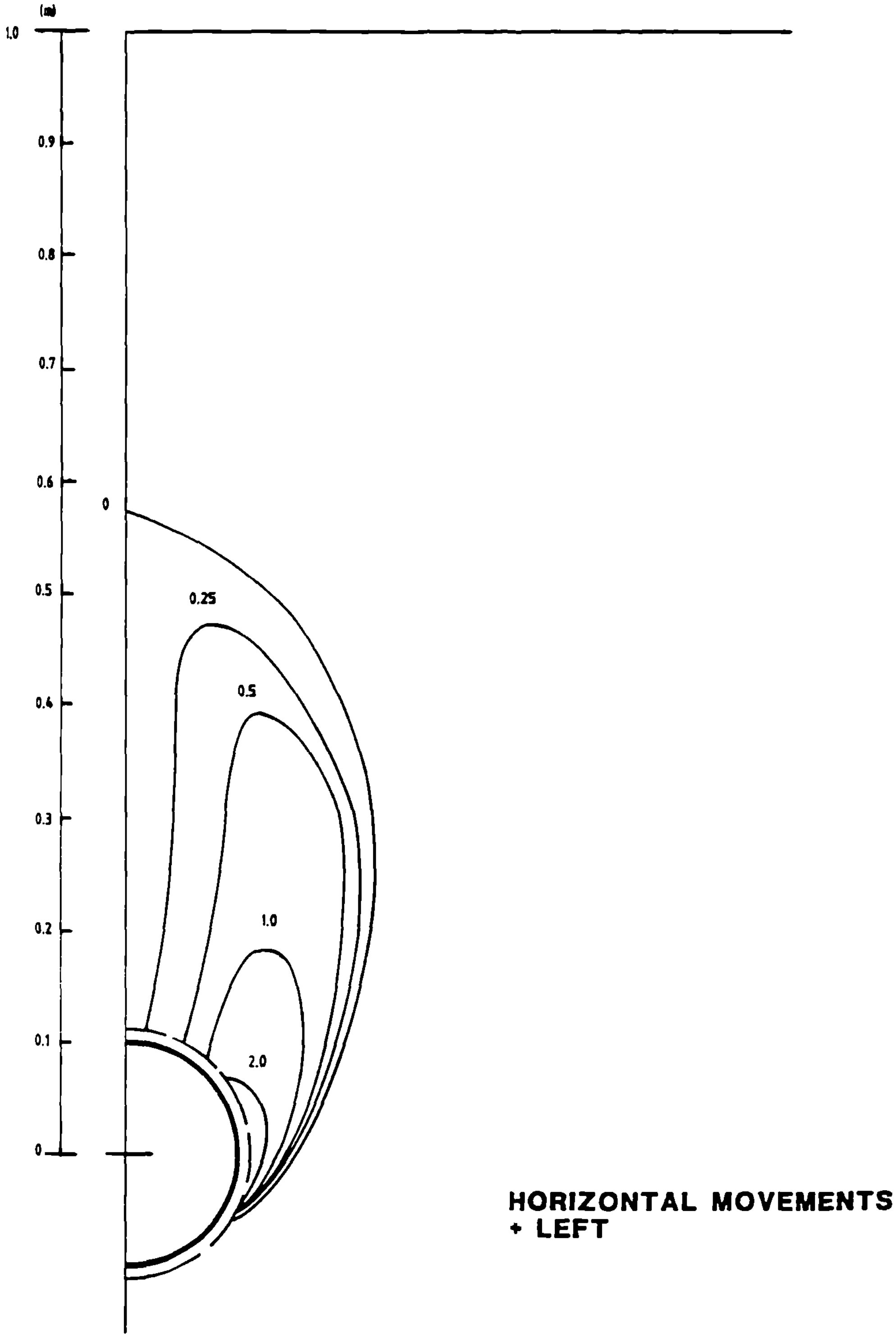

TEST OPJ1

4.5dLB0.1

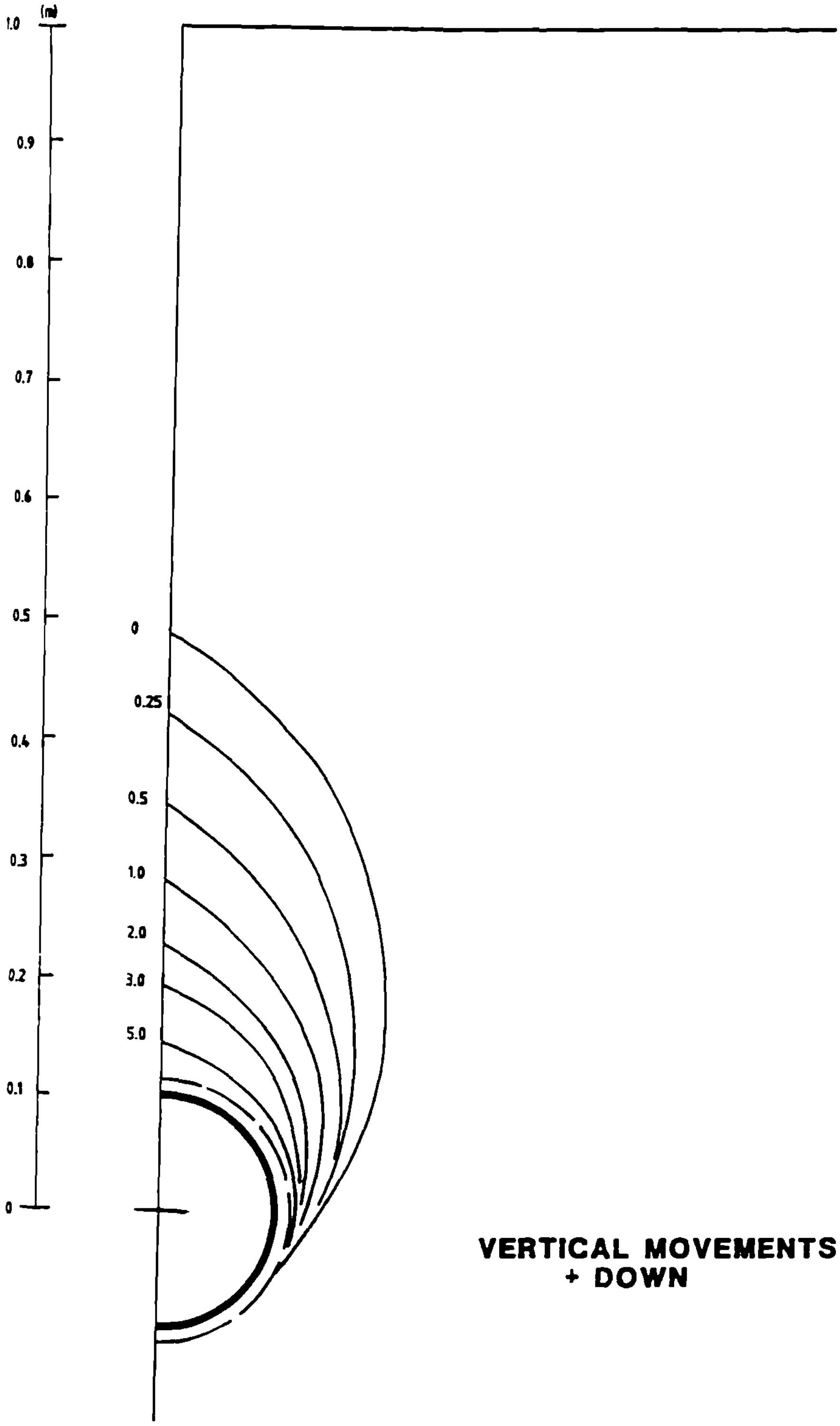

TEST OPJ3
20.0dLB0.1

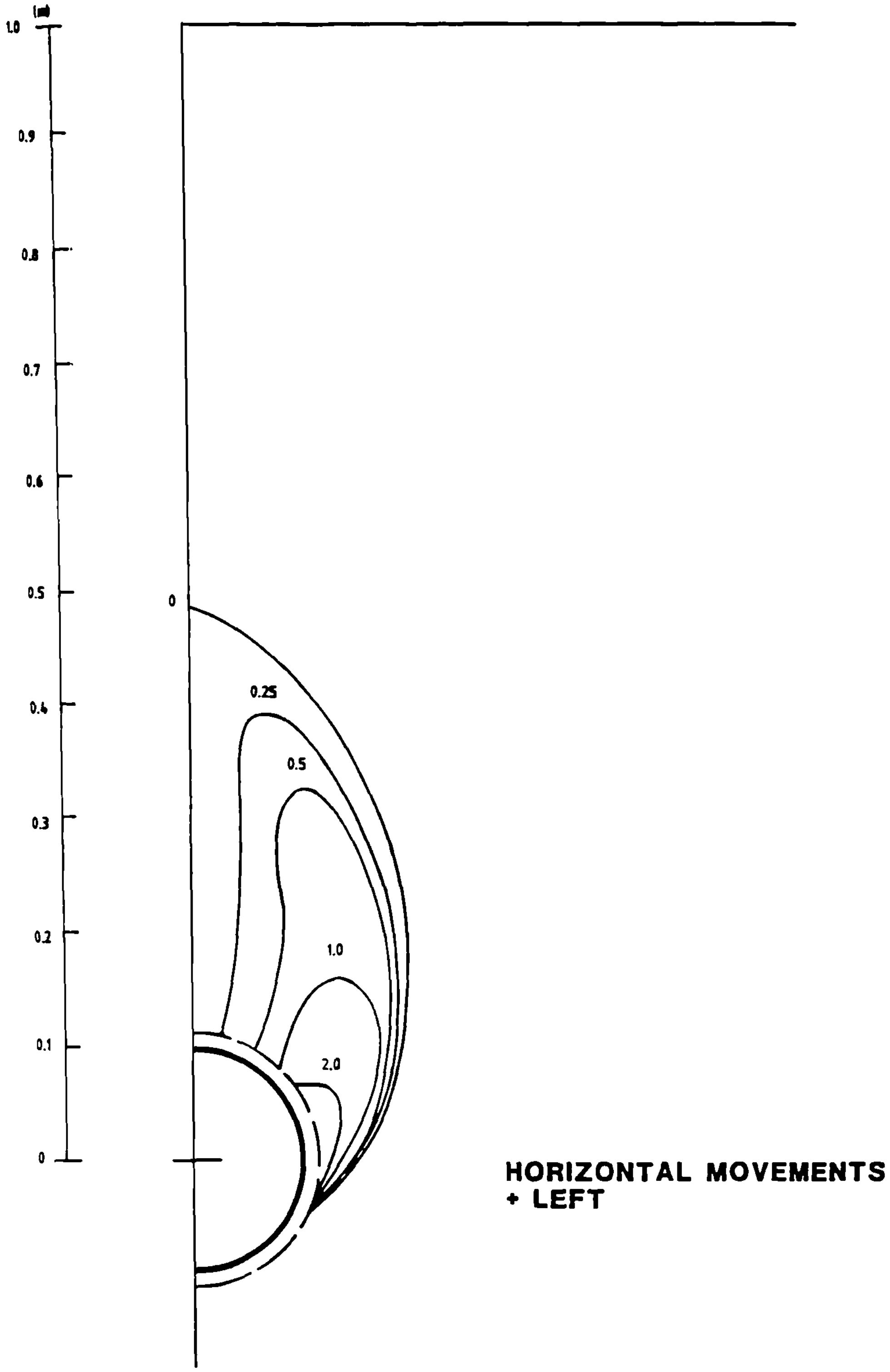

TEST OPJ3

20.0dLB0.1

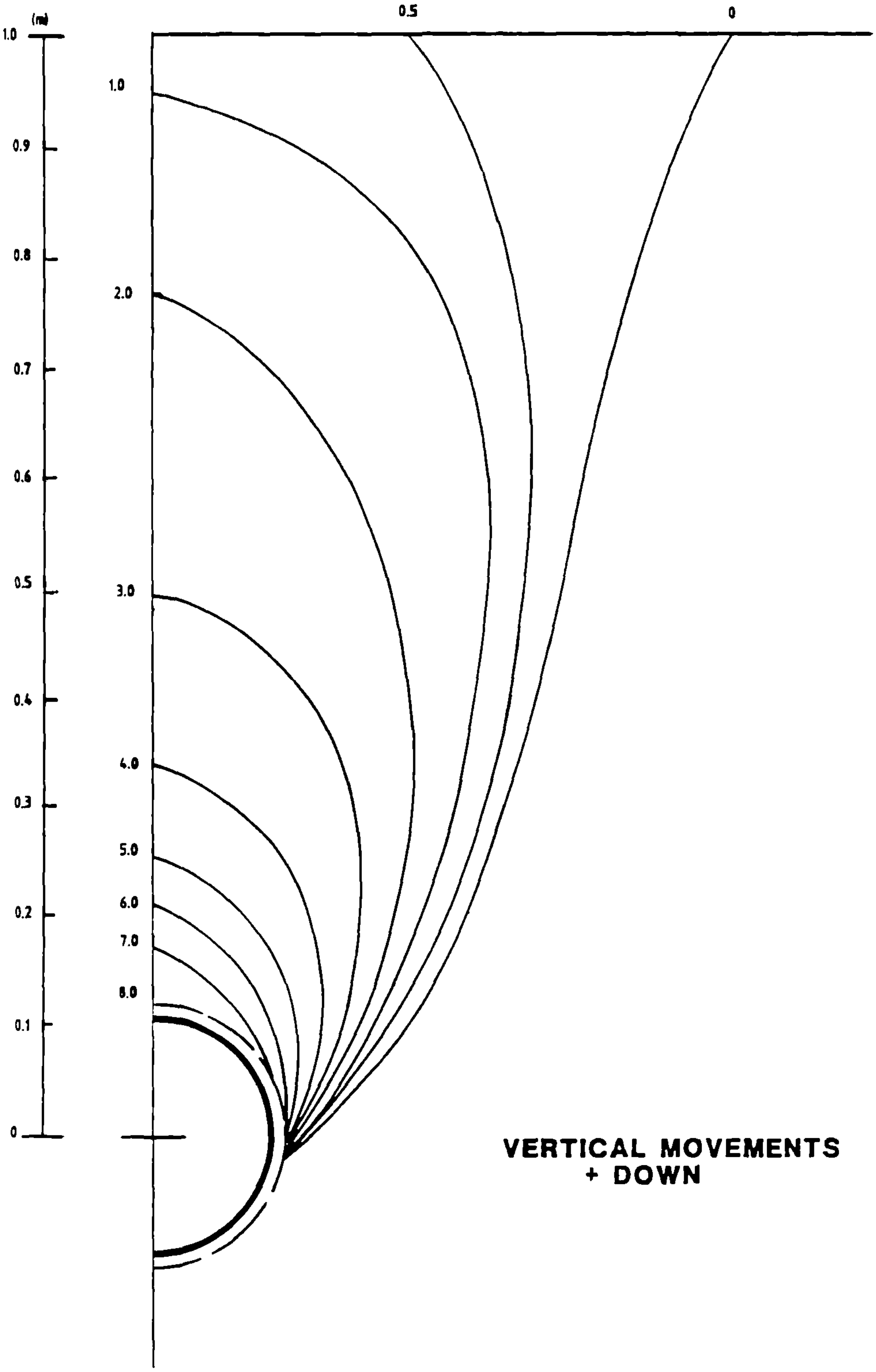

TEST OPJ4

4.5ILB0.1

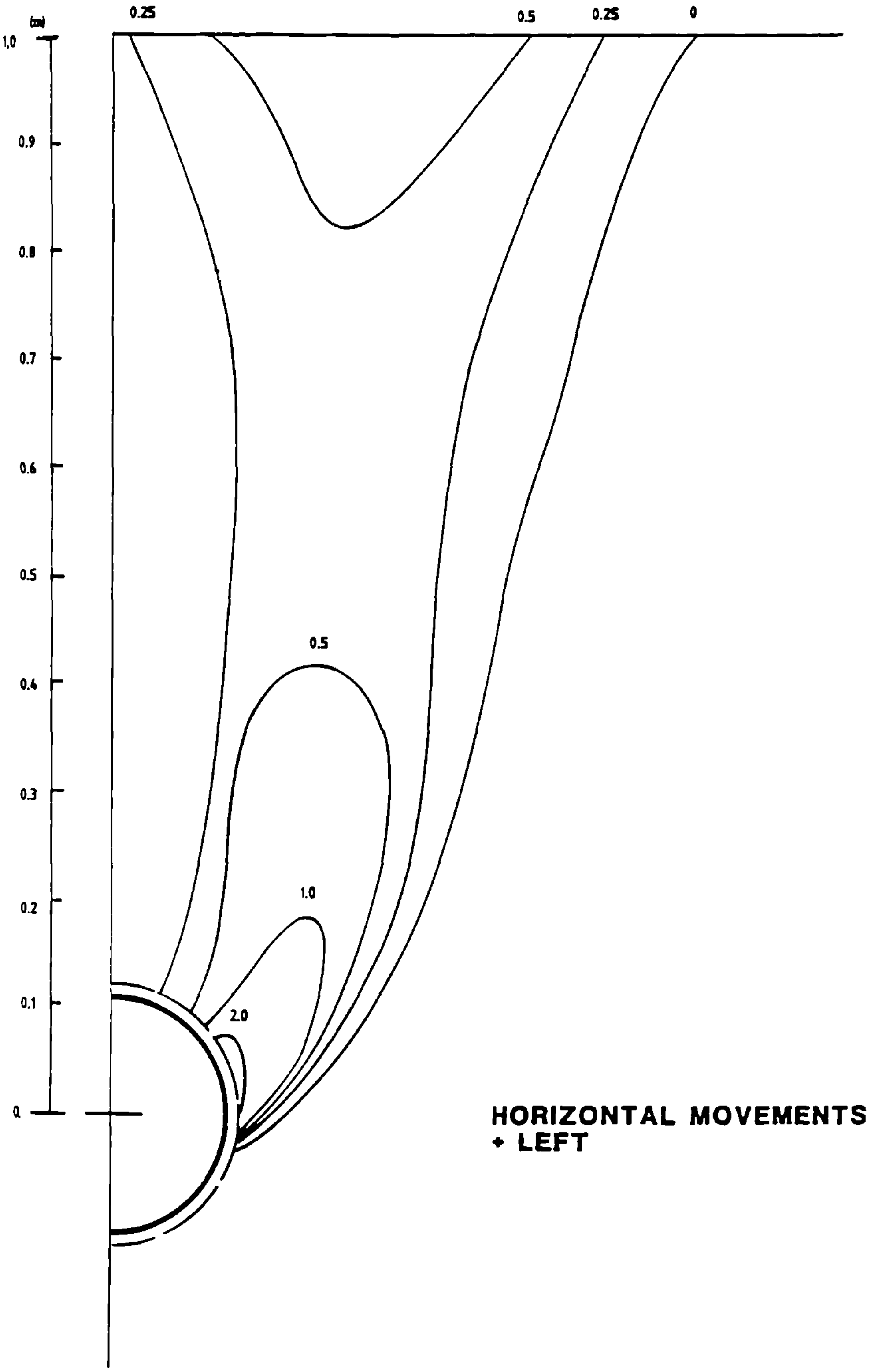

TEST OPJ4

4.5ILB0.1

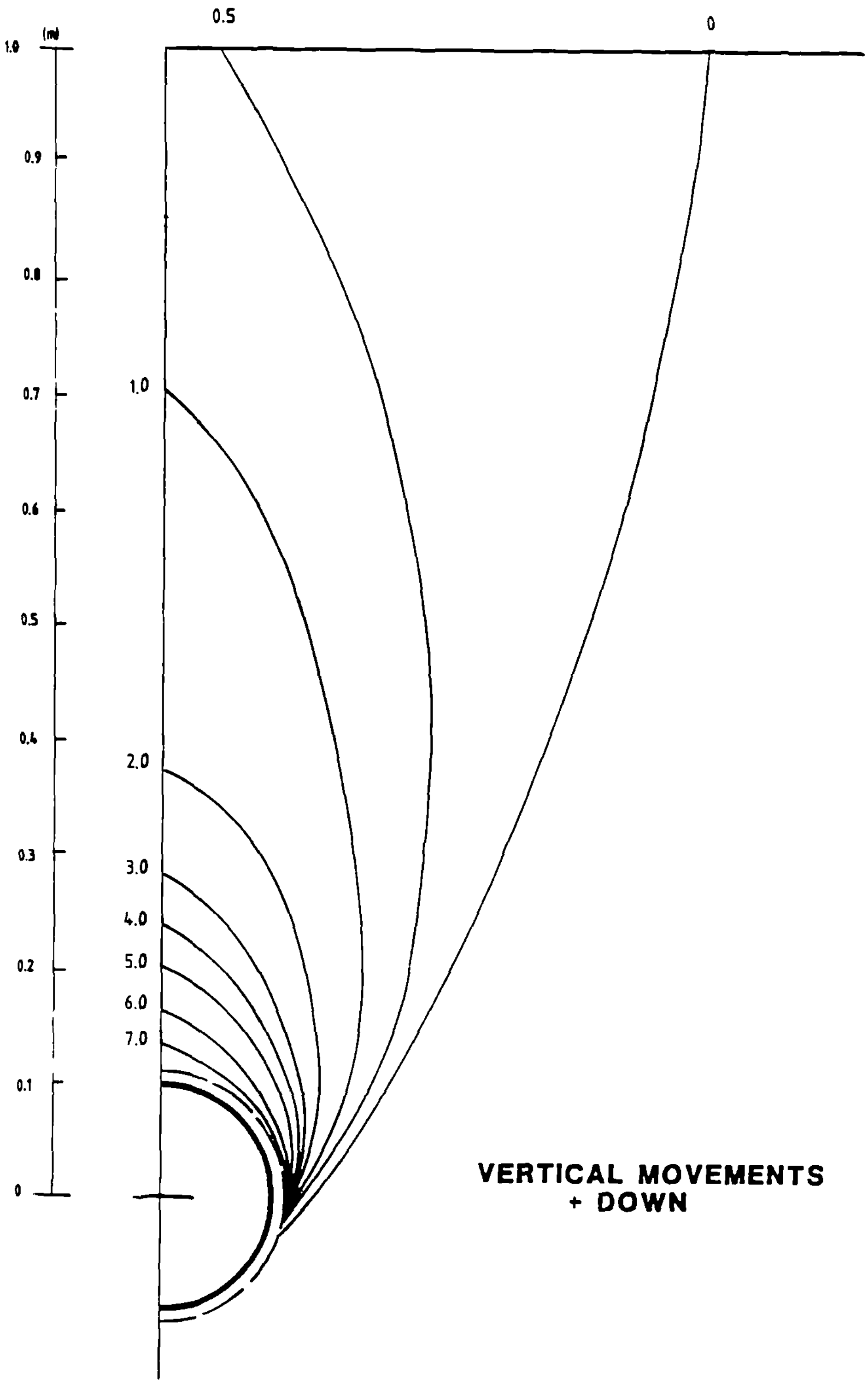

TEST OPJ6
20.01LB0.1

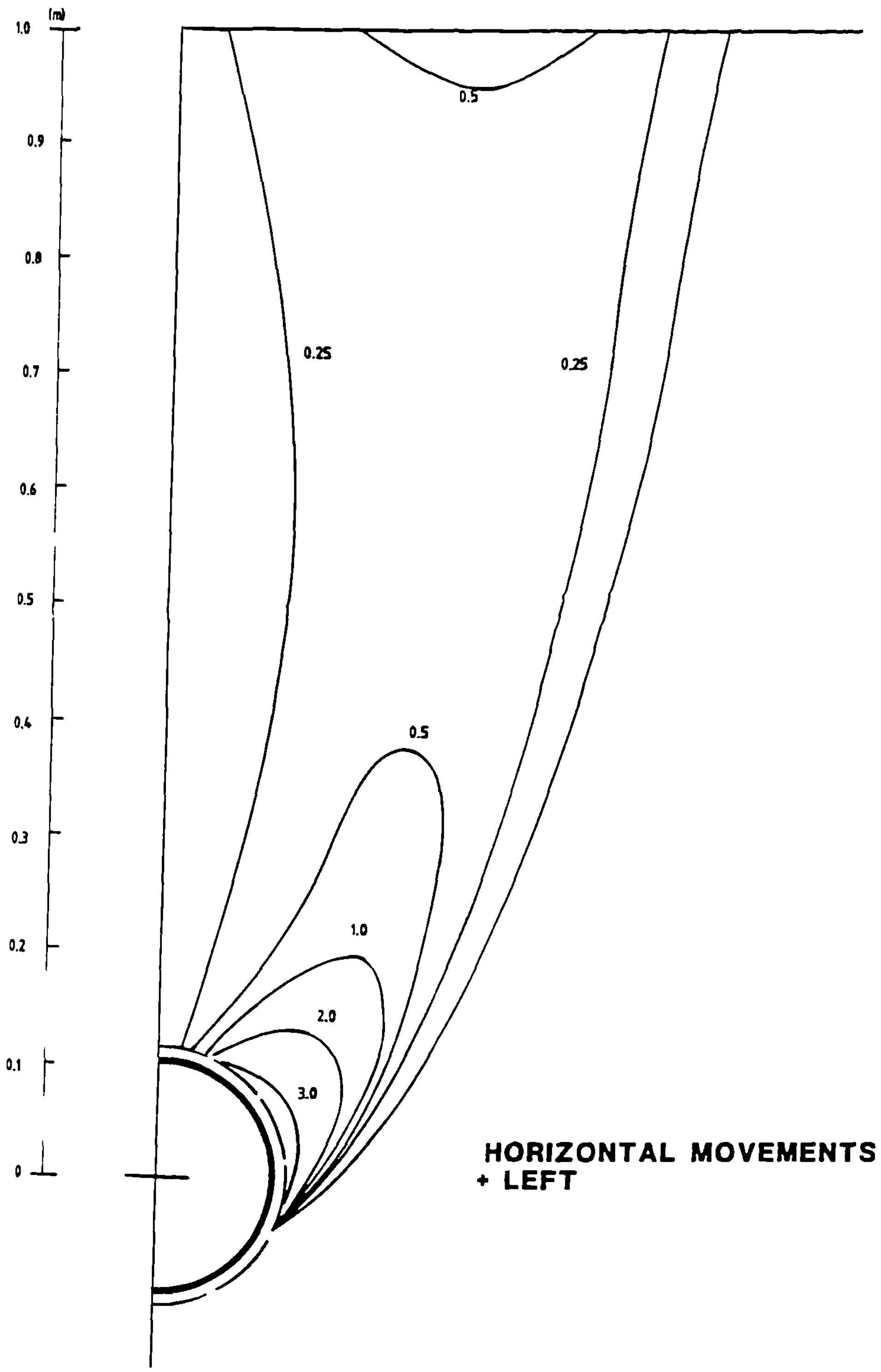

TEST OPJ6
20.0ILB0.1

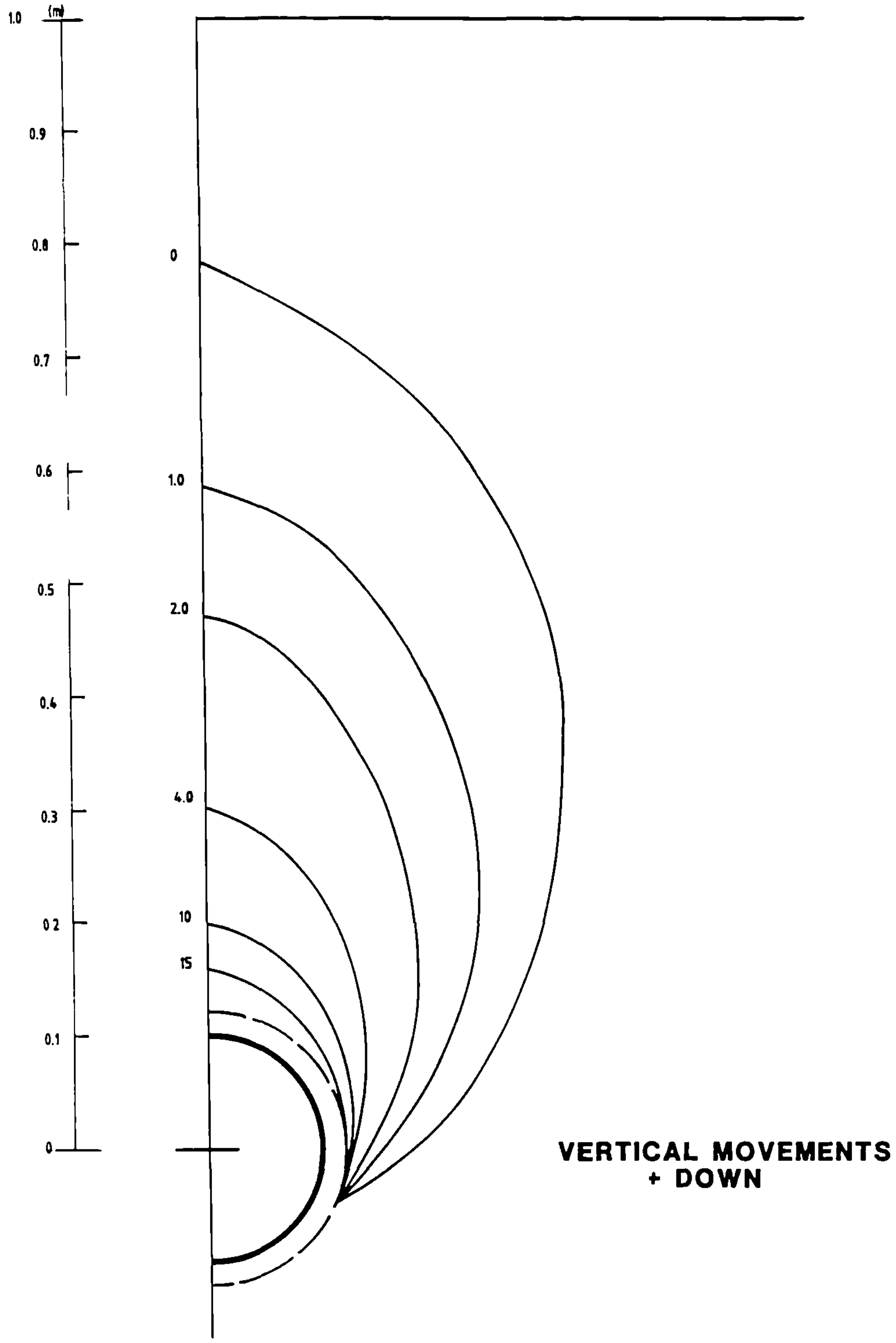

TEST OPJ7
4.5dLB0.2

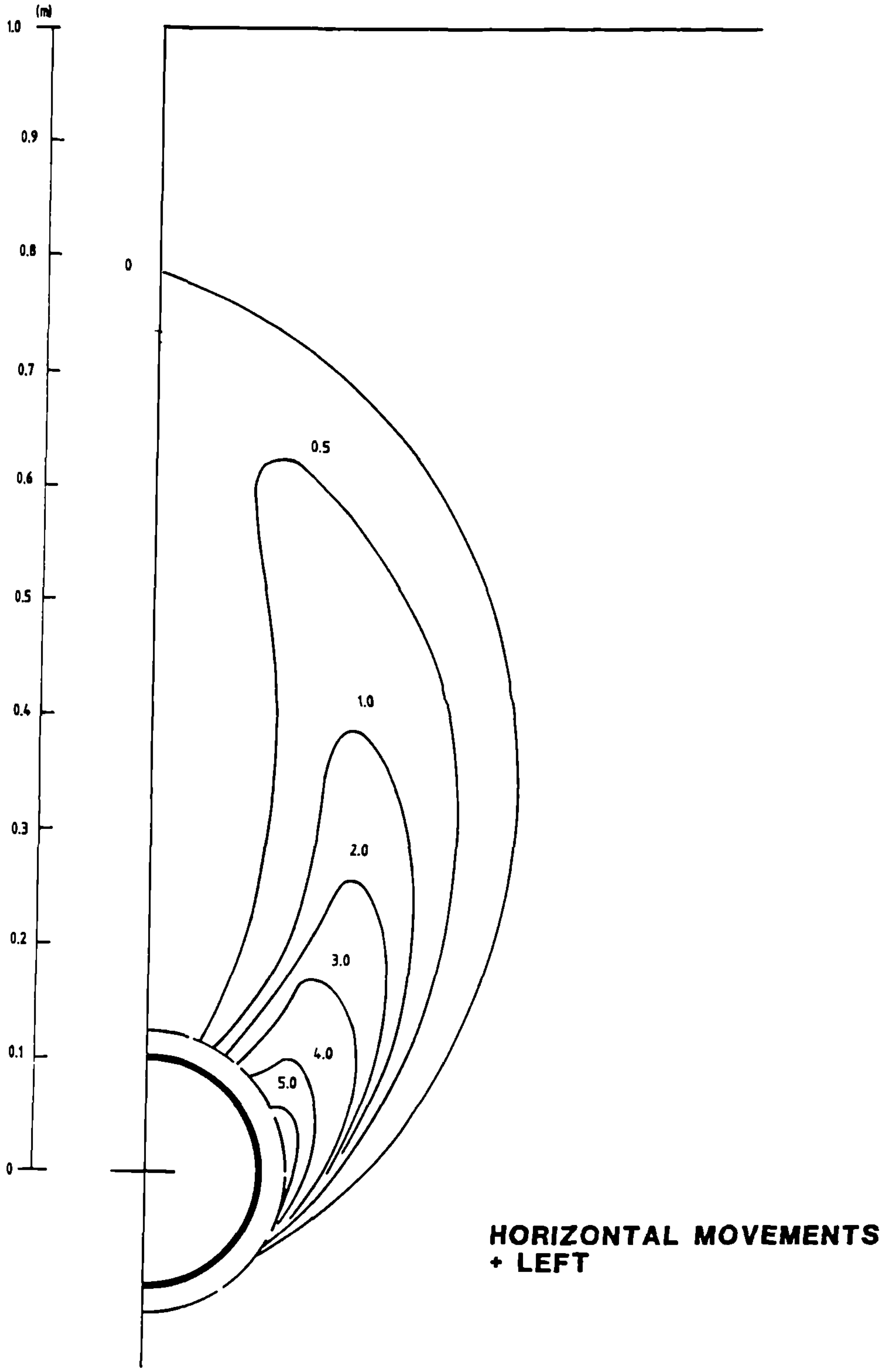

TEST OPJ7

4.5dLB0.2

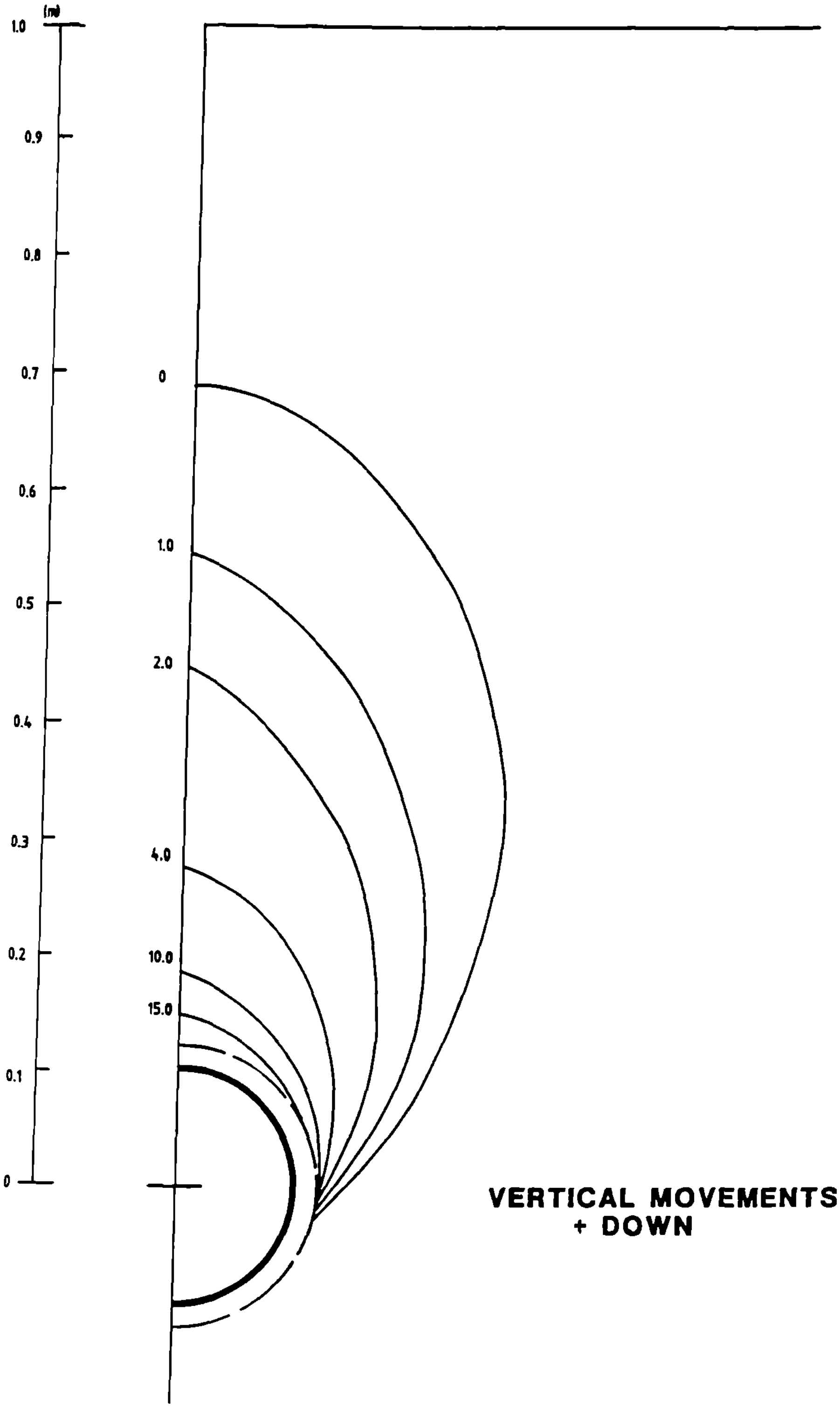

TEST OPJ9
20.0dLB0.2

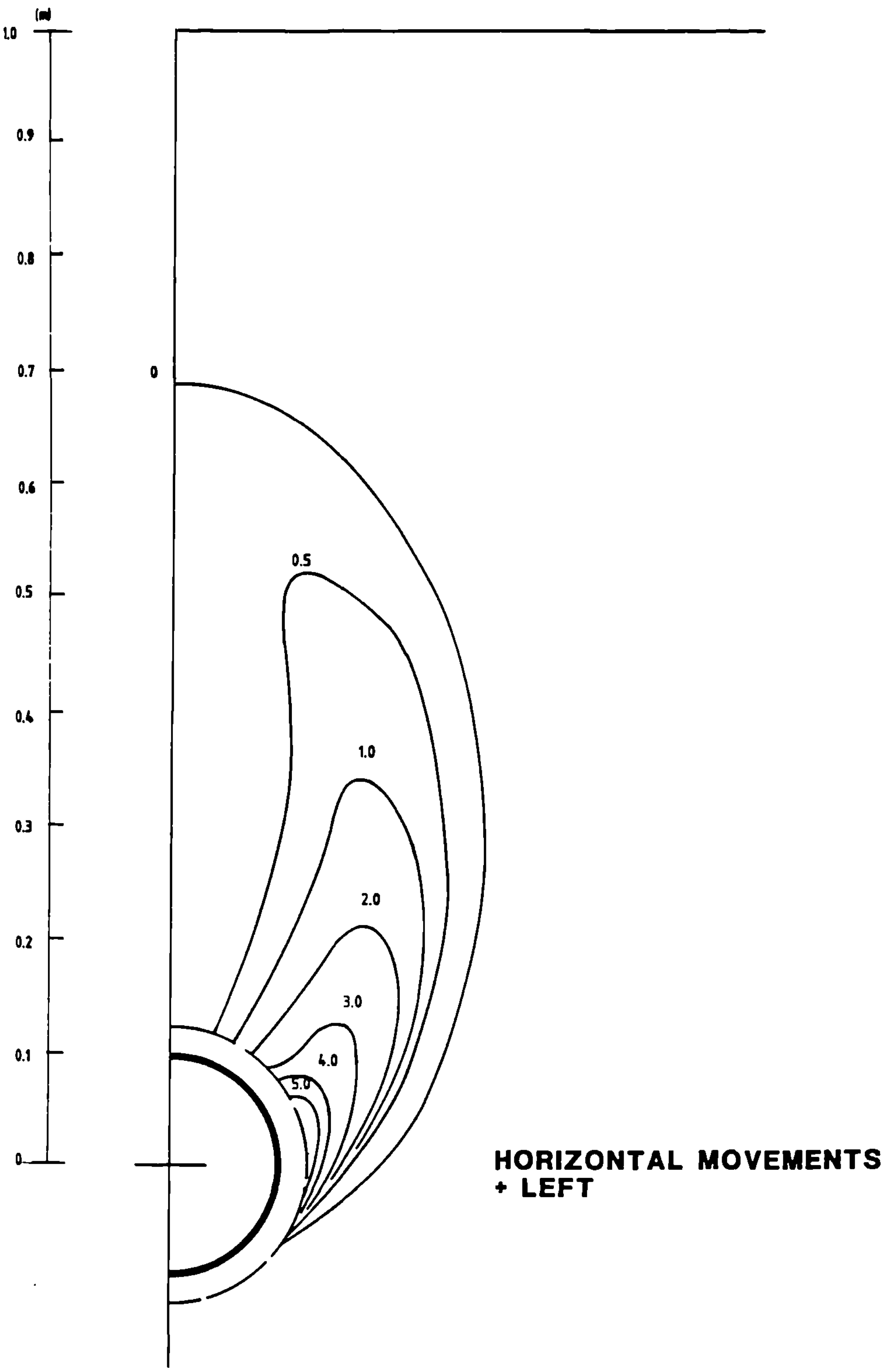

TEST OPJ9
20.0dLB0.2

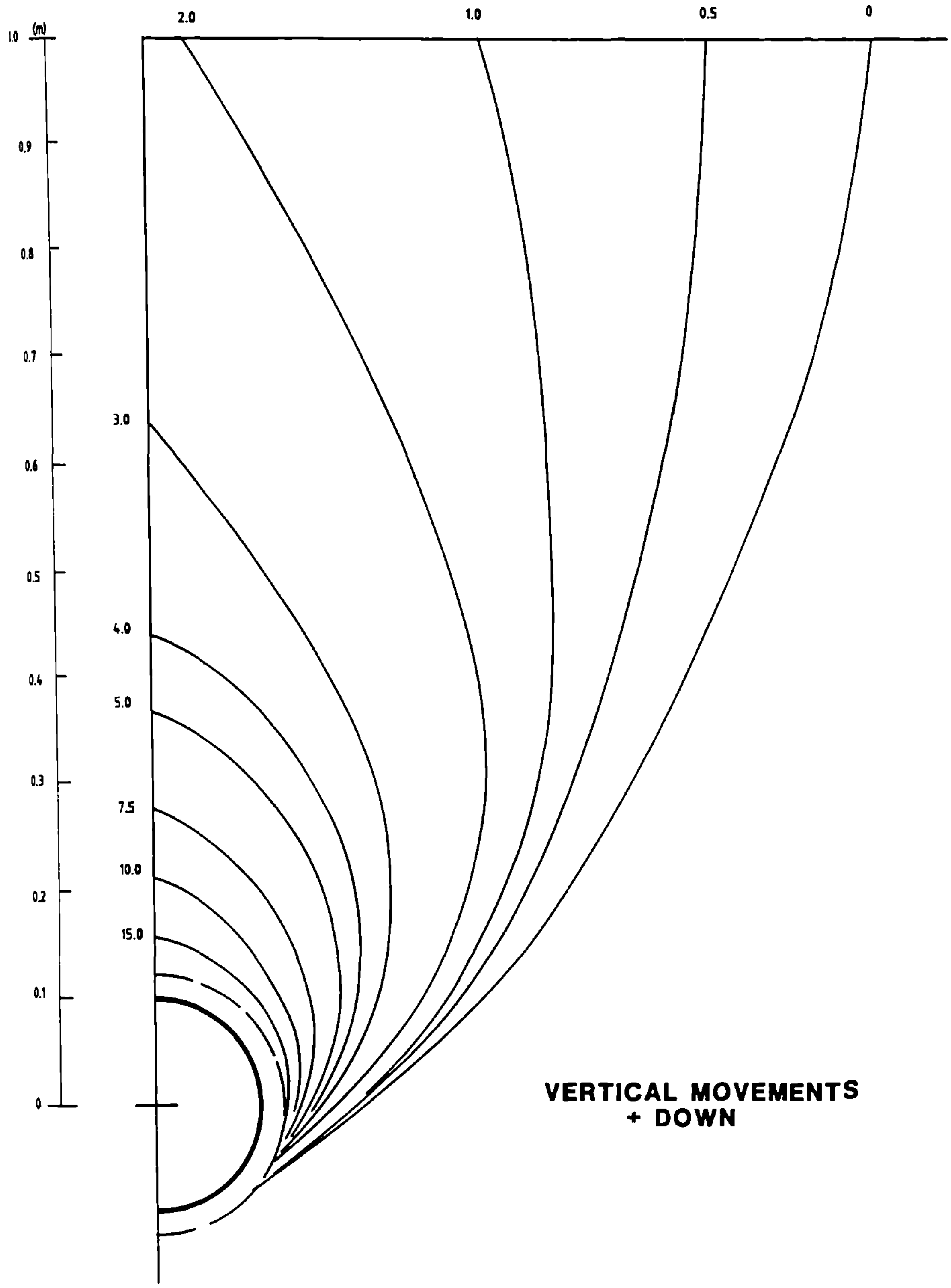

TEST OPJ10

4.5ILB0.2

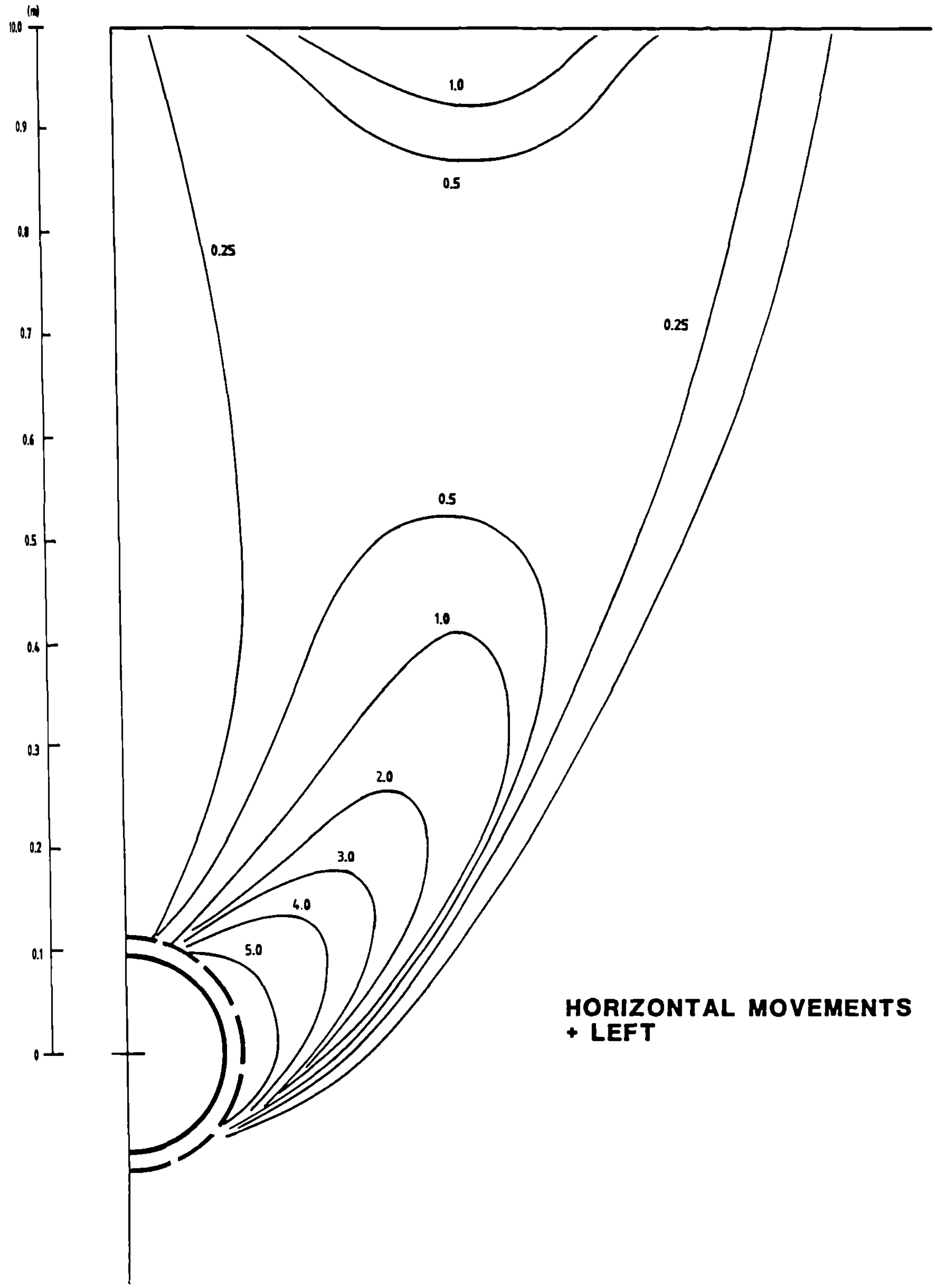

TEST OPJ10

4.5ILB0.2

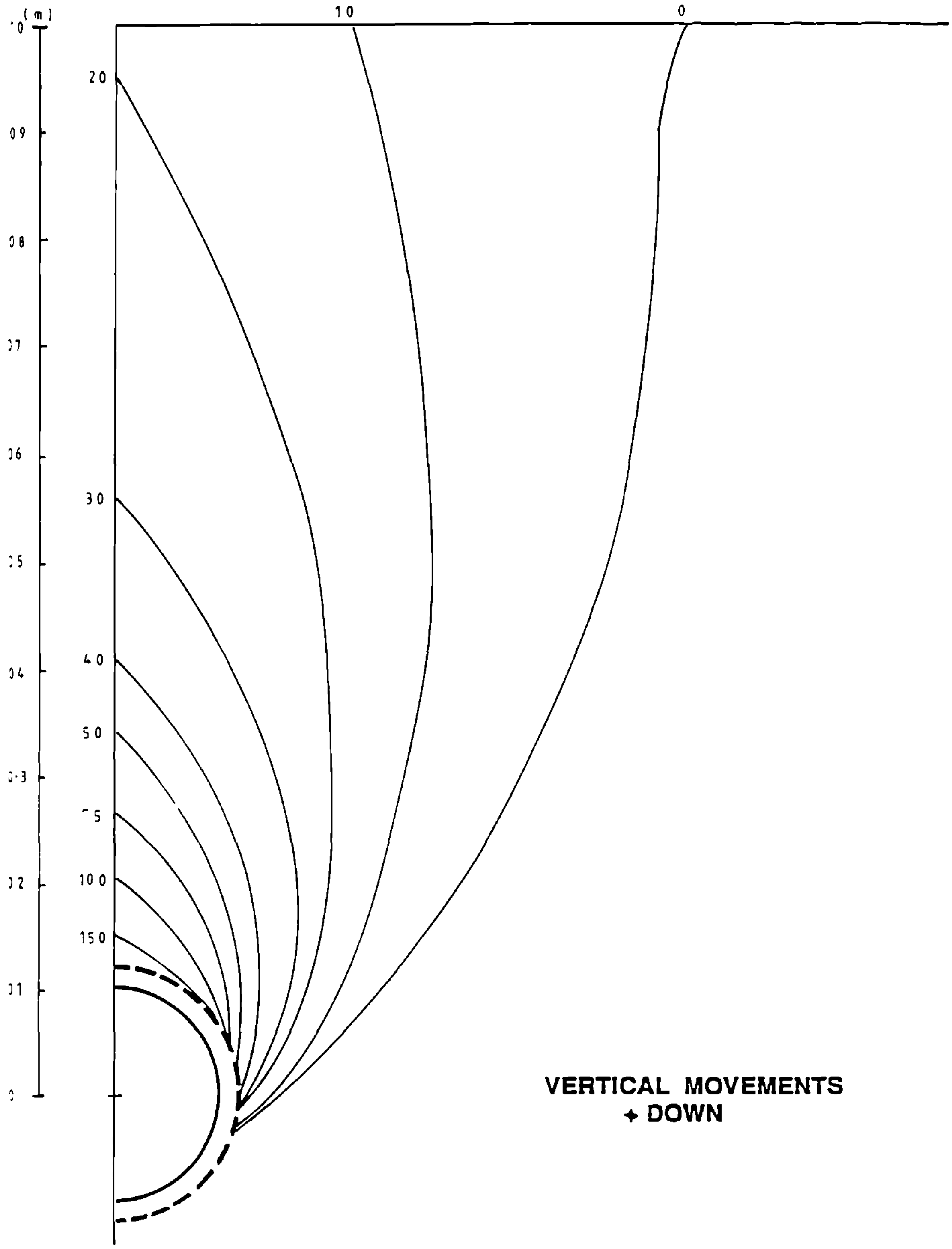

TEST OPJ12
20.01LB0.2

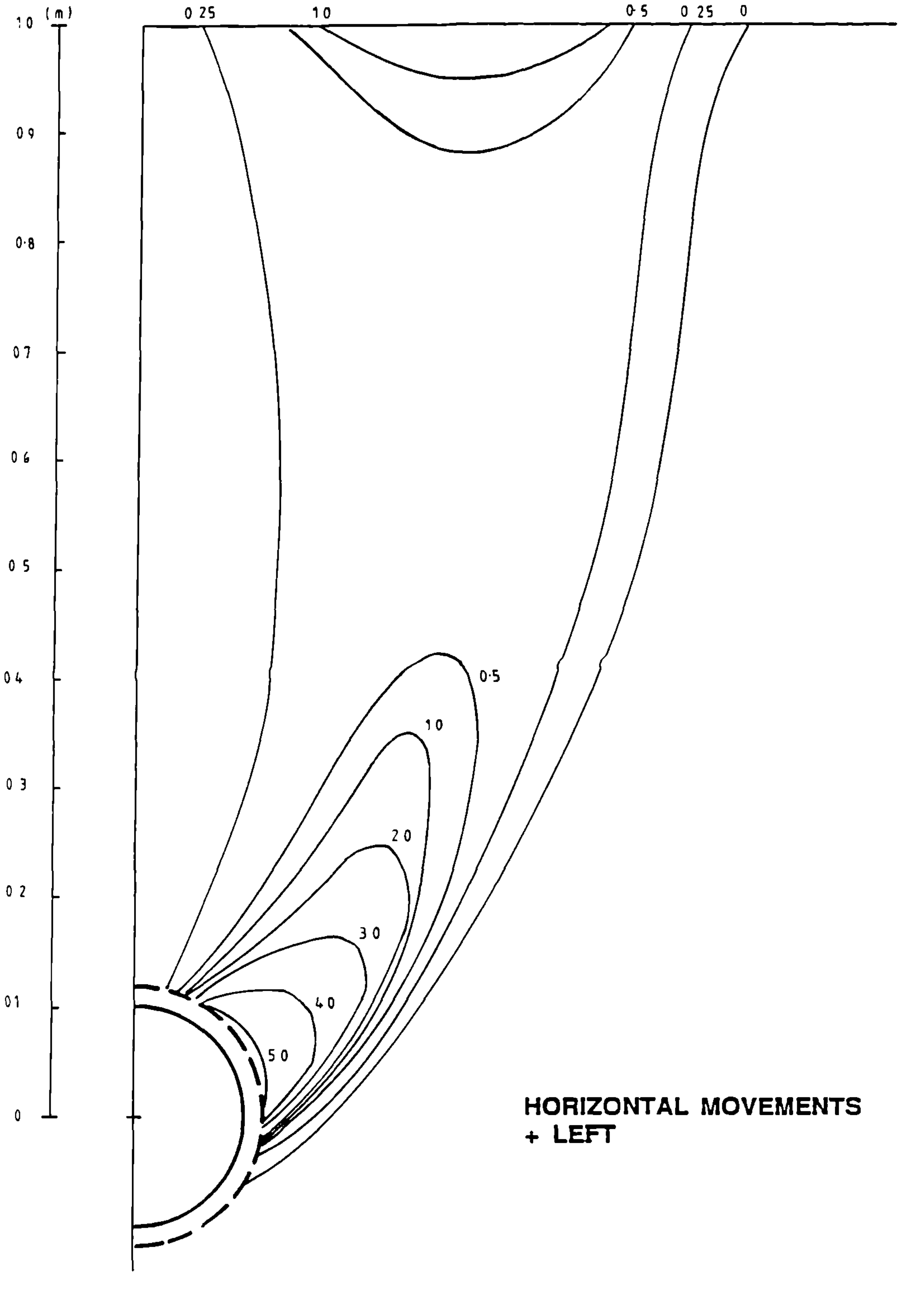

TEST OPJ12

20.01LB0.2

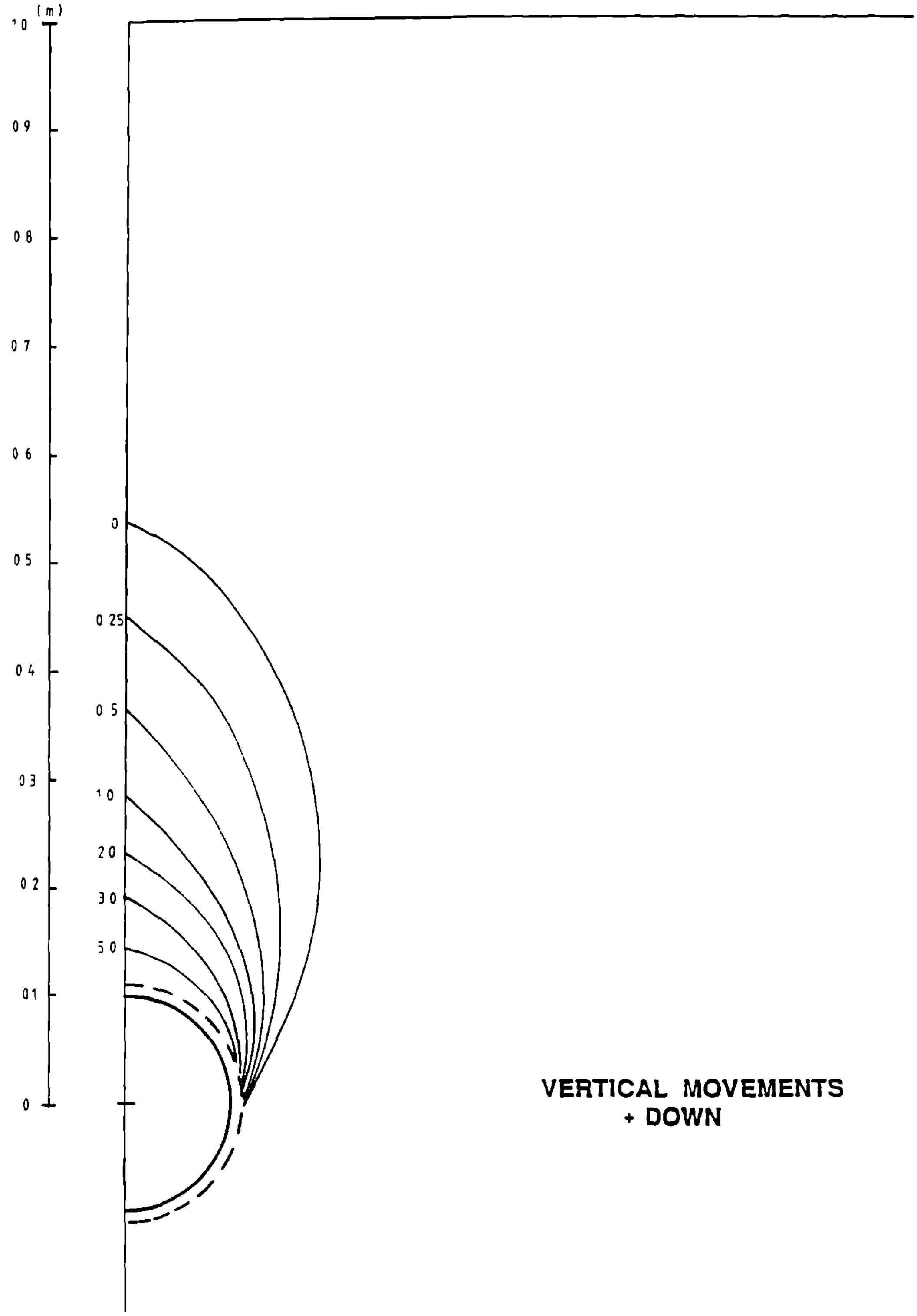

TEST OPJ13

4.5d25B0.1

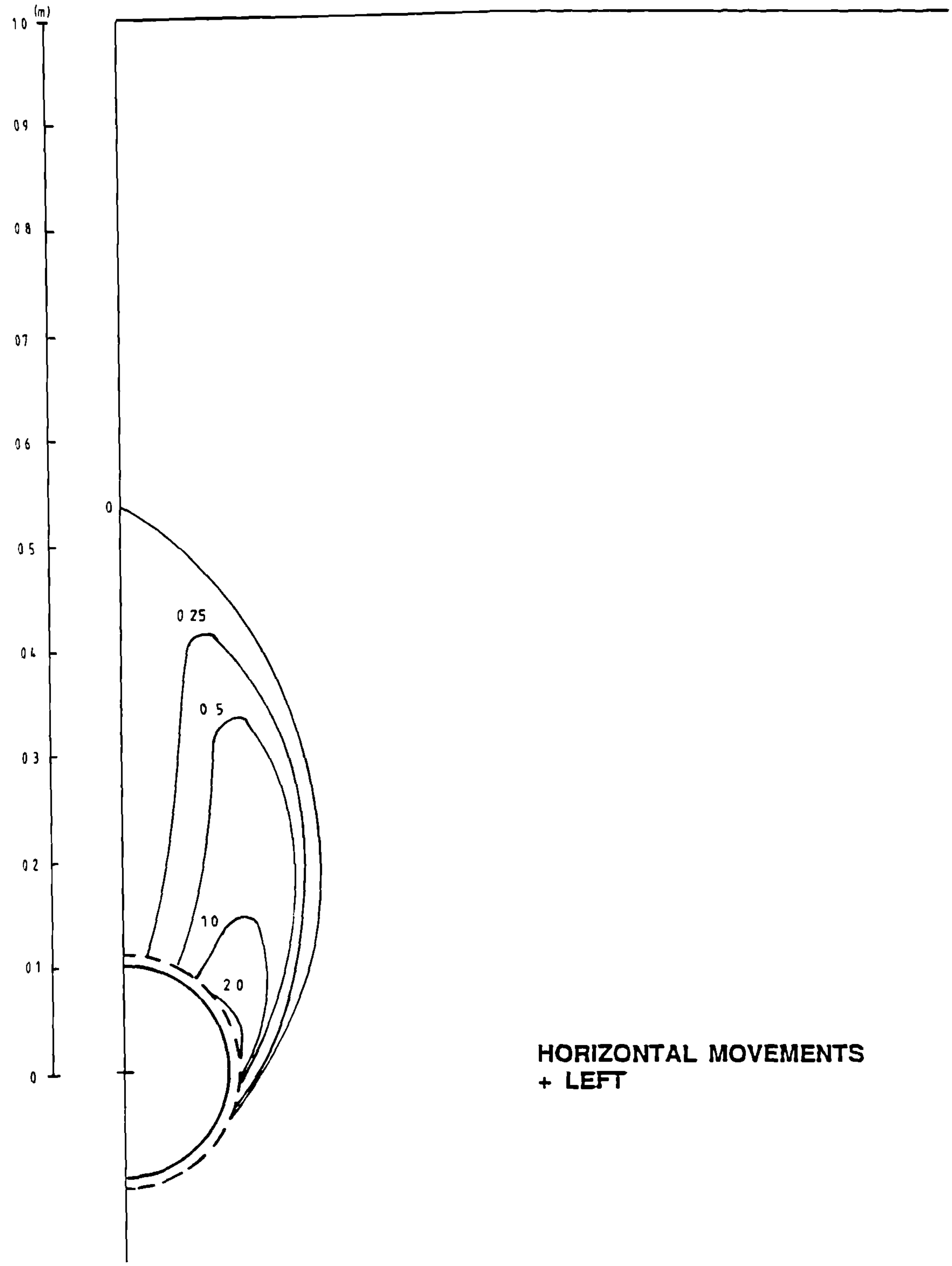

TEST OPJ13

4.5d25B0.1

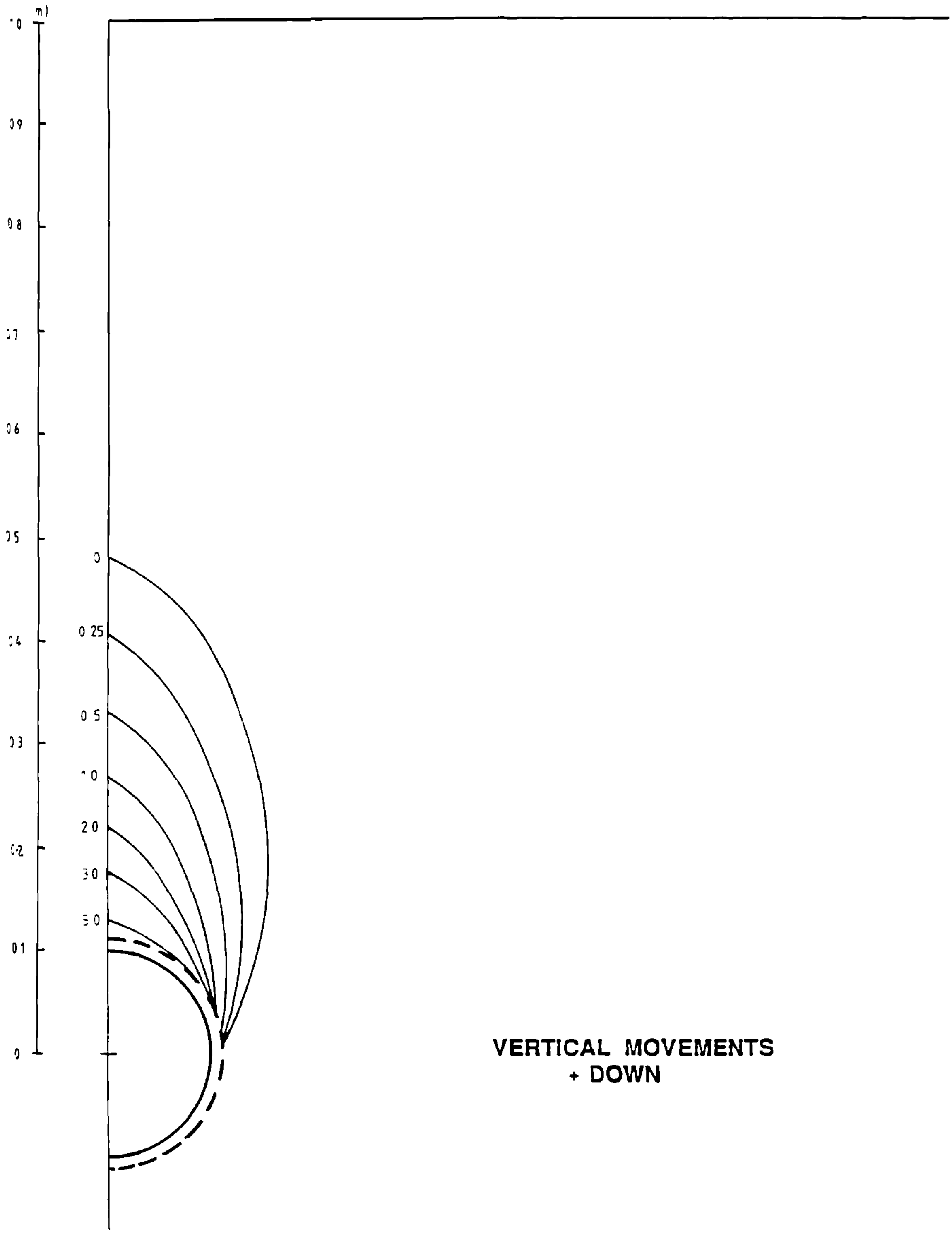

TEST OPJ15

20.0d25B0.1

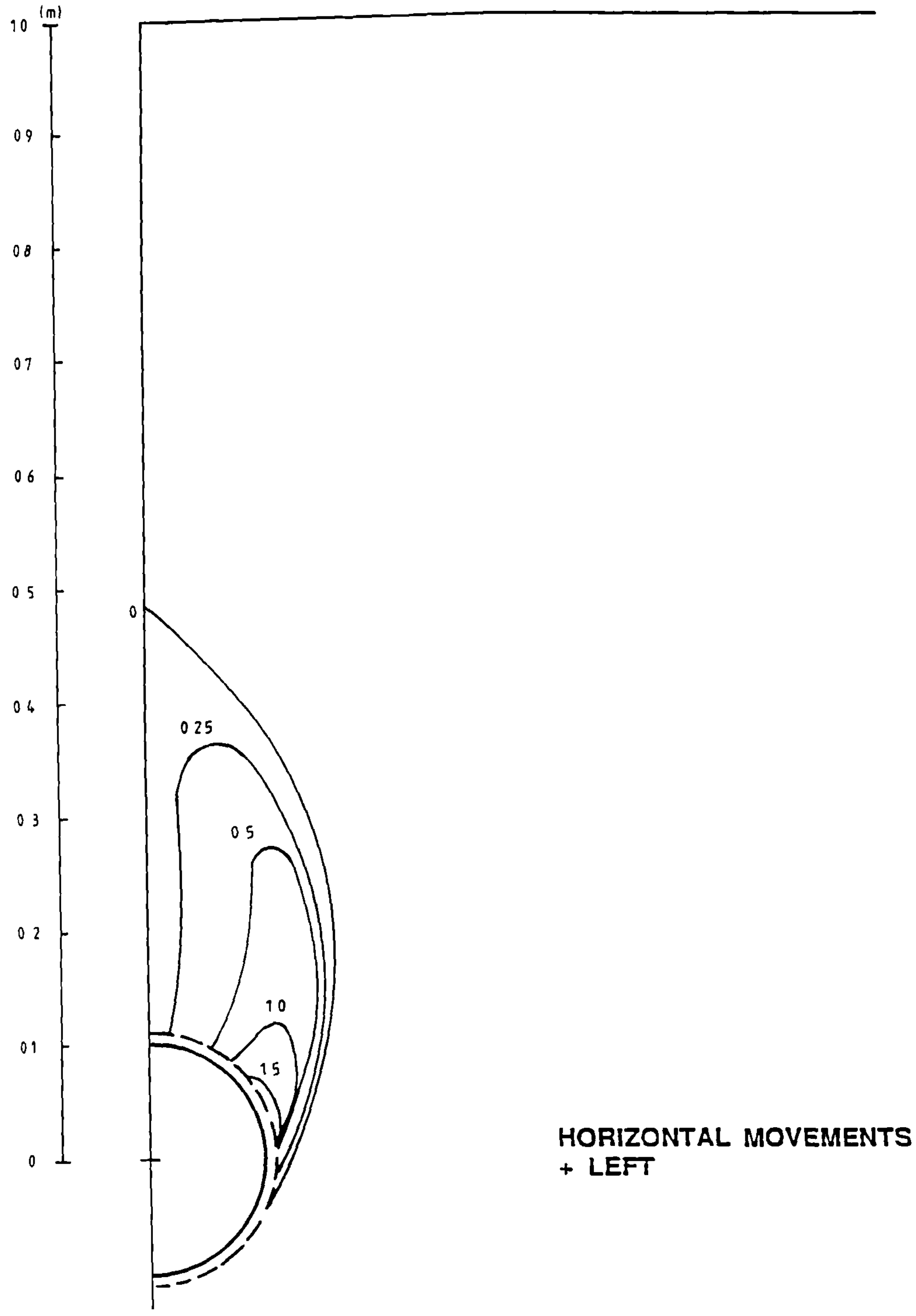

TEST OPJ15

20.0d25B0.1

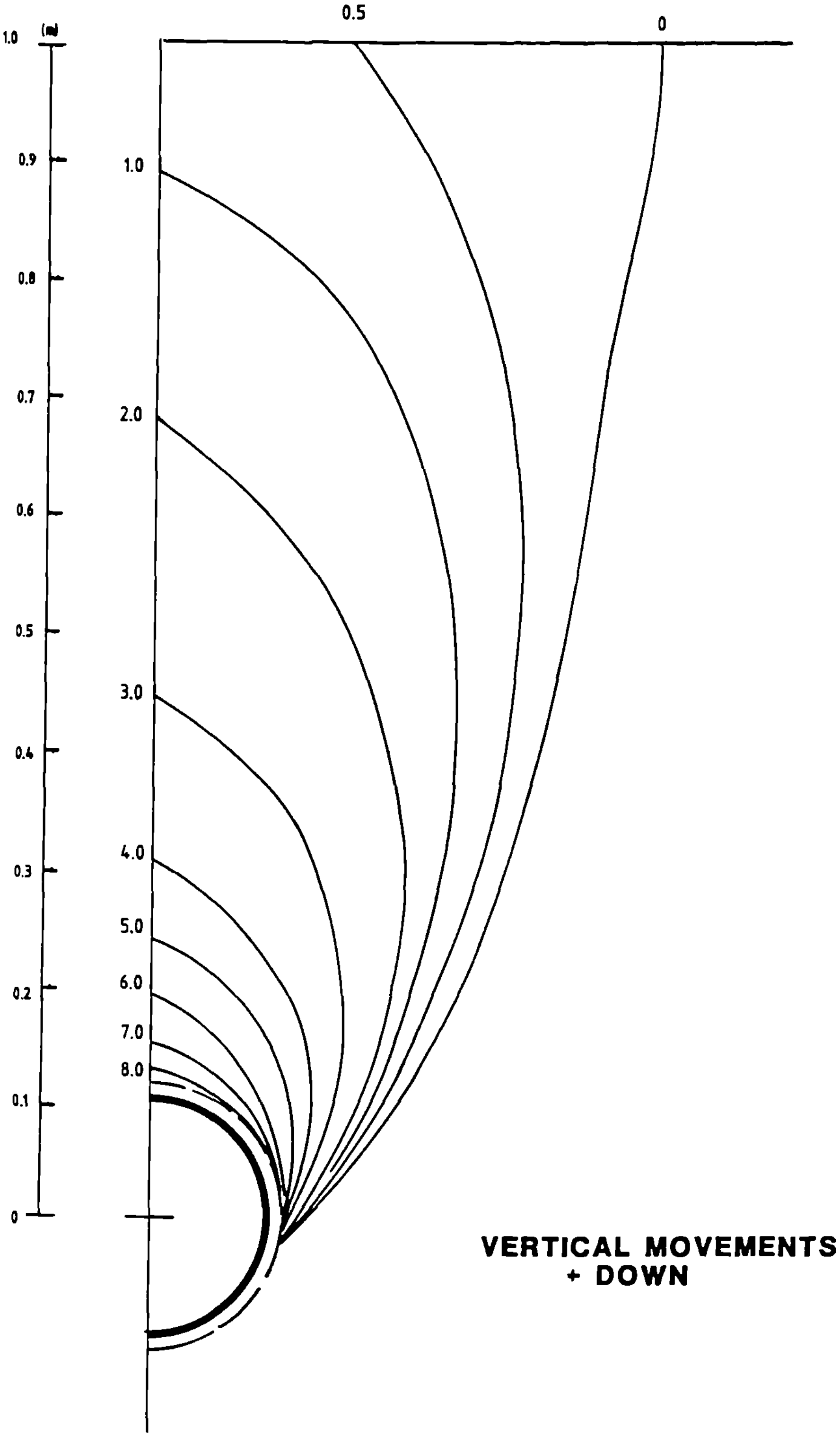

TEST OPJ16
4.5125B0.1

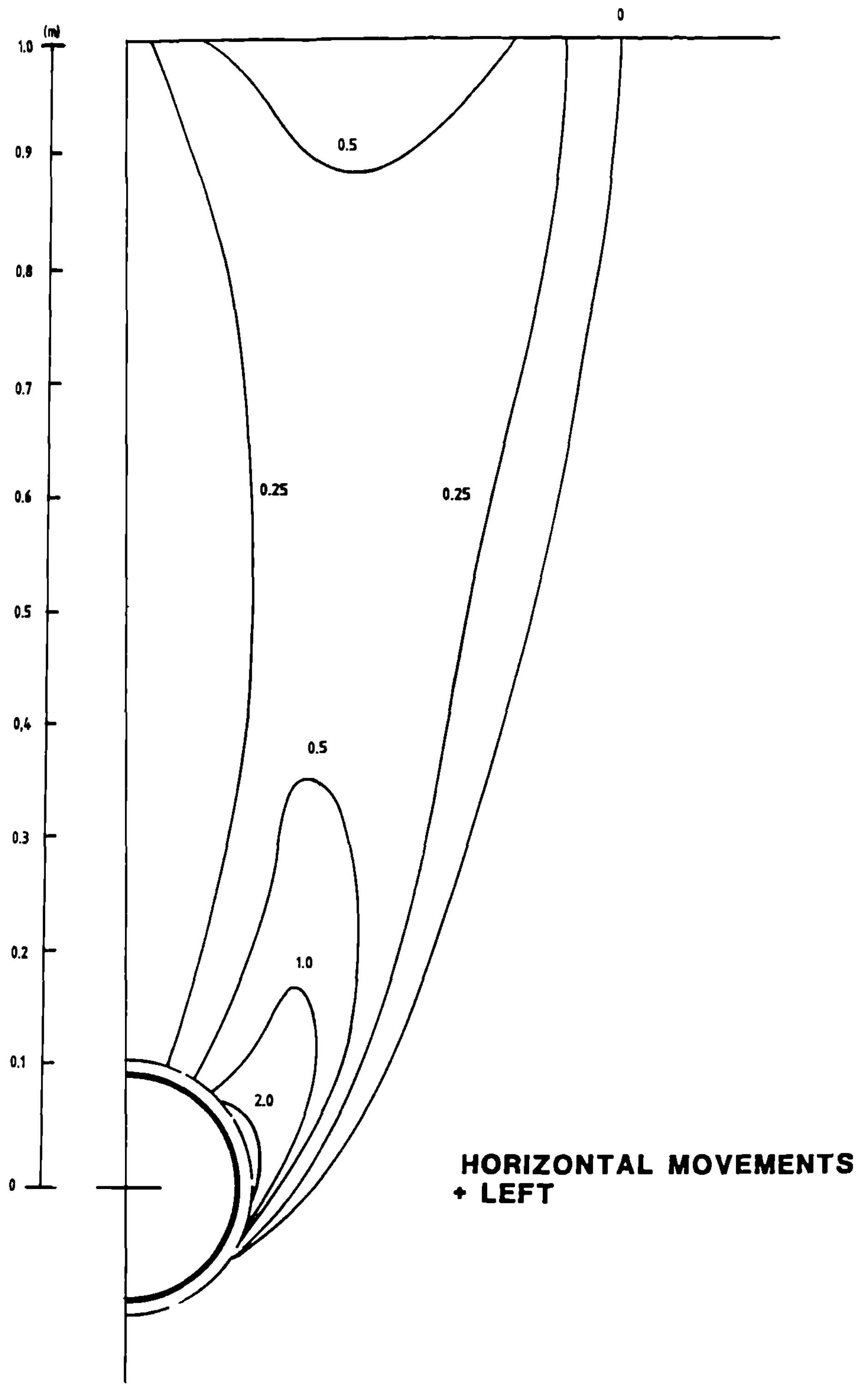

TEST OPJ16

4.5125B0.1

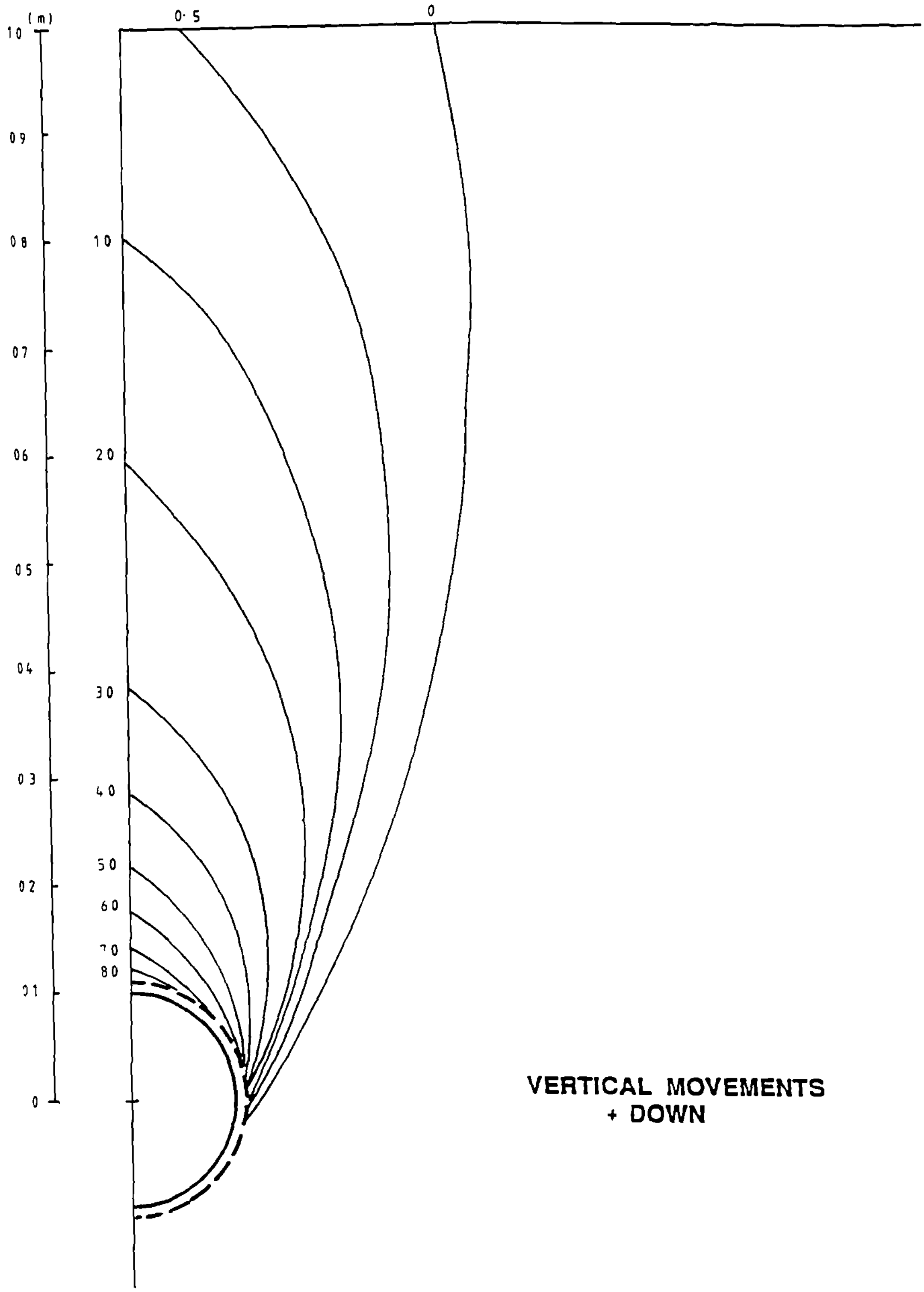

TEST OPJ18

20.0125B0.1

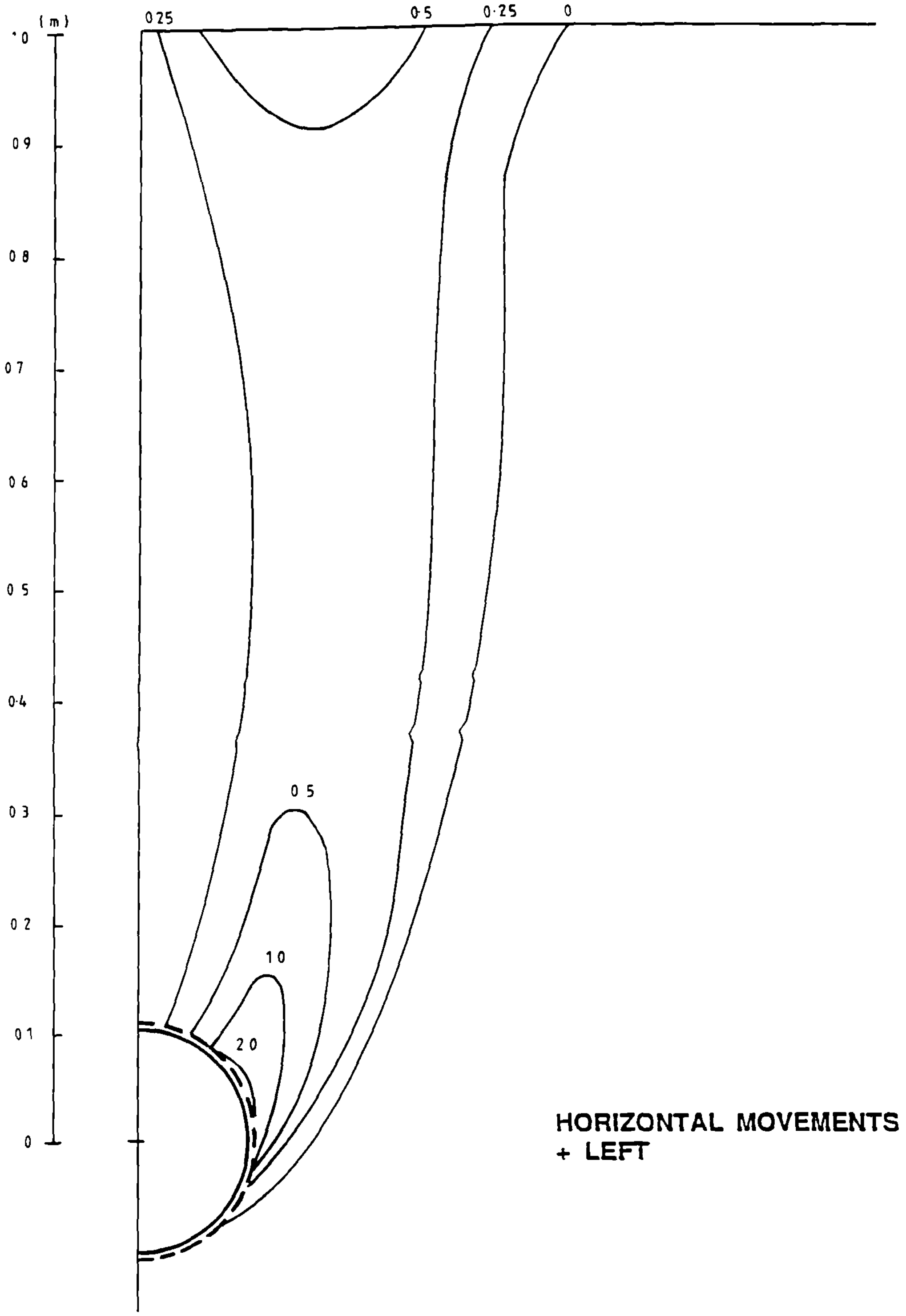

TEST OPJ18
20.0125B0.1

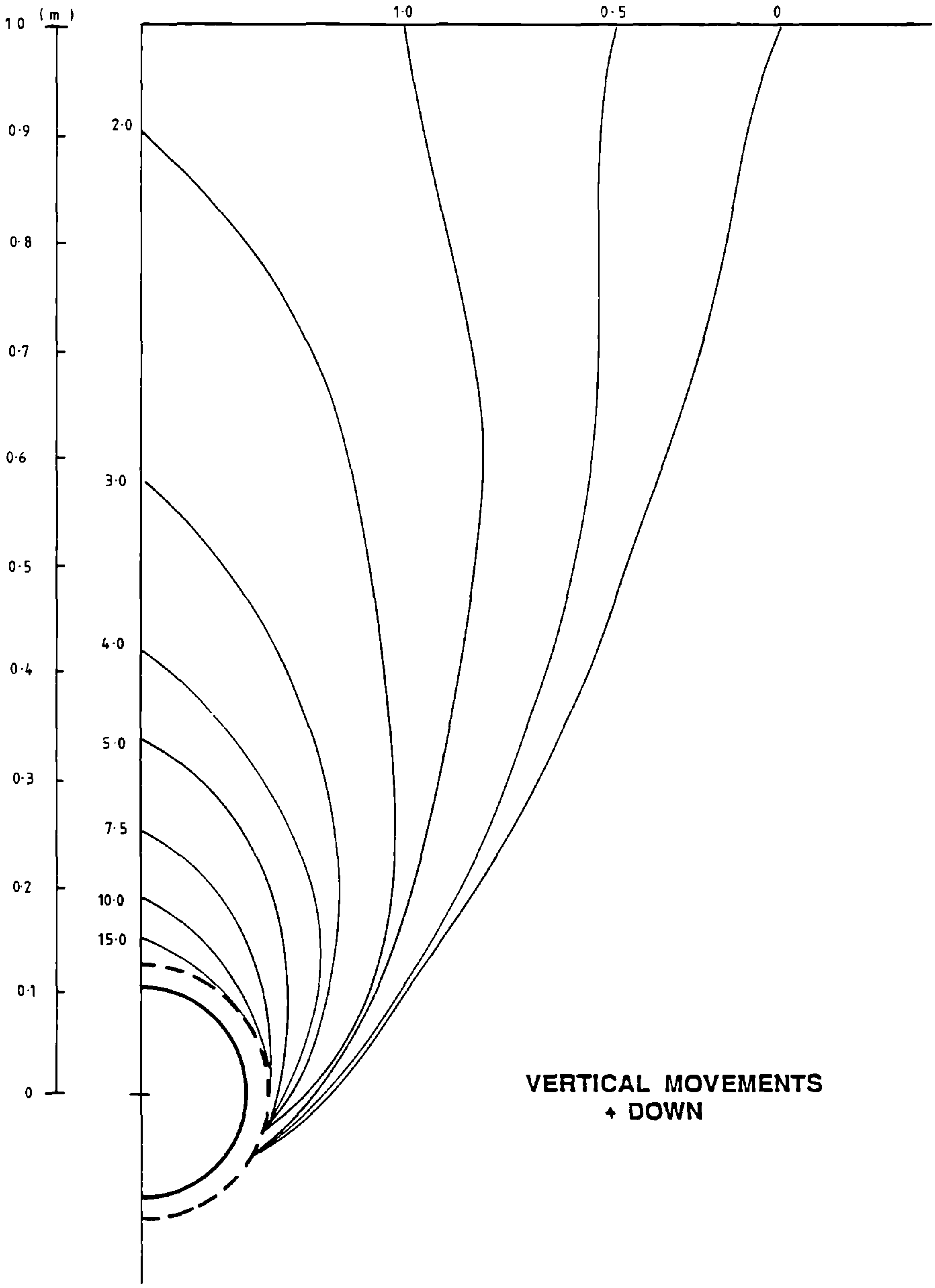

TEST OPJ19
4.5d25B0.2

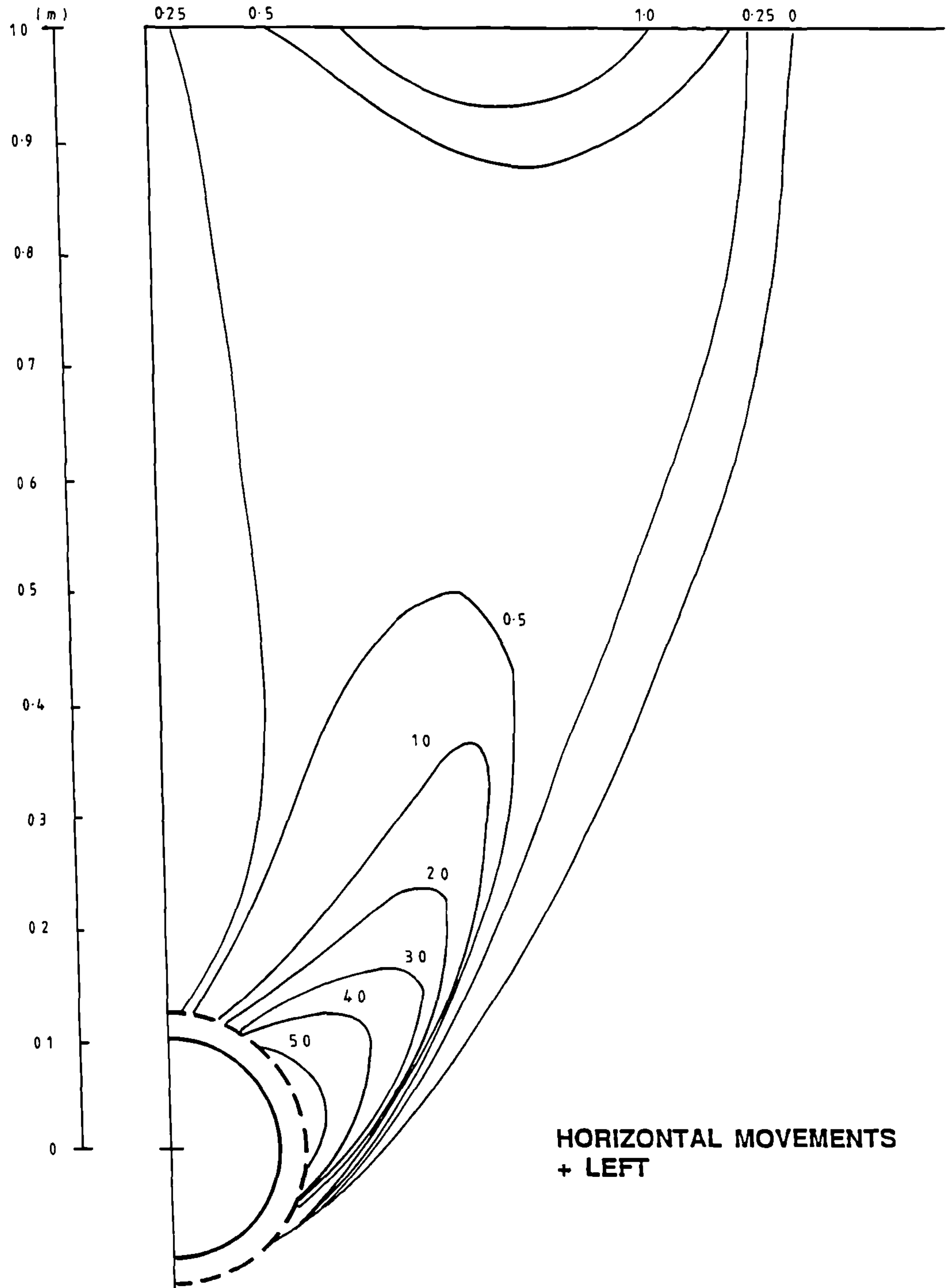

TEST OPJ19
4.5d25B0.2

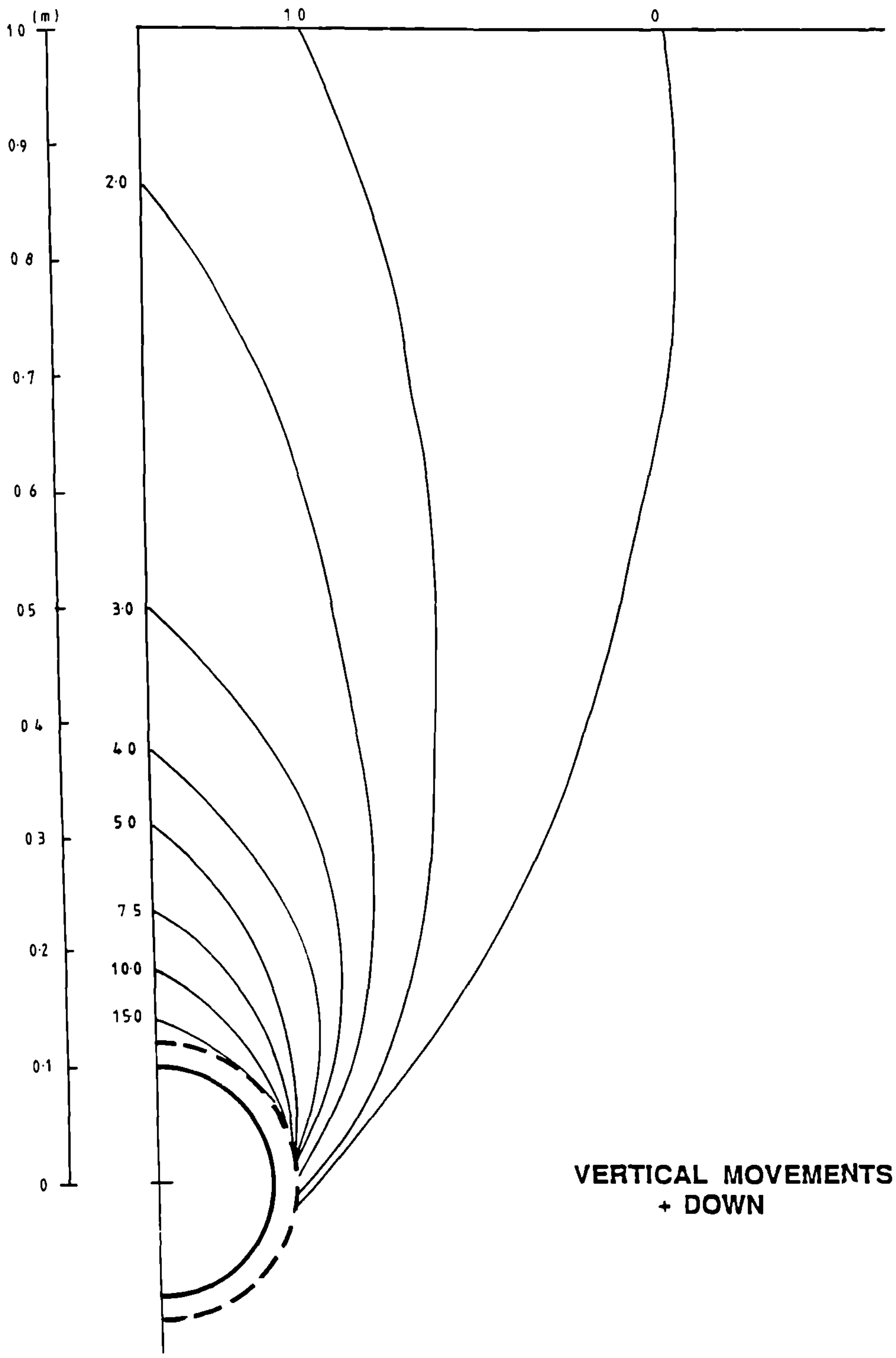

TEST OPJ21

20.0d25B0.2

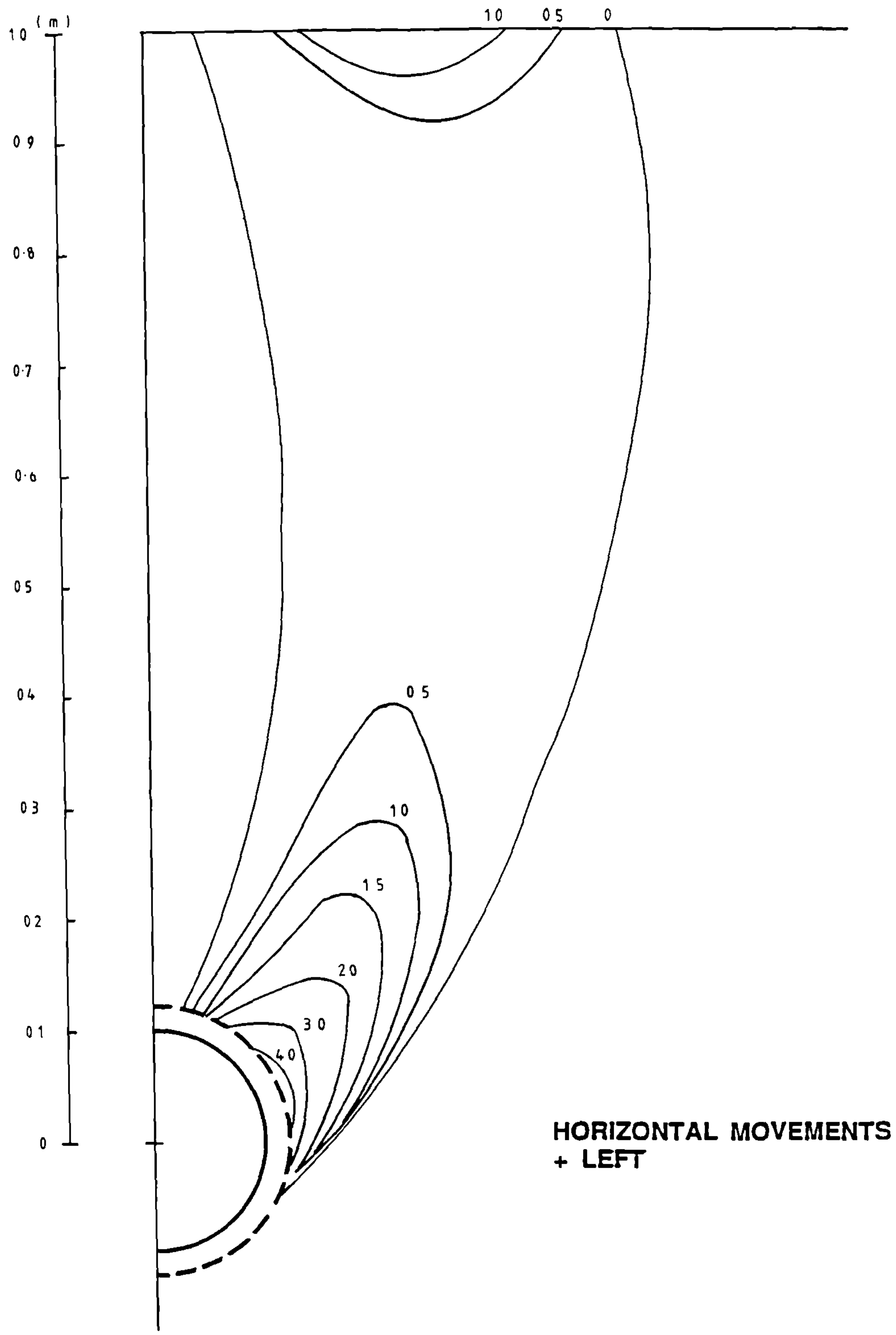

TEST OPJ21

20.0d25B0.2

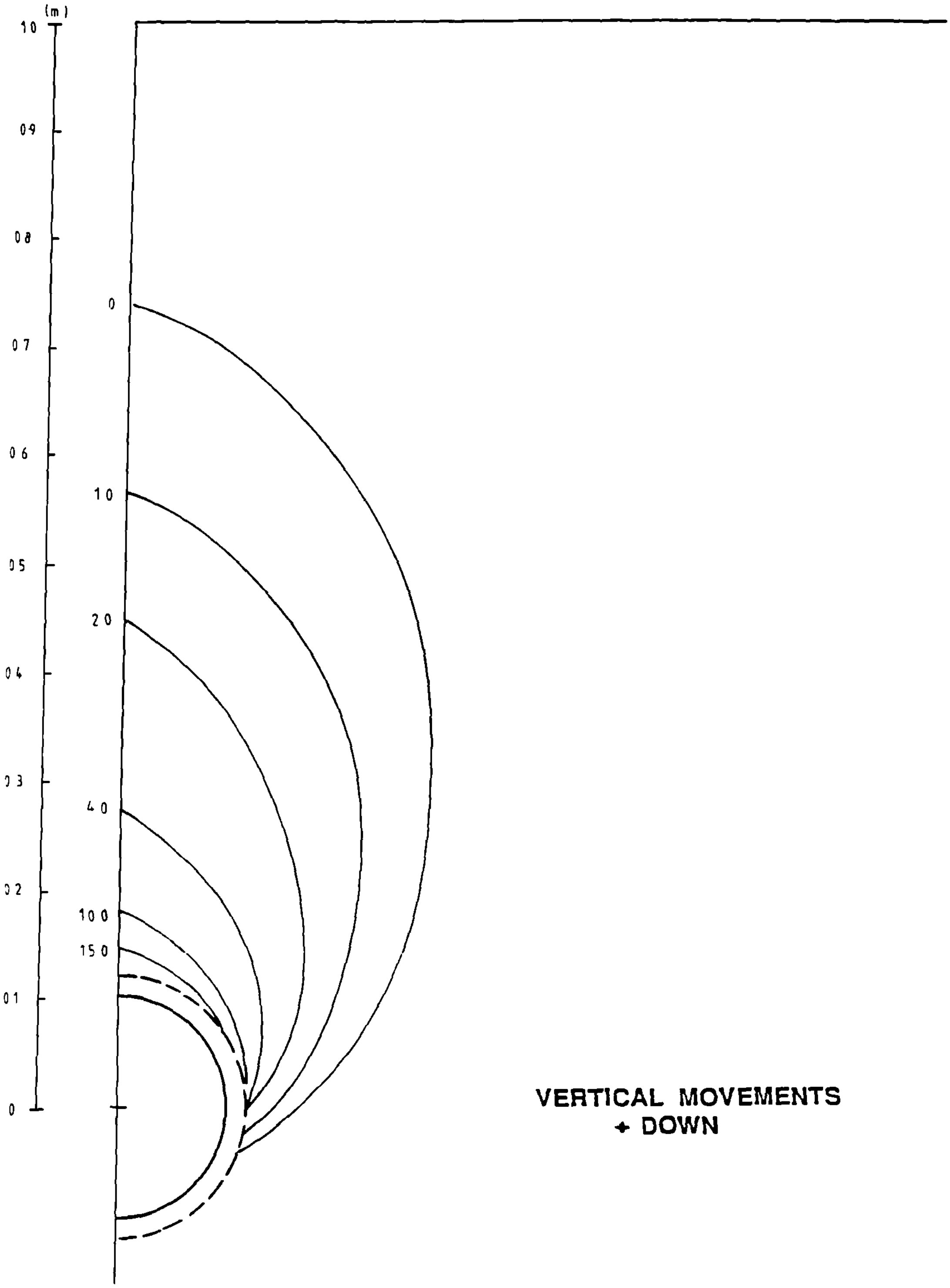

TEST OPJ22

4.5125B0.2

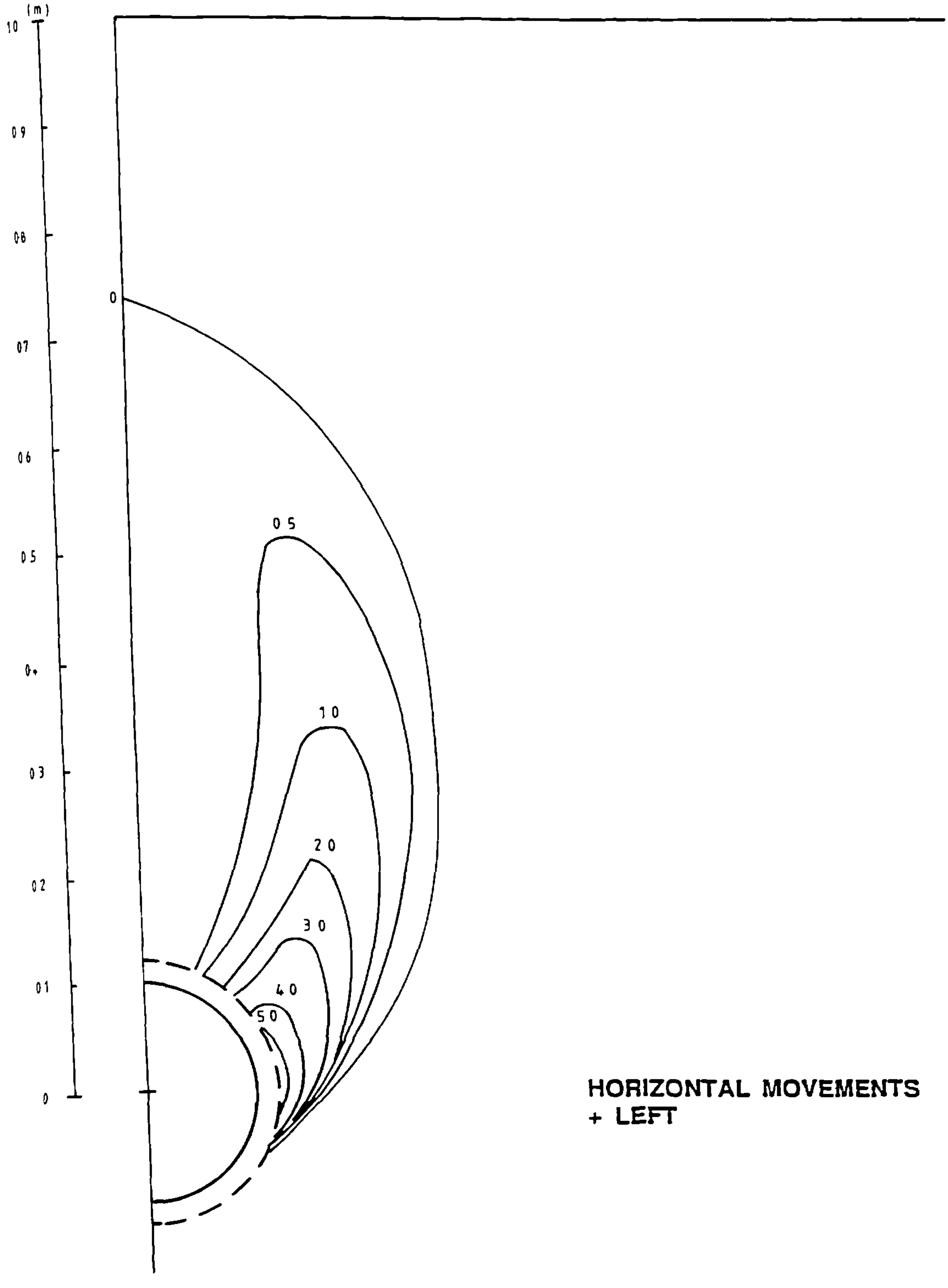

TEST OPJ22
4.5125B0.2

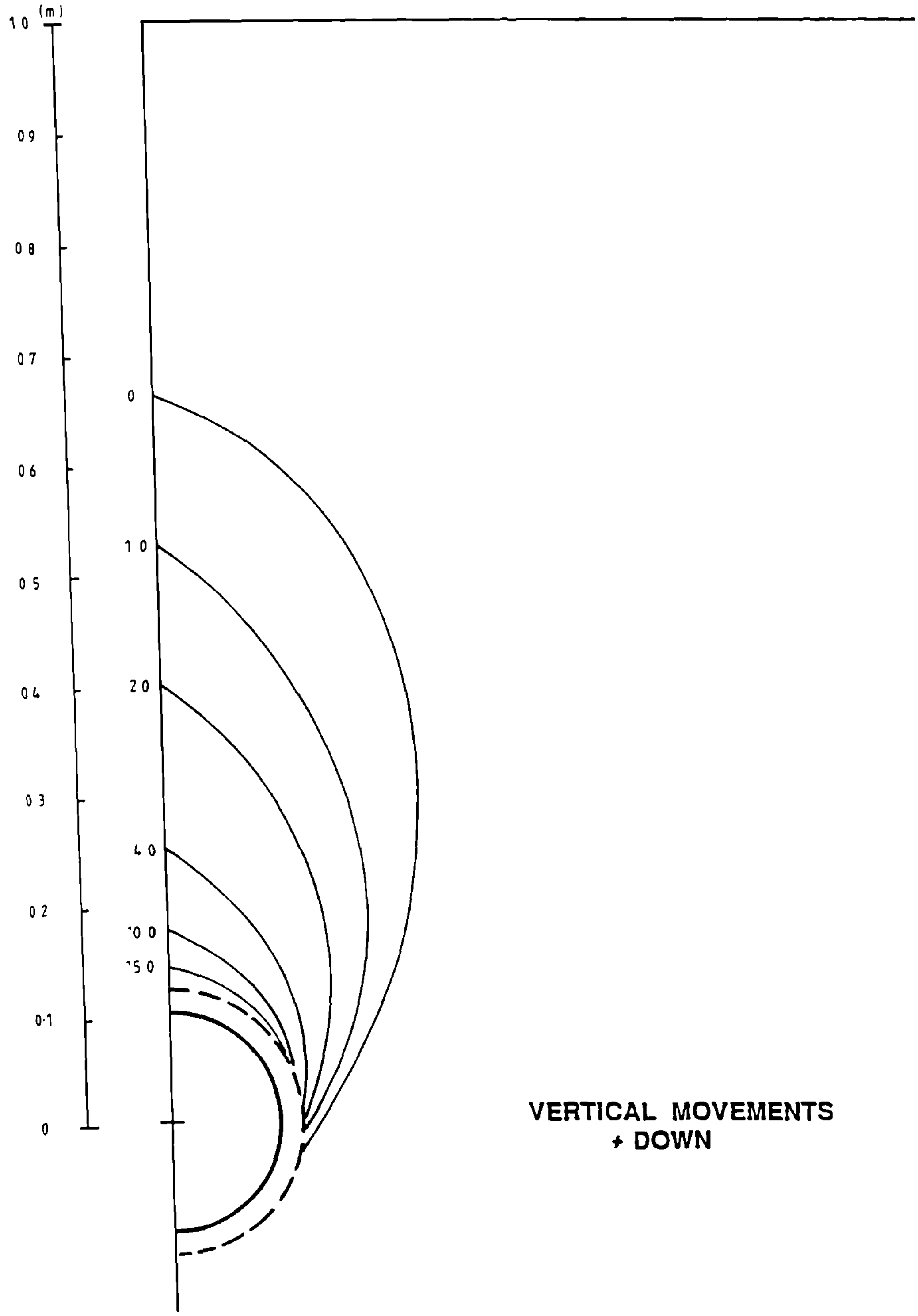

TEST OPJ24

20.0125B0.2

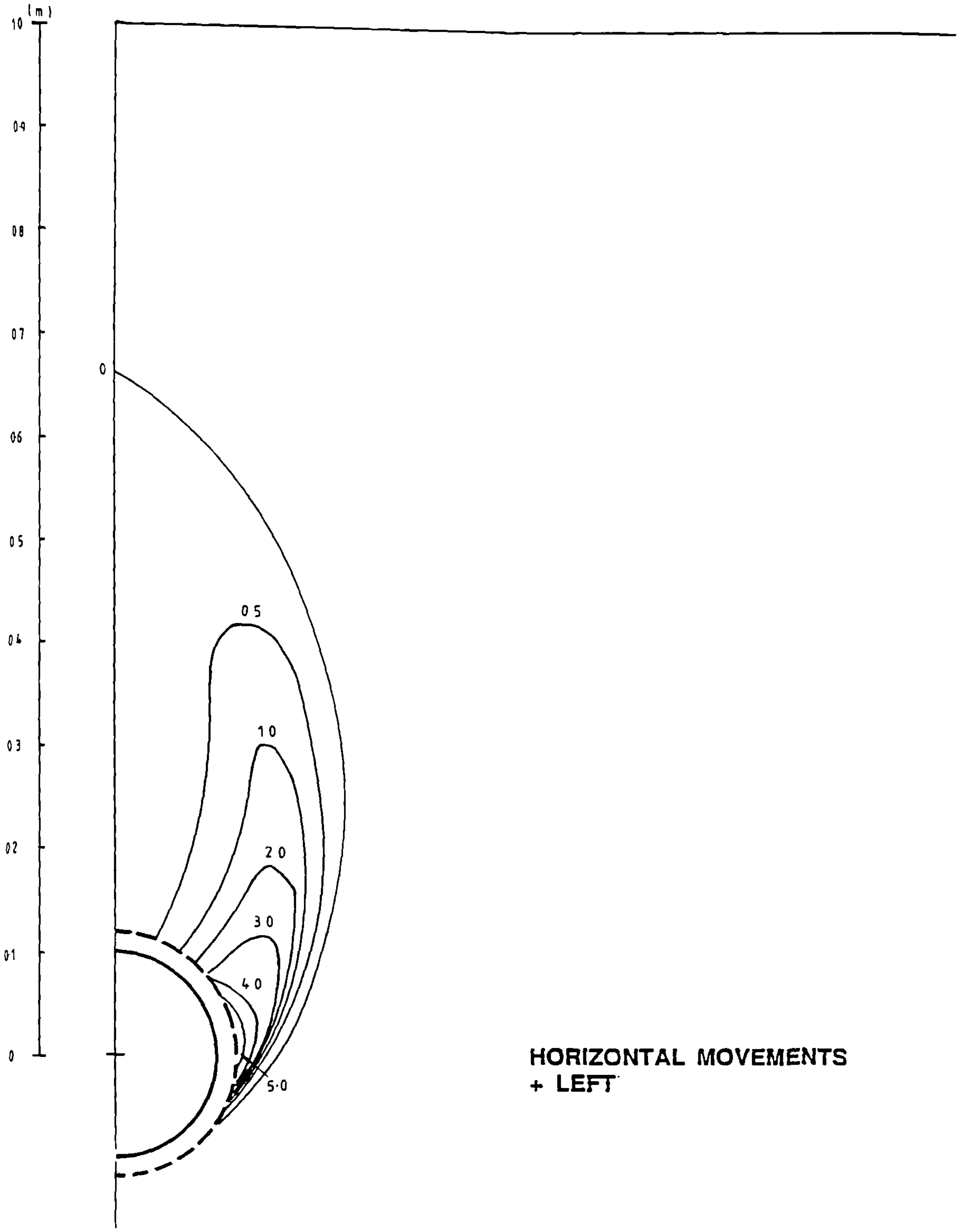

TEST OPJ24

20.0125B0.2

B.3 CLOSED PIPEJACKING TESTS - LONGITUDINAL PLANE RESULTS

The following figures show the horizontal and vertical displacement contour plots for all the closed shield pipejacking tests in the longitudinal plane (5 tests). Results were only obtained in this plane for these tests as the perpendicular plane test results at the shield overcut were identical to those obtained from the open shield tests. The contours are in millimetres and represent the movements of the sand for a 10mm forward jack of the shield and pipe. Test codes are given to aid comparison between results. The test code is defined as: Cover depth to diameter ratio (C/D), density state of sand, sand type, overcut ratio (t/R).

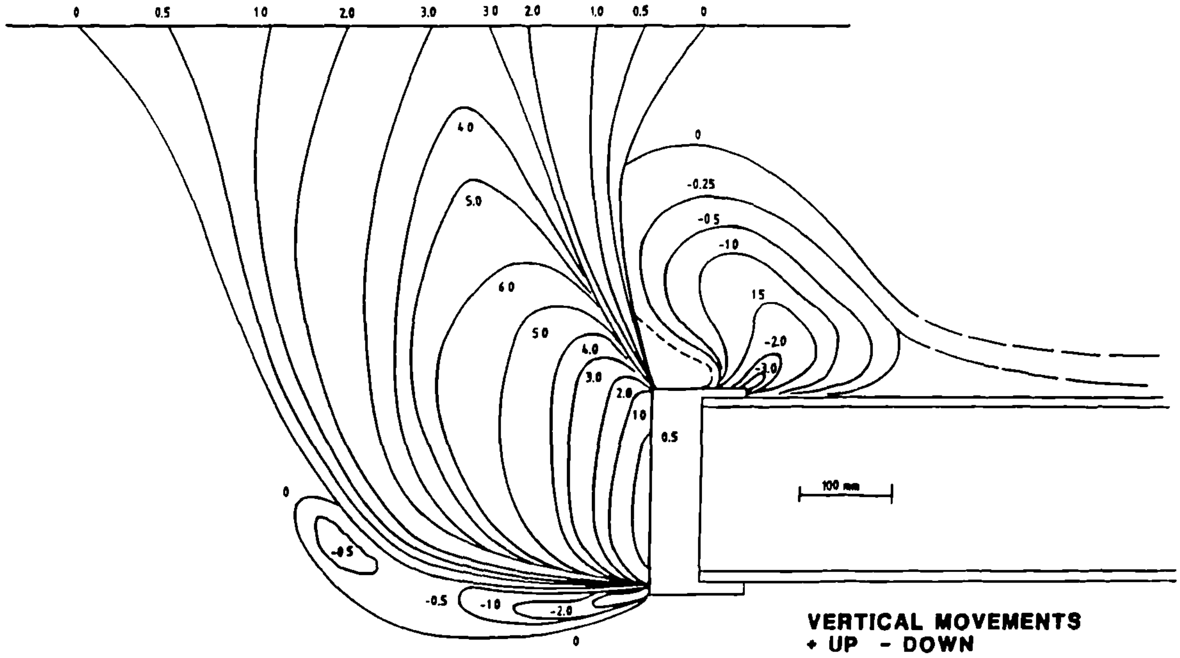

VERTICAL MOVEMENTS
+ UP - DOWN

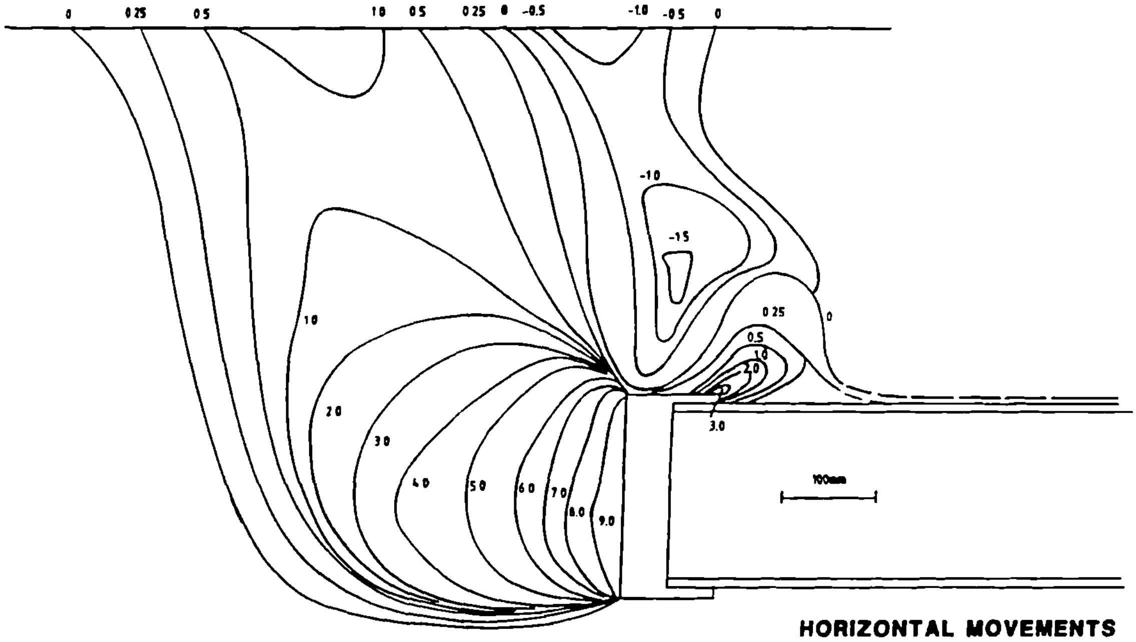

HORIZONTAL MOVEMENTS
+ LEFT - RIGHT

TEST CPJ1

2.0dLB0.1

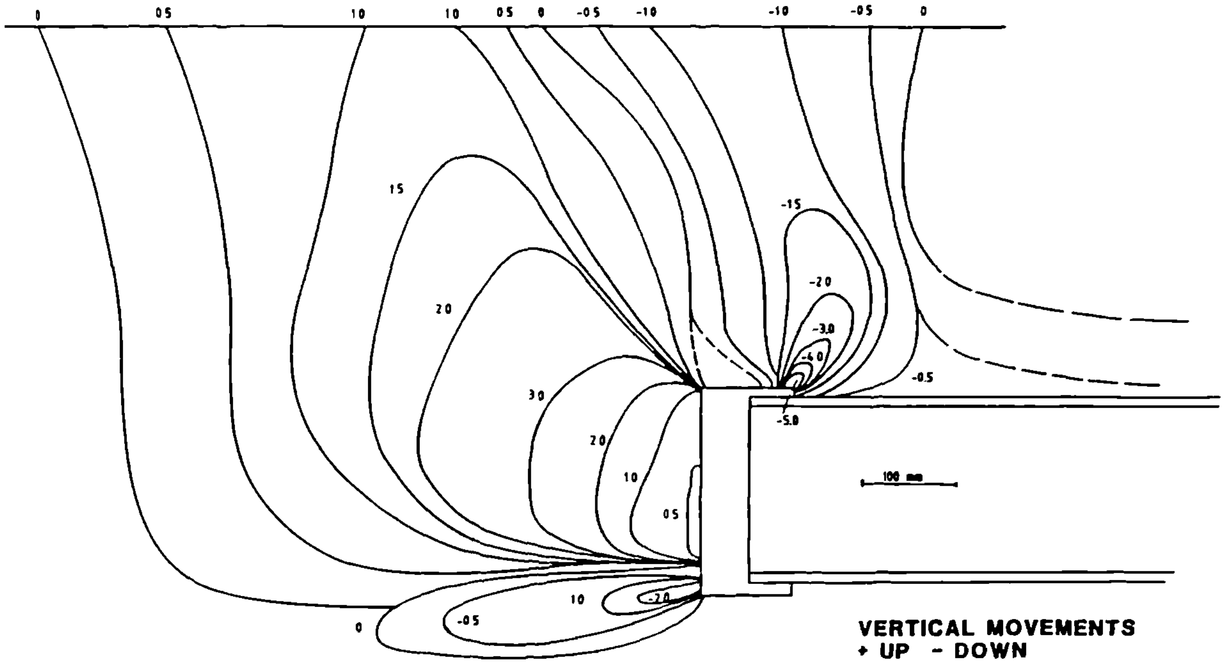

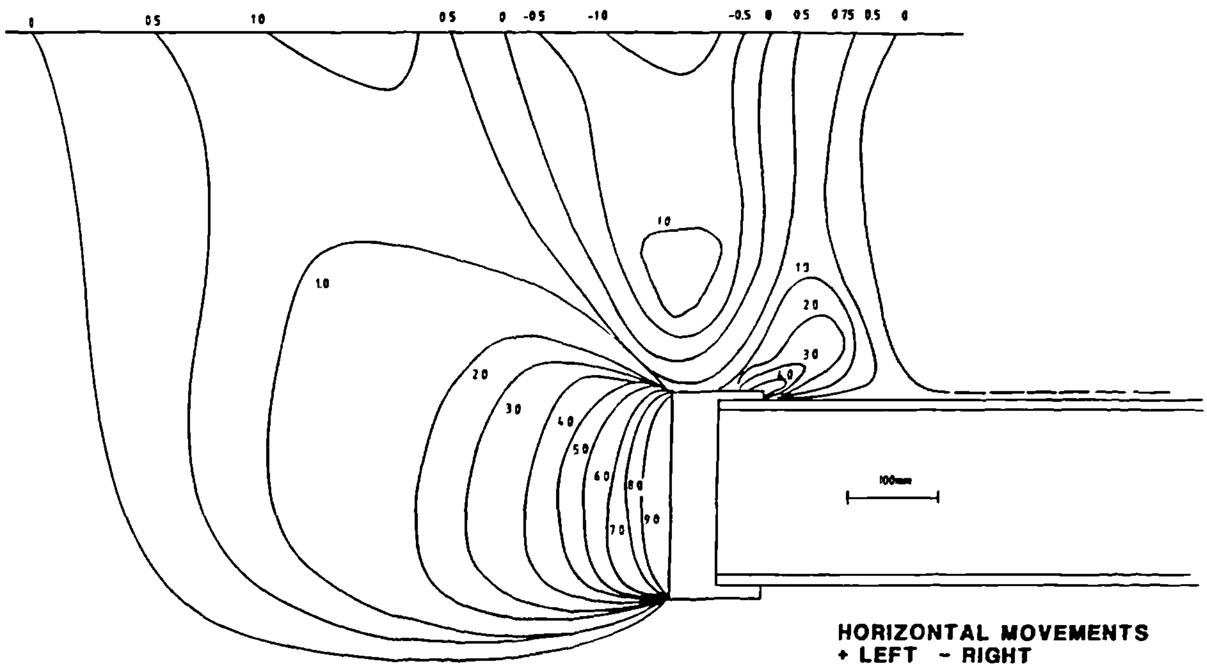

TEST CPJ2

2.0ILB0.1

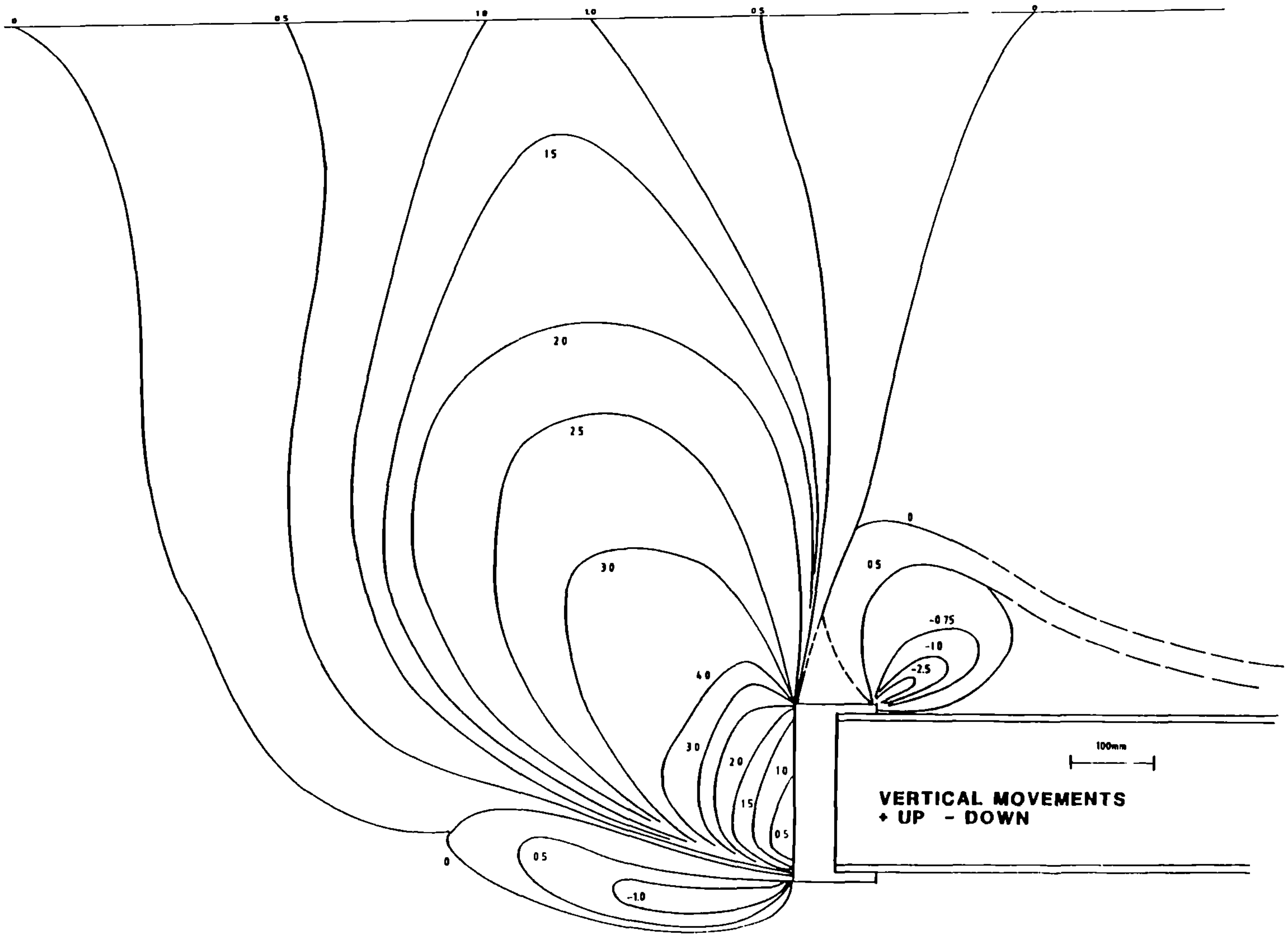

TEST CPJ3
4.5dLB0.1

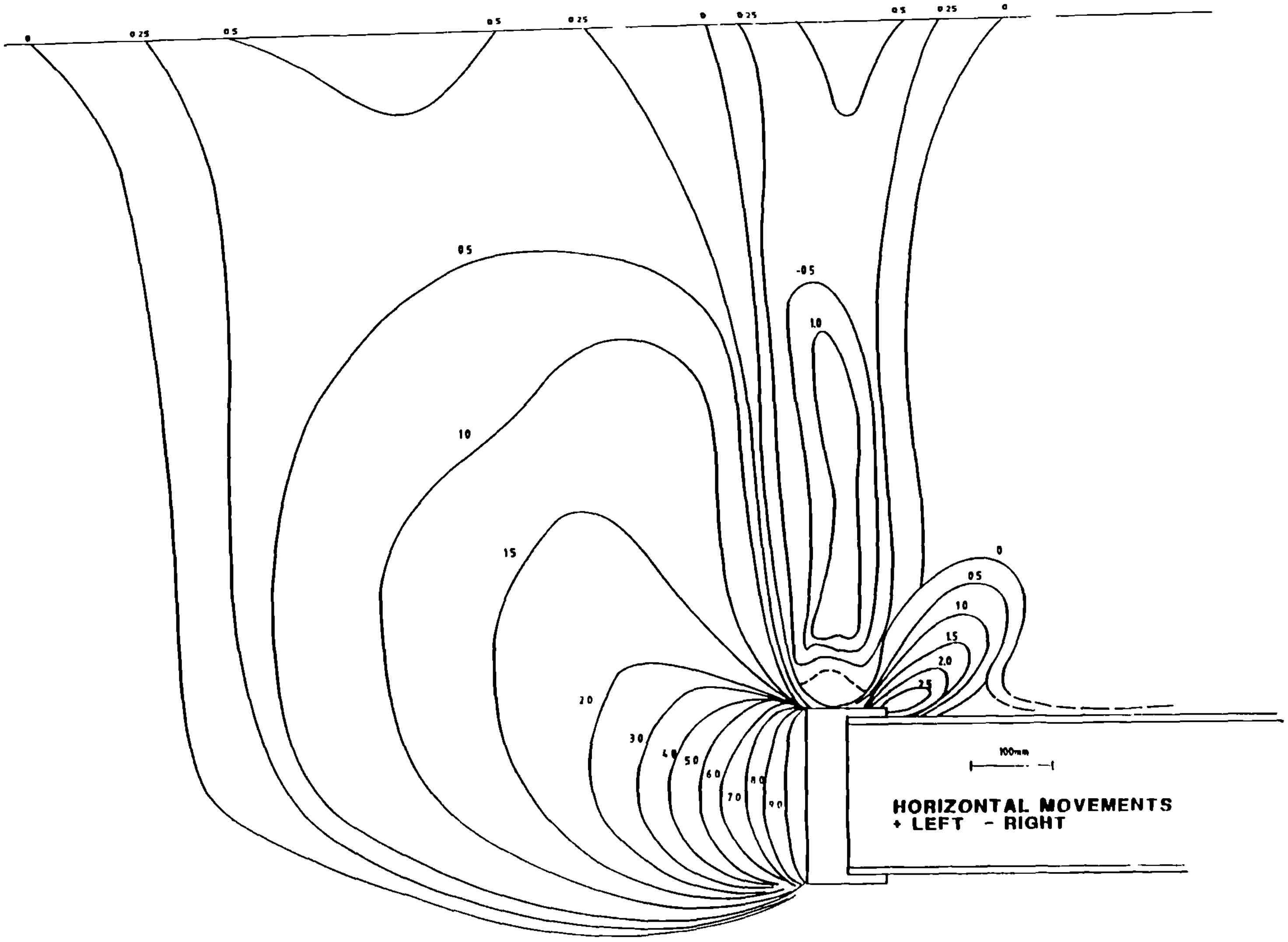

TEST CPJ3
4.5dLB0.1

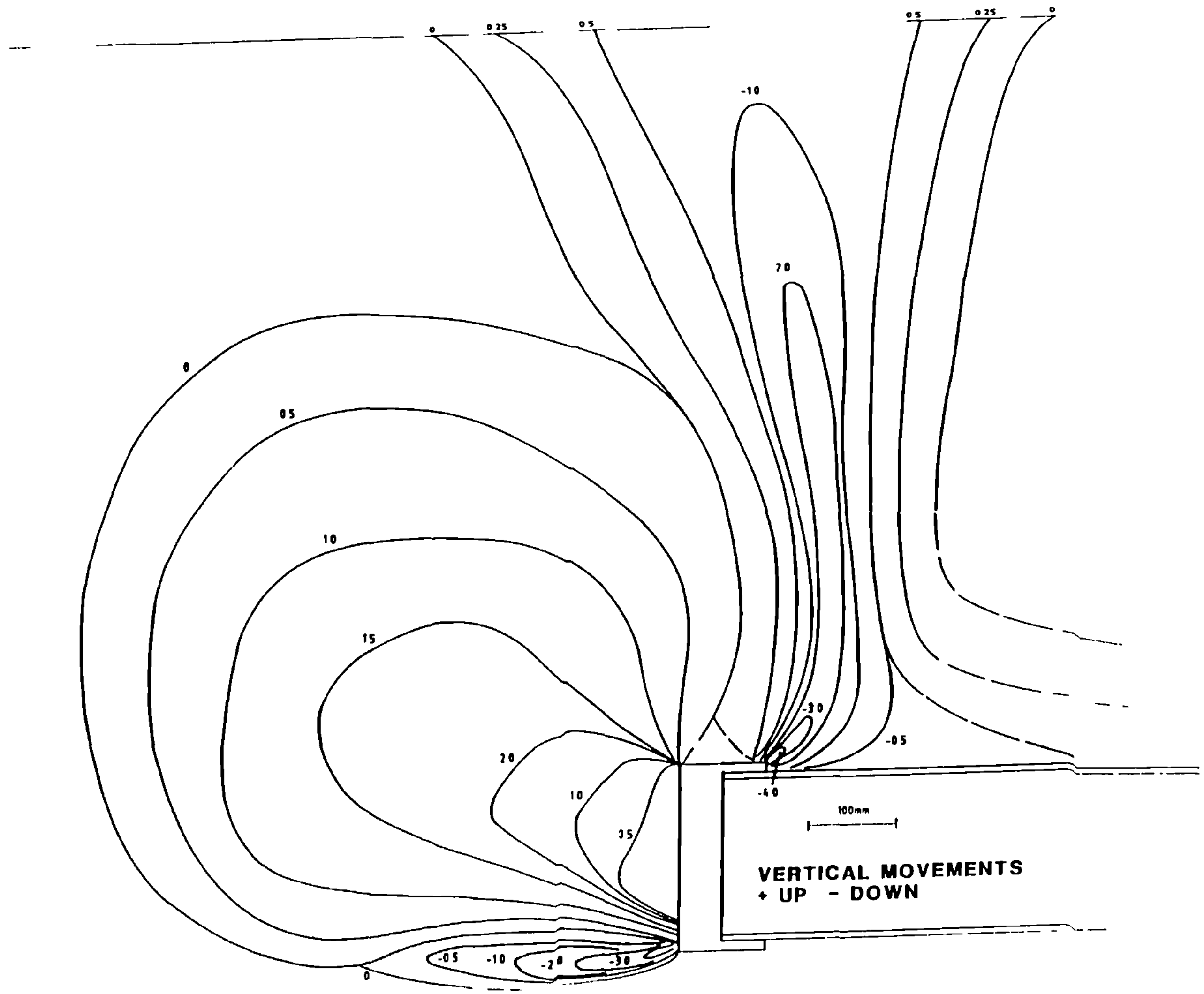

TEST CPJ4

4.5ILB0.1

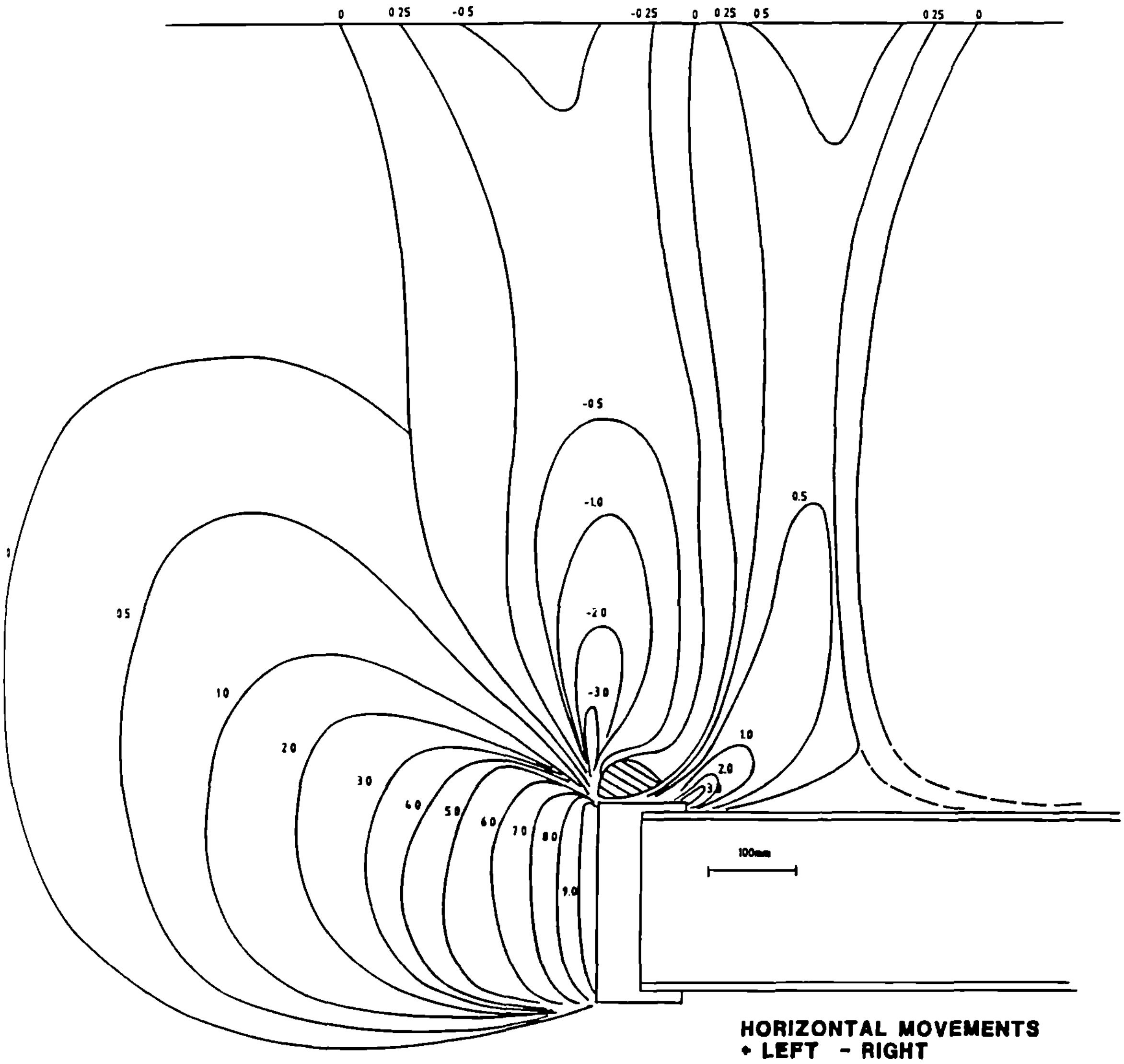

TEST CPJ4

4.5ILB0.1

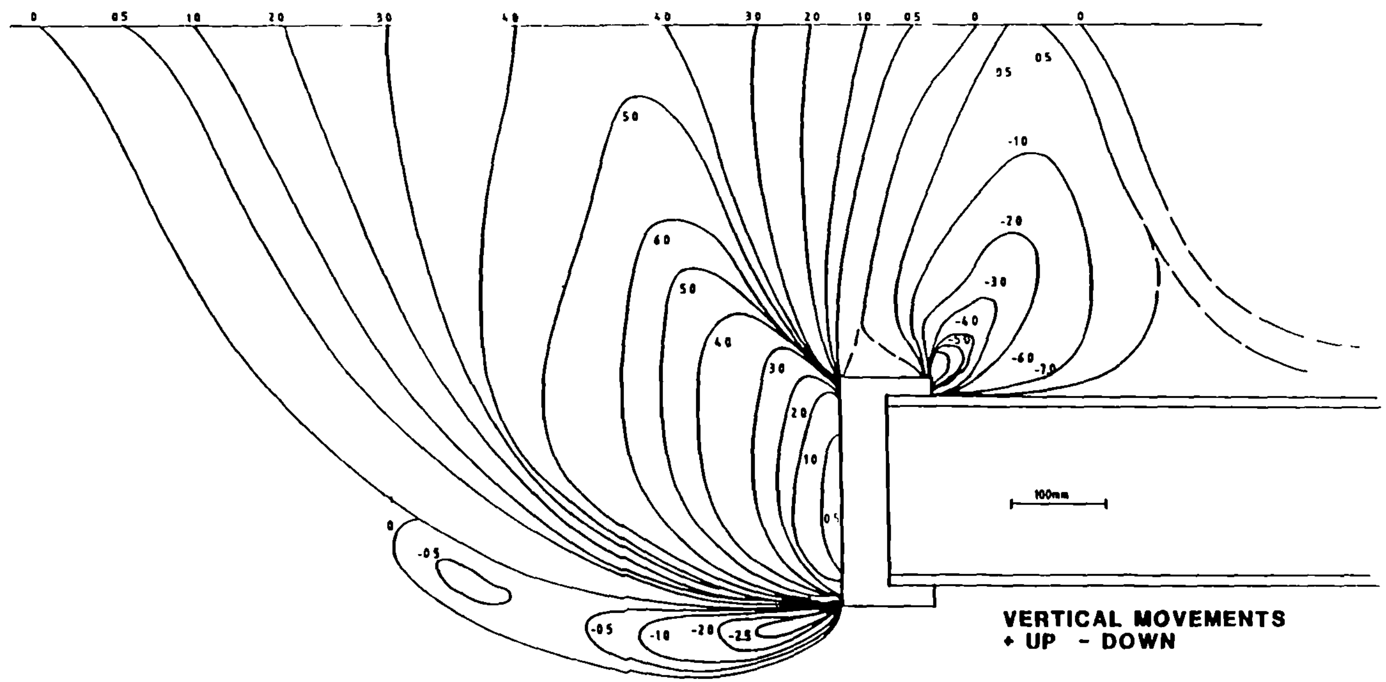

TEST CPJ5
2.0dLB0.2

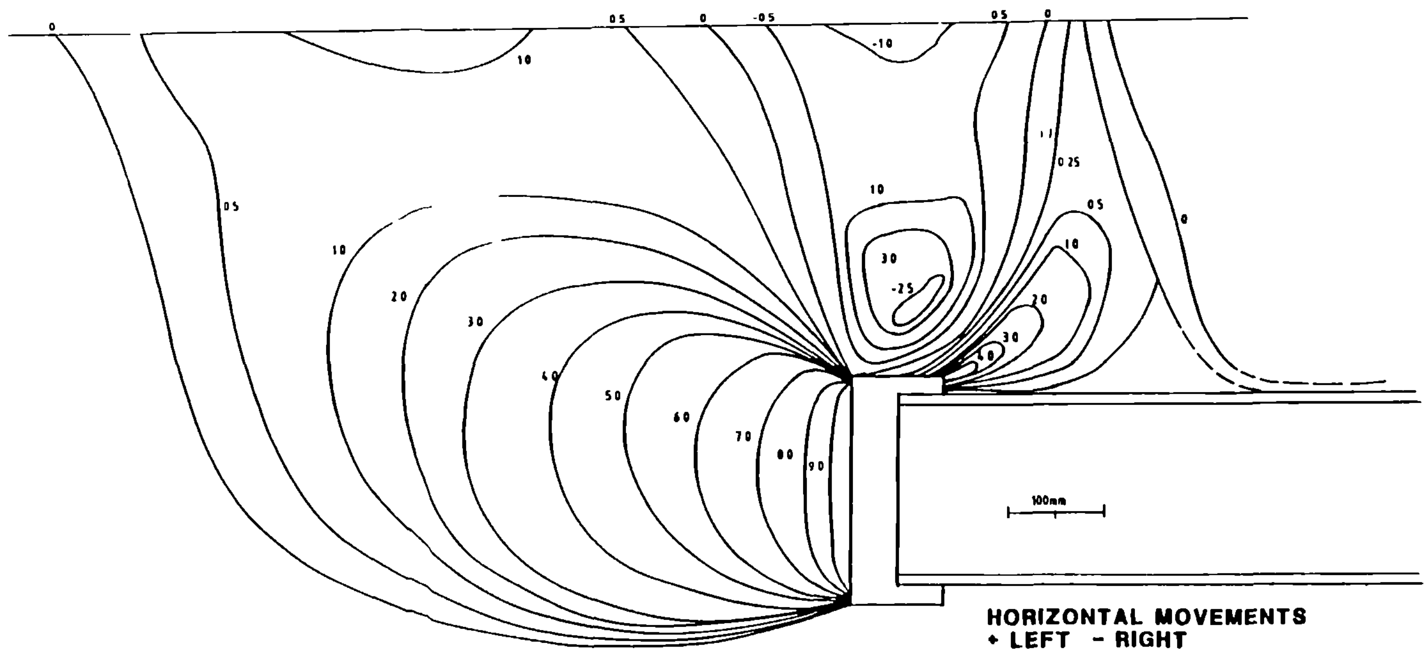

TEST CPJ5
2.0dLB0.2

B.4 PIPEBURSTING TESTS - LONGITUDINAL PLANE RESULTS

The following figures show the horizontal and vertical displacement contour plots for all the pipebursting tests in the longitudinal plane (16 tests). The contours are in millimetres and represent the movements in the sand caused by a 20mm forward jack of the bursting unit and pipe. Test codes are given to aid comparison between results. The test code is defined as: Cover depth to diameter of old pipe (C/D_o), density state of sand, sand type, bursting ratio (D_f/D_o).

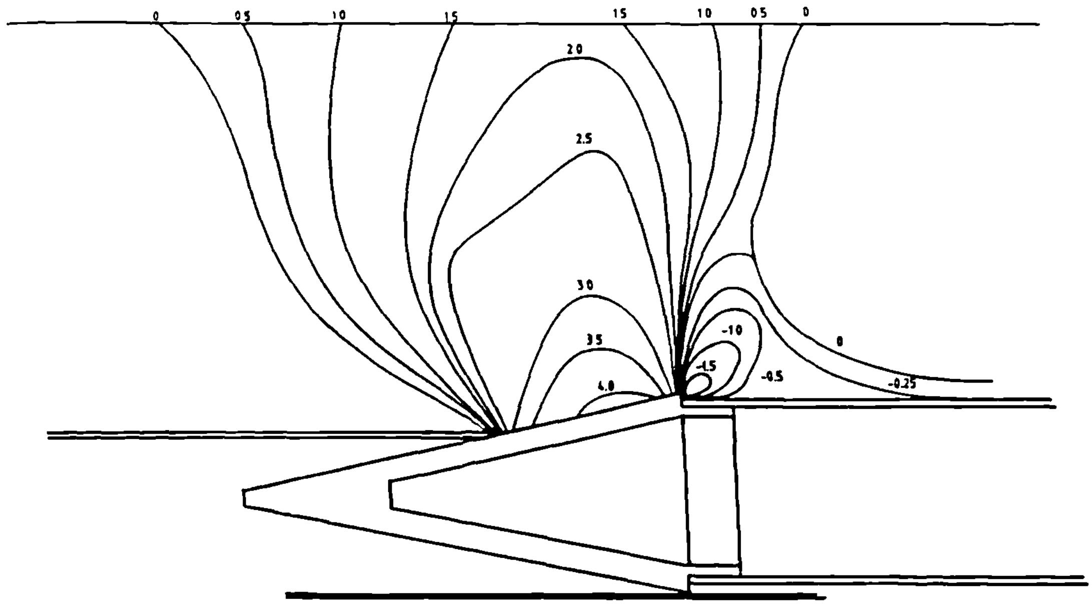

VERTICAL MOVEMENTS
+ UP - DOWN

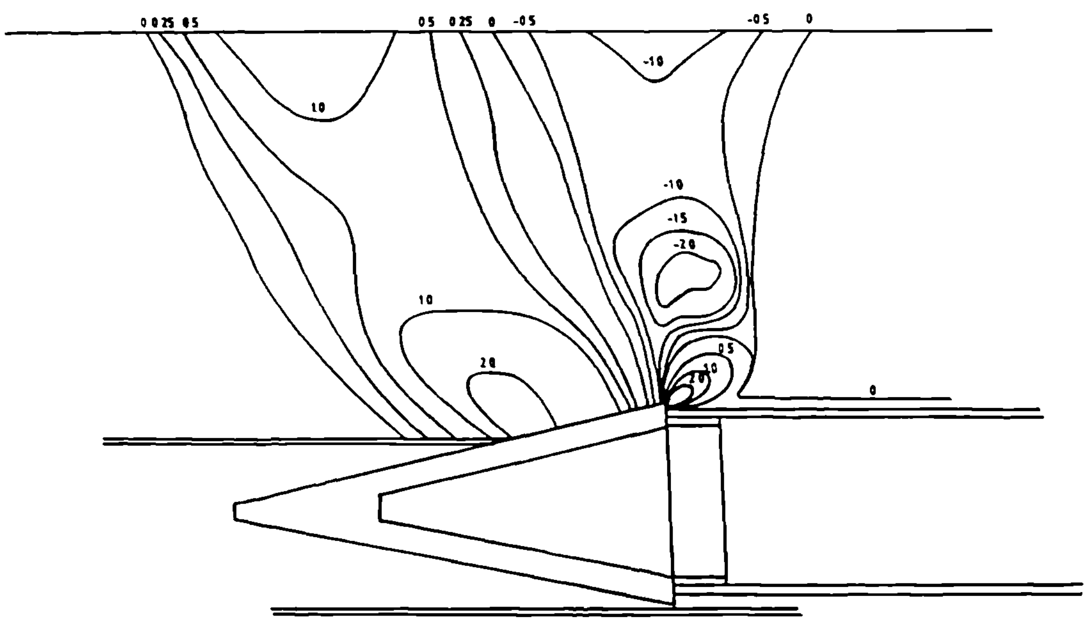

HORIZONTAL MOVEMENTS
+ LEFT - RIGHT

TEST PB1

2.6dLB1.2

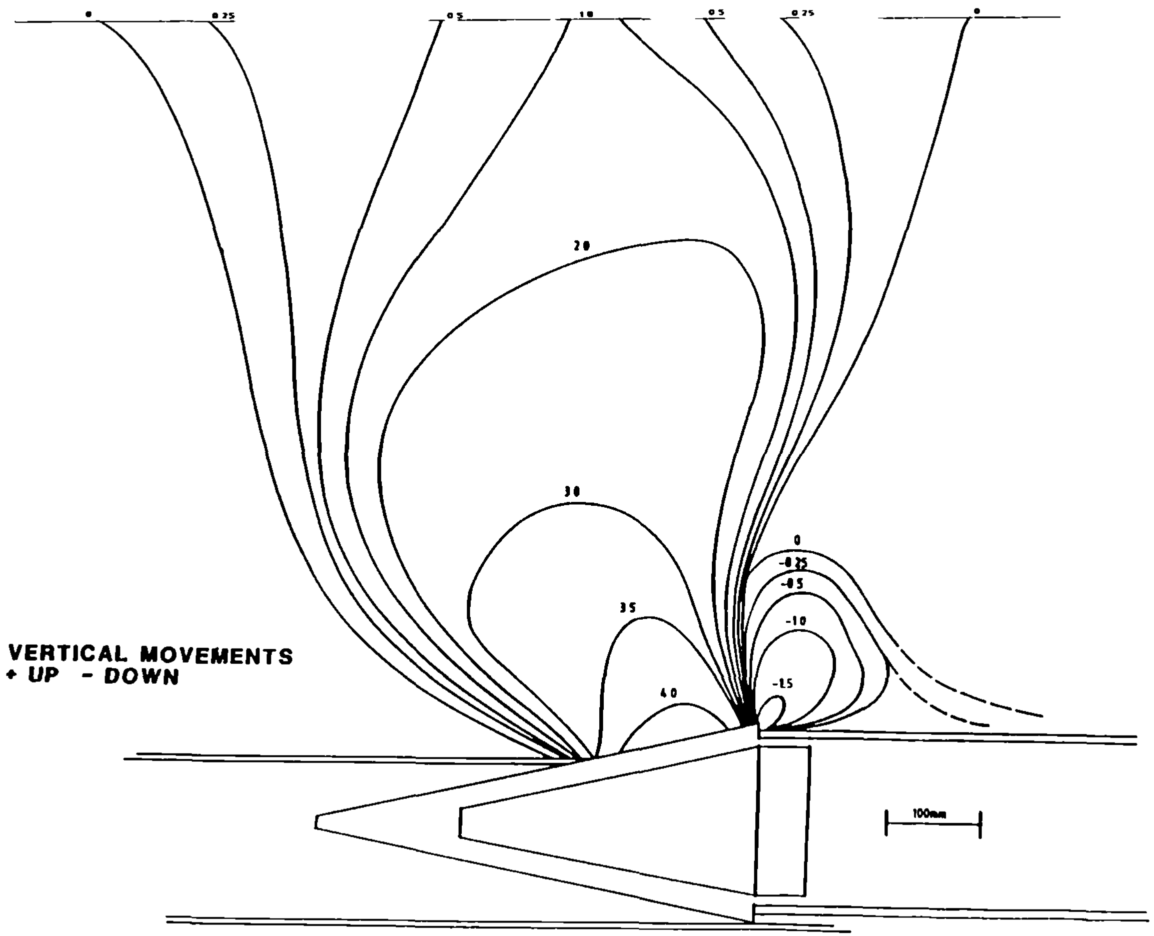

TEST PB2

4.9dLB1.2

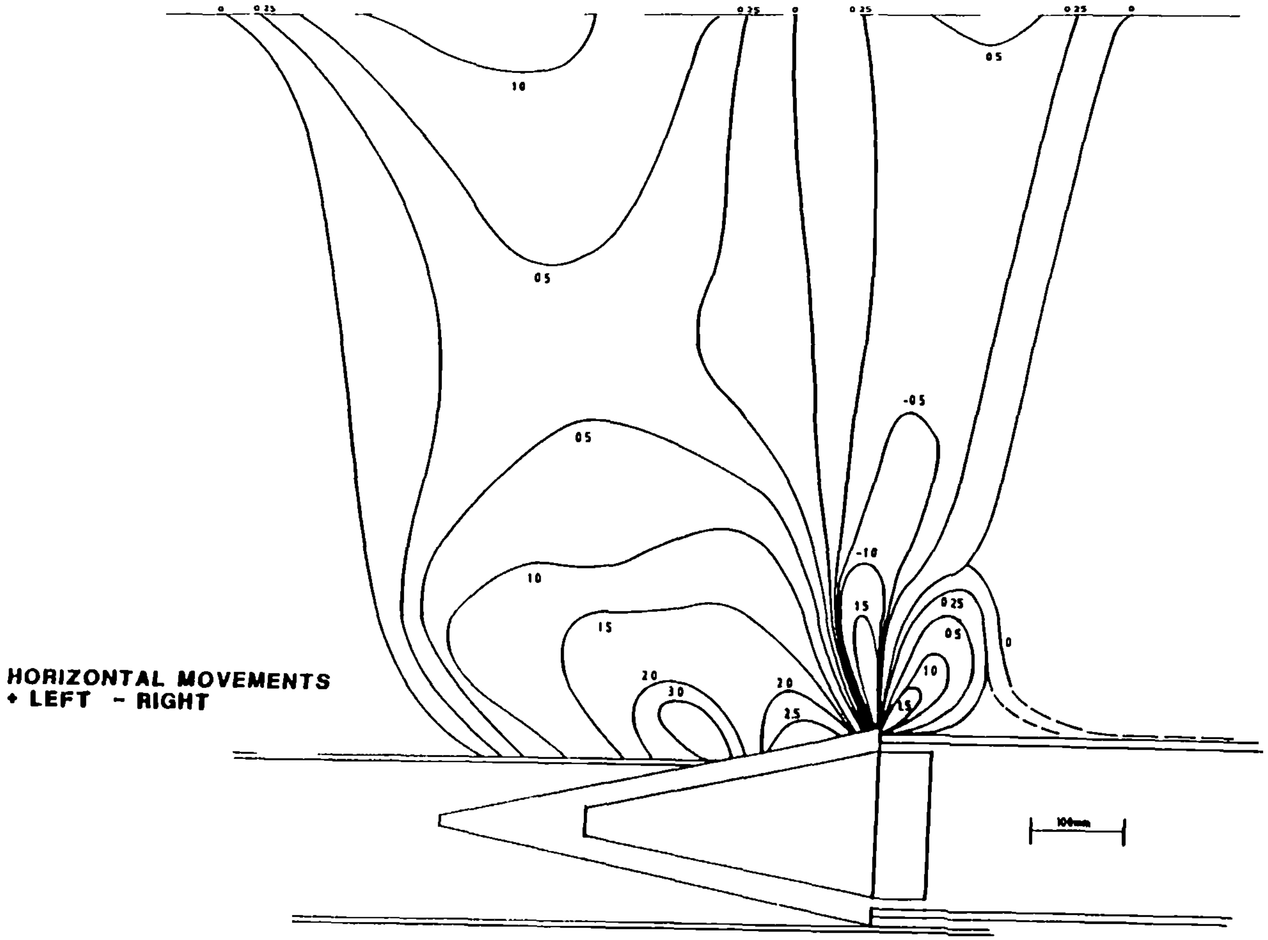

TEST PB2

4.9dLB1.2

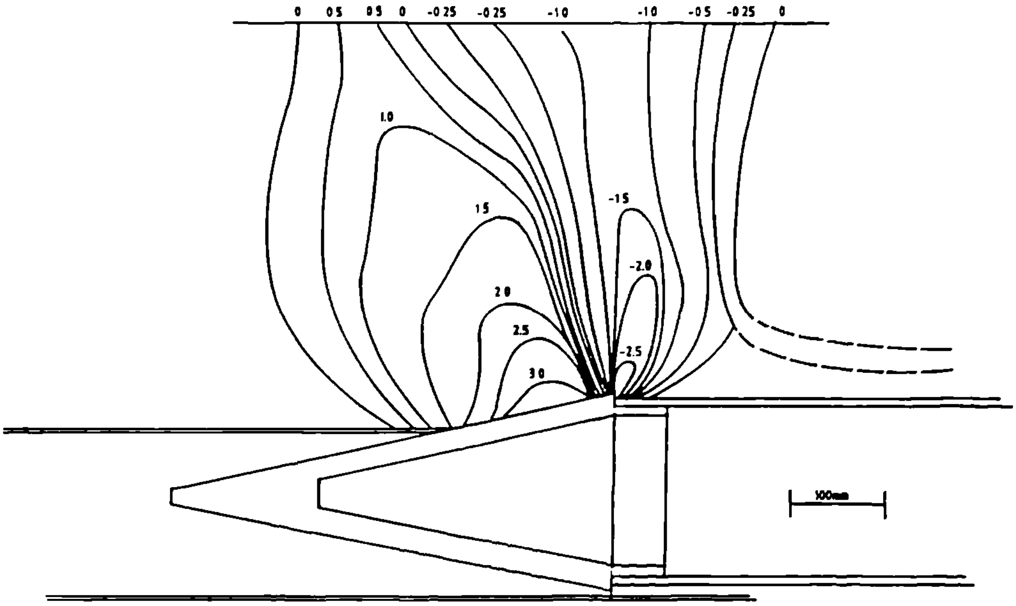

VERTICAL MOVEMENTS
+ UP - DOWN

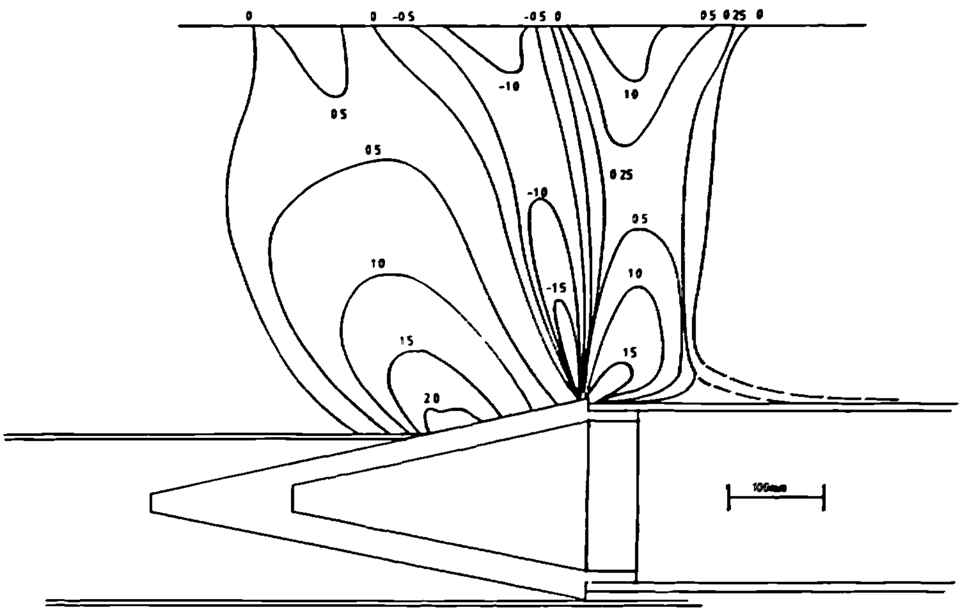

HORIZONTAL MOVEMENTS
+ LEFT - RIGHT

TEST PB3

2.61LB1.2

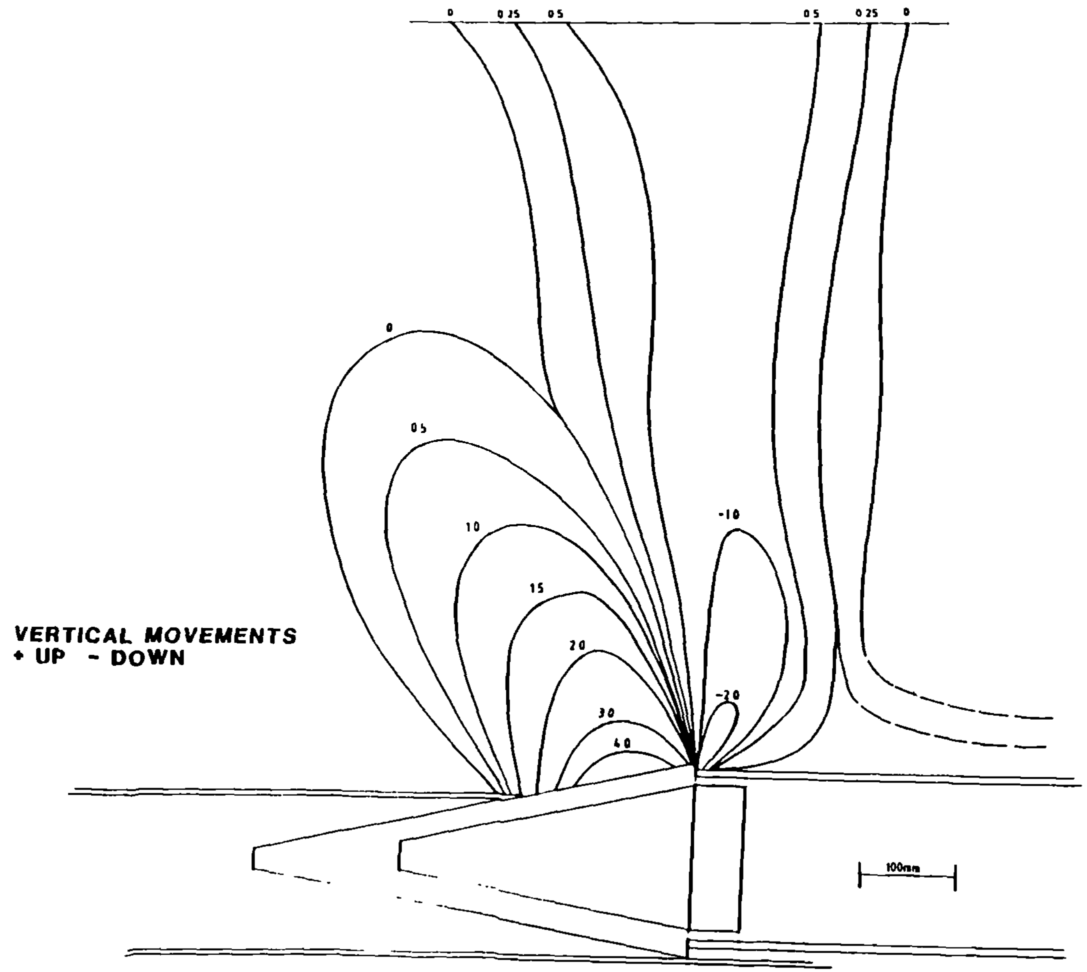

TEST PB4

4.91LB1.2

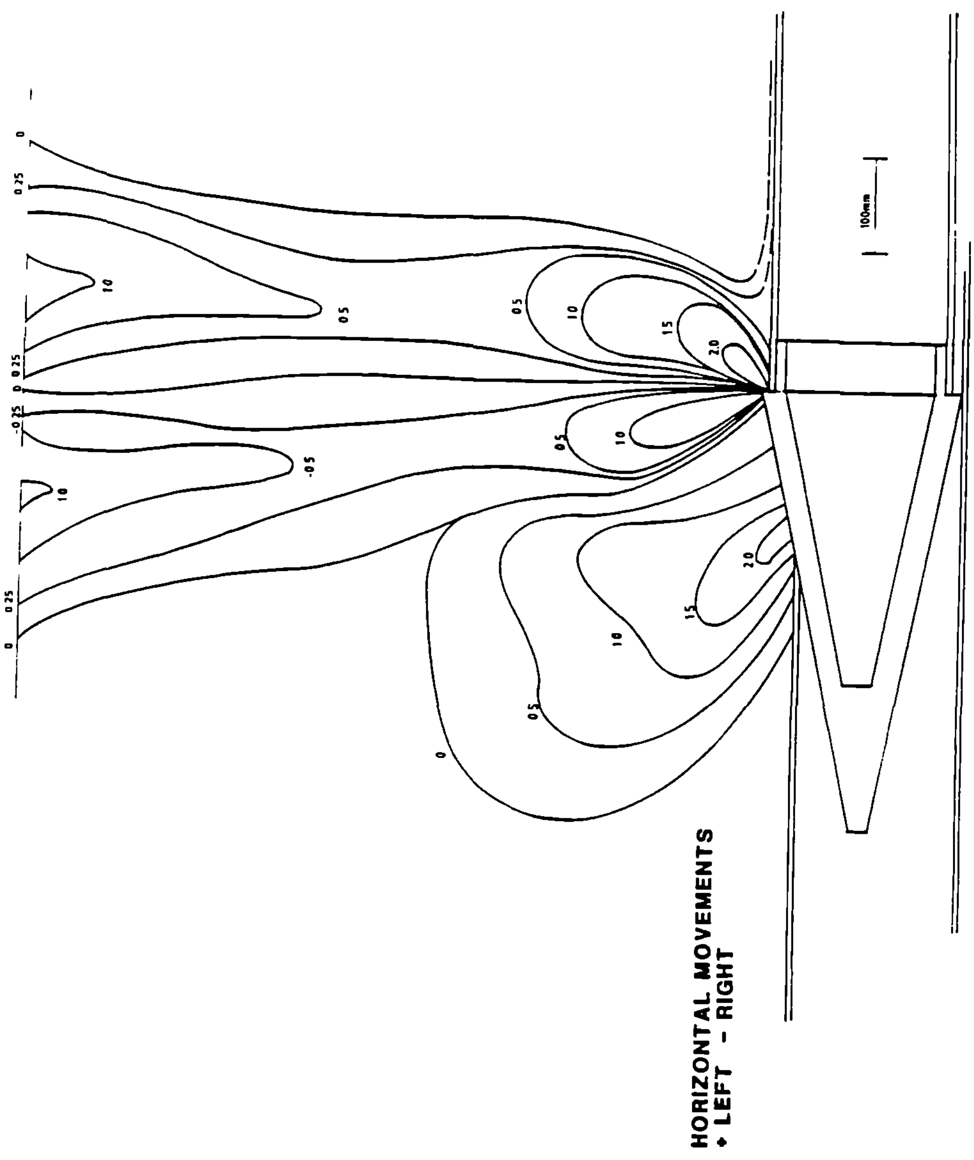

TEST PB4
4.91LB1.2

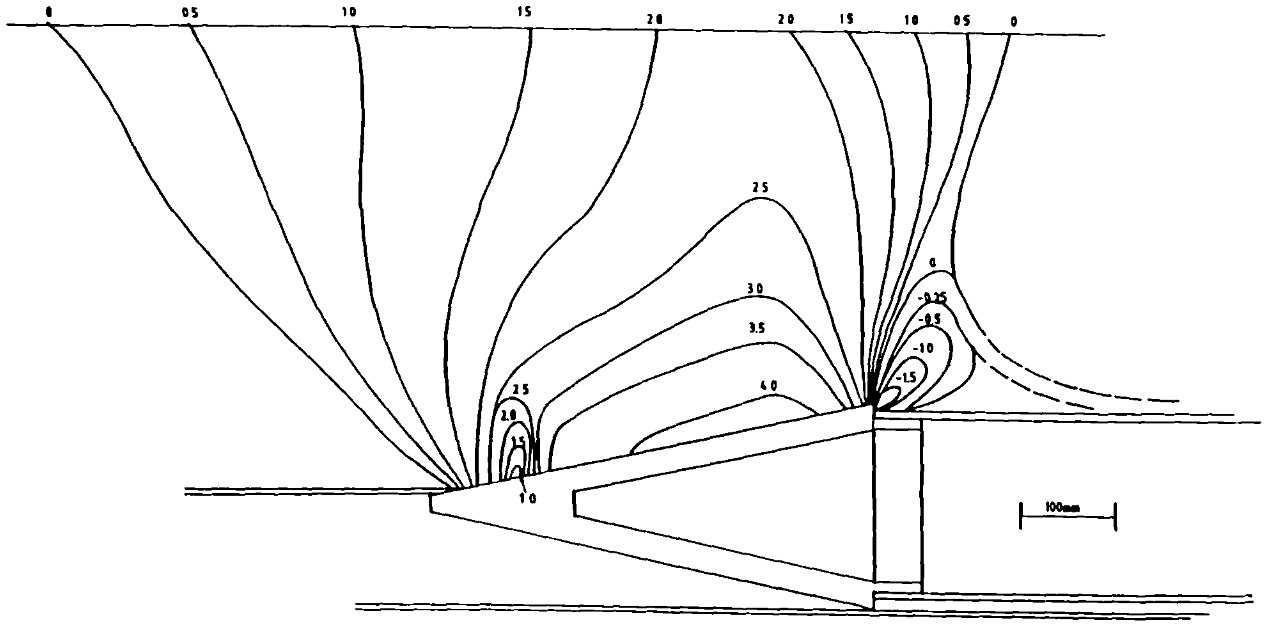

VERTICAL MOVEMENTS
+ UP - DOWN

TEST PB5
3.8dLB1.7

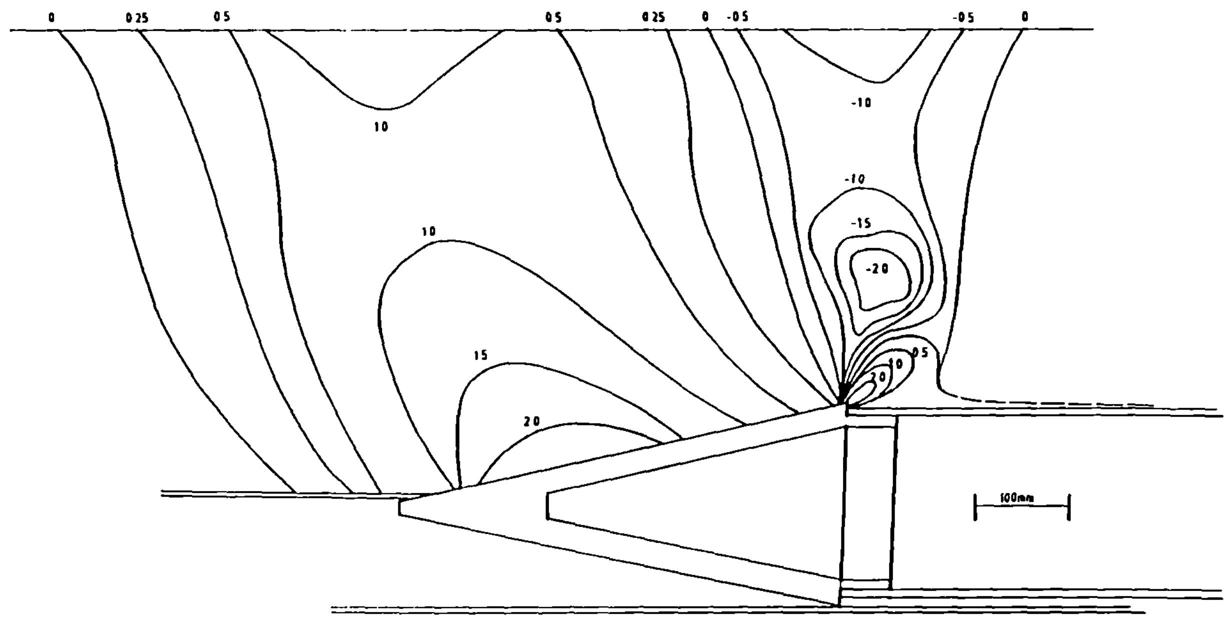

HORIZONTAL MOVEMENTS
+ LEFT - RIGHT

TEST PB5
3.8dLB1.7

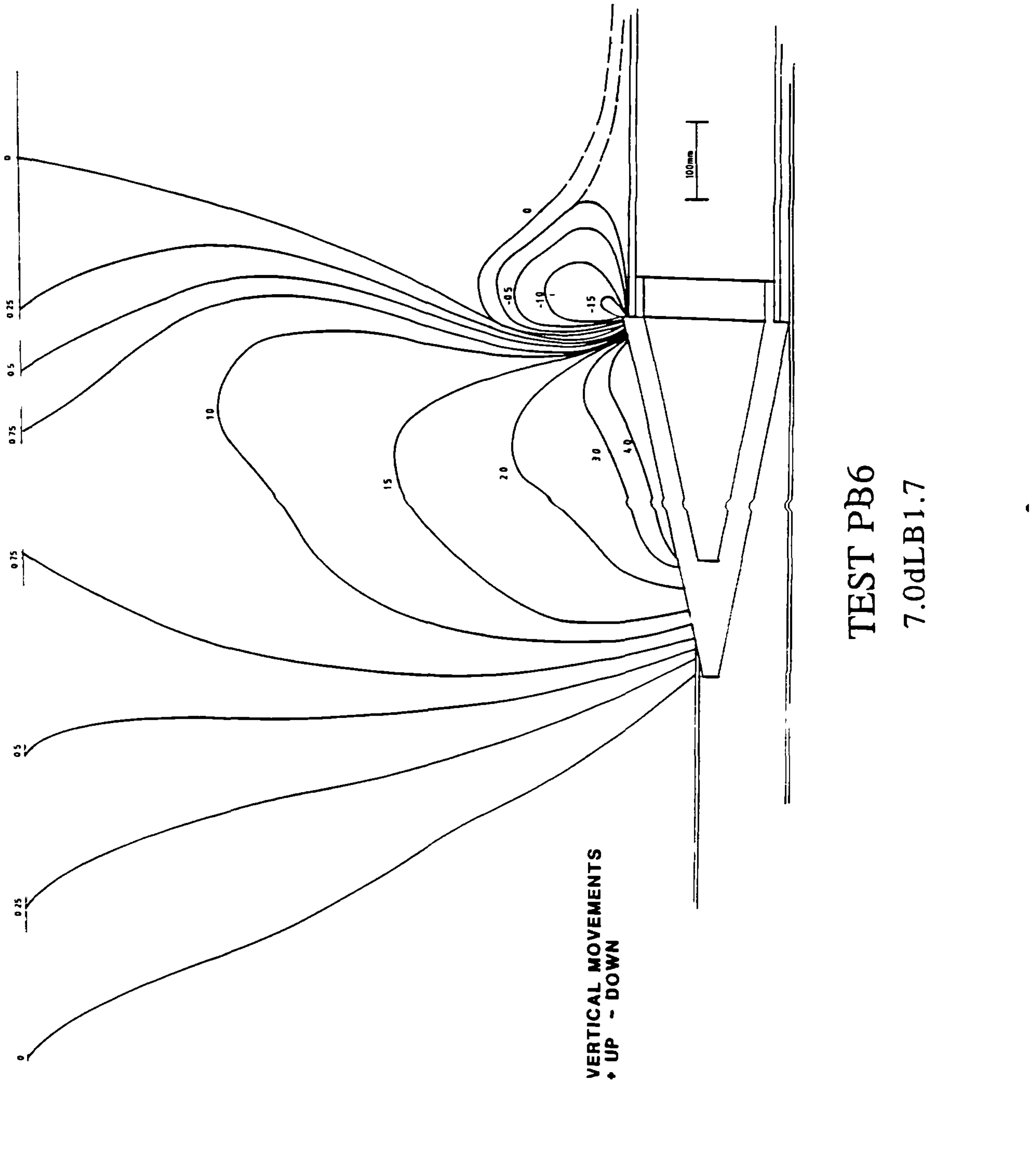
VERTICAL MOVEMENTS
+ UP - DOWN
100mm
0
0.25
0.5
0.75
0.75
0.5
0.25
0
0
-0.5
-1.0
-1.5
1.0
1.5
2.0
3.0
4.0
TEST PB6
7.0dLB1.7

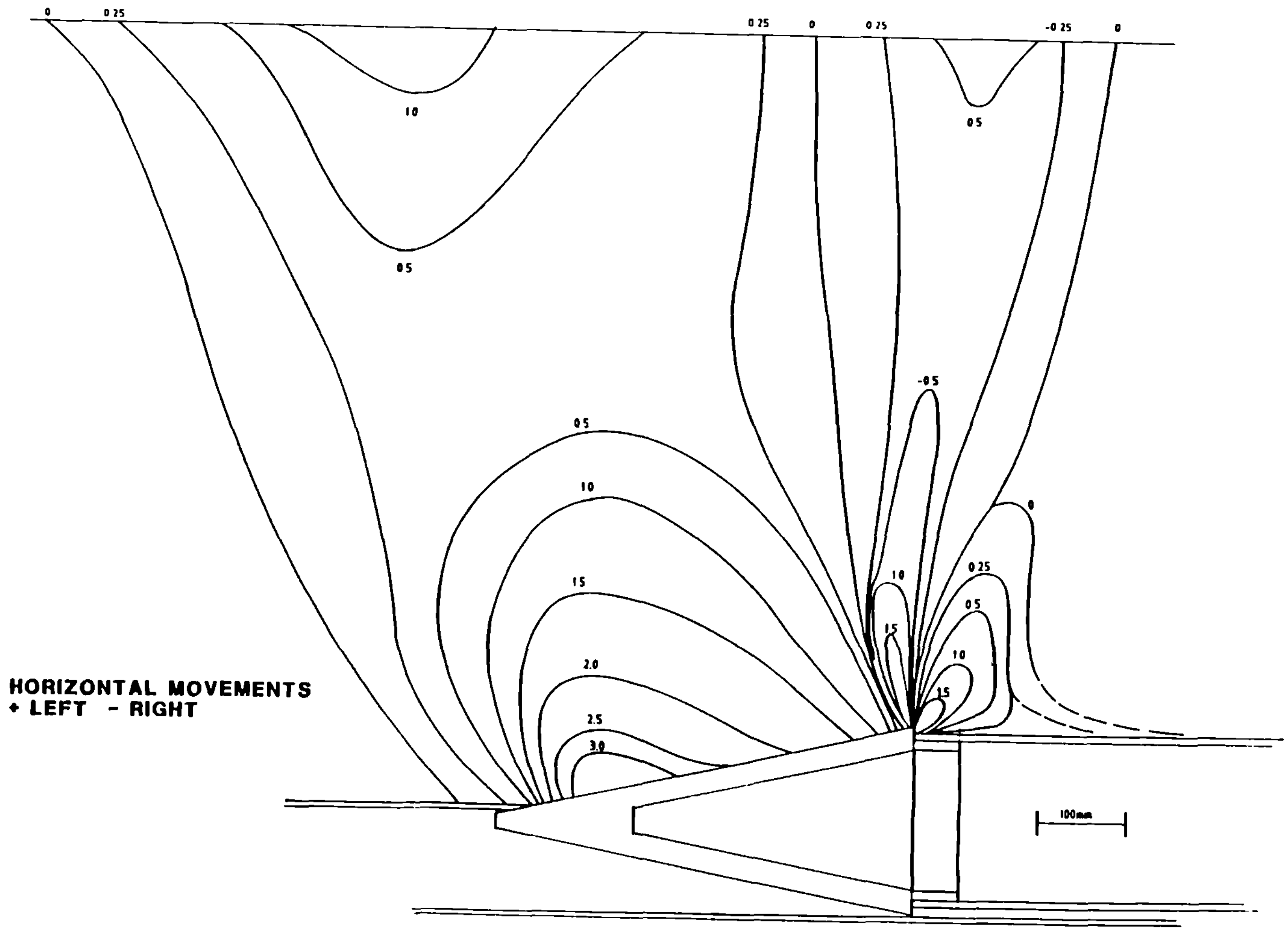

TEST PB6
7.0dLB1.7

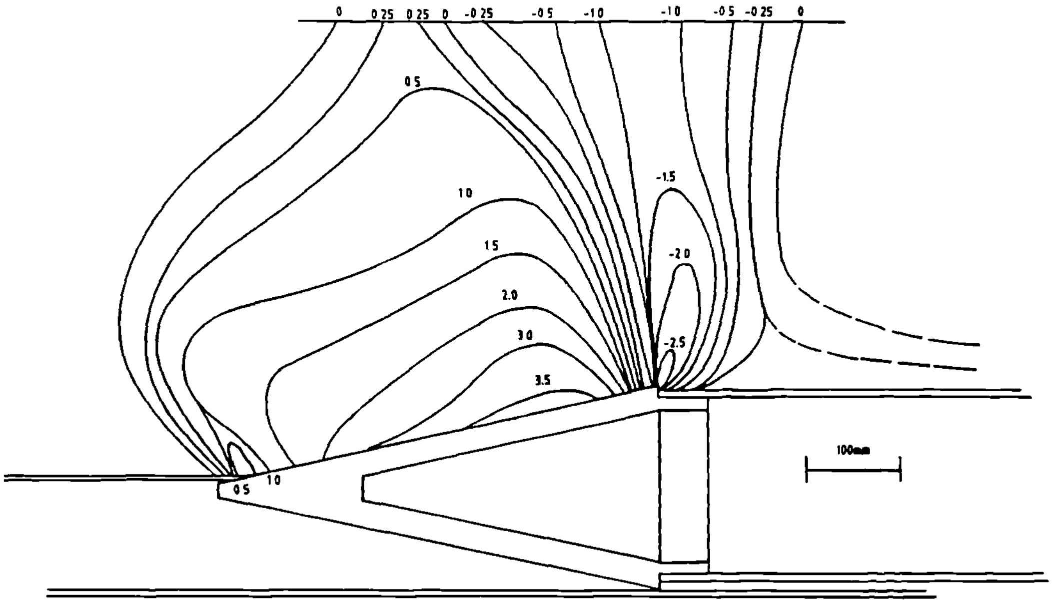

VERTICAL MOVEMENTS
+ UP - DOWN

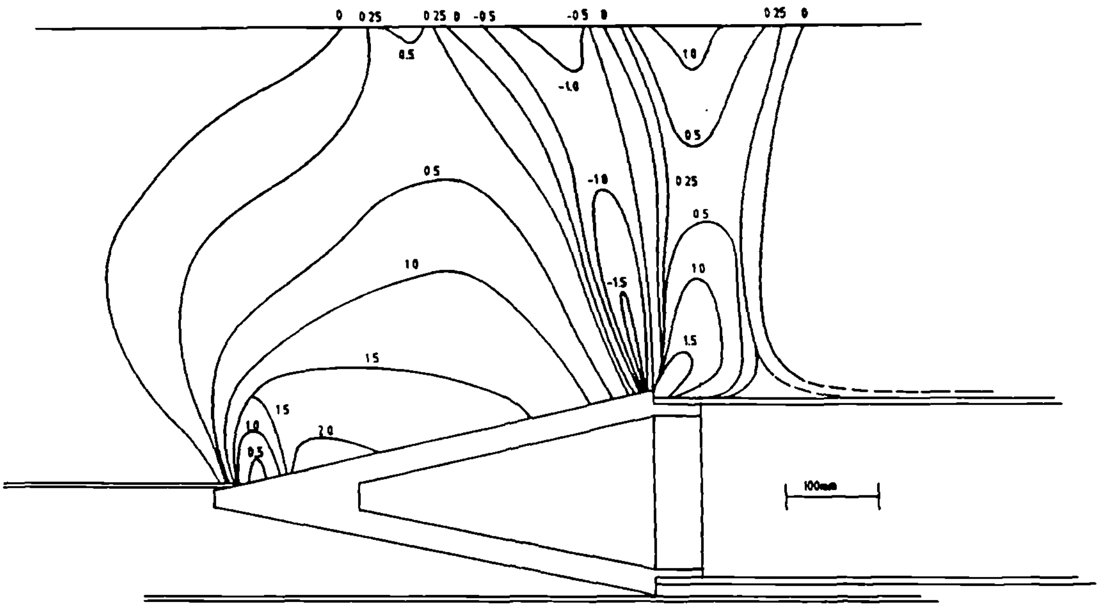

HORIZONTAL MOVEMENTS
+ LEFT - RIGHT

TEST PB7

3.81LB1.7

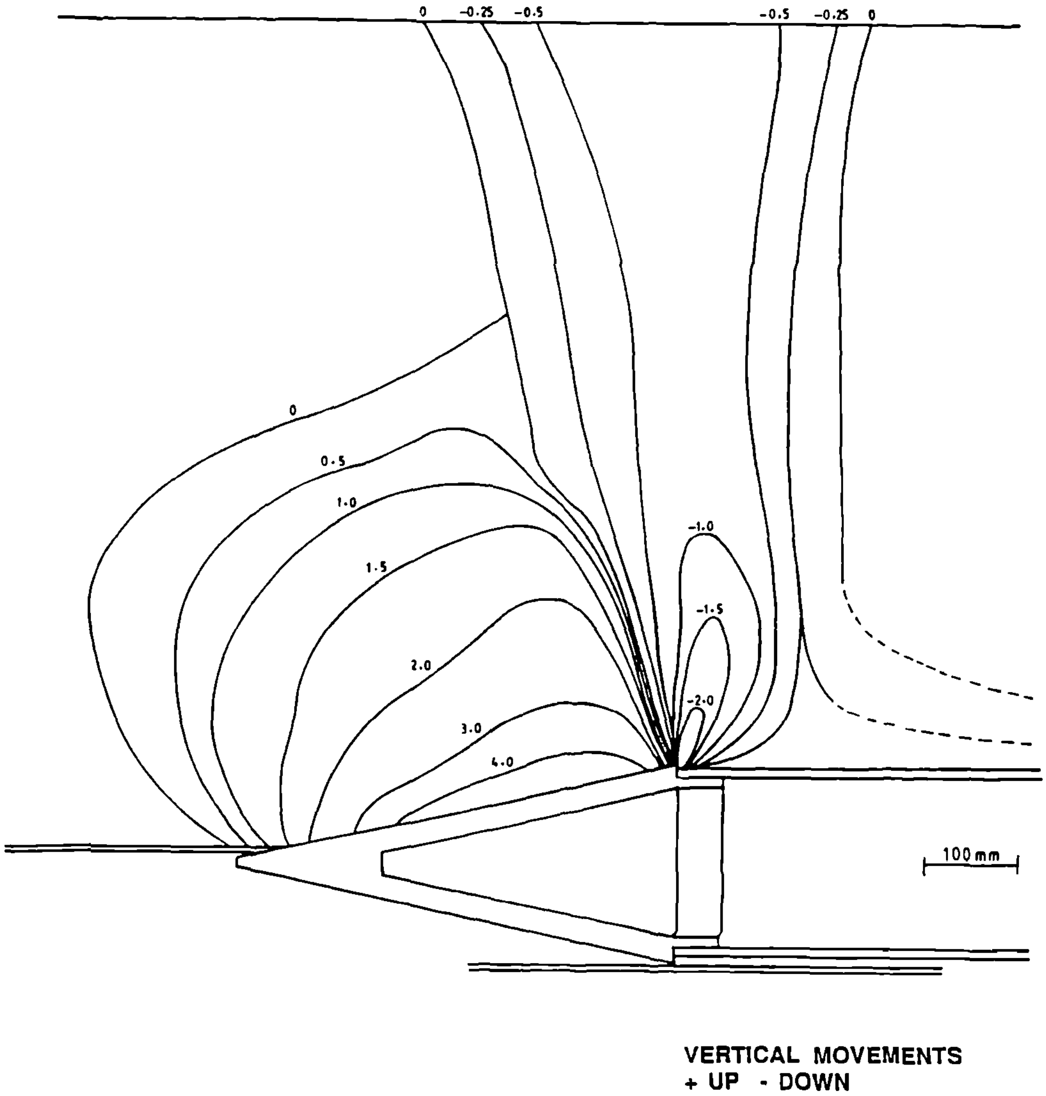

TEST PB8

7.01LB1.7

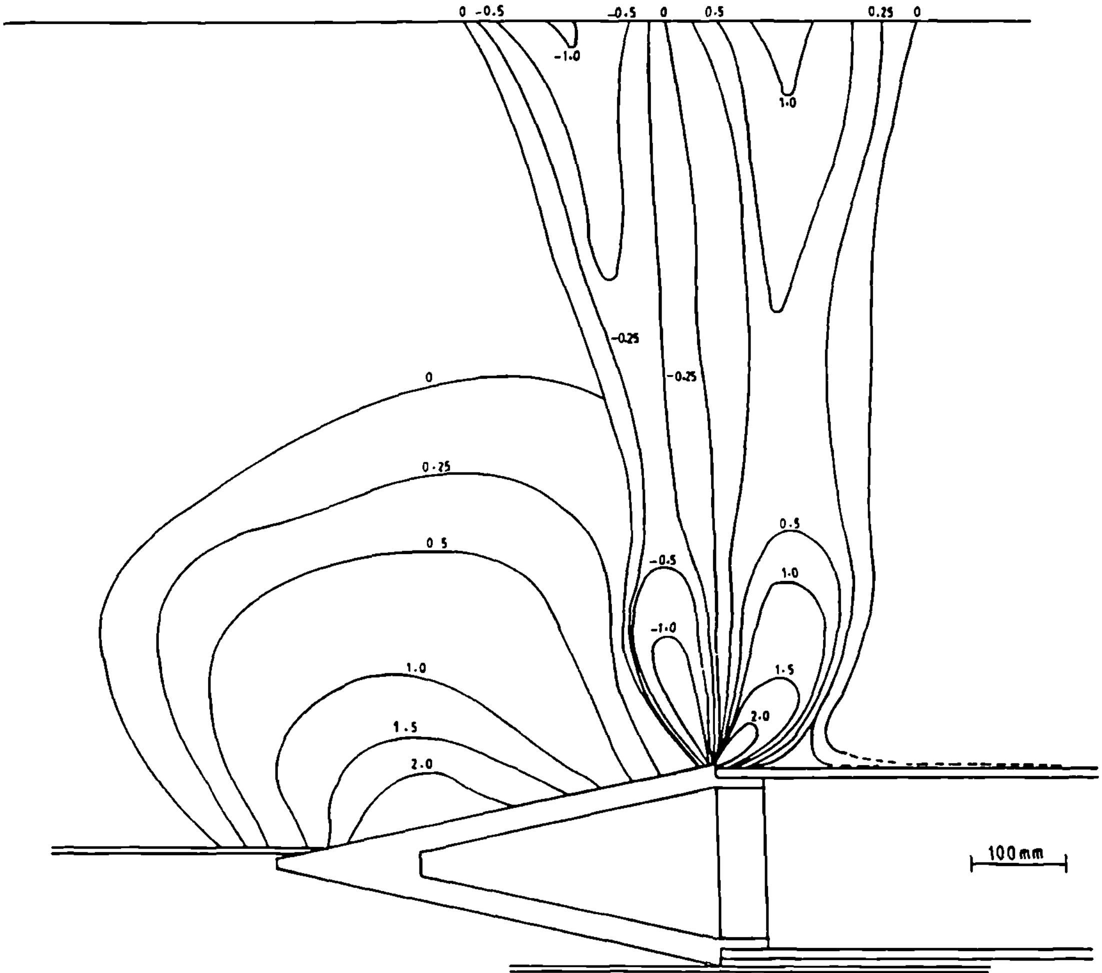

HORIZONTAL MOVEMENTS
+ LEFT - RIGHT

TEST PB8

7.01LB1.7

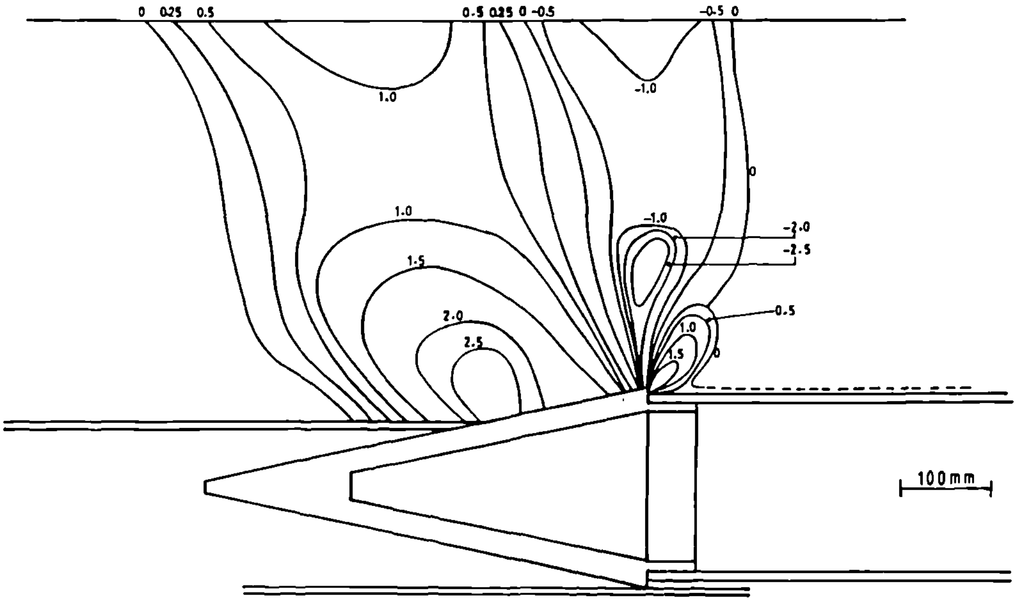

HORIZONTAL MOVEMENTS
+ LEFT - RIGHT

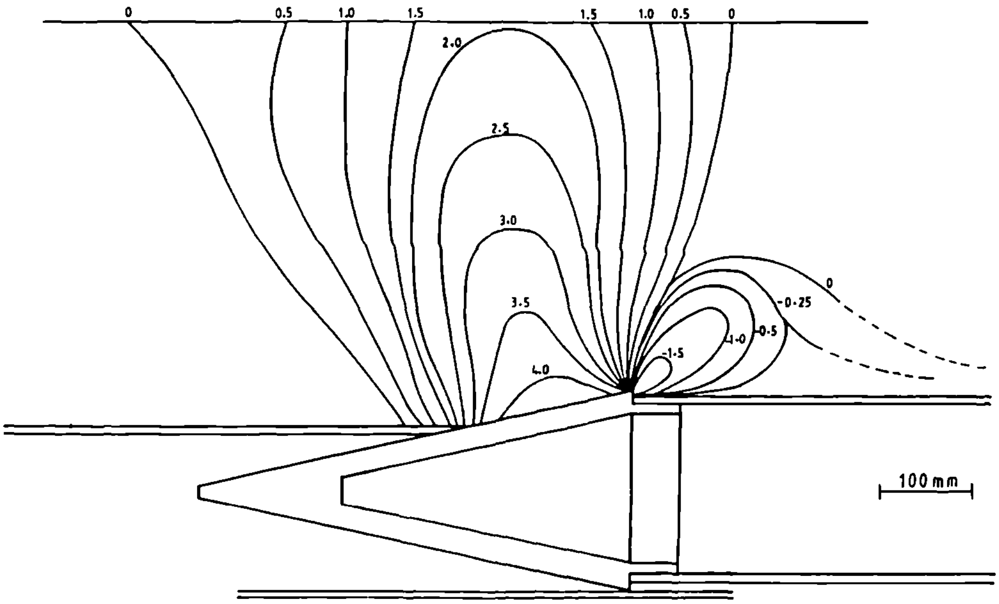

VERTICAL MOVEMENTS
+ UP - DOWN

TEST PB9
2.6d25B1.2

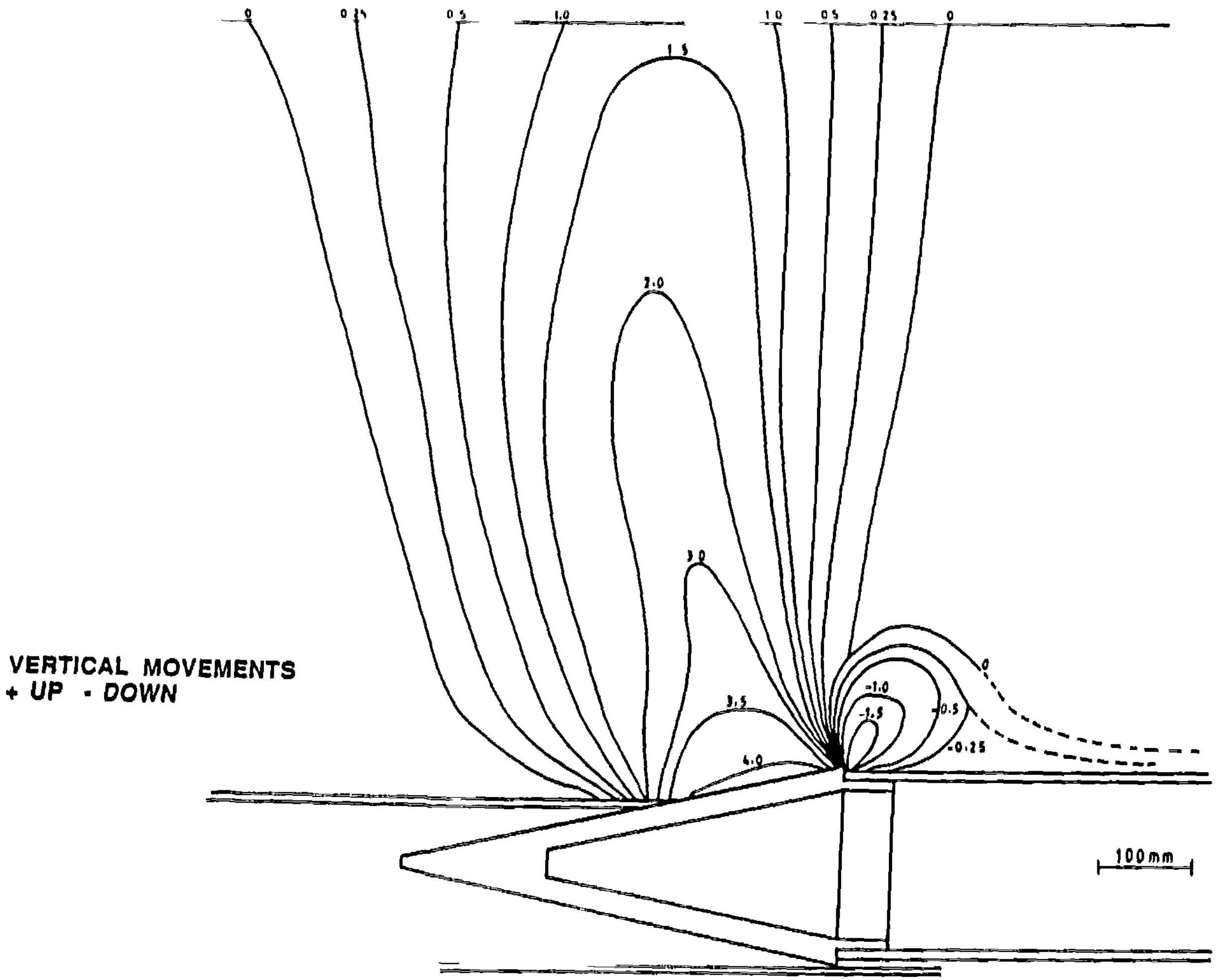

TEST PB10
4.9d25B1.2

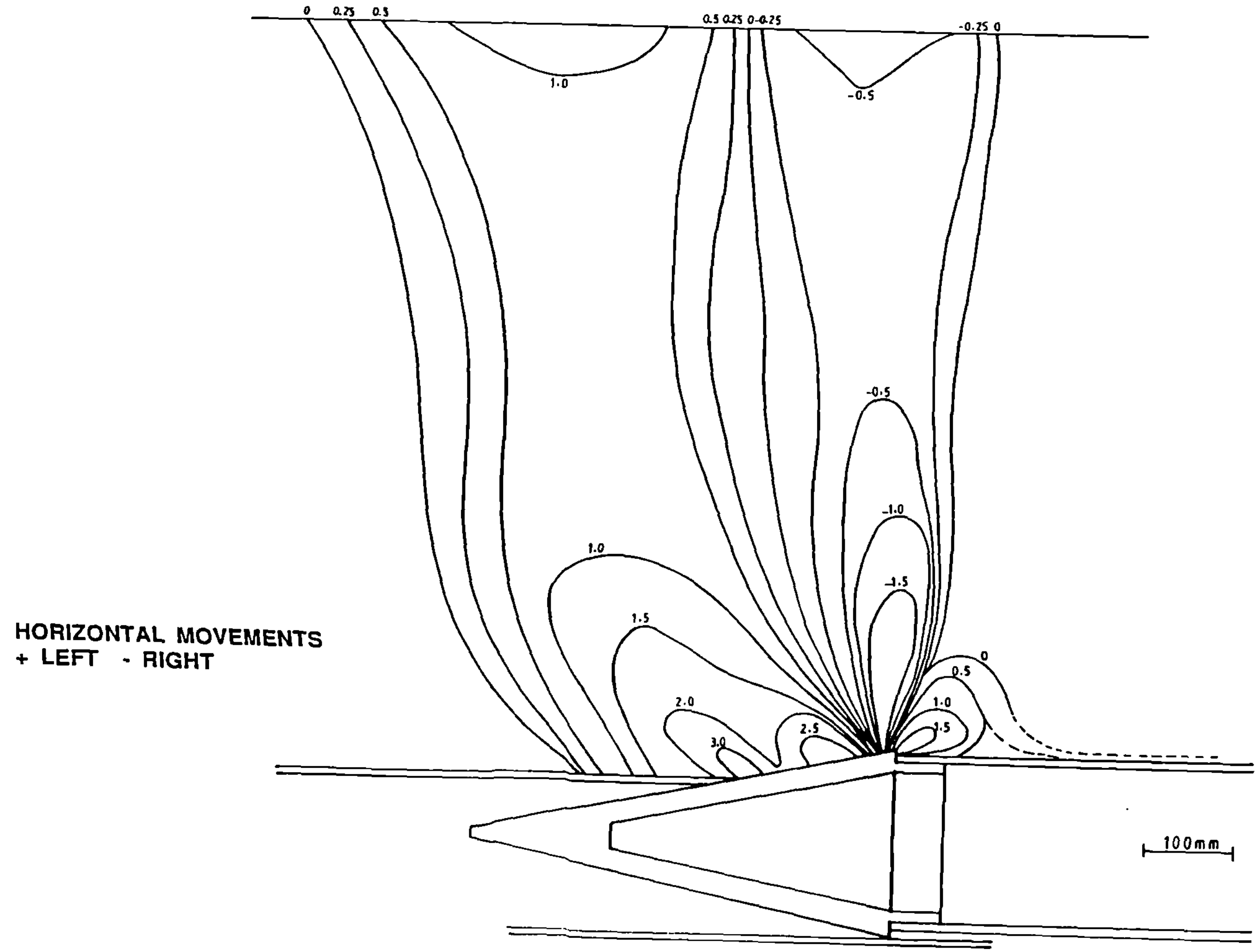

TEST PB10
4.9d25B1.2

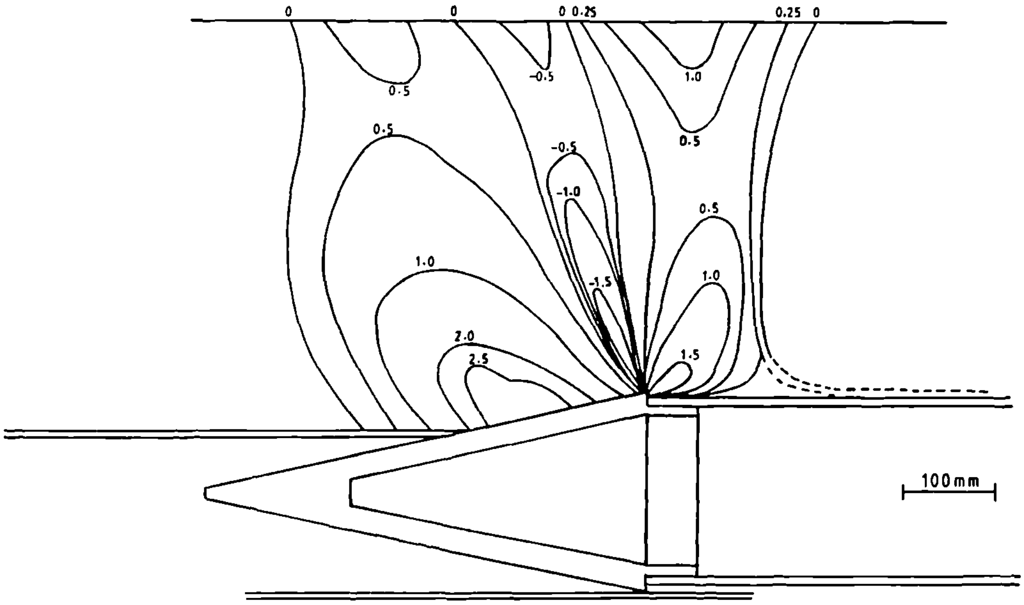

HORIZONTAL MOVEMENTS
+ LEFT - RIGHT

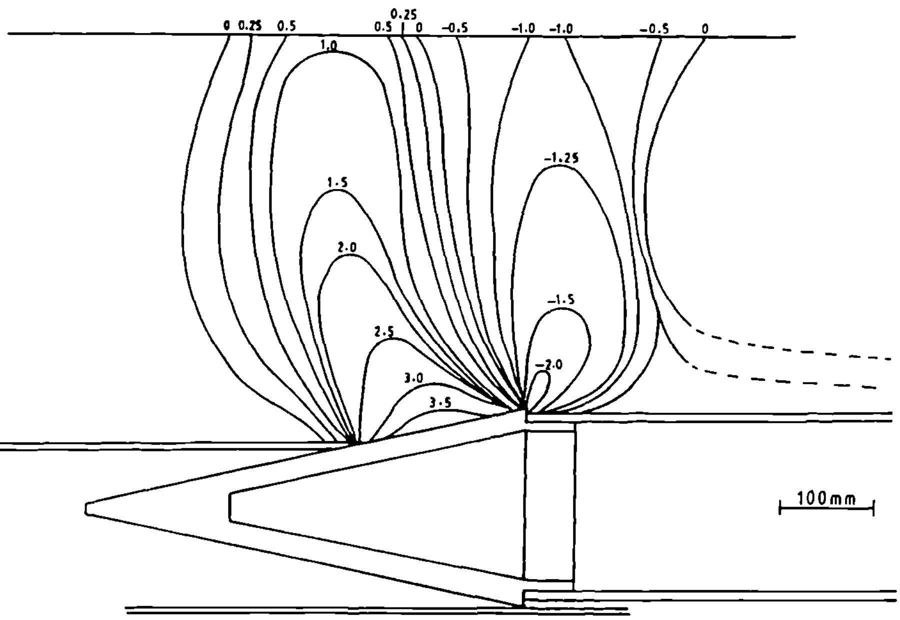

VERTICAL MOVEMENTS
+ UP - DOWN

TEST PB11

2.6125B1.2

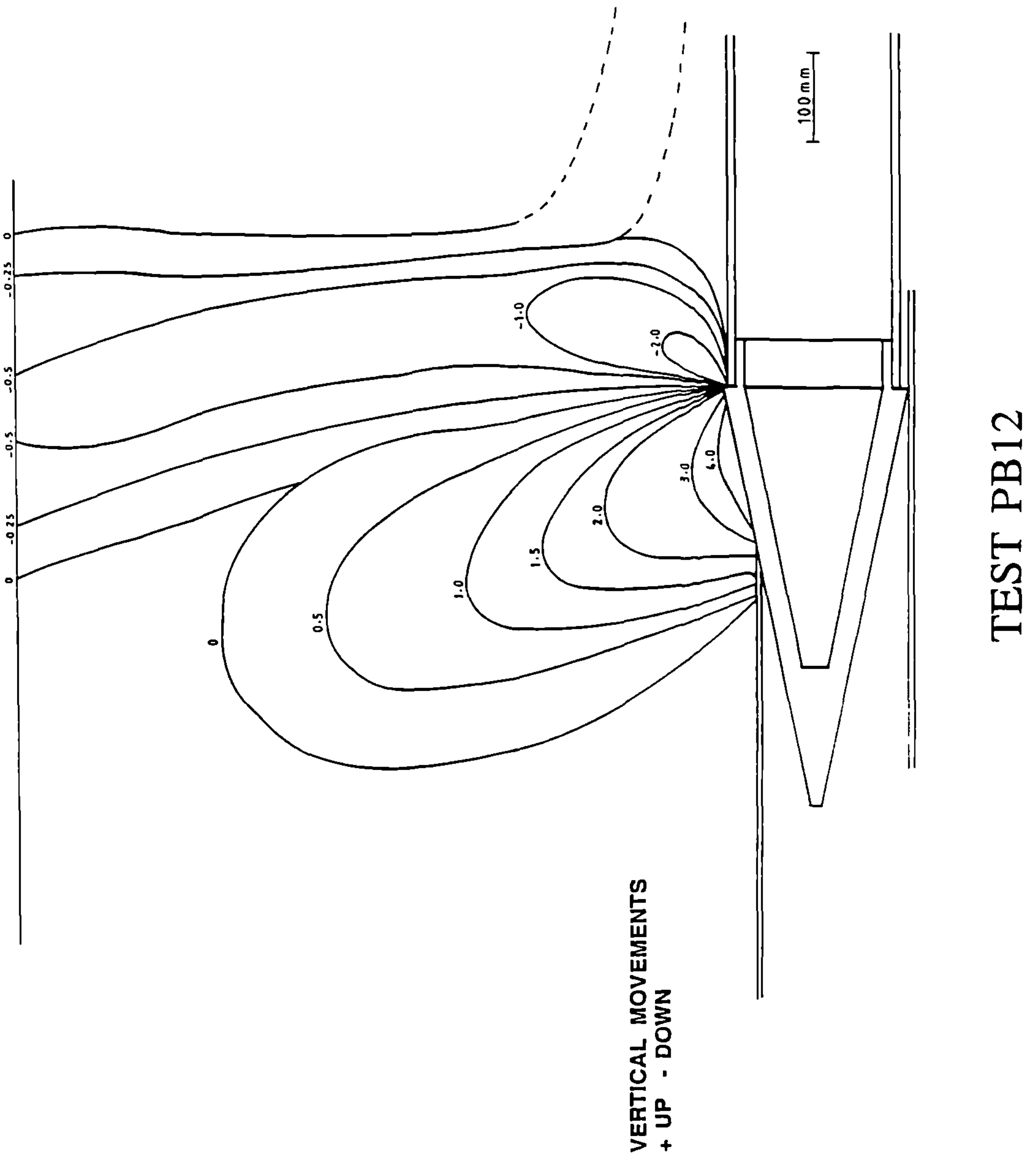

TEST PB12
4.9125B1.2
VERTICAL MOVEMENTS
+ UP - DOWN
100mm

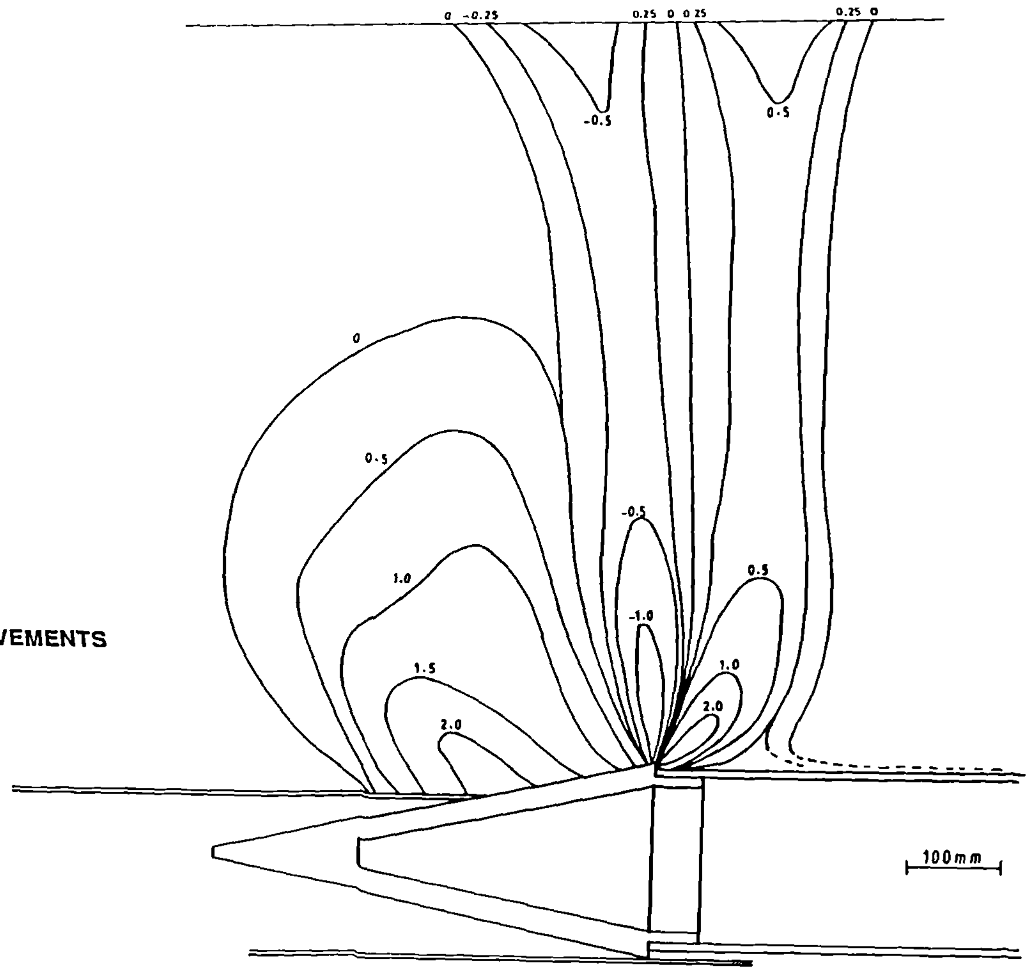

HORIZONTAL MOVEMENTS
+ LEFT - RIGHT

TEST PB12
4.9125B1.2

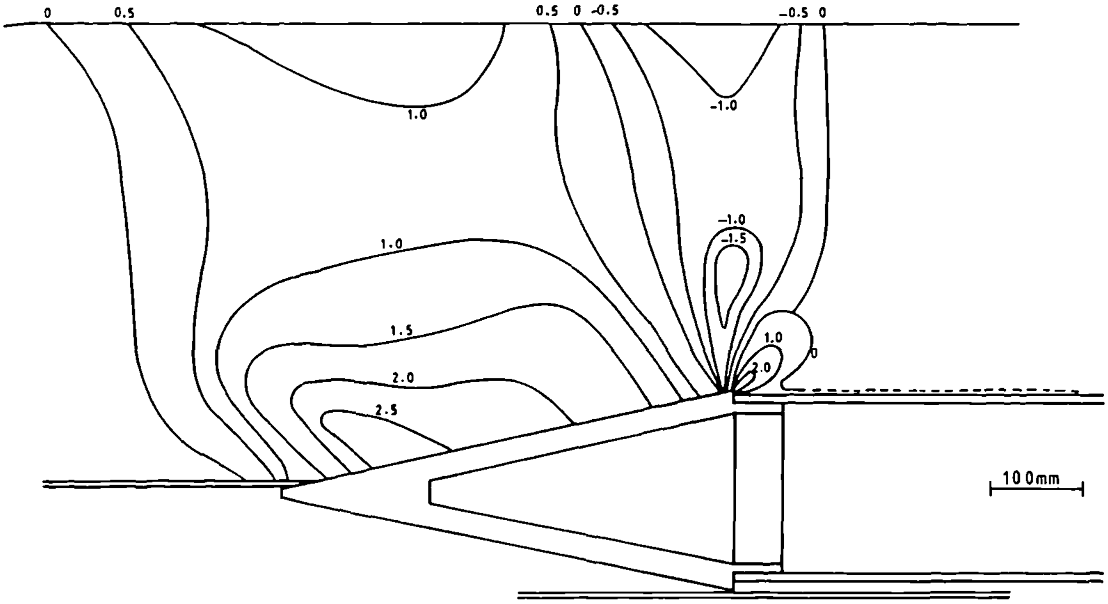

HORIZONTAL MOVEMENTS
+ LEFT - RIGHT

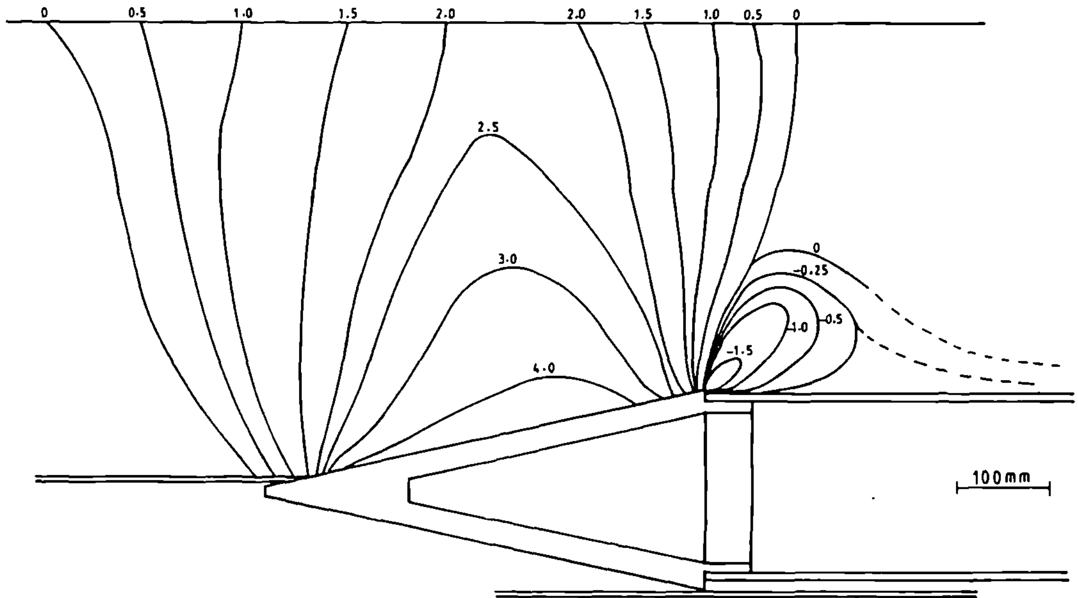

VERTICAL MOVEMENTS
+ UP - DOWN

TEST PB13

3.8d25B1.7

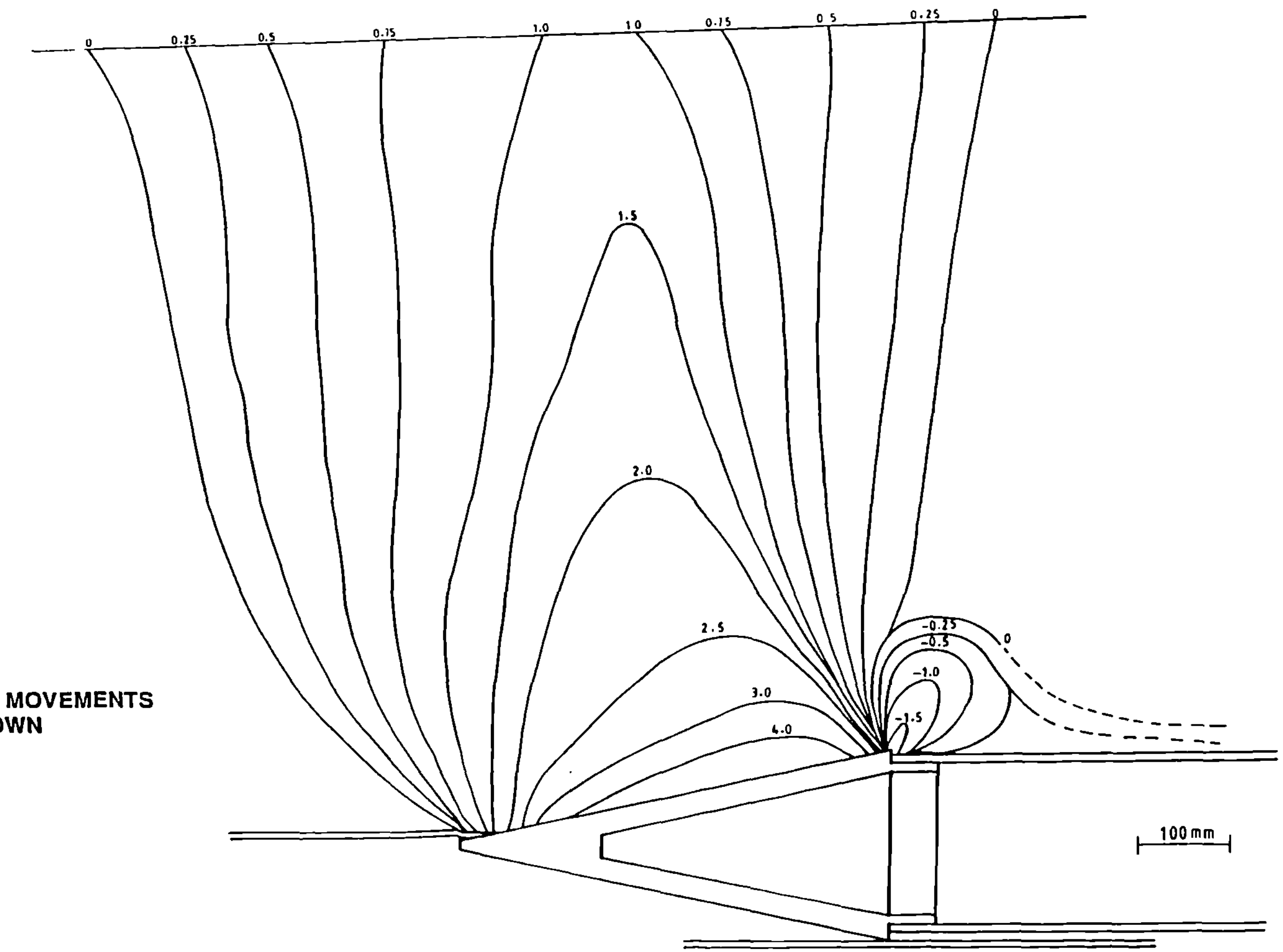

VERTICAL MOVEMENTS
+ UP - DOWN

TEST PB14
7.0d25B1.7

HORIZONTAL MOVEMENTS
+ LEFT - RIGHT

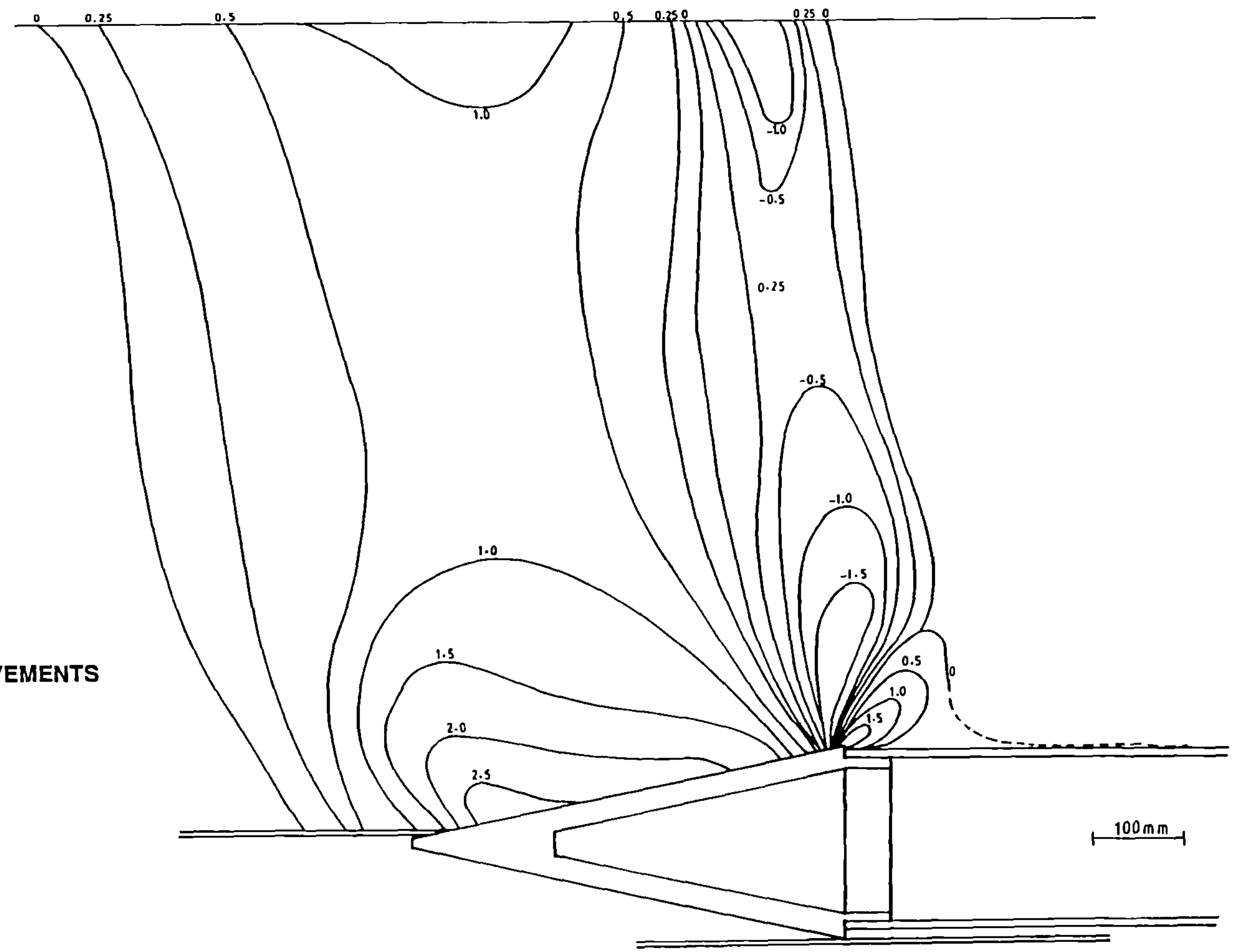

TEST PB14
7.0d25B1.7

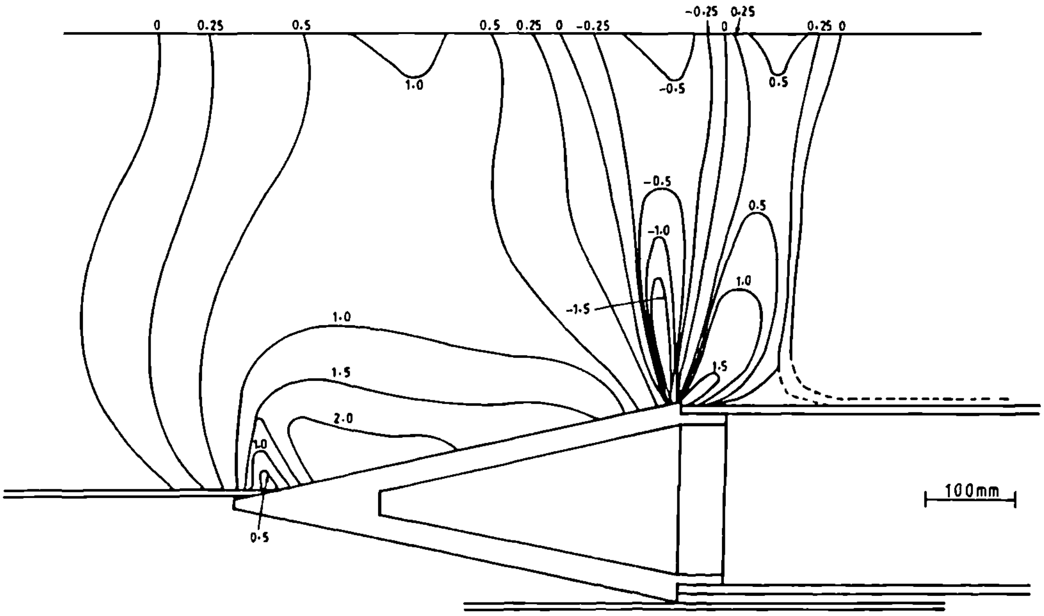

HORIZONTAL MOVEMENTS
+ LEFT - RIGHT

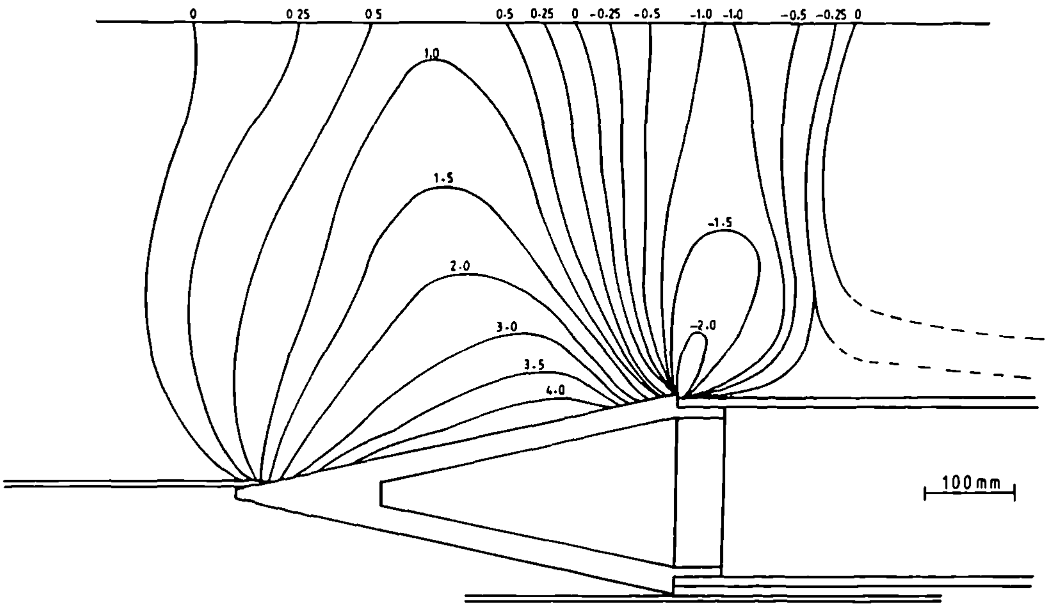

VERTICAL MOVEMENTS
+ UP - DOWN

TEST PB15

3.8125B1.7

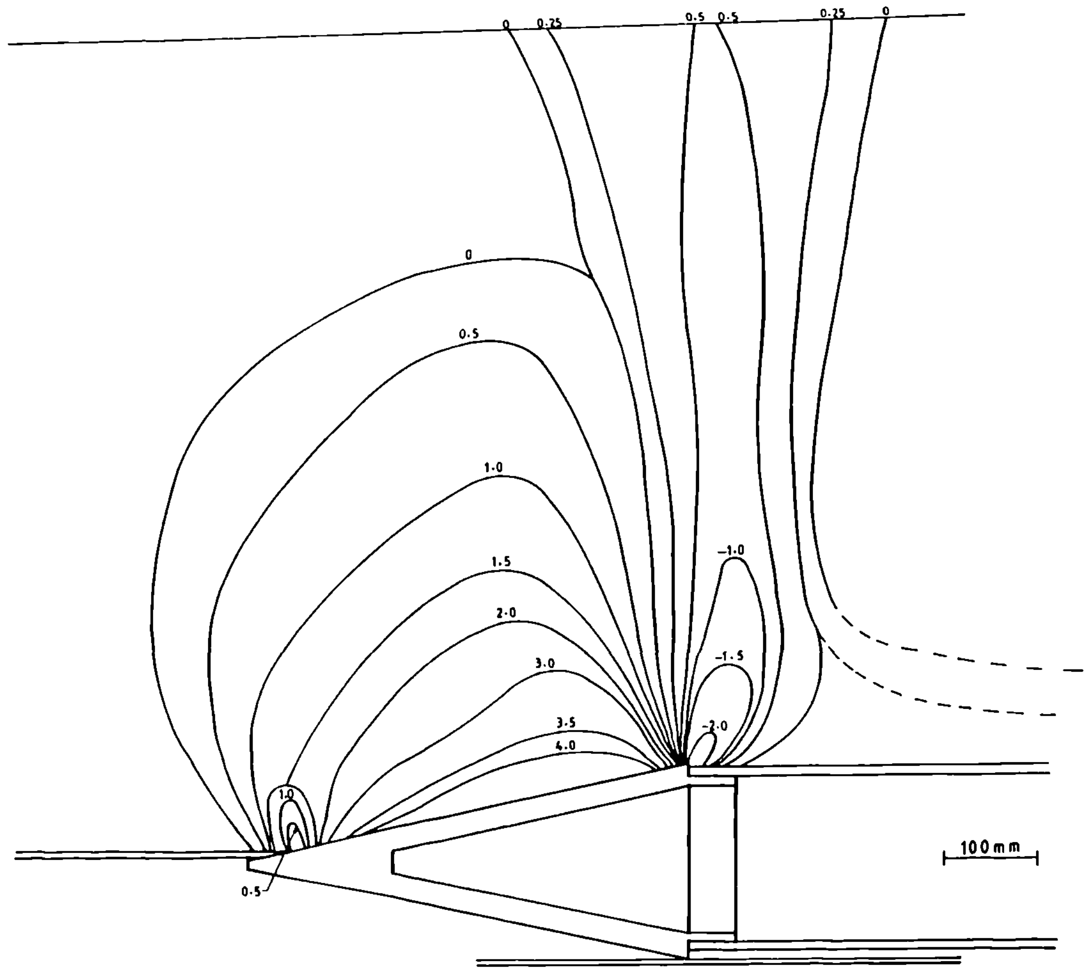

VERTICAL MOVEMENTS
+ UP - DOWN

TEST PB16
7.0125B1.7

HORIZONTAL MOVEMENTS
+ LEFT - RIGHT

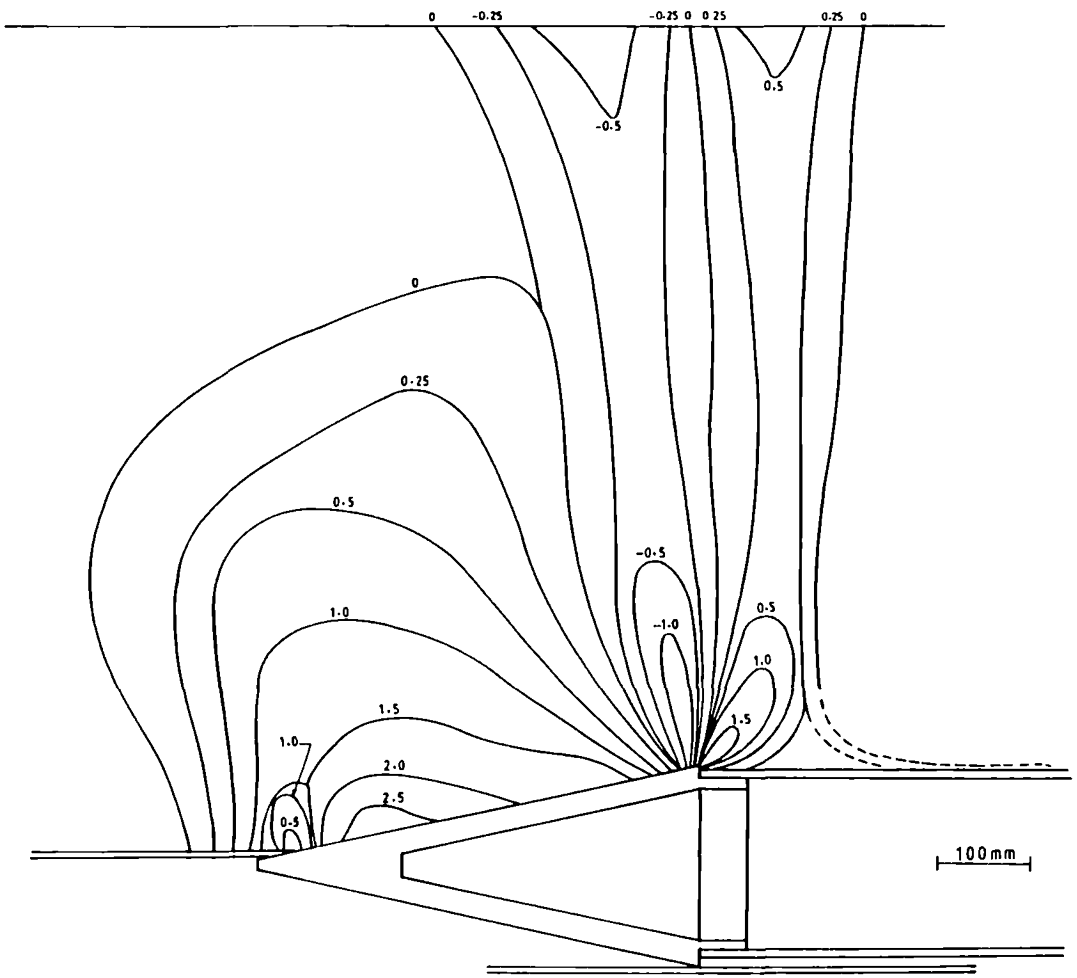

TEST PB16
7.0125B1.7

B.5 PIPEBURSTING TESTS - PERPENDICULAR PLANE RESULTS

The following figures show the horizontal and vertical displacement contour plots for the pipebursting tests in the perpendicular plane. The contours are in millimetres and represent the movements in the sand caused during the expansion process. Some of the test results are shown at different stages of the expansion process to illustrate the build-up of the sand movements. For some of these tests the full expansion movements would have extend to the boundary of the test tank and invalidated the results, so only the movements for part of the expansion process are shown. Test codes are given to aid comparison between results. The test code is defined as: Cover depth to diameter of old pipe (C/D_o), density state of sand, sand type, bursting ratio (D_f/D_o).

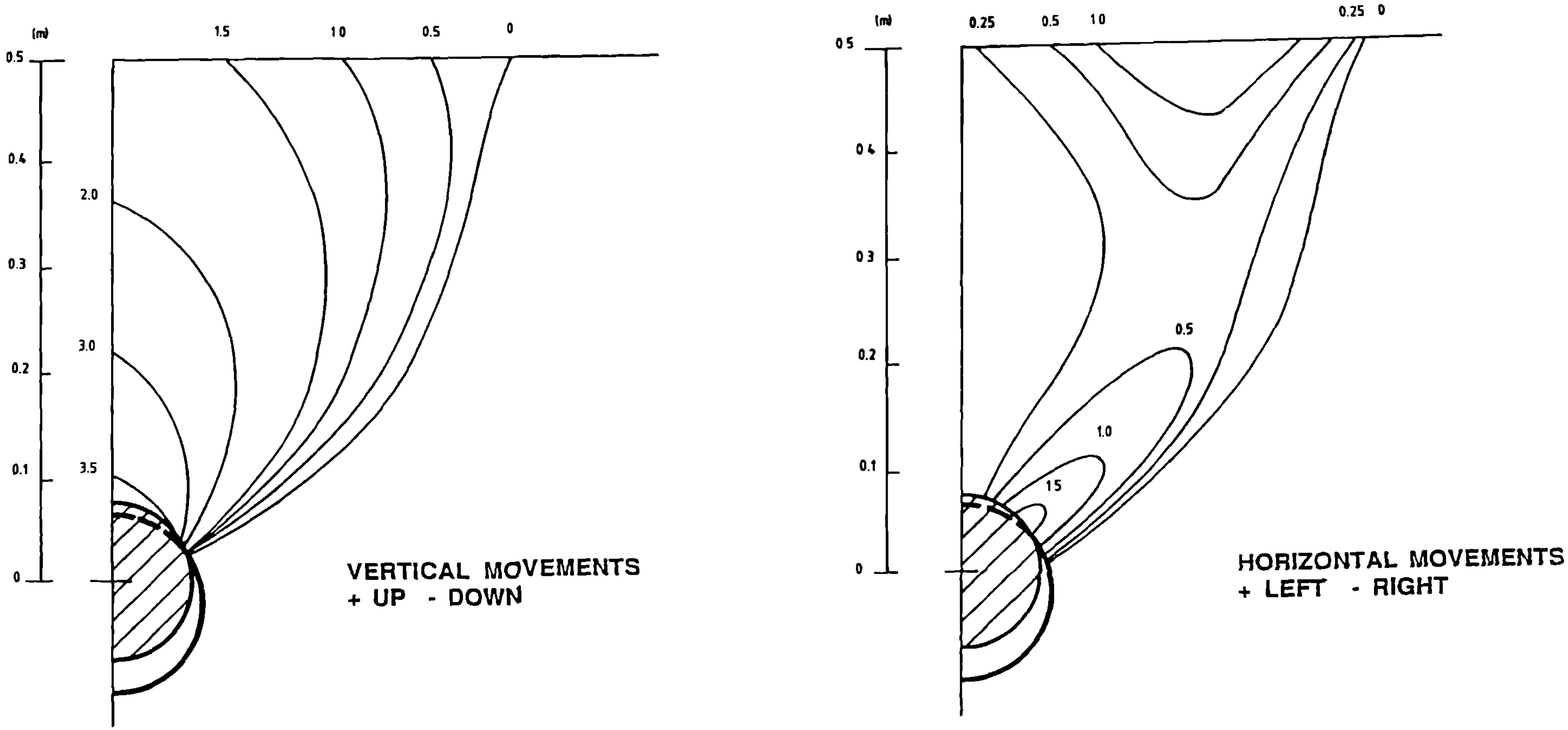

TEST PB1

2.6dLB1.2

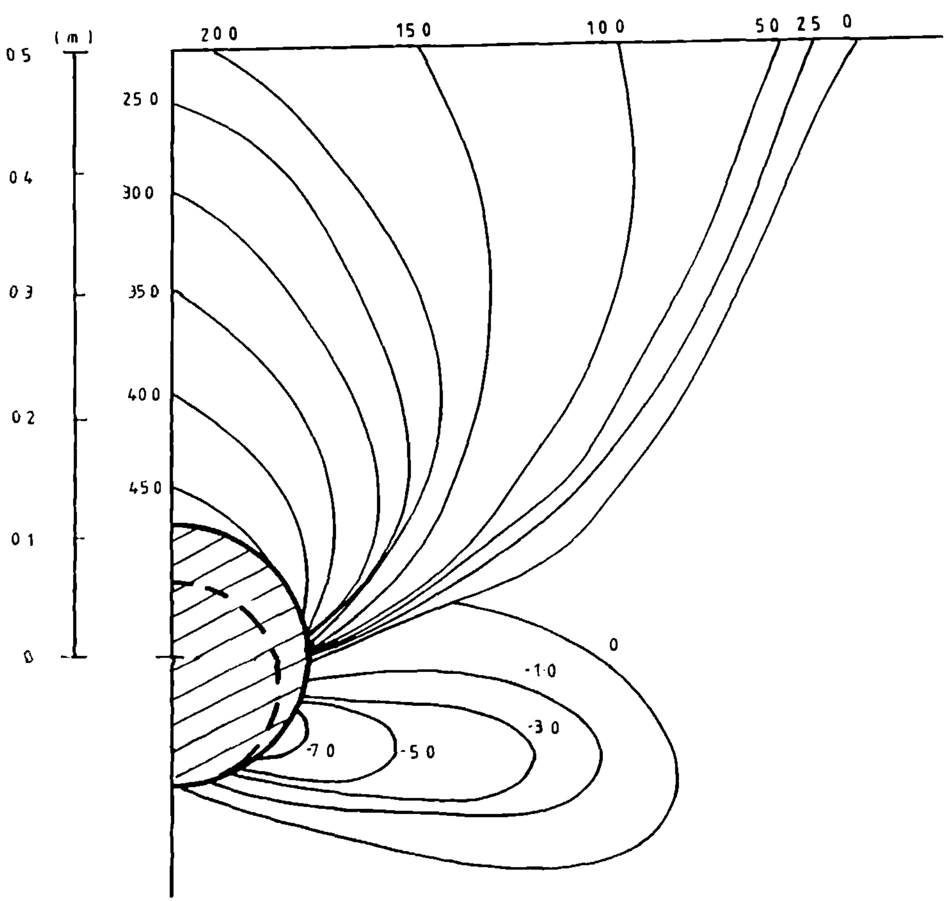

VERTICAL MOVEMENTS
+ UP - DOWN

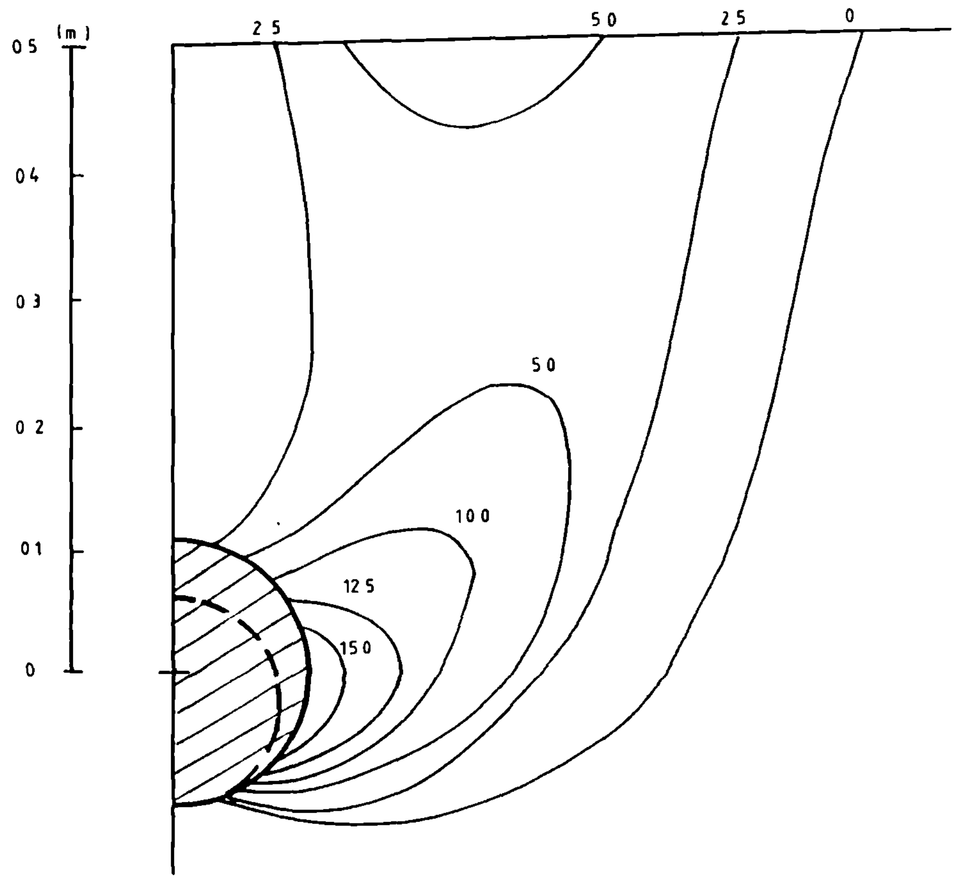

HORIZONTAL MOVEMENTS
+ LEFT - RIGHT

TEST PB1

2.6dLB1.2

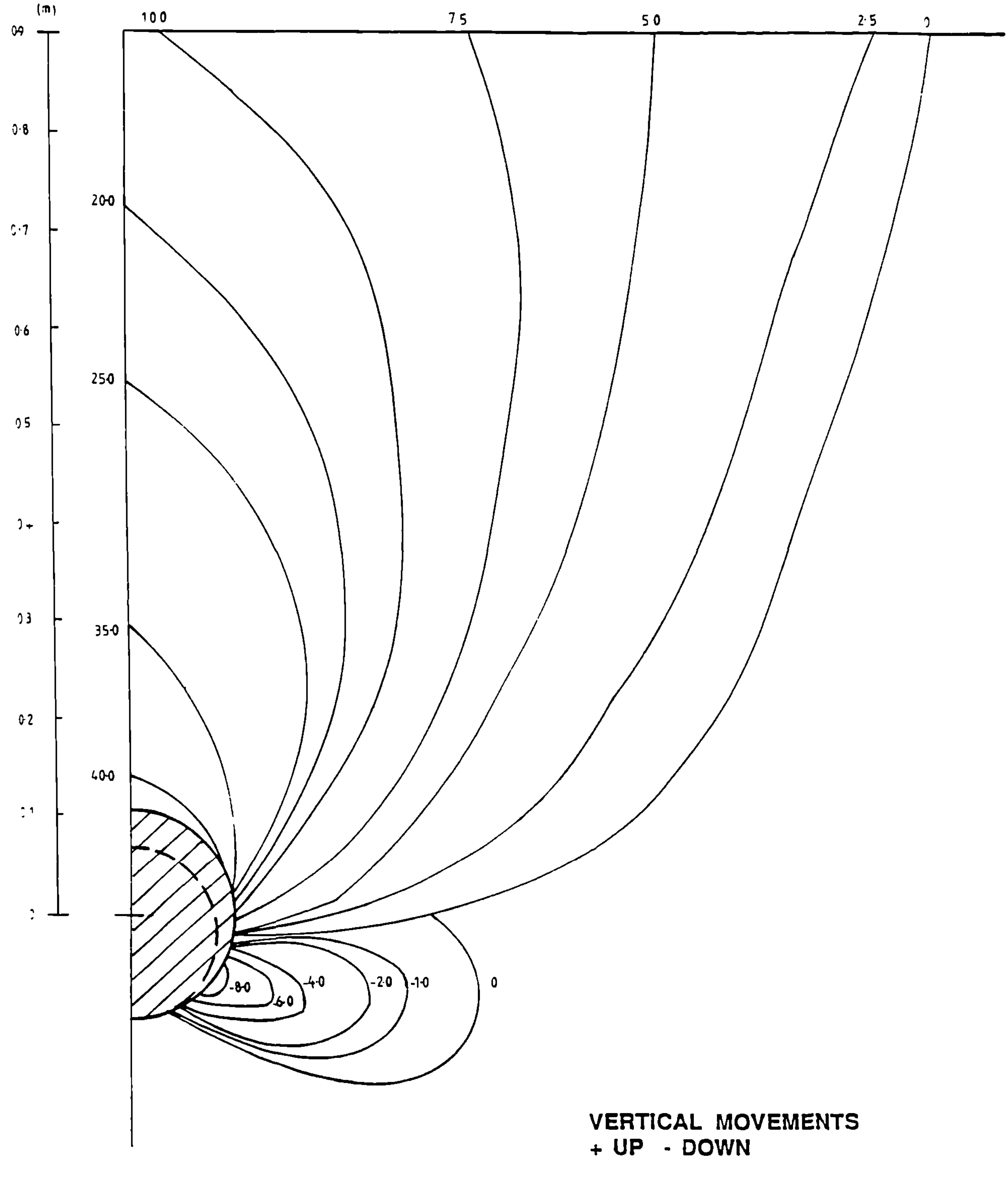

TEST PB2
4.9dLB1.2

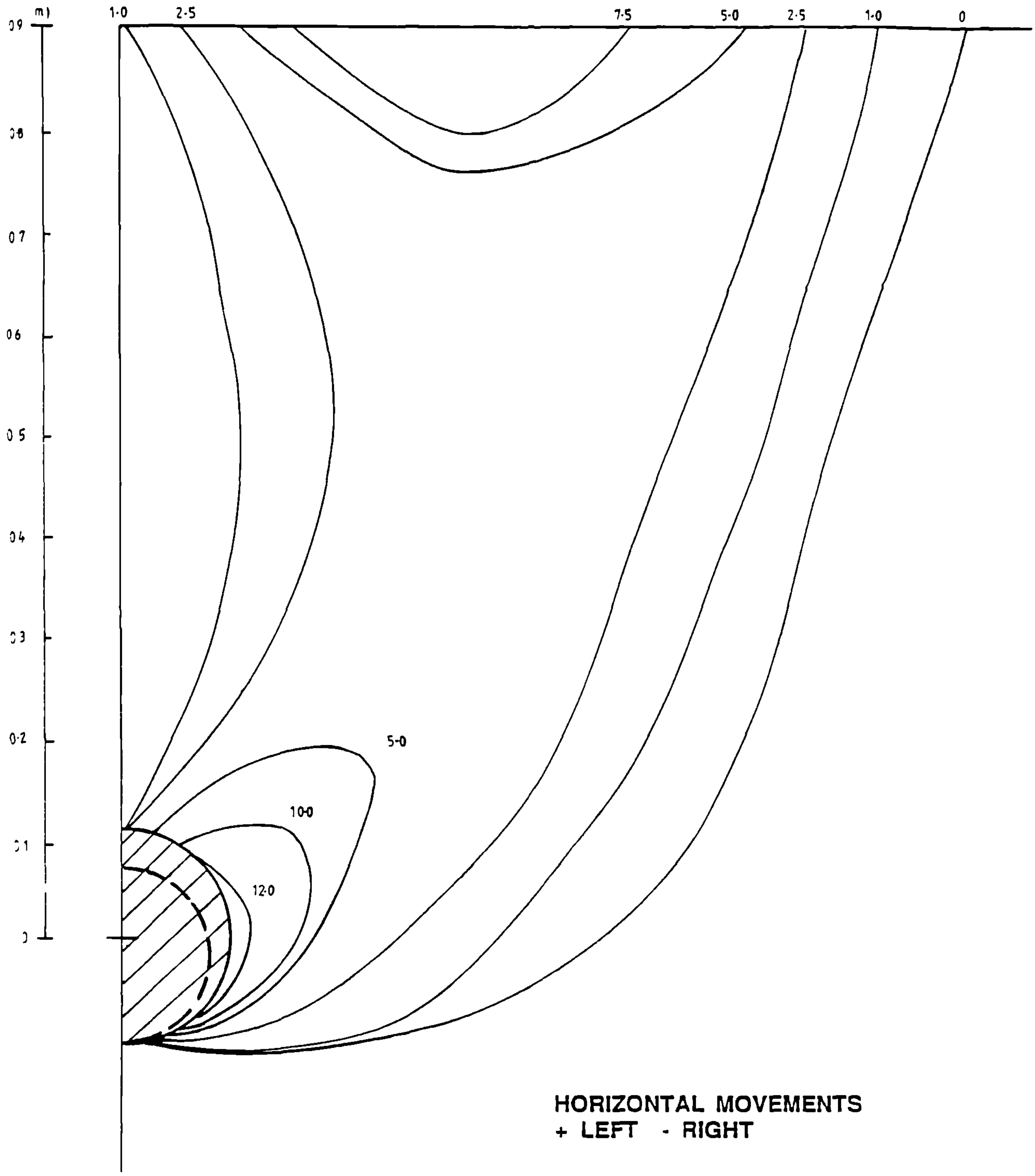

TEST PB2
4.9dLB1.2

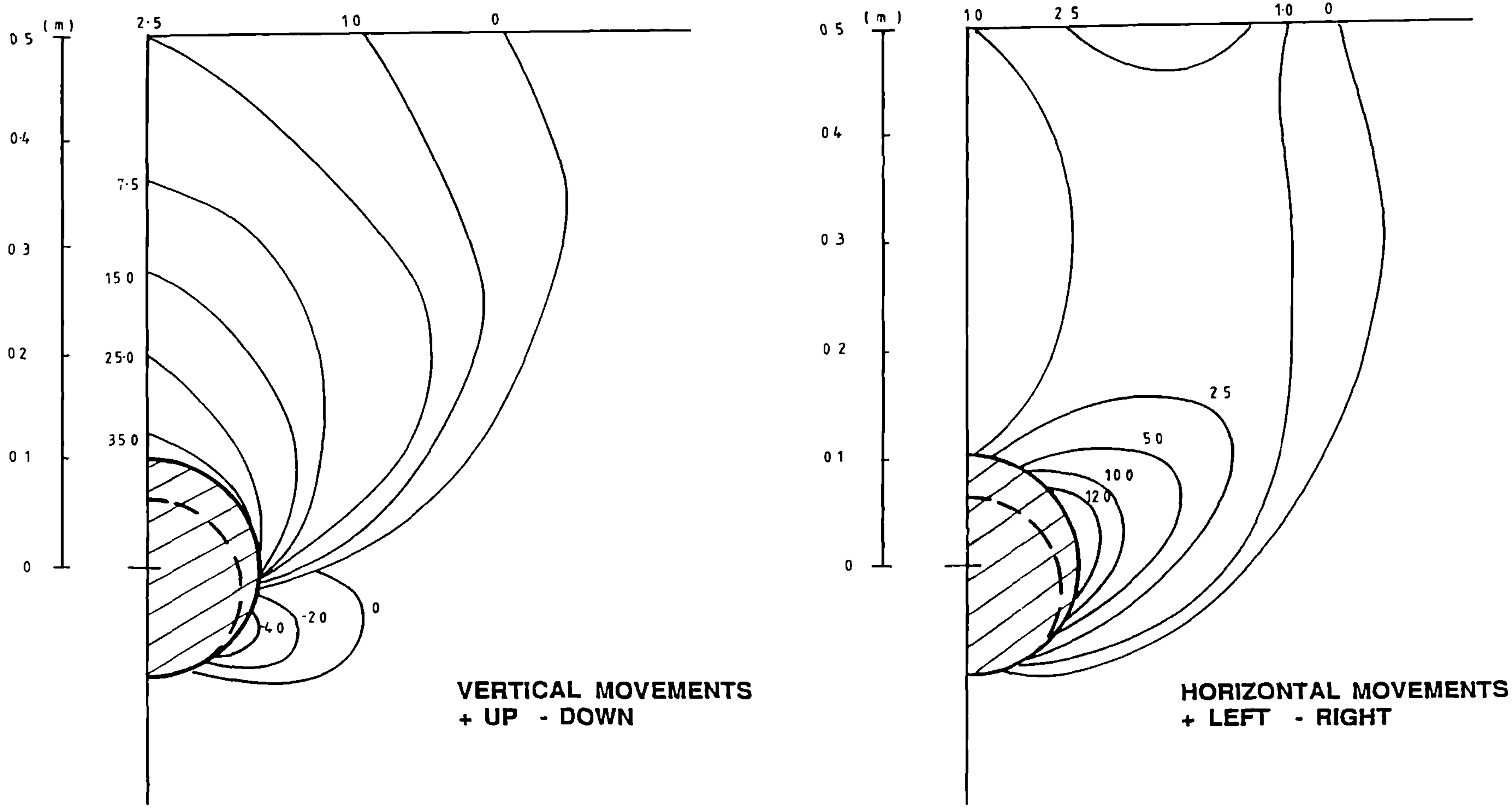

TEST PB3
2.6lLB1.2

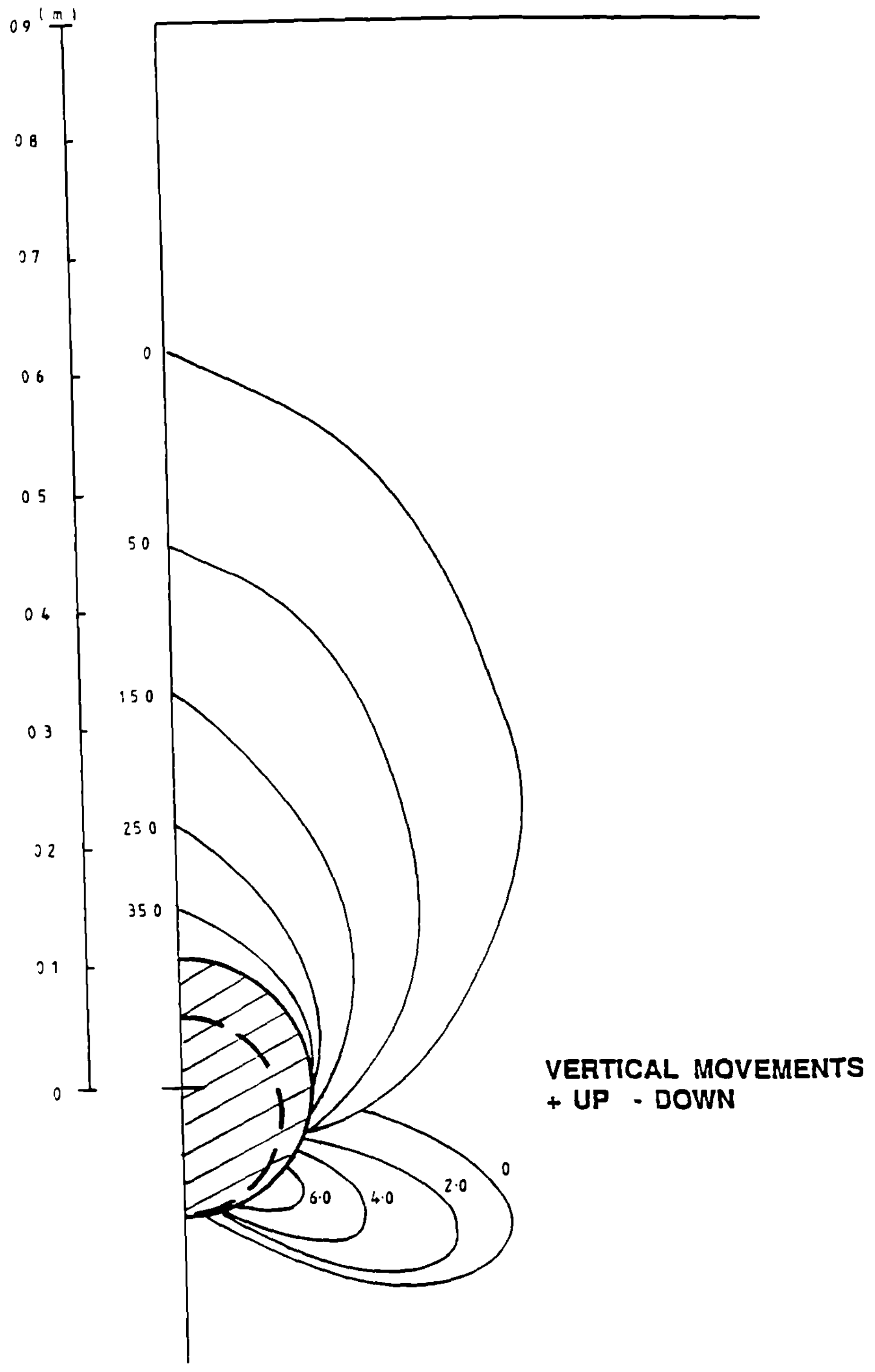

TEST PB4

4.91LB1.2

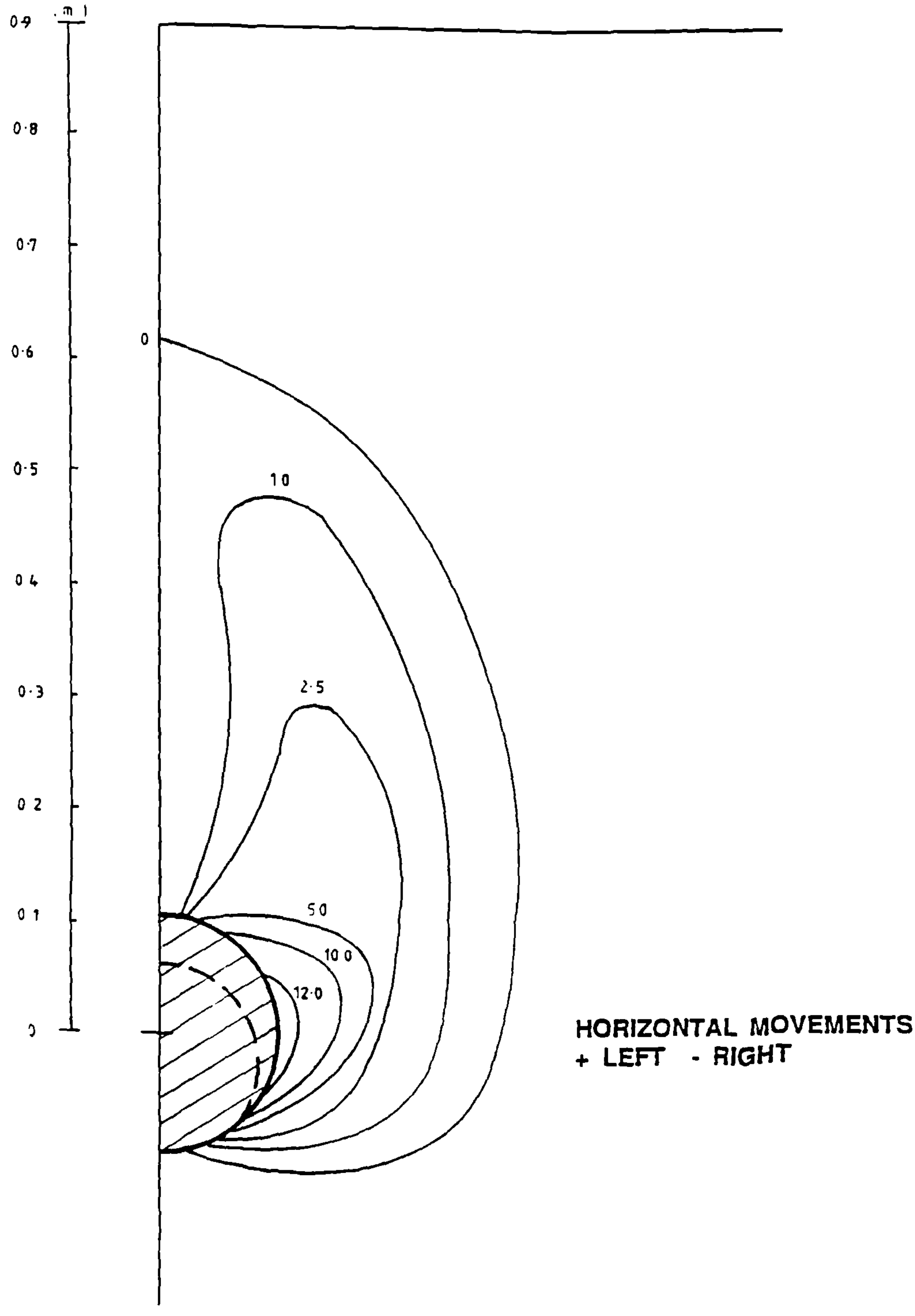

TEST PB4
4.91LB1.2

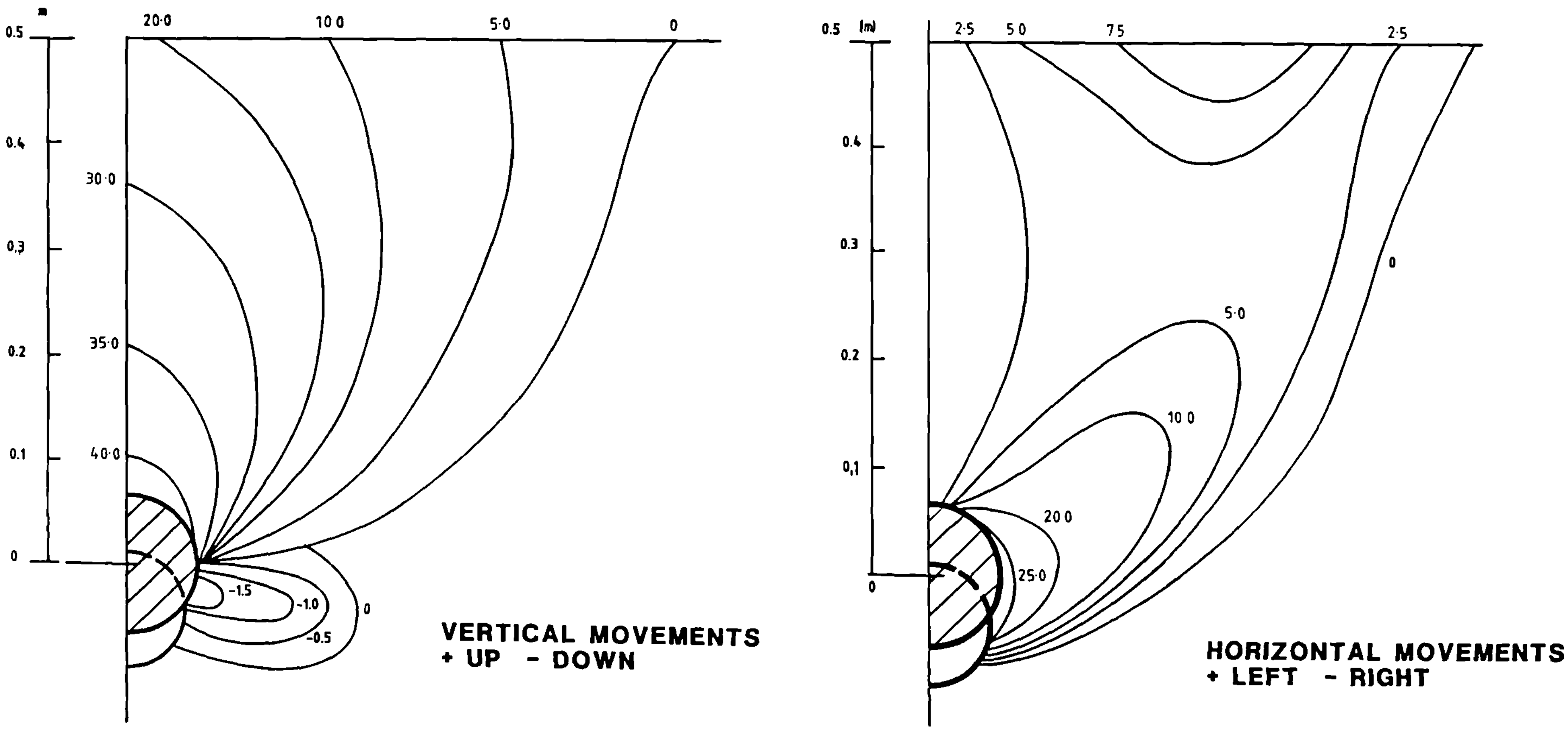

TEST PB5
3.8dLB1.7

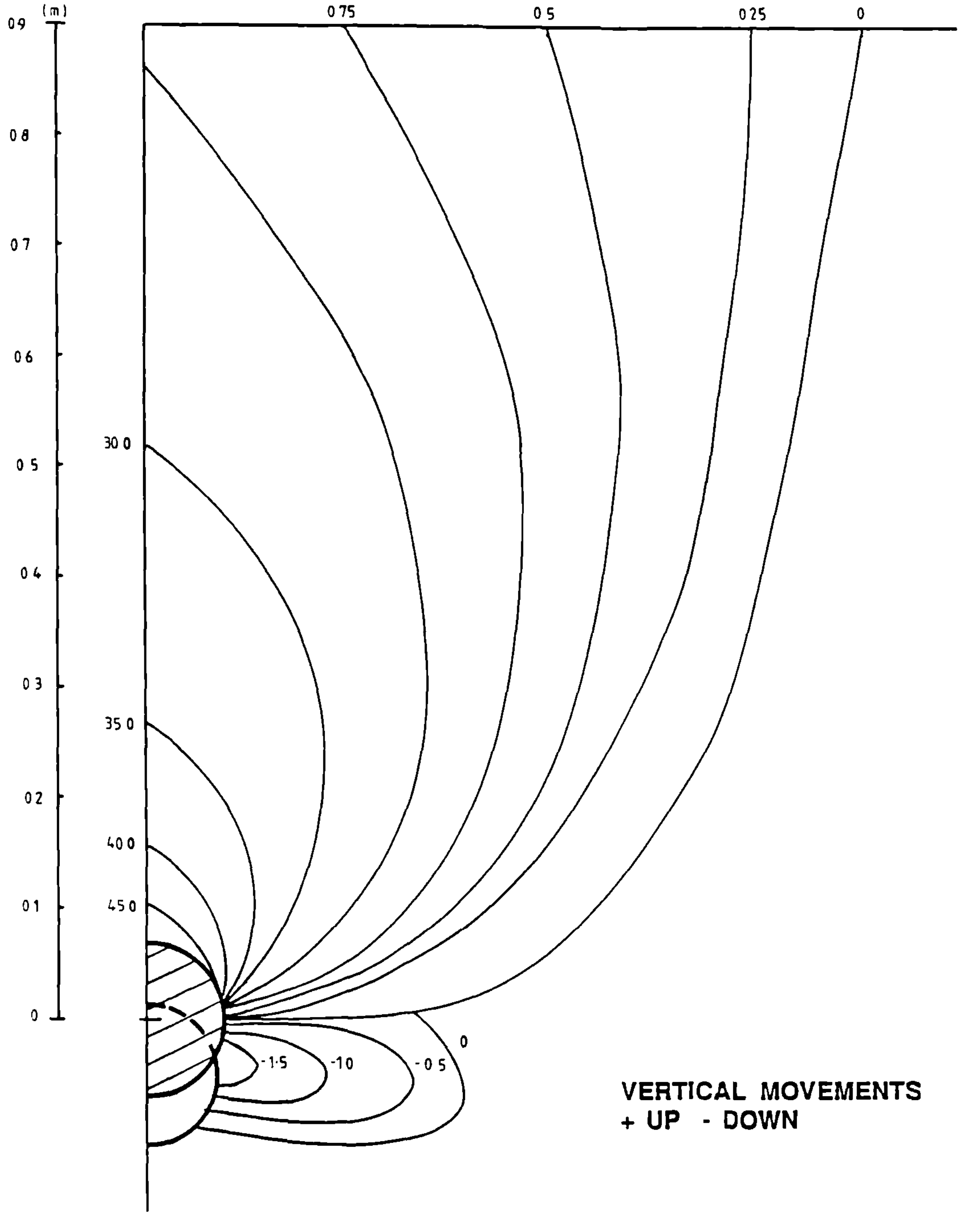

TEST PB6
7.0dLB1.7

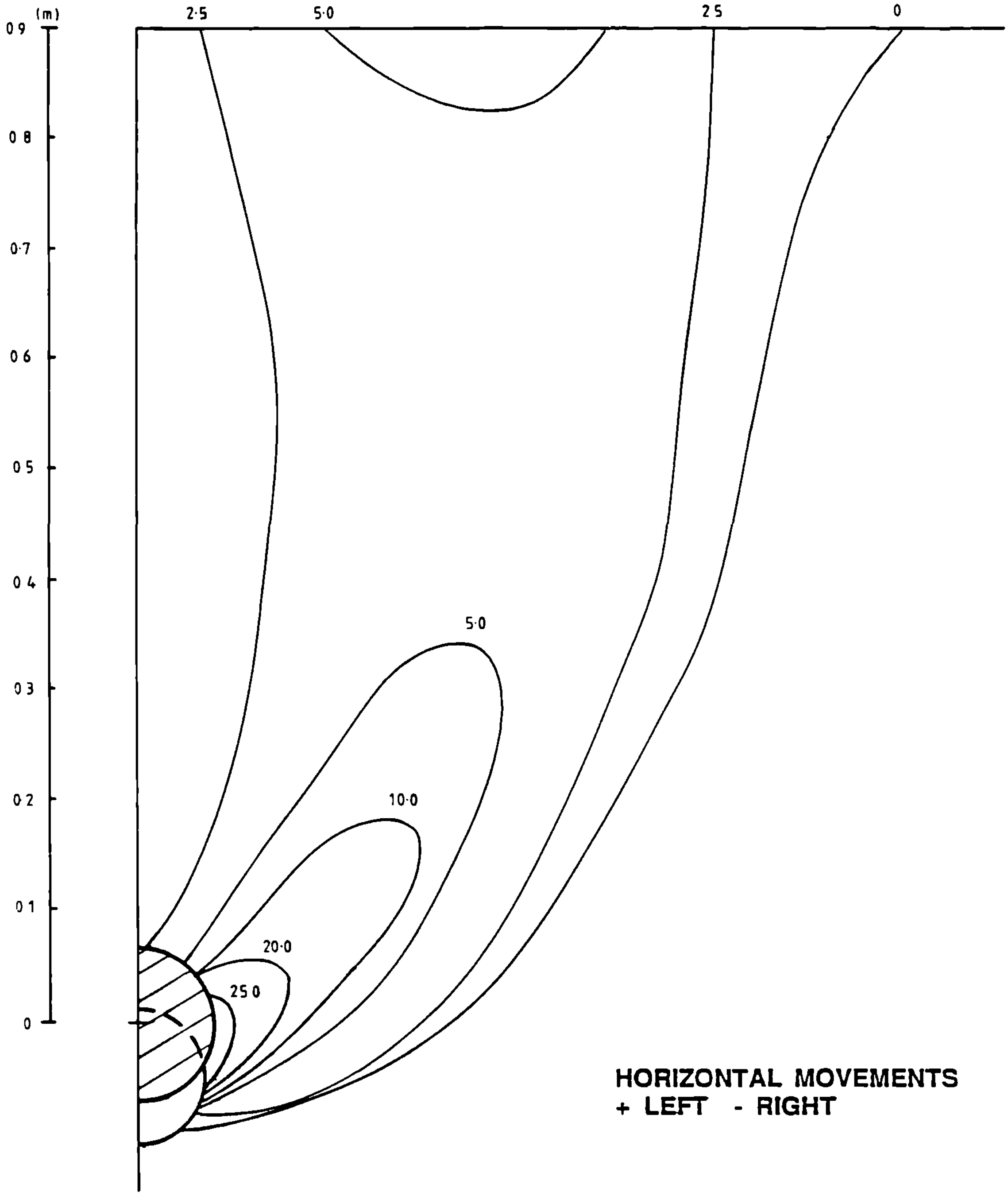

TEST PB6

7.0dLB1.7

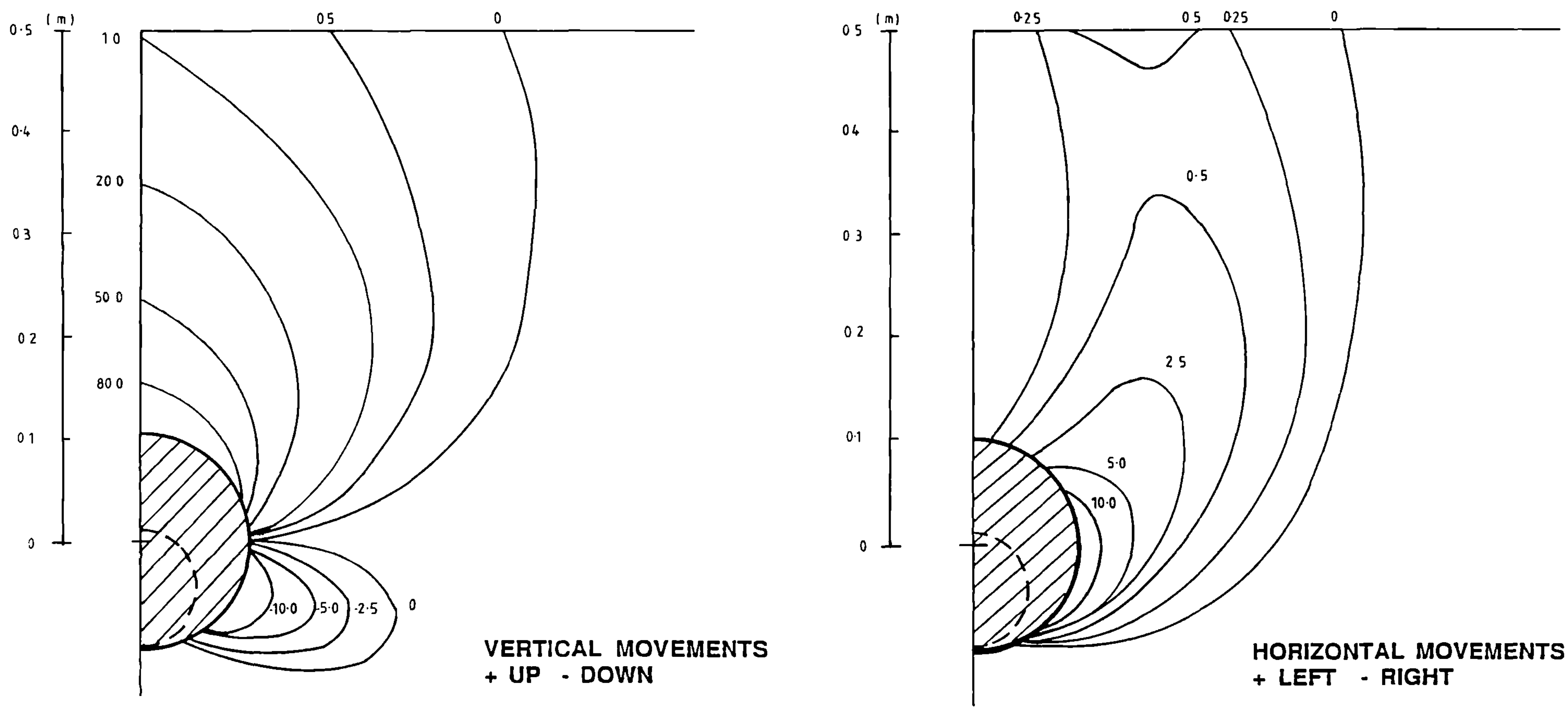

TEST PB7
3.81LB1.7

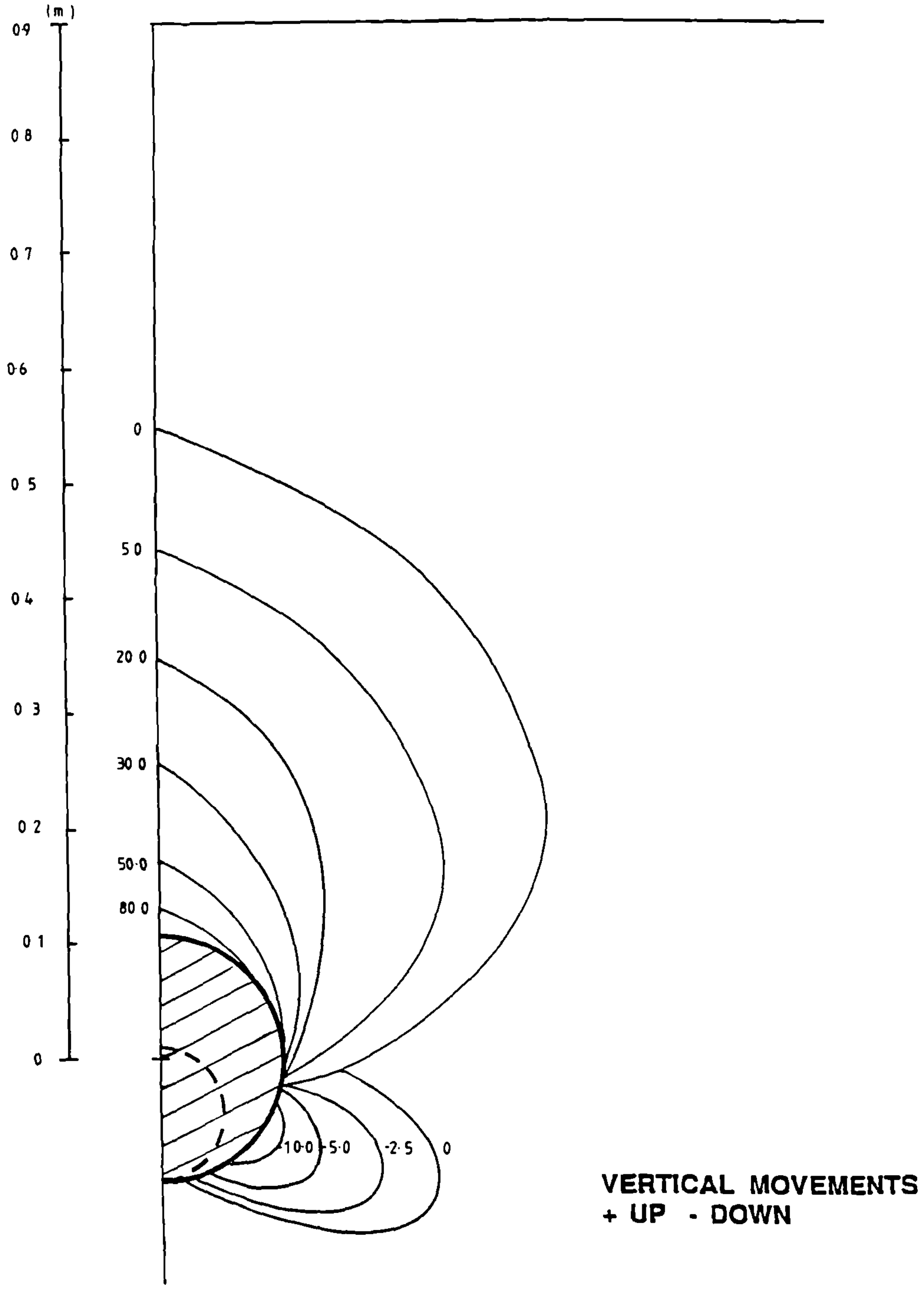

TEST PB8

7.01LB1.7

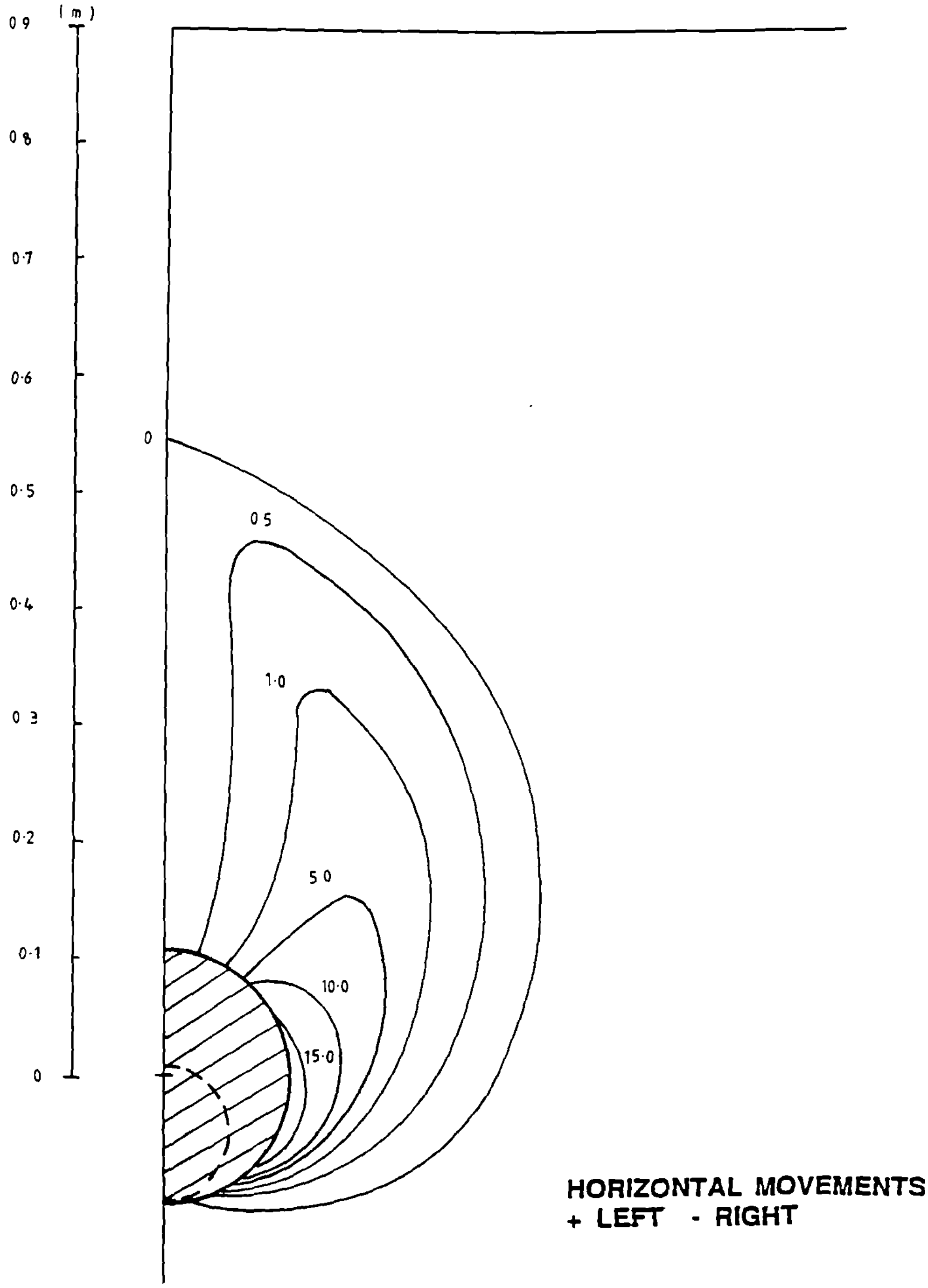

TEST PB8
7.01LB1.7

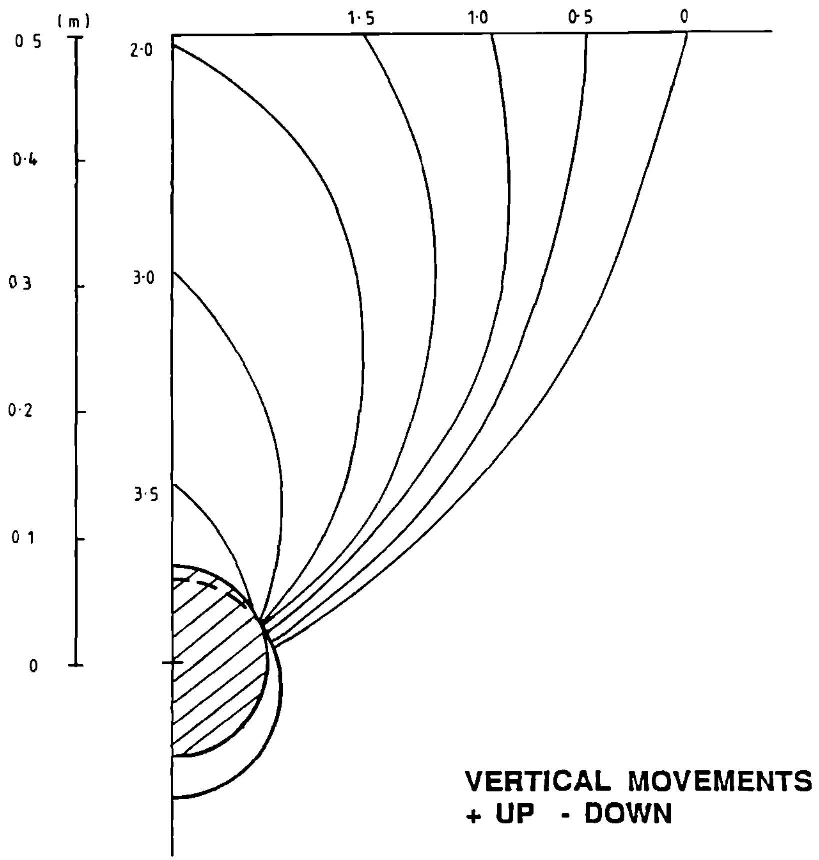

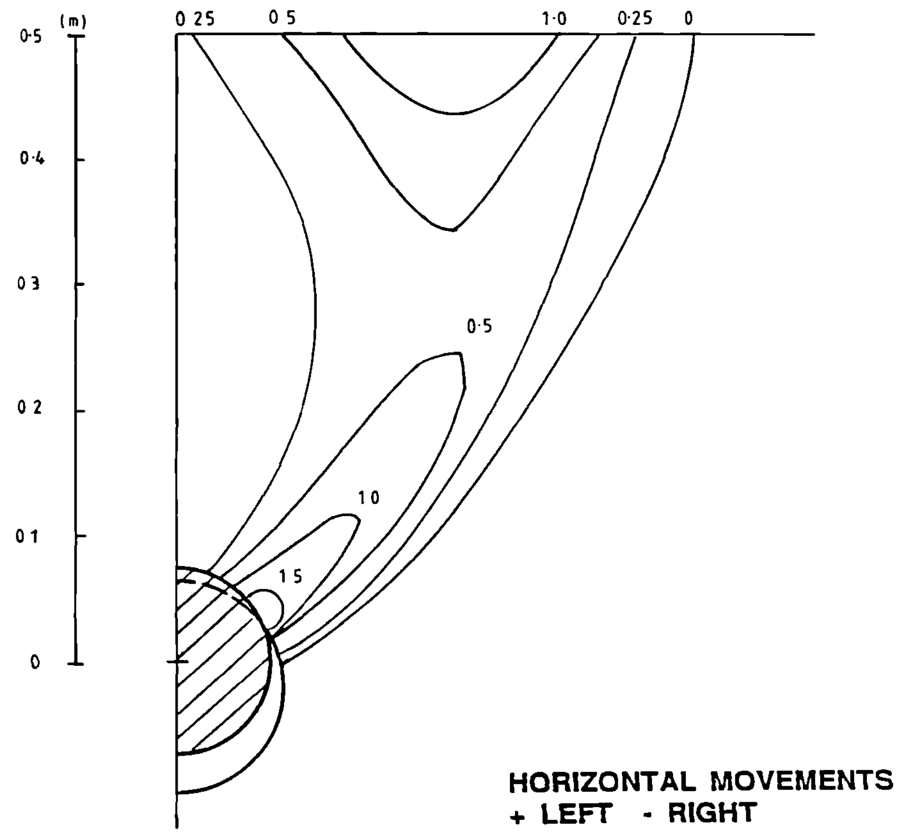

TEST PB9

2.6d25B1.2

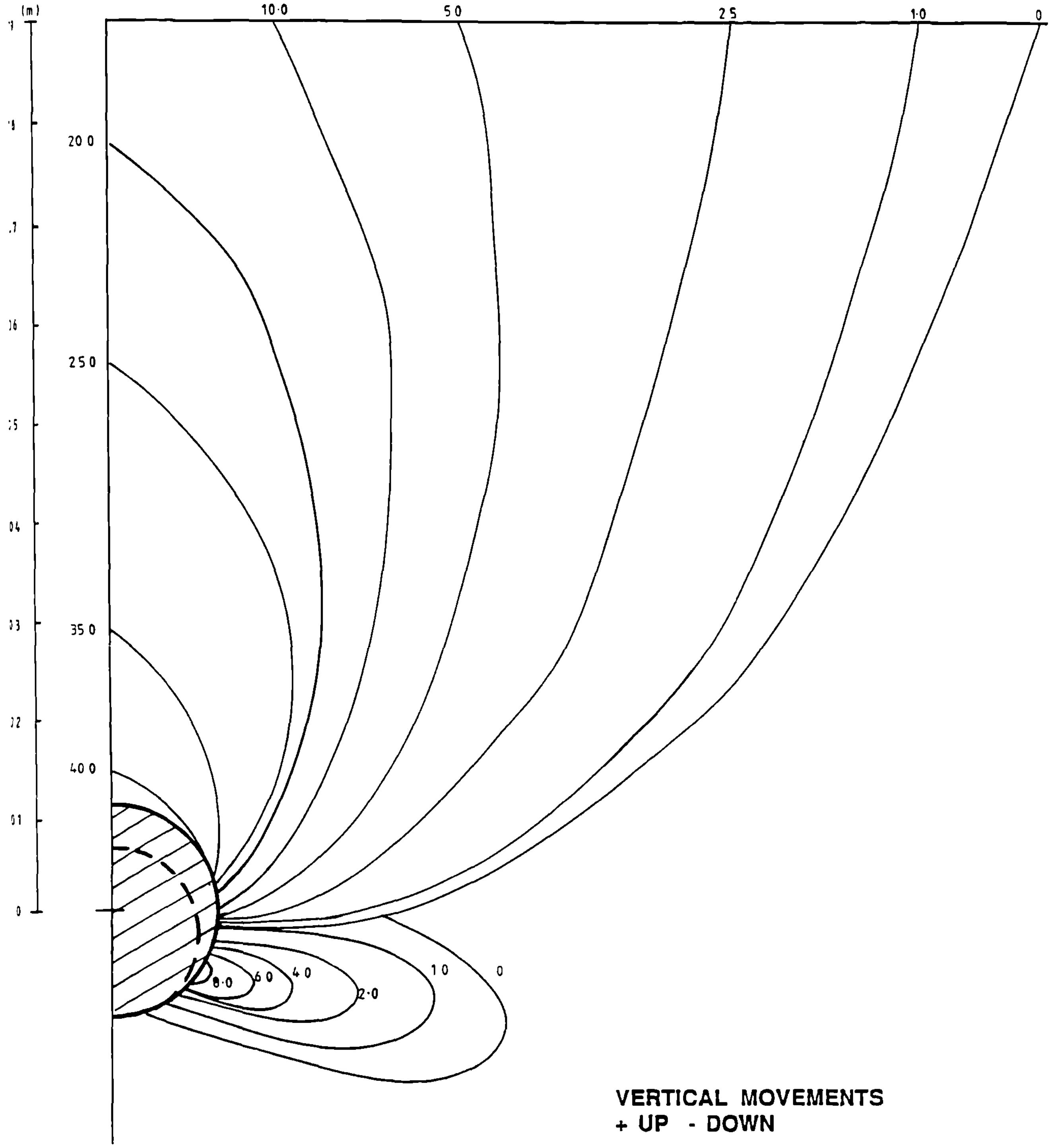

TEST PB10

4.9d25B1.2

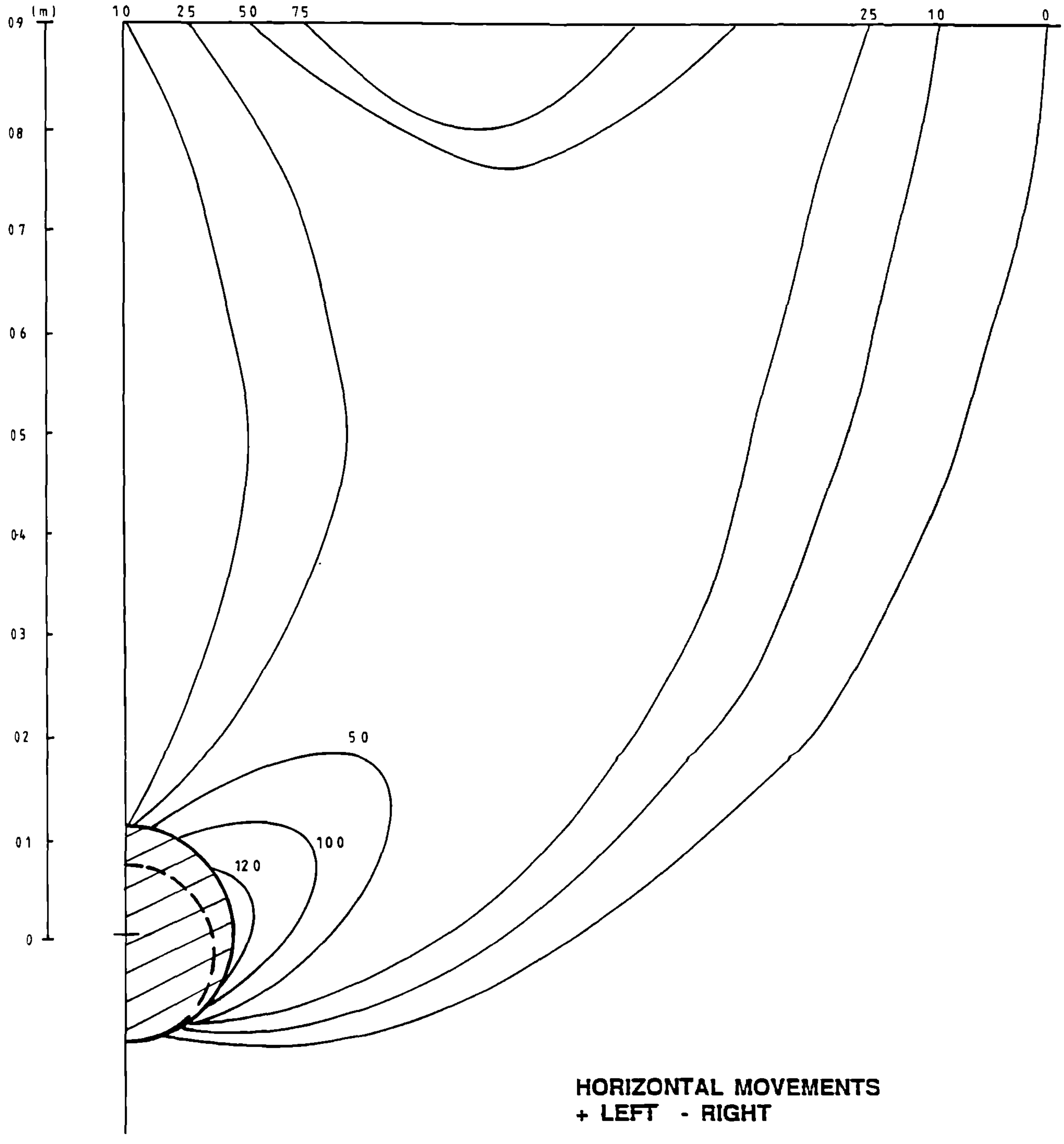

TEST PB10

4.9d25B1.2

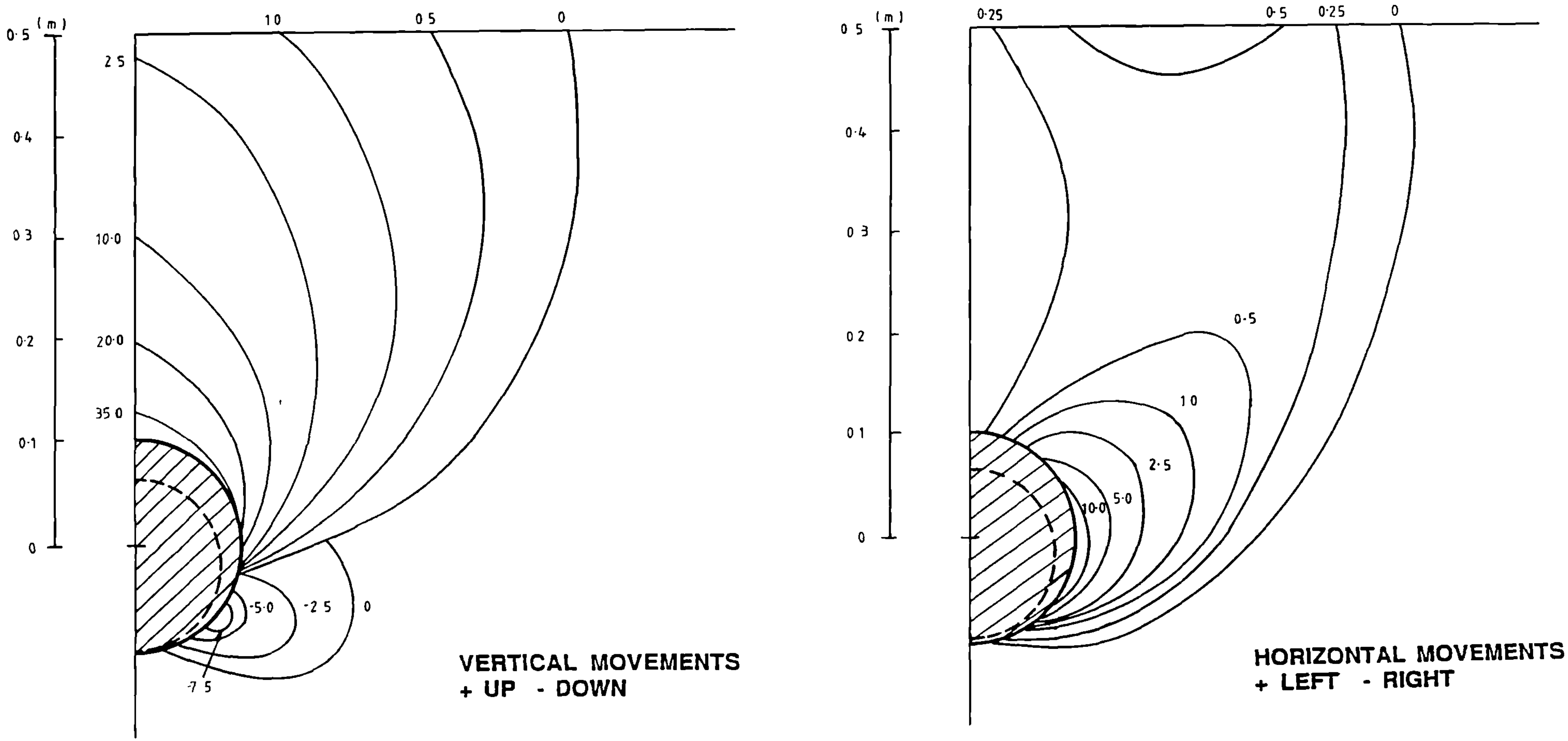

TEST PB11
2.6125B1.2

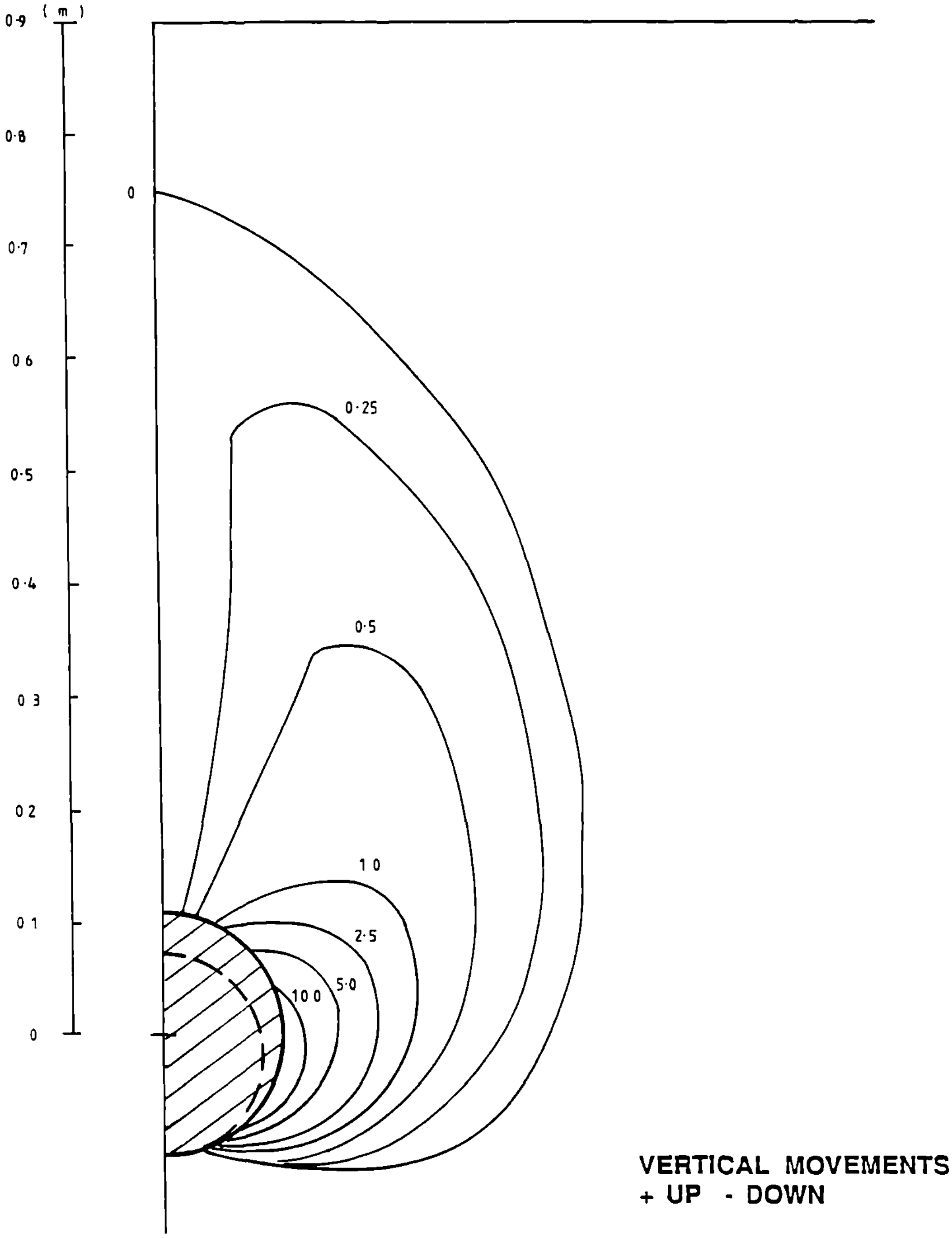

TEST PB12
4.9125B1.2

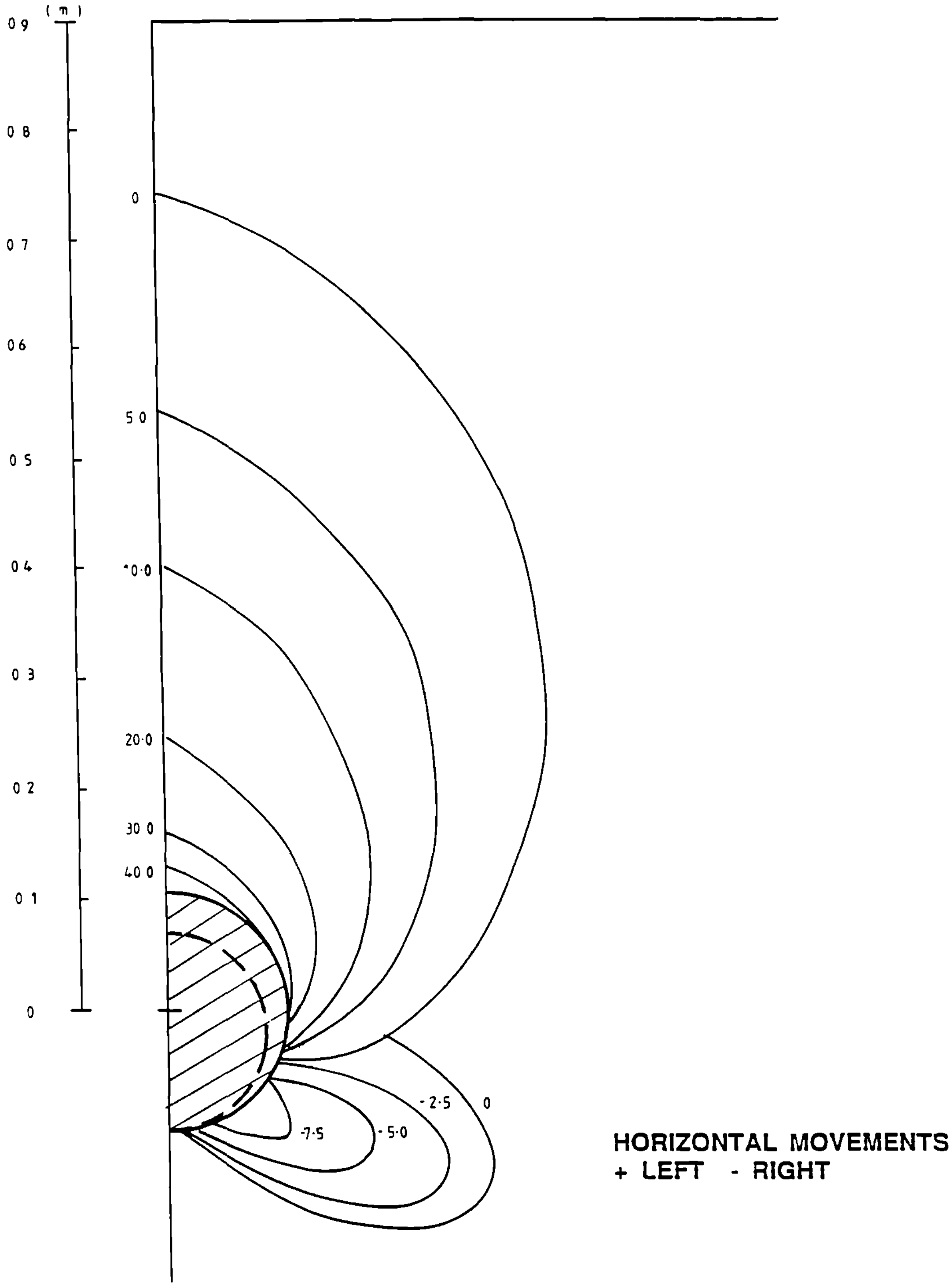

TEST PB12
4.9125B1.2

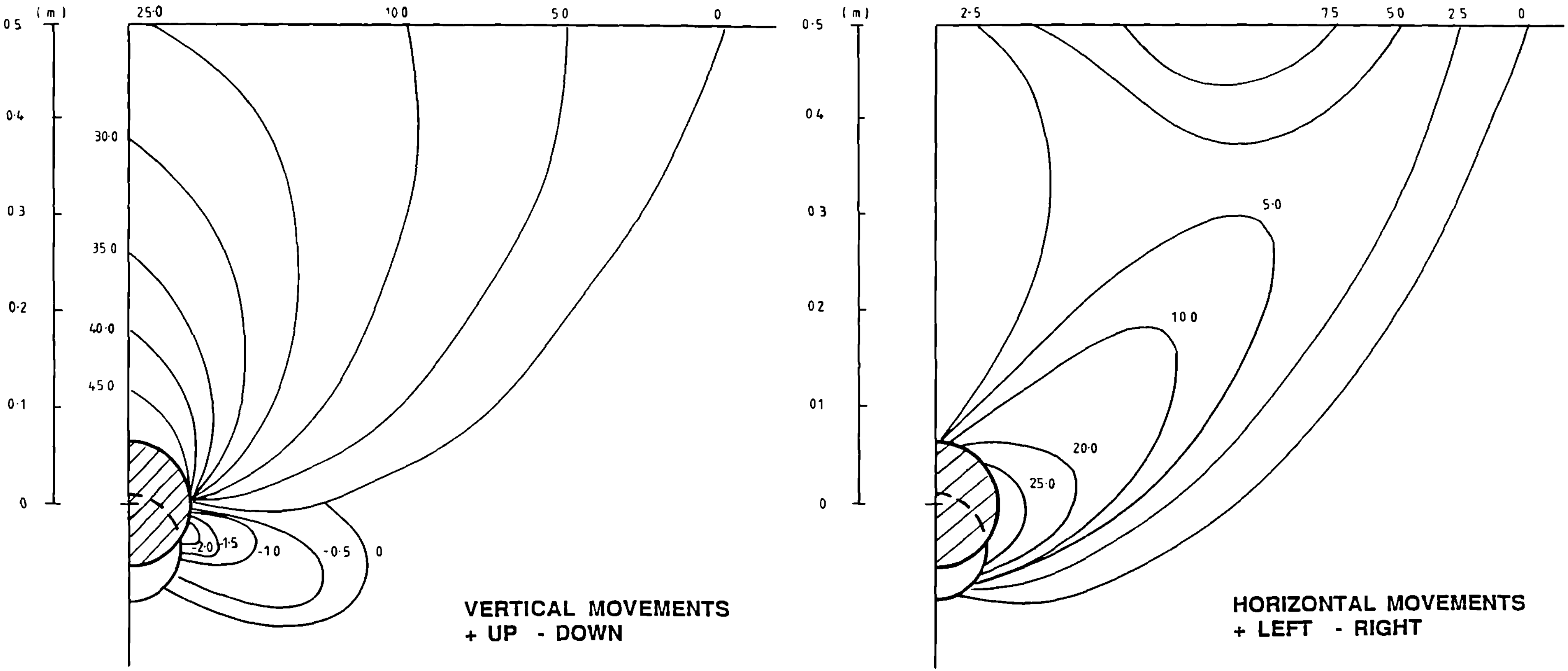

TEST PB13
3.8d25B1.7

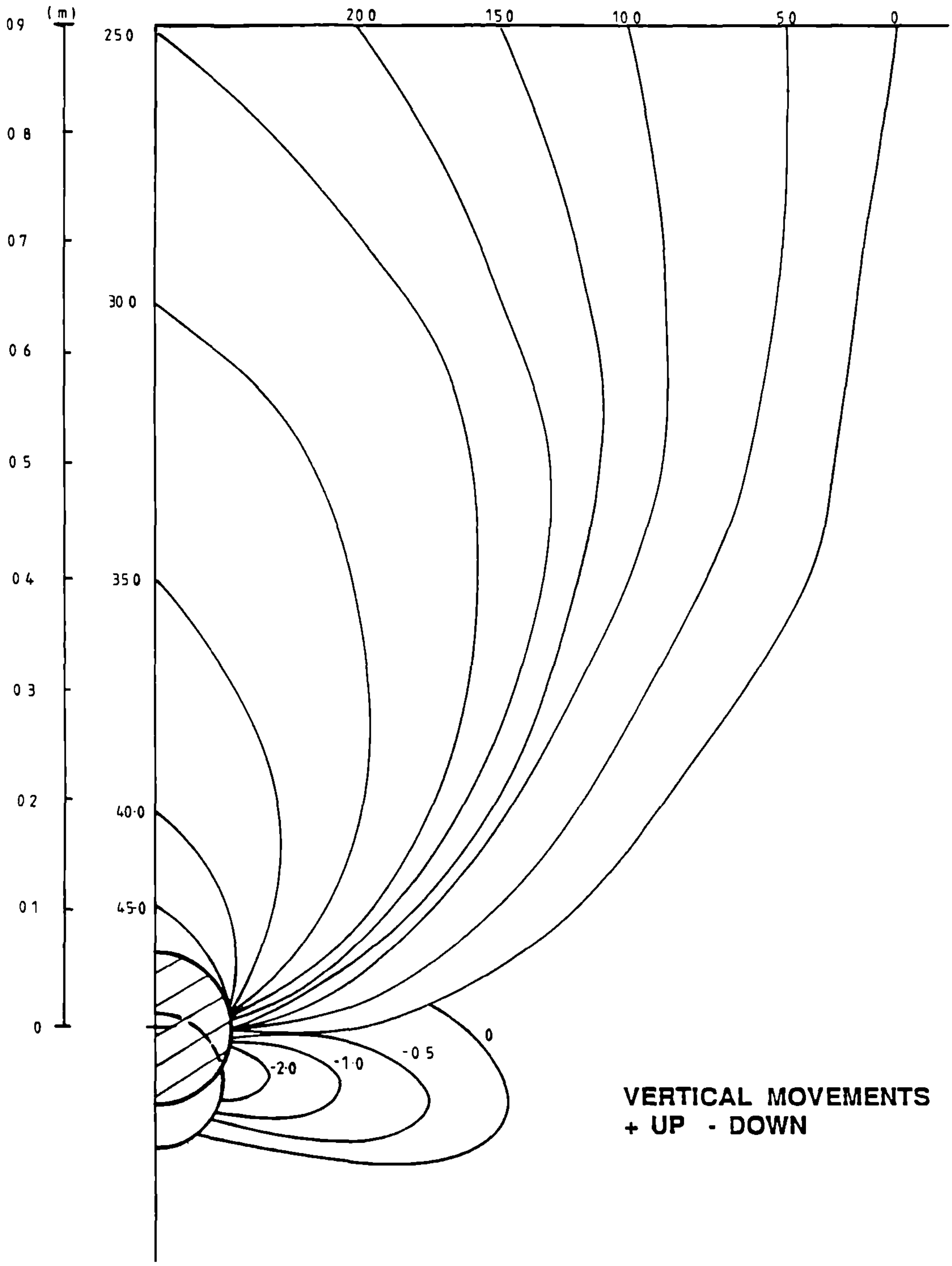

TEST PB14
7.0d25B1.7

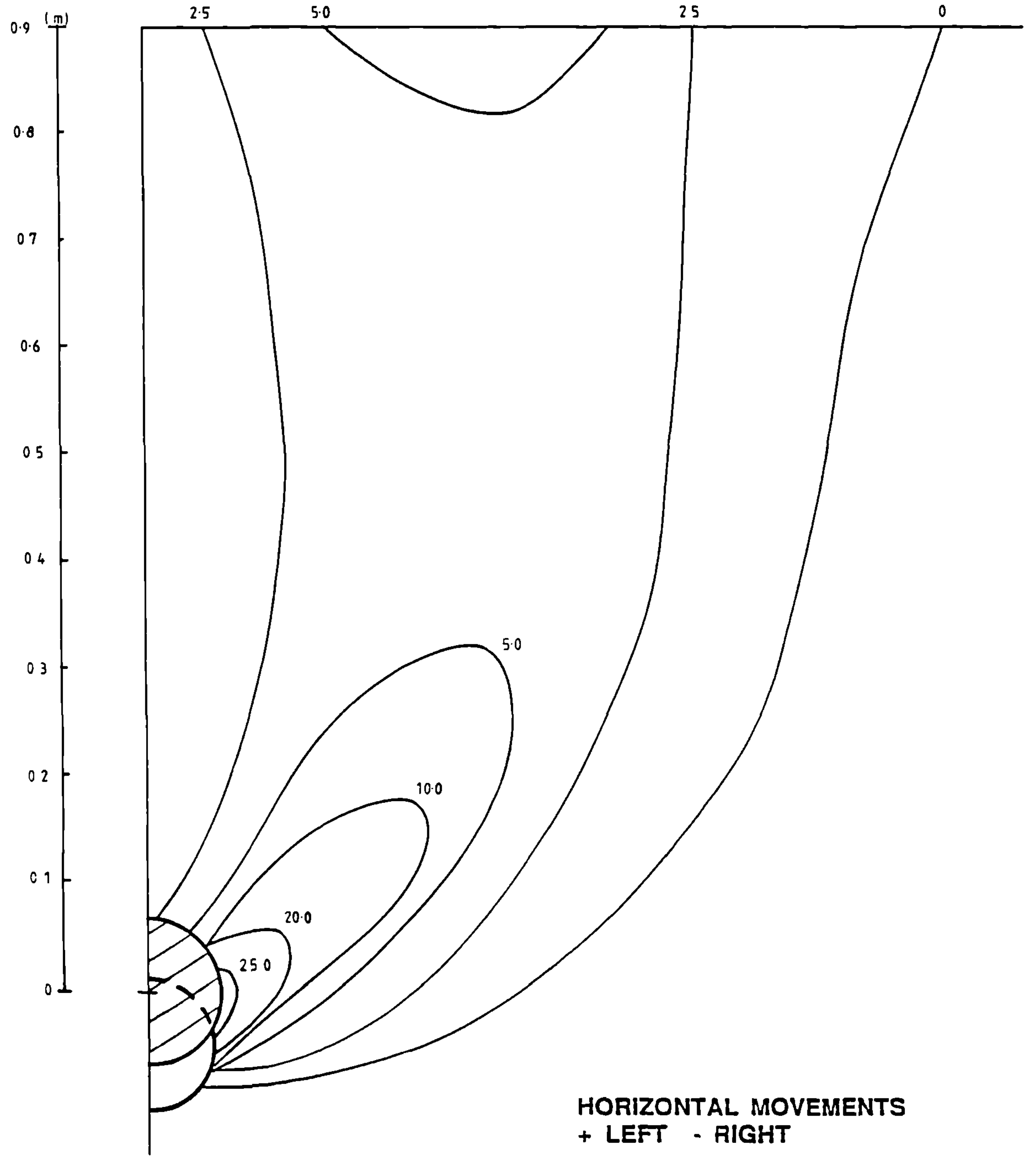

TEST PB14
7.0d25B1.7

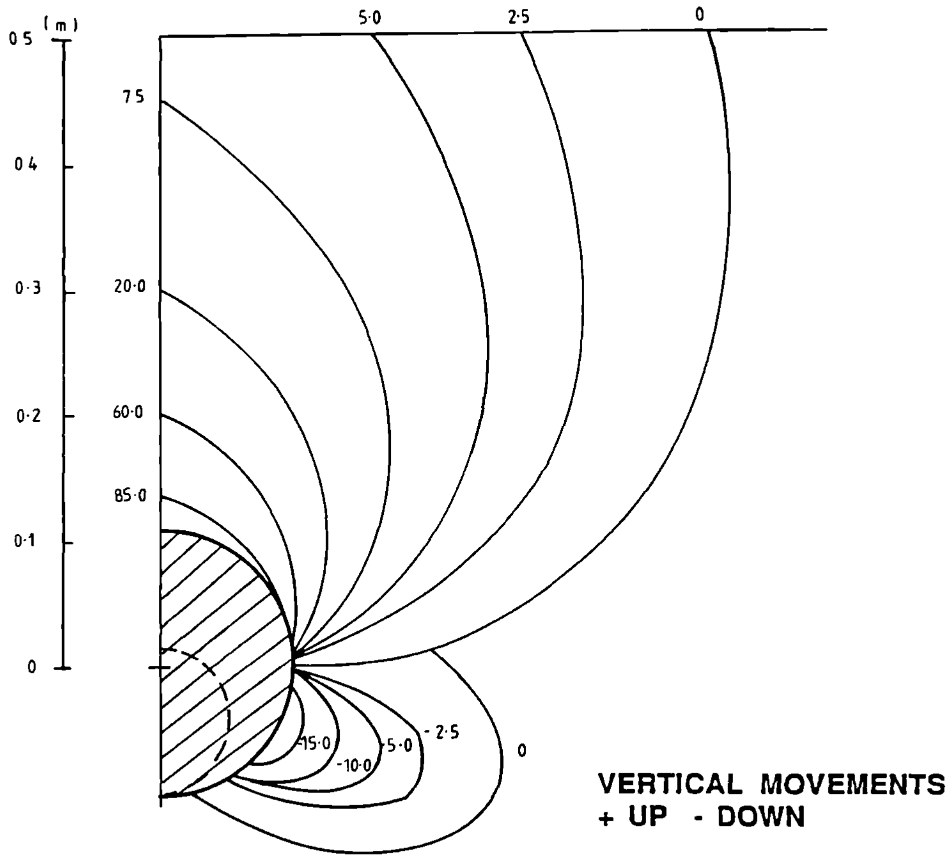

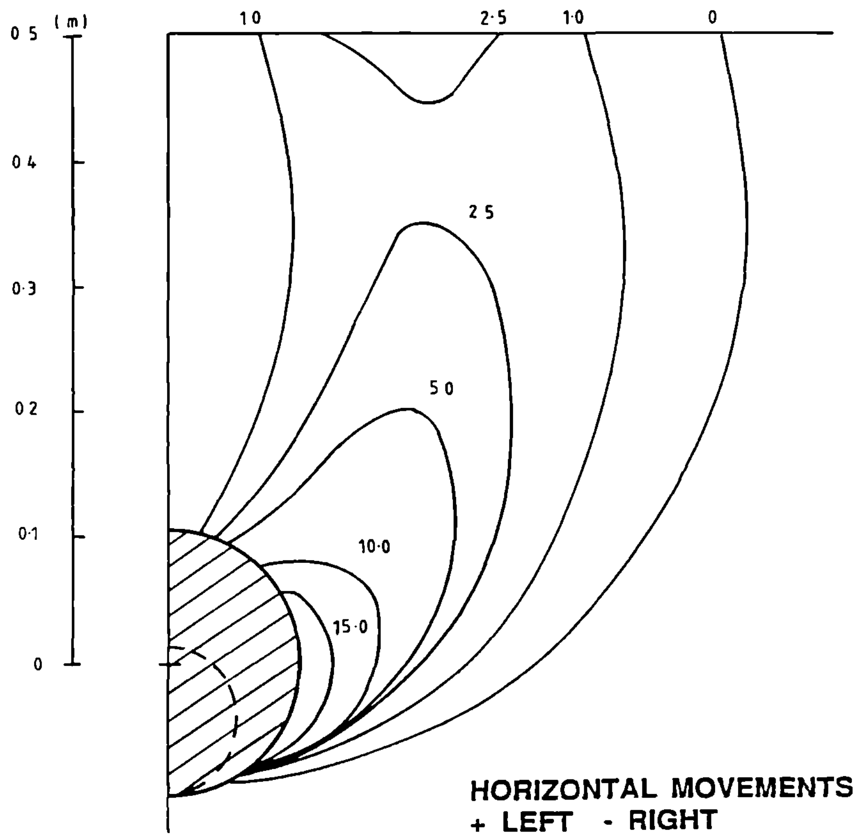

TEST PB15
3.8125B1.7

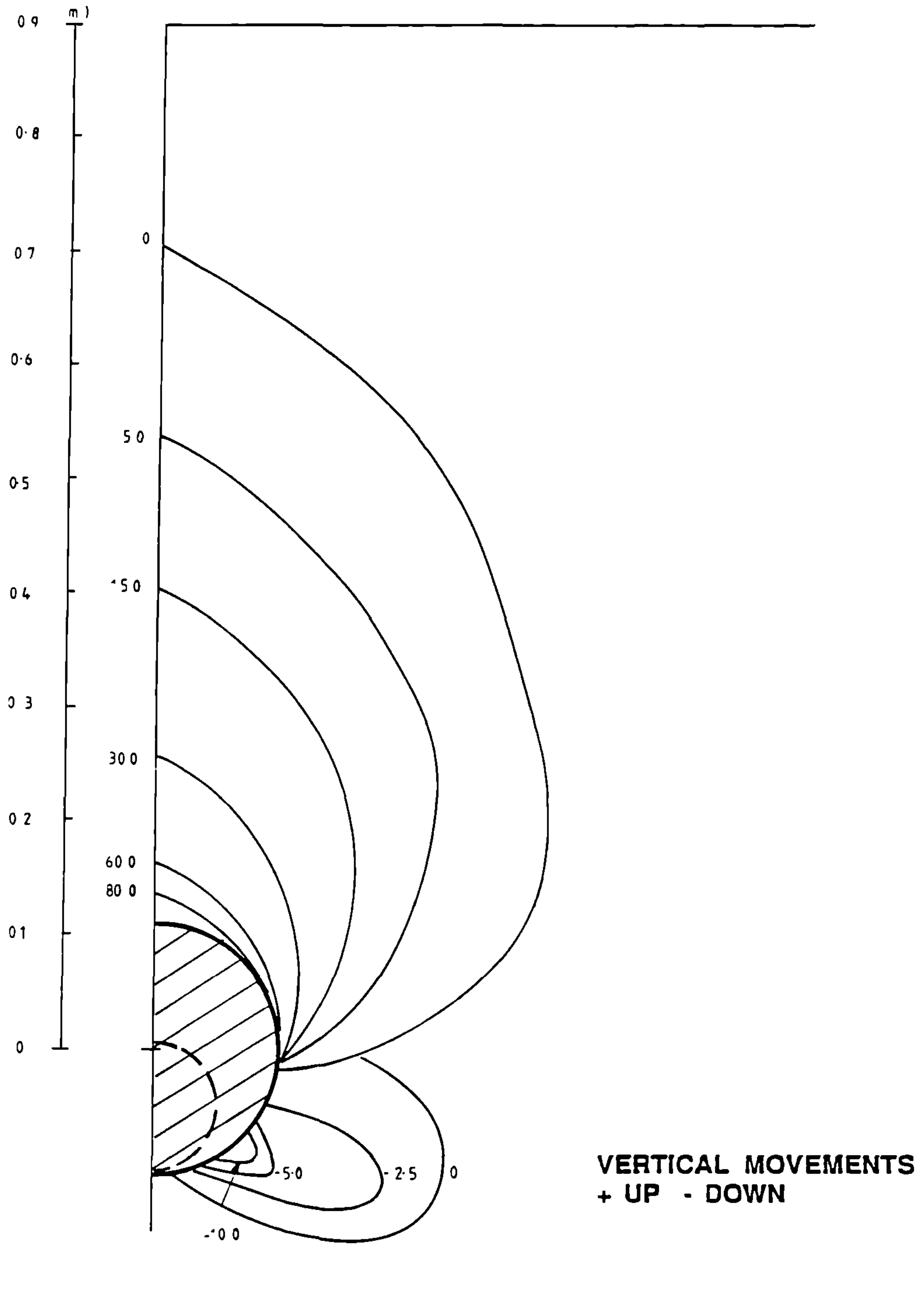

TEST PB16
7.0125B1.7

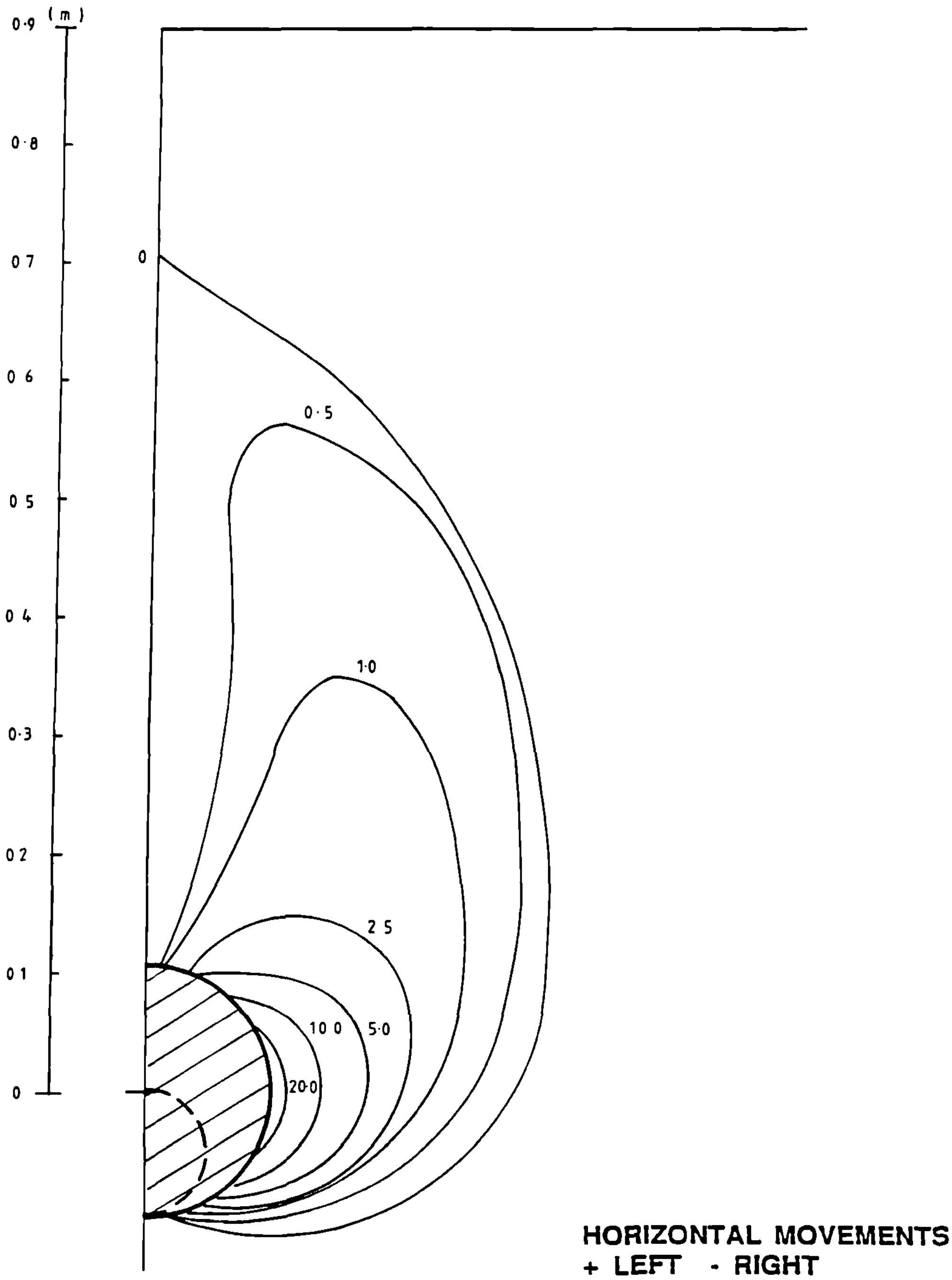

TEST PB16
7.0125B1.7

APPENDIX C

APPENDIX C

C.1 DERIVATIONS FOR THE FLUID FLOW ANALYSIS

C.1.1 Introduction

Volume loss associated with a tunnelling operation, and the requirement to know the resulting ground movements can be considered as a 'Displacement-Displacement' problem (after Sagaseta (1987)). In this case the boundary conditions are only in terms of strains (or displacements), and only strains (or displacements) are wanted. The analysis method consists of the determination of the displacement field in an isotropic and homogeneous incompressible soil (original analysis), when some material is extracted from it at a shallow depth, and the surrounding soil completely fills the void left by the extraction. The formulae given in this appendix will be based on those derived by Sagaseta (1987) for a two-dimensional plane strain situation. The methods for determining the variable volume loss used in the more specific pipejacking and pipebursting analyses are derived. Compressibility and dilation additions to the basic fluid flow method are also outlined.

C.1.2 Incompressible Fluid Flow Analysis

The basic case considered here is that of a point sink which extracts a finite volune of soil at some depth z below the ground surface. The volume loss,V, is considered to be an equivalant cylinder of radius, a, and unit length (Fig. C.1). As outlined in Chapter 6, Section 6.3.1, Step 1 of the analysis involves neglecting the ground surface and treating the soil around the tunnel as an infinite medium. The condition of no volume change implies that points located at a distance r from the sink must have an inward and radial displacement (Fig. C.2).

$$W_r(r) = \frac{a}{n}\left[\frac{a}{r}\right]^{n-1} \qquad (C.1)$$

where $W_r(r)$ is the radial displacement and n=2 in plane strain.

If the sink is at $C(x_o, y_o)$, a point P(x,y) will have displacement components:

$$W_x = -\frac{a^n}{n}\left[\frac{x-x_o}{r^n}\right] \qquad (C.2)$$

$$W_y = -\frac{a^n}{n}\left[\frac{y-y_o}{r^n}\right] \qquad (C.3)$$

where W_x and W_y are the displacements in the horizontal and vertical directions respectively, $r = ((x-x_o)^2 + (y-y_o)^2)^{1/2}$ and x_o and y_o are the origin coordinates in the horizontal and vertical planes respectively.

For Step 2, i.e. the introduction of the ground surface, a virtual image source (Fig. C.3) is used. The displacements caused by this are added to the real sink. The resulting displacements are given below:

$$W_x = -\frac{a^n}{n}\left[\frac{x}{r_1{}^n} - \frac{x}{r_2{}^n}\right] \qquad (C.4)$$

$$W_y = -\frac{a^n}{n}\left[\frac{y-Z}{r_1{}^n} - \frac{y+Z}{r_2{}^n}\right] \qquad (C.5)$$

where

$$r_1 = (x^2 + (y-Z)^2)^{1/2}$$
$$r_2 = (x^2 + (y+Z)^2)^{1/2}$$

The addition of the virtual image, in order take into account the ground surface, does not provide the complete answer and there are resultant shear stresses which need to be eliminated. This is achieved in three stages (Sagaseta (1987):

(a) Evaluate the strains at the surface by differentiation of the displacement field obtained in Steps 1 and 2 of the overall analysis (given in Chapter 6).

(b) From these strains, calculate the corresponding surface stresses.

(c) Obtain the strain field in the a half space subject to a system of forces acting on its surface equal and opposite to those calculated in step (b) above.

The results of Step 3 for the plane strain case are additional displacement componentsfor each point in the soil.

$$W_x = - a^2 \frac{x}{r_2{}^2} \left[1 - \frac{2y(y+Z)}{r_2{}^2} \right] \qquad (C.6)$$

$$W_y = a^2 \frac{y}{r_2{}^2} \left[1 - \frac{2x^2}{r_2{}^2} \right] \qquad (C.7)$$

C.2 APPLICATION OF THE FLUID FLOW ANALYSIS TO PIPEJACKING AND PIPEBURSTING OPERATIONS

As shown in Fig. C.1, the volume loss at the sink (tunnel) is given as $V=\pi a^2$, which can be considered as distributed uniformly at a distance equal to the pipe radius, R, away from the sink. This gives the volume distribution a finite thickness, δR, at this distance.

$$V = \pi.a^2 = \pi.((R+\delta R)^2 - R^2) \qquad (C.8)$$

Multiplying out the right hand side of equation C.8 and ignoring the small term δR^2, gives:

$$a^2 = 2.\delta R.R \qquad (C.9)$$

The general application of the fluid flow theory analysis to pipejacking was shown in Fig. 6.5, of Chapter 6. The origin for the coordinate system in this case is considered at the tunnel axis.

The following relationships are those derived from those originally obtained by Sagaseta, for the pipejacking situation:

$$-W_x = R.\delta R.x\left[\frac{1}{r_1^2} - \frac{1}{r_2^2}\right] \qquad (C.10)$$

$$-W_y = R.\delta R\left[\frac{y}{r_1^2} + \frac{(2.Z-y)}{r_2^2}\right] \qquad (C.11)$$

where $r_1 = (x^2 + y^2)^{1/2}$ and $r_2 = (x^2 + (2Z - y)^2)^{1/2}$.

The equations for the additional stresses, i.e. for Step 3, are given below:

$$-W_x = 2.R.\delta R \frac{x}{r_2^2}\left[1 - \frac{2(Z-y)(2Z-y)}{r_2^2}\right] \qquad (C.12)$$

$$W_y = 2.R.\delta R \frac{(Z-y)}{r_2^2}\left[1 - \frac{2x^2}{r_2^2}\right] \qquad (C.13)$$

The same equations are used in the case of pipebursting by reversing the directions on the displacement components obtained from the above equations.

C.3 VARIABLE VOLUME LOSS DISTRIBUTION

Fig. 6.6 in Chapter 6 shows the volume loss distributions use in the analyses. Initially the uniformly distributed volume loss was used (Section C.2). However, it seemed unlikely that this distribution represented the field situation for pipejacking, as the pipe sections would tend to sit at the invert of the excavated cavity and the resulting volume loss distribution for the overcut would be more like Fig. 6.6b. Fig. C.4 shows how the δR value for this analysis is calculated.

A further concentration of the volume loss around the installed pipe was considered more appropriate for the laboratory model test results, due to the nature of the sand behaviour (Fig.

6.6c). The calculation for the δR value in this situation is shown in Fig. C.5.

C.4 COMPRESSIBILITY AND DILATION EFFECTS

This was discussed in Chapter 6 and it is not proposed to repeat it all here. Equation C.14 shows the basic equation derived for displacements around an expanding cavity:

$$W_r(r) = k\frac{a}{n}\left[\frac{a}{r}\right]^{\alpha} \qquad (C.14)$$

Comparing this with the basic equation used in the fluid flow analysis (equation C.1) shows that the incompressible flow model is one particular solution of equation C.14, when k=1 and α=n-1. Sagaseta (1987) suggested the following relationships for α in equation C.14, in order to take into account compressibility and dilation, i.e. the α power factor reduces or increases the rate at which the displacements vary as one moves away from the sink.

For a sink in a dense soil or a source in a loose soil,

$$\alpha = \frac{(n-1)}{\alpha_a} \qquad (C.15)$$

For a sink in a loose soil or a source in a dense soil,

$$\alpha = (n-1)\,\alpha_a \qquad (C.16)$$

where $\alpha_a = (1-\sin\psi')/(1+\sin\psi')$ and ψ' is the angle of dilatency of the soil. This means that with n=2 and ψ'=0, then the analysis is the same as the original incompressible flow model. In general terms ψ' can be used as a expansion/compressibility factor, values of which can be obtained to represent different soil types encountered in the field.

The general equations for the analysis of pipejacking operations are given in equations C.17 and C.18:

$$-W_x = \frac{Q.x}{\alpha}\left[\frac{1}{r_1\alpha} - \frac{1}{r_2\alpha}\right] \qquad (C.17)$$

$$-W_y = \frac{Q}{\alpha}\left[\frac{y}{r_1\alpha} + \frac{(2.Z-y)}{r_2\alpha}\right] \qquad (C.18)$$

where $Q = ((2.R.\delta R)^{0.5})^{\alpha}$ and $r_1 = (x^2 + y2)^{½}$ and $r_2 = (x^2 + (2Z - y)^2)^{½}$.

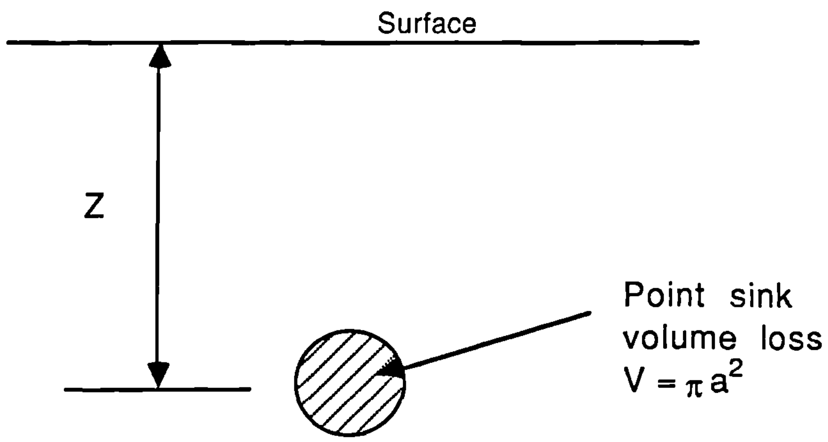

Fig. C.1 Idealisation of the volume loss at a sink (i.e. during tunnel construction)

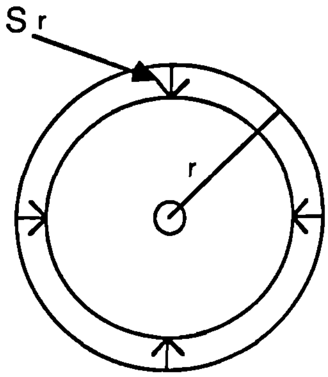

Fig. C.2 Assumption that the displacements are inward and radial

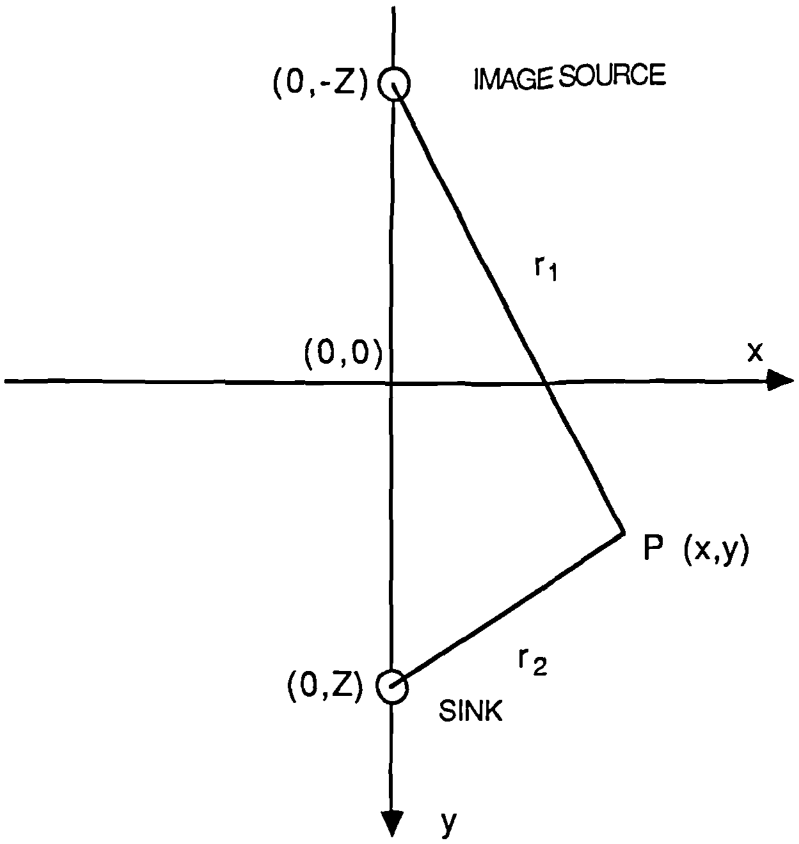

Fig. C.3 A virtual image is used to take into account the ground surface

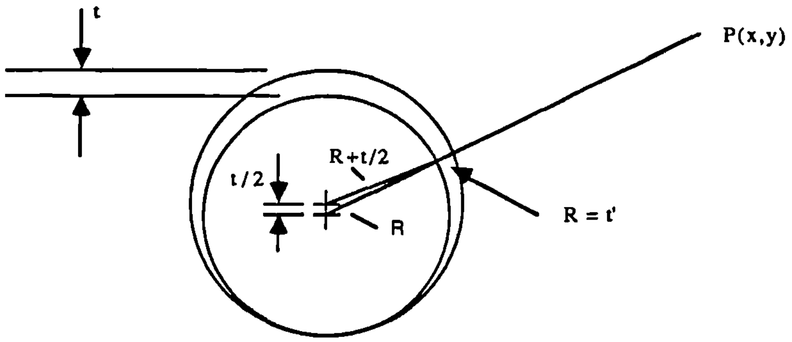

Using the cosine fomula the value
of t' can be calculated

Fig. C.4 Calculation of variable volume loss (zero at invert and maximum at crown)

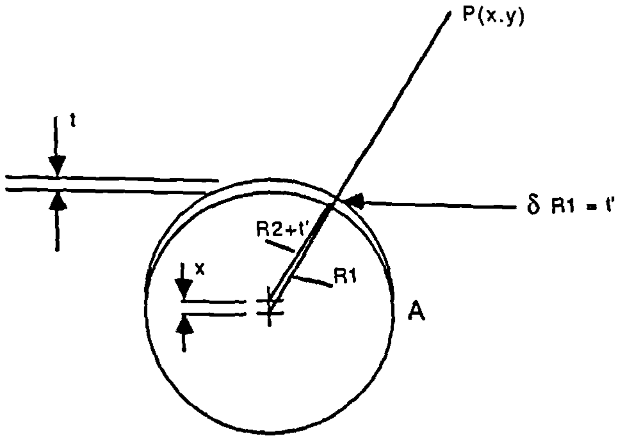

$$R2 = R1 + t \qquad (1)$$

$$x^2 + R1^2 = R2^2 \qquad (2)$$

substituting (1) into (2)

$$\Rightarrow x = (t^2 + 2.R1.t)^{1/2}$$

Using the cosine fomula the value of t' can be calculated

Fig. C.5 Calculation of variable volume loss (zero at the springings and maximum at crown)

APPENDIX D

APPENDIX D CALCULATION OF CURVATURE

The centre of curvature for a particular line, or part of a line, is the point to which the perpendiculars to the tangents to the line meet. The radius of curvature (R) is the distance from the centre of curvature to the line (Fig. D.1). The curvature of the line is defined as the inverse of the radius of curvature.

The derivation for the formula to calculate the curvature of a line joining three points is given below:

$$R.\beta_3 = S \tag{D.1}$$

$$S^2 = (x_1+x_2)^2 + y_2^2 \tag{D.2}$$

From the angles in Fig. D.1

$$\beta_3 = \beta_2 - \beta_1 \tag{D.3}$$

where $\beta_1 = (y_1/x_1)$ and $\beta_2 = (y_2-y_1)/x_2$, assuming distances are small. Substituing equations D.2 and D.3 into D.1 allows R to be calculated.

$$R = \frac{((x_1+x_2)^2 + y_2^2)^{1/2}}{(y_1/x_1) - (y_2-y_1)/x_2} \tag{D.4}$$

As mentioned above the curvature is the inverse of the radius of curvature

$$\text{Curvature} = \frac{(y_1/x_1) - (y_2-y_1)/x_2}{((x_1+x_2)^2 + y_2^2)^{1/2}} \tag{D.5}$$

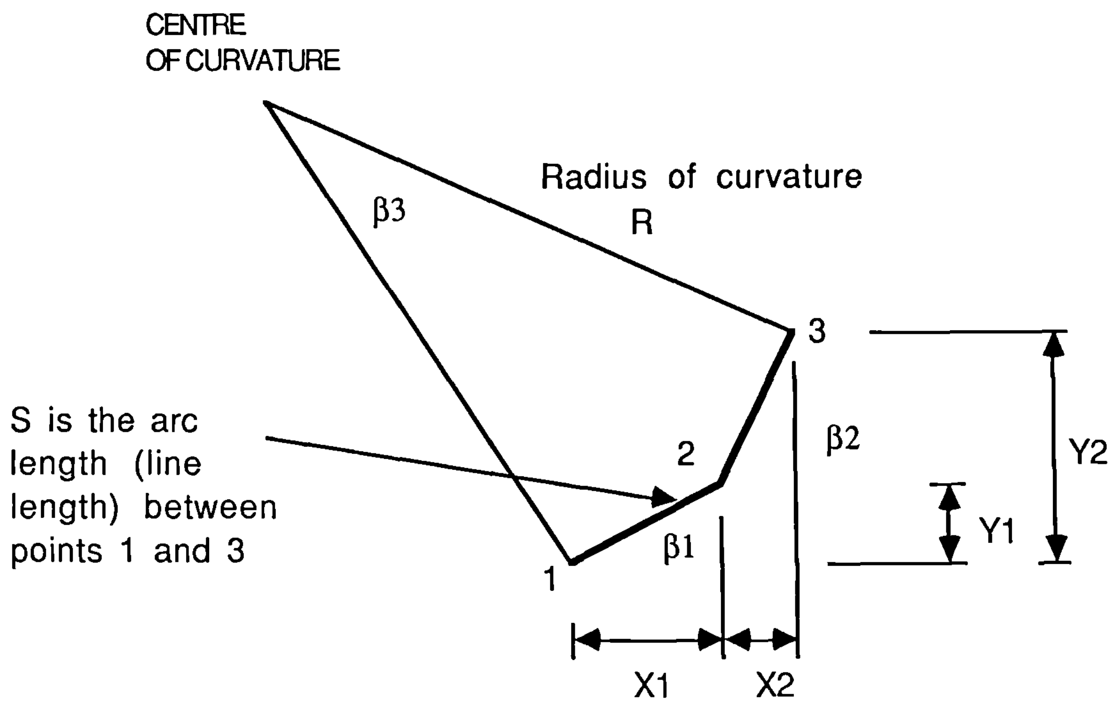

Fig. D.1 The main points required for the calculation of the curvature of a line